BioMed Research International

Impact of Nutritional and Environmental Factors on Inflammation, Oxidative Stress, and the Microbiome 2019

Special Issue Editor in Chief: Gang Liu
Guest Editors: Yan Huang, Filipa S. D. Reis, Deguang Song, and Hengjia Ni

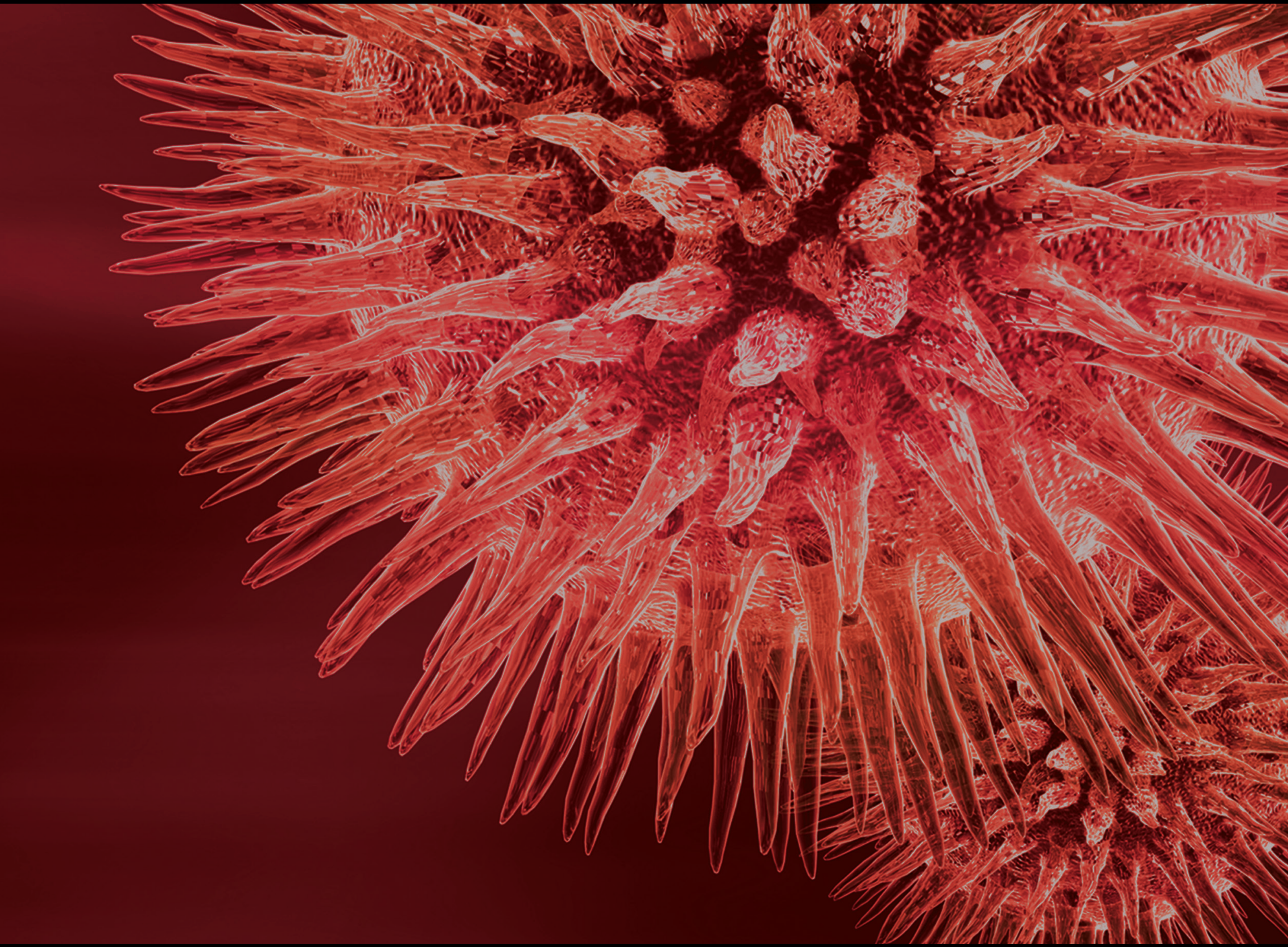

Impact of Nutritional and Environmental Factors on Inflammation, Oxidative Stress, and the Microbiome 2019

BioMed Research International

Impact of Nutritional and Environmental Factors on Inflammation, Oxidative Stress, and the Microbiome 2019

Special Issue Editor in Chief: Gang Liu
Guest Editors: Yan Huang, Filipa S. Reis, Deguang Song, and Hengjia Ni

Copyright © 2019 Hindawi. All rights reserved.

This is a special issue published in "BioMed Research International." All articles are open access articles distributed under the Creative Commons Attribution License, which permits unrestricted use, distribution, and reproduction in any medium, provided the original work is properly cited.

Contents

Impact of Nutritional and Environmental Factors on Inflammation, Oxidative Stress, and the Microbiome 2019
Gang Liu, Yan Huang, Filipa S. Reis, Deguang Song, and Hengjia Ni
Editorial (5 pages), Article ID 5716241, Volume 2019 (2019)

Effects of Proanthocyanidins on Arsenic Methylation Metabolism and Efflux in Human Hepatocytes L-02
Qing-Xin Ren, Meng-Chuan Xu, Qiang Niu, Yun-Hua Hu, Hai-Xia Wang, and Shu-Gang Li
Research Article (11 pages), Article ID 3924581, Volume 2019 (2019)

Biochemical Hallmarks of Oxidative Stress-Induced Overactivation of *Xenopus* Eggs
Alexander A. Tokmakov, Misaki Awamura, and Ken-Ichi Sato
Research Article (7 pages), Article ID 7180540, Volume 2019 (2019)

Prebiotic Effect of Lycopene and Dark Chocolate on Gut Microbiome with Systemic Changes in Liver Metabolism, Skeletal Muscles and Skin in Moderately Obese Persons
Maria Wiese, Yuriy Bashmakov, Natalia Chalyk, Dennis Sandris Nielsen, Łukasz Krych, Witold Kot, Victor Klochkov, Dmitry Pristensky, Tatyana Bandaletova, Marina Chernyshova, Nigel Kyle, and Ivan Petyaev
Clinical Study (15 pages), Article ID 4625279, Volume 2019 (2019)

Systemic Level of Oxidative Stress during Orthodontic Treatment with Fixed Appliances
Vito Kovac, Borut Poljsak, Giuseppe Perinetti, and Jasmina Primozic
Research Article (6 pages), Article ID 5063565, Volume 2019 (2019)

Copper (II) Ions Activate Ligand-Independent Receptor Tyrosine Kinase (RTK) Signaling Pathway
Fang He, Cong Chang, Bowen Liu, Zhu Li, Hao Li, Na Cai, and Hong-Hui Wang
Research Article (8 pages), Article ID 4158415, Volume 2019 (2019)

The Roles of Environmental Factors in Regulation of Oxidative Stress in Plant
Xiulan Xie, Zhouqing He, Nifan Chen, Zizhong Tang, Qiang Wang, and Yi Cai
Review Article (11 pages), Article ID 9732325, Volume 2019 (2019)

Milk Fat Globule Membrane Supplementation Promotes Neonatal Growth and Alleviates Inflammation in Low-Birth-Weight Mice Treated with Lipopolysaccharide
Shimeng Huang, Zhenhua Wu, Cong Liu, Dandan Han, Cuiping Feng, Shilan Wang, and Junjun Wang
Research Article (10 pages), Article ID 4876078, Volume 2019 (2019)

The Bidirectional Interactions between Resveratrol and Gut Microbiota: An Insight into Oxidative Stress and Inflammatory Bowel Disease Therapy
Yaolian Hu, Daiwen Chen, Ping Zheng, Jie Yu, Jun He, Xiangbing Mao, and Bing Yu
Review Article (9 pages), Article ID 5403761, Volume 2019 (2019)

***Dittrichia viscosa* L. Ethanolic Extract Based Ointment with Antiradical, Antioxidant, and Healing Wound Activities**
Wafa Rhimi, Raoudha Hlel, Issam Ben Salem, Abdennacer Boulila, Ahmed Rejeb, and Mouldi Saidi
Research Article (10 pages), Article ID 4081253, Volume 2019 (2019)

The Nutritional Cytokine Leptin Promotes NSCLC by Activating the PI3K/AKT and MAPK/ERK Pathways in NSCLC Cells in a Paracrine Manner
Fengzhou Li, Shilei Zhao, Tao Guo, Jinxiu Li, and Chundong Gu
Research Article (8 pages), Article ID 2585743, Volume 2019 (2019)

Quorum Sensing: A Prospective Therapeutic Target for Bacterial Diseases
Qian Jiang, Jiashun Chen, Chengbo Yang, Yulong Yin, and Kang Yao
Review Article (15 pages), Article ID 2015978, Volume 2019 (2019)

Microarray Based Functional Analysis of Myricetin and Proteomic Study on Its Anti-Inflammatory Property
Tao Li, Jihe Zhu, Fangming Deng, Weiguo Wu, Zhibing Zheng, Chenghao Lv, Yong Li, Wei Xiang, Xiangyang Lu, and Si Qin
Research Article (13 pages), Article ID 3746326, Volume 2019 (2019)

MicroRNA-15a-5p Regulates the Development of Osteoarthritis by Targeting PTHrP in Chondrocytes
Zhi-xi Duan, Peng Huang, Chao Tu, Qing Liu, Shuang-qing Li, Ze-ling Long, and Zhi-hong Li
Research Article (11 pages), Article ID 3904923, Volume 2019 (2019)

Leukemia Inhibitory Factor Receptor Is Involved in Apoptosis in Rat Astrocytes Exposed to Oxygen-Glucose Deprivation
Liang Huo, Yuying Fan, and Hua Wang
Research Article (8 pages), Article ID 1613820, Volume 2019 (2019)

Benzoic Acid Used as Food and Feed Additives Can Regulate Gut Functions
Xiangbing Mao, Qing Yang, Daiwen Chen, Bing Yu, and Jun He
Review Article (6 pages), Article ID 5721585, Volume 2019 (2019)

Comparison of Chromium and Iron Distribution in Serum and Urine among Healthy People and Prediabetes and Diabetes Patients
Qi Zhou, Wenjia Guo, Yanan Jia, and Jiancheng Xu
Research Article (8 pages), Article ID 3801639, Volume 2019 (2019)

The Impact of *Lactobacillus plantarum* on the Gut Microbiota of Mice with DSS-Induced Colitis
Fei Zhang, Yue Li, Xiliang Wang, Shengping Wang, and Dingren Bi
Research Article (10 pages), Article ID 3921315, Volume 2019 (2019)

Orostachys japonicus A. Berger Extracts Induce Immunity-Enhancing Effects on Cyclophosphamide-Treated Immunosuppressed Rats
Hak Yong Lee, Young Mi Park, Jeong Kim, Hong Geun Oh, Kang Sung Kim, Hee Joo Kang, Ri Rang Kim, Min Jung Kim, Sang Hee Kim, Hye Jeong Yang, and Jisun Oh
Research Article (9 pages), Article ID 9461960, Volume 2019 (2019)

Splenectomy Promotes Macrophage Polarization in a Mouse Model of Concanavalin A- (ConA-) Induced Liver Fibrosis
Yongjuan Wang, Xiaopei Guo, Guohui Jiao, Lili Luo, Lu Zhou, Jie Zhang, and Bangmao Wang
Research Article (12 pages), Article ID 5756189, Volume 2019 (2019)

The Ovotransferrin-Derived Peptide IRW Attenuates Lipopolysaccharide-Induced Inflammatory Responses
Huanli Jiao, Qing Zhang, Yuanbang Lin, Ying Gao, and Peng Zhang
Research Article (7 pages), Article ID 8676410, Volume 2019 (2019)

Moringa peregrina Leaves Extracts Induce Apoptosis and Cell Cycle Arrest of Hepatocellular Carcinoma
Mohamed Mansour, Magda F. Mohamed, Abeer Elhalwagi, Hanaiya A. El-Itriby, Hossam H. Shawki, and Ismail A. Abdelhamid
Research Article (13 pages), Article ID 2698570, Volume 2019 (2019)

The Immunogenicity of the C Fragment of Tetanus Neurotoxin in Production of Tetanus Antitoxin
Rui Yu, Chong Ji, Junjie Xu, Denghai Wang, Ting Fang, Yue Jing, Clifton Kwang-Fu Shen, and Wei Chen
Research Article (9 pages), Article ID 6057348, Volume 2018 (2019)

Chlorogenic Acid Functions as a Novel Agonist of PPARγ2 during the Differentiation of Mouse 3T3-L1 Preadipocytes
Shu-guang Peng, Yi-lin Pang, Qi Zhu, Jing-he Kang, Ming-xin Liu, and Zheng Wang
Research Article (14 pages), Article ID 8594767, Volume 2018 (2019)

Effect of Quercetin Monoglycosides on Oxidative Stress and Gut Microbiota Diversity in Mice with Dextran Sodium Sulphate-Induced Colitis
Zhu Hong and Meiyu Piao
Research Article (7 pages), Article ID 8343052, Volume 2018 (2019)

Immunomodulatory Effects of Probiotics on Cytokine Profiles
Md. Abul Kalam Azad, Manobendro Sarker, and Dan Wan
Review Article (10 pages), Article ID 8063647, Volume 2018 (2019)

Hindawi
BioMed Research International
Volume 2019, Article ID 5716241, 5 pages
https://doi.org/10.1155/2019/5716241

Editorial

Impact of Nutritional and Environmental Factors on Inflammation, Oxidative Stress, and the Microbiome 2019

Gang Liu,[1] **Yan Huang**,[2] **Filipa S. Reis**,[3] **Deguang Song**,[4] **and Hengjia Ni**[1]

[1] *Hunan Province Key Laboratory of Animal Nutritional Physiology and Metabolic Process, Key Laboratory of Agro-ecological Processes in Subtropical Region, Institute of Subtropical Agriculture, Chinese Academy of Sciences, National Engineering Laboratory for Pollution Control and Waste Utilization in Livestock and Poultry Production, Changsha, Hunan 410125, China*
[2] *Department of Animal Science, Division of Agriculture, University of Arkansas, Fayetteville, AR 72701, USA*
[3] *Polytechnic Institute of Bragança, Bragança, Portugal*
[4] *Yale School of Medicine, New Haven, USA*

Correspondence should be addressed to Hengjia Ni; nihengjia@isa.ac.cn

Received 1 July 2019; Accepted 1 July 2019; Published 10 July 2019

Copyright © 2019 Gang Liu et al. This is an open access article distributed under the Creative Commons Attribution License, which permits unrestricted use, distribution, and reproduction in any medium, provided the original work is properly cited.

1. Introduction

Metabolically and physiologically, the body is governed by a number of factors: the environment, foodstuffs, the interrelationship and balance of internal microorganisms, and the emotional and physical issues related to stress, inflammation, and illness. Studies show that certain invasive physical and mental issues, possibly caused by surgery, pathogens, or even harmful environmental factors, can lead the body to overgenerate its immune defences, causing inflammation and oxidative stress.

It is known that intestinal microbes react to the immune condition, physiological state, and metabolic activity of their human hosts and that these factors influence health. Extensive but as of yet inconclusive research has identified that probiotics and certain nutrients can assist in the management of oxidative stress, controlling the production of reactive oxygen species (ROS) and reactive nitrogen species (RNS). Some natural compounds and nutraceuticals control the composition of intestinal microbiota, retarding inflammation and allowing the body's natural immune system to control metabolic and physiological processes.

The particular processes that lead to the appearance of disease have yet to be established. The influence of nutrition and the environment, which facilitates the control of inflammation, oxidative stress, and microbiome, requires further study.

This special issue was open to submissions for 9 months from May 2018 to March 2019 and focuses on recent findings on the regulation of inflammation, oxidative stress, and microbiome in diseases and the influence of nutrients, probiotics, and the environment on the development of such diseases.

2. Development Mechanisms and Biomarkers of Disease

A. A. Tokmakov et al. focused on the oxidative stress–induced overactivation of *Xenopus* eggs and studied their biochemical hallmarks. Their study showed that time- and dose-dependent overactivation resulted from high levels of hydrogen peroxide–induced oxidative stress. The overactivated eggs were found to have a decreased volume of soluble cytoplasmic protein content, an accumulated volume of lipofuscin, and depletion of intracellular ATP.

There continues to be a major need for tetanus antitoxin (TAT) in developing and underdeveloped countries. It is a comparatively cheap treatment that is easily administered. Nevertheless, there are questions relating to the production of potent TAT using tetanus toxoid (TT) as an immunogen to elicit an immune response. An immunogenicity study was conducted by R. Yu et al. regarding the involvement of the C fragment of tetanus neurotoxin (TeNT-Hc) in the production of TAT. It was found that TeNT-Hc serves as a totally nontoxic recombinant alternative to TT where liver toxicity is not present, with all of the same benefits, as proven in a lengthy safety study. The results showed that TeNT-Hc was suitable for the production of TAT, either separately or in combination with TT.

Y. Wang et al. investigated the necessity for myeloid-derived suppressor cells (MDSCs) and the nuclear transition factor kappa B (NF-KB) for the protective effects of splenectomy, conducted in a mouse model of ConA-induced liver fibrosis. The results showed that whilst the levels of the M2 macrophage inflammatory factors increased after removal of the spleen, the levels of the M1 macrophages and the volume of macrophages/monocytes decreased. Thus, the operation may promote the polarisation of CD11b+Ly6Chigh MDSCs and limit the level of NF-KB p65-p50 heterodimers, which retard the development of liver fibrosis.

Serum and urinary Cr and Fe levels were investigated by Q. Zhou et al., who studied patients in northeast China with impaired fasting glucose (IFG) and impaired glucose tolerance (IGT) and those with type 1 (T1D) and type 2 (T2D) diabetes. They found that serum creatine (serum cr) level decreased in patients with diabetic retinopathy (DR), nephropathy (DN), and peripheral neuropathy (DPN). The highest level of urinary cr was in T1D samples and was considerably higher than those in T2D groups, with or without complications. The urinary Fe level in T1D increased ($P < 0.05$). Clearly, a positive link existed between serum Cr and serum Fe in T2D patients, indicating that further studies should establish the possible significance of Fe and Cr in diabetes.

Central nervous system cells are protected by leukemia inhibitory factor (LIF) and leukemia inhibitory factor receptor (Lifr), particularly neurons and myelin-sheath oligodendrocytes, in a state of oxygen-glucose deprivation (OGD). L. Huo et al. conducted a study to establish the significance of Lifr in OGD and the mechanism by which it affects hypoxic-ischemic astrocytes. The aim was to derive more information on the neuroprotective role of Lifr. Their findings established the direction and clinical necessity to determine the suitability of Lifr as a repair treatment for neurological and stroke patients.

It has been made increasingly apparent that osteoarthritis (OA) is caused by the degeneration of chondrocytes. Z. Duan et al. showed that parathyroid hormone-related proteins (PTHrP) are targeted by specific microRNAs (miRNAs), which may also control the proliferation and terminal differentiation of chondrocytes. The study further showed that miR-15a-5p was downregulated in OA chondrocytes and that PTHrP was upregulated therein. From these findings, a negative link was established between miR-15a-5p and PTHrP. The reduction of miR-15a-5p encouraged the growth of chondrocytes and restricted calcium build-up, whereas PTHrP was neutralised by the overexpression of miR-15a-5p. These results further clarify the reasons for OA development and signify that miR-15a-5p may be applicable as a biomarker for OA.

V. Kovac et al. conducted a study that examined patients who were undergoing the first 7 days of an orthodontic treatment program with fixed appliances, evaluating various chosen systematic oxidative stress levels. It was found that the treatment may initially lead to the development of systematic oxidative stress, but the effect did not persist. Specifically, increases in ROS and ROS/AD levels were observed only 24 hours after the commencement of treatment. The levels stabilised within 7 days after archwire insertion because of an adaptive endogenous antioxidative response. During subsequent orthodontic treatments, such as archwire reactivation, there was a likelihood that a change of ROS and ROS/AD levels would occur.

Management of oxidative stress in plants has been the subject of several recent studies reviewed by X. Xie et al. This review observed that plants are subject to a number of environmental issues and pressures during their growth, relating to extreme temperature fluctuations, metal toxicity, salinity, and drought. In addition, UV-B radiation, pathogen infection, and pesticides pose challenges to their survival. Plants are able to ameliorate these threats by adapting their molecular, biological, and physiological makeup, in particular via their antioxidant systems. Genetically modified plants, by overexpressing their functional genes, show a marked ability to overcome oxidative stress. This leads to the recommendation that transgenic plants should be cultivated to generate multiple effective genes to combat possibly harmful environments.

A study was performed by F. He et al. to analyse the ligand-independent receptor tyrosine (RTK) cellular signalling pathway and assess its reaction with copper ions (II) (F. He et al.). Copper (II), in the absence of corresponding epidermal growth factor (EGF) and hepatocyte growth factor (HGF) ligands, was used to activate the respective receptor signalling. Two RTK-mediated downstream signal transducers were initiated by copper (II) ions. Proliferation and cellular migration were increased significantly by the use of copper (II). This signifies that cancer treatment may require the growth factors in tumour microenvironments and copper (II) to be points of focus.

3. Regulation of Nutritional Factors on Diseases

3.1. Botanical Extracts and Natural Compounds. Despite increased research on plant extracts and natural compounds, the impact of these materials on regulating physiological and metabolic development has not been fully analysed and requires further investigation.

Research by Q.-X. Ren et al. focused on the effects of arsenic methylation metabolism and efflux in human hepatocytes (L-02) by proanthocyanidins (PC). Their findings that PC can influence arsenic methylation metabolism and efflux in L-02 cells may account for the increased regulation of glutathione peroxidase (GSH), multidrug resistance protein

1 (MRP1), and arsenite methyltransferase (AS3MT) levels by PC.

The role of chlorogenic acid (CGA), a phenolic secondary metabolite in many fruits and vegetables, was evaluated by S. Peng et al. and assessed for its role in the differentiation and lipolysis of mouse 3T3-L1 preadipocytes. As a peroxisome proliferator-activated receptor-gamma (PPARy2) agonist, CGA can stimulate 3T3-L1 preadipocyte differentiation. It was found that rosiglitazone (RG) performed unlike CGA in relation to fat metabolism in the process of adipocyte differentiation. The RG-treated group contained a markedly higher level of triacylglyceride (TAG) than that observed in the CGA-treated group, possibly because of decreased lipid accumulation before preadipocyte differentiation, due to lipolysis rather than lipid synthesis not being operative. The results show CGA to be a different PPARy2 agonist to RG.

Z. Hong et al. investigated the effects of two dietary additions in an experiment to evaluate the protective effects of certain substances on colitis in mice induced by dextran sodium sulfate (DSS). One preparation was based on an onion preparation fortified only with quercetin aglycone (Q). The second onion preparation contained quercetin aglycone and monoglycosides (Q+MQ). Signs of colitis emerged in mice after 7 days of treatment. The symptoms were colonic inflammation and growth reduction. The results showed that both diets reduced the effects of the DSS-induced colitis, even when administered at a low dosage. A range of fruits and vegetables contain quercetin, and these results indicate that a quercetin-supplemented diet (Q or Q+MQ) is a possible ancillary treatment for inflammatory bowel disorder (IBD).

The *Moringa oleifera* tree, one species of the sole-genus plant family *Moringaceae*, grows in several tropical and subtropical regions. M. Mansour et al. examined the reputed anticancer and antimicrobial attributes of the leaf extract of both *Moringa peregrina* and *Moringa oleifera* grown in Egypt. The serial leaf extract of both varieties displayed antimicrobial characteristics against Gram-positive and Gram-negative bacteria and fungi. The extracts also showed cytotoxic effects against HepG2 and MCF-7 cell lines while displaying low toxicity to normal melanocyte cell lines. Cell cycle arrest and apoptosis of HepG2 cells for anticancer activity analysis were conducted effectively with the diethyl ether and ethyl acetate methods. Analysis via gas chromatography-mass spectrometry analysis showed the leaf extracts to be rich in thymol, retinol and ascorbic, palmitic, linoleic and myristic acids, thereby accounting for the displayed activity.

IBD is exacerbated by dysbiosis and oxidative stress in the gut. The current research on the interaction between gut microbiota and resveratrol, combined with new evidence for the treatment of IBD and oxidative stress, was reviewed by Y. Hu et al. Intestinal health, the cellular redox condition, and the inflammatory response in the host organism are all regulated by gut microbiota. The generation of short-chain fatty acids (SCFAs) and proinflammatory cytokines, linked to enteric bacteria, is able to modulate the proinflammatory NF-kB signalling pathway. Resveratrol and its metabolites are able to reduce increased levels of ROS, activate Nrf2 signalling, and ease oxidative stress by inhibiting inflammatory disorders via changes in the gut microbiota. They act to protect epithelial barrier functions and suppress intestinal inflammation and the activation of NF-κB. Resveratrol is thus a new and effective means to treat chronic inflammatory illnesses.

The antioxidant effects of *Dittrichia viscosa*, with its potential for healing wounds, have been authenticated by W. Rhimi et al. Testing involved processing an ethanolic extract of the leaves with other components to form a mass fraction of 2.5% and 5% extracts in beeswax and sesame oil-based ointments. Analysis of the caffeoylquinic acid content (CQC), the phenol content (TPC), and antioxidant activity in the extract was then performed, and the researchers then conducted a wound-healing test using the composite ointments. It was shown that *D. viscosa* was a source of antioxidant compounds, especially caffeoylquinic acid, and was able to prevent oxidative damage and scavenge free radicals. Treatment of wounded animals using these two ointments resulted in complete repair, with good skin regeneration and re-epithelialization in comparison to other control groups. The study identifies the suitability of *D. viscosa* as an additive to pharmaceutical products to heal wounds and in the treatment of oxidative stress.

The immunity effects of *Orostachys japonicus* (OJ) A. Berger were evaluated by H. Y. Lee et al. in a controlled environment. Mouse splenocytes were treated with either extract of OJ or water, both with and without cyclophosphamide (CY). In the presence of OJ extract, an increase was seen in the propagation of splenocytes, and a reduction was seen in CY-induced cytotoxicity. Immunosuppressed rats displayed improved stamina after treatment with OJ extracts when assessed with an obligatory swim test. Treatment with the extract increased the number of immunity-related cells and the levels of plasma cytokines. Thus there is a clear indication that OJ treatment increases immune cell propagation and specific plasma cytokine levels, thereby improving immunity.

An innovative cross-linked omics study was conducted by T. Li et al. The aim was to evaluate the effect of myricetin, a common flavonoid found in many edible plants. They evaluated its anti-inflammatory properties by inspecting the molecular evidence and performing a proteomics assay of gene expressions in a genome-wide analysis, utilising microarrays and specialist analysis tools. The results showed that myricetin exerted a significant anti-inflammatory effect on metabolic disease and lipid metabolism in HepG2 cells and on cardiovascular disease. The indications are that myricetin could have future pharmaceutical health applications. Well-structured research, combining anti-inflammatory proteomics analysis and gene chip data, has led to improved considerations for its multiomic use.

3.2. Probiotics. Probiotics have wide-ranging applications in medical science. Alone or in combination with prebiotics, they are instrumental in controlling gut microbiota, thereby displaying anticancer, angiogenic activities, antipathogenic, antiobesity, diabetic and antidiabetic, anti-inflammatory, and angiogenic activities, in addition to their positive results on the central nervous system and the brain.

M. A. K. Azad et al. reviewed recent research on the effects of probiotic immunomodulators and found that their antiviral properties influenced innate immunity. By stimulating B cells, they improved gut barrier functions and influenced cytokine production, thereby generating host body adaptive responses. More research is needed to establish how probiotics create immunomodulatory effects to combat inflammation.

F. Zhang et al. conducted an experiment using *Lactobacillus plantarum* to investigate its effect on gut inflammation and its interaction with gut microbiota and the immune response. Mice that had been treated with DSS to initiate colitis were fed *Lactobacillus plantarum*. This markedly lowered the production of proinflammatory cytokines during the colitis development phase, and the results indicated that the treatment could improve the pathophysiology of DSS generated colitis. The impact of intestinal microorganisms was lower in the *L. plantarum* group than in the DSS group, showing improved tract stability. The indications are that *L. plantarum* could be used as an IBD treatment because it can manage the symptoms of colitis.

3.3. Other Nutrients. Anti-inflammatory effects are apparent in IRW (Ile-Arg-Trp), which is a bioactive peptide isolated from egg ovotransferrin. An investigation of IRW for use in the treatment of inflammatory cytokines and microbiota was conducted by H. Jiao et al. IRW lowered the serum levels of tumour necrosis factor- (TNF-) a, interleukin- (IL-) 6, and myeloperoxidase (MPO) activity in a lipopolysaccharide- (LPS-) induced rat model. There was an increase in the Shannon and a decrease in the Simpson indices of faecal microbiota. IRW treatment noticeably limited the LPS-enhancement of TNF-a, IL-8, vascular cell adhesion molecule-1 (VCAM-1), and intercellular cell adhesion molecule-1 (ICAM-1) in human umbilical vein endothelial cells (HUVECs). These results indicate that bioactive peptides can be used in anti-inflammatory treatments.

X. Mao et al. investigated the effects of benzoic acid on gut functions. The acid is used as an organic acidifier and is found in a variety of foodstuffs, where it acts as an antifungal and antibacterial preservative. By regulating redox status, immunity, enzyme activity, and microbiota, the acid can aid digestion, barrier, and gut absorption functions. Used as a supplement in foodstuffs, it is particularly effective in improving convalescent health. A benzoic acid dosage of 0.2 to 0.5% is recommended in foodstuffs.

A study was conducted on nutritional cytokine leptin produced by cancer-associated fibroblasts (CAFs) with the aim to study their paracrine effects and mechanisms. Because leptin is the main component of the tumour microenvironment in nonsmall cell lung cancer (NSCLC), a novel *in vitro* cell coculture system was established. F. Li et al. discovered that leptin produced by CAFs can induce the proliferation and migration of NSCLC cells. This probably occurs via the P13K/AKT and MAPK/ERK1/2 paracrine intracellular-signalling pathways. This study indicates that nutritional factors are significant in tumour–tumour microenvironment interactions and suggests there may be a path towards the treatment of NSCLC.

S. Huang et al. investigated the benefits of milk fat globule membrane (MFGM), a protein-lipid complex that surrounds the fat globules in milk. Beneficial for the health of animals, it was seen to enhance the growth rate of low birth weight neonatal (LBW) mice, particularly during their early life. In addition, it relieved intestinal damage incurred from LPS challenge in LBW mice by increasing the messenger RNA (mRNA) levels of tight junction proteins, antioxidant enzymes, and intestinal mucosal barrier proteins. Inhibition of TLR2 and TLR4 signaling reduced the expression of proinflammatory cytokines. These indications showed that MFGM is a beneficial nutrient for the enhancement of growth performance, creating a novel means for the prevention and treatment during the early stages of intestinal inflammation in LBW neonates.

M. Wiese et al. performed an interesting clinical study on moderately obese persons, comprising 15 men and 15 women within an age bracket of 55 ± 5.7 years, to establish the prebiotic effect of lycopene and dark chocolate. These moderately obese subjects ($30<\mathrm{BMI} < 35\ \mathrm{kg/m^2}$) undertook a 1-month trial, and the systematic effects of lycopene or dark chocolate intake were recorded at the end of the trial period. The results were improved blood, gut, and liver lipid metabolism, plus improvements in skeletal muscle and skin conditions. These were deduced to have not been solely a result of the properties of the carotenoid and chocolate, but likely also due to modulation of the gut microbiome, which increased the presence of *Lactobacilli* and *Bifidobacteria* and thus their considerable beneficial effects.

Q. Jiang et al. summarised recent studies of antiquorum sensing (QS) agents, together with their signals in response to pathogens, highlighting the possibility of QS therapy in the treatment of bacterial diseases. Studies have identified many anti-QS agents that can control the pathogenic phenotypes of many types of bacteria. These agents have been shown to limit the pathological damage in infected animal models. They lack the stability of antibiotics and possibly have toxicity, which limits their widespread usage, but when combined with conventional antibiotics they are shown to enhance their effectiveness at a reduced cost, indicating their potential for future bacterial disease treatment.

This issue aims to focus readers' attention on the latest scientific work that is being conducted in relation to nutrients, inflammation, the environment, stress, and microorganisms, highlighting some of the innovative research methods used.

Conflicts of Interest

The editors declare that there are no conflicts of interest regarding the publication of this article.

Acknowledgments

We wish to thank the authors for their eminent studies and the reviewers and editorial staff for their assistance with the many and varied manuscripts submitted. In particular, the

authors thank the editorial office for approving the subject topic for this paper. The hope is that this issue will act as a reference and an inspiration for our readers.

Gang Liu
Yan Huang
Filipa S. Reis
Deguang Song
Hengjia Ni

Hindawi
BioMed Research International
Volume 2019, Article ID 3924581, 11 pages
https://doi.org/10.1155/2019/3924581

Research Article

Effects of Proanthocyanidins on Arsenic Methylation Metabolism and Efflux in Human Hepatocytes L-02

Qing-Xin Ren, Meng-Chuan Xu, Qiang Niu, Yun-Hua Hu,
Hai-Xia Wang, and Shu-Gang Li

Department of Public Health, College of Medicine, Shihezi University, Shihezi 832000, Xinjiang, China

Correspondence should be addressed to Shu-Gang Li; lishugang@ymail.com

Received 20 February 2019; Revised 2 June 2019; Accepted 13 June 2019; Published 4 July 2019

Guest Editor: Hengjia Ni

Copyright © 2019 Qing-Xin Ren et al. This is an open access article distributed under the Creative Commons Attribution License, which permits unrestricted use, distribution, and reproduction in any medium, provided the original work is properly cited.

This study investigated the effects of proanthocyanidins (PC) on arsenic methylation metabolism and efflux in human hepatocytes (L-02), as well as the relationships between PC and GSH, MRP1 and other molecules. Cells were randomly divided into blank control group, arsenic trioxide exposure group (ATO, As_2O_3, 25μmol/L), and PC-treated arsenic exposure group (10, 25, 50mg/L). After 24/48h, the contents of different forms of arsenic were determined, and the methylation indexes were calculated. Intracellular S-adenosyl methionine (SAM), arsenic (+3 oxidation state) methyltransferase (AS3MT), multidrug resistance-associated protein 1 (MRP1), and reduced glutathione (GSH) were ascertained. Changing trends were observed and the correlation between arsenic metabolism and efflux related factors and arsenic metabolites was analyzed. We observed that cells showed increased levels of content/constituent ratio of methyl arsenic, primary/secondary methylation index, methylation growth efficiency/rate, and the difference of methyl arsenic content in cells and culture medium ($P<0.05$, resp.). Compared with ATO exposure group, the intracellular SAM content in PC-treated group decreased, and the contents of GSH, AS3MT, and MRP1 increased ($P<0.05$, resp.). There was a positive correlation between the content of intracellular GSH/AS3MT and methyl arsenic. The content of MRP1 was positively correlated with the difference of methyl arsenic content in cell and culture medium; conversely, the SAM content was negatively correlated with intracellular methyl arsenic content ($P<0.05$, resp.). Taken together, these results prove that PC can promote arsenic methylation metabolism and efflux in L-02 cells, which may be related to the upregulation of GSH, MRP1, and AS3MT levels by PC.

1. Introduction

Arsenic (As) is a ubiquitous harmful element in the environment. At present, there are an estimated 2,102 villages in 14 provinces of China ranked higher in arsenic content, with a population of 1.15 million at risk. High arsenic drinking water has also been reported in the United States, Chile, and other countries in the world [1–3]. Arsenic has the effects of bioaccumulation, toxicity, and carcinogenesis and can cause liver [4] and cardiovascular diseases [5] and nervous system damage [6]. When inorganic arsenic enters the organism, it is mainly converted to organic form by methylation in the liver and then excreted out of the organism. This process is catalyzed by arsenic (+3 oxidation state) methyltransferase (AS3MT). Reduced glutathione (GSH) plays a vital role in arsenic methylation metabolism. IAs^{5+} can be reduced to iAs^{3+} by GSH, combining methyl from its donor S-adenosyl methionine (SAM) [7, 8]. After oxidative methylation, iAs is converted into dimethyl arsenate (DMAV) which is less toxic and is excreted in vitro [9]. Furthermore, GSH can interact with multidrug resistance-associated protein 1 (MRP1) and participate in arsenic efflux [10]. MRP1 could promote the cotransportation of $As(OH)_3$ with GSH out of cells to reduce intracellular drug concentrations, which may induce drug resistance and limit the efficiency of arsenic derived anticancer or antileukemic activity [11]. Leslie E M et al. [12] proposed MRP1 mediated arsenic efflux through a cotransport mechanism with GSH. Consequently, the exploration of the biological effects of GSH, MRP1, and other factors is of great significance in the prevention and treatment of arsenic poisoning.

Human hepatocytes L-02 originate from human body and are closer to the normal human environment. They are convenient to study the mechanism of drug action. In addition, L-02 cells are easy to survive and have a wide range of adaptation conditions, which can reflect the metabolism of arsenic in the liver. Proanthocyanidins (PC) are natural polyphenolic compounds widely distributed in grape seeds, pine bark, and other plant tissues, which can antagonize arsenic-induced liver oxidative damage by upregulating GSH and other protective proteins [13, 14]. However, it has not been elucidated whether PC can affect arsenic methylation metabolism and efflux by affecting GSH and MRP1. In this study, different doses of PC were designed to treat the cell lines with As_2O_3. After a certain period of time, a determination of the contents of related indexes along with an analysis of the effects of arsenic and PC was made. The aim of this study was to explore the effects of PC on arsenic methylation metabolism and efflux in L-02 cells, which may provide a theoretical basis for the application of PC in the prevention and treatment of arsenic poisoning.

2. Materials and Methods

2.1. Reagents. As_2O_3 was purchased from Beijing Chemical Reagent Corp. (Beijing, China). PC which was purified small molecular dimers with purity greater than 98% was obtained from JF-Natural (Tianjin, China). Human Hepatocytes (L-02) were purchased from OBiO Technology (Shanghai) Corp. Fresh fetal bovine serum was acquired from Sijiqing Bioengineering Material Co., Ltd. (Hangzhou, China). Trypsin was purchased from Difco Company (America). KOH was obtained from Shanghai Chemical Reagent Company. KBH_4 and $(NH_4)_2HPO4$ were purchased from China National Pharmaceutical Group Corp. Sodium monomethyl/dimethyl arsenate standard and As^{5+}/As^{3+} ICP-MS standard solution were acquired from American Sigma Company. GSH, ELISA assay kits, phosphate buffer solution (PBS), DMEM cell-culture mediums, syringes, micropipettes, and 96 well enzyme-labeled plates were purchased from Nanjing Jiancheng Bioengineering Institute (Nanjing, China).

2.2. Apparatus. A microplate reader (680) was procured from American Bio-Rad Company. A constant temperature water bath (SHA-B) was purchased from Changzhou Guohua Electric Appliance Co., Ltd. (Changzhou, China). A high-speed refrigerated centrifuge (TGL-16G-A) was acquired from Shanghai Anting Scientific Instrument Factory (Shanghai, China). A manual glass homogenizer was purchased from Shanghai Bioengineering Company (Shanghai, China). An inverted phase-contrast microscope (AE31) was obtained from Motic Group Co., Ltd. (Xiamen, China). A pressure steam sterilizer (TX400Z) was bought from Shanghai SANSHEN Medical Instrument Co., Ltd. (Shanghai, China). A super-clean worktable (SW-CJ-2FD) was ordered from Suzhou Purification Equipment Co., Ltd. (Suzhou, China). A high-performance liquid chromatography-hydride generation atomic fluorescence spectrometry analyzer (SA20) was purchased from Beijing Jitian Instrument Co., Ltd. (Beijing, China). A precision electronic balance was acquired from Shanghai Precision and Scientific Instrument Co., Ltd. (Shanghai, China). A CO_2 incubator (HF151) was purchased from Shanghai LISHEN Scientific Instrument Co., Ltd. (Shanghai, China). A vortex mixer was procured from Shanghai Ya-rong Biochemistry Instrument Factory (Shanghai, China).

2.3. Cell Culture. L-02 cells were cultured in DMEM medium containing 10% fetal bovine serum, 0.0625g/L penicillin, and 0.1g/L streptomycin. The culture medium was put into a CO_2 incubator containing 5% saturated humidity. The temperature was set at 37°C. When cells grew to about 85% ~ 90%, they were processed for digestion with 0.25% trypsin. According to the growth condition, the cells were passaged every 3 to 4 days. Cells in logarithmic growth phase were randomly divided into 5 groups. Through the preliminary experiment, we found that when the intervention dose of ATO was more than 25.0μmol/L, the survival rate of L-02 cells was significantly lower than that in the low gradient dose group in 24/48 hours. So the intervention of 25.0μmol/L ATO can make the survival rate of L-02 cells maintain at a higher level. In this way, we can ensure that our experiments can be carried out and observed obvious results. The grouping is shown in Table 1.

The experimental indexes were detected after 24/48h culture of each group cells. Trypsin (0.5mL) was added to the six-well plates respectively aiming a digestion for 1~2min. When the cells were round and exfoliated, as seen under a microscope, the 2mL complete culture solution was added to each well to terminate digestion. The cells in the six-well plates were collected into the centrifuge tube and separated from the culture solution at 1000 r/min for 5min. Then the cells were washed with PBS 3 times and transferred to the centrifuge tubes (each tube contained about 2.5×10^6 cells). After resuspension, cells were frozen and thawed repeatedly and centrifuged at 1500 r/min for 15 minutes. Afterward, cells were rinsed with 350μL PBS 3 times, and the supernatant was obtained. The cell-culture solution was collected and filtered with 0.2μm pore membrane. Subsequently, the 0.5mL solution was taken for the measurement.

2.4. Determination and Calculation of Arsenic and Its Methylation Metabolites. High-performance liquid chromatography-hydride generation atomic fluorescence spectrometry (HPLC-HGAFS) method was developed for the determination of intracellular and extracellular arsenic with its metabolites. The levels of iAs^{3+}, iAs^{5+}, monomethylated arsenic (MMA), and dimethylated arsenic (DMA) were detected. Total arsenic (TAs) and the ratios of iAs^{3+}, iAs^{5+}, MMA, and DMA (iAs^{3+}%, iAs^{5+}%, MMA%, and DMA %) were calculated. We also calculated primary methylation index (PMI, (MMA+DMA)/TAs×100%), secondary methylation index (SMI, DMA/(MMA+DMA)×100%), monomethylation growth rate ($(MMA_{48h}+DMA_{48h}-MMA_{24h}-DMA_{24h})/24$), dimethylation growth rate ($(DMA_{48h}-DMA_{24h})/24$), monomethylation growth efficiency ($(MMA_{48h}+DMA_{48h}-MMA_{24h}-DMA_{24h})/(TAs_{48h}-MMA_{24h}-DMA_{24h})\times100\%$), dimethylation growth efficiency ($(DMA_{48h}-DMA_{24h})/(MMA_{48h}+DMA_{48h}-DMA_{24h})\times100\%$), and the difference of extracellular and intracellular concentrations of iAs^{3+}, iAs^{5+}, MMA, and DMA ($\triangle iAs^{3+}$, $\triangle iAs^{5+}$, $\triangle$MMA, and $\triangle$DMA).

Table 1: Treatment measures and grouping.

Group	Treatment measures
Blank control group	As_2O_3 + PC (0μmol/L + 0mg/L)
ATO exposure group	As_2O_3 + PC (25μmol/L + 0mg/L)
PC-treated group	As_2O_3 + PC (25μmol/L + 10mg/L)
PC-treated group	As_2O_3 + PC (25μmol/L + 25mg/L)
PC-treated group	As_2O_3 + PC (25μmol/L + 50mg/L)

Note: PC, proanthocyanidins; ATO, arsenic trioxide.

2.5. Methylation Metabolism and Efflux Related Indexes Assay. After 24/48 hours of culture, the cells were tested strictly according to the operation methods of the corresponding apparatus and the instruction manual of the kits. High-performance liquid chromatography (HPLC) was used to determine the content of SAM. AS3MT and MRP1 in cells were determined by ELISA kits, and intracellular GSH was determined by micro ELISA.

2.6. Statistical Analysis. The data were extracted by Excel 2010 software and analyzed using SPSS software for Windows version 21.0. The experimental results were expressed as the mean ± standard deviation. Analysis of variance (ANOVA) was used to detect the differences among the experimental groups. Bonferroni method was used in the pairwise comparison, and Pearson correlation analysis was used in relevance analysis. All tests used a significance level of α=0.05, and a result of $P<0.05$ was considered to be statistically significant.

3. Results

3.1. PC Increased the Contents of Arsenic Metabolites in L-02 Cells Exposed by ATO. The effects of ATO and PC on the contents of arsenic and its metabolites are shown in Figure 1. After 24 hours of intervention, the contents of MMA and DMA were significantly higher in PC (10, 25, 50mg/L)-treated group than in the ATO exposure group. In comparison with PC (10, 25mg/L)-treated group, the treatment of PC (50mg/L) caused an increase of DMA. However, PC (50mg/L)-treated group decreased the level of iAs^{3+} ($P<0.05$, resp.). After 48 hours of intervention, the change trend of each index was basically the same as that of 24h intervention. The TAs content in PC (50mg/L)-treated group was less than that in ATO exposure group and PC (10, 25mg/L)-treated group ($P<0.05$, resp.).

3.2. PC Increased the Ratio of Arsenic Metabolites in L-02 Cells Exposed by ATO. After 24 hours of intervention, compared with ATO exposure group, the constituent ratio of iAs^{3+} decreased and the constituent ratios of iAs^{5+}, MMA, and DMA increased with the increasing PC dosage ($P<0.05$, resp.). The trend of 48h-intervention was basically the same as that of 24h. See Figure 2.

3.3. PC Improved the Level and Capacity of Methylation in L-02 Cells Exposed by ATO. After 24/48h, the PMI and SMI levels in all PC-treated groups increased compared with the ATO exposure group ($P<0.05$, resp.). The SMI of PC (25mg/L)-treated group was higher than that of PC (10mg/L)-treated group, and the PMI and SMI of PC (50mg/L)-treated group were higher than those of PC (10, 25mg/L)-treated group ($P<0.05$, resp.). See Figure 3. As shown in Figure 4, within 24~48 hours of intervention, the methylation growth rate and efficiency in each PC-treated group were higher than those in the ATO exposure group ($P < 0.05$, resp.), showing an upward trend with the increasing PC dosage.

3.4. PC Upregulated the Levels of GSH and AS3MT in L-02 Cells Exposed by ATO. We found out that the intracellular content of GSH in ATO exposure group was lower than that in the blank control group and the AS3MT content was higher than that in the blank control group after 24/48h of intervention ($P<0.05$, resp.). The contents of GSH and AS3MT in the PC-treated group were higher than those of ATO exposure group, and the content of SAM was lower than that of ATO exposure group ($P<0.05$, resp.). See Figure 5.

3.5. The Contents of GSH and AS3MT Were Positively Correlated with Arsenic Metabolites and the Contents of SAM Were Negatively Relevant to Them. We made the correlation between the protein contents of GSH, AS3MT, and SAM and different forms of arsenic content in L-02 cells. As shown in Figure 6, we discovered that MMA and DMA contents were positively correlated with GSH and AS3MT contents and negatively correlated with SAM content ($P < 0.05$, resp.).

3.6. PC Upregulated the Levels of $\triangle$MMA and $\triangle$DMA and Downregulated the Levels of $\triangle iAs^{3+}$ and $\triangle iAs^{5+}$. After 24/48 hours of intervention, the $\triangle$MMA of PC (50mg/L)-treated group was higher than that of ATO exposure group ($P<0.05$), and the $\triangle$DMA of each PC-treated group was higher than that in ATO exposure group ($P<0.001$, resp.), as shown in Table 2. In comparison with the ATO exposure group, the treatment of PC (50mg/L) caused a decrease in $\triangle iAs^{3+}$ ($P=0.002$). In addition, the $\triangle iAs^{5+}$ in PC (50mg/L)-treated group was lower than that in ATO exposure group after the period of 24h ($P=0.009$). See Table 3.

3.7. PC Upgraded the Level of MRP1 in L-02 Cells Exposed by ATO. Compared with the blank control group, MRP1 decreased in 48h-ATO exposure group ($P<0.001$). The level of intracellular MRP1 in the PC (25, 50 mg/L)-treated group for 24 hours was higher than that in the ATO exposure group ($P<0.05$, resp.). After 48 hours of intervention, the MRP1 level of each PC-treated group was higher than that of

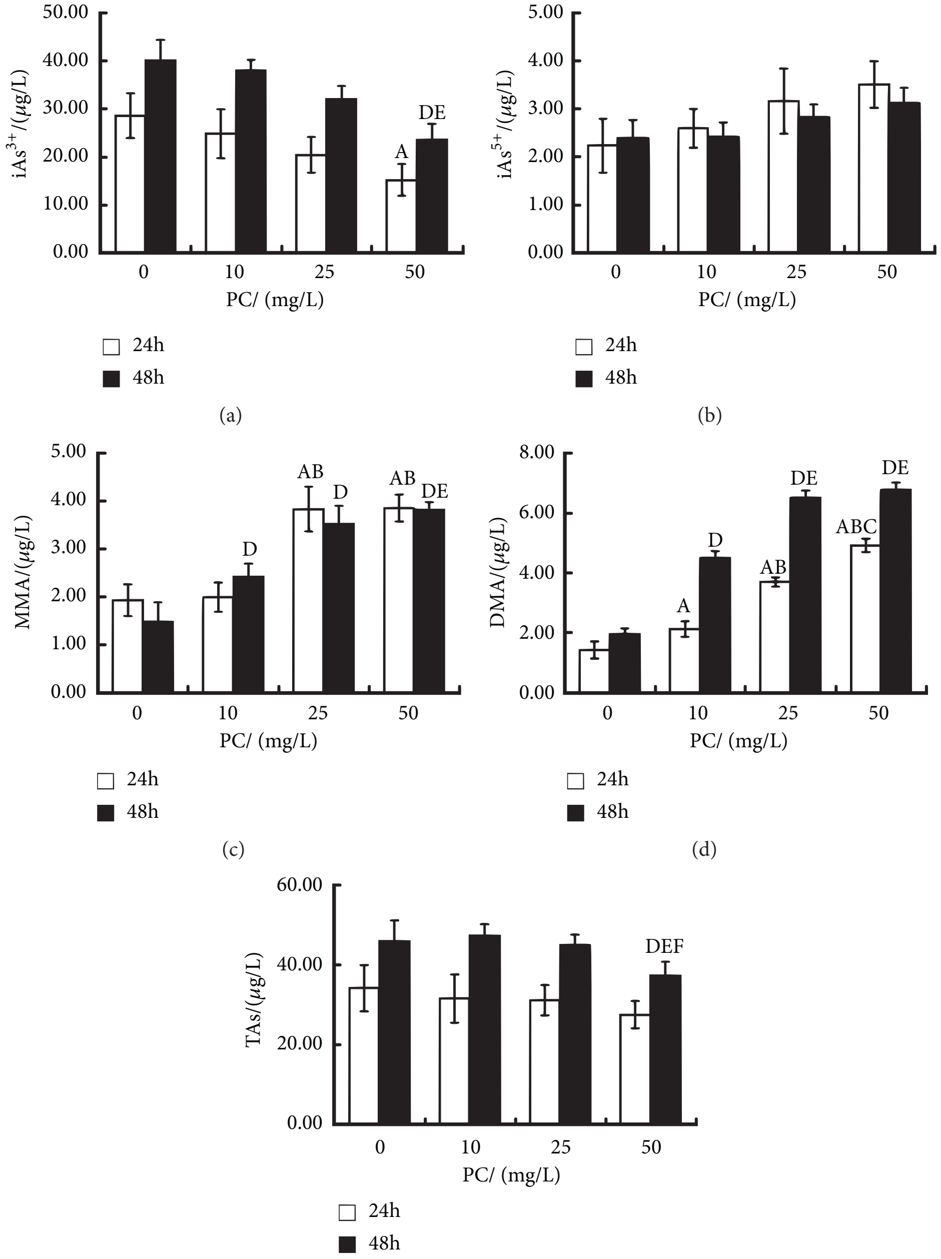

(a) (b)

(c) (d)

(e)

Figure 1: Effects of proanthocyanidins (PC) on inorganic arsenic, arsenic metabolites, and total arsenic (TAs) contents in L-02 cells exposed by arsenic trioxide (ATO). The contents of iAs^{3+} (a), iAs^{5+} (b), MMA (c), DMA (d), and TAs (e) are shown. Values are means (n=3 for each group), with standard deviations represented by vertical bars. ^{A} Indicating significant difference from ATO exposure group with 24h at $P<0.05$. ^{B} Indicating significant difference from PC (10mg/L)-treated group with 24h at $P<0.05$. ^{C} Indicating significant difference from PC (25mg/L)-treated group with 24h at $P<0.05$. ^{D} Indicating significant difference from ATO exposure group with 48h at $P<0.05$. ^{E} Indicating significant difference from PC (10mg/L)-treated group with 48h at $P<0.05$. ^{F} Indicating significant difference from PC (25mg/L)-treated group with 48h at $P<0.05$. iAs, inorganic arsenic; MMA, monomethylated arsenic; DMA, dimethylated arsenic.

ATO exposure group ($P<0.05$, resp.) and increased with the increasing PC dosage. See Figure 7.

3.8. The Content of MRP1 Was Positively Relevant to the Contents of △MMA and △DMA. There was a positive correlation between MRP1 content and △MMA after 24h-intervention ($P=0.002$), and the content of MRP1 was positively correlated with △MMA and △DMA after 48h-intervention ($P<0.05$, resp.), as shown in Figure 8.

4. Discussion

Arsenic is a hazardous element that seriously endangers public health. It widely exists in nature and can cause damage

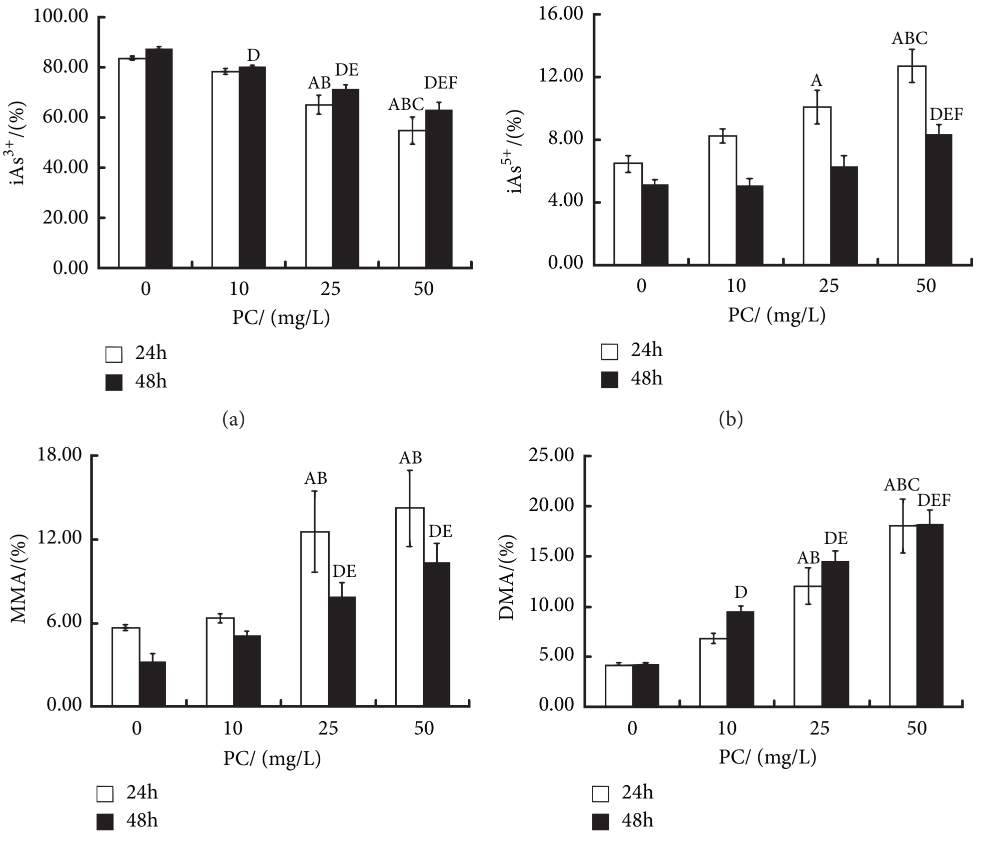

(a) (b)

(c) (d)

Figure 2: Effects of proanthocyanidins (PC) on constituent ratios (%) of various forms of arsenic in L-02 cells exposed by arsenic trioxide (ATO). The constituent ratios of iAs^{3+} (a), iAs^{5+} (b), MMA (c), and DMA (d) are shown. Values are means (n=3 for each group), with standard deviations represented by vertical bars. ^{A} Indicating significant difference from ATO exposure group with 24h at $P<0.05$. ^{B} Indicating significant difference from PC (10mg/L)-treated group with 24h at $P<0.05$. ^{C} Indicating significant difference from PC (25mg/L)-treated group with 24h at $P<0.05$. ^{D} Indicating significant difference from ATO exposure group with 48h at $P<0.05$. ^{E} Indicating significant difference from PC (10mg/L)-treated group with 48h at $P<0.05$. ^{F} Indicating significant difference from PC (25mg/L)-treated group with 48h at $P<0.05$. iAs, inorganic arsenic; MMA, monomethylated arsenic; DMA, dimethylated arsenic.

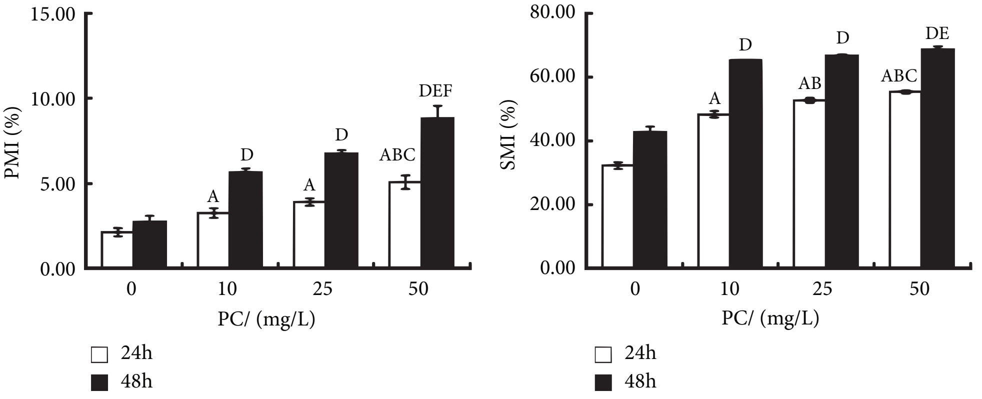

(a) (b)

Figure 3: Effect of proanthocyanidins (PC) on primary methylation index (PMI) and secondary methylation index (SMI) in L-02 cells exposed by arsenic trioxide (ATO). The PMI (a) and SMI (b) are shown. Values are means (n=3 for each group), with standard deviations represented by vertical bars. ^{A} Indicating significant difference from ATO exposure group with 24h at $P<0.05$. ^{B} Indicating significant difference from PC (10mg/L)-treated group with 24h at $P<0.05$. ^{C} Indicating significant difference from PC (25mg/L)-treated group with 24h at $P<0.05$. ^{D} Indicating significant difference from ATO exposure group with 48h at $P<0.05$. ^{E} Indicating significant difference from PC (10mg/L)-treated group with 48h at $P<0.05$. ^{F} Indicating significant difference from PC (25mg/L)-treated group with 48h at $P<0.05$.

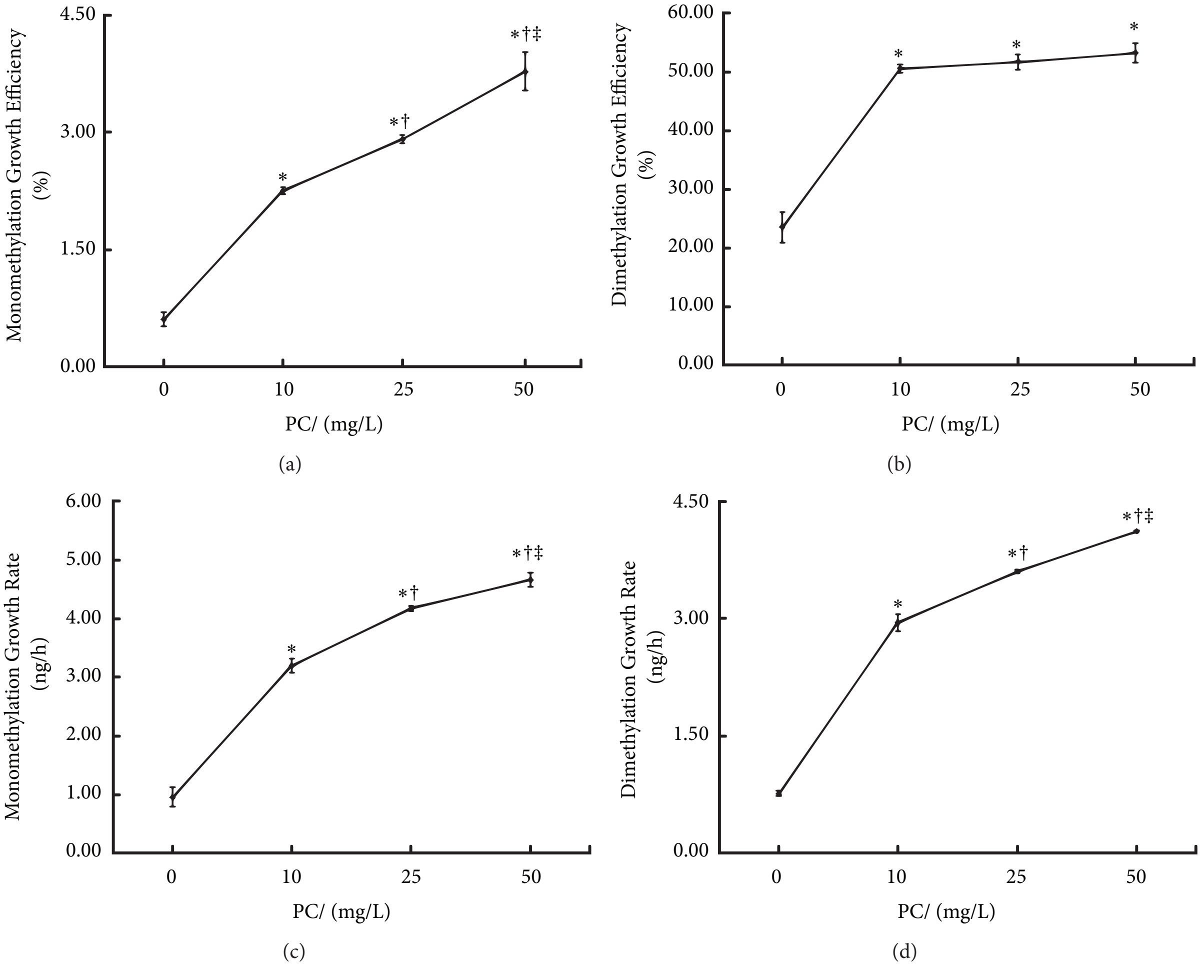

(a) (b)

(c) (d)

FIGURE 4: Effects of proanthocyanidins (PC) on methylation growth rate (ng/h) and efficiency (%) of arsenic in L-02 cells exposed by arsenic trioxide (ATO) within 24~48 hours. The monomethylation growth efficiency (a), dimethylation growth efficiency (b), monomethylation growth rate (c), and dimethylation growth rate (d) are shown. Values are means (n=3 for each group), with standard deviations represented by vertical bars. *Indicating significant difference from ATO exposure group at P<0.05; †indicating significant difference from PC (10mg/L)-treated group at P<0.05; ‡indicating significant difference from PC (25mg/L)-treated group at P<0.05.

TABLE 2: Effects of proanthocyanidins (PC) on the changes of the difference of extracellular and intracellular concentrations of methyl arsenic (n=3).

Group	△MMA (μg/L)		△DMA (μg/L)	
	24h	48h	24h	48h
ATO (25μmol/L)	25.62±2.08	28.46±3.76	11.63±1.47	20.18±1.40
ATO + PC (25μmol/L + 10mg/L)	29.35±1.52	31.87±2.36	27.13±2.01*	59.74±3.40*
ATO + PC (25μmol/L + 25mg/L)	29.11±1.53	36.34±2.02	33.12±2.41$^{*\#}$	73.07±2.48$^{*\#}$
ATO + PC (25μmol/L + 50mg/L)	32.51±1.72*	39.06±2.87*	40.01±1.85$^{*\#\triangle}$	87.23±2.47$^{*\#\triangle}$

Note: the results were described as mean ± SD. *Indicating significant difference from ATO exposure group at P<0.05; $^{\#}$indicating significant difference from PC (10mg/L)-treated group at P<0.05; $^{\triangle}$indicating significant difference from PC (25mg/L)-treated group at P<0.05. △MMA, the difference of extracellular and intracellular concentrations of monomethylated arsenic; △DMA, the difference of extracellular and intracellular concentrations of dimethylated arsenic; ATO, arsenic trioxide.

to tissues and organs [15, 16]. The methylation metabolism of arsenic is one of the most crucial ways of its toxicity, which is related to GSH, AS3MT, and SAM. GSH can interact with MRP1 to participate in the efflux of arsenic [17]. PC is a kind of natural polyphenolic compounds with strong antioxidant activity widely found in grape seeds and other plant tissues. It can upregulate the levels of methylation-related molecules such as GSH. The results showed that PC could increase the indexes and rates of arsenic methylation and the contents of AS3MT and MRP1 in ATO-exposed L-02 cells, suggesting that PC might promote the methylation metabolism and efflux of arsenic in L-02 cells.

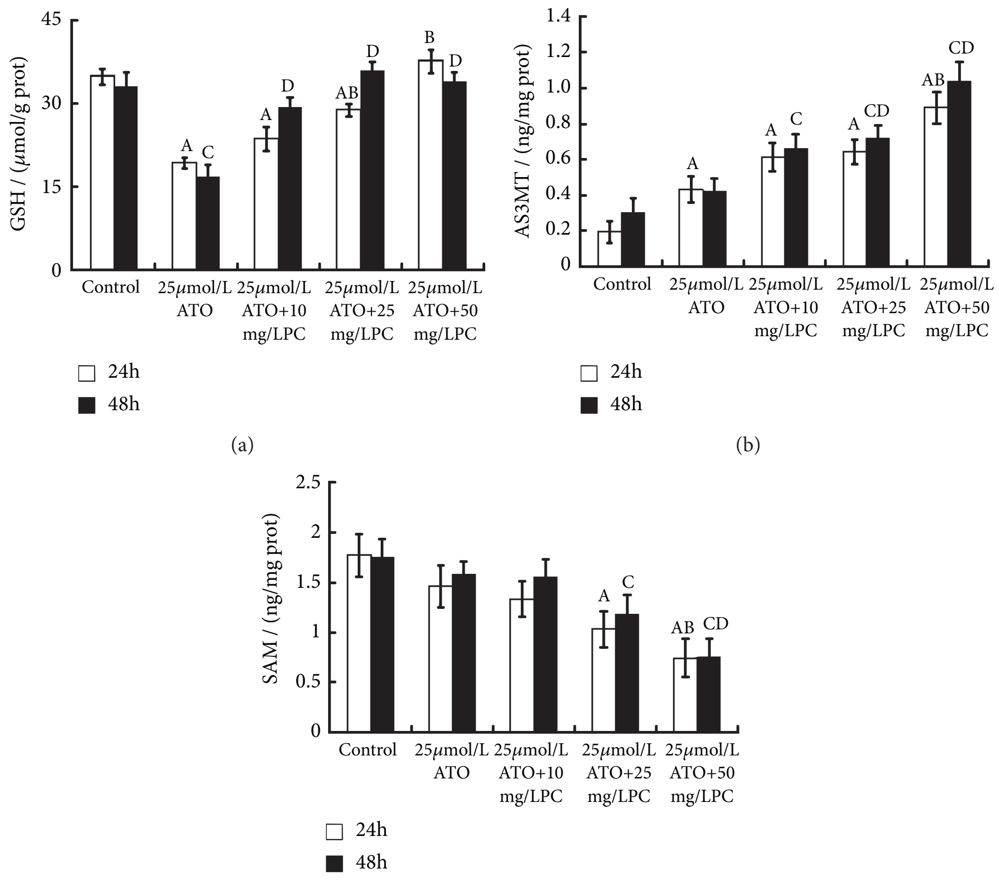

(a)

(b)

(c)

Figure 5: Effects of proanthocyanidins (PC) on the levels of glutathione (GSH, μmol/g), arsenic (+3 oxidation state) methyltransferase (AS3MT, ng/mg) and S-adenosyl methionine (SAM, ng/mg) in L-02 cells exposed by arsenic trioxide (ATO). The GSH (a), AS3MT (b), and SAM (c) are shown. Values are means (n=3 for each group), with standard deviations represented by vertical bars. ^{A} Indicating significant difference from the blank control group with 24h at P<0.05. ^{B} Indicating significant difference from ATO exposure group with 24h at P<0.05. ^{C} Indicating significant difference from the blank control group with 48h at P<0.05. ^{D} Indicating significant difference from ATO exposure group with 48h at P<0.05.

Table 3: Effects of proanthocyanidins (PC) on the changes of the difference of extracellular and intracellular concentrations of inorganic arsenic (n=3).

Group	$\triangle iAs^{3+}$ (μg/L)		$\triangle iAs^{5+}$ (μg/L)	
	24h	48h	24h	48h
ATO (25μmol/L)	1496.72±48.06	1457.89±25.77	372.28±16.58	361.85±36.03
ATO + PC (25μmol/L + 10mg/L)	1440.92±31.28	1305.08±42.56	354.78±16.77	315.03±38.53
ATO + PC (25μmol/L + 25mg/L)	1391.13±34.46	1310.49±14.06	335.11±40.96	317.90±26.00
ATO + PC (25μmol/L + 50mg/L)	$1286.91\pm39.73^{*\#}$	$1129.89\pm94.14^{*\#\triangle}$	$246.43\pm44.77^{*\#}$	276.62±23.17

Note: the results were described as mean ± SD. *Indicating significant difference from ATO exposure group at P<0.05; $^{\#}$indicating significant difference from PC (10mg/L)-treated group at P<0.05; $^{\triangle}$indicating significant difference from PC (25mg/L)-treated group at P<0.05. △iAs, the difference of extracellular and intracellular concentrations of inorganic arsenic; ATO, arsenic trioxide.

Studies have shown that PC can antagonize arsenic-induced oxidative damage in hepatocytes [18]. PMI and SMI are classical indicators to measure the level of arsenic methylation, reflecting the ability of the first methylation of inorganic arsenic to produce methyl arsenic, and the ability of the second methylation to convert MMA into DMA, respectively [19]. In order to avoid the effects of MMA and DMA accumulated in 24 hours on the calculated values of PMI_{48h} and SMI_{48h} and their relationships with PC dosage, the monomethylation and dimethylation growth efficiency measured in this study represent the intracellular conversion levels of inorganic arsenic to methyl arsenic and MMA to DMA in 24~48 hours. It was found out that PMI and SMI and the efficiency and rate of methylation

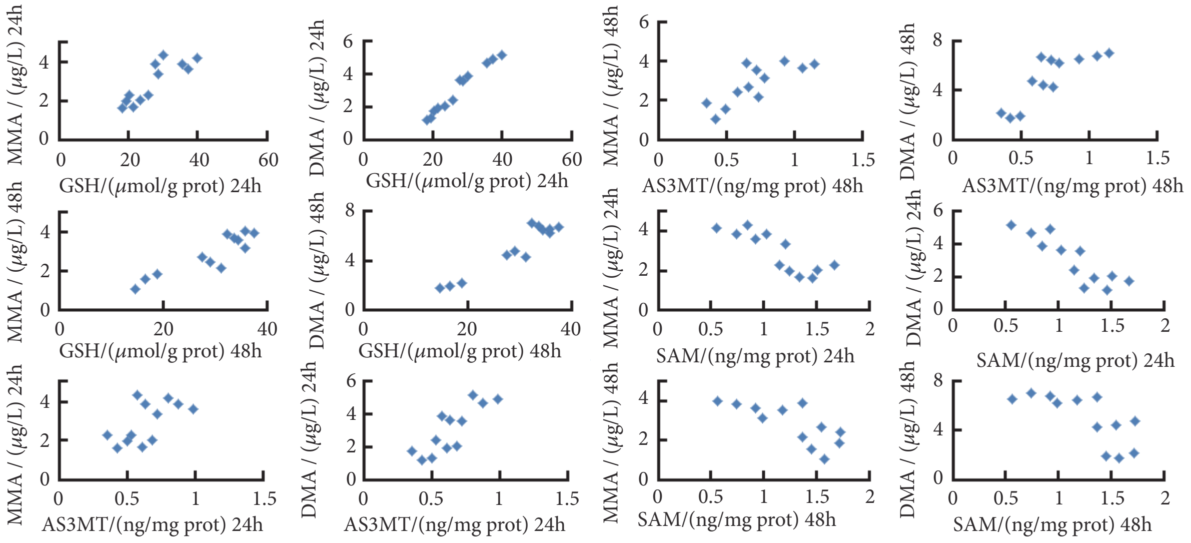

Figure 6: Analysis of the correlation between glutathione (GSH)/arsenic (+3 oxidation state) methyltransferase (AS3MT)/S-adenosyl methionine (SAM) and arsenic metabolites contents in arsenic trioxide (ATO) infected L-02 cells by proanthocyanidins (PC) intervention. The horizontal and vertical coordinates of each data point referred to the contents of GSH, AS3MT, SAM, and corresponding methyl arsenic under the intervention of different doses of PC. MMA, monomethylated arsenic; DMA, dimethylated arsenic.

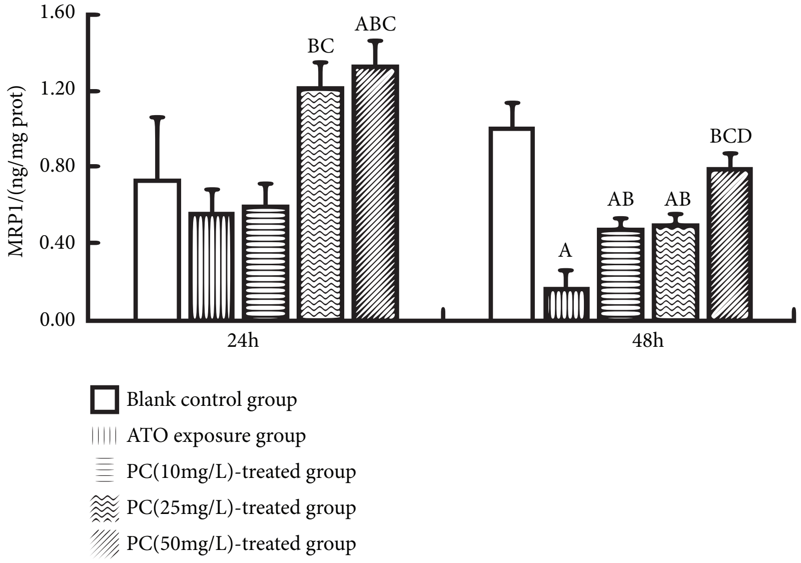

Figure 7: Effects of proanthocyanidins (PC) on the contents of multidrug resistance-associated protein 1 (MRP1, ng/mg) in L-02 cells exposed by ATO. Values are means (n=3 for each group), with standard deviations represented by vertical bars. ^{A} Indicating significant difference from the blank control group at P<0.05. ^{B} Indicating significant difference from ATO exposure group at P<0.05. ^{C} Indicating significant difference from PC(10mg/L)-treated group at P<0.05. ^{D} Indicating significant difference from PC(25mg/L)-treated group at P<0.05.

growth increased with the increase of PC dosage. In addition, with the PC treatment, the content and constituent ratio of inorganic arsenic decreased, while those of methyl arsenic increased, which indicated that PC promoted the methylation of arsenic in L-02 cells. GSH and AS3MT are helpful to the metabolism of arsenic methylation, and SAM can provide methyl for inorganic arsenic [20, 21]. Compared with the blank control group, the content of GSH decreased and the content of AS3MT increased in ATO-exposed group, which was consistent with the results of Hu Yu [22] and Wu Jun [23]. We hypothesize that arsenic could consume intracellular GSH and induce the defensive response of AS3MT. The increased levels of GSH and AS3MT under PC intervention may be related to the activation of phosphoinositide 3-kinase (PI3K)/protein kinase B (PKB/Akt) signal pathway with antioxidant effect [24]. It has also been reported that

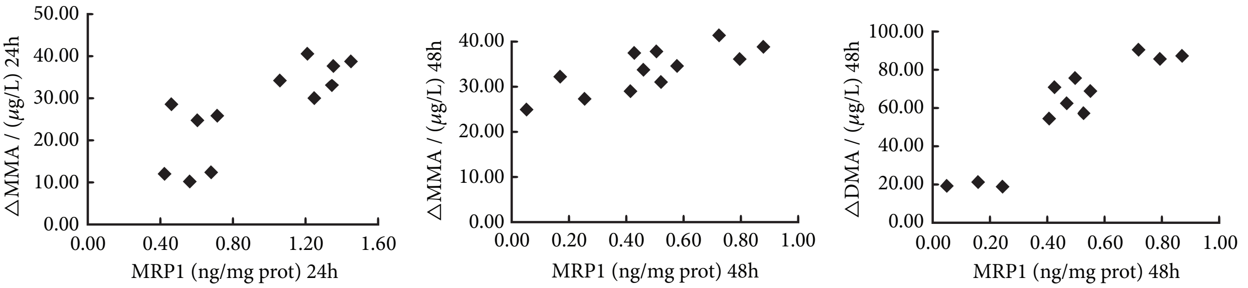

(a) (b) (c)

Figure 8: Analysis of the correlation between multidrug resistance-associated protein 1 (MRP1) contents and the difference of extracellular and intracellular concentrations of monomethylated arsenic (△MMA)/dimethylated arsenic (△DMA).

GSH modulates AS3MT activity [25]. Hence, we speculate that the upregulation of GSH promotes the transfer of methyl from SAM to arsenic in various forms catalyzed by AS3MT to complete methylation metabolism.

MRP1 is a member of adenosine triphosphate binding cassette (ABC) transporter superfamily, which can transport intracellular substance extracellularly in reverse concentration gradients, and is widely distributed in the organism as a kind of GSH transport pump [26, 27]. The results showed that the intracellular TAs decreased with the increasing PC dosage, and the △MMA and △DMA in the PC intervention group were higher than those in the ATO exposure group. The content of MRP1 in ATO-exposed cells was lower than that in the blank control group, but increased after PC intervention, showing a dose-response relationship with PC. The content of MRP1 was positively correlated with △MMA and △DMA. This suggests that MRP1 contributes to the efflux of arsenic from cells, and PC promotes the expression of MRP1. Among several forms of arsenic, DMA has less toxicity and discharges from the organism easily [9, 28]. Therefore, PC can promote arsenic methylation metabolism, which in turn promotes arsenic efflux. Alternatively, PC can antagonize arsenic-induced apoptosis [18, 29]; therefore, PC can affect more active cells to participate in arsenic metabolism and contribute to arsenic efflux. Previous studies have shown that nuclear factor E2 related factor 2 (Nrf2)-antioxidant response element (ARE) signaling pathway could antagonize arsenic-induced oxidative damage [30] and can also upregulate the levels of GSH [31] and MRP1 [32]. Thus, we presume that PC activates this pathway and promotes the expression of MRP1 and GSH. At the same time, GSH upregulates the level of AS3MT and promotes arsenic methylation metabolism. And we speculate that arsenic and its metabolites form complexes with GSH. MRP1 binds to the arsenic-GSH complexes and consumes ATP to pump arsenic out of the cells [33]. It can be seen that PC antagonizes the toxicity of arsenic by promoting the methylation metabolism and efflux of it. Whether PC can prevent arsenic poisoning remains to be further studied.

5. Conclusions

In conclusion, PC can promote arsenic methylation metabolism and efflux in L-02 cells, which may be related to the upregulation of GSH, MRP1, and AS3MT levels by PC. However, this study is a cell-based experiment, and further investigation in different cell lines and in vivo is needed to clarify these findings. This way our findings could help provide a better understanding of the mechanism and achieve better development and utilization of PC. Moreover, we can also provide a theoretical basis for preventing arsenic poisoning and improving public health.

Data Availability

The data used to support the findings of this study are available from the corresponding author upon request.

Conflicts of Interest

The authors declare that there are no conflicts of interest regarding the publication of this paper.

Authors' Contributions

Qing-Xin Ren and Meng-Chuan Xu contributed equally to the present work.

Acknowledgments

The authors would like to thank the Department of Public Health, Shihezi University School of Medicine for assistance with this work. The authors acknowledge funding from the National Natural Science Foundation of China (Nos. 81560517, 81760584, and 81860559), the Key Areas of Science and Technology Research Project of Xinjiang Production and Construction Corps (Nos. 2014BA039 and 2015AG014), the Research Project of Shihezi University (Nos. KYPT201804, GJHZ201602, and ZZZC201801A), and Opening Project of Key Laboratory of Xinjiang Endemic and Ethnic Diseases (Ministry of Education, KF2018-4).

References

[1] Y.-H. Gao and D.-J. Sun, "Study on biogeochemical diseases, ancient and new field," *Chinese Journal of Disease Control & Prevention*, vol. 02, pp. 107–108+121, 2018.

[2] O. L. Valenzuela, V. H. Borja-Aburto, G. G. Garcia-Vargas et al., “Urinary trivalent methylated arsenic species in a population chronically exposed to inorganic arsenic,” *Environmental Health Perspectives*, vol. 113, no. 3, pp. 250–254, 2005.

[3] Committee on Toxicology, National Research Council, and National Academy of Sciences, *Arsenic in Drinking Water: 2001 Update*, National Academies Press, Washington, DC, USA, 2001.

[4] S. Wu, J. Li, and X. Jin, “iTRAQ-based quantitative proteomic analysis reveals important metabolic pathways for arsenic-induced liver fibrosis in rats,” *Scientific Reports*, vol. 8, no. 1, 2018.

[5] M. Wu, H. Chiou, Y. Hsueh et al., “Effect of plasma homocysteine level and urinary monomethylarsonic acid on the risk of arsenic-associated carotid atherosclerosis,” *Toxicology and Applied Pharmacology*, vol. 216, no. 1, pp. 168–175, 2006.

[6] G. M. Kannan, N. Tripathi, S. N. Dube, M. Gupta, S. Flora, and S. J. Flora, “Toxic effects of arsenic (III) on some hematopoietic and central nervous system variables in rats and guinea pigs,” *Journal of Toxicology - Clinical Toxicology*, vol. 39, no. 7, pp. 675–682, 2001.

[7] T. Watanabe and S. Hirano, “Metabolism of arsenic and its toxicological relevance,” *Archives of Toxicology*, vol. 87, no. 6, pp. 969–979, 2013.

[8] T. Hayakawa, Y. Kobayashi, X. Cui, and S. A. Hirano, “A new metabolic pathway of arsenite: Arsenic-glutathione complexes are substrates for human arsenic methyltransferase Cyt19,” *Archives of Toxicology*, vol. 79, no. 4, pp. 183–191, 2005.

[9] X. WANG, Y. DONG, A.-J. GENG et al., “Comparison of pharmacokinetics and subacute toxicity for four arsenic species in rats,” *Chinese Journal of Food Hygiene*, vol. 29, no. 4, pp. 400–406, 2017.

[10] K. Sodani, A. Patel, R. J. Kathawala, and Z. Chen, “Multidrug resistance associated proteins in multidrug resistance,” *Chinese Journal of Cancer*, vol. 31, no. 2, pp. 58–72, 2012.

[11] M. Salerno, M. Petroutsa, and A. Garnier-Suillerot, “The MRP1-mediated effluxes of arsenic and antimony do not require arsenic–glutathione and antimony–glutathione complex formation,” *Journal of Bioenergetics and Biomembranes*, vol. 34, no. 2, pp. 135–145, 2002.

[12] E. M. Leslie, A. Haimeur, and M. P. Waalkes, “Arsenic transport by the human multidrug resistance protein 1 (MRP1/ABCC1),” *The Journal of Biological Chemistry*, vol. 279, no. 31, pp. 32700–32708, 2004.

[13] R. Taheri, B. A. Connolly, M. H. Brand, and B. W. Bolling, “Underutilized chokeberry (Aronia melanocarpa, Aronia arbutifolia, Aronia prunifolia) accessions are rich sources of anthocyanins, flavonoids, hydroxycinnamic acids, and proanthocyanidins,” *Journal of Agricultural and Food Chemistry*, vol. 61, no. 36, pp. 8581–8588, 2013.

[14] Y. Kim, Y. Choi, H. Ham, H.-S. Jeong, and J. Lee, “Protective effects of oligomeric and polymeric procyanidin fractions from defatted grape seeds on tert-butyl hydroperoxide-induced oxidative damage in HepG2 cells,” *Food Chemistry*, vol. 137, no. 1–4, pp. 136–141, 2013.

[15] S. Alarifi, D. Ali, S. Alkahtani, M. A. Siddiqui, and B. A. Ali, “Arsenic trioxide-mediated oxidative stress and genotoxicity in human hepatocellular carcinoma cells,” *OncoTargets and Therapy*, vol. 6, pp. 75–84, 2013.

[16] M. F. Naujokas, B. Anderson, H. Ahsan et al., “The broad scope of health effects from chronic arsenic exposure: update on a worldwide public health problem,” *Environmental Health Perspectives*, vol. 121, no. 3, pp. 295–302, 2013.

[17] S. Hui, L. Shugang, N. Qiang et al., “Factors affecting arsenic methylation in arsenic-exposed humans: a systematic review and Meta-analysis,” *Chinese Journal of Endemiology*, vol. 35, no. 12, pp. 869–874, 2016.

[18] M. Xu, S. Li, Y. Ding et al., “Protective mechanism of grape seed proanthocyanidin extract against oxidative damage induced by arsenic in HL-7702 cells,” *Food Science*, vol. 39, no. 3, pp. 176–181, 2018.

[19] S.-G. Li, Q. Niu, S.-Z. Xu et al., “The changing levels of hepatic function and arsenic methylation of mice induced by arsenic trioxide,” *Journal of Toxicology*, vol. 29, no. 1, pp. 23–26, 2015.

[20] X. Song, Z. Geng, X. Li et al., “Functional and structural evaluation of cysteine residues in the human arsenic (+3 oxidation state) methyltransferase (hAS3MT),” *Biochimie*, vol. 93, no. 2, pp. 369–375, 2011.

[21] L. F. N. Silva, M. Lemaire, C. A. Lemarié et al., “Effects of inorganic arsenic, methylated arsenicals, and arsenobetaine on atherosclerosis in the, mouse model and the role of As3mt-mediated methylation,” *Environmental Health Perspectives*, vol. 125, no. 7, Article ID 077001, 2017.

[22] Y. Hu, X.-M. Jin, G.-Q. Wang et al., “Effect of arsenic on GSH level: its related enzyme activity and gene expression in NIH 3T3 cells,” *Journal of Environmental & Occupational Medicine*, vol. 20, no. 6, pp. 396–402, 2003.

[23] J. Wu, Z. Shi, Y.-J. Zheng et al., “Effects of sodium arsenite and sodium arsenate on expression of DNA and arsenic methyltransferases in rats,” *Journal of Environment and Health*, vol. 29, no. 1, pp. 20–25, 2012.

[24] P. Wang, X. Peng, Z. Wei et al., “Geraniin exerts cytoprotective effect against cellular oxidative stress by upregulation of Nrf2-mediated antioxidant enzyme expression via PI3K/AKT and ERK1/2 pathway,” *Biochimica et Biophysica Acta (BBA) - General Subjects*, vol. 1850, no. 9, pp. 1751–1761, 2015.

[25] L. Ding, R. J. Saunders, Z. Drobná et al., “Methylation of arsenic by recombinant human wild-type arsenic (+3 oxidation state) methyltransferase and its methionine 287 threonine (M287T) polymorph: Role of glutathione,” *Toxicology and Applied Pharmacology*, vol. 264, no. 1, pp. 121–130, 2012.

[26] B. D. Stride, G. Valdimarsson, J. H. Gerlach, G. M. Wilson, S. P. C. Cole, and R. G. Deeley, “Structure and expression of the messenger RNA encoding the murine multidrug resistance protein, an ATP-binding cassette transporter,” *Molecular Pharmacology*, vol. 49, no. 6, pp. 962–971, 1996.

[27] D. Keppler, I. Leier, G. Jedlitschky, and J. König, “ATP-dependent transport of glutathione S-conjugates by the multidrug resistance protein MRP1 and its apical isoform MRP2,” *Chemico-Biological Interactions*, vol. 111-112, pp. 153–161, 1998.

[28] H. Naranmandura, M. W. Carew, S. Xu et al., “Comparative toxicity of arsenic metabolites in human bladder cancer EJ-1 cells,” *Chemical Research in Toxicology*, vol. 24, no. 9, pp. 1586–1596, 2011.

[29] M. Wei, F. Guo, D. Rui et al., “Alleviation of arsenic-induced pulmonary oxidative damage by GSPE as shown during in vivo and in vitro experiments,” *Biological Trace Element Research*, vol. 183, no. 1, pp. 80–91, 2018.

[30] M.-F. Feng, Q.-X. Ren, Y.-X. Jiang et al., “Effects of proanthocyanidins on oxidative damage via Nrf2 signaling pathway: a systematic review and meta-analysis,” *Natural Product Research and Development*, vol. 30, no. 3, pp. 526–533, 2018.

[31] S. Nishimoto, S. Koike, N. Inoue, T. Suzuki, and Y. Ogasawara, “Activation of Nrf2 attenuates carbonyl stress induced by

methylglyoxal in human neuroblastoma cells: Increase in GSH levels is a critical event for the detoxification mechanism," *Biochemical and Biophysical Research Communications*, vol. 483, no. 2, pp. 874–879, 2017.

[32] L. Ji, H. Li, P. Gao et al., "Nrf2 pathway regulates multidrug-resistance-associated protein 1 in small cell lung cancer," *PLoS ONE*, vol. 8, no. 5, Article ID e63404, 2013.

[33] J. Lankelma, O. V. Tellingen, J. Beijnen et al., "Role of glutathione in the export of compounds from cells by the multidrug-resistance-associated protein," *Proceedings of the National Acadamy of Sciences of the United States of America*, vol. 92, no. 17, pp. 7690–7694, 1995.

Hindawi
BioMed Research International
Volume 2019, Article ID 7180540, 7 pages
https://doi.org/10.1155/2019/7180540

Research Article

Biochemical Hallmarks of Oxidative Stress-Induced Overactivation of *Xenopus* Eggs

Alexander A. Tokmakov, Misaki Awamura, and Ken-Ichi Sato

Department of Molecular Biosciences, Kyoto Sangyo University, Kamigamo-motoyama, Kita-ku, Kyoto 603-8555, Japan

Correspondence should be addressed to Alexander A. Tokmakov; tokmak@cc.kyoto-su.ac.jp

Received 31 January 2019; Revised 28 March 2019; Accepted 28 May 2019; Published 2 July 2019

Guest Editor: Yan Huang

Copyright © 2019 Alexander A. Tokmakov et al. This is an open access article distributed under the Creative Commons Attribution License, which permits unrestricted use, distribution, and reproduction in any medium, provided the original work is properly cited.

Egg overactivation occurs with a low frequency in the populations of naturally ovulated frog eggs. At present, its natural inducers, molecular mechanisms, and intracellular events remain unknown. Using microscopic and biochemical analyses, we demonstrate here that high levels of hydrogen peroxide-induced oxidative stress can cause time- and dose-dependent overactivation of *Xenopus* eggs. Lipofuscin accumulation, decrease of soluble cytoplasmic protein content, and depletion of intracellular ATP were found to take place in the overactivated eggs. Progressive development of these processes suggests that egg overactivation unfolds in a sequential and ordered fashion.

1. Introduction

Oocytes and eggs of the African clawed frog *Xenopus laevis* provide the most common model for studying oogenesis, fertilization, meiotic and mitotic cell cycle progression, and apoptosis because of their large size and high biochemical tractability. The term “eggs” is generally used in the frog model for mature ovulated oocytes arrested in metaphase of the second meiotic division by high activity of the key meiotic regulators, such as the maturation promoting factor (MPF) and the cytostatic factor (CSF) [1]. The meiotic metaphase arrest prevents cell cycle progression and parthenogenesis prior to fertilization. Meiotically arrested eggs awaiting fertilization can experience various injuries leading to the loss of their quality. The stress- and age-triggered damage leads to decreased rates of fertilization, polyspermy, parthenogenesis, and abnormal development of embryos. Poor quality of oocytes and eggs is considered to be a cause of infertility and abnormal embryo development in different animals, including mammals [2, 3]. In addition, spontaneous egg activation and exit from the meiotic metaphase arrest make successful fertilization impossible [4, 5]. It was reported that unfertilized *Xenopus* eggs spontaneously activate, exit the meiotic arrest, and degrade by a robust apoptotic process within 48 hours after ovulation [6, 7].

The intracellular pathways involved in spontaneous egg activation are poorly investigated. It has been suggested that this process might engage a calcium-dependent mechanism in mammalian eggs [4, 8–10]. Indeed, artificial elevation of intracellular calcium concentration is known to initiate parthenogenetic activation of eggs in various species. However, spontaneous activation may also utilize calcium-independent mechanisms. In aging unfertilized sea urchin eggs, apoptosis was shown to be triggered by progressive inactivation of MAPK [11, 12]. Also, it was demonstrated that aged mouse and pig eggs have decreased activities of major CSF and MPF components [13, 14]. The gradual decrease in the content and/or activity of the key meiotic regulators below a threshold level necessary to maintain the meiotic metaphase arrest was hypothesized to cause meiotic exit in the absence of intracellular calcium signal [5].

At present, physiological inducers of spontaneous egg activation remain unidentified. It was suggested that oxidative stress might act as the initiator for a cascade of events that lead to expedited aging and deterioration of postovulatory oocytes [15]. Using *Xenopus* eggs, it was demonstrated previously that hydrogen peroxide initiates tyrosine phosphorylation and elevates intracellular calcium, resulting in Src kinase-dependent egg activation [16]. The study also reported that prolonged treatment with hydrogen peroxide led to excessive cortical contraction, egg swelling, and overactivation with a very distinctive egg phenotype. Studies of overactivated eggs are important because they can expand our understanding of cell death by unveiling alternative physiological mechanisms. So far, the intracellular events that occur in eggs upon overactivation have not been investigated in detail. Considering that hydrogen peroxide can easily diffuse through the cell plasma and subcellular compartment membranes to directly inflict oxidative damage [17], it could be expected that the drug might interfere with various intracellular processes and severely damage egg homeostasis.

In this work, we investigated oxidative stress-induced overactivation of *Xenopus* eggs using light and fluorescent microscopy, histochemical staining, protein, and bioluminescent assays. It was found that lipofuscin accumulation, decrease of soluble cytoplasmic protein content, and depletion of intracellular ATP occur in the eggs overactivated by strong oxidative stress. To the best of our knowledge, this is the first report concerning the changes of cellular homeostasis in overactivated eggs.

2. Materials and Methods

2.1. Materials. Anesthetic MS-222, water-soluble progesterone, and ATP Bioluminescence Assay Kit CLS II were purchased from Sigma (St. Louis, MO). Collagenase (280 U/mg) was obtained from Wako (Osaka, Japan) and human chorionic gonadotropin was from Teikoku Zoki (Tokyo Japan). Hydrogen peroxide, Sudan Black B (SBB), and protein assay CBB solution were from Nacalai Tesque (Kyoto, Japan). Hydrogen peroxide colorimetric/fluorometric assay kit was from BioVision (Milpitas, CA). Other chemicals were obtained from Wako and Nacalai Tesque. Slide glasses and cover slips for microscopy were purchased from Matsunami Glass (Osaka, Japan).

2.2. Animals, Cell, and Extracts. Adult female frogs of wild-type of *Xenopus laevis* were purchased from Shimizu (Kyoto, Japan) and maintained in dechlorinated water at the ambient temperature of 21-23°C. The experiments with the animals were conducted according to the Kyoto Sangyo University Animal Experimentation Regulations. Egg ovulation was induced by injection of 500 U/animal of human chorionic gonadotropin in the dorsal lymph sac of female frogs. Eggs were collected by squeezing the abdominal parts of the animals in about 10 hours after injection and kept in OR-2 buffer at the ambient temperature. Oocytes were isolated as described previously [6]. Briefly, frogs were anesthetized in 2 mg/ml solution of MS-222 and put on ice; then ovaries were surgically removed and placed into OR-2 solution containing 82.5 mM NaCl, 2.5 mM KCl, 1 mM $CaCl_2$, 1 mM $MgCl_2$, 1 mM Na_2HPO_4, 5 mM HEPES, and pH 7.6. Ovaries were manually dissected into clumps of 50–100 oocytes and extensively washed with OR-2 solution. Clumps of oocytes were treated with 5 mg/ml collagenase (280 U/mg) in OR-2 at 23°C for 2-3 hours by shaking at 60 rpm. Oocytes were extensively washed in OR-2 solution and left for stabilization over 4 h. Undamaged defolliculated oocytes of stage VI were manually selected and used in the experiments. *In vitro* oocyte maturation was induced by addition of 5 μM progesterone and monitored by appearance of a white spot on the animal hemisphere of oocytes. To obtain cytosolic fractions, eggs were homogenized by pipetting in tenfold volume of cold OR-2 buffer containing protease inhibitors APMSF and leupeptin and then centrifuged at 10,000 rpm, 4°C, for 10 min. Supernatant fractions were collected and stored on ice until following biochemical analysis.

2.3. Microscopic Observations. Egg observation and imaging were carried out using SZX16 stereo zoom microscope (Olympus, Japan) equipped with high-frame digital microscope CCD camera DP73, CCD interface *U*-TV0.5XC-*3*, wide-angle objective SDF PLAPO 1xPF. The CellSens Standard software (Olympus) was used for image acquisition. Acquired images were further processed with the ImageJ software of the National Institute of Health [18] freely available at https://imagej.nih.gov/ij/.

2.4. Treatment of Eggs with Hydrogen Peroxide. Hydrogen peroxide was added at the specified concentrations (1-100 mM) to the oocytes matured *in vitro* for 10-12 hours in the presence of progesterone. The cells were washed with OR-2 buffer before peroxide administration to remove the hormone. The precise concentration of hydrogen peroxide was determined by titration using the hydrogen peroxide colorimetric/fluorometric assay kit, according to the manufacturer's manual.

2.5. Detection of Lipofuscin. Lipofuscin is a nondegradable aggregate of oxidized lipids and proteins that accumulates within lysosomes. Two major methods are currently employed for lipofuscin detection. One of them is based on evaluation of lipofuscin autofluorescence and another one on Sudan Black B (SBB) staining [19]. In this study, autofluorescence of lipofuscin in the insoluble particulate fraction of *Xenopus* eggs and staining of egg intracellular compartments with SBB were performed as described previously [20].

2.6. Measurements of Intracellular ATP. To measure intracellular ATP contents, the ATP Bioluminescence Assay Kit CLS II was used according to manufacturer's manual. Egg cytosolic fractions were obtained as described in Section 2.2. 1-μl fraction aliquots were taken into 100-μl bioluminescence assays. Intensity of luminescence was quantified using a GeneLight GL-220 compact luminometer (Microtec, Funabashi, Japan) within one minute after initiation of luciferase reaction by sample addition.

2.7. Other Methods. Protein content in egg cytosolic fractions was determined with the CBB protein assay. Sample absorbance was measured using a NanoDrop 1000 Spectrophotometer (Thermo Fisher, Waltham, MA). Bovine serum albumin was applied as a calibration standard. Quantified data in figures are presented as means ± SD values of four to six measurements taken in single-batch experiments.

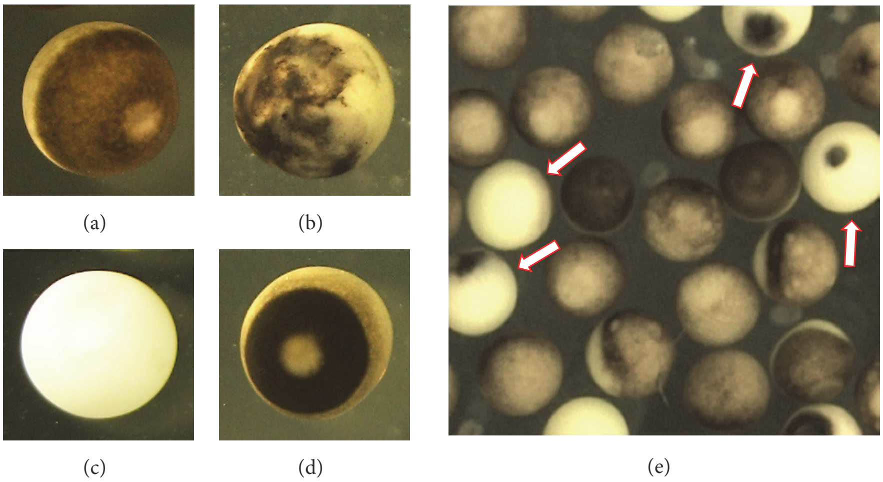

Figure 1: Morphological types of eggs observed in populations of naturally ovulated *Xenopus* eggs. Panels (a), (b), (c), and (d) present mature fertilization-competent, apoptotic, overactivated, and cortically contracted eggs, respectively. Panel (e) shows population of eggs matured *in vitro* in the presence of progesterone and aged by overnight incubation on bench. Arrows point to overactivated eggs.

The experiments were repeated with the separate batches of oocytes and eggs obtained from four different animals. From 50 to 100 eggs were observed in the experiments that concerned counting overactivated egg phenotype.

3. Results

3.1. Overactivated Xenopus Eggs Are Distinguishable by Their Phenotype. Several types of eggs can be found in aging populations of ovulated unfertilized *Xenopus* eggs. The major types are presented in Figures 1(a)–1(d). They include the eggs arrested in the second meiotic metaphase, as it can be judged by the presence of a white spot on the dark animal hemisphere (Figure 1(a)); apoptotic eggs that lost the white spot after activation and experience progressive decoloring of the pigment layer (Figure 1(b)); overactivated eggs that lost their pigmentation and became near completely white (Figure 1(c)); and the eggs with the contracted pigment layer of the animal hemisphere (Figure 1(d)). The proportion of contracted eggs is usually low in egg populations because cortical contraction is transient and completes within 15 min (see next section for details). Importantly, overactivated eggs can clearly be distinguished by their specific phenotype in aging populations of frog eggs (Figure 1(e)), making easy their observation and collection for following biochemical analysis.

3.2. High Levels of Oxidative Stress Induce Time- and Dose-Dependent Overactivation of Xenopus Eggs. The proportion of overactivated eggs in the populations of naturally ovulated frog eggs is quite low, not exceeding normally 2-3%. However, the mature meiotically arrested eggs can be effectively overactivated in the presence of millimolar concentrations of hydrogen peroxide. Strong oxidative stress induces fast cortical contraction of the egg pigment layer that can be detected within 15 min of peroxide administration (Figure 2(a)). In contrast to physiological egg activation, the cortical contraction induced by the prolonged incubation with hydrogen peroxide is not reversible. The pigmented area progressively shrinks, producing overcontracted phenotypes by 30 minutes. Further cortical contraction results in overactivated egg phenotypes with nearly complete loss of egg pigmentation (Figure 2(a)). The proportion of overactivated eggs increases steadily with time, approaching 100% within 4 hours of peroxide administration. Thus, oxidative stress induces time-dependent egg overactivation, and dynamics of this process is presented in Figure 2(b). In addition, the rate of egg overactivation also depends on concentration of hydrogen peroxide, as presented in Figure 2(c). In our experiments, the lowest effective concentration of peroxide capable of inducing overactivation was found to be 1 mM (Figure 2(c)).

3.3. Oxidative Stress Stimulates Lipofuscin Accumulation in Xenopus Eggs. The results presented in Figures 1 and 2 are based on observations of egg morphology. To gain a deeper insight into the oxidative stress-induced egg overactivation, we further attempted to pinpoint biochemical features of this process. As hydrogen peroxide is known to induce oxidation of proteins and lipids, the content of lipofuscin, a nondegradable aggregate of oxidized lipids, proteins, and metals, was investigated in the insoluble particulate fractions of peroxide-treated *Xenopus* eggs.

No significant changes in the lipofuscin level were observed in the eggs within 30 min of peroxide treatment; however lipofuscin content was elevated in the eggs incubated with peroxide for more than 1 hour, as revealed by monitoring lipofuscin-specific autofluorescence [Figures 3(a) and 3(b)]. Of note, a decrease in lipofuscin content was evident at the longer exposure times of 4 and 8 hours. This could probably be attributed to a gradual decrease of peroxide concentration in the egg incubation medium over that time. Indeed, it was found that peroxide concentration falls in the incubation dishes to about 30% of its original level

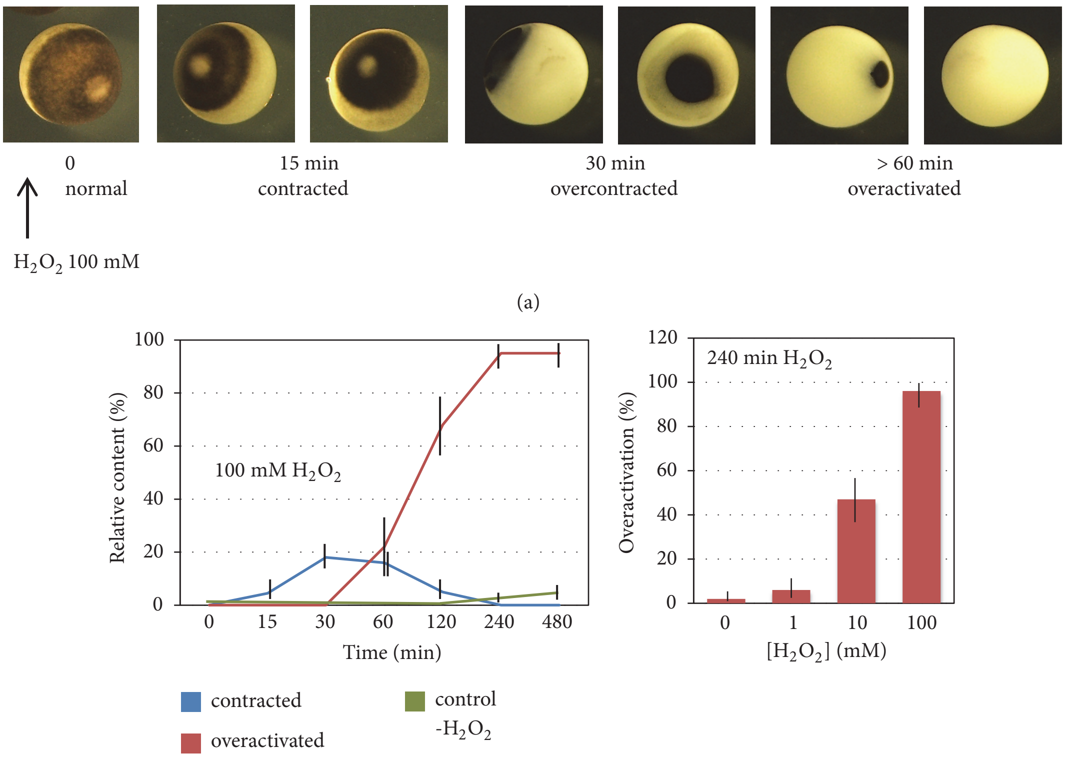

(a)

(b)

(c)

Figure 2: Time and dose dependencies of egg overactivation by hydrogen peroxide. Panel (a) shows dynamics of morphological changes in the eggs overactivated by 100 mM hydrogen peroxide. Panel (b) presents time course of egg cortical contraction and overactivation after addition of 100 mM hydrogen peroxide. The untreated control (-H_20_2) in panel (b) refers to overactivated phenotype. Panel (c) shows dose dependency of egg overactivation. Overactivated phenotype in panel (c) was counted in 240 min after addition of peroxide.

after 8 hours (data not shown). The results of fluorescent analysis were further confirmed by an alternative method of lipofuscin detection. Staining egg particulate fractions with SBB, a lipophilic histochemical dye that reacts with lipids and lipofuscin, revealed color augmentation at 1 and 2 hours followed by color reduction at 4 and 8 hours of peroxide treatment [Figure 3(c)].

3.4. Strong Oxidative Stress Disrupts Protein and Energy Homeostases in Xenopus Eggs. At present, intracellular events that occur upon egg overactivation remain unknown. We hypothesized that the major metabolic traits, such as protein and energy homeostases, might be significantly affected by overactivation and measured the contents of soluble cytoplasmic protein and intracellular ATP in the hydrogen peroxide-treated eggs. A gradual decrease in the content of soluble protein and rapid drop in cellular ATP were observed in overactivated eggs (Figure 4). A statistically significant decrease in the protein content to about 60% level was registered in eggs after 1 hour of hydrogen peroxide treatment (Figure 4(a)), and nearly complete depletion of intracellular ATP (a decrease of almost two orders of magnitude) occurred within 30 minutes (Figure 4(b)). These findings indicate that the oxidative stress applied exerts highly detrimental impact on egg metabolism, resulting in progressive disruption of protein and energy homeostases.

4. Discussion

Egg overactivation happens with a low frequency in the populations of naturally ovulated *Xenopus* eggs (Figure 1). Also, quite rare, spontaneous overactivation of *Xenopus* eggs can be observed in the absence of activation stimuli *in vitro* (Figure 2(b)). Presently, it is viewed as a pathological, spontaneous, and uncontrollable process that renders eggs fertilization incompetent. The results of our study indicate that egg overactivation occurs in the time- and dose-dependent fashion in response to strong oxidative stress (Figure 2), resulting in progressive disruption of cellular homeostasis. Lipofuscin accumulation, protein degradation, and ATP depletion represent biochemical hallmarks of the oxidative stress-induced egg overactivation process (Figures 3 and 4).

Natural inducers of egg overactivation are unknown. In the present study, we used hydrogen peroxide to impose oxidative stress on eggs. It was found that high concentrations of peroxide (10-100 mM) elicit most robust and synchronized egg overactivation (Figure 2(c)), providing a convenient biochemically tractable model of strong oxidative stress. However, physiological relevance of these concentrations is questionable. It seems that much lower peroxide concentrations (below ~1 mM) are actually relevant. Indeed, the average intracellular steady-state concentration of peroxide was

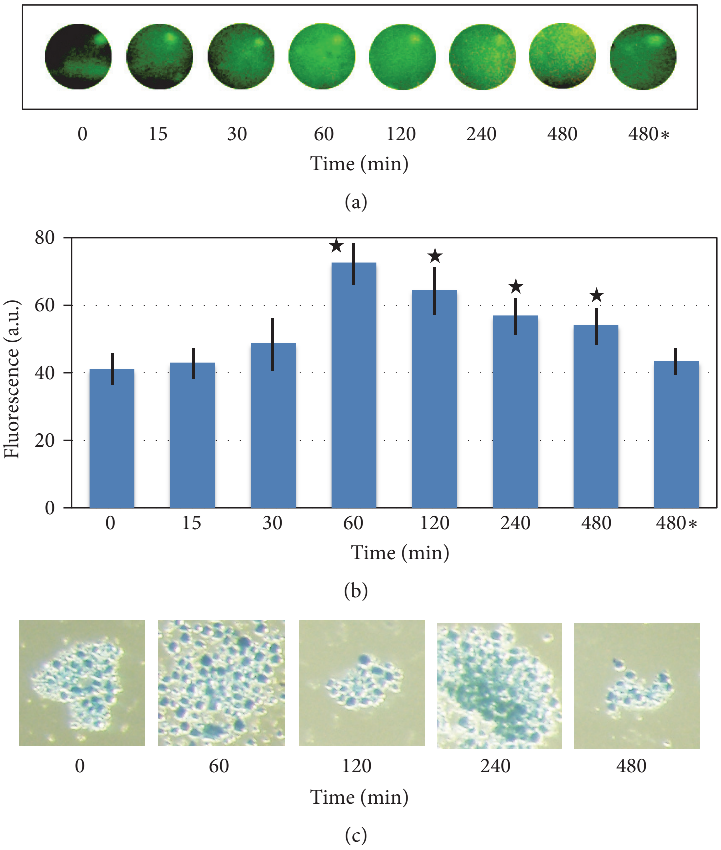

FIGURE 3: Oxidative stress-induced accumulation of lipofuscin in *Xenopus* eggs. Spot assay of lipofuscin autofluorescence in the insoluble particulate fractions of the peroxide-treated eggs and its quantification are presented in panels (a) and (b), respectively. The items labeled as 480∗ refer to control eggs incubated for 480 min in the absence of peroxide. Stars in panel (b) indicate statistical significance from the untreated control ($p<0.05$). Panel (c) shows SBB staining of the egg endosomal compartment. Hydrogen peroxide (f.c. 100 mM) was added to the eggs at 0 time.

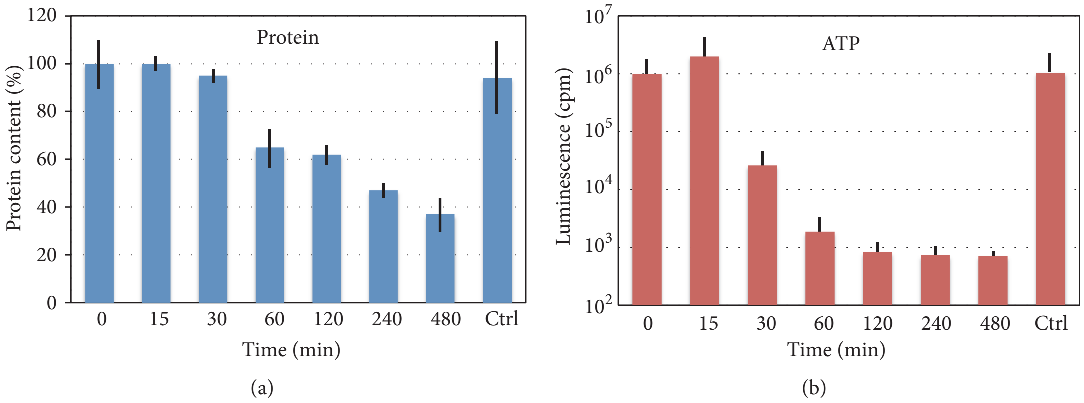

FIGURE 4: Protein and ATP contents in overactivated *Xenopus* eggs. The contents of soluble cytosolic protein and intracellular ATP in the eggs overactivated by addition of 100 mM hydrogen peroxide are shown in panels (a) and (b), respectively. Control (Ctrl) in the panels refers to the eggs incubated for 480 min in the absence of hydrogen peroxide.

reported to be about 10 nM, and the blood plasma concentration was estimated to be 100–5000 times higher [21]. Thus, peroxide concentration can reach the submillimolar range in biological fluids, and it can contribute, hypothetically, to the low-frequency overactivation observed in naturally ovulated frog eggs. Of note, egg stability and sensitivity to oxidative stress vary significantly between experiments. For instance, sensitivity of the eggs to oxidative stress in a previous study [16] was substantially higher, with a threshold of 0.1 mM hydrogen peroxide vs 1 mM in the present work, reflecting, most probably, differences in egg quality between individual egg batches. It is well known that the quality of *Xenopus* eggs greatly depends on the health and husbandry conditions of the adult females producing the eggs. Factors that affect oocyte quality include season of the year, nutrition, lightning, and water quality [22, 23].

It is established that strong oxidative stress can damage lysosomes, mitochondria, and other intracellular compartments, directly and potently affecting cellular homeostasis. Reactive oxygen species were shown to induce chemical modification of lysosomal membrane lipids and proteins, as well as lysosomal membrane permeabilization [24]. Accordingly, our present study revealed accumulation of lipofuscin, a nondegradable aggregate of oxidized lipids, proteins, and metals, in the insoluble particulate fraction of hydrogen peroxide-treated eggs (Figure 3). It was reported recently that lipofuscin is predominantly localized in specialized large-sized late acidic endosomes that store protein and lipids in *Xenopus* eggs. These endosomes were identified in colocalization studies as a subpopulation of yolk platelets, the organelles abundantly present in frog oocytes and eggs [20].

In addition, oxidative damage is known to lead to disruption of mitochondrial function, loss of mitochondrial membrane potential, mitochondrial membrane permeabilization, inhibition of the respiratory chain and ATP production, and release of mitochondrial proteins to the cytoplasm [25]. Correspondingly, our study revealed the depletion of intracellular ATP in hydrogen peroxide-treated eggs within 30 minutes (Figure 4(b)), suggesting severe damage of mitochondrial function by oxidative stress at that time.

At present, executive mechanisms of egg overactivation and ensuing cell death are unknown. Although disruption of mitochondrial function and release of mitochondrial proteins, such as cytochrome C, can promote caspase-dependent apoptotic cell death, it is highly unlikely that apoptosis is involved in degradation of overactivated *Xenopus* eggs. The pace of egg degradation by an apoptotic process that unfolds in the eggs after their activation is much slower than that of the process initiated by overactivation. For example, ATP depletion in apoptotic eggs can be observed only after many hours following egg activation [6]; however it occurs within 30 minutes of oxidative stress-induced egg overactivation (Figure 3(b)). Of note, ATP depletion occurs typically quite late in apoptosis because high ATP levels are necessary to maintain this process [26].

Alternatively, oxidative stress has been reported to initiate autophagy, a homeostatic process that allows cells to degrade cytoplasmic proteins and organelles [27, 28]. For example, mitochondria damaged in Alzheimer disease by oxidative stress in neurons are subjected to autophagic degradation, leading to neurodegeneration [29]. Markedly, autophagy also requires certain levels of intracellular ATP, making this process incompatible with the early ATP depletion that takes place during egg overactivation (Figure 3(b)). In the future, it would be interesting to delineate intracellular molecular events in the overactivated eggs and elucidate the exact pattern of their cell death.

5. Conclusions

This study demonstrates that (i) overactivated *Xenopus* eggs have a distinctive phenotype in the populations of naturally ovulated unfertilized eggs, (ii) egg overactivation can be induced time- and dose-dependently by high levels of oxidative stress, and (iii) oxidative stress-induced overactivation is accompanied by progressive disruption of cellular protein and energy homeostases. It is revealed for the first time that lipofuscin accumulation, decrease of soluble cytoplasmic protein content, and depletion of intracellular ATP take place in the eggs overactivated by strong oxidative stress. These intracellular events may serve as biochemical markers of egg overactivation. In addition, it appears that egg overactivation unfolds as a sequential and ordered process. Further investigations are necessary to delineate in detail the sequence of intracellular events during this process.

Data Availability

All the data are available from the corresponding author upon request.

Conflicts of Interest

The authors declare that there are no conflicts of interest regarding the publication of this article.

Acknowledgments

The work was supported in part by the Collaboration Research Grant 281027 from the Kobe University, Japan (to A. Tokmakov) and by the Grant-in-Aid for Scientific Research 15K07083 from the Ministry of Education, Culture, Sports, Science and Technology (to K.-I. Sato). Publication costs were covered by institutional funds.

References

[1] Y. Masui and C. L. Markert, “Cytoplasmic control of nuclear behavior during meiotic maturation of frog oocytes,” *Journal of Experimental Zoology*, vol. 177, no. 2, pp. 129–145, 1971.

[2] Y.-L. Miao, K. Kikuchi, Q.-Y. Sun, and H. Schatten, “Oocyte aging: cellular and molecular changes, developmental potential and reversal possibility,” *Human Reproduction Update*, vol. 15, no. 5, pp. 573–585, 2009.

[3] S. Prasad, M. Tiwari, B. Koch, and S. K. Chaube, “Morphological, cellular and molecular changes during postovulatory egg aging in mammals,” *Journal of Biomedical Science*, vol. 22, article no. 36, 2015.

[4] T. Chebotareva, J. Taylor, J. J. Mullins, and I. Wilmut, “Rat eggs cannot wait: Spontaneous exit from meiotic metaphase-II arrest,” *Molecular Reproduction and Development*, vol. 78, no. 10-11, pp. 795–807, 2011.

[5] A. A. Tokmakov, K.-I. Sato, and V. E. Stefanov, “Postovulatory cell death: why eggs die via apoptosis in biological species with external fertilization,” *The Journal of Reproduction and Development*, vol. 64, no. 1, pp. 1–6, 2018.

[6] A. A. Tokmakov, S. Iguchi, T. Iwasaki, and Y. Fukami, “Unfertilized frog eggs die by apoptosis following meiotic exit,” *BMC Cell Biology*, vol. 12, article no. 56, 2011.

[7] S. Iguchi, T. Iwasaki, Y. Fukami, and A. A. Tokmakov, “Unlaid Xenopus eggs degrade by apoptosis in the genital tract,” *BMC Cell Biology*, vol. 14, no. 1, article no. 11, 2013.

[8] K. V. Premkumar and S. K. Chaube, “An insufficient increase of cytosolic free calcium level results postovulatory aging-induced abortive spontaneous egg activation in rat,” *Journal of Assisted Reproduction and Genetics*, vol. 30, no. 1, pp. 117–123, 2013.

[9] K. V. Premkumar and S. K. Chaube, “RyR channel-mediated increase of cytosolic free calcium level signals cyclin B1 degradation during abortive spontaneous egg activation in rat,” *In Vitro Cellular & Developmental Biology - Animal*, vol. 50, no. 7, pp. 640–647, 2014.

[10] M. Whitaker, “Calcium at fertilization and in early development,” *Physiological Reviews*, vol. 86, no. 1, pp. 25–88, 2006.

[11] L. Houel-Renault, L. Philippe, M. Piquemal, and B. Ciapa, “Autophagy is used as a survival program in unfertilized sea urchin eggs that are destined to die by apoptosis after inactivation of MAPK1/3 (ERK2/1),” *Autophagy*, vol. 9, no. 10, pp. 1527–1539, 2013.

[12] L. Philippe, L. Tosca, W. L. Zhang, M. Piquemal, and B. Ciapa, “Different routes lead to apoptosis in unfertilized sea urchin eggs,” *Apoptosis*, vol. 19, no. 3, pp. 436–450, 2014.

[13] Z. Xu, A. Abbott, G. S. Kopf, R. M. Schultz, and T. Ducibella, “Spontaneous activation of ovulated mouse eggs: Time-dependent effects on M-phase exit, cortical granule exocytosis, maternal messenger ribonucleic acid recruitment, and inositol 1,4,5-trisphosphate sensitivity,” *Biology of Reproduction*, vol. 57, no. 4, pp. 743–750, 1997.

[14] W. Ma, D. Zhang, Y. Hou et al., “Reduced expression of MAD2, BCL2, and MAP kinase activity in pig oocytes after in vitro aging are associated with defects in sister chromatid segregation during meiosis II and embryo fragmentation after activation,” *Biology of Reproduction*, vol. 72, no. 2, pp. 373–383, 2005.

[15] T. Lord and R. John Aitken, “Oxidative stress and ageing of the post-ovulatory oocyte,” *Reproduction*, vol. 146, no. 6, pp. R217–R227, 2013.

[16] K.-I. Sato, K. Ogawa, A. A. Tokmakov, T. Iwasaki, and Y. Fukami, “Hydrogen peroxide induces Src family tyrosine kinase-dependent activation of Xenopus eggs,” *Development, Growth & Differentiation*, vol. 43, no. 1, pp. 55–72, 2001.

[17] G. P. Bienert, J. K. Schjoerring, and T. P. Jahn, “Membrane transport of hydrogen peroxide,” *Biochimica et Biophysica Acta (BBA) - Biomembranes*, vol. 1758, no. 8, pp. 994–1003, 2006.

[18] M. D. Abramoff, P. J. Magalhaes, and S. J. Ram, “Image processing with imagej,” *Biophotonics International*, vol. 11, pp. 36–42, 2004.

[19] E. A. Georgakopoulou, K. Tsimaratou, K. Evangelou et al., “Specific lipofuscin staining as a novel biomarker to detect replicative and stress-induced senescence. A method applicable in cryo-preserved and archival tissues,” *Aging*, vol. 5, no. 1, pp. 37–50, 2013.

[20] A. A. Tokmakov and K. Sato, “Activity and intracellular localization of senescence-associated β-galactosidase in aging Xenopus oocytes and eggs,” *Experimental Gerontology*, vol. 119, pp. 157–167, 2019.

[21] H. J. Forman, A. Bernardo, and K. J. A. Davies, “What is the concentration of hydrogen peroxide in blood and plasma?” *Archives of Biochemistry and Biophysics*, vol. 603, pp. 48–53, 2016.

[22] H. L. Sive, R. M. Grainger, and R. M. Harland, *Early Development of Xenopus Laevis*, Cold Spring Harbor Laboratory Press, Cold Spring Harbor, New York, NY, USA, 1997.

[23] M. Wu and J. Gerhart, “Raising Xenopus in the laboratory,” in *Methods in Cell Biology*, H. B. Peng and B. Kay, Eds., vol. 36, pp. 3–18, Academic Press, San Diego, Calif, USA, 1991.

[24] R. Gómez-Sintes, M. D. Ledesma, and P. Boya, “Lysosomal cell death mechanisms in aging,” *Ageing Research Reviews*, vol. 32, pp. 150–168, 2016.

[25] H. Cui, Y. Kong, and H. Zhang, “Oxidative stress, mitochondrial dysfunction, and aging,” *Journal of Signal Transduction*, vol. 2012, Article ID 646354, 13 pages, 2012.

[26] V. Nikoletopoulou, M. Markaki, K. Palikaras, and N. Tavernarakis, “Crosstalk between apoptosis, necrosis and autophagy,” *Biochimica et Biophysica Acta*, vol. 1833, no. 12, pp. 3448–3459, 2013.

[27] H. K. Eun, S. Sohn, J. K. Hyuk et al., “Sodium selenite induces superoxide-mediated mitochondrial damage and subsequent autophagic cell death in malignant glioma cells,” *Cancer Research*, vol. 67, no. 13, pp. 6314–6324, 2007.

[28] R. A. Kirkland, R. M. Adibhatla, J. F. Hatcher, and J. L. Franklin, “Loss of cardiolipin and mitochondria during programmed neuronal death: evidence of a role for lipid peroxidation and autophagy,” *Neuroscience*, vol. 115, no. 2, pp. 587–602, 2002.

[29] P. I. Moreira, S. L. Siedlak, X. Wang et al., “Increased autophagic degradation of mitochondria in alzheimer disease,” *Autophagy*, vol. 3, no. 6, pp. 614-615, 2007.

Hindawi
BioMed Research International
Volume 2019, Article ID 4625279, 15 pages
https://doi.org/10.1155/2019/4625279

Clinical Study

Prebiotic Effect of Lycopene and Dark Chocolate on Gut Microbiome with Systemic Changes in Liver Metabolism, Skeletal Muscles and Skin in Moderately Obese Persons

Maria Wiese,[1] Yuriy Bashmakov ,[2] Natalia Chalyk,[3] Dennis Sandris Nielsen ,[1] Łukasz Krych,[1] Witold Kot,[4] Victor Klochkov,[3] Dmitry Pristensky,[2] Tatyana Bandaletova,[5] Marina Chernyshova,[2] Nigel Kyle,[2] and Ivan Petyaev [2]

[1] *Department of Food Science, University of Copenhagen, Rolighedsvej 26, 1958, Frederiksberg, Denmark*
[2] *Lycotec Ltd., Granta Park, Cambridge, CB21 6GP, UK*
[3] *State Medical University, Research Institute of Cardiology, 12 Chenyshevskogo Str, 410028 Saratov, Russia*
[4] *Department of Environmental Sciences, Aarhus University, Denmark*
[5] *DiagNodus Ltd., Granta Park, Cambridge, CB21 6GP, UK*

Correspondence should be addressed to Ivan Petyaev; ykb75035@aol.com

Received 21 January 2019; Revised 1 April 2019; Accepted 18 April 2019; Published 2 June 2019

Guest Editor: Yan Huang

Copyright © 2019 Maria Wiese et al. This is an open access article distributed under the Creative Commons Attribution License, which permits unrestricted use, distribution, and reproduction in any medium, provided the original work is properly cited.

Lycopene rich food and dark chocolate are among the best-documented products with a broad health benefit. This study explored the systemic effect of lycopene and dark chocolate (DC) on gut microbiota, blood, liver metabolism, skeletal muscle tissue oxygenation and skin. 30 volunteers were recruited for this trial, 15 women and 15 men with a mean age of 55 ± 5.7 years and with moderate obesity, $30 < \mathrm{BMI} < 35\,\mathrm{kg/m^2}$. They were randomized and divided into five equal interventional groups: three received different formulations of lycopene, one of them with a 7 mg daily dose and two with 30 mg; another group was given 10 g of DC with 7 mg lycopene embedded into its matrix, and the last group received 10 g DC. The trial was double-blinded for the three lycopene groups and separately for the 2 DC groups; the trial lasted for 1 month. By the end of the trial there were dose-dependent changes in the gut microbiota profile in all three lycopene groups with an increase of relative abundance of, e.g., *Bifidobacterium adolescentis* and *Bifidobacterium longum*. This was also accompanied by dose-dependent changes in the blood, liver metabolism, skeletal muscle and skin parameters. Consumption of DC resulted in increased relative abundance of, e.g., *Lactobacillus* and a reduction of corneocyte exfoliation. This is the first study which reports the prebiotic potential of lycopene and DC.

1. Introduction

Carotenoids are essential micronutrients, which cannot be synthesized by humans and must be obtained from food. Lycopene, the red pigment of tomatoes, watermelon, and some other fruits, is one major carotenoids. Intake of lycopene rich food has been linked to lower prevalence of cardiovascular disease, stroke [1] and some forms of cancer [2, 3]. Limited interventional clinical studies have indicated its therapeutic ability to slow down development of carotid atherosclerosis [4], anti-infective and anti-inflammatory properties [5], improvement of parameters associated with prostate hyperplasia [6], benefit in management of prostate cancer [7] and help to protect skin from UV damage [8, 9].

The concentration of lycopene in blood and body tissues is highly variable and depends on dietary habits and age and has also been related to health status. For example, the plasma or serum concentration could vary from about 60 ng/ml, or below, to 600 ng/ml or above [10]. A reduced level in the body could be due to three major reasons: either low dietary intake, impaired lycopene absorption and processing for example in older persons or those with metabolic syndrome, which results in poor bioavailability of this carotenoid or due to its accelerated depletion as a result of ongoing free radical pathologies in the body.

The current consensus on the broad beneficial effects of lycopene on health exists with regard to its powerful antioxidant properties and the related protection of lipoproteins and other lipid structures from oxidative damage, which typically are associated with a number of pathological conditions [1, 11].

It has been demonstrated that cocoa flavanols have a systemic effect in healthy volunteers with prebiotic activity on the gut microbiome and reduction of blood lipoproteins produced by the liver [12]. However, in real life these flavanols usually consumed by humans in a food form of chocolate, which contains cocoa butter, triglyceride lipids, other cocoa ingredients, and cocobiota metabolites [13]. Therefore, another objective of our study was to assess whether regular consumption of dark chocolate, DC, would have a similar effect as the cocoa flavanols drink. Although there were a number of reports, which demonstrated a positive impact of DC on blood lipids [14, 15], to the best of our knowledge this is the first study investigating the effect of lycopene and DC on the gut microbiota in middle-aged subjects with moderate obesity, 30 < Body Mass Index, BMI < 35 kg/m^2. For this purpose we used GA lycopene, which is specifically formulated to overcome reduced bioavailability of this carotenoid in older people and in individuals with metabolic syndrome (Lycotec, UK). We found that continuous administration of this product for 4 weeks resulted in significant prebiotic effects. These positive changes in the gut microbiota profile were accompanied by systemic improvement of different physiological parameters of the participants from blood and liver metabolism to peripheral tissues including skin.

2. Methods

Study Design. In total 30 volunteers were recruited to take part in the study, 15 male and 15 female, all Caucasian within the age span of 40–68 and median 55 ± 5.7 years. They were randomized and divided into five groups of equal size. Group I received a daily dose of 10 g dark chocolate with 7 mg lycopene by a proprietary protocol guaranteeing its maximum embedment into the lipid part of the chocolate, L-Tug, and on another optimal lycopene coating of chocolate crystals and formation of coco- lycosomes, DCL [16]. Group II received daily one capsule of 7 mg GA lycopene formulated with medium saturated fatty acids, GAL-MSFA, Group III one capsule daily of 30 mg GAL-MSFA, group IV one capsule daily 30 mg of GA lycopene formulated with polyunsaturated fatty acids, GAL-PUFA, and group V 10 g of the control dark chocolate daily. Three GAL groups received blinded lycopene capsules, as two other groups received blinded DC products.

Products. All products for the trial were developed and made by Lycotec Ltd. (Cambridge, United Kingdom). The product was especially designed to improve lycopene bioavailability in middle-aged persons, 50 years old or above, or in those who have such conditions as metabolic syndrome, fatty liver, etc. [17]. It contained phosphatidylcholine, which serves as a principle scaffolding element for incorporation of lycopene during lipoprotein intracellular reassembly, the process that is essential for lycopene transportation but impaired in the above individuals.

There were two formulations of GAL, for two different nutraceutical applications, which were applied in this study. The first was with a blend of MSFA to facilitate formation of small-medium chylomicrons, which would be transported by the portal vein for liver targeting delivery of lycopene. The second one was a blend with PUFA to facilitate formation of larger chylomicrons, which would be transported by the thoracic duct for the systemic blood circulation bypassing the liver. All GAL products were made in gelatin capsule.

For the control DC and DCL Green & Black's 70% dark chocolate was used. It was made from Trinitario cocoa beans and contained 42% fat, of which saturates were 25%; carbohydrates 36.5%, of which sugars were 28.5%; fibre 10%, protein 9.1%, salt 0.13%. Each 10 g bar contained 1.5 mg of catechins, 6.6 mg of epicatechins, 1.9 mg of dimer-B2, 7.5 mg of caffeine, 75 mg of theobromine, 75 μg of phenylethylamine, 55 μg of serotonin, and ≤ 0.1 μg of resveratrol.

Both capsule and chocolate products were advised to be taken once a day after the main meal.

The duration of the trial was 1 month.

The treatment part of the study and the blood analysis were conducted at the Institute of Cardiology, the Ministry of Health of the Russian Federation (Saratov, Russian Federation) by Lycotec Ltd. (Cambridge, United Kingdom). The protocol was approved by the Local Ethics Committee (FGBU SarNIIK18.02.2014). Trial registration number was ACTRN12618000715279. All patients were informed of the purpose and goals of the study and had signed a consent form before enrolment and participation in the study.

The stool microbiota analysis was made by the Department of Food Science in the Section of Food Microbiology, at the University of Copenhagen in Denmark.

The skin samples were analysed by Lycotec in Cambridge.

2.1. Inclusion/Exclusion Criteria

Inclusion Criteria were as follows:

(i) ability to sign an informed consent,

(ii) nonsmokers or light-to-moderate smokers (≤10 cigarettes daily),

(iii) moderately obese with BMI between 30 and 35 kg/m^2,

(iv) with elevated serum markers of inflammatory oxidative damage, IOD ≥ 40 μM/mL and oxidative stress, LDL-Px, ELISA × 10^3 ≥ 200,

(v) no participation in other dietary trials during the last 3 months before enrolment and duration of study,

(vi) willingness and ability to comply with the study protocol for the duration of the study.

Exclusion criteria were as follows:

(i) unwillingness to sign informed consent,

(ii) unable to comply with the protocol for the duration of the study,

(iii) history of myocardial infarction in the 3 months preceding the study, ejection fraction (EF) < 45%,

(iv) significant medical condition that would impact safety considerations (e.g., significantly elevated liver enzymes, hepatitis, severe dermatitis, uncontrolled diabetes, cancer, severe GI disease, fibromyalgia, renal failure, recent CVA (cerebrovascular accident), pancreatitis, respiratory diseases, epilepsy, etc.),

(v) compulsive alcohol abuse (>10 drinks weekly),

(vi) or regular exposure to other substances of abuse,

(vii) participation in other nutritional or pharmaceutical studies,

(viii) resting heart rate of >100 beats per minute or <50 beats per minute,

(ix) positive test for tuberculosis, HIV, or hepatitis B,

(x) inability to tolerate phlebotomy,

(xi) special diets in the 4 weeks prior to the study (e.g., liquid, protein, and raw food diet),

(xii) tomato or DC intolerance.

2.2. BMI, Pulse Rate, and Systolic and Diastolic Blood Pressure. Measurements of body mass index, BMI, body mass of the patients and their height were carried out in the morning and BMI was calculated in kg/m^2. Pulse rate, systolic and diastolic blood pressure, SBP, and DBP were recorded three times on the left arm of the seated patient after 15 min of rest. The time between measurements was greater than 2 minutes. The mean result for each parameter was calculated. All body and vascular parameters were recorded in the morning between 8 and 10 am.

Tissue Oxygenation. Thenar eminence and forearm muscles of the patients were used as a tissue target for the assessment of oxygen saturation, StO_2, or combined level of oxygenated haemoglobin and myoglobin. StO_2 was assessed by continuous wavelength near-infrared spectroscopy, NIRS, with wide-gap second-derivative (In Spectra, Hutchinson Technology, MN, USA). The measurements were taken at different time points. The recording was initiated after 15 min of rest in a supine position before occlusion of the brachial artery. It was then continued during stagnant ischemia induced by rapidly inflating the cuff to 50 mm Hg above systolic BP. The ischemia lasted for 3 min, and the recording period lasted for another 5 min after that until StO_2 was stabilized. The area under the hyperaemic curve, AUC, of the recorded signal for the settling time in the postocclusion period was then calculated as described earlier in % O_2/minute [17, 18].

Samples Collection. Blood was collected by phlebotomy in the morning, in the hospital, and from the arm veins of patients following night fast. The serum was separated from the rest of the clotted mass by centrifugation; aliquots were then stored in code-labeled tubes for blinded analysis and stored at −80°C until use.

For sample collection from the surface of the facial skin and samples of the cerumen all study participants were requested to avoid facial and ear hygienic manipulations for 24 hours before sampling, which was carried out in the morning in parallel with blood sample collection. Skin surface sample collection and preparation were performed as previously described [19]. Briefly, samples were collected using polyester swabs from the surface of the facial skin (the sides of the nose). During the procedure two samples were taken (one swab per side). Each collected sample was placed on the surface of a microscope slide. A second microscope slide was pressed against the surface of the first one. This procedure provided a pair of identical smears. All slides with collected samples were coded to provide sample anonymity for blinded analysis and stored at −20°C until further analysis.

The stool samples were collected either on the morning or night before the day of the visit to the hospital. Participants did this collection themselves, at the convenience of their home, in the morning on the day of visiting clinic. A special kit and sample containers were provided by the trial team. The collected samples were labeled and stored at −80°C until analysis.

2.3. Gut Microbiome Analysis

2.3.1. DNA Extraction. Genomic DNA was extracted from 200 mg stomached fecal material (stomacher 2x 60 sec at mid speed) using the Power Soil Kit protocol (MoBio Laboratories). The FastPrep bead-beating step was performed in 3 cycles of 15 s each at a speed of 6.5 M/s in a FastPrep-24TM Homogenizer (MP). DNA quantity and quality were measured using a NanoDrop 1000 (Thermo Scientific), 16S rRNA gene library preparation. The fecal microbiota composition was determined using tag-encoded 16S rRNA gene MiSeq-based (Illumina, CA, USA) high throughput sequencing. In brief the V3 region of the 16S rRNA gene was amplified using primers compatible with the Nextera Index Kit (Illumina) NXt_338_F:5′- TCGTCGGCAGCGTCAGATGTGTATAAGAGACAGACWCCTACGGGWGGCAGCAG -3′ and NXt_518_R: 5′- GTCTCGTGGGCTCGGAGATGTGTATAAGAGACAGATTACCGCGGCTGCTGG -3′·· [20]; the PCR reactions and library preparation were conducted as described in [21].

2.3.2. High throughput Sequencing and Data Treatment. The raw dataset containing pair-ended reads with corresponding quality scores were merged and trimmed using fastq_mergepairs and fastq_filter scripts implemented in the UPARSE pipeline. The minimum overlap length was set to 10 base pairs (bp). The minimum length of merged reads was 150 bp, the maximum expected error E was 2.0, and the first truncating position with a quality score was N≤4. Purging the dataset from chimeric reads and constructing de novo Operational Taxonomic Units (OTU) was conducted using the UPARSE pipeline [22]. The Green Genes (13.8) 16S rRNA gene collection was used as a reference database [23]. Quantitative Insight Into Microbial Ecology (QIIME) open source software [24] (1.7.0 and 1.8.0) was used for the subsequent analysis steps. Principal coordinate analysis (PCoA) plots were generated with the Jackknifed Beta Diversity workflow based on 10 UniFrac distance metrics calculated using 10 subsampled OTU tables. The number of sequences taken for each jackknife subset was set to 90% of the sequence number within the most indigent sample, hence 10000 reads per sample. Permutational Multivariate Analysis of Variance (PERMANOVA) was used to evaluate group differences using weighted, unweighted, and generalized UniFrac distance metrics that were generated based on rarefied (10000 reads/sample) OTU tables. The relative distribution of the genera registered was calculated for unified and summarized in genus level OTU tables. Alpha diversity measures expressed as observed species values (sequence similarity 97%) were computed for rarefied OTU tables (10000 reads/sample) using the alpha rarefaction workflow. Differences in alpha diversity were determined using a t-test-based approach employing the nonparametric (Monte Carlo) method (999 permutations) implemented in the comparative alpha diversity workflow. The ANOVA determined significance of quantitative (relative abundance) association of OTUs with given categories; p values were False Discovery Rate (FDR) corrected. These were calculated based on 1000 subsampled OTU tables rarefied to an equal number of reads (10000 reads/sample). Spearman correlations between the taxa relative abundance (at the OTU level and summarized to the species level) and the host parameters were conducted using observation metadata correlations script (Qiime 1.9.1). Fisher z-transformation method with 1000 permutations was used for calculating p values. The influence of explanatory variables (host parameters) and OTUs relative abundance (species level) was tested with the rda function (vegan R-package), using the ANOVA-like permutation tests (1,000) to determine the significance of the putative constrains effects [25].

Biochemistry. Glucose, total cholesterol, triglycerides, high density cholesterol, low density cholesterol and C-reactive protein were determined using commercially available analytical kits according to the manufacturers' instructions (ByoSystems, R&D Systems).

Lycopene Quantitative Analysis. The lycopene concentration in all serum samples was measured in duplicate by high-performance liquid chromatography [26] with modifications. Briefly, 400 μl of serum was mixed with 400 μl of ethanol and was extracted twice with 2 ml hexane. The combined hexane layers were evaporated to dryness in a vacuum (Scan Speed 32 centrifuge) and the residue reconstituted to a volume of 100 μl in sample solution (absolute ethanol – methylene chloride, 5:1, v/v). The specimens were centrifuged again (15 minutes at 10,000 g) and clear supernatant was transferred to HPLC vials. Five microliters of the extract was injected into an Acquity HSS T3 75x 2.1mm 1.8 μm column (Waters, USA) preceded by a Acquity HSS T3 1.8 μm VanGuard precolumn (Waters, USA) and eluted isocratically at 45°C with the mobile phase (acetonitrile – 0.08% phosphoric acid solution - tert-Butyl methyl ether, 70:5:25, v/v/v) at a flow rate of 0.5 ml/min. The lycopene peak was detected by a Photodiode Array Detector (Waters, USA) at 474 nm. The peak area was measured using Empower 3 software (Waters, MA). The lycopene concentration in serum samples was calculated by reference to an analytical standard (lycopene from tomato, L9879, Sigma, USA).

Inflammatory Oxidative Damage (IOD). Serum samples were incubated in 0.05 M PBS acetate buffer (pH 5.6) overnight, to imitate the type of oxidative damage which occurs during the release of lysosomes following neutrophil degranulation. The following morning the reaction was stopped using trichloroacetic acid. The concentration of the end products such as malondialdehyde (MDA), and other possible thiobarbituric acid reactive substances (TBARS), was then measured by colorimetry [27] using reagents and kits from Cayman Chemical (MC, USA).

LDL-Px and Lipoprotein O_2. Activity of serum LDL peroxidase proteins, which include IgG with superoxide dismutase activity, was measured as described previously [28]. Plasma oxygen, which carried by blood lipids/lipoproteins, was measured by catalymetry [29].

Statistics. For the assessment of normally distributed parameters the Shapiro-Wilk method was used. Student's *t*-test was then applied for both paired and unpaired samples. In cases where parameters were not normally distributed the Mann–Whitney test and Kruskal-Wallis test were used. ANOVA and ANCOVA were used with post hoc analysis (Statistica 9 suite, StatSoft, Inc.). Statistical significance between two-tailed parameters was considered to be $P<0.05$.

3. Results

Baseline characteristics of the participants are presented in Table 1 and were comparable between all five groups.

3.1. Blood and Liver Metabolism.

Ingestion of lycopene products for one month, either in the capsule format or in the chocolate matrix, resulted in a significant increase of its concentration both in the serum and in the ear skin excretion (Table 2).

Supplementation with GAL-MSFA resulted in a dose-dependent significant reduction of markers of oxidative damage and inflammation. 7 mg of lycopene was able to reduce IOD and LDL-Px, by the end of the month, by 49 μM MDA, or by 35%, and by 200 ELISA units, or by 36%, while 30 mg reduced these parameters by 69, or by 60%, and 285, by 43%, accordingly. 30 mg of GAL-MSFA was 3 fold more effective in inhibiting IOD than the same dose of lycopene but in the GAL-PUFA formulation. This may potentially indicate on the liver origin of this blood marker. Effect of two formulations of lycopene on LDL-Px was similar (Table 2).

DC with or without lycopene had a similar effect on the inhibition of IOD as 7 mg of lycopene. Although both chocolate products were able to reduce LDL-Px, their effectiveness was below that of lycopene itself.

Administration of either formulation of GAL, or lycopene with DC complex, resulted in significant changes in the profile of fasting lipoproteins, which are assembled and produced by the liver. GAL-MSFA reduced in a dose-dependent

Table 1: Baseline values.

	BASELINE CHARACTERISTICS OF THE ENROLLED VOLUNTEERS(Mean +/- SD)				
	Groups				
	I	II	III	IV	V
Number of Patients	6	6	6	6	6
Males	3	2	4	3	3
Females	3	4	2	3	3
Age	61.8±5.9	56.2±5.9	56.1±5.8	52.1±5.1	63.2±6.1
Light/Moderate Smokers	1	1	1	1	1
Body Mass Index in kg/m^2	32.1±2.4	32.7±3.3	33.8±3.5	31.1±3.2	31.8±2.9
Fasting Glucose mmol/dL	6.1±0.42	6.0±0.45	5.7±0.49	5.4±0.43	5.5±0.56
Total Cholesterol mg/dL	185 ± 14.3	181 ± 15.2	175 ± 14.7	187 ± 16.2	180 ± 13.9
Triglycerides mg/dl	135±14.9	136±13.8	136±13.8	127±13.1	122±13.5
LDL mg/dL	144±11.8	143±12.7	121±12.2	137±13.6	131±12.1
HDL mg/dL	41.9±3.2	46.5±4.4	51.2±4.7	49.8±4.4	44.0±4.4
Pulse rate per min	66.7±4.2	67.7±3.5	65.2±3.4	70.5±3.9	66.6±5.1
Blood Pressure					
Systolic	112±5.5	123±7.4	117±6.9	124±8.5	118±6.7
Diastolic	77.6±4.4	78.7±5.0	77.6±4.4	76.7±4.6	79±5.6

manner both LDL concentration and triglycerides. This liver targeting formulation of lycopene, in 30 mg dose, was able to reduce the first parameter by 17 mg/dL and the second by 18 mg/dL. Supplementation with GAL-PUFA resulted in LDL reduction by 13 mg/dL and triglycerides by only 3 mg/dL. Lycopene in the L-Tug complex with dark chocolate was also able to reduce LDL; however, changes caused by the ingestion of the control DC were not significant (Table 2).

By the end of the trial there were no changes in the serum concentration of HDL, glucose and liver enzymes, ALT and AST (results are not presented).

There were noticeable improvements in the molecular oxygen metabolism in all groups. In groups supplemented with GAL-MSFA O_2 concentration and its transportation by blood lipoproteins was significantly increased by 18-19%, $p < 0.05$. In the group that received GAL-PUFA this increase was lower, by 12%, $p > 0.05$. In the group, which received control DC, the increase in the lipoprotein O_2 was the highest, by 44%, $p < 0.01$.

These changes in the plasma oxygen transportation translated to benefit for peripheral tissue oxygenation but not in the control DC group. Ingestion of all lycopene products also resulted in a significant boost of tissue oxygenation in skeletal muscles. Administration of GAL-MSFA demonstrated a dose-dependent effect in changes of this parameter. However, 30 mg of lycopene in GAL-PUFA formulation was 25%, $p < 0.05$, more effective than the same dose of lycopene but in the GAL-MSFA formulation (Table 2).

3.2. Skin Parameters. Supplementation of the participants with all formulations of lycopene for one month resulted in significant reversal of age-associated parameters of sebum and corneocytes. Also for the GAL-PUFA a reduction was observed, though statistically not significant. The GAL-PUFA formulation was more effective in improving cellular parameters of the skin, while GAL-MSFA was more effective for sebum parameters.

However, different to the blood parameters, observed changes in the skin, apart from those related to the sebum, did not have dose-dependency. This may indicate that even the dose of 7 mg of daily supplementation with lycopene was sufficient to reach its saturated level in this tissue by the end of the trial.

The viscosity of the sebum, in terms of the size of the lipid droplets collected from the surface of the skin, was increased on average by 390 nm during this trial after supplementation by all formulations of lycopene. However, GAL-PUFA only slightly increased the diameter of the droplets, by 50 nm, while GAL-MSFA was much more effective and did it in a dose-dependent manner, by 180 nm for 7 mg of lycopene and by 480 nm for 30 mg (Table 3 and Figure 1 top images).

The rate of corneocyte exfoliation was reduced by about 23% for the former formulation and by 9-11% for the latter. Moreover, not just the rate of exfoliation was reduced by lycopene supplementation but also the damage of these cells too. The number of the clusters of cross-linked corneocytes was reduced by 36% for GAL-PUFA and by 29 to 47% by GAL-MSFA (Table 3 and Figure 1, images in the middle).

It was interesting to observe that these improvements of the sebum (Figure 1(a)) and corneocyte (Figure 1(b)) parameters were accompanied by significant reduction of the total load of the gram-negative bacteria on the surface of the skin, but only by supplementation with GAL-MSFA. In the group of GAL-PUFA there was a similar trend, but it was statistically insignificant.

In the control DC group the sebum and corneocytes parameters by the end of the trial were not affected.

Table 2: Changes in blood and tissue parameters after supplementation with GA lycopene for one month.

Parameters before and after 4 weeks of the trial	Groups I	II	III	IV	V
Lycopene in serum, in ng/ml					
before	110 ± 17	110 ± 12	210 ± 19	90 ± 8.4	120 ± 22
after	500 ± 52**	310 ± 30**	430 ± 30**	190 ± 14*	170 ± 27
Lycopene in cerumen, in ng/g					
before	53 ± 9.5	40 ± 5.5	70 ± 10.2	750 ± 93	14 ± 7.6
after	102 ± 12.4*	100 ± 12.5*	90 ± 11.5	2,500 ± 237**	12 ± 5.5
Triglycerides mg/dL					
before	135±14.9	155 ± 12.1	128 ± 9.7	126 ± 10.2	122±13.5
after	133± 11.5	150 ± 11.3	110 ± 8.5*	123 ± 10.1	118 ± 11.7
LDL, in mg/dL					
before	144±12.5	143 ± 12.4	121 ± 10.5	137 ± 11.7	131±12.1
after	139 ± 10.1*	134 ± 11.2*	104 ± 9.8*	124 ± 10.3*	129 ± 10.2
HDL, in mg/dL					
before	41.9±2.9	46.5 ± 3.7	49.8 ± 3.9	50.1 ± 4.2	44.0±2.2
after	42.2 ± 3.1	47.8 ± 3.9	50.0 ± 4.6	51.2 ± 4.4	45.1 ± 2.4
IOD, in μM MDA					
before	142 ± 9.2	141 ± 12.7	115 ± 10.9	164 ± 5.8	177 ± 12.1
after	101 ± 8.7**	92 ± 8.8**	46 ± 4.5**	42 ± 3.7*	153 ± 11.9*
LDL-Px, in ELISA $\times 10^3$					
before	310 ± 29	550 ± 61	664 ± 63	420 ± 45	450 ± 41
after	250 ± 24*	350 ± 29**	379 ± 34**	130 ± 12**	370 ± 32*
Lipoprotein O_2, in μM					
before	4.07 ± 0.29	3.89 ± 0.35	3.86 ± 0.32	3.07 ± 0.29	3.67 ± 0.31
after	5.26 ± 0.33*	4.64 ± 0.33*	4.55 ± 0.39*	3.44 ± 0.27	5.27 ± 0.39*
StO_2, in AUC mm					
before	81 ± 6.4	66 ± 5.2	67 ± 5.1	59 ± 4.4	76 ± 5.5
after	88 ± 6.9*	79 ± 6.1*	83 ± 7.1*	79 ± 6.3*	76 ± 6.3

$* p < 0.05$, $** p < 0.001$.

Table 3: Changes in sebum, and corneocyte parameters of the skin after supplementation with GA lycopene for one month.

Parameters before and after 4 weeks of trial	Groups with GA Lycopene supplementation				
	I	II	III	IV	V
Sebum droplet size, in μm					
before	4.6 ± 1.11	3.96 ± 0.17	3.72 ± 0.43	3.89 ± 0.21	4.9 ± 0.53
after	5.1 ± 0.75∗	4.14 ± 0.11∗	4.20 ± 0.88∗	3.94 ± 0.22	4.9 ± 0.57
Corneocyte exfoliation rate§					
before	66 ± 6.8	82 ± 7.8	83 ± 9.3	87 ± 9.5	61 ± 6.2
after	63 ± 6.2	73 ± 12.0∗	76 ± 7.7∗	67 ± 13.5∗	60 ± 6.9
Corneocyte damage§§					
before	4.2 ± 0.98	7.19 ± 2.47	3.40 ± 0.97	3.50 ± 1.16	2.0 ± 1.98
after	2.5 ± 0.43∗	3.80 ± 1.23∗∗	2.41 ± 0.76∗	2.17 ± 0.52∗	1.8 ± 1.23

∗ $p < 0.05$, ∗∗$p < 0.001$.

§as an average number of single corneocytes in stratum cornea, §§as an average number of cross-linked damaged corneocyte clusters in stratum cornea; each parameter was calculated in 40 randomly selected microscopic areas (x 1,000).

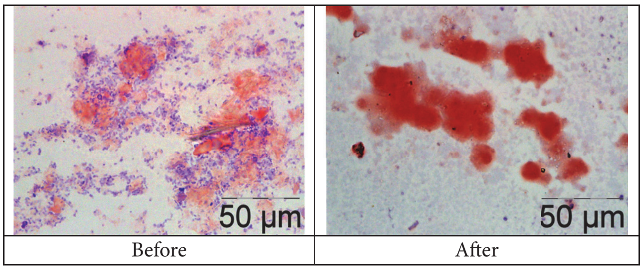

(a) Sebum

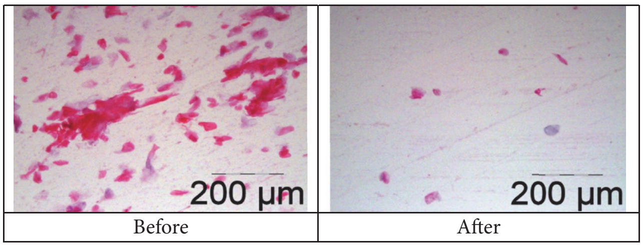

(b) Exfoliated corneocytes

Figure 1: Changes in skin parameters after supplementation with 7 mg of GA lycopene for one month. Typical skin smear samples: lipid droplets of the sebum were stained with Oil Red O, and corneocytes with hematoxylin, eosin at 1,000× magnification.

3.3. Gut Microbiome. After 4 weeks of supplementation with GA lycopene, a shift in the gut microbial communities was detected in the stool of the participants. The relative abundance of OTUs on Phyla level changed to increased relative abundance in Actinobacteria in all intervention groups, Group IV (30mg lycopene liver targeting) 4.5%- 7.12%, Group II (7mg lycopene capsule) 2.52%- 2.85%, and a significant increase was detected for Group III (30 mg lycopene cardiovascular targeting) with 1.12%- 3.22% p=0.04 (FDR corrected)(Figure 2). The separation between the week zero and week 4 of the intervention Group III is also shown in Figure 2; PERMANOVA analysis indicated a separation R= 0.250, p=0.04)

An increased dose of lycopene 30 mg Group III and IV versus Group II, 7 mg, was also reflected in an increased relative abundance of Actinobacteria (+2.6 Group IV, Group III +2.1%, Group II +0.33%). Bacteroidetes decreased in the relative abundance in all groups even though not being statistically significant (Group IV 4.92%-2.72%, Group III 12.4% to 7.2%, Group II 31.3% to 21.1%), p >0.5 (FDR corrected). No significant changes were detected for the remaining GM composition on Phyla level.

Relative abundances on the OTU species level at week 0 and week 4 for the GAL intervention groups (Group II, III, IV) with regard to formulations and dose effect are shown in Table 4.

It is evident that three different OTUs (species level cut-off), namely, OTUs representing Bifidobacterium species increased in relative abundance; these were Bifidobacterium longum, B. adolescentis, and an assigned species.

Whereas several OTUs belonging to the Prevotella genera had decreased in relative abundance over the course of the intervention, the statistically insignificant decrease in Bacteroidetes by GAL formulations seems hence to be genera specific (Table 4).

Looking at Groups I, II, and V the DC and DC-GAL (7 mg) and GAL-MSFA (7 mg) on the Phyla level we have detected a decreased relative abundance of Actinobacteria 4.4-3.4%, though not statistically significant (p>0.9) for the DC intervention; no significant changes were detected in the relative abundance of Bacteroidetes 6.4%-6.3%, Proteobacteria 6.6 -2.4% (p>0.9) for this intervention group after 4 weeks of DC intervention.

Whereas the relative abundance of Actinobacteria increased in the DC-GAL group (I) from 1.9% to 3.3% after 4 weeks of intervention, Bacteroidetes on the other hand increased slightly from 23.4 to 25.8%, Firmicutes decreased 71.7-67.8%, Proteobacteria decreased from 0.49 to 0.24%, p>0.4; these changes were not statistically significant. The relative abundance of bacteria on the species level of the DC intervention and 7 mg GAL-DC versus GAL-MSFA formulations can be seen in Table 5. For the DC intervention we detected a decrease in OTUs belonging to

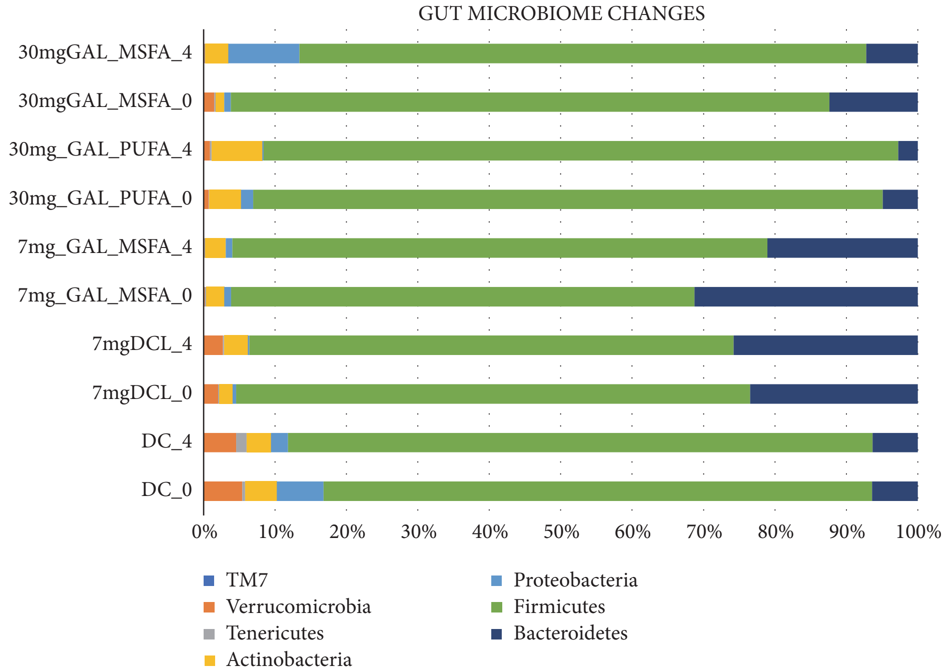

Figure 2: Bacterial relative abundance (Phylum level) of the different intervention groups before and after the 4 weeks of intervention as determined by 16S rRNA gene amplicon sequencing. (Group I) fortified with 7 mg lycopene - 10 g dark chocolate 7 mg DCL, (Group II) 7 mg of lycopene in a capsule 7 mg GAL-MSFA, (Group III) 30 mg of lycopene in cardiovascular GAL-MSFA, (Group IV) 30 mg lycopene liver targeting/liver health GAL-PUFA. (Group V) 10 g of dark chocolate DC.

the Actinobacteria and an increase in Lactobacillus genera, though not statistically significant p>0.1.

There were no significant correlations between the tested parameters and taxa relative abundance (raw OTU level nor summarized to the species level). No relationship between the bacterial relative abundance and host parameters could be found using the redundancy analysis (Figure 3).

4. Discussion

Interconnection between intestine and its flora, liver metabolism and the skin is the subject of intensive investigations [30, 31]. Therefore, in order to correct parameters of one of these organs, it is important to assess possible changes, which may develop in parallel in others. However, this alteration may not be noticeable or be minimal, and ultimately a correction will not be needed, if targeted persons are healthy and analysed parameters are within their healthy norm. Therefore, in our study we have included middle-age subjects with a mild form of obesity with blood markers of subclinical inflammation and oxidative damage.

Development of metabolic syndrome, age associated skeletal muscle loss and frailty are accompanied by ongoing, often at a subclinical level, processes of inflammatory and oxidative damage, which may lead to changes in liver metabolism, vascular functions, increased body mass and development of subclinical systemic tissue hypoxia [32, 33]. In our study we observed that supplementation with lycopene, especially formulated for effective bioavailability, in middle-aged people, had antioxidant, anti-inflammatory, and blood lipid-lowering effects, which are in accordance with earlier reports [34]. These changes in the blood markers were accompanied by or maybe resulting in the improvement of

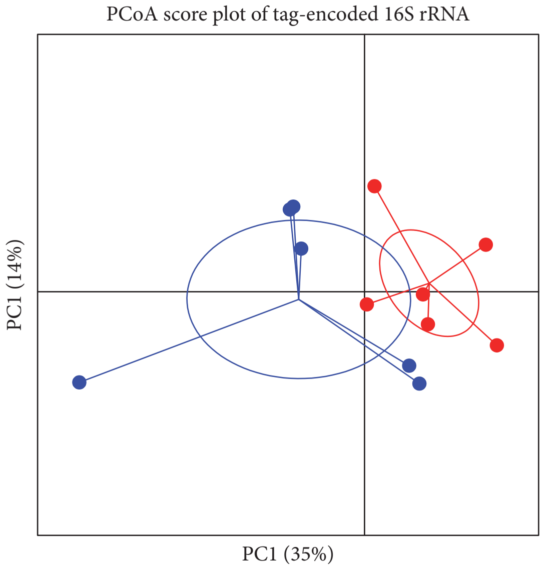

Figure 3: PCoA score plot of tag-encoded 16S rRNA gene amplicon sequencing data based on generalized UniFrac distance metrics ($n = 6$, for each time point) of week 0 (red dots) and week 4 (blue dots) intervention Group III. R = 0.250, p=0.04.

Table 4: Average relative species compositions of gut microbial communities for the intervention groups 7 mg GAL-MSFA, 30 mg GAL-MSFA, 30 GAL-PUFA at different doses at the beginning and at the end of the intervention study.

Phyla	Family	Genera	Species	7 mg II_Day_0	GAL MSFA II_Week_4	30 mg III_Day_0	GAL MSFA III_Week_4	30 mg IV_Day_0	GAL PUFA IV_Week_4
Bacteroidetes	Porphyromonadaceae	*Parabacteroides*	*distasonis*	0,36	0,09	0,04	0,04	0,04	0,05
Bacteroidetes	S24-7			0,73	1,72	0,15	0,48	0,07	0,2
Bacteroidetes	Porphyromonadaceae	*Parabacteroides*		0,33	0,1	0,68	0,09	0,05	0,24
Bacteroidetes	[Paraprevotellaceae]	*Paraprevotella*		0,11	0,05	0,26	0,03	0,01	0
Bacteroidetes	Bacteroidaceae	*Bacteroides*		8,59	2,58	0,91	3,14	0,74	0,95
Bacteroidetes	Bacteroidaceae	*Bacteroides*	*ovatus*	0,08	0,04	0,03	0,02	0,01	0
Bacteroidetes				0,77	1,14	0,31	0	0,08	0,02
Bacteroidetes	Prevotellaceae	*Prevotella*	*copri*	13,52	12,2	8,52	0,38	0,8	0,13
Bacteroidetes	Bacteroidaceae	*Bacteroides*	*caccae*	0,09	0,01	0,02	0,01	0	0
Bacteroidetes	Bacteroidaceae	*Bacteroides*	*Other*	0,15	0,04	0,04	0,1	0,09	0,26
Bacteroidetes	Prevotellaceae	*Prevotella*		0,26	0,19	0,38	0	0,2	0
Bacteroidetes	Prevotellaceae	*Prevotella*	*stercorea*	1,24	0,52	0,15	0	0,11	0,03
Bacteroidetes	Rikenellaceae			2,18	0,57	0,2	1,33	0,34	0,39
Bacteroidetes	Bacteroidaceae	*Bacteroides*	*plebeius*	0,49	0,99	0,15	1,22	2	0,01
Bacteroidetes	[Odoribacteraceae]	*Butyricimonas*		0,08	0,03	0,03	0,04	0,02	0,01
Bacteroidetes	[Paraprevotellaceae]	*[Prevotella]*		1,16	0,5	0,21	0	0,04	0,02
Bacteroidetes	[Barnesiellaceae]			0,71	0,07	0,02	0,1	0,05	0,06
Bacteroidetes	Bacteroidaceae	*Bacteroides*	*uniformis*	0,24	0,03	0,08	0,11	0,03	0,34
Actinobacteria	Bifidobacteriaceae	*Bifidobacterium*	*longum*	0,09	0,11	0,04	0,16	0,11	0,16
Actinobacteria	Bifidobacteriaceae	*Bifidobacterium*		0,15	0,54	0,03	0,5	0,73	2,31
Actinobacteria	Bifidobacteriaceae	*Bifidobacterium*	*adolescentis*	0,33	1,09	0,05	0,24	0,69	2,93
Actinobacteria	Actinomycetaceae	*Actinomyces*		0,02	0,01	0,04	0,35	0,04	0,02
Actinobacteria	Coriobacteriaceae	*Other*	*Other*	0	0	0,02	0,03	0,01	0,01
Actinobacteria	Coriobacteriaceae	*Eggerthella*	*lenta*	0,01	0	0,01	0,02	0,09	0,07
Actinobacteria	Coriobacteriaceae	*Atopobium*		0,01	0,01	0,01	0,09	0,02	0,02
Actinobacteria	Coriobacteriaceae	*Collinsella*	*aerofaciens*	0,96	0,58	0,59	1,2	1,57	0,94
Actinobacteria	Coriobacteriaceae			0,83	0,41	0,21	0,27	0,91	0,52
Actinobacteria	Coriobacteriaceae	*Adlercreutzia*		0,02	0,01	0,06	0,1	0,09	0,07
Actinobacteria	Coriobacteriaceae	*Slackia*		0,09	0,09	0,07	0,1	0,23	0,04
Firmicutes	Veillonellaceae	*Dialister*		0,3	0,82	1,54	0,09	1,2	7,23
Firmicutes	Lachnospiraceae	*Anaerostipes*		0,04	0,02	0,02	0,04	0,03	0,11
Firmicutes	Clostridiaceae	*Caloramator*		0,01	0	0,01	0,04	0,1	0
Firmicutes	Streptococcaceae	*Streptococcus*		0,13	0,21	0,8	8,14	0,19	2,26
Firmicutes	Clostridiaceae			0,95	0,75	0,82	4,8	5,63	0,94
Firmicutes	Lachnospiraceae	*Roseburia*		0,08	0,14	0,04	0,03	0,09	0,05
Firmicutes				6,99	6,64	16,32	10,2	8,45	5,98
Firmicutes	Clostridiaceae	*Other*	*Other*	0,03	0,01	0,03	0,22	0,53	0,04
Firmicutes	Lachnospiraceae	*[Ruminococcus]*	*Other*	0,01	0,01	0,02	0	0	0,01
Firmicutes	Lachnospiraceae	*[Ruminococcus]*	*gnavus*	0,04	0,04	0,05	0,06	0,13	0,06

Table 4: Continued.

Phyla	Family	Genera	Species	7 mg II_Day_0	GAL MSFA II_Week_4	30 mg III_Day_0	GAL MSFA III_Week_4	30 mg IV_Day_0	GAL PUFA IV_Week_4
Firmicutes	Lachnospiraceae	*Blautia*	*Other*	0,86	0,68	1,09	1,02	1,72	2,23
Firmicutes	Lachnospiraceae	*Blautia*		3,08	2,23	3,78	4,24	7,24	9,07
Firmicutes	Lachnospiraceae	*Coprococcus*	*Other*	0,13	0,22	0,36	0,15	0,15	0,15
Firmicutes	Ruminococcaceae	*Faecalibacterium*	*prausnitzii*	1,39	2,42	1,04	1	0,98	1,13
Firmicutes	Veillonellaceae	*Phascolarctobacterium*		0,39	0,17	0,04	0,02	3,69	0,01
Firmicutes	Ruminococcaceae			20,99	30,92	25,11	15,39	20,02	23,35
Firmicutes	Other	*Other*	*Other*	1,31	0,77	1,59	6,12	4,79	1,8
Firmicutes	Streptococcaceae	*Streptococcus*	*anginosus*	0,01	0	0,02	0,08	0	0,11
Firmicutes	Lachnospiraceae	*[Ruminococcus]*		0,2	0,31	0,17	0,19	0,26	0,17
Firmicutes	Erysipelotrichaceae			0,08	0,04	0,02	0,09	0,2	0,05
Firmicutes	Christensenellaceae			0,23	0,28	0,18	0,04	0,93	0,24
Firmicutes	Lachnospiraceae	*Shuttleworthia*		0,12	0,1	0,13	0,15	0,18	0,21
Firmicutes	Clostridiaceae	*Clostridium*		0,32	0,45	0,3	0,42	0,3	0,27
Firmicutes	Lachnospiraceae			7,01	8,06	8,82	7,27	9,5	8,18
Firmicutes	Ruminococcaceae	*Oscillospira*		1,71	1,44	1,69	2,56	1,98	1,66
Firmicutes	Erysipelotrichaceae	*[Eubacterium]*	*biforme*	0,53	0,27	0,38	1,03	0,78	0,09
Firmicutes	Lachnospiraceae	*Lachnospira*		0,25	0,11	0,23	0,04	0,23	0,21
Firmicutes	[Mogibacteriaceae]			0,17	0,11	0,06	0,08	0,29	0,11
Firmicutes	Lachnospiraceae	*Other*	*Other*	4,85	5,88	5,46	4,67	7,47	6,19
Firmicutes	Lachnospiraceae	*Coprococcus*		1,78	2,07	2,2	2,56	3,41	3,43
Firmicutes	Ruminococcaceae	*Ruminococcus*		1,85	2,11	4,7	2,11	1,49	4,73
Firmicutes	Lachnospiraceae	*Dorea*		1,88	2,8	1,77	2,15	2,76	2,13
Firmicutes	Ruminococcaceae	*Other*	*Other*	5,54	3,82	2,47	1,85	0,62	3,46
Firmicutes	Erysipelotrichaceae	*Catenibacterium*		0,63	0,38	2,25	1,18	2,4	2,88
Proteobacteria	Desulfovibrionaceae	*Bilophila*		0,02	0,01	0,01	0,01	0,11	0,02
Proteobacteria	Enterobacteriaceae			0,66	0,74	0,33	9,8	0,95	0,08
Proteobacteria	Alcaligenaceae	*Sutterella*		0,04	0,06	0,01	0	0,01	0
Verrucomicrobia	Verrucomicrobiaceae	*Akkermansia*	*muciniphila*	0,17	0,12	1,49	0,13	0,72	0,91
Tenericutes				0,19	0,12	0,2	0,08	0,01	0,21
TM7				0	0	0,01	0,01	0,02	0,01
Cyanobacteria				0,01	0,01	0,01	0,01	0,03	0,02

Table 5: Average relative species compositions of gut microbial communities for the intervention groups 7 mg DCL, 7 mg GAL-MSFA and DC at the beginning and at the end of the intervention study.

				7 mg_DCL I_Day_0	7 mg_DCL I_Week_4	7 mg_GAL-MSFA II_Day_0	7 mg_GAL-MSFA II_Week_4	DC V_Day_0	DC V_Week_4
Bacteroidetes	Bacteroidaceae	*Bacteroides*	*Other*	1,08	0,21	0,15	0,04	0,12	0,04
Bacteroidetes	Bacteroidaceae	*Bacteroides*	*uniformis*	1,71	0,41	0,24	0,03	0,21	0,07
Bacteroidetes	Bacteroidaceae	*Bacteroides*		7,54	1,84	8,60	2,57	1,64	0,57
Bacteroidetes	Bacteroidaceae	*Bacteroides*	*eggerthii*	1,43	0,17	0,01	0,00	0,30	0,00
Bacteroidetes	Prevotellaceae	*Prevotella*	*copri*	2,05	22,30	13,55	12,19	0,28	2,72
Bacteroidetes	[Odoribacteraceae]	*Butyricimonas*		0,11	0,01	0,08	0,03	0,06	0,01
Bacteroidetes	Porphyromonadaceae	*Parabacteroides*	*distasonis*	0,46	0,07	0,36	0,09	0,13	0,05
Bacteroidetes	Porphyromonadaceae	Parabacteroides		0,48	0,05	0,33	0,10	0,26	0,32
TM7				0,02	0,00	0,01	0,00	0,00	0,01
Bacteroidetes	S24-7			0,00	0,00	0,72	1,71	1,55	1,56
Bacteroidetes	[Paraprevotellaceae]	*Paraprevotella*		0,58	0,05	0,11	0,05	0,04	0,00
Bacteroidetes	Bacteroidaceae	*Bacteroides*	*ovatus*	0,08	0,03	0,08	0,04	0,09	0,00
Bacteroidetes	Bacteroidaceae	*Bacteroides*	*caccae*	0,09	0,01	0,09	0,01	0,04	0,01
Bacteroidetes	[Barnesiellaceae]			0,22	0,06	0,70	0,07	0,03	0,01
Bacteroidetes	Prevotellaceae	*Prevotella*	*stercorea*	0,02	0,00	1,25	0,52	0,09	0,13
Bacteroidetes	Prevotellaceae	*Prevotella*		0,42	0,00	0,27	0,19	0,08	0,64
Bacteroidetes	Rikenellaceae			1,12	0,58	2,18	0,57	0,38	0,08
Actinobacteria	Coriobacteriaceae	*Collinsella*	*aerofaciens*	0,47	0,70	0,95	0,57	0,24	0,57
Actinobacteria	Coriobacteriaceae	*Slackia*		0,02	0,06	0,09	0,09	0,07	0,15
Actinobacteria	Bifidobacteriaceae	*Bifidobacterium*	*adolescentis*	0,06	0,62	0,33	1,09	1,13	0,58
Actinobacteria	Bifidobacteriaceae	*Bifidobacterium*	*longum*	0,37	0,83	0,09	0,11	0,23	0,08
Actinobacteria	Bifidobacteriaceae	*Bifidobacterium*		0,66	0,42	0,16	0,54	1,29	0,41
Actinobacteria	Coriobacteriaceae			0,20	0,52	0,83	0,41	1,36	1,50
Actinobacteria	Coriobacteriaceae	*Adlercreutzia*		0,03	0,03	0,02	0,01	0,03	0,05
Actinobacteria	Coriobacteriaceae	*Atopobium*		0,01	0,01	0,01	0,01	0,01	0,02
Actinobacteria	Actinomycetaceae	*Actinomyces*		0,03	0,04	0,02	0,01	0,02	0,04
Firmicutes	Ruminococcaceae	*Ruminococcus*		1,52	1,01	1,86	2,11	1,45	1,92
Firmicutes	Clostridiaceae	*Clostridium*		0,50	0,29	0,32	0,45	0,61	0,75
Firmicutes	Lachnospiraceae	*Shuttleworthia*		0,10	0,12	0,12	0,10	0,07	0,09
Firmicutes				7,10	7,06	6,98	6,65	5,43	5,16
Firmicutes	Lachnospiraceae	*Coprococcus*		2,19	2,06	1,78	2,06	1,66	1,76
Firmicutes	Ruminococcaceae	*Other*		0,83	1,10	5,54	3,82	0,87	0,54
Firmicutes	Clostridiaceae			1,88	0,99	0,95	0,75	0,58	0,94
Firmicutes	Lachnospiraceae	*Blautia*		1,22	1,61	0,87	0,68	1,37	1,49
Firmicutes	Christensenellaceae			0,51	0,52	0,23	0,27	0,36	1,61
Firmicutes	Other	*Other*		1,55	1,29	1,31	0,78	1,06	1,22
Firmicutes	Erysipelotrichaceae	*Catenibacterium*		0,10	0,79	0,63	0,38	0,83	1,11

Table 5: Continued.

				7 mg_DCL I_Day_0	7 mg_DCL I_Week_4	7 mg_GAL-MSFA II_Day_0	7 mg_GAL-MSFA II_Week_4	DC V_Day_0	DC V_Week_4
Firmicutes	Lachnospiraceae	*Roseburia*		0,10	0,05	0,08	0,14	0,20	0,25
Firmicutes	Ruminococcaceae	*Ruminococcus*	*flavefaciens*	0,22	0,10	0,07	0,03	0,00	0,02
Firmicutes	Lachnospiraceae	*Blautia*		3,78	5,86	3,08	2,24	4,21	4,65
Firmicutes	Veillonellaceae	*Dialister*		1,08	1,00	0,30	0,82	3,64	1,25
Firmicutes	Ruminococcaceae	*Faecalibacterium*	*prausnitzii*	2,21	3,35	1,39	2,43	2,00	2,34
Firmicutes	Ruminococcaceae	*Oscillospira*		1,22	1,24	1,71	1,44	2,63	1,02
Firmicutes	Erysipelotrichaceae			0,06	0,06	0,08	0,04	0,06	0,02
Firmicutes	Streptococcaceae	*Streptococcus*		0,36	0,59	0,13	0,21	0,26	3,29
Firmicutes	Lactobacillaceae	*Lactobacillus*		0,02	0,01	0,00	0,02	0,02	0,14
Firmicutes	Ruminococcaceae			20,67	19,42	20,96	30,93	33,04	26,33
Firmicutes	Lachnospiraceae	*[Ruminococcus]*	*Other*	0,01	0,01	0,01	0,01	0,01	0,02
Firmicutes	[Mogibacteriaceae]			0,04	0,05	0,18	0,11	0,09	0,11
Firmicutes	Lachnospiraceae	*[Ruminococcus]*	*gnavus*	0,06	0,04	0,04	0,04	0,05	0,07
Firmicutes	Erysipelotrichaceae	*Bulleidia*	*p-1630-c5*	0,01	0,00	0,59	0,09	0,08	0,07
Firmicutes	Lachnospiraceae	*Anaerostipes*		0,04	0,04	0,04	0,02	0,05	0,09
Firmicutes	Lachnospiraceae	*Dorea*		3,64	2,31	1,87	2,81	1,61	3,00
Firmicutes	Veillonellaceae	*Veillonella*	*dispar*	0,04	0,05	0,01	0,03	0,16	0,27
Firmicutes	Veillonellaceae	*Phascolarctobacterium*		0,22	0,12	0,39	0,17	0,08	0,01
Firmicutes	Lachnospiraceae	*[Ruminococcus]*		0,27	0,17	0,20	0,30	0,24	0,41
Firmicutes	Clostridiaceae	*Other*	*Other*	0,06	0,03	0,03	0,01	0,01	0,01
Firmicutes	Lachnospiraceae	*Coprococcus*	*Other*	0,53	0,37	0,13	0,22	0,21	0,25
Firmicutes	Lachnospiraceae	*Lachnospira*		0,73	0,36	0,25	0,11	0,44	0,84
Firmicutes	Lachnospiraceae	*Other*	*Other*	7,50	5,93	4,84	5,90	6,08	10,35
Firmicutes	Erysipelotrichaceae	*[Eubacterium]*	*biforme*	0,14	0,13	0,53	0,27	0,09	0,32
Firmicutes	Lachnospiraceae			11,09	9,48	7,01	8,05	6,73	9,18
Proteobacteria	Enterobacteriaceae			0,35	0,08	0,67	0,74	2,51	0,65
Proteobacteria	Alcaligenaceae	*Sutterella*		0,07	0,04	0,04	0,06	0,03	0,19
Proteobacteria	Desulfovibrionaceae	*Bilophila*		0,01	0,01	0,02	0,01	0,02	0,01
Tenericutes				0,14	0,16	0,18	0,12	0,40	1,44
Verrucomicrobia	Verrucomicrobiaceae	*Akkermansia*	*muciniphila*	2,02	2,68	0,17	0,12	5,41	4,58

the peripheral tissue StO_2. The main contributor into this parameter is the skeletal muscle respiration, although skin oxygenation is part of it too.

It was observed that supplementation with lycopene can increase its level in the skin tissue, which results in improving its protection from UV damage [9]. However, the fact that lycopene can be secreted to the surface of the human body either with the cerumen, which we are reporting here, or sebum (results not shown), to the best of our knowledge, has not been reported earlier.

Sebum is not only essential for skin lubrication, which prevents it from dehydration, but is also an important part of its immune system and its antibacterial acid mantle.

The sebum is also supplying antioxidants and perhaps other beneficial molecules to the surface of the skin [35]. It has been reported that with ageing the quality of the sebum is impaired, and in particular its viscosity, is increased, which is accompanied by accelerated corneocyte desquamation [19]. In our study we observed that supplementation of the diet with lycopene of middle-aged persons resulted in the restoration of the sebum viscosity, reduction of the corneocyte damage, and desquamation.

Continuous ingestion of DC had also a significant positive effect on liver associated markers of IOD and LDL-Px and also on the concentration of lipoprotein transported O_2. However, these positive changes were not translated in improvement of skeletal muscle respiration and analysed skin parameters.

The absence of any direct correlations between relative abundance of gut taxa and analysed parameters of the blood, skeletal muscle and skin indicates a complex intertwined relationship between gut microbiome environment and the host metabolic pathways.

Prebiotics are traditionally considered to be non-digestable food ingredients, which can reach the intestine and be selectively utilized by host microorganisms conferring a health benefit [36, 37].

There are a number of molecules within food, which are not fully digestible; hence, they can reach the colon and its microbiota. Carotenoids and lycopene in particular belong to these types of partially digestible molecules [38, 39].

In our study we observed that regular intake for one month middle-aged mildly obese persons of lycopene, either in the GA formulations or in L-Tug chocolate resulted in significant changes in the profile of the gut microbiota.

GAL formulations led to a dose-dependent increase of members of the Phyla Actinobacteria, mainly driven by an increase in the relative abundance of *Bifidobacterium* spp. such as *B. longum* and *B. adolescentis*, indicating a prebiotic potential of these formulations. Further, in the DC intervention we observed an increase in a *Lactobacillus* related OTUs indicating a selective prebiotic potential of DC.

Bifidobacteria are one of the best studied genera of beneficial bacteria and often marketed as probiotics, presumably conferring a broad range of health benefits not only in the gut environment but in the whole body. This involves their ability to control bacterial and viral pathogens, stimulate local intestinal and systemic immune system, and improve lipid metabolism and weight management [40, 41]. The loss or reduction of the bifidobacterial gut associated population could be a significant factor associated with ageing-associated frailty development [42].

There is emerging evidence that dysbiosis of the gut microbiome and alteration of the associated bacterial gene pool and metabolic pathways may contribute to the development of pathogenesis of obesity [43–45] although it is still under debate whether the relative abundance of *Bacteroides* within the microbiome has been associated with obesity [46, 47].

In our study we observed that continuous intervention with GAL, DC, and DCL resulted in significant decrease in the abundance of Bacteroidetes. This could be explained either by direct action of this carotenoid, or its indirect activity via stimulation of some species of *Bifidobacteria*, or a combination of both factors.

It was interesting that observed lycopene effects on the gut bacteria, blood markers of inflammation and oxidation, lipids produced by the liver and by the skin (sebum) and peripheral tissue oxygenation were all dose-dependent.

This indicates that the observed complex of positive systemic changes could not only be a result of direct action of lycopene but also a conseqence of its indirect activity via stimulation of production of signaling metabolites *Bifidobacteria adolescentis* population with the blood, liver, skeletal; muscles and skin, which lycopene can control.

Continuous ingestion of the DC resulted in an increase in the abundance of *Lactobacillus* spp., which also constitutes a genus where several strains have been investigated and also marketed as probiotics. Increased relative abundance was also accompanied by reduction of liver associated blood markers of oxidative damage and inflammation. However, these positive changes did not positively affect skin parameters in this study group.

These results raised a number of unanswered questions, one of them being whether the observed systemic effects are specific to the lycopene molecule or other carotenoids would have similar properties.

The other question, to which we do not have an answer, is whether lycopene or dark chocolate molecules directly affected growth of the *Bifidobacteria adolescentis, B. longum,* and *Lactobacillus* or if it was their indirect effect via systemic changes. The improvement of metabolism and physiology of the gut tissues may lead to its better control of the microbiota and boost the growth of bacteria with proposed health benefits.

Whatever the nature of the prebiotic effect of lycopene, this, to the best of our knowledge, is the first report that ingestion of a carotenoid may have this new property. It is also for the first time our study demonstrated that dark chocolate has a similar effect albeit selective for a different putatively beneficial bacteria.

To conclude, the observed systemic effect of lycopene supplementation, or dark chocolate ingestion, which includes improvement of gut, blood, liver lipid metabolism and, for the former, skeletal muscles and skin parameters could be not just due to the carotenoid and dark chocolate properties themselves, but are likely also to modulate the gut microbiome increasing the relative abundance of putatively beneficial bifidobacteria and lactobacilli.

Data Availability

The supporting results will be displayed on the publicly available website Lycotec.com. Moreover, the data that support the findings of this study are available from the corresponding author, Dr. Ivan M Petyaev, upon reasonable request.

Conflicts of Interest

The authors declare no conflicts of interest involved.

Authors' Contributions

Maria Wiese, Yuriy Bashmakov and Ivan Petyaev designed research; Natalia Chalyk, and Tatyana Bandaletova conducted clinical work; Dennis Sandris Nielsen, Łukasz Krych, and Witold Kot performed microbiota analysis; Dmitry Pristensky, Marina Chernyshova, and Natalia Chalyk conducted analytic and morphological assays; Maria Wiese and Ivan Petyaev analysed results and wrote the paper; Ivan Petyaev, Maria Wiese, and Yuriy Bashmakov had primary responsibility for final content of the manuscript. All authors read and approved the final manuscript.

Acknowledgments

We thank Kristina Kaasik for help with gDNA extraction from stool samples and PCR.

References

[1] A. F. M. Kardinaal, P. van't Veer, F. Kok et al., "Antioxidants in adipose tissue and risk of myocardial infarction: the EURAMIC study," *The Lancet*, vol. 342, no. 8884, pp. 1379–1384, 1993.

[2] N. J. Barber and J. Barber, "Lycopene and prostate cancer," *Prostate Cancer and Prostatic Diseases*, vol. 5, no. 1, pp. 6–12, 2002.

[3] M. J. Kim and H. Kim, "Anticancer effect of lycopene in gastric carcinogenesis," *Journal of Cancer Prevention*, vol. 20, no. 2, pp. 92–96, 2015.

[4] Z.-Y. Zou, X.-R. Xu, X.-M. Lin et al., "Effects of lutein and lycopene on carotid intima–media thickness in Chinese subjects with subclinical atherosclerosis: a randomised, double-blind, placebo-controlled trial," *British Journal of Nutrition*, vol. 111, no. 3, pp. 474–480, 2014.

[5] N. A. Zigangirova, E. Y. Morgunova, E. D. Fedina et al., "Lycopene inhibits propagation of chlamydia infection," *Scientifica*, vol. 2017, Article ID 1478625, 11 pages, 2017.

[6] S. Schwarz, U. C. Obermüller-Jevic, E. Hellmis, W. Koch, G. Jacobi, and H.-K. Biesalski, "Lycopene inhibits disease progression in patients with benign prostate hyperplasia," *Journal of Nutrition*, vol. 138, no. 1, pp. 49–53, 2008.

[7] I. Paur, W. Lilleby, S. K. Bøhn et al., "Tomato-based randomized controlled trial in prostate cancer patients: Effect on PSA," *Clinical Nutrition*, vol. 36, no. 3, pp. 672–679, 2017.

[8] W. Stahl, U. Heinrich, O. Aust, H. Tronnier, and H. Sies, "Lycopene-rich products and dietary photoprotection," *Photochemical & Photobiological Sciences*, vol. 5, no. 2, pp. 238–242, 2006.

[9] S. Grether-Beck, A. Marini, T. Jaenicke, W. Stahl, and J. Krutmann, "Molecular evidence that oral supplementation with lycopene or lutein protects human skin against ultraviolet radiation: results from a double-blinded, placebo-controlled, crossover study," *British Journal of Dermatology*, vol. 176, no. 5, pp. 1231–1240, 2017.

[10] V. Ganji and M. R. Kafai, "Population determinants of serum lycopene concentrations in the United States: Data from the Third National Health and Nutrition Examination Survey, 1988-1994," *Journal of Nutrition*, vol. 135, no. 3, pp. 567–572, 2005.

[11] L. Müller, C. Caris-Veyrat, G. Lowe, and V. Böhm, "Lycopene and its antioxidant role in the prevention of cardiovascular diseases—a critical review," *Critical Reviews in Food Science and Nutrition*, vol. 56, no. 11, pp. 1868–1879, 2016.

[12] X. Tzounis, A. Rodriguez-Mateos, J. Vulevic, G. R. Gibson, C. Kwik-Uribe, and J. P. E. Spencer, "Prebiotic evaluation of cocoa-derived flavanols in healthy humans by using a randomized, controlled, double-blind, crossover intervention study," *American Journal of Clinical Nutrition*, vol. 93, no. 1, pp. 62–72, 2011.

[13] I. M. Petyaev and Y. K. Bashmakov, "Cocobiota: implications for human health," *Journal of Nutrition and Metabolism*, vol. 2016, Article ID 7906927, 3 pages, 2016.

[14] J. Mursu, S. Voutilainen, T. Nurmi et al., "Dark chocolate consumption increases HDL cholesterol concentration and chocolate fatty acids may inhibit lipid peroxidation in healthy humans," *Free Radical Biology & Medicine*, vol. 37, no. 9, pp. 1351–1359, 2004.

[15] O. A. Tokede, J. M. Gaziano, and L. Djoussé, "Effects of cocoa products/dark chocolate on serum lipids: A meta-analysis," *European Journal of Clinical Nutrition*, vol. 65, no. 8, pp. 879–886, 2011.

[16] I. M. Petyaev, P. Y. Dovgalevsky, N. E. Chalyk, V. A. Klochkov, and N. H. Kyle, "Lycopene embedded into cocoa butter micelles of dark chocolate causes dose dependent decrease in serum lipids of hypercholesterolemic volunteers," *British Journal of Medicine Medical Research*, vol. 13, no. 11, pp. 1–11, 2016.

[17] I. M. Petyaev, P. Y. Dovgalevsky, V. A. Klochkov et al., "Effect of lycopene supplementation on cardiovascular parameters and markers of inflammation and oxidation in patients with coronary vascular disease," *Food Science & Nutrition*, vol. 6, no. 6, pp. 1770–1777, 2018.

[18] H. Gómez, J. Mesquida, P. Simon et al., "Characterization of tissue oxygen saturation and the vascular occlusion test: influence of measurement sites, probe sizes and deflation thresholds," *Circulation*, vol. 13, 13 Suppl, pp. 1–7, 2009.

[19] N. E. Chalyk, T. Y. Bandaletova, N. H. Kyle, and I. M. Petyaev, "Age-related differences in morphological characteristics of residual skin surface components collected from the surface of facial skin of healthy male volunteers," *Skin Research and Technology*, vol. 23, no. 2, pp. 212–220, 2017.

[20] L. Øvreås, L. Forney, F. L. Daae, and V. Torsvik, "Distribution of bacterioplankton in meromictic lake Saelenvannet, as determined by denaturing gradient gel electrophoresis of PCR-amplified gene fragments coding for 16S rRNA," *Applied and Environmental Microbiology*, vol. 63, no. 9, pp. 3367–3373, 1997.

[21] Ł. Krych, W. Kot, K. M. B. Bendtsen, A. K. Hansen, F. K. Vogensen, and D. S. Nielsen, "Have you tried spermine? A rapid and cost-effective method to eliminate dextran sodium sulfate inhibition of PCR and RT-PCR," *Journal of Microbiological Methods*, vol. 144, pp. 1–7, 2018.

[22] R. C. Edgar, "UPARSE: highly accurate OTU sequences from microbial amplicon reads," *Nature Methods*, vol. 10, no. 10, pp. 996–998, 2013.

[23] D. McDonald, M. N. Price, J. Goodrich et al., "An improved Greengenes taxonomy with explicit ranks for ecological and evolutionary analyses of bacteria and archaea," *The ISME Journal*, vol. 6, no. 3, pp. 610–618, 2012.

[24] J. G. Caporaso, J. Kuczynski, J. Stombaugh et al., "QIIME allows analysis of high-throughput community sequencing data," *Nature Methods*, vol. 7, no. 5, pp. 335-336, 2010.

[25] A. J. Oksanen, F. G. Blanchet, R. Kindt et al., "vegan: Community Ecology Package. R Package," 2015.

[26] V. Diwadkar-Navsariwala, J. A. Novotny, D. M. Gustin et al., "A physiological pharmacokinetic model describing the disposition of lycopene in healthy men," *Journal of Lipid Research*, vol. 44, no. 10, pp. 1927–1939, 2003.

[27] K. Yagi, "Lipid peroxide and human disease," *Chemistry and Physics of Lipids*, vol. 45, no. 2, pp. 337–351, 1978.

[28] I. Petyaev, M. M. J. Mitchinson, J. V. Hunt, and P. J. Coussons, "Superoxide dismutase activity of antibodies purified from the human arteries andatherosclerotic lesions," *Biochemical Society Transactions*, vol. 26, no. 1, pp. S43–S45, 1998.

[29] I. M. Petyaev, A. Vuylsteke, D. W. Bethune, and J. V. Hunt, "Plasma oxygen during cardiopulmonary bypass: A comparison of blood oxygen levels with oxygen present in plasma lipid," *Clinical Science*, vol. 94, no. 1, pp. 35–41, 1998.

[30] C. A. O'Neill, G. Monteleone, J. T. McLaughlin, and R. Paus, "The gut-skin axis in health and disease: A paradigm with therapeutic implications," *BioEssays*, vol. 38, no. 11, pp. 1167–1176, 2016.

[31] Q. Feng, W. Chen, and Y. Wang, "Gut microbiota: an integral moderator in health and disease," *Frontiers in Microbiology*, vol. 9, article no. 151, 2018.

[32] L. Marseglia, S. Manti, G. D'Angelo et al., "Oxidative stress in obesity: a critical component in human diseases," *International Journal of Molecular Sciences*, vol. 16, no. 1, pp. 378–400, 2014.

[33] F. Costes, C. Denis, F. Roche, F. Prieur, F. Enjolras, and J.-C. Barthélémy, "Age-associated alteration of muscle oxygenation measured by near infrared spectroscopy during exercise," *Archives of Physiology and Biochemistry*, vol. 107, no. 2, pp. 159–167, 1999.

[34] I. M. Petyaev, P. Y. Dovgalevsky, V. A. Klochkov, N. E. Chalyk, and N. Kyle, "Clinical study: whey protein lycosome formulation improves vascular functions and plasma lipids with reduction of markers of inflammation and oxidative stress in prehypertension," *The Scientific World Journal*, vol. 2012, Article ID 269476, 7 pages, 2012.

[35] S. Passi, O. De Pità, P. Puddu, and G. P. Littarru, "Lipophilic antioxidants in human sebum and aging," *Free Radical Research*, vol. 36, no. 4, pp. 471–477, 2002.

[36] G. Macfarlane and J. Cummings, "Probiotics and prebiotics: Can regulating the activities of intestinal bacteria benefit health?" *BMJ*, vol. 318, no. 7189, pp. 999–1003, 1999.

[37] G. R. Gibson, R. Hutkins, M. E. Sanders et al., "Expert consensus document: the international scientific association for probiotics and prebiotics (ISAPP) consensus statement on the definition and scope of prebiotics," *Nature Reviews Gastroenterology & Hepatology*, vol. 14, no. 8, pp. 491–502, 2017.

[38] K. Schnäbele, K. Briviba, A. Bub, S. Roser, B. L. Pool-Zobel, and G. Rechkemmer, "Effects of carrot and tomato juice consumption on faecal markers relevant to colon carcinogenesis in humans," *British Journal of Nutrition*, vol. 99, no. 3, pp. 606–613, 2008.

[39] D. Głąbska, D. Guzek, P. Zakrzewska, D. Włodarek, and G. Lech, "Lycopene, lutein and zeaxanthin may reduce faecal blood, mucus and pus but not abdominal pain in individuals with ulcerative colitis," *Nutrients*, vol. 8, no. 10, Article ID E613, 2016.

[40] A. L. Servin, "Antagonistic activities of lactobacilli and bifidobacteria against microbial pathogens," *FEMS Microbiology Reviews*, vol. 28, no. 4, pp. 405–440, 2004.

[41] A. O'Callaghan and D. van Sinderen, "Bifidobacteria and their role as members of the human gut microbiota," *Frontiers in Microbiology*, vol. 7, 2016.

[42] S. Arboleya, C. Watkins, C. Stanton, and R. P. Ross, "Gut Bifidobacteria Populations in Human Health and Aging," *Frontiers in Microbiology*, vol. 19, article no. 1204, no. 7, 2016.

[43] F. Bäckhed, H. Ding, T. Wang et al., "The gut microbiota as an environmental factor that regulates fat storage," *Proceedings of the National Acadamy of Sciences of the United States of America*, vol. 101, no. 44, pp. 15718–15723, 2004.

[44] P. J. Turnbaugh, R. E. Ley, M. A. Mahowald, V. Magrini, E. R. Mardis, and J. I. Gordon, "An obesity-associated gut microbiome with increased capacity for energy harvest," *Nature*, vol. 444, no. 7122, pp. 1027–1031, 2006.

[45] P. J. Turnbaugh, M. Hamady, T. Yatsunenko et al., "A core gut microbiome in obese and lean twins," *Nature*, vol. 457, no. 7228, pp. 480–484, 2009.

[46] R. Liu, J. Hong, X. Xu et al., "Gut microbiome and serum metabolome alterations in obesity and after weight-loss intervention," *Nature Medicine*, vol. 23, no. 7, pp. 859–868, 2017.

[47] Y. Qin, J. D. Roberts, S. A. Grimm et al., "An obesity-associated gut microbiome reprograms the intestinal epigenome and leads to altered colonic gene expression," *Genome Biology*, vol. 19, article no. 7, no. 1, 2018.

Hindawi
BioMed Research International
Volume 2019, Article ID 5063565, 6 pages
https://doi.org/10.1155/2019/5063565

Research Article

Systemic Level of Oxidative Stress during Orthodontic Treatment with Fixed Appliances

Vito Kovac,[1] Borut Poljsak,[1] Giuseppe Perinetti,[2] and Jasmina Primozic[3]

[1] *Faculty of Health Sciences, University of Ljubljana, Slovenia*
[2] *Private Practice, Nocciano (PE), Italy*
[3] *Medical Faculty, University of Ljubljana, Slovenia*

Correspondence should be addressed to Jasmina Primozic; jasminaprimozic@gmail.com

Received 1 March 2019; Revised 8 April 2019; Accepted 24 April 2019; Published 23 May 2019

Guest Editor: Filipa S. Reis

Copyright © 2019 Vito Kovac et al. This is an open access article distributed under the Creative Commons Attribution License, which permits unrestricted use, distribution, and reproduction in any medium, provided the original work is properly cited.

The aim of the study was to assess the level of selected systemic oxidative stress parameters during the first week of orthodontic treatment with fixed appliances. Fifty-four males with malocclusion and having a similar lifestyle were randomized using a computer based procedure and allocated to either the treatment group (TG; n=27;24.6 ± 1.7 years) or control group (CG; n=27;24.7 ± 1.7 years). Capillary blood was collected at baseline and 6 hours, 24 hours, and 7 days after archwire insertion. At the same time points, capillary blood was retrieved in the CG. In order to determine the oxidative stress, both the reactive oxygen species (ROS) formation and the antioxidative defense (AD) potential were measured using the ROS testing and oxygen free radicals defense (equivalent to antioxidant defense) testing, respectively, by a blinded operator. The ratio between ROS and AD (ROS/AD) was calculated and data were analyzed using nonparametric tests. No drop-outs or harms were detected. At baseline, neither ROS (1.54 [1.22; 2.12] and 1.74 [1.40; 2.01] for the TG and CG, respectively), AD (1.19 [0.66; 1.50] and 1.19 [0.57; 1.42] for the TG and CG, respectively), nor ROS/AD levels were significantly different (p>0.05). After 24 hours, the ROS level significantly increased in the TG (2.05 [1.71; 2.26]) and was higher compared to the CG ROS level (1.67 [1.29; 1.95]; p=0.025), while for the AD level, no marked between and within group differences were detected. A notable change of ROS/AD ratio was observed over time only within the TG (p=0.026). Moreover, a significantly higher ROS/AD ratio was detected 24 hours after archwire insertion in the TG compared to the CG (2.69 [1.44; 3.89] and 1.79 [1.45; 2.35], respectively), followed by a decrease. Orthodontic treatment with fixed appliances might induce systemic oxidative stress in the short-term, since ROS levels and ROS/AD levels are normalized within 7 days after archwire insertion.

1. Introduction

The oral cavity is subjected to various external factors, including dental materials that have substantial oxidizing potential and have the ability to generate reactive oxygen species (ROS) [1]. Increased reactive oxygen species (ROS) cause oxidative stress, which is defined as the imbalance between ROS and antioxidant defense (AD) in favor of the former. During orthodontic treatment with fixed appliances, the subjects are exposed to heavy metals released from corroded appliances, which might increase the levels of ROS through metal-catalyzed free radical reactions (Fenton and Fenton-like reactions). Many metal ions such as chromium undergo redox cycling, thus directly producing ROS [2]:

$$\left(\mathrm{Mn}^{+}\right) + \mathrm{H_2O_2} \longrightarrow \left(\mathrm{M}^{n+1}\right) + \mathrm{OH}^{-} + \mathrm{OH}^{\bullet} \qquad (1)$$

Moreover, during orthodontic treatment various inflammatory mediators (i.e., cytokines) causing aseptic inflammation in the periodontal ligament are being released after mechanical force application to the teeth inducing a cascade of reactions in the periodontal tissue, which leads to tissue remodeling and tooth movement. Since there is sound evidence indicating that periodontal inflammation is one of the main sources of ROS in the mouth [3], it is plausible that also aseptic inflammation might be associated with oxidative stress induced damage.

Several in vitro studies showed that both orthodontic brackets [4] and archwires [2] induce oxidative stress, associated with heavy metals release. In vivo studies that aimed to assess either salivary biomarkers [5, 6] of oxidative stress or biomarkers in the gingival crevicular fluid [7], reported different results. On the one hand Olteanu et al. [6] and Buczko et al. [5] reported that orthodontic treatment modifies the oxidative-antioxidative balance in the patients' saliva. In particular, Olteanu et al. [6] demonstrated that markers of oxidative stress (ceruloplasmin and malondialdehyde) increased to their highest levels 24 hours after orthodontic appliance insertion and decreased back to their initial levels 7 days after insertion. Similarly, Buczko et al. [5] evidenced a marked increase in salivary oxidative stress biomarkers one week after orthodontic appliance insertion and a decrease to normal values at the 24-week follow-up. On the other hand Atung Ozcan et al. [7] concluded that the levels of examined oxidative stress biomarkers did not change after one and six months of orthodontic treatment.

The varying results might be due to the different methodologies used and due to the different materials of orthodontic appliances to which the subjects were exposed. Moreover, the use of single biomarkers for estimating the oxidative stress is limiting, since oxidative stress is a result of an imbalance between ROS and AD in favor of the former [8, 9]. Therefore, the ratio between ROS and AD appears to be a more accurate indicator of oxidative stress [10]. To establish the complex relationship between ROS and AD direct and indirect methods can be used [11]. Direct methods relate to ROS measurements of superoxide, H2O2, $OH^{\bullet}$. These species are very reactive and their quantitation can be assessed only with electron paramagnetic resonance. Therefore, indirect methods are usually used, which include measurement of the balance between ROS and AD and measurements of each antioxidant separately (i.e., catalase, superoxide dismutase, vitamin C, reduced glutathione, vitamin E, etc.). The main limitation of the latter is that it does not assess the synergistic effect between different antioxidants [11].

Apart from the above-mentioned in vitro and in vivo studies of oxidative stress biomarkers changes in the local environment due to exposure to orthodontic fixed appliances, there is still paucity of data regarding oxidative stress induction at the systemic level during orthodontic treatment. Therefore, the aim of the present study was to assess the systemic level of oxidative stress during orthodontic treatment with fixed appliances, determined from capillary blood samples. The hypothesis tested was that selected oxidative stress parameters in capillary blood do change during the first week of orthodontic treatment with fixed appliances.

2. Material and Methods

2.1. Subjects and Study Design. Ethical approval for this study was gained (No. 0120-523/2018/8) from the National Medical Ethics Committee and informed consent was obtained from all subjects before inclusion. The study protocol was designed and performed following the Declaration of Helsinki for medical research involving human subjects. The data used to support the findings of this study are available from the corresponding author upon request.

A group of 54 male subjects aged between 19.7 and 28.2 years who were seeking orthodontic treatment at the Department of Orthodontics of the University Medical Centre of Ljubljana, Slovenia, due to mild crowding and teeth malalignment were recruited based on a preliminary questionnaire regarding their lifestyle habits. Subjects with oral pathology (including periodontal disease), poor oral hygiene, and known allergies as well as smoking subjects or subjects undergoing any pharmaceutical therapy, including food additives with antioxidant properties intake, were excluded. Females were not included due to possible false results as a consequence of hormonal fluctuation. Randomization was performed according to a computer based procedure having groups of equal numerosity. Twenty-seven subjects were allocated to the treatment group (TG, aged 24.6 ± 1.7 years), while the control group (CG, aged 24.7 ± 1.7 years) consisted of 27 age-matched subjects. No subject left the study.

During the study, the subjects of both groups were asked to follow a similar diet regimen (3 portions [400 g] of fruit and vegetable/day, avoidance of antioxidant supplements, and no alcohol intake) and to perform very similar activities (avoidance of extreme sport activities and sun exposure; avoidance of nocturnal life).

The fixed orthodontic appliance used in the TG was composed by stainless steel brackets (Gemini brackets, 3M Unitek; USA) attached to the upper and lower teeth and two Nickel-Titanium archwires (3M Unitek; USA) inserted in the bracket's slots.

For the evaluation of oxidative stress the balance between ROS and AD was assessed from capillary blood. The FORT (free oxygen radicals testing) and FORD (free oxygen radicals defense) assays were performed as previously described [12], using a dedicated spectrophotometer Free Oxygen Radical Monitor (FORM®, CR 3000, Callegari, Parma, Italy). Blood samples of 50 μl for FORD and 20 μl for FORT were collected in a sterile regimen from the tip of the subject's finger into a heparinized tube, mixed with provided reagents, centrifuged, and analyzed in the spectrophotometer by measuring light absorption at a wavelength of 505 nm. FORT and FORD values were measured immediately after blood collection. The FORT test results are given as FORT units (0,26 mg/l H2O2), while the results of the FORD test are expressed as mmol/l of Trolox (6-hydroxy-2,5,7,8-tetramethylchroman-2-carboxylic acid; a water-soluble analog of vitamin E). Principles of the determination of oxidative stress in human blood using FORD and FORT tests were previously described [13–15]. FORT and FORD analyses were performed by a blinded operator.

Capillary blood was collected before the insertion of the fixed orthodontic appliance and at 6 hours, 24 hours, and 7 days' time point. At the same time points, blood was collected and analyzed also from the matched controls. To exclude any possible influence of periodontal inflammation on the measurements of oxidative stress parameters, two weeks before the beginning of the study, all the participants were instructed regarding oral hygiene activities. At baseline, the periodontal status was assessed by measuring probing depth at six sites around every erupted tooth of each subject. Furthermore, the bleeding on probing index was used at each time point to determine the presence of inflammation.

2.2. Sample Size Calculation. Sample size of at least 26 subjects for each group was needed to detect an effect size coefficient of 0.8 (which is regarded as “large effect” [16]) for the measured parameters in any comparison between the groups, with an alpha set at 0.05 and a power of 0.80.

2.3. Statistical Analysis. The Statistical Package for Social Sciences Software release 20.0 (SPSS Inc., Chicago, Illinois, USA) was used for data analysis. The balancing of experimental groups by age was tested with a Mann-Whitney U-test. After testing the normality of the data with the Shapiro-Wilk test and Q-Q normality plots and the equality of variance among the datasets using a Levene test, nonparametric methods were used for data analysis.

A Friedman test was used to assess the significance of the differences in every parameter (FORT, FORD, and FORT/FORD ratio) over the time points within each group. When significant interactions were seen, a Bonferroni-corrected Wilcoxon test was used for pairwise comparisons. A Mann-Whitney U-test was used to assess the significance of the differences in every parameter between the two groups within each time point.

The results were considered to be significant at p-values below 0.05.

The intra-assay and inter-assay coefficients of variation were reported to be 3.7% and 6.2%, respectively, for the FORT and 4.2% and 6.6%, respectively, for the FORD [12].

3. Results

The results of the FORT and FORD assays for the TG and CG group at different time points are reported in Table 1. At baseline, no significant differences were detected between the TG and CG, neither for FORT (p>0.05) nor FORD (p>0.05) levels.

The FORT level in the TG increased to significantly higher values than those in the CG (p=0.025) at the 24 hours' time point, and decreased to normal values similar to those seen in the CG at the 7 days' time point. Although a decrease of the FORD level was detected in the TG at the 24 hours' time point, this was not statistically significantly different from the CG.

A significant change of the FORT level over time was seen within the TG (p=0.026), while no notable changes were detected for the FORD level (p>0.05). In the CG, neither FORT nor FORD levels changed markedly over time (P>0.05).

The FORT/FORD ratio, expressing the balance between ROS and AD is represented in Figure 1. At baseline and 6 hours, no significant differences regarding the FORT/FORD ratio were observed between the TG and CG (p=0.897 and p=0.528, respectively). At 24 hours, the FORT/FORD ratio increased significantly in the TG as compared to the CG (p=0.044). Finally, at the 7 days' time point, no significant differences regarding the FORT/FORD ratio were measured between the two groups (p=0.299). None of the subjects had signs of periodontal disease/inflammation over the observational period.

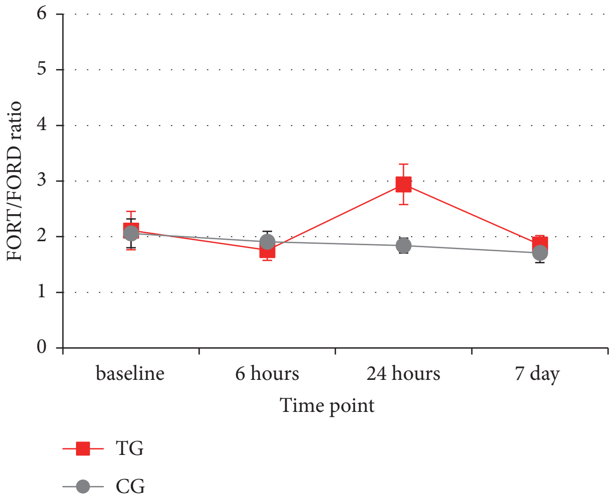

Figure 1: Mean values and standard errors of the longitudinal changes of the FORT/FORD ratio in the treated (TG) and control (CG) groups.

4. Discussion

It has been postulated, that orthodontic treatment with fixed appliances might play an important role in inducing oxidative stress and related damage [1]. Until recently, only local environment levels of ROS and/or antioxidant defense were assessed during orthodontic treatment, by examining either saliva [5–7, 17] or the gingival crevicular fluid [7]. To our best knowledge, the present study is the first attempt to determine the oxidative stress induced at the systemic level by orthodontic treatment. Both, the ROS formation as well as the AD potential were measured in blood/serum, and the ratio between them was calculated [12] in subjects undergoing orthodontic treatment and in a control group.

The results evidenced a marked short-term systemic increase of ROS as well as an increase in the ratio between ROS and AD, among subjects undergoing orthodontic treatment. In accordance with the study of Olteanu et al. [6] that revealed maximum levels of salivary oxidative stress biomarkers 24 hours after the start of orthodontic treatment, the present study also denoted a significant increase of the systemic (blood/serum) ROS/AD ratio 24 hours after the start of treatment. Similarly to the previous report [6], after 7 days of treatment, a decrease of the ROS/AD ratio to normal values as those measured in the CG was observed also in the present study. A recent study by Buczko et al. [5] evidenced significant changes of the total oxidative status index (ratio between the total oxidative status and total antioxidative status) in unstimulated and stimulated saliva during orthodontic treatment. The authors [5] revealed an increase of the total oxidative status in saliva at 1 week and a significant decrease of it at 24 weeks follow-up, which is in contrast with the results of the present study, as the systemic ROS/AD ratio normalized after 7 days.

It could be hypothesized that oxidative stress during orthodontic treatment might be induced by different factors: local and systemic exposure to heavy metals, inflammation of

Table 1: The FORT and FORD levels among the treated and control groups over the observational period.

Parameter	Group	Baseline	6 hours	24 hours	7 days	Diff.
FORT	TG	1.54 (1.22;2.12)	1.78 (1.22;2.15)	2.05 (1.71;2.26), *a*	1.64 (1.22;2.08), *b*	0.026; *S*
	CG	1.74 (1.40;2.01)	1.71 (1.22;2.01)	1.67 (1.29;1.95)	1.64 (1.29;1.92)	0.100; *NS*
	Diff.	0.602; *NS*	0.376; *NS*	0.025; *S*	0.910; *NS*	
FORD	TG	1.19 (0.66;1.50)	1.23 (0.89;1.45)	1.04 (0.51;1.45)	0.96 (0.66;1.49)	0.331; *NS*
	CG	1.19 (0.57;1.42)	1.07 (0.66;1.44)	0.91 (0.66;1.41)	1.20 (0.72;1.57)	0.887; *NS*
	Diff.	0.775; *NS*	0.276; *NS*	0.431; *NS*	0.307; *NS*	

Data is presented as median (25th; 75th percentile). *TG*, treated group, n=27; *CG*, control group, n=27. *Diff.*, p-values; significance of the difference between the groups within each time point or over time within either group. Results of the pairwise comparisons between time points: *a*, significantly different from the baseline; *b*, significantly different from 24 hours. *NS*, not statistically significant; *S*, statistically significant.

the periodontal tissues due to poor oral hygiene, and aseptic inflammation in the periodontal ligament due to mechanical force application.

In vitro studies [2, 4] have shown that metal ions such as nickel, cobalt, and chromium, released either from corroded orthodontic brackets and archwires, induce oxidative stress. Despite the smaller corrosion susceptibility of titanium alloys, due to the protective titanium oxide layer, mechanical friction in the contact between bracket and archwire during orthodontic treatment leads to the disruption of the protective titanium oxide layer [18, 19], causing corrosion and release of titanium ions, which might increase ROS production [1]. Likewise, the in vivo study by Buczko et al. [5] explained the increase of ROS/AD ratio in saliva after one week as an effect of heavy metal exposure during orthodontic treatment, since the highest concentration of nickel ions was measured simultaneously.

Also in the present study, patients could have been exposed to nickel, cobalt, chromium, and titanium released from the parts of the orthodontic appliance used, all of which might have induced the systemic elevation of the ROS/AD ratio after 24 hours of orthodontic treatment. However, at the 7 days' time point, contrasting the results of salivary oxidative stress biomarkers [5], the ROS/AD ratio normalized, most probably due to adaptive stress responses and induction of antioxidative endogenous defense. This is in accordance with two other in vivo studies [7, 17] that reported no marked changes of the salivary [7, 17] and gingival crevicular fluid [7] oxidative stress biomarkers after 4-5 weeks and six months of orthodontic treatment. Of note, the contrasting results could also be due to the great variability in the timing of nickel ions increase in saliva, which ranges from 10 minutes to four weeks after orthodontic appliance insertion [20, 21].

A second cause of the significant systemic elevation of ROS and ROS/AD ratio could be the periodontal inflammation induced by increased plaque apposition due to the orthodontic appliance. Although periodontal inflammation has been associated with ROS formation [3], Portelli et al. [17] reported no notable correlation between oxidative stress biomarkers and oral hygiene in patients undergoing orthodontic treatment. Similarly, periodontal inflammation as a cause of oxidative stress could be excluded in the present study, as all the subjects had excellent oral hygiene without any signs of periodontal inflammation at each time point.

A final explanation for the increase in ROS and ROS/AD ratio detected in the present study 24 hours after the start of orthodontic treatment could be a result of the expression of proinflammatory mediators in the periodontal ligament induced by mechanical force application on the tooth. In fact, the mechanism of orthodontic tooth movement with fixed appliances is characterized by a cascade of events, triggered by the strain of the periodontal ligament fibers, leading to an inflammatory process that allows appropriate tissue remodeling. It has been shown that this inflammation might occur only at a subclinical (i.e., molecular level) and might be limited to the alveolar bone, with no systemic consequences in terms of elevation of C-Reactive Protein [22]. However, this does not exclude, that the short-term elevation of systemic ROS and ROS/AD ratio seen in the present study is a consequence of the aseptic inflammation in the periodontal ligament due to force application induced by the orthodontic appliance.

Limitations of the Study. It is generally accepted that two or more assays should be utilized to assess oxidative stress status, whenever possible to enhance validity, since each technique measures something different and has its own inherent limitations and no method by itself can be said to be a completely accurate measure of antioxidant status and ROS formation [11]. In the present study ROS and different antioxidants present in the blood as well as their interactions were assessed with FORT and FORD. Although changes in the ROS/AD ratio were observed over time, their main cause(s) could not be determined. In fact, the observed ROS/AD ratio changes can be related to many factors (i.e., endogenous antioxidants activation, inflammation, and blood metal ions), the assessment of which was beyond the scope of the present study. On the other hand, the possible influence of periodontal inflammation on the measured systemic oxidative stress parameters could be excluded, since no signs of inflammation were detected in any of the subjects over the observed period of time, the influence of sterile periodontal inflammation due to force application and blood metal ions content could not be excluded as the cause of increased ROS observed in the TG. In fact, due to ethical reasons it was not feasible to retrieve consecutive larger venous blood samples four times over a period of one week for assessing any possible changes of inflammation mediators as well as heavy metals in venous blood. Moreover, previous studies [23] reported that heavy metal ions (i.e., nickel) are detectable in blood only after long-term exposure.

Given that the results presented here are descriptive and future research is needed for a better understanding of which factors (presence of heavy metals and/or inflammation) have a direct causative impact on increased parameters of ROS and ROS/AD ratio observed in the blood of the treated group. Nevertheless, due to the short-term elevation of oxidative stress parameters during the first week of orthodontic treatment, increased intake of natural antioxidants would be recommended. However, a study on the efficacy of antioxidant treatment during orthodontic therapy should be performed to determine the rational and dosage of their use. In fact, an excess use of antioxidants might also induce harmful health effects [24, 25].

5. Conclusions

Orthodontic treatment with fixed appliances might induce systemic oxidative stress, but only in the short-term. In particular, the elevation of ROS and ROS/AD levels is seen only 24 hours after the start of orthodontic treatment, while normalization of the levels occurs within 7 days after archwire insertion most probably due to adaptive endogenous antioxidative response. However, intermittent changes of the ROS and AD levels during orthodontic treatment (i.e., at each archwire reactivation) could not be excluded. Future studies should be performed to confirm the activation of endogenous antioxidant defense (superoxide dismutase, catalase, and glutathione peroxidase activity) as well as the main cause of increased oxidative stress (heavy metal release and/or inflammation) during orthodontic treatment with fixed appliances.

Data Availability

The data used to support the findings of this study are available from the corresponding author upon request.

Conflicts of Interest

The authors declare no conflicts of interest.

Acknowledgments

The study was funded by the Slovenian Research Agency and Croatian Science Foundation (P3-0388; J3-8199/2014-09-7500).

References

[1] P. Żukowski, M. Maciejczyk, and D. Waszkiel, "Sources of free radicals and oxidative stress in the oral cavity," *Archives of Oral Biolog*, vol. 92, pp. 8–17, 2018.

[2] S. Spalj, M. Mlacovic Zrinski, V. Tudor Spalj, and Z. Ivankovic Buljan, "In-vitro assessment of oxidative stress generated by orthodontic archwires," *American Journal of Orthodontics and Dentofacial Orthopedics*, vol. 141, no. 5, pp. 583–589, 2012.

[3] L. Tóthová and P. Celec, "Oxidative stress and antioxidants in the diagnosis and therapy of periodontitis," *Frontiers in Physiology*, vol. 8, article 1055, 2017.

[4] Z. I. Buljan, S. P. Ribaric, M. Abram, A. Ivankovic, and S. Spalj, "In vitro oxidative stress induced by conventional and self-ligating brackets," *The Angle Orthodontist*, vol. 82, no. 2, pp. 340–345, 2012.

[5] P. Buczko, M. Knaś, M. Grycz, I. Szarmach, and A. Zalewska, "Orthodontic treatment modifies the oxidant–antioxidant balance in saliva of clinically healthy subjects," *Advances in Medical Sciences*, vol. 62, no. 1, pp. 129–135, 2017.

[6] C. Olteanu, A. Muresan, D. Daicovicin et al., "Variations of some saliva markers of the oxidative stress in patients with orthodontic appliances," *Physiology*, vol. 19, pp. 26–29, 2009.

[7] S. S. Atug Ozcan, I. Ceylan, E. Ozcan, N. Kurt, I. M. Dagsuyu, and C. F. Canakci, "Evaluation of oxidative stress biomarkers in patients with fixed orthodontic appliances," *Dis Markers*, vol. 2014, Article ID 597892, p. 10, 2014.

[8] L. Deguillaume, M. Leriche, and N. Chaumerliac, "Impact of radical versus non-radical pathway in the Fenton chemistry on the iron redox cycle in clouds," *Chemosphere*, vol. 60, no. 5, pp. 718–724, 2005.

[9] P. A. Riley, "Free radicals in biology: oxidative stress and the effects of ionizing radiation," *International Journal of Radiation Biology*, vol. 65, no. 1, pp. 27–33, 1994.

[10] J. Wang, H. M. Schipper, A. M. Velly, S. Mohit, and M. Gornitsky, "Salivary biomarkers of oxidative stress: a critical review," *Free Radical Biology & Medicine*, vol. 85, pp. 95–104, 2015.

[11] B. Poljsak and P. Jamnik, "Methodology for oxidative state detection in biological systems," in *Handbook of Free Radicals : Formation, Types and Effects*, D. Kozyrev and V. Slutsky, Eds., pp. 421–448, Nova Science Publishers, New York, NY, USA, 2010.

[12] M. G. Pavlatou, M. Papastamataki, F. Apostolakou, I. Papassotiriou, and N. Tentolouris, "FORT and FORD: two simple and rapid assays in the evaluation of oxidative stress in patients with type 2 diabetes mellitus," *Metabolism*, vol. 58, no. 11, pp. 1657–1662, 2009.

[13] B. Palmieri and V. Sblendorio, "Oxidative stress tests: overview on reliability and use. Part II," *European Review for Medical and Pharmacological Sciences*, vol. 11, pp. 383–399, 2007.

[14] B. Palmieri and V. Sblendorio, "Current status of measuring oxidative stress," *Methods in Molecular Biology*, vol. 594, pp. 3–17, 2010.

[15] J. Ogrin Papić and B. Poljšak, "Antioxidant potential of selected supplements in vitro and the problem of its extrapolation for in vivo," *Journal of Health Sciences*, vol. 2, no. 1, pp. 5–12, 2012.

[16] J. Cohen, "A power primer," *Psychological Bulletin*, vol. 112, no. 1, pp. 155–159, 1992.

[17] M. Portelli, A. Militi, G. Cervino et al., "Oxidative stress evaluation in patients treated with orthodontic self-ligating multibracket appliances: an in vivo case-control study," *The Open Dentistry Journal*, vol. 11, no. 1, pp. 257–265, 2017.

[18] M. Abedini, H. M. Ghasemi, and M. Nili Ahmadabadi, "Tribological behavior of NiTi alloy in martensitic and austenitic states," *Materials and Corrosion*, vol. 30, no. 10, pp. 4493–4497, 2009.

[19] P. Močnik, T. Kosec, J. Kovač, and M. Bizjak, "The effect of pH, fluoride and tribocorrosion on the surface properties of dental archwires," *Materials Science and Engineering C: Materials for Biological Applications*, vol. 78, pp. 682–689, 2017.

[20] R. M. De Souza and L. M. De Menezes, "Nickel, chromium and iron levels in the saliva of patients with simulated fixed orthodontic appliances," *The Angle Orthodontist*, vol. 78, no. 2, pp. 345–350, 2008.

[21] M. Natarajan, S. Padmanabhan, A. Chitharanjan, and M. Narasimhan, "Evaluation of the genotoxic effects of fixed appliances on oral mucosal cells and the relationship to nickel and chromium concentrations: an in-vivo study," *American Journal of Orthodontics and Dentofacial Orthopedics*, vol. 140, no. 3, pp. 383–388, 2011.

[22] J. K. MacLaine, A. B. Rabie, and R. Wong, "Does orthodontic tooth movement cause an elevation in systemic inflammatory markers?" *European Journal of Orthodontics*, vol. 32, no. 4, pp. 435–440, 2010.

[23] M. Mikulewicz and K. Chojnacka, "Trace Metal release from orthodontic appliances by in vivo studies: A systematic literature review," *Biological Trace Element Research*, vol. 137, no. 2, pp. 127–138, 2010.

[24] B. Poljsak and I. Milisav, "The neglected significance of "antioxidative stress"," *Oxidative Medicine and Cellular Longevity*, vol. 2012, Article ID 480895, 12 pages, 2012.

[25] B. Poljsak, D. Šuput, and I. Milisav, "Achieving the balance between ros and antioxidants: when to use the synthetic antioxidants," *Oxidative Medicine and Cellular Longevity*, vol. 2013, Article ID 956792, 11 pages, 2013.

Hindawi
BioMed Research International
Volume 2019, Article ID 4158415, 8 pages
https://doi.org/10.1155/2019/4158415

Research Article

Copper (II) Ions Activate Ligand-Independent Receptor Tyrosine Kinase (RTK) Signaling Pathway

Fang He,[1] Cong Chang,[1] Bowen Liu,[1] Zhu Li,[2] Hao Li,[3] Na Cai ,[2] and Hong-Hui Wang [1]

[1] *Institute of Nanotechnology and Tissue Engineering, College of Biology, Hunan University, Changsha, 410082, China*
[2] *CellWay Bio, Changsha, 410000, China*
[3] *State Key Laboratory of Chemo/Bio-Sensing and Chemometrics, College of Chemistry and Chemical Engineering, Hunan University, Changsha, 410082, China*

Correspondence should be addressed to Na Cai; cainaya@hotmail.com and Hong-Hui Wang; wanghonghui@hnu.edu.cn

Received 28 February 2019; Revised 15 April 2019; Accepted 28 April 2019; Published 14 May 2019

Guest Editor: Hengjia Ni

Copyright © 2019 Fang He et al. This is an open access article distributed under the Creative Commons Attribution License, which permits unrestricted use, distribution, and reproduction in any medium, provided the original work is properly cited.

Receptor tyrosine kinase (RTK) is activated by its natural ligand, mediating multiple essential biological processes. Copper (II) ions are bioactive ions and are crucial in the regulation of cell signaling pathway. However, the crosstalk between copper (II) ions and RTK-mediated cellular signaling remains unclear. Herein, we reported the effect of copper (II) ions on the ligand-independent RTK cellular signaling pathway. Our results indicate that both EGFR and MET signaling were activated by copper (II) in the absence of the corresponding ligands, EGF and HGF, respectively. Consequently, copper (II) ions initiate two RTK-mediated downstream signal transductions, including AKT and ERK. Moreover, copper (II) significantly increased proliferation and cellular migration. Our study proposes a novel role of copper in RTK-mediated signaling for growth factor-independent cancer cell proliferation and migration, implying that targeting both the copper (II) and growth factor in tumor microenvironments may be necessary for cancer treatment.

1. Introduction

Receptor tyrosine kinase (RTK) is the most abundant type of enzyme-linked receptor, and it is both a receptor and an enzyme that can bind to the ligand and phosphorylate tyrosine residues of target proteins. RTK is a class of single transmembrane receptors with endogenous protein tyrosine kinase activity in cell receptors [1]. So far, more than 50 RTKs have been identified, including hepatocyte growth factor receptor (MET), epidermal growth factor receptor (EGFR), vascular endothelial growth factor receptor (VEGFR), platelet-derived growth factor receptor (PDGFR), and fibroblast growth factor receptor (FGFR) [2, 3]. All members of RTK have similar protein structures: extracellular ligand binding domain, single transmembrane helical domain, near-membrane regulatory domain, a tyrosine kinase domain, and carboxyl-terminal region. Most ligands that specifically activate RTK are soluble secretory proteins, called growth factors. When the growth factor binds to the extracellular domain of RTKs, the receptor is induced to dimer by ligand, and the protein conformation changes to enhance the kinase activity of RTK [4]. The RTK signaling pathway is strictly regulated by various positive feedback loops [5]. The RTK signaling pathway regulates cell proliferation, and differentiation promotes cell survival and regulates and corrects cell metabolism [6]. At present, the RTK signaling pathway has become the primary target in tumor therapy such as breast cancer, prostate cancer, glioblastoma, pancreatic cancer, and lung cancer [7]. EGFR (epidermal growth factor receptor) is a receptor for cell proliferation and signal transduction in epithelial growth factor (EGF). EGFR dimerization activates its intracellular kinase pathway and directs downstream phosphorylation, including the MAPK, AKT, and JNK pathways, to induce cell proliferation [8, 9]. MET (hepatocyte growth factor receptor, HGFR) plays a vital role in cell morphology, proliferation, differentiation, migration, and survival. The signal transduction pathway, which is of great significance, is shown to be active in many tumors. MET-HGF/SF is a potential therapeutic target [10]. AKT (a.k.a. protein kinase B, PKB) is a protein serine/threonine kinase activated by inositol phosphate recruitment to the plasma membrane, which plays a significant role in cell survival and apoptosis [11]. ERK (extracellular regulated protein kinases) refers to extracellular regulated protein kinases, including ERK1 and ERK2, which are the key to transmitting signals from surface receptors to the nucleus. ERK is engaged in many biological reactions such as apoptosis, cell carcinogenesis, cell proliferation and differentiation, cell morphology maintenance, and cytoskeleton construction [12].

Copper is a necessary metal in biology and is widely found in prokaryotes, fungi, mammals, plants, and humans [13]. The vital role of copper in a series of critical physiological processes is increasingly demonstrated in various research fields including wound healing, angiogenesis, protection of reactive oxygen species, synthesis of neurotransmitters, regulation of normal cells, and tumor growth [14]. For example, increased copper content in tumor microenvironments is directly related to the progression of many malignant tumors. It has been reported that CD 147 autocorrelation induced by copper targeting is a new tumor therapy strategy [15]. Copper has been involved in the regulation of the immune response and plays an essential role in regulating gene expression and the maturation of fine hypertrophic cells [16]. Copper has excellent antibacterial properties, and it is not easy for bacterial resistance to develop in response to it. Copper ions can slow down inflammation and have high potential applications in the pharmaceutical, health, food industry, agricultural, and other sectors [17]. The role that copper ions play in inflammatory reactions, oxidation pressures, and microbial environments should not be underestimated. Wound healing is related to hemostasis, inflammation, proliferation, scabbing, and so on [18, 19]. Copper is also known to promote angiogenesis and the development of new blood vessels that are essential to feeding rapidly growing and dividing cells, including rampantly dividing cancer cells. Indeed, copper stimulates the formation of vascular and mature factors such as vascular endothelial growth factor (VEGF) [20]. On the other hand, copper exists in either a reduced (Cu^+) state or an oxidized copper (II) ($Cu2^+$) state in structure and catalysis [21]. Although copper is involved in many aspects of cell signal transduction and cellular functions, the mechanisms of this activity remain less well understood.

Herein, we hypothesized that copper (II) ions promote cell proliferation via an RTK-mediated signaling pathway. Therefore, we investigated the effect of copper (II) on the RTK-mediated cellular signaling pathway. The current study aimed at finding out the influences of copper (II) ions on RTK-mediated cellular signaling pathway and cellular responses including proliferation and wound healing, providing useful data for further study on the mechanism of copper (II) ions' actions in cell behaviors.

2. Materials and Methods

All experiments in this study were performed in the Institute of Nanotechnology and Tissue Engineering, College of Biology, Hunan University.

2.1. Reagents and Instruments

2.1.1. Reagents. Copper dichloride ($CuCl_2$) was purchased from Sangon Biotech (Shang Hai, China). 3-(4,5-Dimethyl-2-thiazolyl)-2,5-diphenyl-2-H-tetrazolium bromide (CCK-8) was purchased from Sigma-Aldrich (China). The primary antibody for phospho-EGFR (Y1068, #4064) and phospho-AKT (S473, #4007) was obtained from Bioworld Technology. The primary antibody for phospho-MET (Y1234/Y1235, #3077), total-MET (#8198), and phospho-ERK (T202/Y204, #3510) was obtained from Cell Signaling Technology. The secondary antibody (goat anti-rabbit IgG(H&L)-HRP, goat anti-mouse IgG(H&L)-HRP) was obtained from Invitrogen. The α-tubulin primary antibody was purchased from Cellway Biological Co., Ltd. Recombinant Human Hepatocyte Growth Factor (hHGF) and Recombinant Human Epidermal growth factor (hEGF) were obtained from Peprotech. Forenitib, a MET inhibitor, was purchased from Selleck. The nitrocellulose membrane was obtained from Merck Millipore (Germany). RPMI1640, DMEM medium was purchased from neuronbc (Beijing, China); fetal bovine serum (FBS) was purchased from Biological Industries USA. Penicillin-Streptomycin (100X), 0.25% Trypsin-EDTA (1X), and ECL substrate solution were purchased from NCM Biotech (Suzhou, China).

2.1.2. Instruments. Electrophoresis apparatus was purchased from Beijing Liuyi Co., Ltd. The transmembrane instrument was purchased from Biotool. Western blot images were acquired on a chemiluminescence imaging system (Micro-Chemi4.2). Microporous plate detector was purchased from PerkinElmer, Inc. The inverted fluorescence microscope with no eyepiece was purchased from AMG Co., Ltd. (EVOS f1, America).

2.2. Cell Culture. All cells were cultured in 5% CO_2 in an incubator (Thermo Fisher) at 37°C. A549 cells and DU145 cells were cultured in RPMI1640 with 10% fetal bovine serum and 1% penicillin and streptomycin.

2.3. Preparation of Cell Lysates. Cells were seeded in 35 mm dishes. When the cells reached 80% confluence, they were starved for 24 h in 1640 supplemented with 0.2 % FBS. After the starvation, the medium was changed and incubated with different concentration of copper ion for 12 min in the incubator. Then the dishes were put on the ice to stop the stimulation and washed twice by precooling PBS and then lysed with lysis buffer (RIPA buffer with 1% phosphatase inhibitors and protease inhibitor). The cell lysates were centrifuged at 14000 rcf for 10 min; then retain the supernatant, saved in the -20°C before use.

2.4. Western Blot Assay. The cell lysates were separated by 8% SDS-PAGE electrophoresis and then transferred to nitrocellulose membrane by semidry electrophoretic transfer unit for 10 min. After blocking with 5 % BSA-PBST (1×PBS with 0.1% Tween-20) solution for 1 h, the membrane reacted with primary antibody (1:1000 dilution) overnight in 4°C and secondary antibody (1:5000 dilution) for 1 h in room temperature. Before imaging, the membranes were reacted with ECL substrate solution (NCM Biotech Co., Ltd). Chemiluminescent images were obtained using Bio-Imaging Systems (MicroChemi4.2), and the density of bands was quantified using Image Studio Lite software (Ver 3.1, Li-Cor).

2.5. Cell Viability Assay. The A549 and DU145 (5.0×10^2 cells) were seeded at 96-well plate for 24 h. Then, the medium was removed, and the cells were pretreated with copper (II) ions at various concentrations of 0 μM, 5 μM, 10 μM, 20 μM, 50 μM, and 100 μM. Next, the cells were incubated under 5% CO_2 in a humidified incubator at 37°C. After 2 days, cell viability was evaluated using CCK-8 according to the manufacturer's instruction. CCK8 solution (10 μl) was added to each well, and the mixtures were incubated for 2 h at 37°C. Absorbance was then measured using a plate detector at 450 nm.

2.6. Wound Scratch Assay. Firstly, A549 cells were seeded in a 12-well plate at a density that they should reach ~70-80% confluence as a monolayer after 24h of growth. Do not change the medium, and wounds were then scratched in each cell monolayer using a sterile 1 ml pipette tip. After scratching, gently wash the well twice with medium to remove the detached cells. Then, cells were further cultured with 50 μM copper (II) in the 1640 medium with 0.2 % FBS. The cell motility was measured at 24 h by an inverted microscope. The rate of wound healing was related to the ability of cell migration and cell proliferation.

2.7. Statistical Analysis. Statistical analyses were performed using GraphPad Prism 5 software (GraphPad Software, Inc., San Diego, CA). All data are presented as means ± SD, and Student's non-paired t-test was used for statistical analyses. An overall variation among the different groups was analyzed by One-way ANOVA statistical analyses. The asterisk marks significant differences ($*P<0.05$, $**P<0.001$).

3. Results

3.1. Copper (II) Promotes Ligand-Independent Activation of RTK. RTK-mediated cellular signal pathway plays an essential role in the human body [1]. In order to explore the effect of copper (II) on RTK-mediated cellular signal pathway, we selected human lung cancer cell A549 and human prostate cancer cell DU145. We firstly investigated the effects of copper (II) on RTK phosphorylation and growth factors (HGF or EGF). The results showed that copper (II) significantly promoted the phosphorylation of EGFR in DU145 cells (Figures 1(a) and 1(b)). Similarly, copper (II) induced the phosphorylation of MET in A549 cells (Figures 1(c) and 1(d)). Both results demonstrated that RTK was able to be activated by copper (II) ions. To investigate whether the kinase activity plays a role in copper (II)-induced RTK activation, foretinib, a potent inhibitor for MET, was utilized, and the result showed that the pretreatment of foretinib significantly inhibited the copper (II)-induced phosphorylation of MET in A549 cells (Figures 1(e) and 1(f)). In conclusion, these data indicated that copper (II)-promoted RTK activation is dependent on RTK-dimerization and autophosphorylation (Figure 2(a)). Both the phosphorylation of EGFR and that of MET were upregulated when the concentration of copper (II) was increased to 100 μM (Figures 2(b) and 2(c)). Interestingly, the phosphorylation of EGFR was significantly enhanced in the presence of 100 μM copper (II), suggesting the RTK is dose-dependently activated by the treatment of copper (II). We further characterized the time course of the copper (II)-promoted RTK signal pathway to determine the optimal time for copper (II) to stimulate the RTK-mediated cellular signal pathway. Based on the time-dependent activation of MET by copper (II), the best stimulation time for copper (II) is 10 min (Figures 3(a) and 3(b)).

3.2. Copper (II) Triggers RTK-Mediated Downstream Signal Pathways. We evaluated the RTK-mediated downstream signaling pathways including Ras/mitogen-activated protein kinase (Ras/MAPK) and phosphoinositide 3-kinase/protein kinase B (PI3K/AKT). The A549 cells were cultured in the different concentrations of copper (II) for 10 min and to explore their effect on AKT and ERK phosphorylation. The phosphorylation of both ERK and AKT was remarkably upregulated with the increase of copper (II) concentration (Figures 2(d) and 2(e)). We further characterized the time course of copper (II)-activated RTK signaling. The A549 cells were cultured in 100 μM of copper (II) for 0, 10, 20, and 30 min, respectively, and the phosphorylation level of AKT and ERK1/2 in DU145 cell lysates was measured by western blotting analysis. The data demonstrated that the phosphorylation level of ERK1/2 at T202/Y204 residues was significantly increased in the presence of copper (II) compared with that in the control cells (Figure 3(a)). On the other hand, PI3K phosphorylates and activates AKT, contributing to migratory cell behavior [11]. We observed robust time-dependent activation of AKT by copper (II) (Figure 3(c)). In summary, both EGFR and MET signaling were activated upon copper (II) ion stimulation. When the concentration of copper (II) ion increased to 50 μM, the elevated phosphorylation of MET, AKT, and ERK signals was observed as the copper (II) concentration increased, suggesting that the RTK-mediated downstream signaling pathways were promoted by copper (II) in a time-dependent manner.

3.3. Copper (II) Promotes Cell Migration and Proliferation. To study the impacts of copper (II) ion on cell viability, A549 and DU145 cells were exposed to copper (II) at different concentrations for analysis. The A549 cells were exposed to 0 μM, 5 μM, 10 μM, 20 μM, 50 μM, and 100 μM copper (II) for 48 h resulting in 100.0 ± 0.3%, 122.1 ± 6.2%, 125.1 ± 0.6%, 124.7 ± 0.8%, 125.0 ± 0.4%, and 82.3 ± 6.0% survival rates, respectively (Figure 4(a)). The survival rates of DU145 cells treated with the different concentrations of copper ion were 99.98 ± 0.9%, 100.3 ± 2.4%, 97.3 ± 0.5%, 92.4 ± 0.9%, 94.7 ± 3.0%, and 104.3 ± 0.0%, respectively (Figure 4(b)). There was no remarkable change in the cell viability after exposure with up to 50 μM copper (II). Next, we used the

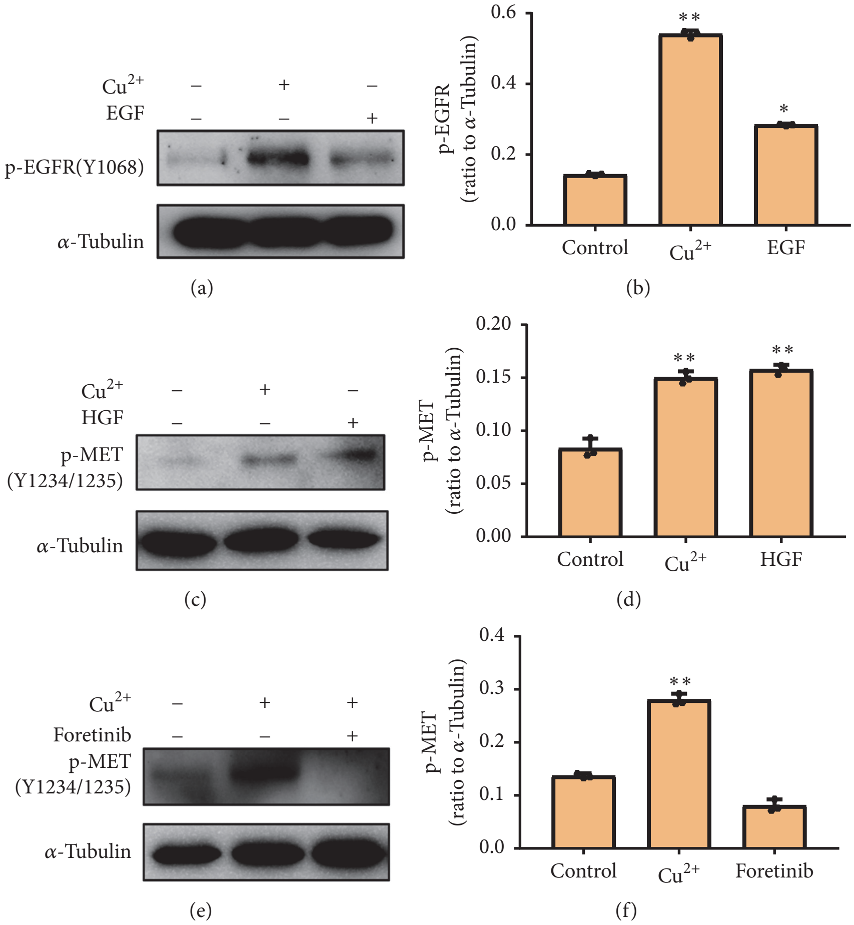

Figure 1: *Copper (II) promotes RTK activation analogous to the ligand-activated pathway*. (a) DU145 cells serum-starved for 24 hours were stimulated with 50 μM copper (II) ion and 99 ng/ml EGF for 10 min, respectively. Copper (II) ion and growth factor on EGFR activation were evaluated by western blotting. (b) The phosphorylation level of EGFR in each experiment was quantified and analyzed. Data are represented as means ± S.D. of triplicate experiments ($*$P<0.05, $**$P<0.001). (c) A549 cells were serum-starved for 24 hours and stimulated with 50 μM copper (II) ion and 50 ng/ml HGF for 10 min, respectively. (d) The phosphorylation level of MET in each experiment was quantified and analyzed. Data are represented as mean ± S.D. of triplicate experiments ($*$P<0.05, $**$P<0.001). (e) A549 cells were serum-starved for 24 hours and pretreated without or with foretinib (100 nM) for 2 h. Then the cells were stimulated with 50 μM copper (II) ion for 10 min and subjected to western blotting analysis. (f) The phosphorylation level of MET in each experiment was quantified and analyzed. Data are represented as mean ± S.D. of triplicate experiments ($*$P<0.05, $**$P<0.001).

scratch wound assay to mimic the wound healing in vitro and studied cell migration upon the stimulation of copper (II). We investigated the effect of copper (II) on wound-closure events after making an artificial wound in the monolayer of A549 cells (Figure 5(a)). The treatment of copper (II) ion significantly increased the wound-closure rates (34.7%) of A549 cells (Figure 5(b)), indicating that copper (II) enhanced the cancer cell migration. Moreover, copper (II) ion remarkably promoted cell proliferation (Figure 5(c)). Taken together, copper (II) ion enhanced the cell functions including proliferation and migration via the ligand-independent RTK signaling pathway.

4. Discussion

In the present study, we validated that copper could initiate the RTK-mediated signaling pathway and cell functions analogues to the natural ligand biological effect. Interestingly, copper ions used in the treatment of diseases are not suitable for clinical use because of their toxicity, irritability, and absorbability. However, the chelation of the copper ions can reduce their toxicity and irritation and facilitate the cells to absorb copper ions for biological functions [22]. A previous study identified that copper chelate inhibits vascular injury response and promotes angiogenesis for tissue repair [23]. In our experiments, we have titrated the optimal concentration of copper (II) for minimal toxicity to cells and demonstrated that the cells survive and proliferate at the concentration up to 100 μM.

On the other hand, in this experiment, we mainly discussed the effect of divalent copper (II) on the cell signaling pathway and cellular responses. It has been reported that the monovalent copper ion is unstable in the solution, and it is proved that the bivalent copper ion acts on the cell [15].

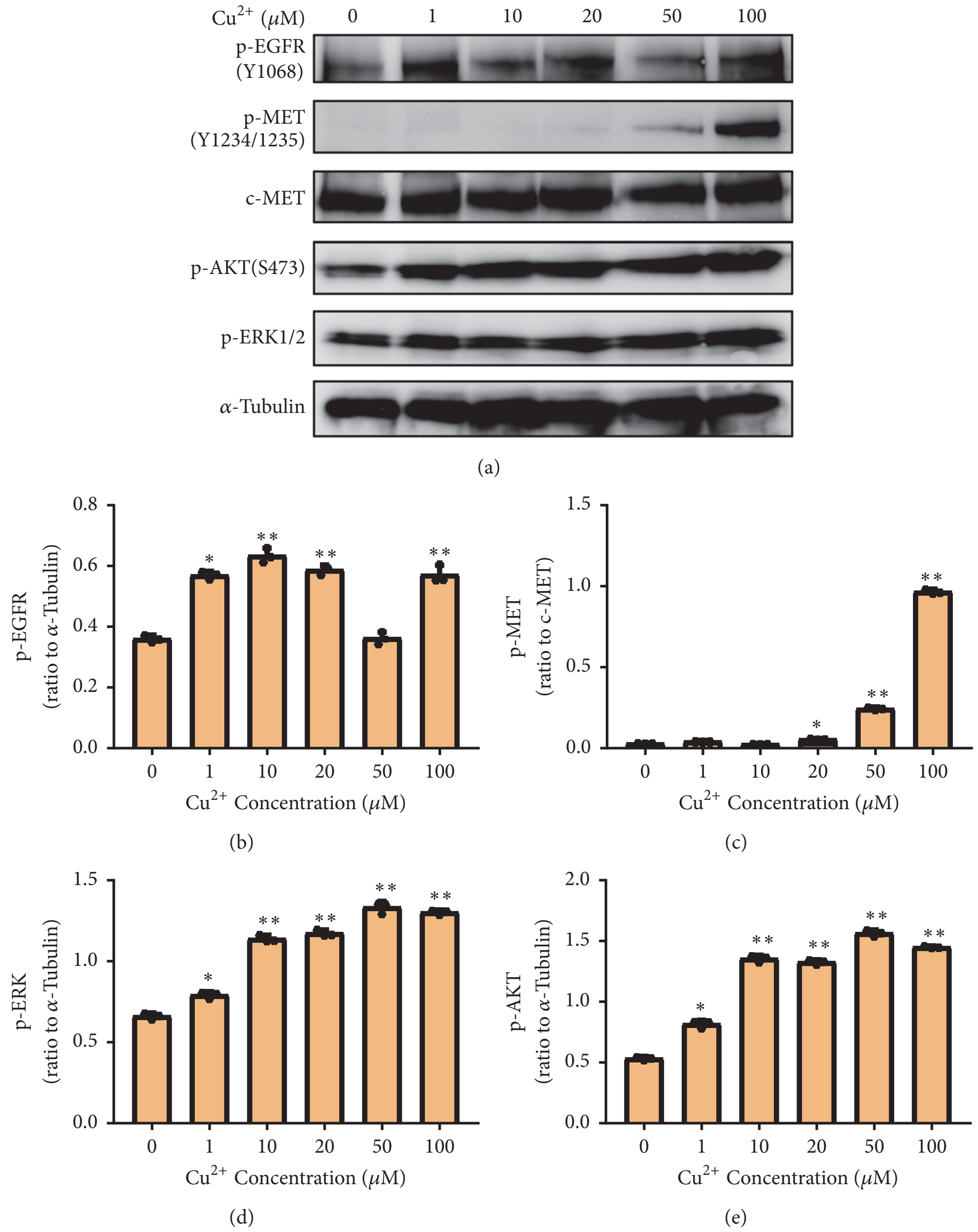

Figure 2: *Copper (II) induced the RTK-mediated cellular signal pathway in a concentration-dependent manner*. (a) A549 cells were treated with different concentrations of copper (II) ion for 10 min and the phosphorylation of EGFR, MET, AKT, and ERK was examined using western blotting. The phosphorylation level of EGFR (b), MET (c), ERK (d), and AKT (e) in each experiment was quantified and analyzed. Data are represented as mean ± S.D. of triplicate experiments ($*P<0.05$, $**P<0.001$).

We determined the optimal time and concentration of the response of the RTK signaling pathway upon copper (II) stimulation. We demonstrated that copper (II) stimulated cells with enhanced phosphorylation levels of RTK (EGFR and MET). The potent inhibitor of MET abolished the effect of copper (II) on phosphorylated-MET, suggesting copper (II) might promote the dimerization-mediated autophosphorylation of RTKs. However, the detailed mechanism should be further investigated. As the critical downstream signaling events, the phosphorylation of ERK and AKT was significantly elevated in the presence of copper (II) in both time-dependent and dose-dependent manners. However, copper transporter 1 was previously reported to be essential for MAPK signal transduction induced by FGF, PDGF, and EGF [24]. A potential explanation is that the major copper influx transporter, CTR1, maintains copper-dependent enzyme SOD1 which serves to inhibit phosphatases that limit RTK signaling, thus activating the central elements of RTK downstream signaling pathways. It has been reported that copper transporters and copper chaperones play essential roles in cardiovascular physiology and disease, including cell growth, migration, angiogenesis, and wound repair [25, 26].

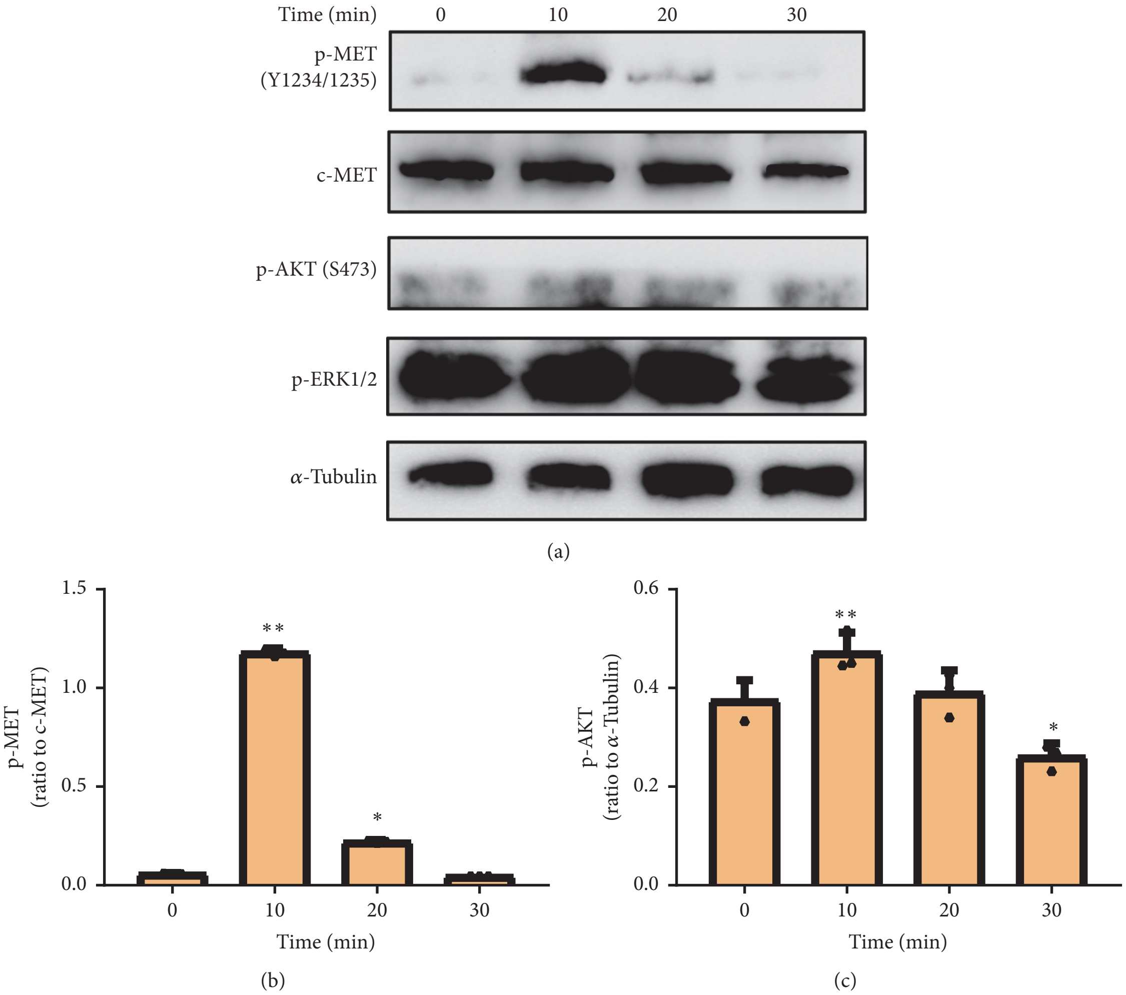

(a)

(b)

(c)

FIGURE 3: *Copper (II) ion stimulated the RTK-mediated signal pathway time-dependently*. (a) The A549 cells were serum-starved and treated with 100 μM copper (II) for 0, 10, 20, and 30 min, respectively. The phosphorylation of MET, AKT, and ERK1/2 was examined using western blot analysis. The phosphorylation level of MET (b) and AKT (c) in each experiment was quantified and analyzed. Data are represented as mean ± S.D. of triplicate experiments ($*P<0.05$, $**P<0.001$).

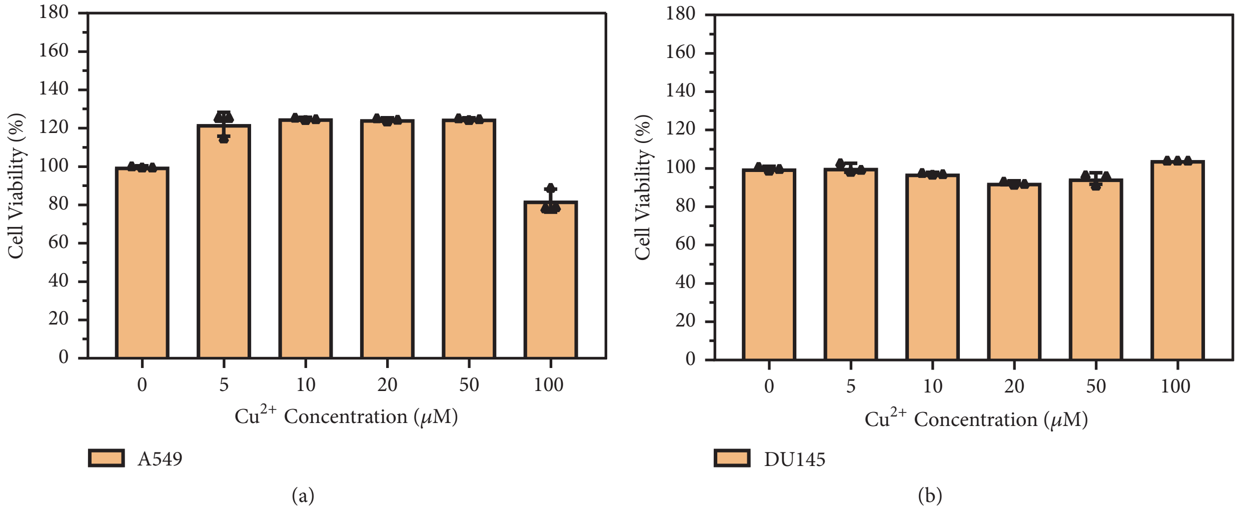

(a)

(b)

FIGURE 4: *Copper (II) ion exhibited minimal cytotoxicity on A549 and DU145 cells*. A549 (a) and DU145 (b) cells are incubated with different concentrations of copper (II) ions for 48 h. The cell viability in each experiment was determined using CCK8 assay. Data are represented as mean ± S.D. of triplicate experiments.

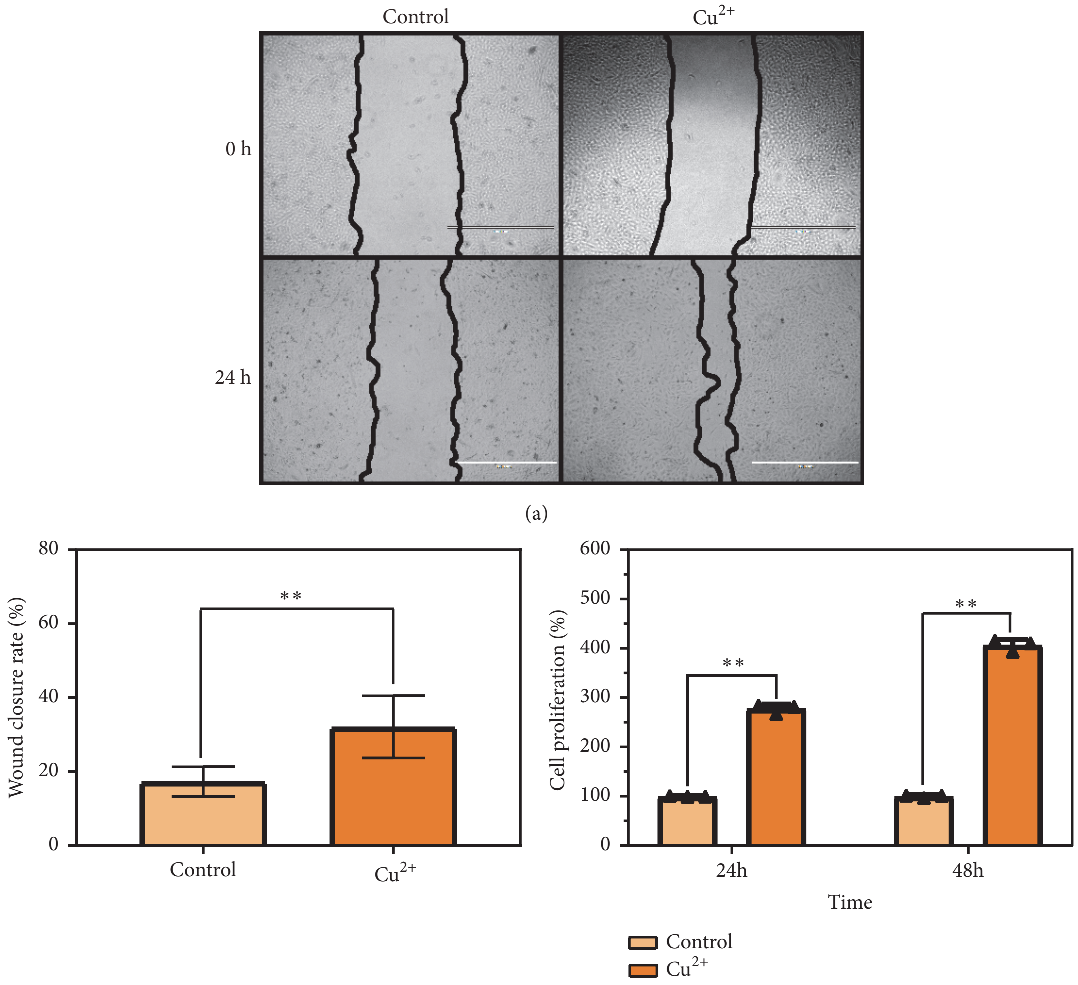

(a)

(b)

(c)

Figure 5: *Copper (II) promoted wound healing and proliferation.* (a) Copper (II) ion enhanced wound healing. The A549 cells were treated with or without copper (II) ion (50 μM), and the wound-closure events were captured by a light microscope. The images were taken at 0 and 24 h. The black lines indicate boundaries between cells in the monolayer and the scratched areas uncovered by cells. Scale bar: 1000 μm. (b) Relative wound-closure rate was measured and analyzed. Data are presented as means ± S.D. (n = 5) ($**P<0.001$). (c) A549 cells were treated with 50 μM copper (II) and the relative cell proliferation at 24 h and 48 h was determined using CCK8 assay. Data are presented as means ± S.D. (n = 5) ($**P<0.001$).

Our data propose a new hypothesis that copper (II) might directly activate RTK signaling probably via the enhanced dimerization between monomer RTKs, which needs ultimate validation. Moreover, in addition to Ras/MAPK, and PI3K/PKB, the signal pathways mediated by RTK also include JNK, P38 MAPK, Rac, and the JAK/STAT pathway [1]. There are potential effects of copper (II) on other downstream signaling pathways of RTK activation. Finally, copper was previously demonstrated to be necessary for carcinogenic BRAF signals and tumorigenesis via the binding-enhanced kinase activity of copper (I) on intracellular MAPK [27]. Therefore, whether copper (II) can stimulate other signaling pathways to affect the cancer cell behavior remains to be further studied. In our research, we clearly evidenced that copper (II) promotes the phosphorylation of RTK as well as essential intracellular AKT and ERK pathways in two different cancer cells, i.e., A549 and DU145, supporting the hypothesis that the presence of high amounts of copper (II) in a tumor microenvironment may promote the cancer cell proliferation even if the natural ligands are deficient [28]. Thus, our results suggest that copper (II) significantly induces ligand-independent RTK signal pathways and promotes both cell migration and proliferation of malignant cells, which provides useful data for the further study of the mechanism of the effect of copper (II) on cancer cells. Thus, the understanding of role of copper (II) in cancer cell behaviors would contribute to the careful clinical preevaluation on not only the detectable ligands for RTK but also the concentration of copper (II) in the tumor microenvironment. Nevertheless, developing additive or synergistic treatment of copper (II) chelation combined with RTK inhibitors may lead to a potential survival advantage in cancer treatment.

5. Conclusion

Our results demonstrated that copper (II) ions could induce ligand-independent RTK-mediated signaling, promoting cell proliferation and wound healing. Copper (II) ions are bioactive ions and are crucial in the regulation of cell signaling pathway and cellular behaviors.

Data Availability

The data used to support the findings of this study are available from the corresponding author upon request.

Conflicts of Interest

The authors declare no competing financial interest.

Authors' Contributions

Fang He and Cong Chang contributed equally.

Acknowledgments

This work was supported by the Natural Science Foundation of Hunan Province (2016JJ3035).

References

[1] J. Schlessinger, "Cell signaling by receptor tyrosine kinases," *Cell*, vol. 103, no. 2, pp. 211–225, 2000.

[2] W. Zhu and L. Qin, "GOLM1-regulated EGFR/RTK recycling is a novel target for combating HCC metastasis," *Science China Life Sciences*, vol. 60, no. 1, pp. 98–101, 2017.

[3] Q. Liu, J. Zhang, H. Gao et al., "Role of EGFL7/EGFR-signaling pathway in migration and invasion of growth hormone-producing pituitary adenomas," *Science China Life Sciences*, vol. 61, no. 8, pp. 893–901, 2018.

[4] A. Zinkle and M. Mohammadi, "A threshold model for receptor tyrosine kinase signaling specificity and cell fate determination," *F1000Research*, vol. 7, p. 872, 2018.

[5] A. Östman and F.-D. Böhmer, "Regulation of receptor tyrosine kinase signaling by protein tyrosine phosphatases," *Trends in Cell Biology*, vol. 11, no. 6, pp. 258–266, 2001.

[6] F. G. Haj, B. Markova, L. D. Klaman, F. D. Bohmer, and B. G. Neel, "Regulation of receptor tyrosine kinase signaling by protein tyrosine phosphatase-1B," *The Journal of Biological Chemistry*, vol. 278, no. 2, pp. 739–744, 2003.

[7] T. Regad, "Targeting RTK signaling pathways in cancer," *Cancers*, vol. 7, no. 3, pp. 1758–1784, 2015.

[8] S. Barberán and F. Cebrià, "The role of the EGFR signaling pathway in stem cell differentiation during planarian regeneration and homeostasis," *Seminars in Cell & Developmental Biology*, vol. 87, pp. 45–57, 2019.

[9] N. Lv, S. Hao, and C. Luo, "miR-137 inhibits melanoma cell proliferation through downregulation of GLO1," *Science China Life Sciences*, vol. 61, no. 5, pp. 541–549, 2018.

[10] G. Skead and D. Govender, "Gene of the month: MET," *Journal of Clinical Pathology*, vol. 68, no. 6, pp. 405–409, 2015.

[11] J. A. Fresno Vara, E. Casado, J. de Castro, P. Cejas, C. Belda-Iniesta, and M. González-Barón, "PI3K/Akt signalling pathway and cancer," *Cancer Treatment Reviews*, vol. 30, no. 2, pp. 193–204, 2004.

[12] F. Tang, M. T. F. Pacheco, P. Chen, D. Liang, and W. Li, "Secretogranin III promotes angiogenesis through MEK/ERK signaling pathway," *Biochemical and Biophysical Research Communications*, vol. 495, no. 1, pp. 781–786, 2018.

[13] R. A. Festa and D. J. Thiele, "Copper: An essential metal in biology," *Current Biology*, vol. 21, no. 21, pp. R877–R883, 2011.

[14] J. H. Kaplan and E. B. Maryon, "How mammalian cells acquire copper: an essential but potentially toxic metal," *Biophysical Journal*, vol. 110, no. 1, pp. 7–13, 2016.

[15] P. Ding, X. Zhang, S. Jin et al., "CD147 functions as the signaling receptor for extracellular divalent copper in hepatocellular carcinoma cells," *Oncotarget* , vol. 8, no. 31, pp. 51151–51163, 2017.

[16] J. M. Hu Frisk, L. Kjellén, S. G. Kaler, G. Pejler, and H. Öhrvik, "Copper regulates maturation and expression of an MITF: tryptase axis in mast cells," *The Journal of Immunology*, vol. 199, no. 12, pp. 4132–4141, 2017.

[17] A. Gopal, V. Kant, A. Gopalakrishnan, S. K. Tandan, and D. Kumar, "Chitosan-based copper nanocomposite accelerates healing in excision wound model in rats," *European Journal of Pharmacology*, vol. 731, no. 1, pp. 8–19, 2014.

[18] A. P. Kornblatt, V. G. Nicoletti, and A. Travaglia, "The neglected role of copper ions in wound healing," *Journal of Inorganic Biochemistry*, vol. 161, pp. 1–8, 2016.

[19] L. Weichselbaum and O. D. Klein, "The intestinal epithelial response to damage," *Science China Life Sciences*, vol. 61, no. 10, pp. 1205–1211, 2018.

[20] H. Xie and Y. J. Kang, "Role of copper in angiogenesis and its medicinal implications," *Current Medicinal Chemistry*, vol. 16, no. 10, pp. 1304–1314, 2009.

[21] X. Shi, C. Stoj, A. Romeo, D. J. Kosman, and Z. Zhu, "Fre1p Cu2+ reduction and Fet3p Cu1+ oxidation modulate copper toxicity in saccharomyces cerevisiae," *The Journal of Biological Chemistry*, vol. 278, no. 50, pp. 50309–50315, 2003.

[22] K. R. Closson and E. A. Paul, "Comparison of the toxicity of two chelated copper algaecides and copper sulfate to non-target fish," *Bulletin of Environmental Contamination and Toxicology*, vol. 93, no. 6, pp. 660–665, 2014.

[23] L. Mandinov, A. Mandinova, S. Kyurkchiev et al., "Copper chelation represses the vascular response to injury," *Proceedings of the National Acadamy of Sciences of the United States of America*, vol. 100, no. 11, pp. 6700–6705, 2003.

[24] C.-Y. Tsai, J. C. Finley, S. S. Ali, H. H. Patel, and S. B. Howell, "Copper influx transporter 1 is required for FGF, PDGF and EGF-induced MAPK signaling," *Biochemical Pharmacology*, vol. 84, no. 8, pp. 1007–1013, 2012.

[25] E. Urso and M. Maffia, "Behind the link between copper and angiogenesis: established mechanisms and an overview on the role of vascular copper transport systems," *Journal of Vascular Research*, vol. 52, no. 3, pp. 172–196, 2015.

[26] T. Fukai, M. Ushio-Fukai, and J. H. Kaplan, "Copper transporters and copper chaperones: Roles in cardiovascular physiology and disease," *American Journal of Physiology-Cell Physiology*, vol. 315, no. 2, pp. C186–C201, 2018.

[27] D. C. Brady, M. S. Crowe, M. L. Turski et al., "Copper is required for oncogenic BRAF signalling and tumorigenesis," *Nature*, vol. 509, no. 7501, pp. 492–496, 2014.

[28] D. C. Brady, M. S. Crowe, D. N. Greenberg, and C. M. Counter, "Copper chelation inhibits BRAFV600E-driven melanomagenesis and counters resistance to BRAFV600E and MEK1/2 inhibitors," *Cancer Research*, vol. 77, no. 22, pp. 6240–6252, 2017.

Hindawi
BioMed Research International
Volume 2019, Article ID 9732325, 11 pages
https://doi.org/10.1155/2019/9732325

Review Article

The Roles of Environmental Factors in Regulation of Oxidative Stress in Plant

Xiulan Xie,[1] Zhouqing He,[1] Nifan Chen,[1] Zizhong Tang,[1] Qiang Wang,[2] and Yi Cai[1]

[1] *School of Life Sciences, Sichuan Agricultural University, Ya'an 625014, China*
[2] *Institute of Ecological Agriculture, Sichuan Agricultural University, Chengdu 611130, China*

Correspondence should be addressed to Yi Cai; yicai@sicau.edu.cn

Received 26 February 2019; Accepted 16 April 2019; Published 8 May 2019

Guest Editor: Hengjia Ni

Copyright © 2019 Xiulan Xie et al. This is an open access article distributed under the Creative Commons Attribution License, which permits unrestricted use, distribution, and reproduction in any medium, provided the original work is properly cited.

Exposure to a variety of environmental factors such as salinity, drought, metal toxicity, extreme temperature, air pollutants, ultraviolet-B (UV-B) radiation, pesticides, and pathogen infection leads to subject oxidative stress in plants, which in turn affects multiple biological processes via reactive oxygen species (ROS) generation. ROS include hydroxyl radicals, singlet oxygen, and hydrogen peroxide in the plant cells and activates signaling pathways leading to some changes of physiological, biochemical, and molecular mechanisms in cellular metabolism. Excessive ROS, however, cause oxidative stress, a state of imbalance between the production of ROS and the neutralization of free radicals by antioxidants, resulting in damage of cellular components including lipids, nucleic acids, metabolites, and proteins, which finally leads to the death of cells in plants. Thus, maintaining a physiological level of ROS is crucial for aerobic organisms, which relies on the combined operation of enzymatic and nonenzymatic antioxidants. In order to improve plants' tolerance towards the harsh environment, it is vital to reinforce the comprehension of oxidative stress and antioxidant systems. In this review, recent findings on the metabolism of ROS as well as the antioxidative defense machinery are briefly updated. The latest findings on differential regulation of antioxidants at multiple levels under adverse environment are also discussed here.

1. Introduction

The environment consists of a set of relationships between livings and nonliving things and is perfectly balanced by various natural processes. Each species influences its environment and, in turn, gets influenced by it. In general, numerous environmental factors including salinity, drought, extreme temperature, metal toxicity, air pollutants, ultraviolet light [1], and high doses of pesticides as well as pathogen infection can lead to subject oxidative stress in plants [2–6]. The oxidative stress is caused either by the direct effects of environmental stress or by indirect reactive oxygen species (ROS) generation and accumulation, which damage a cell before elimination. In order to evade stressors, animals are able to move and escape. Plants as sessile organisms, however, have developed complex strategies to release stressors. The plant cells will be in a state of "oxidative stress" if the ROS quantity is more than the inside defense mechanisms. It then exhibits growth retardation under oxidative stress, including flower and leaf abscission [7, 8], root gravitropism [9], seed germination [10], polar cell growth [11], lignin biosynthesis in cell wall [12], and cell senescence [13].

ROS include superoxide radical ($O_2^{\bullet -}$), hydroxyl radical ($OH^{\bullet}$), hydrogen peroxide (H_2O_2), singlet oxygen ($^1O_2$), and so on [14, 15]. They are regarded as natural byproducts of the aerobic way of life and are generated in different cellular compartments like chloroplasts, peroxisomes, mitochondria, and plasma membrane [16]. It is significant that the increase of ROS level is highly reactive and affects a large variety of cellular, physiological, and biochemical functions, such as the disruption of plasma membrane via carbohydrate deoxidation, lipid peroxidation, protein denaturation, and the destruction of DNA, RNA, enzymes, and pigments [17–20]. All of those result in the loss of crop yield and quality [6, 21–27]. For example, in potatoes (*Solanum tuberosum L.*), overexpression of *AtCYP21-4*, a protein involved in oxidative stress tolerance, resulted in heavier tubers [28]. Similarly, in rice (*Oryza sativa L.*), *OsCYP21-4* overexpressing transgenic plants exhibited higher biomass and productivity with 10-15% higher seed weight than in the WT [28]. Besides, in sweet oranges (*Citrus sinensis L. Osbeck*), overexpression of *CitERF13* in citrus fruit peel resulted in rapid chlorophyll degradation and led to the accumulation of ROS [29, 30]. Moreover, in Arabidopsis (*Arabidopsis thaliana*), mutants of the singlet oxygen ($^1O_2$) overproducing flu and chlorina1 (ch1) have shown that $^1O_2$-induced changes in gene expression can lead to either PCD or acclimation [31]. In conclusion, all of those observations demonstrate that ROS have a significant impact on crop yield and quality.

In the past several decades, research on oxidative stress was mainly focused on *Escherichia coli*. In the past ten years, however, it has moved beyond animals (e.g., human) to plants, particularly model plants and crops (e.g., *Arabidopsis thaliana*, rice). It has substantially increased the understanding of the role and action of oxidative stress in general development-defense and environment-related responses [32–35]. Plants evolved their own antioxidant protection mechanism to maintain a dynamic balance of ROS, since the overcounteraction of ROS leads to the loss of an important intracellular signaling molecule [36].

This review primarily deals with the metabolism of ROS in plants and gives a brief introduction to the types, generation sites, and induced oxidative stresses of ROS. Then, we will focus on the antioxidative defense machinery in resisting the risk of overproduced ROS under disadvantageous environments and summarize recent researches on different environmental factors in regulating oxidative stress in plants.

2. The Metabolism of ROS in Plants

2.1. The Types of ROS. The most common ROS include $O_2^{\bullet -}$, $^1O_2$, H_2O_2, and $OH^\bullet$. The environment of molecular oxygen (O_2) is generally inactive due to its electron configuration [37]. But the unbalanced metabolism of O_2 can lead to the production of ROS, which include both free radicals ($O_2^{\bullet -}$, superoxide radical; $OH^\bullet$, hydroxyl radical; $HO_2^\bullet$, perhydroxyl radical; and $RO^\bullet$, alkoxy radicals) and nonradical molecules (H_2O_2, hydrogen peroxide; and $^1O_2$, singlet oxygen) [5, 15, 38].

Among the various types of ROS, H_2O_2 received most attention. It plays a vital role in the regulation of senescence process [39], stomatal behavior [40], cell wall crosslinking [41], regulation of the cell cycle [42], photosynthesis [43], stress acclimation [44], and antioxidative defense [45]. In addition, it is indicated that H_2O_2 can interact with other signal molecules such as abscisic acid (ABA), auxin, brassinosteroid (BR), and ethylene, which are important for plant development and senescence [46–48]. Both ABA and BR induce heat and paraquat tolerance via H_2O_2 produced by *RBOH1* in tomato (*Solanum lycopersicum* L.) [49]. Moreover, ethylene mediates UV-B-induced stomatal closure through peroxidase-dependent H_2O_2 production in *Vicia faba* [50]. Besides, ethylene-induced stomatal closure is required for H_2O_2 synthesis, and both ethylene and H_2O_2 signaling mediate in guard cells in *Arabidopsis* [51]. The specificity of these responses allowing different signaling transduction pathways to act according to surrounding environmental triggers perceived and the physiological status of the plants is likely to be determined by spatial-temporal changes in H_2O_2 production and accumulation.

Several recent studies have demonstrated that H_2O_2 is involved in stress signal transduction pathways, which can activate multiple acclamatory responses that reinforce resistance to various biotic and abiotic stressors. Overexpression of pepper (*Capsicum annuum*) *CaWRKY41* in *Arabidopsis* indicated that it impaired Cd tolerance, enhanced Cd levels through activating Zn transporters, and accelerated H_2O_2 accumulation. On the contrary, *CaWRKY41* silenced via VIGS in pepper plants displayed increased Cd tolerance and reduced H_2O_2 levels [52]. Mutations of *Cu/Zn-SOD1* (*csd1*), *csd2,* and *sodx* led to enhanced resistance to *Magnaporthe oryzae* and increased H_2O_2 accumulation in rice. Further studies revealed that they altered the expression of CSDs and other SOD family members, resulting in increased total SOD enzyme activity and leading to higher H_2O_2 production compared to WT [53]. These transgenic studies established the role of H_2O_2 in the formation of plant tolerance to different biotic and abiotic stresses.

2.2. The Production Sites of ROS. ROS are generated in both unstressed and stressed plant cells. Gradual reduction of O_2 by high-energy exposure or electron-transfer reactions leads to the production of highly reactive ROS. In plants, the activation of ROS is energy dependent and requires an unavoidable leakage of electron from the electron transport activities of chloroplasts, peroxisomes, mitochondria, plasma membranes, endoplasmic reticulum (ER), apoplasts, and cell wall or as a byproduct of various metabolic pathways localized in different cellular compartments [48, 54–59].

Chloroplasts and peroxisomes are the main ROS generators in the presence of light, whilst the mitochondria are the chief sources of ROS production under dark conditions [1]. The chloroplast consists of a highly ordered system of thylakoids, which harbors the efficient light-capturing photosynthetic machinery. Photosystem (PS) I and PSII form the core of the light-harvesting systems in the thylakoids and are the primary sources of ROS generation [60, 61]. Near the reaction centers of PSII, O_2 may produce $^1O_2$ when there is overexcitation of chlorophyll under stress conditions. Besides, $O_2^{\bullet -}$ may also be formed at PSI via Mehler reaction [62] or at PSII during electron transfer to O_2 through Q_A and Q_B [55]. Additionally, due to the activities of flavin oxidases, peroxisomes are the main sites of H_2O_2 generation [58, 63]. In mitochondria, $O_2^{\bullet -}$ and H_2O_2 may be generated by univalent reduction of O_2 near electron transport chain in plant cell [57].

Apart from those organelles, there are cellular sites mediated in the generation of ROS. At plasma membrane that plays a vital role in sensing environmental conditions, localized NADPH-dependent oxidase transfers electrons from NADPH on cytoplasmic side to O_2 producing $O_2^{\bullet -}$ [59]. ER also mediates the generation of $O_2^{\bullet -}$ by Cyt P_{450} [64]. During harsh environmental conditions, the apoplast is rendered for H_2O_2 production by stress signals combined with ABA [65]. As cell wall localized peroxidase(s), diamine/polyamine oxidases and oxalate oxidase produce H_2O_2 that may, in turn, be metabolized to $OH^{\bullet}$ by the activity of class III peroxidases [66, 67].

2.3. Oxidative Damage. When the level of ROS is low or moderate, they function as second messenger that mediates a series of reactions in plant cells, including stomatal closure, programmed cell death (PCD) [23], gravitropism [81], and acquisition of tolerance to both abiotic and biotic stresses [82]. However, in the past two decades, it has become more and more evident that all types of ROS at a high concentration are significantly harmful to organisms. Constant environmental stresses for plants will lead to the generation of superfluous ROS which cannot be completely disposed by the active oxygen scavenging system. Therefore, important physiological actions should be exerted, such as peroxidation of lipids, oxidation of nucleic acids, denaturation of proteins, inhibition of enzyme activity, and even activation of PCD pathway [55, 59].

The major targets of oxidative damage caused by ROS are lipids and proteins in plant cell. The oxidative decomposition of polyunsaturated lipids in plasma membrane, which is known as lipid peroxidation, occurs in every organism and is often considered as an indicator to determine the extent of lipid damage under severe conditions [83–85]. It is now well demonstrated that lipid peroxidation starts a reaction chain that can also create other reactive products such as ketones, aldehydes, and hydroxyl acids and can modify proteins, by oxidation of some amino acid residues [86, 87]. The activity of the protein is altered due to modifications such as glutathionylation, carbonylation, nitrosylation, and disulfide bond formation [88].

3. Antioxidative Defense System in Plants

Environmental factors such as salinity, drought, chilling, metal toxicity, air pollutants, UV-B radiation, and high doses of pesticides as well as pathogen infection lead to enhanced production of ROS in plant cells [89, 90]. Plenty of studies demonstrated the significance of intracellular antioxidant defense machinery against a variety of stresses [91–93]. This antioxidant defense machinery includes enzymatic and nonenzymatic components to scavenge ROS, and it operates at different subcellular compartments such as chloroplasts, peroxisomes, plasma membranes, and ER [59]. Enzymatic antioxidants contain enzymes such as superoxide dismutase (SOD), catalase [84], guaiacol peroxidase (GPX), ascorbate peroxidase (APX), guaiacol peroxidase (GPOX), monodehydroascorbate reductase (MDHAR), dehydroascorbate reductase (DHAR), glutathione reductase (GR), and glutathione S-transferases (GST) and nonenzymatic antioxidants which are ascorbic acid, glutathione, carotenoids, tocopherols, proline, glycine betaine, and flavonoids [94]. Additionally, NADPH oxidases and respiratory burst oxidase homologues (RBOHs) are also known to be major components of ROS production system in plants [95].

Initially, most of the studies on antioxidative defense system were focused on enzymatic characteristics due to the limitations of the experimental conditions. The enzymes of SOD, APX, CAT, etc. have been widely investigated in order to understand the antioxidative defense mechanisms in response to oxidative stress induced by various environmental factors. For instance, in alfalfa (*Medicago sativa* L.), after NaCl treatment, Xinmu No. 1 exhibited higher enzymatic activity of SOD, APX, and CAT in its shoots and roots than Northstar and, meanwhile, showed lower levels of H_2O_2 production and lipid peroxidation [96]. In another example, blue light illumination increased fruit color index, enhanced the activities of SOD, CAT, and APX, and maintained lower levels of H_2O_2 in strawberry (*Fragaria vesca*), which demonstrated that the treatment of blue light maintains fruit quality and increases nutritional value in strawberries due to the strengthening of both antioxidant systems and free radical elimination capabilities [97].

Subsequently, with the development of molecular cloning technology, researches on the functions of antioxidant genes generated many new insights into this area. The dynamic transcription activity of ROS-scavenging enzymatic genes has been widely characterized. In pear (*Pyrus communis* L.), the expression of *SOD*, *CAT,* and *APX* were significantly upregulated over 24, 48, 72, and 96 h after inoculation of *Erwinia amylovora*, comparing to the controls [98]. In cotton (*Gossypium hirsutum*), the expression patterns of 18 *GhSOD* genes were tested in different abiotic stresses, which indicated that they may play a very crucial role in ROS scavenging caused by various stresses through genome-wide characterization [99]. These expression patterns of *SOD*, *CAT,* and *APX* in pear and *GhSOD* suggest that they are associated with the antioxidative defense process. There have been a large number of similar studies on antioxidant genes expression in plants, focused mainly on the mRNA level, but further functional studies are limited.

In recent years, numbers of transgenic plants such as *Arabidopsis*, tomato, rice, tobacco, and maize have been developed with disposed expression of antioxidant enzymes that exhibited increased tolerance to salinity, extreme temperatures, and drought stress [100]. Jing et al. reported that overexpressing *Kandelia candel KcCSD* (a Cu/Zn SOD) in tobacco showed salinity tolerance in the aspect of lipid peroxidation, root growth, and survival rate and enhanced SOD and CAT activity compared to wild type (WT)[68]. Likewise, overexpression of Chinese cabbage (*Brassica campestris*) *BcAPX2* and *BcAPX3* in *Arabidopsis* improved seed germination rate and showed amazing high temperature tolerance via efficient scavenging of cellular H_2O_2 [73]. In *Arachis hypogaea*, transgenic *AhCuZnSOD* in tobacco plants resulted in enhanced salinity and drought tolerance as indicated by better seed germination and higher chlorophyll content compared to WT [69]. Notably, overexpression of a single gene could increase plant tolerance to different stresses and many researchers paid close attention to transgenics with overexpression of *SOD* for enhancing stress tolerance [90].

As science advances, a growing amount of researches show that the stress tolerance can develop markedly by applying the simultaneous coexpression of genes involved in metabolic pathways. Xu et al. (2014) coexpressed *MeCu/ZnSOD* and *MeAPX2* in cassava (*Manihot esculenta* Crantz) and tested the tolerance of transgenic plants against oxidative and chilling stresses. After exposure to 100 μM methyl viologen and 0.5 M H_2O_2, the result exhibited a lower level of chlorophyll degreening, lipid peroxidation, and H_2O_2 accumulation along with a higher level of activities of SOD and APX in transgenic plants than the WT [75]. Similarly, coexpression of *Brassica rapa BrMDHAR* and *BrDHAR* genes via hybridization conferred tolerance to freezing [101]; cotransformation of *cytSOD* and *cytAPX* led to salinity tolerance in transgenic plums [102]; coexpression of *PaSOD* and *RaAPX* genes from *Potentilla atrosanguinea* and *Rheum austral,* respectively, in transgenic *Arabidopsis* showed increased salt tolerance through regulating lignin deposition [70].

Genes encoding enzymes required for antioxidative defense have been widely studied in several types of plants. However, research on the transcriptional regulation of antioxidant enzymes remains limited and mainly focuses on the oxidative stress-related transcription factors including AP2/ERF, NAC, MYB, and bHLH family [15, 103–105]. For example, overexpression of the buckwheat (*Fagopyrum tataricum*) *FtbHLH3* in *Arabidopsis* resulted in enhanced drought tolerance, which was attributed to not only the lower level of H_2O_2 but also the higher activities of SOD and CAT as well as the higher photosynthetic efficiency in transgenic lines compared to WT [106]. Overexpressing of rice miR529a led to enhanced plant resistance to high level of H_2O_2, which manifested as improved seed germination rate and increased SOD and POD activities, as well as reduced leaf rolling rate and chlorophyll content [107]. However, the underlying regulatory mechanisms specific to antioxidant enzymes are still not fully characterized and should be further explored.

4. The Impact of Environmental Factors on Plant Oxidative Stress

4.1. Salinity. Soil salinity is a major issue that limits the productivity and quality of the agricultural crops in many arid and semiarid regions of the world. Hypersaline conditions impact the stressed crops at multiple aspects such as oxidative stress, genotoxicity, ionic imbalance and toxicity, nutrition deficiency, and osmotic stress, resulting in subhealthy status of the plants [108]. As a consequence, plant cells decrease photosynthetic electron transport and generate excessive ROS. To counteract the deleterious effects mentioned above, plants have developed various strategies, including salt compartmentalization and exclusion [109].

In plants, all enzymatic scavengers operate together to conquer salt stress for better growth and development. In maize seedlings organs including roots, mature leaves, and young leaves, the activities of CAT and DHAR increased in all organs of salt-treated plants, while SOD, APX, GST, and GR increased specifically in the roots after NaCl treatment [110]. Two local wheat salt-tolerant cultivars, BARI Gom 27 and 28, displayed reduced accumulations of H_2O_2 and higher activities of CAT, peroxidase, and APX than salt-sensitive cultivars in virtue of reduced oxidative damage [111]. In the above reports, higher expression level of enzymatic antioxidants induced by salt treatment suggests an efficient way to decrease saline toxicities. However, some studies also indicated that differential expression behavior of these enzyme genes, the salinity extent, and the exposure time as well as the plant developmental stage will make the expression levels different [53, 71, 72].

Due to the significance of antioxidant enzymes, genetic engineering with altered antioxidant entities through overexpression of their pathway genes has been conducted to improve salt tolerance in various crops [72]. Zhou et al. (2018) demonstrated that Tyr-210 is a major phosphorylation site in CatC and is activated by STRK1 (receptor-like cytoplasmic kinase). Moreover, phosphorylating and activating CatC by overexpressing STRK1 regulated H_2O_2 homeostasis and indeed improved salt and oxidative tolerance. Importantly, overexpression of *STRK1* in rice enhanced rice seedling growth status; meanwhile, the loss of grain yield under salt stress was significantly limited [112]. Guan et al. (2015) found that the expression of *PutAPX* was upregulated with extended exposure to $NaHCO_3$, NaCl, H_2O_2, and PEG6000 treatment in *Puccinellia tenuiflora*. Furthermore, when grown with 150 or 175 mM NaCl, transgenic Arabidopsis plants overexpressing *PutAPX* displayed increased tolerance of saline toxicity and decreased level of lipid peroxidation [71].

4.2. Drought. Drought is an important environmental stress for plant growth that ultimately causes the reduction in crops yield in a global warming world, especially for commercial crops including rice, wheat, and maize [113]. Nevertheless, plants have evolved multiple strategies to minimize the damage during drought conditions [108]. It is demonstrated that the key process in plant physiological response to drought is the production of ROS, which causes progressive oxidative damage, stunted growth, and eventual cell death when ROS level reaches a certain threshold [89].

Several researches indicated that sustainable tolerance to drought stress could be achieved by increasing the expression/activity of ROS scavenging-related genes/enzymes [96]. For example, overexpression (OE) of *OsLG3* (a ERF family transcription factor) increased rice drought tolerance by modulating ROS homeostasis through upregulation in the OE lines and downregulation in the RNAi lines of the expression of 10 ROS scavenging-related genes (*APX1*, *APX2*, *APX4*, *APX6*, *APX8*, *CATB*, *POD1*, *POD2*, *SODcc1*, and *FeSOD*) [114]. Moreover, Xu et al. (2016) reported that the increasing cytokinin production through overexpression of *isopentenyl transferase* (*ipt*) alleviated drought damage and promoted root growth in *Agrostis stolonifera*. Further enzymatic assays and transcript abundance analysis showed that CAT, SOD, POD, and DHAR were much higher in roots of a transgenic line overexpressing *ipt* under drought stress [74]. In another example, *Arabidopsis* ZAT18 (a C2H2 zinc finger protein) OE plants exhibited less leaf water loss, lower content of H_2O_2, higher leaf water content, and higher activities of POD and CAT after drought treatment when compared with the WT [115].

The significant roles of oxidant enzymes in ROS scavenging also have been suggested by studies with transgenic plants. Wang et al. (2005) demonstrated that overexpression of pea (*Pisum sativum*) *MnSOD* in rice showed reduced electrolyte leakage compared to WT leaf slices after polyethylene glycol 6000 treatment, which could induce drought stress

Table 1: Antioxidant enzymatic defense mechanism in response to oxidative stress induced by various environmental factors.

Environmental factors	Antioxidant enzymes	Plant species/source crop	Recipient crop	References
salinity	Cu/ZnSOD, CAT	*Kandelia candel*	*tobacco*	[68]
	SOD	*Arachis hypogaea*		[69]
	PaSOD, RaAPX	*Potentilla atrosanguinea* *Rheum austral*	*Arabidopsis*	[70]
	PutAPX	*Puccinellia tenuiflora*	*Arabidopsis*	[71]
	OsAPX	*Oryza sativa*	*knockout*	[72]
drought	APX	*Solanum melongena*	*Oryza sativa*	[73]
				[74]
chilling	SOD, APX	*Manihot esculenta*		[75]
	Glutaredoxins	*Arabidopsis thaliana*	*Solanum lycopersicum*	[76]
metal toxicity	GR	*Cannabis sativa*	*Cannabis sativa*	[77]
	GSH	synthetic	*Oryza sativa*	[78]
UV-B radiations	APX, SOD, POD, CAT	*Pisum sativum* *Cassia auriculata*		[79]
pathogens	peroxidase expression	*Oryza sativa*	mutation	[80]

[116]. Lu et al. (2010) reported that overexpressing *APX* and *Cu/ZnSOD* in chloroplasts of sweet potato improved the capacity of drought tolerance and recovery in plants. It also exhibited enhanced photosynthetic activity when suffered drought stress, compared to WT [117].

4.3. Chilling. Chilling stress is a major restriction of crops growth, production, and distribution. Enhancing crop chilling tolerance is thus vital to crops yield increase. As chilling induces oxidative stress and results in lipid peroxidation, chlorophyll degradation, etc., chilling tolerance is thus mainly associated with antioxidant enzyme activities enhancement and corresponding H_2O_2 accumulation reduction (Table 1).

Glutaredoxins (GRXs), as common oxidoreductases, mainly utilize the reducing power of glutathione to break disulfide bonds of substrate proteins and maintain cellular redox homeostasis. It has been reported that the expression of *AtGRXS17* in tomato conferred transgenic tomato chilling stress tolerance without any growth defects showing up. Compared with wild-type plants, tomato expressing *AtGRXS17* exhibits lower ion leakage and increased maximal photochemical efficiency when challenged by cold [76]. Soluble sugar in those transgenic tomato plants also accumulates to a higher level.

Xu et al. (2014) coexpressed *MeCu/ZnSOD* and *MeAPX2* in cassava (*Manihot esculenta* Crantz) to enhance tolerance against oxidative attributed to chilling stresses. Specifically, higher levels of antioxidative enzymes activities and lower levels of chlorophyll degradation, lipid peroxidation, and H_2O_2 accumulation were detected in transgenic plants after exposure to H_2O_2 and methyl viologen, a ROS-generating reagent [75]. Similarly, *BrMDHAR* and *BrDHAR* coexpression in *Brassica rapa* via hybridization elevated the plant resistance to freezing [101].

4.4. Metal Toxicity. Since the industrial revolution, heavy metal environmental pollution has become so serious that an increasing number of scientists are engaged in relevant scientific research. Usually, the concentrations of heavy metals determine their negative impacts on plants and the environment [118]. Plants then exhibit their ability to avoid the detrimental impacts when the amount of heavy metals is controlled in a natural level [119]. There has already been evidence suggesting that excessive level of heavy metals impairs homeostasis and increases ROS production in the plant cells [120].

Due to the redox ability, heavy metals absorbed by plants are involved in several mechanisms that produce free radicals. As redox-active elements, iron (Fe), copper (Cu), chromium [121], etc., can participate in a redox-cycling reaction, resulting in the production of toxic hydroxyl radicals which seriously damage the living cells. Mannitol exhibits the ability to activate the antioxidant enzyme which might be helpful to alleviating pathological symptoms in wheat (*Triticum aestivum* L.) when challenged by Cr stress [122]. As for other metals without redox capacity, such as lead (Li), cadmium (Cd), mercury (Hg), zinc (Zn), and nickel (Ni), the primary route for their toxicity is to suppress the antioxidative system, which can be achieved by depleting glutathione and binding sulfhydryl groups of antioxidative enzymes including reductases, superoxide dismutase, and catalases [77]. They also meddle with photosynthetic process and consequently increase the superoxide and singlet oxygen generation within the cells [123]. As highlighted by several authors, the intensity of oxidative stress induced by heavy metals depends on species and varies across disparate genotypes, tissues, and/or developmental stages. In general, metal-susceptible plants display marked symptoms under oxidative stress, while metal-resistant plants display only mild or even no oxidative damages [119].

In addition to the antioxidant responses in plants, there have been a number of chemicals reported that may reduce the uptake of heavy metals and ameliorate the oxidative stress in plants. For example, the biochar derived from *Citrus epicarp* inhibited *Abelmoschus esculentus* (L.) Moench (okra) to absorb Cd from low Cd stress environment [124]. Decreasing Cu uptake and oxidative damage through applying exogenous SNP (Sodium Nitroprusside) and GSH (Glutathione) also alleviated copper toxicity in rice seedlings [78]. Besides, some fungus can provide plants with protections via mycorrhization [125].

4.5. UV-B Radiations. UV-B radiation (280 - 315 nm) accompanies exposure to sunlight and is an inevitable abiotic factor for photosynthetic organisms. When plants are exposed to high level of UV-B radiation, a plethora of cell components, particularly the cellular macromolecules (DNA and protein), are interfered, and oxygen radicals are induced as a consequence. The effects of these radiations vary from the applied dose and sensitivity of living plant cells to the action of radiation type [126].

It has been known for many years that exposure of crop plants to physical radiations such as ionizing FN and nonionizing UV-B generates excessive free radicals which give rise to cytogenetic changes in plants [79]. A current study observed that almost all irradiation exposure doses of FN and UV-B exhibited special interference with meiotic-pollen mother cells and pollen grains leading to the genotoxic effect in *Vicia faba* L. [127]. The RUS1/RUS2 (Root UV-B Sensitive) complex, which works in UV-B-sensing pathway in root, is involved in seedling morphogenesis and development at early stages in Arabidopsis. In the absence of RUS1/RUS2 complex, the development of seedling is interfered with due to the dramatically increased signal generated from photoreceptors after the perception of UV-B [128].

4.6. Pathogens. Pathogen infection which causes plant diseases and epidemics has threatened plant growth, crop yield, and food security worldwide. Diverse and rapidly evolving characters make pathogen one of the most disastrous threats for plants. Different from vertebrates, sessile plants developed a conserved, unique yet sophisticated immune system to combat invading pathogens. Physical and chemical barriers deal with most of the microbes, while specific resistance responses termed host resistance handle the rest of them. When plants perceive PAMPs (Pathogen-associated Molecular Patterns), a multitude of immune responses within the cells will be triggered [129, 130].

ROS production is one of the responses mentioned above that bursts rapidly and transiently. It is mediated by NADPH oxidases located in plasma membrane, belonging to the respiratory burst oxidase homolog (RBOH) family [131–133], as well as apoplastic peroxidases (PRXs). The mechanism of RBOH in stress response is well studied [134]. Kadota *et al.* (2014) has demonstrated that RBOHD phosphorylation mediated by BIK1 has biological significance for stomatal closure, ROS burst, and disease resistance against bacterial pathogens in PTI (PAMP-triggered immunity) [95]. Another example of ROS-related defense response is regulated by ACD11, whose binding partners are Arabidopsis BPA1 and its homologs. Those binding partners can be targeted by an effector, RxLR207, derived from *Phytophthora capsici.*, and then ROS-mediated cell death, which is indispensable for virulence of *P. capsici.*, is activated [135].

Another way to enhance plant disease resistance is to prevent H_2O_2 degradation catalyzed by peroxidases and to increase ROS burst to eliminate invading pathogens. A recent discovery found a natural mutation of the transcription factor that suppresses peroxidase expression and confers broad-spectrum blast resistance in rice [80].

Nevertheless, the transcriptional regulation of ROS-related genes in the apoplast remains largely controversial. For example, the expression of the apoplastic peroxidases coding genes *PRX33* and *PRX34* enhanced cytokinin-mediated stomatal immunity and plant resistance to bacteria [136]. It has also been reported that plants knocked down *PRX33* and *PRX34* exhibited enhanced disease resistance to the necrotrophic fungus *Alternaria brassicicola* [137].

Although ROS burst and accumulation cause damage to plant cells, the generation of ROS is indispensable in plant immunity. Owing to the signaling and bactericidal functions of ROS, short-term oxidative stress is utilized by plant immune system as an effective way to defend against pathogens. The dual roles of ROS in signal transduction help plants detect pathogen invasion. Still, the production of ROS needs to be strictly regulated to control its function.

ROS and Ca^{2+} waves contribute to rapid systemic signaling, which is crucial to plant adaptation to abiotic stresses [138]. Besides, plant resistance to pathogens can be attenuated or enhanced by abiotic stress factors [139]. ROS production bursts in a few minutes after immunogenic treatment; thus, this biological process can be detected to uncover the contribution of those plant components that are necessary in the burst of early immune responses [133].

5. Conclusions

Plants face a variety of pressure during their growth, especially environmental pressure including salinity, drought, extreme temperature, metal toxicity, UV-B radiation, pesticides, and pathogen infection. They adapt to those conditions with adjustments at molecular, biochemical, and physiological levels, especially via antioxidant systems. Although the general process of ROS formation as well as the antioxidative defense of plants (Figure 1) are understood, it is still unclear how plants detect stresses and prepare themselves for the incoming threats because of the extremely reactive nature and

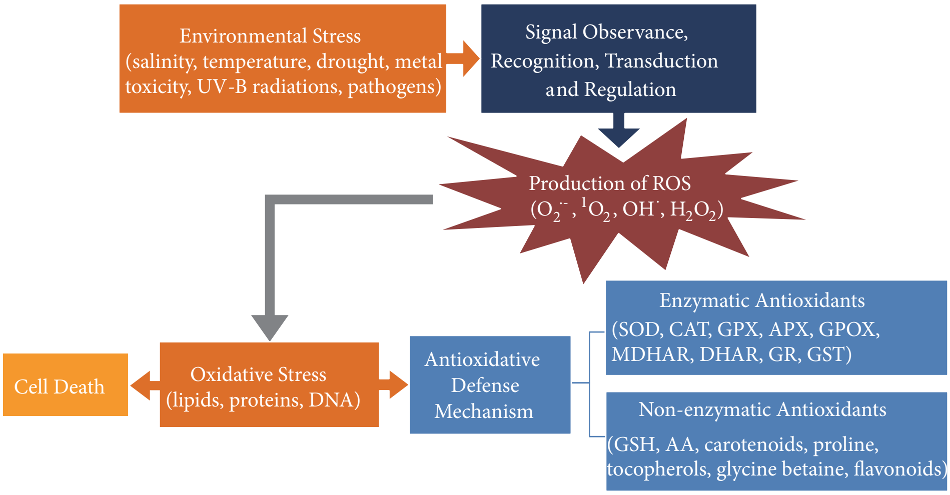
Environmental Stress
(salinity, temperature, drought, metal toxicity, UV-B radiations, pathogens)
Signal Observance, Recognition, Transduction and Regulation
Production of ROS
($O_2^{\cdot-}$, $^1O_2$, $OH^{\cdot}$, H_2O_2)
Enzymatic Antioxidants
(SOD, CAT, GPX, APX, GPOX, MDHAR, DHAR, GR, GST)
Cell Death
Oxidative Stress
(lipids, proteins, DNA)
Antioxidative Defense Mechanism
Non-enzymatic Antioxidants
(GSH, AA, carotenoids, proline, tocopherols, glycine betaine, flavonoids)

FIGURE 1: Environmental stress induced ROS generation, antioxidative defense, and cell death in plant.

short half-life of ROS. In recent studies, genetically modified plants with overexpressing functional genes have shown promising traits in combating oxidative stress. Moreover, to achieve high tolerance against various adverse environments, efforts should be made to generate transgenic plants by coexpressing multiple effective genes.

Conflicts of Interest

The authors declare that there are no conflicts of interest regarding the publication of this paper.

Authors' Contributions

Xiulan Xie and Zhouqing He contributed equally to this work.

Acknowledgments

This work was supported by the National Natural Science Foundation of China (31801839); the Henry Fok Foundation (151104); Ministry of Human Resources and Social Security, China; Sichuan Provincial Department of Science and Technology, China (2018HH0042, 2016JQ0009); Sichuan Provincial Department of Education, China (16TD0005, 15ZA0001).

References

[1] S. Choudhury, P. Panda, L. Sahoo, and S. K. Panda, "Reactive oxygen species signaling in plants under abiotic stress," *Plant Signaling and Behavior*, vol. 8, no. 4, Article ID e236811, 2013.

[2] J. H. L. Pacheco, M. A. Carballo, and M. E. Gonsebatt, "Antioxidants against environmental factor-induced oxidative stress," in *Nutritional Antioxidant Therapies: Treatments and Perspectives*, K. H. Al-Gubory, Ed., vol. 8, pp. 189–215, Springer, Cham, Switzerland, 2018.

[3] F. S. Farnese, P. E. Menezes-Silva, G. S. Gusman, and J. A. Oliveira, "When bad guys become good ones: the key role of reactive Oxygen species and Nitric Oxide in the plant responses to abiotic stress," *Frontiers in Plant Science*, vol. 7, p. 471, 2016.

[4] R. C. Foley, B. N. Kidd, J. K. Hane, J. P. Anderson, and K. B. Singh, "Reactive oxygen species play a role in the infection of the necrotrophic fungi, Rhizoctonia solani in wheat," *PLoS ONE*, vol. 11, no. 3, Article ID e0152548, 2016.

[5] M. A. Hossain, S. Bhattacharjee, S. Armin et al., "Hydrogen peroxide priming modulates abiotic oxidative stress tolerance: insights from ROS detoxification and scavenging," *Frontiers in Plant Science*, vol. 6, no. 420, 2015.

[6] M. Sabir, E. A. Waraich, K. R. Hakeem, M. Öztürk, H. R. Ahmad, and M. Shahid, "Chapter 4 -phytoremediation: mechanisms and adaptations," in *Soil Remediation and Plants*, K. R. Hakeem, M. Sabir, M. Öztürk, and A. R. Mermut, Eds., pp. 85–105, Academic Press, San Diego, Calif, USA, 2015.

[7] P. Muñoz and S. Munné-Bosch, "Photo-oxidative stress during leaf, flower and fruit development," *Plant Physiology*, vol. 176, no. 2, pp. 1004–1014, 2018.

[8] S. Goldental-Cohen, C. Burstein, I. Biton et al., "Ethephon induced oxidative stress in the olive leaf abscission zone enables development of a selective abscission compound," *BMC Plant Biology*, vol. 17, no. 1, p. 87, 2017.

[9] S. Mugnai, C. Pandolfi, E. Masi et al., "Oxidative stress and NO signalling in the root apex as an early response to changes in gravity conditions," *BioMed Research International*, vol. 2014, Article ID 834134, 10 pages, 2014.

[10] Y. Shi, Y. Zhang, H. Yao, J. Wu, H. Sun, and H. Gong, "Silicon improves seed germination and alleviates oxidative stress of bud seedlings in tomato under water deficit stress," *Plant Physiology and Biochemistry*, vol. 78, pp. 27–36, 2014.

[11] S. Mangano, S. P. D. Juárez, and J. M. Estevez, "ROS regulation of polar growth in plant cells," *Plant Physiology*, vol. 171, no. 3, pp. 1593–1605, 2016.

[12] M. Chialva, A. Salvioli di Fossalunga, S. Daghino et al., "Native soils with their microbiotas elicit a state of alert in tomato plants," *New Phytologist*, vol. 220, no. 4, pp. 1296–1308, 2018.

[13] H. Bu, S. Wedel, M. Cavinato, and P. Jansen-Dürr, "MicroRNA regulation of oxidative stress-induced cellular senescence," *Oxidative Medicine and Cellular Longevity*, vol. 2017, Article ID 2398696, 12 pages, 2017.

[14] D. K. Gupta, L. B. Pena, M. C. Romero-Puertas et al., "NADPH oxidases differentially regulate ROS metabolism and nutrient uptake under cadmium toxicity," *Plant Cell & Environment*, vol. 40, no. 4, 2016.

[15] R. Kalia, S. Sareen, A. Nagpal et al., "ROS-induced transcription factors during oxidative stress in plants: a tabulated review," in *Reactive Oxygen Species and Antioxidant Systems in Plants: Role and Regulation under Abiotic Stress*, M. Khan and N. Khan, Eds., pp. 129–158, Springer, Singapore, 2017.

[16] K. Apel and H. Hirt, "Reactive oxygen species: metabolism, oxidative stress, and signal transduction," *Annual Review of Plant Biology*, vol. 55, pp. 373–399, 2004.

[17] S. Li, X. Sun, and X. Ma, "Effects of cyclic tensile strain on oxidative stress and the function of schwann cells," *BioMed Research International*, vol. 2018, Article ID 5746525, 6 pages, 2018.

[18] V. Van Ruyskensvelde, F. Van Breusegem, and K. Van Der Kelen, "Post-transcriptional regulation of the oxidative stress response in plants," *Free Radical Biology & Medicine*, vol. 122, pp. 181–192, 2018.

[19] Y. Martínez, X. Li, G. Liu et al., "The role of methionine on metabolism, oxidative stress, and diseases," *Amino Acids*, vol. 49, no. 12, pp. 2091–2098, 2017.

[20] S. Bose, Y. Du, P. Takhistov, and B. Michniak-Kohn, "Formulation optimization and topical delivery of quercetin from solid lipid based nanosystems," *International Journal of Pharmaceutics*, vol. 441, no. 1-2, pp. 56–66, 2013.

[21] M. Sharma, S. Gupta, F. Deeba et al., "Effects of reactive oxygen species on crop productivity: an overview," in *Reactive Oxygen Species in Plants*, V. P. Singh, S. Singh, D. K. Tripathi, S. M. Prasad, and D. K. Chauhan, Eds., John Wiley & Sons Ltd., 2017.

[22] S. Fulda, "Regulation of necroptosis signaling and cell death by reactive oxygen species," *biological chemistry*, vol. 397, no. 7, pp. 657–660, 2016.

[23] V. Petrov, J. Hille, B. Mueller-Roeber, and T. S. Gechev, "ROS-mediated abiotic stress-induced programmed cell death in plants," *Frontiers in Plant Science*, vol. 6, article no. 69, 2015.

[24] M. Shahid, S. Khalid, G. Abbas et al., "Heavy metal stress and crop productivity," in *Crop Production and Global Environmental Issues*, K. Hakeem, Ed., pp. 1–25, Springer, Cham, Switzerland, 2015.

[25] M. L. Reshi, Y. C. Su, and J. R. Hong, "RNA viruses: ROS-mediated cell death," *International Journal of Cell Biology*, vol. 2014, Article ID 467452, 16 pages, 2014.

[26] Y. Guo and S.-S. Gan, "Translational researches on leaf senescence for enhancing plant productivity and quality," *Journal of Experimental Botany*, vol. 65, no. 14, pp. 3901–3913, 2014.

[27] J. You and Z. Chan, "Ros regulation during abiotic stress responses in crop plants," *Frontiers in Plant Science*, vol. 6, p. 1092, 2015.

[28] H. J. Park, A. Lee, S. S. Lee et al., "Overexpression of golgi protein CYP21-4s improves crop productivity in potato and rice by increasing the abundance of mannosidic glycoproteins," *Frontiers in Plant Science*, vol. 8, p. 1250, 2017.

[29] X.-L. Xie, X.-J. Xia, S. Kuang et al., "A novel ethylene responsive factor CitERF13 plays a role in photosynthesis regulation," *Journal of Plant Sciences*, vol. 256, pp. 112–119, 2017.

[30] X. Yin, X. Xie, X. Xia et al., "Involvement of an ethylene response factor in chlorophyll degradation during citrus fruit degreening," *The Plant Journal*, vol. 86, no. 5, pp. 403–412, 2016.

[31] L. Shumbe, A. Chevalier, B. Legeret, L. Taconnat, F. Monnet, and M. Havaux, "Singlet oxygen-induced cell death in arabidopsis under high-light stress is controlled by OXI1 kinase," *Plant Physiology*, vol. 170, no. 3, pp. 1757–1771, 2016.

[32] A. C. B. A. Lopes, T. S. Peixe, A. E. Mesas et al., "Lead exposure and oxidative stress: a systematic review," *Reviews of Environmental Contamination & Toxicology*, vol. 236, p. 193, 2016.

[33] A. M. Pisoschi and A. Pop, "The role of antioxidants in the chemistry of oxidative stress: a review," *European Journal of Medicinal Chemistry*, vol. 97, pp. 55–74, 2015.

[34] A. C. Maritim and R. A. Sanders, "Diabetes, oxidative stress, and antioxidants: a review," *Journal of Biochemical & Molecular Toxicology*, vol. 17, no. 1, pp. 24–38, 2010.

[35] G. Guan and S. Lan, "Implications of antioxidant systems in inflammatory bowel disease," *BioMed Research International*, vol. 2018, Article ID 1290179, 7 pages, 2018.

[36] F. Afzal, R. Khurshid, M. Ashraf et al., "Chapter 13 – reactive oxygen species and antioxidants in response to pathogens and wounding," in *Oxidative Damage to Plants*, P. Ahmad, Ed., vol. 13, pp. 397–424, Academic Press, 2014.

[37] E. F. Elstner, "Metabolism of activated oxygen species," in *The Biochemistry of Plants: A Comprehensive Treatise*, D. D. Davies, Ed., vol. 8, pp. 253–315, Elsevier, 1987.

[38] A. Trchounian, M. Petrosyan, and N. Sahakyan, "Plant cell redox homeostasis and reactive oxygen species," in *Redox State as a Central Regulator of Plant-Cell Stress Responses*, D. Gupta, J. Palma, and F. Corpas, Eds., pp. 25–50, Springer, Cham, Switzerland, 2016.

[39] I. Jajic, T. Sarna, and K. Strzalka, "Senescence, stress, and reactive oxygen species," *Plants*, vol. 4, no. 3, pp. 393–411, 2015.

[40] O. Rodrigues, G. Reshetnyak, A. Grondin et al., "Aquaporins facilitate hydrogen peroxide entry into guard cells to mediate ABA- and pathogen-triggered stomatal closure," *Proceedings of the National Acadamy of Sciences of the United States of America*, vol. 114, no. 34, pp. 9200–9205, 2017.

[41] J. Li, R. Zhong, and E. T. Palva, "WRKY70 and its homolog WRKY54 negatively modulate the cell wall-associated defenses to necrotrophic pathogens in Arabidopsis," *PLoS ONE*, vol. 12, no. 8, Article ID e0183731, 2017.

[42] W. Pokora, A. Aksmann, A. Baścik-Remisiewicz et al., "Changes in nitric oxide/hydrogen peroxide content and cell cycle progression: study with synchronized cultures of green alga Chlamydomonas reinhardtii," *Journal of Plant Physiology*, vol. 208, pp. 84–93, 2017.

[43] M. Exposito-Rodriguez, P. P. Laissue, G. Yvon-Durocher, N. Smirnoff, and P. M. Mullineaux, "Photosynthesis-dependent H2O2 transfer from chloroplasts to nuclei provides a high-light signalling mechanism," *Nature Communications*, vol. 8, no. 1, p. 49, 2017.

[44] X. Lv, H. Li, X. Chen et al., "The role of calcium-dependent protein kinase in hydrogen peroxide, nitric oxide and ABA-dependent cold acclimation," *Journal of Experimental Botany*, vol. 69, no. 16, pp. 4127–4139, 2018.

[45] Y. Liu, L. Wang, H. Liu et al., "The antioxidative defense system is involved in the premature senescence in transgenic tobacco (Nicotiana tabacum NC89)," *Biological Research*, vol. 49, no. 1, p. 30, 2016.

[46] A. Krishnamurthy and B. Rathinasabapathi, "Oxidative stress tolerance in plants: novel interplay between auxin and reactive oxygen species signaling," *Plant Signaling and Behavior*, vol. 8, no. 10, Article ID e25761, 2013.

[47] M. Alqurashi, L. Thomas, C. Gehring, and C. Marondedze, "A microsomal proteomics view of H2O2- and ABA-dependent responses," *Proteomes*, vol. 5, no. 3, p. 22, 2017.

[48] X.-J. Xia, Y.-H. Zhou, K. Shi, J. Zhou, C. H. Foyer, and J.-Q. Yu, "Interplay between reactive oxygen species and hormones in the control of plant development and stress tolerance," *Journal of Experimental Botany*, vol. 66, no. 10, pp. 2839–2856, 2015.

[49] J. Zhou, J. Wang, X. Li et al., "H2O2 mediates the crosstalk of brassinosteroid and abscisic acid in tomato responses to heat and oxidative stresses," *Journal of Experimental Botany*, vol. 65, no. 15, pp. 4371–4383, 2014.

[50] J. He, X. Yue, R. Wang, and Y. Zhang, "Ethylene mediates UV-B-induced stomatal closure via peroxidase-dependent hydrogen peroxide synthesis in Vicia faba L.," *Journal of Experimental Botany*, vol. 62, no. 8, pp. 2657–2666, 2011.

[51] X.-M. Ge, H.-L. Cai, L. Xue et al., "Heterotrimeric G protein mediates ethylene-induced stomatal closure via hydrogen peroxide synthesis in Arabidopsis," *Plant Journal for Cell & Molecular Biology*, vol. 82, no. 1, pp. 138–150, 2015.

[52] F. Dang, J. Lin, Y. Chen et al., "A feedback loop between CaWRKY41 and H2O2 coordinates the response to Ralstonia solanacearum and excess cadmium in pepper," *Journal of Experimental Botany*, vol. 70, no. 5, pp. 1581–1595, 2019.

[53] Y. Li, X. L. Cao, Y. Zhu et al., "Osa-miR398b boosts H2O2 production and rice blast disease-resistance via multiple superoxide dismutases," *New Phytologist*, 2019.

[54] F. J. Corpas, D. K. Gupta, and J. M. Palma, "Production sites of reactive oxygen species (ROS) in organelles from plant cells," in *Reactive Oxygen Species and Oxidative Damage in Plants Under Stress*, D. Gupta, J. Palma, and F. Corpas, Eds., pp. 1–22, Springer, Cham, Switzerland, 2015.

[55] K. Das and A. Roychoudhury, "Reactive oxygen species (ROS) and response of antioxidants as ROS-scavengers during environmental stress in plants," *Frontiers in Environmental Science*, vol. 2, p. 53, 2014.

[56] A. Saed-Moucheshi, H. Pakniyat, H. Pirasteh-Anosheh et al., "Chapter 20 - role of ROS as signaling molecules in plants," in *Oxidative Damage to Plants*, P. Ahmad, Ed., pp. 585–620, Academic Press, 2014.

[57] N. Navrot, N. Rouhier, E. Gelhaye, and J.-P. Jacquot, "Reactive oxygen species generation and antioxidant systems in plant mitochondria," *Physiologia Plantarum*, vol. 129, no. 1, pp. 185–195, 2007.

[58] L. A. del Río, L. M. Sandalio, F. J. Corpas, J. M. Palma, and J. B. Barroso, "Reactive oxygen species and reactive nitrogen species in peroxisomes. Production, scavenging, and role in cell signaling," *Plant Physiology*, vol. 141, no. 2, pp. 330–335, 2006.

[59] P. I. Sharma, A. B. Jha, R. S. Dubey, and M. Pessarakli, "Reactive oxygen species, oxidative damage, and antioxidative defense mechanism in plants under stressful conditions," *Journal of Botany*, vol. 2012, Article ID 217037, 26 pages, 2012.

[60] B. C. H. Tripathy and R. Oelmüller, "Reactive oxygen species generation and signaling in plants," *Plant Signaling and Behavior*, vol. 7, no. 12, pp. 1621–1633, 2012.

[61] M. I. Dar, M. I. Naikoo, F. A. Khan et al., "An introduction to reactive oxygen species metabolism under changing climate in plants," in *Reactive Oxygen Species and Antioxidant Systems in Plants: Role and Regulation under Abiotic Stress*, M. Iqbal, R. Khan, and N. A. Khan, Eds., pp. 25–52, Singapore, 2017.

[62] T. Karuppanapandian, J.-C. Moon, C. Kim, K. Manoharan, and W. Kim, "Reactive oxygen species in plants: their generation, signal transduction, and scavenging mechanisms," *Australian Journal of Crop Science*, vol. 5, no. 6, pp. 709–725, 2011.

[63] J. M. Palms, F. J. Corpas, and L. A. Del Río, "Proteome of plant peroxisomes: new perspectives on the role of these organelles in cell biology," *Proteomics*, vol. 9, no. 9, pp. 2301–2312, 2009.

[64] R. Mittler, "Oxidative stress, antioxidants and stress tolerance," *Trends in Plant Science*, vol. 7, no. 9, pp. 405–410, 2002.

[65] X. Hu, A. Zhang, J. Zhang, and M. Jiang, "Abscisic acid is a key inducer of hydrogen peroxide production in leaves of maize plants exposed to water stress," *Plant & Cell Physiology (PCP)*, vol. 47, no. 11, pp. 1484–1495, 2006.

[66] A. Kärkönen and K. Kuchitsu, "Reactive oxygen species in cell wall metabolism and development in plants," *Phytochemistry*, vol. 112, no. 1, pp. 22–32, 2015.

[67] R. K. Kar, "ROS signaling: relevance with site of production and metabolism of ROS," 2015.

[68] X. Jing, P. Hou, Y. Lu et al., "Overexpression of copper/zinc superoxide dismutase from mangrove Kandelia candel in tobacco enhances salinity tolerance by the reduction of reactive oxygen species in chloroplast," *Frontiers in Plant Science*, vol. 6, p. 23, 2015.

[69] N. P. Negi, D. C. Shrivastava, V. Sharma, and N. B. Sarin, "Overexpression of CuZnSOD from Arachis hypogaea alleviates salinity and drought stress in tobacco," *Plant Cell Reports*, vol. 34, no. 7, pp. 1109–1126, 2015.

[70] A. Shafi, R. Chauhan, T. Gill et al., "Expression of SOD and APX genes positively regulates secondary cell wall biosynthesis and promotes plant growth and yield in *Arabidopsis* under salt stress," *Plant Molecular Biology*, vol. 87, no. 6, pp. 615–631, 2015.

[71] Q. Guan, Z. Wang, X. Wang, T. Takano, and S. Liu, "A peroxisomal APX from *Puccinellia tenuiflora* improves the abiotic stress tolerance of transgenic *Arabidopsis thaliana* through decreasing of H_2O_2 accumulation," *Journal of Plant Physiology*, vol. 175, pp. 183–191, 2015.

[72] J. R. Cunha, M. C. L. Neto, F. E. L. Carvalho et al., "Salinity and osmotic stress trigger different antioxidant responses related to cytosolic ascorbate peroxidase knockdown in rice roots," *Environmental & Experimental Botany*, vol. 131, pp. 58–67, 2016.

[73] C. M. Chiang, H. L. Chien, L. F. O. Chen et al., "Overexpression of the genes coding ascorbate peroxidase from Brassica campestris enhances heat tolerance in transgenic Arabidopsis thaliana," *Biologia Plantarum*, vol. 59, no. 2, pp. 305–315, 2015.

[74] Y. Xu, P. Burgess, X. Zhang, and B. Huang, "Enhancing cytokinin synthesis by overexpressing ipt alleviated drought inhibition of root growth through activating ROS-scavenging systems in Agrostis stolonifera," *Journal of Experimental Botany*, vol. 67, no. 6, pp. 1979–1992, 2016.

[75] J. Xu, J. Yang, X. Duan, Y. Jiang, and P. Zhang, "Increased expression of native cytosolic Cu/Zn superoxide dismutase and ascorbate peroxidase improves tolerance to oxidative and chilling stresses in cassava (Manihot esculenta Crantz)," *BMC Plant Biology*, vol. 14, no. 1, p. 208, 2014.

[76] Y. Hu, Q. Wu, S. A. Sprague et al., "Tomato expressing Arabidopsis glutaredoxin gene AtGRXS17 confers tolerance to chilling stress via modulating cold responsive components," *Horticulture Research*, vol. 2, p. 15051, 2015.

[77] R. Fryzova, M. Pohanka, P. Martinkova et al., "Oxidative stress and heavy metals in plants," in *Reviews of Environmental Contamination and Toxicology*, vol. 245 of *Reviews of Environmental Contamination and Toxicology*, pp. 129–156, Springer International Publishing, Cham, Switzerland, 2018.

[78] M. G. Mostofa, Z. I. Seraj, and M. Fujita, “Exogenous sodium nitroprusside and glutathione alleviate copper toxicity by reducing copper uptake and oxidative damage in rice (*Oryza sativa* L.) seedlings,” *Protoplasma*, vol. 251, no. 6, pp. 1373–1386, 2014.

[79] S. B. Agrawal, S. Singh, and M. Agrawal, “Chapter 3 ultraviolet-B induced changes in gene expression and antioxidants in plants,” *Advances in Botanical Research*, vol. 52, pp. 47–86, 2009.

[80] W. Li, Z. Zhu, M. Chern et al., “A natural allele of a transcription factor in rice confers broad-spectrum blast resistance,” *Cell*, vol. 170, no. 1, pp. 114–126, 2017.

[81] A. Wassim, B. R. Ichrak, and A. Saïda, “Putative role of proteins involved in detoxification of reactive oxygen species in the early response to gravitropic stimulation of poplar stems,” *Plant Signaling and Behavior*, vol. 8, no. 1, pp. 1–6, 2013.

[82] M. Nath, D. Bhatt, R. Prasad et al., “Reactive oxygen species (ROS) metabolism and signaling in plant-mycorrhizal association under biotic and abiotic stress conditions,” in *Mycorrhiza - Eco-Physiology, Secondary Metabolites, Nanomaterials*, A. Varma, R. Prasad, and N. Tuteja, Eds., pp. 223–232, Springer, Cham, Switzerland, 2017.

[83] M. M. Gaschler and B. R. Stockwell, “Lipid peroxidation in cell death,” *Biochemical and Biophysical Research Communications*, vol. 482, no. 3, pp. 419–425, 2017.

[84] A. Catalá and M. Díaz, “Editorial: impact of lipid peroxidation on the physiology and pathophysiology of cell membranes,” *Frontiers in Physiology*, vol. 7, p. 423, 2016.

[85] M. Repetto, J. Semprine, and A. Boveris, “Lipid peroxidation: chemical mechanism, biological implications and analytical determination,” in *Lipid Peroxidation*, A. Catala, Ed., Angel Catala IntechOpen, 2012.

[86] E. E. Farmer and M. J. Mueller, “ROS-mediated lipid peroxidation and RES-activated signaling,” *Annual Review of Plant Biology*, vol. 64, pp. 429–450, 2013.

[87] M. Reginato, C. Varela, A. M. Cenzano et al., “Role of polyphenols as antioxidants in native species from argentina under drought and salinization,” in *Reactive Oxygen Species and Oxidative Damage in Plants Under Stress*, D. Gupta, J. Palma, and F. Corpas, Eds., pp. 247–267, Springer, Cham, Switzerland, 2015.

[88] S. Grimm, A. Höhn, and T. Grune, “Oxidative protein damage and the proteasome,” *Amino Acids*, vol. 42, no. 1, pp. 23–38, 2012.

[89] A. Molassiotis, D. Job, V. Ziogas, and G. Tanou, “Citrus plants: a model system for unlocking the secrets of NO and ROS-inspired priming against salinity and drought,” *Frontiers in Plant Science*, vol. 7, p. 553, 2016.

[90] A. Caverzan, A. Casassola, and S. P. Brammer, “Antioxidant responses of wheat plants under stress,” *Genetics and Molecular Biology*, vol. 39, no. 1, pp. 1–6, 2016.

[91] G. Cavallini, A. Sgarbossa, I. Parentini et al., “Dolichol: a component of the cellular antioxidant machinery,” *Lipids*, vol. 51, no. 4, pp. 477–486, 2016.

[92] A. Delaunay-Moisan and C. Appenzeller-Herzog, “The antioxidant machinery of the endoplasmic reticulum: protection and signaling,” *Free Radical Biology & Medicine*, vol. 83, pp. 341–351, 2015.

[93] N. Tuteja, “Mechanisms of high salinity tolerance in plants,” *Methods in Enzymology*, vol. 428, pp. 419–438, 2007.

[94] S. Pandey, D. Fartyal, A. Agarwal et al., “Abiotic stress tolerance in plants: myriad roles of ascorbate peroxidase,” *Frontiers in Plant Science*, vol. 8, p. 581, 2017.

[95] Y. Kadota, K. Shirasu, and C. Zipfel, “Regulation of the NADPH oxidase RBOHD during plant immunity,” *Plant & Cell Physiology (PCP)*, vol. 56, no. 8, pp. 1472–1480, 2015.

[96] W. B. Wang, Y. H. Kim, H. S. Lee et al., “Analysis of antioxidant enzyme activity during germination of alfalfa under salt and drought stresses,” *Plant Physiology & Biochemistry*, vol. 47, no. 7, pp. 570–577, 2009.

[97] F. Xu, L. Shi, W. Chen, S. Cao, X. Su, and Z. Yang, “Effect of blue light treatment on fruit quality, antioxidant enzymes and radical-scavenging activity in strawberry fruit,” *Scientia Horticulturae*, vol. 175, pp. 181–186, 2014.

[98] S. Azarabadi, H. Abdollahi, M. Torabi, Z. Salehi, and J. Nasiri, “ROS generation, oxidative burst and dynamic expression profiles of ROS-scavenging enzymes of superoxide dismutase (*SOD*), catalase (*CAT*) and ascorbate peroxidase (*APX*) in response to *Erwinia amylovora* in pear (*Pyrus communis* L),” *European Journal of Plant Pathology*, vol. 147, no. 2, pp. 279–294, 2017.

[99] W. Wang, X. Zhang, F. Deng, R. Yuan, and F. Shen, “Genome-wide characterization and expression analyses of superoxide dismutase (SOD) genes in Gossypium hirsutum,” *BMC Genomics*, vol. 18, no. 1, p. 376, 2017.

[100] T. Chakradhar, S. Mahanty, R. A. Reddy et al., “Biotechnological perspective of reactive oxygen species (ROS)-mediated stress tolerance in plants,” in *Reactive Oxygen Species and Antioxidant Systems in Plants: Role and Regulation under Abiotic Stress*, M. Khan and N. Khan, Eds., pp. 53–87, Springer, Singapore, 2017.

[101] S.-Y. Shin, M.-H. Kim, Y.-H. Kim, H.-M. Park, and H.-S. Yoon, “Co-expression of monodehydroascorbate reductase and dehydroascorbate reductase from Brassica rapa effectively confers tolerance to freezing-induced oxidative stress,” *Molecules and Cells*, vol. 36, no. 4, pp. 304–315, 2013.

[102] P. Diaz-Vivancos, M. Faize, G. Barba-Espin et al., “Ectopic expression of cytosolic superoxide dismutase and ascorbate peroxidase leads to salt stress tolerance in transgenic plums,” *Plant Biotechnology Journal*, vol. 11, no. 8, pp. 976–985, 2013.

[103] H. S. Marinho, C. Real, L. Cyrne, H. Soares, and F. Antunes, “Hydrogen peroxide sensing, signaling and regulation of transcription factors,” *Redox Biology*, vol. 2, pp. 535–562, 2014.

[104] K.-J. Dietz, “Redox regulation of transcription factors in plant stress acclimation and development,” *Antioxidants & Redox Signaling*, vol. 21, no. 9, pp. 1356–1372, 2014.

[105] P. Woodrow, G. Pontecorvo, L. F. Ciarmiello, M. G. Annunziata, A. Fuggi, and P. Carillo, “Transcription factors and genes in abiotic stress,” in *Crop Stress and Its Management: Perspectives and Strategies*, B. Venkateswarlu, A. Shanker, C. Shanker, and M. Maheswari, Eds., pp. 317–357, Springer, Netherlands, 2012.

[106] P.-F. Yao, C.-L. Li, X.-R. Zhao et al., “Overexpression of a tartary buckwheat gene, FtbHLH3, enhances drought/oxidative stress tolerance in transgenic Arabidopsis,” *Frontiers in Plant Science*, vol. 8, p. 625, 2017.

[107] E. Yue, Z. Liu, C. Li, Y. Li, Q. Liu, and J.-H. Xu, “Overexpression of miR529a confers enhanced resistance to oxidative stress in rice (Oryza sativa L.),” *Plant Cell Reports*, vol. 36, no. 7, pp. 1171–1182, 2017.

[108] Z. H. Shah, H. M. Rehman, T. Akhtar et al., “Redox and ionic homeostasis regulations against oxidative, salinity and drought stress in wheat (a systems biology approach),” *Frontiers in Genetics*, vol. 8, p. 141, 2017.

[109] W.-H. Wang, E.-M. He, Y. Guo, Q.-X. Tong, and H.-L. Zheng, “Chloroplast calcium and ROS signaling networks potentially

facilitate the primed state for stomatal closure under multiple stresses," *Environmental and Experimental Botany*, vol. 122, pp. 85–93, 2016.

[110] H. AbdElgawad, G. Zinta, M. M. Hegab, R. Pandey, H. Asard, and W. Abuelsoud, "High salinity induces different oxidative stress and antioxidant responses in maize seedlings organs," *Frontiers in Plant Science*, vol. 7, p. 580, 2016.

[111] M. N. Siddiqui, M. G. Mostofa, M. M. Akter et al., "Impact of salt-induced toxicity on growth and yield-potential of local wheat cultivars: oxidative stress and ion toxicity are among the major determinants of salt-tolerant capacity," *Chemosphere*, vol. 187, pp. 385–394, 2017.

[112] Y. Zhou, C. Liu, D. Tang et al., "The receptor-like cytoplasmic kinase STRK1 phosphorylates and activates CatC, thereby regulating H2O2 homeostasis and improving salt tolerance in rice," *The Plant Cell*, vol. 30, no. 5, pp. 1100–1118, 2018.

[113] A. L. Furlan, E. Bianucci, and S. Castro, "Signaling role of ROS in modulating drought stress tolerance," in *Drought Stress Tolerance in Plants, Vol 1: Physiology and Biochemistry*, L. S. Tran, Ed., Springer, Cham, Switzerland, 2016.

[114] H. Xiong, J. Yu, J. Miao et al., "Natural variation in OsLG3 increases drought tolerance in rice by inducing ROS scavenging," *Plant Physiology*, vol. 178, no. 1, pp. 451–467, 2018.

[115] M. Yin, Y. Wang, L. Zhang et al., "The Arabidopsis Cys2/His2 zinc finger transcription factor ZAT18 is a positive regulator of plant tolerance to drought stress," *Journal of Experimental Botany*, vol. 68, no. 11, pp. 2991–3005, 2017.

[116] F.-Z. Wang, Q.-B. Wang, S.-Y. Kwon, S.-S. Kwak, and W.-A. Su, "Enhanced drought tolerance of transgenic rice plants expressing a pea manganese superoxide dismutase," *Journal of Plant Physiology*, vol. 162, no. 4, pp. 465–472, 2005.

[117] Y.-Y. Lu, X.-P. Deng, and S.-S. Kwak, "Over expression of CuZn superoxide dismutase (CuZn SOD) and ascorbate peroxidase (APX) in transgenic sweet potato enhances tolerance and recovery from drought stress," *African Journal of Biotechnology*, vol. 9, no. 49, pp. 8378–8391, 2010.

[118] S. Stankovic, P. Kalaba, and A. R. Stankovic, "Biota as toxic metal indicators," *Environmental Chemistry Letters*, vol. 12, no. 1, pp. 63–84, 2014.

[119] R. Juknys, G. Vitkauskaitė, M. Račaitė, and J. Venclovienė, "The impacts of heavy metals on oxidative stress and growth of spring barley," *Open Life Sciences*, vol. 7, no. 2, pp. 299–306, 2012.

[120] M. Shahid, B. Pourrut, C. Dumat, M. Nadeem, M. Aslam, and E. Pinelli, "Heavy-metal-induced reactive oxygen species: phytotoxicity and physicochemical changes in plants," *Reviews of Environmental Contamination and Toxicology*, vol. 232, pp. 1–44, 2014.

[121] M. Valko, H. Morris, and M. T. D. Cronin, "Metals, toxicity and oxidative stress," *Current Medicinal Chemistry*, vol. 12, no. 10, pp. 1161–1208, 2005.

[122] M. Adrees, S. Ali, M. Iqbal et al., "Mannitol alleviates chromium toxicity in wheat plants in relation to growth, yield, stimulation of anti-oxidative enzymes, oxidative stress and Cr uptake in sand and soil media," *Ecotoxicology and Environmental Safety*, vol. 122, pp. 1–8, 2015.

[123] S. S. Sharma and K. J. Dietz, "The relationship between metal toxicity and cellular redox imbalance," *Trends in Plant Science*, vol. 14, no. 1, pp. 43–50, 2009.

[124] C. O. Ogunkunle, M. Varun, I. G. Ogundele, K. S. Olorunmaiye, and M. S. Paul, "Citrus epicarp-derived biochar reduced Cd uptake and ameliorates oxidative stress in young Abelmoschus esculentus (L.) Moench (okra) under low Cd stress," *Bulletin of Environmental Contamination and Toxicology*, vol. 100, no. 6, pp. 827–833, 2018.

[125] A. Schützendübel and A. Polle, "Plant responses to abiotic stresses: heavy metal-induced oxidative stress and protection by mycorrhization," *Journal of Experimental Botany*, vol. 53, no. 372, pp. 1351–1365, 2002.

[126] C. Barta, T. Kálai, K. Hideg, I. Vass, and É. Hideg, "Differences in the ROS-generating efficacy of various ultraviolet wavelengths in detached spinach leaves," *Functional Plant Biology*, vol. 31, no. 1, pp. 23–28, 2004.

[127] E. Abdel Haliem, H. Abdullah, and A. A. Al-Huqail, "Oxidative damage and mutagenic potency of fast neutron and uv-b radiation in pollen mother cells and seed yield of Vicia faba L," *BioMed Research International*, vol. 2013, Article ID 824656, 12 pages, 2013.

[128] C. D. Leasure, H. Tong, G. Yuen, X. Hou, X. Sun, and Z.-H. He, "Root UV-B sensitive2 acts with root UV-B sensitive1 in a root ultraviolet B-sensing pathway," *Plant Physiology*, vol. 150, no. 4, pp. 1902–1915, 2009.

[129] X. Luo, N. Xu, J. Huang et al., "A lectin receptor-like kinase mediates pattern-triggered salicylic acid signaling," *Plant Physiology*, vol. 174, no. 4, pp. 2501–2514, 2017.

[130] D. Couto and C. Zipfel, "Regulation of pattern recognition receptor signalling in plants," *Nature Reviews Immunology*, vol. 16, no. 9, pp. 537–552, 2016.

[131] M. A. Torres and J. L. Dangl, "Functions of the respiratory burst oxidase in biotic interactions, abiotic stress and development," *Current Opinion in Plant Biology*, vol. 8, no. 4, pp. 397–403, 2005.

[132] M. Sagi and R. Fluhr, "Superoxide production by plant homologues of the gp91phox NADPH oxidase. Modulation of activity by calcium and by tobacco mosaic virus infection," *Plant Physiology*, vol. 126, no. 3, pp. 1281–1290, 2001.

[133] Y. Sang and A. P. Macho, "Analysis of PAMP-triggered ROS burst in plant immunity," in *Plant Pattern Recognition Receptors: Methods and Protocols*, L. Shan and P. He, Eds., pp. 143–153, Springer, New York, NY, USA, 2017.

[134] Y. Liu and C. He, "Regulation of plant reactive oxygen species (ROS) in stress responses: learning from AtRBOHD," *Plant Cell Reports*, vol. 35, no. 5, pp. 995–1007, 2016.

[135] Q. Li, G. Ai, D. Shen et al., "A phytophthora capsici effector targets ACD11 binding partners that regulate ROS-mediated defense response in arabidopsis," *Molecular Plant*, vol. 12, no. 4, pp. 565–581, 2019.

[136] D. Arnaud, S. Lee, Y. Takebayashi et al., "Cytokinin-mediated regulation of reactive oxygen species homeostasis modulates stomatal immunity in arabidopsis," *The Plant Cell*, vol. 29, no. 3, pp. 543–559, 2017.

[137] E. Kámán-Tóth, T. Dankó, G. Gullner, Z. Bozsó, L. Palkovics, and M. Pogány, " Contribution of cell wall peroxidase- and NADPH oxidase-derived reactive oxygen species to *Alternaria brassicicola* -induced oxidative burst in *Arabidopsis*," *Molecular Plant Pathology*, vol. 20, no. 4, pp. 485–499, 2019.

[138] S. Gilroy, N. Suzuki, G. Miller et al., "A tidal wave of signals: calcium and ROS at the forefront of rapid systemic signaling," *Trends in Plant Science*, vol. 19, no. 10, pp. 623–630, 2014.

[139] Y. Bai, C. Kissoudis, Z. Yan, R. G. F. Visser, and G. van der Linden, "Plant behaviour under combined stress: tomato responses to combined salinity and pathogen stress," *The Plant Journal*, vol. 93, no. 4, pp. 781–793, 2018.

Hindawi
BioMed Research International
Volume 2019, Article ID 4876078, 10 pages
https://doi.org/10.1155/2019/4876078

Research Article

Milk Fat Globule Membrane Supplementation Promotes Neonatal Growth and Alleviates Inflammation in Low-Birth-Weight Mice Treated with Lipopolysaccharide

Shimeng Huang,[1] Zhenhua Wu,[1] Cong Liu,[1] Dandan Han,[1] Cuiping Feng,[2] Shilan Wang,[1] and Junjun Wang[1]

[1]*State Key Laboratory of Animal Nutrition, College of Animal Science and Technology, China Agricultural University, Beijing 100193, China*
[2]*Department of Obstetrics and Gynecology, China-Japan Friendship Hospital, Beijing 100029, China*

Correspondence should be addressed to Junjun Wang; wangjj@cau.edu.cn

Received 24 February 2019; Accepted 15 April 2019; Published 2 May 2019

Guest Editor: Deguang Song

Copyright © 2019 Shimeng Huang et al. This is an open access article distributed under the Creative Commons Attribution License, which permits unrestricted use, distribution, and reproduction in any medium, provided the original work is properly cited.

Impaired intestinal mucosal integrity and immunity are frequently observed in low-birth-weight (LBW) animals, which lead to inadequate growth and high neonatal mortality. However, the mechanisms of intestinal dysfunction in LBW animals are still unclear. Milk fat globule membrane (MFGM), a protein-lipid complex surrounding the fat globules in milk, has many healthful benefits for animals. Therefore, this study was conducted to explore the effect of MFGM supplementation on intestinal injury and inflammation in LBW mouse pups while being challenged with lipopolysaccharide (LPS). C57BL/6J LBW female neonatal mice were fed on breast milk and divided into four groups, including two normal diet groups (ND; CON group and LPS group) and the diet supplemented with two dosages of MFGM, namely, MFGM100 (ND plus MFGM at 100 mg/kg BW) and MFGM200 (ND plus MFGM at 200 mg/kg BW) from postnatal day (PND) 4 to PND 21. At PND21, pups from the LPS group, MFGM100 group, and MFGM200 group were injected intraperitoneally with LPS while the pups from the CON group were injected with equivalent volume of sterile saline. After 4 h of LPS administration, all pups were slaughtered and then the plasma, mid-ileum, and mid-colon tissue samples were collected. Our results showed that MFGM supplementation promoted the body weight from PND16 to PND21 and attenuated intestinal inflammation manifested by reduced histological damage, decreased secretion of TNF-α, IL-6, IFN-γ, and IL-1β, and improved oxidative stress characterized by increased SOD activity and decreased secretion of MDA. Expression of tight junction proteins (ZO-1, occludin, and claudin-1), MUC1, and MUC2 was increased in MFGM presupplemented groups compared to the LPS-challenged mice with normal diet. Meanwhile, the expression of proinflammatory cytokines and TLRs was decreased by MFGM presupplementation. Collectively, MFGM is a critical nutrient with an ability to improve the growth performance of LBW mouse pups, especially during the LPS challenge, by promoting the intestinal epithelial integrity and inhibiting inflammation through activating of TLR2 and TLR4 signals.

1. Introduction

Infants with low birth weight (LBW) have higher morbidity and mortality than normal birth weight infants during their neonatal period as an outcome of intrauterine growth restriction (IUGR) [1], which was defined as impaired growth and development of the mammalian embryo/fetus or its organs during pregnancy [2]. Despite advanced prenatal care for both mothers and fetuses, approximately 15% of human infants suffer from LBW worldwide [3] and approximately 15-20% of newborn piglets suffer from IUGR [4]. Neonates with LBW show impaired intestinal development, nutrient metabolism, and immune function in both human-beings [5, 6] and animal models [2, 7, 8]. Metabolic programming and the alterations in early physiological may proceed to intestinal dysfunction during the neonatal period [9]. During this critical window, nutrition is the principal contributor to the development of immune and metabolic and the establishment of microbes [10]. Epidemiological studies also indicated that the LBW humans or animals are in high risk of metabolic disease in their later life [11]. Therefore, exploring novel strategies to improve the development of LBW animals or human infants during their suckling period is paramount and has prospects for practical applications.

Milk fat globule membrane (MFGM), derived from the apical surface of mammary epithelial cells and composed of proteins and lipids [12], could protect the milk fat globules and retard their physical destabilization in milk [13, 14]. Several studies have found that supplementation of the MFGM could decrease the infection and inflammation in rodent models [15] and promote the gut mucosal integrity during lipopolysaccharide (LPS)-induced intestine inflammation in male BALB/c adult mice [16], suggesting that MFGM possess a function of antibacterial and anti-inflammatory activity [16]. In addition, MFGM has attracting attentions in related metabolic disorders in high fat diet induced obese mice [17]. MFGM treatment on human infants and neonatal piglets could improve the neurodevelopment and increase the cognitive as compared to the control formula, reaching a similar effect to those of breastfed infants [18–20]. However, previous studies showed no significant effects of MFGM supplementation on weight gain and feed intake of normal birth weight mice during early life and adulthood time [16, 21]. Whether MFGM can promote the growth of LBW newborns or alleviate the intestinal inflammation and injury induced by LPS challenge is unknown. We hypothesized that MFGM supplementation could attenuate the intestinal inflammation and damage in LBW pups, especially while being challenged with LPS. Therefore, the present study was conducted to investigate the protective effect of MFGM against intestinal injury in LBW mice during neonatal growth and LPS challenge, as well as the possible mechanisms.

2. Materials and Methods

2.1. Animals and Treatments. All experiments were performed in accordance with the Health Guide for Care and Use of Laboratory Animals by China Agricultural University. C57BL/6J female mice were obtained from Sibeifu Inc. (Beijing, China). All mice were housed under a 12 h light/dark cycle, a constant temperature (24°C), and 50% humidity. Pregnant mice were housed individually with *ad libitum* access to normal chow diet (KeAoXieLi Feed Co., Ltd., Beijing, China). At birth, pups were spontaneously delivered from female mice and their body weights were recorded. A low-birth-weight (LBW) pup was defined when its birth weight was lower than 2 SD (standard deviations) of the mean birth weight of their littermates [22, 23]. On postnatal day (PND) 4, LBW female mice ($n = 32$) were cross-fostered to adjust the litter size among these groups and were divided into four groups ($n = 8$ pups/group), including two normal diet groups (ND; CON group and LPS group) and the diet supplemented with two dosages of MFGM, namely, MFGM100 (ND plus MFGM at 100 mg/kg BW) and MFGM200 (ND plus MFGM at 200 mg/kg BW) from PND4 to PND 21. Meanwhile, body weight was measured every day and dosage of MFGM administration was adjusted. From PND4 to PND11, pups were administered in a volume averaged 20 μL and 50 μL from PND11 to PND21. At PND21, pups from the LPS group, MFGM100 group and MFGM200 group were injected intraperitoneally with LPS (10 mg/kg BW; E. coli serotype 055: B5, Sigma Chemical) while the pups from the CON group were injected with equivalent amount of sterile saline.

2.2. Tissue Sampling. After 4 h of LPS treatment, all the pups were anesthetized with tribromoethanol (500 mg/kg) and blood was taken to collect plasma and the mid-ileum and mid-colon were dissected. The blood was centrifuged for 15 minutes at 3000 rpm and plasma stored at -20°C. Intestinal tissues (mid-ileum and mid-colon) were harvested immediately and fixed in 4% buffered formalin overnight and processed for routine histological analysis. Meanwhile, the mid-ileum and mid-colon were washed with normal saline, snapped frozen in liquid nitrogen, and stored at -80° C prior to processing for ELISA and qRT-PCR analysis of the cytokines.

2.3. Histological Analysis. The paraformaldehyde-fixed mid-ileum and mid-colon were dehydrated in graded alcohol and embedded in paraffin wax. Then, hematoxylin and eosin (H&E) stained paraffin sections were viewed under bright field on a Zeiss Axio Imager microscope as outlined previously. Microscopic intestinal damage was observed in images using the measurement tool on CaseViewer software at 200x magnification. The degree of intestinal tissue damage was scored as described by Ji et al. [24] and Nishiyama et al. [25], where the extent of epithelial loss on intestinal villi and inflammatory infiltration was evaluated and included in the histopathological examination.

2.4. Plasma Inflammatory Profile Analysis. The concentrations of proinflammatory cytokines (TNF-α, IL-6, and IL-1β) were detected using enzyme-linked immunosorbent assay (ELISA) kits according to the protocol provided (eBioscience, CA, USA). Meanwhile, the concentrations of malonyldialdehyde (MDA) and superoxide dismutase (SOD) were analyzed by kits from Nanjing Jiancheng Bioengineering Institute (Nanjing, China).

2.5. RNA Extraction and Quantitative Real-Time PCR Analysis. Total RNA from mid-ileum and mid-colon were extracted using TRIzol kit (Invitrogen, Carlsbad, CA, USA) following the protocol. cDNA was obtained using PrimeScript™ RT Kit (Takara, Japan). The qPCR was performed according to the SYBR Premix Ex Taq™ II instructions (Takara, Japan). The reaction was performed on a LightCycler® System (Roche, Germany). Primers for RT-qPCR were synthesized by Shanghai Generay Biotech Co., Ltd. (Supplementary Table S1). Amplifications were performed in triplicate for each sample. The relative abundances of target genes to that of the reference gene (β-actin) were calculated according to $2^{-\Delta\Delta \mathrm{Ct}}$ method.

2.6. Statistical Analysis. The statistical significance of differences among means was assessed with one-way analyses of variance (ANOVA) and Student-Newman-Keuls test. All the

Table 1: Effect of MFGM supplementation from postnatal d 4 to d 21 on plasma proinflammatory cytokines, antioxidant enzyme activity, and oxidant products in LPS-challenged LBW mice[a].

Items	CON	LPS	MFGM100	MFGM200
TNF-α (pg/ml)	19.14±1.80a	37.02±4.84c	27.84±3.16b	24.63±2.51b
IL-6 (pg/ml)	227.03±15.68a	325.00±10.70d	282.04±15.97c	251.99±12.94b
IL-1β (pg/ml)	15.56±4.12a	26.01±3.49c	20.14±3.94b	25.69±3.45c
T-SOD (U/ml)	109.69±3.30a	101.45±11.58a	127.18±7.92c	111.70±8.05ab
MDA (nmol/ml)	5.09±0.83	5.38±0.80	5.06±0.83	5.32±0.45

[a] Mean values with their standard errors of the mean (SEM) (n = 8/group). Within a row, means without a common letter (a, b, c, and d) differ ($p < 0.05$).

data are expressed as mean ± standard deviations (SD). $P < 0.05$ was regarded as statistically significant. The Prism software (Graphpad, San Diego, CA, USA) was used for all statistical analyses.

3. Results

3.1. MFGM Supplementation during Neonatal Stage Improved the Growth Performance of LBW Mice. As shown in Figure 1(a), there was no difference in the body weight of LBW mice among the CON, LPS, MFGM100 and MFGM200 groups at beginning of the experiment (PND4). From PND16 to PND21, the body weight of MFGM100 and MFGM200 groups became significantly higher ($P < 0.05$) than that of the PBS gavaged treatments, due to the higher average daily gain with MFGM treatment ($P < 0.05$) (Figure 1(b)). Finally, at PND21, the body weight of pups from the MFGM100 and MFGM200 groups were higher ($P < 0.05$) (Figure 1(c)) than the pups from the normal diet groups (CON and LPS).

3.2. MFGM Presupplementation Prevented the Intestinal Inflammatory Alterations Induced by LPS Challenge in LBW Mice. As shown in Figures 2 and 3, LPS-challenged mice had increased infiltration of inflammatory cells in the mucosal layer of ileal and colonic tissue compared with the control pup (CON), while these harmful effects of LPS were significantly mitigated ($P < 0.05$) in MFGM100 and MFGM200 groups (Figures 2 and 3), suggesting that MFGM supplementation during the neonatal stage alleviated the LPS-induced intestinal injury in LBW pups. Meanwhile, feeding of the 100 mg/kg BW MFGM showed better effects than MFGM200 in mitigating ($P < 0.05$) the LPS-induced intestinal damage.

To gain an insight into the effects of MFGM on secretional level of inflammatory cytokines in LPS-induced LBW pups, we assessed the concentrations of cytokines including TNF-α, IL-6, and IL-1β in the plasma. As shown in Table 1, pups challenged with LPS (LPS group) had higher levels of TNF-α, IL-6, and IL-1β than the CON group ($P < 0.05$), which was largely relieved ($P < 0.05$) by MFGM supplementation, suggesting an effect of MFGM (MFGM100 and MFGM200 group) in inhibiting the secretion of proinflammatory cytokines. Furthermore, the supplementation of 100 mg/kg BW MFGM resulted in significantly lower concentrations of the proinflammatory cytokines (IL-6 and IL-1β) ($P < 0.05$) in pups than the MFGM200 group.

Expression level of the proinflammatory genes such as TNF-α, IL-6, IFN-γ, and IL-1β was provided in Figures 4 and 5. In the ileum (Figure 4(a)), the pups challenged with LPS had higher expression of TNF-α, IL-6, IFN-γ, and IL-1β ($P < 0.05$), compared to the mice in CON group. However, the MFGM presupplementation (MFGM100 or MFGM200 group) relieved ($P < 0.05$) the LPS-induced intestinal damage by decreasing the gene expression levels of TNF-α, IL-6, and IL-1β. In the colon (Figure 5(a)), compared to the controls, the genes expressions of TNF-α and IL-1β were significantly increased ($P < 0.05$) in the LPS group, which were decreased ($P < 0.05$) by MFGM treatment (MFGM100 or MFGM200 group).

3.3. MFGM Presupplementation Prevented the Alterations of Plasma Antioxidant Index and Intestinal Antioxidant Gene Expressions Induced by LPS Challenge in LBW Mice. As shown in Table 1, the plasma activity of T-SOD was increased ($P < 0.05$) by MFGM presupplementation compared with the LPS group, and the MFGM100 had higher ($P < 0.05$) activity of T-SOD than MFGM200. LBW pups fed with 100 mg/kg BW MFGM (MFGM100 group) had also higher ($P < 0.05$) mRNA levels of CAT and SOD as compared with the controls in both ileum and colon, whereas there was no difference ($P > 0.05$) between the LPS group and CON group in ileum (Figures 4(c) and 5(c)). However, the expression level of SOD was lower ($P < 0.05$) in colon of the LPS group than those in other groups.

3.4. MFGM Presupplementation Regulated the Gene Expressions of Tight Junction and Inflammatory Pathway and Prevented Activation of the Toll-Like Receptors Induced by LPS Challenge in LBW Mice. To investigate whether the MFGM supplementation regulates intestinal tight junction, the gene expressions of ZO-1, claudin-1, and occludin in ileum and colon were measured. As shown in Figures 4 and 5, there were significant interactions ($P < 0.05$) between LPS challenge and intestinal tight junction or MUCs genes expression in ileum and colon. After the LBW pups were injected intraperitoneally with LPS for 4 h, presupplementation of MFGM increased the mRNA expression levels of ZO-1, claudin-1, and occludin ($P < 0.05$) (Figures 4(b) and 5(b)). At the same time, the expression of MUC1 and MUC2 was significantly increased ($P < 0.05$) by MFGM administration (MFGM100 and MFGM200 groups) in both ileum and colon (Figures 4(b) and 5(b)), compared with the CON and LPS group.

Compared with the MFGM200 group, MFGM100 group had higher ($P < 0.05$) mRNA expression levels of ZO-1, claudin-1, and occludin in both ileum and colon. After

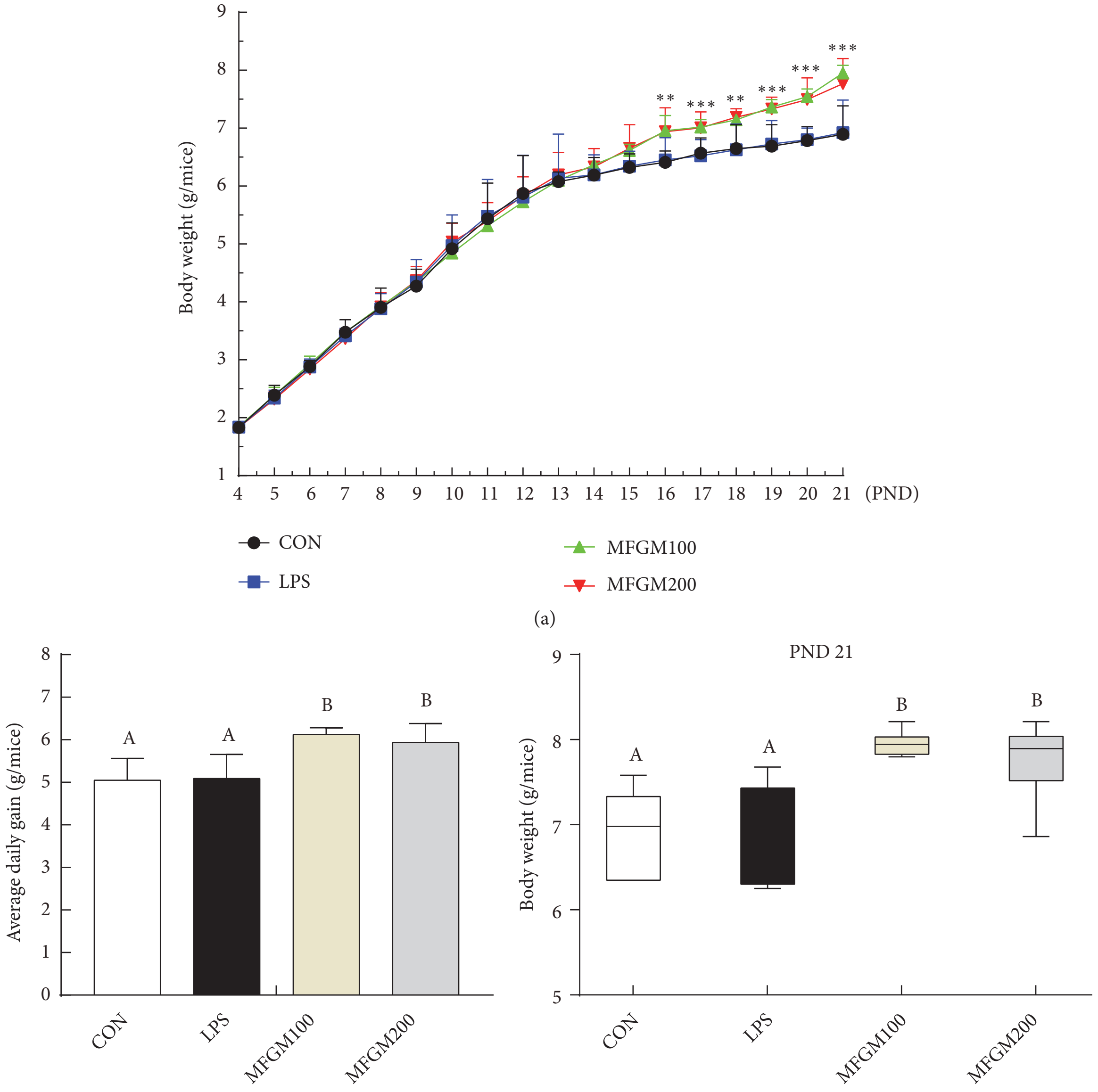

(a)

(b)

(c)

Figure 1: *Effects of MFGM supplementation from postnatal d 4 to d 21 on the body weight gain in LBW mice*. Before LPS being injected, pups were fed with phosphate buffered solution (CON and LPS group), MFGM at 100 mg/kg BW (MFGM100), and 200 mg/kg BW (MFGM200) from PND4 to PND21. (a) Body weight from PND4 to PND21. (b) Average daily gain. (c) The body weight of pups at PND21. Mean values with their standard errors of the mean (SEM) (n = 8 pups/group). Within a row, means without a common letter (A, B, and C) differ ($p < 0.05$).

4 h of LPS injection (Figures 4(d) and 5(d)), the gene expressions of TLR2 and TLR4 in ileum and colon were higher ($P < 0.05$) in LPS group than those in the CON group, while were significantly decreased ($P < 0.05$) by MFGM presupplementation (MFGM100 and MFGM200 groups).

4. Discussion

The gastrointestinal tract (GIT) is of paramount importance in postnatal nutrient digestion and acquisition, where the epithelial barrier of the GIT plays an important function in immune system during neonatal period [26]. However, LBW or IUGR predispose the offspring to malnutrition and endanger the development of intestine and other organs after birth [2, 27, 28]. In current study, our results showed that MFGM supplementation from PND4 to PND21 improved the growth performance of LBW mice, and the MFGM presupplementation mitigated LPS-induced intestinal damage and inflammation at PND21. Our results suggested that this protective effect of MFGM is associated with reduced secretion of proinflammatory cytokines, increased antioxidant enzyme activity, and reduced gene expressions of TLR2 and TLR4.

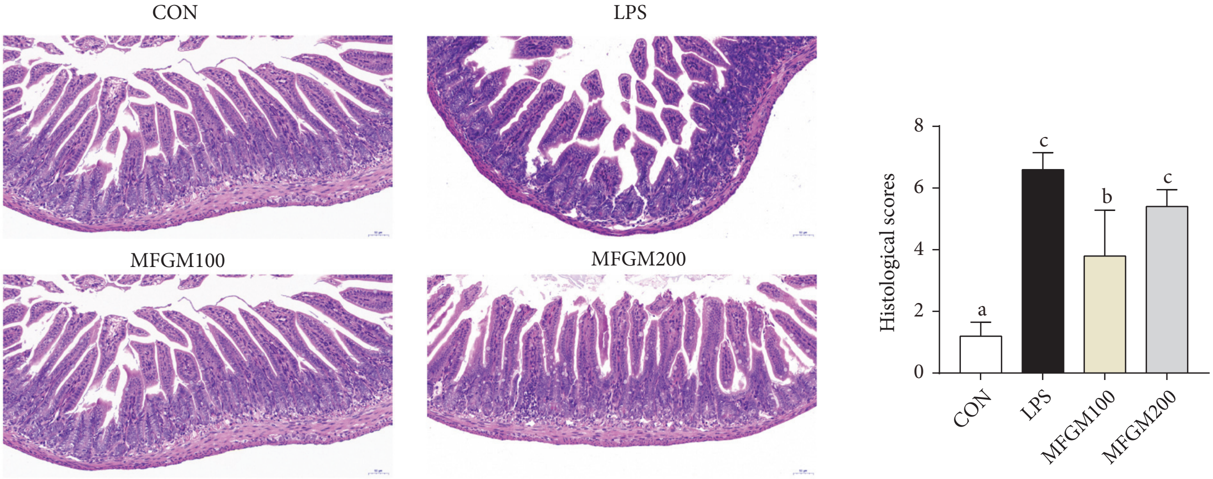

Figure 2: *Effect of MFGM presupplementation from postnatal d 4 to d 21 on ileum damage in LBW mice after LPS challenge*. Mean values with their standard errors of the mean (SEM) (n = 8 pups/group). Within a row, means without a common letter (a, b, and c) differ ($p < 0.05$).

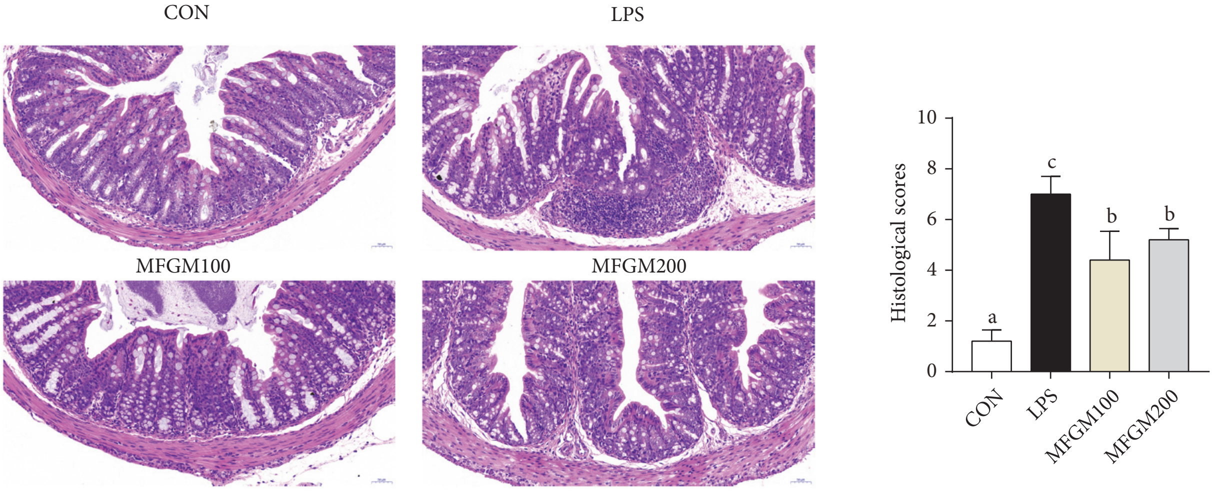

Figure 3: *Effect of MFGM presupplementation from postnatal d 4 to d 21 on colon damage in LBW mice after LPS challenge*. Mean values with their standard errors of the mean (SEM) (n = 8 pups/group). Within a row, means without a common letter (a, b, and c) differ ($p < 0.05$).

To the best of our knowledge, this is the first to report that MFGM supplementation affects the epithelium integrity and toll-like receptors pathway in LBW neonatal mice.

First, MFGM supplementation from PND4 to PND21 improved the weight gain and growth performance in LBW pups. Studies showed that milk contains various bioactive compounds for infants, playing vital roles in regulating GIT development and protecting against infections during the early life of infants [29]. Milk fat globule membrane is a bioactive molecule better for gut health [13]. MFGM supplementation could increase the villus lengths and decrease crypt depths in the neonatal period of mice and, therefore, usually increase the utilization of nutrients [30, 31]. In this study, our results showed that MFGM supplementation (100 mg/kg BW or 200 mg/kg BW) could improve the growth performance of LBW pups from PND16 to PND21, which is consistent with the previous study [22]. The growth-promoting effects during this time zone could be explained by the increased needs of the neonates for growth but gradually decreased amount of secreted breast milk from PND14 [8, 32]. Consequently, further studies need to be done to elucidate how MFGM supplementation affects the growth performance at different ages.

Second, MFGM presupplementation improved the intestinal structure and barrier function and alleviated the intestinal inflammation after LPS challenge. In link with previous studies [33], intestinal villus was damaged by LPS challenge, suggesting that LPS could cause obstruction of intestinal development and histological damage during early life. As mentioned before, the GIT was important for postnatal nutrient acquisition [26]; damage of the intestinal morphology and structure was associated with

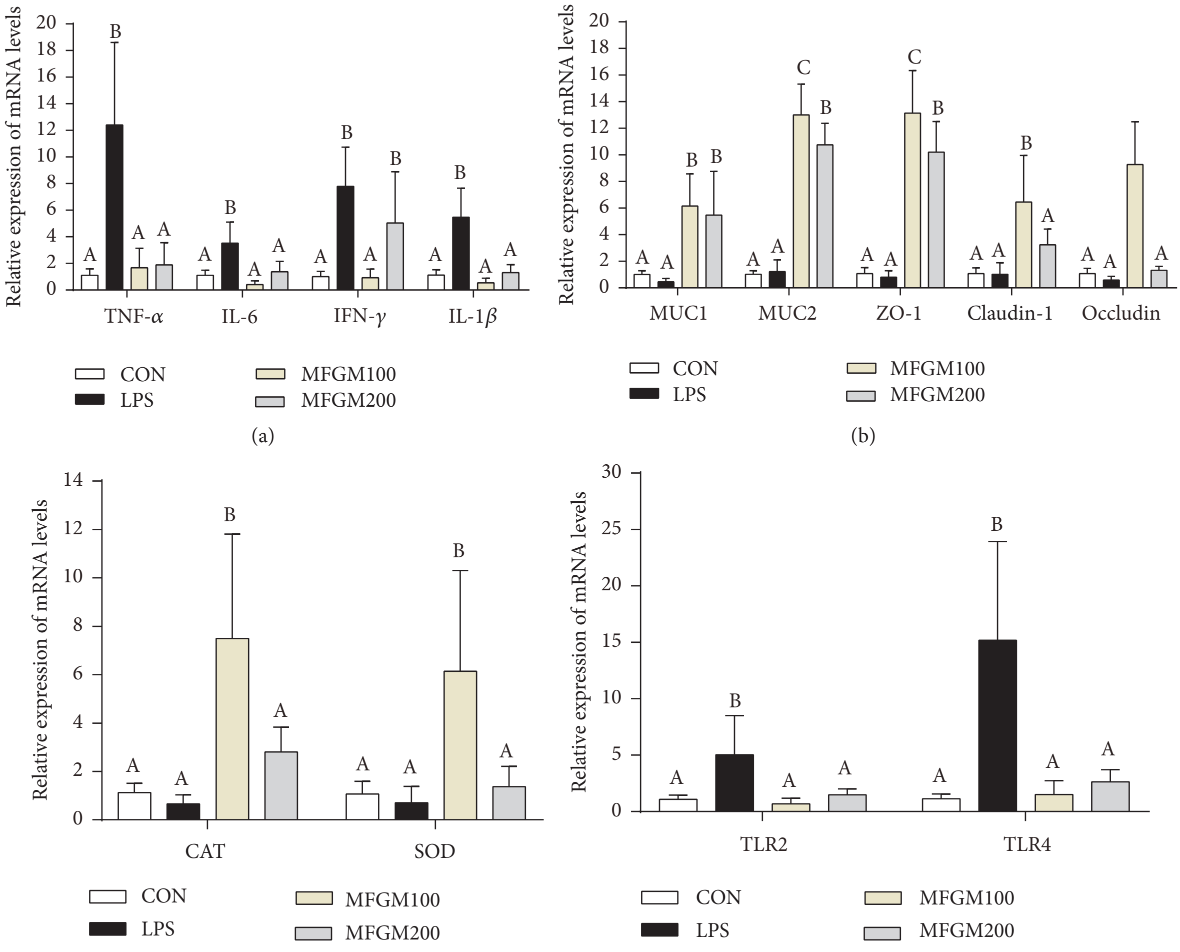

(c) (d)

Figure 4: *Effect of MFGM presupplementation from postnatal d 4 to d 21 on the mRNA abundance of genes in the ileum of LBW mice after LPS challenge*. Mean values with their standard errors of the mean (SEM) (n = 8 pups/group). Within a row, means without a common letter (A, B, and C) differ ($p < 0.05$).

disorder of digestion and absorption. In the current study, our results showed that MFGM presupplementation from PND 4 to PND 21 mitigated the intestinal histological damage and decreased the infiltration of intestinal lamina propria in ileum and colon of LBW mice challenged by LPS, which were in accordance with study carried out by Snow et al. [16]. Previous studies have also found that the intestinal epithelium forms the most important barrier among the internal and external environments [34]. The barrier is maintained by the tight junctions, including ZO-1, occludin, and claudin-1 [8, 33, 35]. Meanwhile, mucins (MUCs), the major components of mucous and a kind of glycoproteins, act as various roles in homeostasis [36] and can protect and lubricate the epithelial mucosa [37]. Our results showed that MFGM presupplementation increased the mRNA levels of ZO-1, claudin-1, and occludin in ileum and colon of the LPS-induced LBW mice and improved the expression of MUC1 and MUC2, in accordance with the study carried out by Snow et al. [16]. These results suggested that MFGM supplementation improves the development of villi morphology, as well as maintaining the intestinal integrity and barrier function by improving the expression levels of tight junction and MUCs.

Third, MFGM presupplementation improved the intestinal oxidative stress during LPS challenge. Due to the suddenly increased oxygen concentration at birth, a large number of oxygen free radicals were produced in the intestine [8, 38–40], ultimately leading to oxidative stress in the GIT of the neonates [38, 41]. According to previous studies [8, 10, 28, 38, 42], the impaired GIT of IUGR neonates is prone to produce a large amount of oxygen free radicals, thereby exacerbating their oxidative stress. The intestinal morphology and barrier of neonatal mice were disturbed by LPS, leading to increased intestinal permeability and damaged tight junction, ultimately resulting in oxidative stress [43–45]. Oxidative stress is frequently associated with intestinal epithelial barrier and inflammatory cytokines, such as tight junction and proinflammatory cytokines, respectively [8, 46]. Previous studies showed that oxidative stress could increase the proinflammatory cytokine (TNF-α) expression and decreased the tight junction mRNA level in the intestinal mucosa of piglets [16, 46, 47], where oxidative stress could be

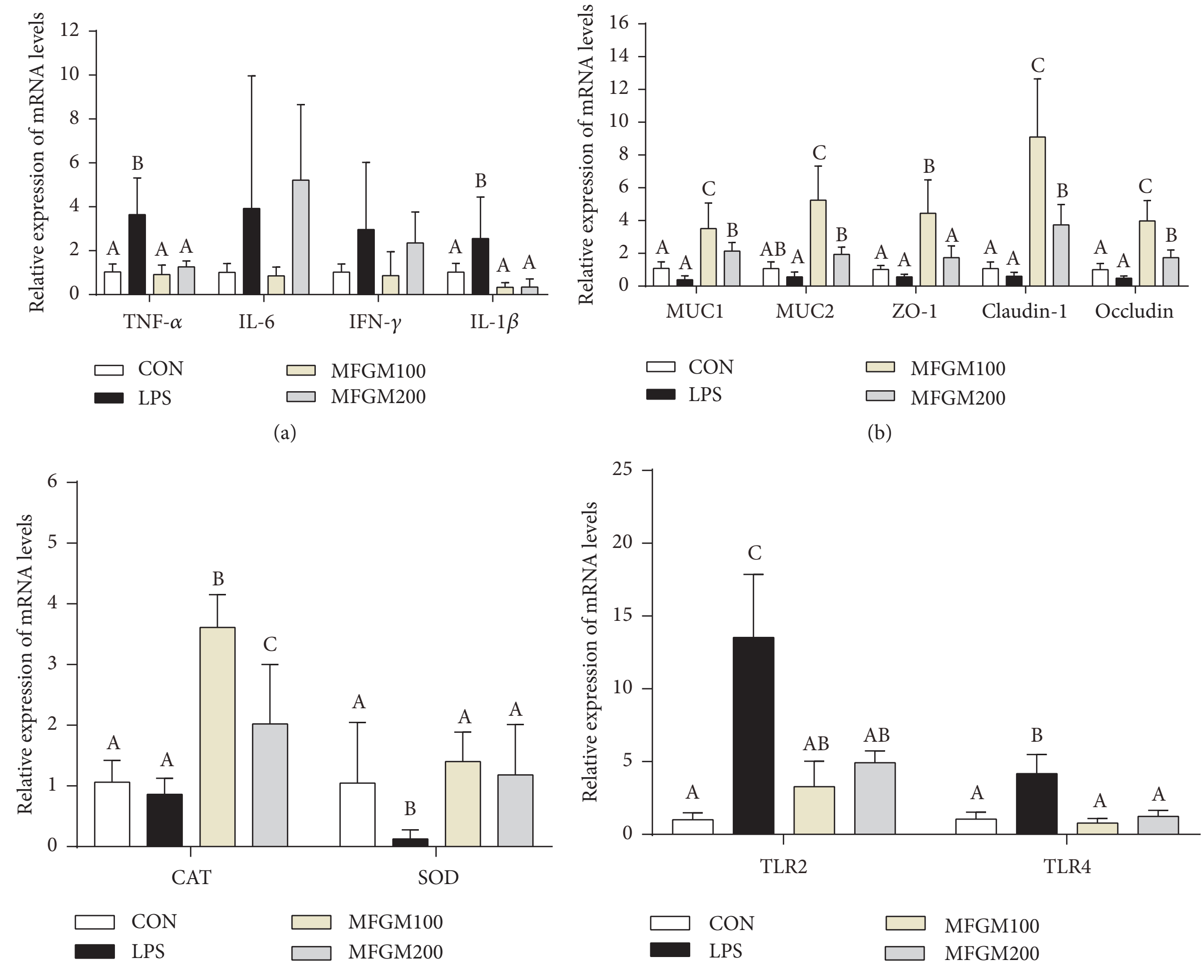

(a)

(b)

(c)

(d)

Figure 5: *Effect of MFGM presupplementation from postnatal d 4 to d 21 on the mRNA abundance of genes in the colon of LBW mice after LPS challenge*. Mean values with their standard errors of the mean (SEM) (n = 8 pups/group). Within a row, means without a common letter (A, B, and C) differ ($p < 0.05$).

a vital factor leading to intestinal dysfunction in LBW piglets [8]. To investigate the oxidative stress in LBW pups after LPS challenge, the redox status of plasma and intestine was determined. In the current study, the plasma concentration of SOD was increased by MFGM presupplementation from PND4 to PND21 in LPS-induced LBW mice. Meanwhile, MFGM presupplementation increased the expression levels of SOD and CAT in both ileum and colon after LPS challenge. It was well known that SOD and CAT are antioxidant enzyme systems to maintain cellular integrity and tissue redox homeostasis [48, 49]. And MDA is the most important biomarker of lipid peroxidation products and may impair intestinal integrity and intestinal permeability [8]. Thus, MFGM supplementation could ameliorate intestinal dysfunction in LBW pups by enhancing the antioxidant systems.

Fourth, mammalian toll-like receptors (TLRs) play a vital role in signal transduction during pathogen invasion, inflammatory, and immune response [50, 51]. Previous studies revealed that TLR2 played important role in inflammatory response [50, 51]. Meanwhile, it was well known that intestinal epithelium cells recognize LPS through the membrane protein of TLR4. LPS can cause intestinal inflammatory and promote the expression levels of proinflammatory cytokines via activation of the TLR4/NF-κB signaling pathway [52]. According to our results, the expression levels of TLR4 and TLR2 were increased in the ileum and colon of LPS-challenged LBW mice, while being significantly abolished by MFGM presupplementation. Meanwhile, the genes expression of proinflammatory cytokines was decreased in the MFGM presupplementation group. In summary, our results showed that MFGM presupplementation decreased the expression level of proinflammatory cytokines by modulating TLR signaling pathway in LPS-induced LBW mice, which was consistent with previous studies [16, 33].

In conclusion, using the LPS-induced neonatal LBW mice model, we demonstrated that MFGM supplementation improved the growth performance of the neonatal mice during their early life. MFGM presupplementation could also alleviate the intestinal damage induced by LPS challenge in LBW mice through increasing the mRNA levels of tight junction, intestinal mucosal barrier, and antioxidant enzyme, while reducing the expression of proinflammatory cytokines by inhibiting TLR2 and TLR4 signaling. This study disclosed that MFGM is a functional nutrient with an ability to improve the growth performance of LBW mouse pups, especially during the LPS challenge, and provides a new approach for treatment or prevention of intestinal inflammatory in LBW neonates during their early life.

Abbreviations

LBW:	Low birth weight
PND:	Postnatal day
LPS:	Lipopolysaccharides
ANOVA:	One-way analysis of variance
IL-1β:	Interleukin-1 beta
IL-6:	Interleukin-6
TNF-α:	Tumor necrosis factor alpha
IFN-γ:	Interferon-gamma
SD:	Standard deviation
CAT:	Catalase
SOD:	Superoxide dismutase
TLRs:	Toll-like receptors
TLR2:	Toll-like receptor 2
TLR4:	Toll-like receptor 4
MUC1:	Mucin 1
MUC2:	Mucin 2.

Data Availability

The data used to support the findings of this study are available from the corresponding author (jkywjj@hotmail.com) upon request.

Conflicts of Interest

The authors declare that the research was conducted in the absence of any commercial or financial relationships that could be construed as potential conflicts of interest.

Authors' Contributions

Junjun Wang, Shimeng Huang, Dandan Han, and Cuiping Feng designed the experiments. Shimeng Huang and Zhenhua Wu conducted the experiment. Shimeng Huang and Zhenhua Wu carried out the experiments and collected the samples. Shimeng Huang, Zhenhua Wu, and Cong Liu performed the analysis of samples. Shimeng Huang, Cong Liu, Dandan Han, Shilan Wang, and Zhenhua Wu analyzed the data. Shimeng Huang, Cong Liu, and Junjun Wang wrote the manuscript. All authors read and approved the final manuscript.

Acknowledgments

The MFGM was provided by the Sanyuan Foods Co. Ltd. in Beijing, China. We thank the experimental animal platform of China Agricultural University in Beijing, China, for the assistances in this study. This work was supported by the Beijing Municipal Natural Science Foundation (S170001), the National Natural Science Foundation of China (31630074), the National Key Research and Development Program of China (2016YFD0500506 and 2018YDF0501002), the 111 Project (B16044), and the Jinxinnong Animal Science Developmental Foundation.

Supplementary Materials

Supplementary Table S1: the information of primer sequences used for qRT-PCR quantification of related genes. *(Supplementary Materials)*

References

[1] M. A. Selak, B. T. Storey, I. Peterside, and R. A. Simmons, "Impaired oxidative phosphorylation in skeletal muscle of intrauterine growth-retarded rats," *American Journal of Physiology-Endocrinology and Metabolism*, vol. 285, no. 1, pp. E130–E137, 2003.

[2] G. Wu, F. W. Bazer, J. M. Wallace, and T. E. Spencer, "Board-invited review: Intrauterine growth retardation: Implications for the animal sciences," *Journal of Animal Science*, vol. 84, no. 9, pp. 2316–2337, 2006.

[3] X. Wang, Y. Zhu, C. Feng et al., "Innate differences and colostrum-induced alterations of jejunal mucosal proteins in piglets with intra-uterine growth restriction," *British Journal of Nutrition*, vol. 119, no. 7, pp. 734–747, 2018.

[4] G. Su, M. S. Lund, and D. Sorensen, "Selection for litter size at day five to improve litter size at weaning and piglet survival rate," *Journal of Animal Science*, vol. 85, no. 6, pp. 1385–1392, 2007.

[5] H. Aly, J. Davies, M. El-Dib, and A. Massaro, "Renal function is impaired in small for gestational age premature infants," *The Journal of Maternal-Fetal and Neonatal Medicine*, vol. 26, no. 4, pp. 388–391, 2013.

[6] A. Tzschoppe, E. Struwe, W. Rascher et al., "Intrauterine growth restriction (IUGR) is associated with increased leptin synthesis and binding capability in neonates," *Clinical Endocrinology*, vol. 74, no. 4, pp. 459–466, 2011.

[7] L. Hu, Y. Liu, C. Yan et al., "Postnatal nutritional restriction affects growth and immune function of piglets with intra-uterine growth restriction," *British Journal of Nutrition*, vol. 114, no. 1, pp. 53–62, 2015.

[8] P. Zheng, Y. Song, Y. Tian et al., "Dietary arginine supplementation affects intestinal function by enhancing antioxidant capacity of a nitric oxide–independent pathway in low-birth-weight piglets," *Journal of Nutrition*, vol. 148, no. 11, pp. 1751–1759, 2018.

[9] S. E. Pinney and R. A. Simmons, "Metabolic programming, Epigenetics, and gestational diabetes mellitus," *Current Diabetes Reports*, vol. 12, no. 1, pp. 67–74, 2012.

[10] N. Li, W. Wang, G. Wu, and J. Wang, "Nutritional support for low birth weight infants: Insights from animal studies," *British Journal of Nutrition*, vol. 117, no. 10, pp. 1390–1402, 2017.

[11] P. D. Gluckman, M. A. Hanson, C. Cooper, and K. L. Thornburg, "Effect of in utero and early-life conditions on adult health and disease," *The New England Journal of Medicine*, vol. 359, no. 1, pp. 61–73, 2008.

[12] X. Zou, Z. Guo, Q. Jin et al., "Composition and microstructure of colostrum and mature bovine milk fat globule membrane," *Food Chemistry*, vol. 185, pp. 362–370, 2015.

[13] C. Bourlieu and M.-C. Michalski, “Structure-function relationship of the milk fat globule,” *Current Opinion in Clinical Nutrition & Metabolic Care*, vol. 18, no. 2, pp. 118–127, 2015.

[14] C. Bourlieu, K. Bouzerzour, S. Ferret-Bernard et al., “Infant formula interface and fat source impact on neonatal digestion and gut microbiota,” *European Journal of Lipid Science and Technology*, vol. 117, no. 10, pp. 1500–1512, 2015.

[15] R. C. Sprong, M. F. E. Hulstein, T. T. Lambers, and R. Van Der Meer, “Sweet buttermilk intake reduces colonisation and translocation of Listeria monocytogenes in rats by inhibiting mucosal pathogen adherence,” *British Journal of Nutrition*, vol. 108, no. 11, pp. 2026–2033, 2012.

[16] D. R. Snow, R. E. Ward, A. Olsen, R. Jimenez-Flores, and K. J. Hintze, “Membrane-rich milk fat diet provides protection against gastrointestinal leakiness in mice treated with lipopolysaccharide,” *Journal of Dairy Science*, vol. 94, no. 5, pp. 2201–2212, 2011.

[17] T. Li, J. Gao, M. Du, J. Song, and X. Mao, “Milk fat globule membrane attenuates high-fat diet-induced obesity by inhibiting adipogenesis and increasing uncoupling protein 1 expression in white adipose tissue of mice,” *Nutrients*, vol. 10, no. 3, pp. 331–342, 2018.

[18] A. T. Mudd, L. S. Alexander, K. Berding et al., “Dietary prebiotics, milk fat globule membrane, and lactoferrin affects structural neurodevelopment in the young piglet,” *Frontiers in Pediatrics*, vol. 4, pp. 1–10, 2016.

[19] N. Timby, E. Domellöf, O. Hernell, B. Lönnerdal, and M. Domellöf, “Neurodevelopment, nutrition, and growth until 12 mo of age in infants fed a low-energy, low-protein formula supplemented with bovine milk fat globule membranes: a randomized controlled trial,” *American Journal of Clinical Nutrition*, vol. 99, no. 4, pp. 860–868, 2014.

[20] O. Hernell, N. Timby, M. Domellöf, and B. Lönnerdal, “Clinical benefits of milk fat globule membranes for infants and children,” *Journal of Pediatrics*, vol. 173, pp. S60–S65, 2016.

[21] G. Bhinder, J. M. Allaire, C. Garcia et al., “Milk fat globule membrane supplementation in formula modulates the neonatal gut microbiome and normalizes intestinal development,” *Scientific Reports*, vol. 7, pp. 1–15, 2017.

[22] L. R. Brink and B. Lönnerdal, “The role of milk fat globule membranes in behavior and cognitive function using a suckling rat pup supplementation model,” *The Journal of Nutritional Biochemistry*, vol. 58, pp. 131–137, 2018.

[23] G. Lin, C. Liu, C. Feng et al., “Metabolomic analysis reveals differences in umbilical vein plasma metabolites between normal and growth-restricted fetal pigs during late gestation,” *Journal of Nutrition*, vol. 142, no. 6, pp. 990–998, 2012.

[24] Y. Ji, Z. Dai, S. Sun et al., “Hydroxyproline attenuates dextran sulfate sodium-induced colitis in mice: involvment of the NF-κB signaling and oxidative stress,” *Molecular Nutrition & Food Research*, vol. 62, no. 21, Article ID e1800494, 2018.

[25] Y. Nishiyama, T. Kataoka, K. Yamato, T. Taguchi, and K. Yamaoka, “Suppression of dextran sulfate sodium-induced colitis in mice by radon inhalation,” *Mediators of Inflammation*, vol. 2012, Article ID 239617, 11 pages, 2012.

[26] R. D’Inca, C. Gras-Le Guen, L. Che, P. T. Sangild, and I. Le Huërou-Luron, “Intrauterine growth restriction delays feeding-induced gut adaptation in term newborn pigs,” *Neonatology*, vol. 99, no. 3, pp. 208–216, 2011.

[27] J. Wang, L. Chen, D. Li et al., “Intrauterine growth restriction affects the proteomes of the small intestine, liver, and skeletal muscle in newborn pigs,” *Journal of Nutrition*, vol. 138, no. 1, pp. 60–66, 2008.

[28] J. Wang, Z. Wu, D. Li et al., “Nutrition, epigenetics, and metabolic syndrome,” *Antioxidants & Redox Signaling*, vol. 17, no. 2, pp. 282–301, 2012.

[29] W. Z. Wu, X. Q. Wang, G. Y. Wu, S. W. Kim, F. Chen, and J. J. Wang, “Differential composition of proteomes in sow colostrum and milk from anterior and posterior mammary glands,” *Journal of Animal Science*, vol. 88, no. 8, pp. 2657–2664, 2010.

[30] K.-Y. Yeh and M. Yeh, “Use of pup in a cup model to study gastrointestinal development: Interaction of nutrition and pituitary hormones,” *Journal of Nutrition*, vol. 123, no. 2, pp. 378–381, 1993.

[31] I. C. Teller, H. Hoyer-Kuhn, H. Brönneke et al., “Complex lipid globules in early-life nutrition improve long-term metabolic phenotype in intra-uterine growth-restricted rats,” *British Journal of Nutrition*, vol. 120, no. 7, pp. 763–776, 2018.

[32] Y. Chen, D. Mou, L. Hu et al., “Effects of maternal low-energy diet during gestation on intestinal morphology, disaccharidase activity, and immune response to lipopolysaccharide challenge in pig offspring,” *Nutrients*, vol. 9, no. 10, 2017.

[33] H. Zhu, H. Wang, S. Wang et al., “Flaxseed oil attenuates intestinal damage and inflammation by regulating necroptosis and TLR4/NOD signaling pathways following lipopolysaccharide challenge in a piglet model,” *Molecular Nutrition & Food Research*, vol. 62, no. 9, Article ID e1700814, 2018.

[34] K. R. Groschwitz and S. P. Hogan, “Intestinal barrier function: molecular regulation and disease pathogenesis,” *The Journal of Allergy and Clinical Immunology*, vol. 124, no. 1, pp. 3–20, 2009.

[35] E. Dejana, “Endothelial cell-cell junctions: happy together,” *Nature Reviews Molecular Cell Biology*, vol. 5, no. 4, pp. 261–270, 2004.

[36] E. Levi, D. S. Klimstra, N. V. Adsay, A. Andea, and O. Basturk, “MUC1 and MUC2 in pancreatic neoplasia,” *Journal of Clinical Pathology*, vol. 57, no. 5, pp. 456–462, 2004.

[37] A. P. Corfield, D. Carroll, N. Myerscough, and C. S. Probert, “Mucins in the gastrointestinal tract in health and disease,” *Frontiers in Bioscience: A Journal and Virtual Library*, vol. 6, pp. D1321–1357, 2001.

[38] W. Wang, J. Degroote, C. Van Ginneken et al., “Intrauterine growth restriction in neonatal piglets affects small intestinal mucosal permeability and mRNA expression of redox-sensitive genes,” *The FASEB Journal*, vol. 30, no. 2, pp. 863–873, 2016.

[39] J. Yin, W. Ren, G. Liu et al., “Birth oxidative stress and the development of an antioxidant system in newborn piglets,” *Free Radical Research*, vol. 47, no. 12, pp. 1027–1035, 2013.

[40] Y. Surh, J. K. Kundu, H. Na, and J. Lee, “Redox-sensitive transcription factors as prime targets for chemoprevention with anti-inflammatory and antioxidative phytochemicals,” *Journal of Nutrition*, vol. 135, no. 12, pp. 2993S–3001S, 2005.

[41] J. K. Friel, R. W. Friesen, S. V. Harding, and L. J. Roberts, “Evidence of oxidative stress in full-term healthy infants,” *Pediatric Research*, vol. 56, no. 6, pp. 878–882, 2004.

[42] X. Wang, G. Lin, C. Liu et al., “Temporal proteomic analysis reveals defects in small-intestinal development of porcine fetuses with intrauterine growth restriction,” *The Journal of Nutritional Biochemistry*, vol. 25, no. 7, pp. 785–795, 2014.

[43] M. Mittal, M. R. Siddiqui, K. Tran, S. P. Reddy, and A. B. Malik, “Reactive oxygen species in inflammation and tissue injury,” *Antioxidants & Redox Signaling*, vol. 20, no. 7, pp. 1126–1167, 2014.

[44] N. R. P. G. Kallapura, X. H. Velasco, B. Hargisand, and G. Tellez, "Mechanisms involved in lipopolysaccharide derived ROS and RNS oxidative stress and septic shock," *Journal of Microbiology Research and Reviews*, vol. 2, pp. 6–11, 2014.

[45] P. Libby, "Inflammatory mechanisms: the molecular basis of inflammation and disease," *Nutrition Reviews*, vol. 65, no. 3, pp. S140–S146, 2007.

[46] B. Rada, P. Gardina, T. G. Myers, and T. L. Leto, "Reactive oxygen species mediate inflammatory cytokine release and EGFR-dependent mucin secretion in airway epithelial cells exposed to Pseudomonas pyocyanin," *Mucosal Immunology*, vol. 4, no. 2, pp. 158–171, 2011.

[47] G. Buonocore, F. Bazzini, F. Proietti et al., "The free radical diseases of newborn," *Journal of Pediatric Biochemistry*, vol. 6, no. 2, pp. 73–78, 2016.

[48] Y. Ozsurekci and K. Aykac, "Oxidative Stress Related Diseases in Newborns," *Oxidative Medicine and Cellular Longevity*, vol. 2016, 2016.

[49] L. He, T. He, S. Farrar, L. Ji, T. Liu, and X. Ma, "Antioxidants maintain cellular redox homeostasis by elimination of reactive oxygen species," *Cellular Physiology and Biochemistry*, vol. 44, no. 2, pp. 532–553, 2017.

[50] E.-K. Jo, "Mycobacterial interaction with innate receptors: TLRs, C-type lectins, and NLRs," *Current Opinion in Infectious Diseases*, vol. 21, no. 3, pp. 279–286, 2008.

[51] S. Janssens and R. Beyaert, "Role of Toll-like receptors in pathogen recognition," *Clinical Microbiology Reviews*, vol. 16, no. 4, pp. 637–646, 2003.

[52] T. Liu, L. Zhang, D. Joo, and S. Sun, "NF-κB signaling in inflammation," *Signal Transduction and Targeted Therapy*, vol. 2, pp. 1–9, 2017.

Hindawi
BioMed Research International
Volume 2019, Article ID 5403761, 9 pages
https://doi.org/10.1155/2019/5403761

Review Article

The Bidirectional Interactions between Resveratrol and Gut Microbiota: An Insight into Oxidative Stress and Inflammatory Bowel Disease Therapy

Yaolian Hu,[1,2,3] Daiwen Chen,[1,2,3] Ping Zheng,[1,2,3] Jie Yu,[1,2,3] Jun He,[1,2,3]
Xiangbing Mao ,[1,2,3] and Bing Yu [1,2,3]

[1] *Key Laboratory of Animal Disease-Resistant Nutrition, Sichuan Province, China*
[2] *Key Laboratory of Animal Disease-Resistant Nutrition, Ministry of Education, China*
[3] *Animal Nutrition Institute, Sichuan Agricultural University, Ya'an, 625014, China*

Correspondence should be addressed to Bing Yu; ybingtian@163.com

Received 27 February 2019; Revised 10 April 2019; Accepted 15 April 2019; Published 24 April 2019

Academic Editor: Gang Liu

Copyright © 2019 Yaolian Hu et al. This is an open access article distributed under the Creative Commons Attribution License, which permits unrestricted use, distribution, and reproduction in any medium, provided the original work is properly cited.

Dysbiosis and oxidative stress in the gut have contributed to the progression of intestinal inflammatory bowel disease (IBD). The current study has reported that enteric bacteria mediate redox homeostasis through the regulation of reactive oxygen species (ROS) production. Resveratrol, one of the most abundant polyphenols, with poor oral bioavailability, is considered as a scavenger of ROS and other free radicals. Recent studies have shown that resveratrol effectively enhances the growth of *Lactococcus lactis* and inhibits the growth of *Enterococcus faecalis*. (1) In terms of the two-way relationship between gut microbiota and resveratrol, resveratrol modulates gut microbiota; (2) in terms of resveratrol biotransformation by gut microbiota, we speculate that gut microbiota could be a target of resveratrol to maintain gut homeostasis. Here, we reviewed the current researches about the cellular signaling pathways in intestinal epithelial cells triggered by gut microbiota in response to oxidative stress. These results suggest that the modulation of the gut microbiota through resveratrol supplementation appears as a promising potential approach for the therapy of inflammatory bowel disease.

1. Introduction

Oxidative stress is caused by an imbalance between reactive oxygen species (ROS) production and cellular antioxidant capacity with accumulation of excessive ROS in cells [1, 2]. Prolonged oxidative stress plays a key role in the initiation and development of inflammatory bowel disease (IBD), including Crohn's disease (CD) and ulcerative colitis (UC) [3–5]. IBD is an inappropriate immune response caused by a range of genetic, microbial, and environmental factors, characterized by chronic inflammation with alternating periods of remissions and relapses [6–8]. Recent evidence further identified that oxidative stress also appears to play a pathogenic role in chronic inflammatory diseases [9–11]. The inhibition of NF-E2 related factor-2 (Nrf2) attenuated anti-oxidative stress pathway and induced inflammation in Nrf2 knockout mice [12]. The intestinal mucosae of patients with IBD have high levels of ROS and decreased antioxidant defense capacity [13]. Excessive production of ROS can increase membrane permeability and cellular stress, finally resulting in the expansion of facultative anaerobic bacteria, gut barrier dysfunction, and inflammation [14, 15]. Moreover, experimental UC in mice is attenuated by antioxidant interventions [16]. Notably, certain intestinal epithelial cells have been reported to rapidly generate ROS in response to microbial signals [17]. The enteric bacteria in the intestinal lumen have been identified as a large source of redox-based effector signals. They regulate multiple cell signaling via promoting the generation of ROS in intestinal epithelial cells, leading to the initiation and progression of many diseases such as IBD, metabolic syndrome, and cancer [18, 19]. The pathogenic bacteria-induced ROS will cause DNA damage in epithelial cells, which can give rise to genomic instability and the dysregulation of epithelial barrier function

[20, 21]. It is generally accepted that chronic inflammation is associated with the inability of the gut immune system to manage microflora and the alteration in the microbial composition in the gastrointestinal tract [22–25]. Furthermore, the metabolism disorder of bacterial fermentation products short-chain fatty acids (SCFAs) may stimulate the immune responses, resulting in increased intestinal epithelial permeability [26]. In all, the ROS overproduction in intestinal epithelial cells is the main consequence of intestinal dysbiosis that can be considered a significant risk factor of IBD. Thus, targeting gut microbiota to improve of oxidative stress and inflammation in the gut could be a promising potential therapy for IBD.

Resveratrol (3,5,4′-trihydroxy-trans-stilbene), a nonflavonoid polyphenol compound, is found in various plants, including *Vitis vinifera*, *Arachis hypogaea*, and *Polygonum cuspidatum* [27, 28]. It is proved to be a potent antioxidant, antibacterial, antiobesity, anti-inflammatory, and anticancer agent in *in vitro* and *in vivo* experiments [29–33]. Notably, resveratrol is considered as a strong scavenger of ROS and other free radicals [34]. In a review, Manach et al. [35] proposed that polyphenols are the major dietary antioxidants present in the colon, as other antioxidants, such as vitamins E and C, are absorbed in the small intestine. Although resveratrol has shown beneficial effects on host metabolism, measurements of plasma levels of the parent drug suggest that resveratrol exhibits poor bioavailability and high rate of metabolism when administered orally [36, 37]. Resveratrol can be metabolized by hepatic and gut microbial enzymes [38, 39]. The metabolite of resveratrol, dihydroresveratrol (DH-RES), is formed in cecum, colon, and rectum by gut microbiota fermentation, and the level of DH-RES is much higher than that of resveratrol. Therefore, this metabolite may also contribute to pharmacological activity in the human large intestine [36]. Besides, many studies have assessed the effect of resveratrol on gut microbiota diversity and composition, including inhibiting the growth of *Enterococcus faecalis*, increasing the Bacteroidetes-to-Firmicutes ratios, and increasing the *Lactobacillus* and *Bifidobacterium* populations [40, 41]. Here, we discuss the cellular signaling triggered by enteric bacteria in host defense and disease development. In addition, we review the reciprocal interactions between resveratrol and gut microbiota, as well as the new evidence for the treatment of oxidative stress and inflammatory bowel disease.

2. The Role of Gut Microbiota in IBD

The intestine contains a complex microbial community of 100 trillion bacterial cells with more than 1,000 species, most of which are beneficial to our health [42, 43]. The gut microbiota affect human metabolism due to their ability to interact with receptors on gut epithelial cells and other effector cells [25, 44, 45]. Given the development of novel diagnostic and therapeutic approaches for human diseases, a critical need exists for a deeper understanding of the underlying mechanism of cellular signaling induced by gut microbiota, and the symbiotic relationship between gut microbiota and the host.

In response to symbiotic microbes, intestinal epithelial cells can use NADPH oxidase (NOX) family to generate ROS, which have been detected in different multicellular organisms [46, 47]. NOX-produced H_2O_2, a major nonradical ROS production in the epithelial cells after the formylated peptide receptors sense and bind to a specific N-formyl group of the *Lactobacilli*, is well documented as a second messenger in signal transduction networks. These changes in H_2O_2 do not cause a significant imbalance between oxidant production and antioxidant levels [48–50]. H_2O_2 generated by the cells can oxidize redox-sensitive cysteine residues on Kelch-like ECH-associated protein 1 (Keap1), resulting in the activation of Nrf2 (see Figure 1) [51]. Of note, high levels of H_2O_2 further oxidize thiolate anions of the peroxidatic Cys to sulfinic (SO_2H) or sulfonic (SO_3H) species. This irreversible modification can lead to cellular damage and oxidative stress [52]. In fact, the diverse biological outcomes of different ROS depend on the specificity and selectivity of ROS on their targets and the compartmentalization of ROS production in cells [53]. *Lactococcus lactis* was found to diminish oxidative stress, by releasing cytoplasmic superoxide dismutase A (SodA) due to host lysozyme-mediated lysis at inflamed colonic sites [54]. Interestingly, *Lactobacillus* appears to modify the natural course of the disease through the upregulation of Nrf2-dependent antioxidant enzymes. *Enterococcus faecalis* near the oxygenated colonic luminal surface generates extracellular O^{2-} at high rate causing intestinal injury [23, 55]. For example, germ-free interleukin-10 knockout (IL-10 KO) mice developed IBD after colonization with *Enterococcus faecalis* but not in the *Lactococcus lactis* colonized mice [56]. Indeed, unlike *Lactococcus lactis*, intestinal ROS overproduction is induced by opportunistic pathogens under certain conditions, and this can aggravate intestinal damage. The bacterial-derived uracil is responsible for dual oxidase (DUOX)-dependent ROS generation in human mucosal epithelial cells, which can lead to overexpression of DUOX2 and oxidative stress in the gut (see Figure 1) [57]. Oxygen radical generation by opportunistic pathogens promotes epithelial cell DNA damage and exacerbates intestine inflammation [58]. Taken together, the microbiota composition is thought to be a major determinant of health and disease of the host, because of the potential of intestinal microbiota to modulate ROS production and antioxidant defense.

Culture-independent methods to analyze the gut microbial composition allow a more detailed understanding of the alterations in gut microbe and IBD. The high levels of mucosa-associated bacteria were detected in those patients [59, 60]. As mentioned above, the studies have demonstrated an association between microbiota composition and redox state of enterocytes; that is, several enteric bacteria could produce extracellular ROS, which may dysregulate intestinal homeostasis (see Figure 1). Moreover, anaerobic intestinal bacteria can downregulate proinflammatory cytokines expression and modulate the host mucosal immune response by inhibiting peroxisome proliferator-activated receptor gamma-mediated nuclear factor-kappaB (NF-κB) activation [61, 62]. Furthermore, anaerobic bacterial fermentation gives rise to the production of SCFAs, including acetate, propionate, and butyrate. SCFAs have been

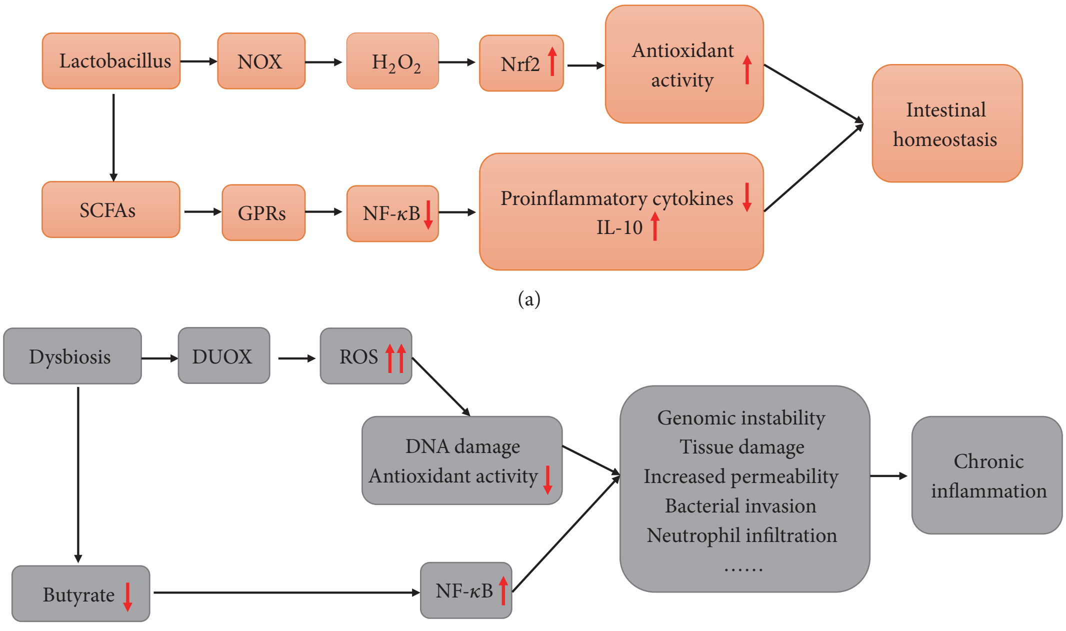

(a)

(b)

Figure 1: The associations between gut microbiota, intestinal inflammation, and oxidative stress. (a) Intestinal homeostasis is associated with enteric bacteria residing in the intestinal lumen. (b) Dysbiosis and oxidative stress in the gut have been shown as contributors of the pathogenesis of intestinal diseases.

suggested to bind to the intestinal epithelial cell-surface G-protein-coupled receptors (GPRs) in the surface of intestinal epithelial cells, such as GPR41, GPR43, and GPR109A [63–66]. They maintain intestinal homeostasis by suppressing NF-κB activation, reducing the production of proinflammatory factors, increasing intestinal mucus synthesis, and decreasing the intestinal epithelial permeability (see Figure 1) [67–69]. Moreover, the metabolism of butyrate in the colonocytes has been shown to drive the oxygen consumption, which leads to a significant reduction of H_2O_2-induced DNA damage [26, 70]. A hypoxic environment induced by the oxygen consumption is also essential for preventing the expansion of facultative anaerobic bacteria. However, continued oxidative stress can alter the colonocyte metabolism and damage the hypoxic environment in large intestine, leading to the expansion of facultative anaerobic bacteria during dysbiosis [71]. The disorder of butyrate metabolism can give rise to an increasing number of macrophages and NF-κB activation in colonocytes of patients with UC (see Figure 1) [72].

Several clinical studies have shown that the fecal microbiota transplantation (FMT) from the healthy donor promotes intestinal microbiota recovery and inflammation resolution in IBD patients [73, 74]. Therefore, a new potent approach by normalizing the intestinal dysbiosis and improving redox imbalance may open a new era for patients with chronic inflammation in the gut.

3. The Relationship between Resveratrol and Gut Microbiota

Resveratrol and its derivatives have shown therapeutic potential for the prevention and treatment of different chronic diseases such as diabetes and IBD [75–78]. Resveratrol, as a phytoalexin, shows antioxidant and anti-inflammatory activities to improve oxidative stress and chronic inflammation [30, 79]. For instance, resveratrol protects the porcine intestinal epithelial cell line (IPEC-J2) from mycotoxin-induced increases in intracellular ROS level and cell damage through the regulation of the Nrf2 signaling pathway [80]. The supplementation with 500 mg resveratrol can reduce levels of proinflammatory mediators and inhibit activity of NF-κB in patients with active UC [81]. However, the low water solubility of resveratrol leads to poor oral bioavailability, which has limits for resveratrol's concentration in plasma [82, 83]. It seems to be a controversial issue about multiple biological activities of resveratrol. It can be speculated that enteric bacteria might represent a major contributor to the effects of resveratrol on the functional modifications of host cells [35, 84]. Using ultrahigh-performance liquid chromatography (UHPLC), coupled with a linear ion trap mass spectrometer, this hypothesis has been confirmed by these determinations of resveratrol metabolites in plasma and colon. Resveratrol was shown to be metabolized into various derivatives by pharmacokinetic profiling [85]. Resveratrol cannot be absorbed in the native form but is present at a very low concentration in plasma in conjugated forms such as sulfate and glucuronide conjugates [86–88]. An accumulation of resveratrol in the large intestine after oral administration has been reported, because of its poor absorption [37, 39]. It has been reported that resveratrol can modulate gut microbial composition while microbiota can also regulate resveratrol biotransformation [89, 90].

However, it is debated whether the effects of resveratrol on gut microbiome modulation are enough to be responsible

Table 1: The effects of resveratrol administration are partly dependent on the gut microbiota.

Animal model	Treatment	Alerted bacterial taxa	Biological effects	Reference
Kunming mice	High-fat diet	Increasing *Lactobacillus* and *Bifidobacterium* abundance; decreasing *Enterococcus faecalis* abundance	Anti-obesity effects	Qiao et al. [41]
Wistar rats	High-fat sucrose diet	Decreasing the abundance of *Parabacteroides* genus	Altering the mRNA expression of tight-junction proteins and inflammation-associated genes	Etxeberria et al. [90]
Fischer F344 rats	DSS	Increasing *Lactobacillus* and *Bifidobacterium* abundance; decreasing *Enterococcus faecalis* abundance	Protecting the colonic mucosa architecture and reducing systemic inflammation markers	Larrosa et al. [84]
Wistar rats	High-fat diet	Inhibiting the growth of *Bacteroides* and *Desulfovibrionaceae sp.*; enhancing the proportion of *Blautia* and *Dorea* in the *Lachnospiraceae* family	Reducing fasting blood glucose levels and increasing the HDL-c levels	Yang et al. [91]
C57BL/6J mice	Choline or Trimethylamine	Increasing the relative abundance of *Bacteroides*, *Lactobacillus*, *Bifidobacterium*, and *Akkermansia*; decreasing the relative abundance of *Prevotella*, uncultured *Ruminococcaceae*, *Anaerotruncus*, *Alistipes*, *Helicobacter*, and uncultured *Peptococcaceae*	Anti-atherosclerosis effects	Chen et al. [93]

for its antioxidant and anti-inflammatory activities and these effects are associated with the improvement of gut diseases in the process of bacteria-mediated ROS overproduction. The definitive mechanisms remain to be obtained. Based on the current evidence, the potential mechanisms will be discussed in the following sections.

3.1. Alterations of the Intestinal Microbiota by Resveratrol. Resveratrol is known to modulate the composition of the gut microbiota with a decrease in opportunistic pathogenic bacteria *in vivo*. Yang et al. [91] showed a significant decrease in the diversity of the gut microbiota and an increase in oxidative stress in high-fat-diet-fed rats compared with that in controls. Resveratrol supplementation (400 mg resveratrol per kg of feed for 8 weeks) increases the population of butyrate producer *Blautia* and *Dorea* in the *Lachnospiraceae* family. However, they noted that the supplementation of resveratrol had no significant influence on the levels of SCFAs. SCFAs are rapidly absorbed in the colon. This may result in the inaccuracy of SCFAs measurement. Additionally, resveratrol administration decreased the population of Bacteroidetes. Most *Bacteroides*, as antibiotic-resistant bacteria, may become highly pathogenic bacteria. The increased levels of *Bacteroides* can result in inflammation [92]. However, Qiao et al. [41] demonstrated that resveratrol supplementation (200 mg/kg/d for 12 weeks) promotes a higher Bacteroidetes-to-Firmicutes ratio in Western-diet-fed mice. Species (rats vs. mice) and/or housing environments (isolated vs. conventional) being studied could potentially explain the differences in specific microbial changes. In addition, the number of *Lactobacillus* and *Bifidobacterium* was significantly increased in resveratrol-fed animals. These genera, as noted above, are closely linked with redox signaling in mucosal epithelial cells, which plays a critical role in maintaining gut homeostasis. Moreover, *Enterococcus faecalis*, which is linked with the high levels of extracellular O^{2-}, was significantly decreased in resveratrol-fed mice. Similarly, recent evidence suggests that the relative abundance of *Bacteroides*, *Lactobacillus*, *Bifidobacterium*, and *Akkermansia* is increased with resveratrol supplementation [93]. Previous studies have also shown that resveratrol administration leads to the increases in the number of *Lactobacilli* and the decrease in the number of *Enterococcus faecalis* and *Escherichia coli* species in high-fat-fed mice. Both *Escherichia coli* and *Enterococcus faecalis* are positively correlated with colonic ROS and MDA levels, while several bacteria such as *Lactobacilli* are significantly associated with colonic T-AOC [94]. Cellular studies also indicated an antimicrobial activity of natural phenolic compounds such as resveratrol and kaempferol, which is a growth inhibition of *Enterococcus faecalis* [95]. Thus, it is speculated that resveratrol alleviates oxidative stress by ROS and subsequent intestinal damage through gut microbiota (see Table 1).

A previous study, using the dextran sulfate sodium-induced colitis (DSS-colitis) rat model, has demonstrated that resveratrol treatment (1 mg/kg/day for 25 days) provides beneficial effects on the colon, including altering the expression of inflammation-associated genes, protecting the colonic mucosa architecture, and modulating intracellular signaling such as NF-κB signaling pathway [84]. In addition, resveratrol administration can also restore normal intestinal microbiota in bacterial composition under DSS treatment. These include some anti-inflammatory gut microbiota, such as *Lactobacilli* and *Bifidobacteria*. More recently, Wellman et al. [96] reported that aged mice with deletion of Sirtuin1 in the intestinal epithelium (SIRT1 iKO mice) exhibited a reduced abundance of *Bacilli*, particularly *Lactobacillus*. Compared to wild-type DSS-colitis mice, aged SIRT1 iKO mice experienced enhanced rectal bleeding, increased colonic shortening, and elevated colonic crypt erosion after DSS challenge. Therefore, SIRT1 has been shown to improve intestinal barrier function and maintain epithelial cell homeostasis. Interestedly, depletion of gut microbiota by the antibiotic cocktail in SIRT1 iKO mice shows minimal colonic spontaneous inflammation. Hence, SIRT1 deficiency-induced intestinal mucosal damage is highly associated with alterations in gut microbiota upon DSS treatment. In view of the proved associations between gut microbiota, intestinal inflammation, and SIRT1, among them, gut microbiota is the main target of SIRT1 to reduce inflammation markers. Resveratrol, a well-known activator of SIRT1, has been shown to significantly increase SIRT1 activity [97, 98]. It has been postulated that health benefits of resveratrol in the gut are largely dependent on the gut microbiota.

3.2. Antioxidant and Anti-Inflammatory Properties of Resveratrol-Derived Microbial Metabolites. As mentioned previously, large quantities of resveratrol and its metabolites were found in the content of gastrointestinal tract in resveratrol-fed animals. The new data suggested that most unabsorbed resveratrol was transformed by gut microbiota into various bioactive metabolites, including DH-RES, 3,4'-dihydroxy-trans-stilbene, and piceid [99]. The enzymes of these bacteria, such as *Slackia equolifaciens* and *Adlercreutzia equolifaciens,* are responsible for the hydrogenation of resveratrol to yield DH-RES [100]. In addition, Jung et al. [101] showed that DH-RES was also synthesized by *E. lenta ATCC 43055* and *B. uniformis ATCC 8492* in vitro. For piceid, studies have demonstrated that *Bacillus cereus* could transform resveratrol into piceid. Of note, though the biological activity of resveratrol is generally attributed to the parent drug, bacterial-derived metabolites have demonstrated equal or similar activity.

In *in vitro* experiments, Lin et al. [102] indicate that 3,4'-dihydroxy-trans-stilbene has cytoprotection function against t-BHP-induced oxidative insult through activating the Keap1-Nrf2-ARE signaling pathway and the downstream antioxidant genes in HepG2 cells. This bacterial metabolite exhibits similar antioxidant effects in gut tract. Moreover, recent evidence has established that DH-RES, whose solubility is higher than that of resveratrol, can participate in the inhibition of NF-κB activity in the cerulein-treated rats [103]. Piceid and resveratrol show similar activities as inhibitors of the lipid peroxidation. Piceid may be more efficacious than resveratrol due to the slow reactivity [104]. Piceid administration can alter the transfer of electrons from NADPH to oxygen and the production of ROS, increasing the availability of GSH and the activity of SOD in rotenone-induced Parkinson's disease rat models [105]. Plant callus is considered as a source of valuable secondary metabolites. Several studies have reported that rice callus suspension culture (RCSC) exhibits strong anti-inflammatory and antiproliferative activity. RCSC treatment has been shown to exhibit strong ROS modulating effects and reduce the effect of inflammation on cell death in cell lines treated with the proinflammatory cytokine cocktail. Piceid, 4-deoxyphloridzin, 5$'$-methoxycurcumin and lupeol, identified through HPLC and mass spectroscopy, are responsible for biological activities of RCSC [106]. Zhu et al. [107] demonstrated that DH-RES, an extract of *Dendrobium*, quenches intracellular ROS in a more efficient manner than vitamin E. In experimental acute pancreatitis rats, the levels of proinflammatory cytokines were notably reduced, and the nuclear expression of NF-κB was remarkably decreased with the administration of DH-RES at 10, 20, and 50mg/kg [108]. Furthermore, Kim et al. [109] recently reported that resveratrol-FMT recipients, which are obese mice receiving FMTs from healthy resveratrol-fed mice, showed significantly lower inflammatory cytokine levels in the colon when compared with Chow-FMT recipients. These results indicated that resveratrol and/or its metabolites suppressed mucosal inflammation through the inhibition of NF-κB activation. Sung et al. [110] previously demonstrated that bacterial-derived metabolites induced by resveratrol are capable of modulating energy metabolism in high-fat high-salt-fed mice receiving FMTs and increasing SCFAs production. It is suggested that the biological activity of metabolites or nonliving microorganisms in the gut is also associated with SCFAs production.

4. Conclusions

Gut microbiota regulates the cellular redox state in the host organism. *Lactobacillus*-mediated ROS production within gut epithelial cells in low levels maintains gut homeostasis, whereas high levels of extracellular O2− induced by *Enterococcus faecalis* cause epithelial cell DNA damage, intestinal injury, and inflammatory responses. Additionally, proinflammatory cytokines expression and the production of SCFAs, which are associated with enteric bacteria, can both modulate the proinflammatory NF-κB signaling pathway.

Resveratrol can inhibit inflammatory disorders through the changes in the gut microbiota. Resveratrol and its microbial metabolites can reduce the increased levels of ROS, activate Nrf2 signaling, and improve oxidative stress. They protect epithelial barrier function and suppress the activation of NF-κB and intestinal inflammation. However, questions remain regarding the bidirectional interactions between resveratrol and gut microbiota, and if these interactions can fully afford resveratrol's biological activity. The mechanism of how resveratrol and its derivatives regulate ROS production in intestinal epithelial cells has yet to be fully elucidated. Considering the health benefits of resveratrol and its metabolic characteristics, the administration of resveratrol is a novel and rational strategy for the treatment of chronic inflammatory diseases.

Conflicts of Interest

There are no conflicts of interest regarding this manuscript.

Acknowledgments

This work was supported by the Key Program of the National Natural Science Foundation of China (31730091). We thank Dr. Hui Yan of Washington University in St. Louis for editing the manuscript and are grateful to Yong Zhang and Jin Wan of Sichuan Agricultural University for helpful advice.

References

[1] A. Abdal Dayem, H.-Y. Choi, J.-H. Kim, and S.-G. Cho, "Role of oxidative stress in stem, cancer, and cancer stem cells," *Cancers*, vol. 2, no. 2, pp. 859–884, 2010.

[2] P. Newsholme, V. F. Cruzat, K. N. Keane, R. Carlessi, and P. I. de Bittencourt, "Molecular mechanisms of ROS production andoxidative stress in diabetes," *Biochemical Journal*, vol. 473, no. 24, pp. 4527–4550, 2016.

[3] J. Li, H. Chen, B. Wang et al., "ZnO nanoparticles act as supportive therapy in DSS-induced ulcerative colitis in mice by maintaining gut homeostasis and activating Nrf2 signaling," *Scientific Reports*, vol. 7, Article ID 43126, 2017.

[4] E. Dudzińska, M. Gryzinska, K. Ognik, P. Gil-Kulik, and J. Kocki, "Oxidative stress and effect of treatment on the oxidation product decomposition processes in IBD," *Oxidative Medicine and Cellular Longevity*, vol. 2018, no. 4, pp. 1–7, 2018.

[5] R. D'Incà, R. Cardin, L. Benazzato, I. Angriman, D. Martines, and G. C. Sturniolo, "Oxidative DNA damage in the mucosa of ulcerative colitis increases with disease duration and dysplasia," *Inflammatory Bowel Diseases*, vol. 10, no. 1, pp. 23–27, 2004.

[6] F. Zhang, Y. Li, X. Wang, S. Wang, and D. Bi, "The impact of lactobacillus plantarum on the gut microbiota of mice with DSS-induced colitis," *BioMed Research International*, vol. 2019, Article ID 3921315, 10 pages, 2019.

[7] Z. Hong and M. Piao, "Effect of quercetin monoglycosides on oxidative stress and gut microbiota diversity in mice with dextran sodium sulphate-induced colitis," *BioMed Research International*, vol. 2018, Article ID 8343052, 7 pages, 2018.

[8] L. Huang, R. Gao, N. Yu, Y. Zhu, Y. Ding, and H. Qin, "Dysbiosis of gut microbiota was closely associated with psoriasis," *SCIENCE CHINA Life Sciences*, 2018.

[9] Guiping Guan and Shile Lan, "Implications of antioxidant systems in inflammatory bowel disease," *BioMed Research International*, vol. 2018, Article ID 1290179, 7 pages, 2018.

[10] J. Chen, B. Yu, D. Chen et al., "Chlorogenic acid improves intestinal barrier functions by suppressing mucosa inflammation and improving antioxidant capacity in weaned pigs," *The Journal of Nutritional Biochemistry*, vol. 59, pp. 84–92, 2018.

[11] L. Kruidenier and H. W. Verspaget, "Oxidative stress as a pathogenic factor in inflammatory bowel disease—radicals or ridiculous?" *Alimentary Pharmacology & Therapeutics*, vol. 16, no. 12, pp. 1997–2015, 2002.

[12] K. L. Cheung, J. H. Lee, T. O. Khor et al., "Nrf2 knockout enhances intestinal tumorigenesis in Apcmin/+ mice due to attenuation of anti-oxidative stress pathway while potentiates inflammation," *Molecular Carcinogenesis*, vol. 53, no. 1, pp. 77–84, 2014.

[13] D. S. Wilson, G. Dalmasso, L. Wang, S. V. Sitaraman, D. Merlin, and N. Murthy, "193 orally delivered thioketal-nanoparticles loaded with TNFα-SiRNA target inflammation and inhibit gene expression in the intestines," *Gastroenterology*, vol. 138, no. 5, pp. S-35–S-36, 2010.

[14] M.-K. Sung, J.-Y. Yeon, S.-Y. Park, J. H. Y. Park, and M.-S. Choi, "Obesity-induced metabolic stresses in breast and colon cancer," *Annals of the New York Academy of Sciences*, vol. 1229, no. 1, pp. 61–68, 2011.

[15] X. Mao, Q. Yang, D. Chen, B. Yu, and J. He, "Benzoic acid used as food and feed additives can regulate gut functions," *BioMed Research International*, vol. 2019, Article ID 5721585, 6 pages, 2019.

[16] A. E. Khodir, E. Said, H. Atif, H. A. ElKashef, and H. A. Salem, "Targeting Nrf2/HO-1 signaling by crocin: Role in attenuation of AA-induced ulcerative colitis in rats," *Biomedicine & Pharmacotherapy*, vol. 110, pp. 389–399, 2019.

[17] A. Kumar, H. Wu, L. S. Collier-Hyams et al., "Commensal bacteria modulate cullin-dependent signaling via generation of reactive oxygen species," *EMBO Journal*, vol. 26, no. 21, pp. 4457–4466, 2007.

[18] W.-J. Lee, "Bacterial-modulated signaling pathways in gut homeostasis," *Science Signaling*, vol. 1, no. 21, article pe24, 2008.

[19] P. J. Daschner, M. B. Grisham, and M. G. Espey, "Redox relationships in gut-microbiome interactions," *Free Radical Biology & Medicine*, vol. 105, pp. 1-2, 2017.

[20] J.-P. Nougayrède, S. Homburg, F. Taieb et al., "Escherichia coli induces DNA double-strand breaks in eukaryotic cells," *Science*, vol. 313, no. 5788, pp. 848–851, 2006.

[21] Y. Liu, H. J. Van Kruiningen, A. B. West, R. W. Cartun, A. Cortot, and J.-F. Colombel, "Immunocytochemical evidence of Listeria, Escherichia coil, and Streptococcus antigens in Crohn's disease," *Gastroenterology*, vol. 108, no. 5, pp. 1396–1404, 1995.

[22] I. Koboziev, W. C. Reinoso, K. L. Furr, and M. B. Grisham, "Role of the enteric microbiota in intestinal homeostasis and inflammation," *Free Radical Biology & Medicine*, vol. 68, pp. 122–133, 2014.

[23] M. M. Huycke, V. Abrams, and D. R. Moore, "Enterococcus faecalis produces extracellular superoxide and hydrogen peroxide that damages colonic epithelial cell DNA," *Carcinogenesis*, vol. 23, no. 3, pp. 529–536, 2002.

[24] P. Bercik, E. Denou, J. Collins et al., "The intestinal microbiota affect central levels of brain-derived neurotropic factor and behavior in mice," *Gastroenterology*, vol. 141, no. 2, article e593, pp. 599–609, 2011.

[25] W. Ren, P. Wang, J. Yan et al., "Melatonin alleviates weanling stress in mice: Involvement of intestinal microbiota," *Journal of Pineal Research*, vol. 64, no. 2, Article ID e12448, 2018.

[26] H. M. Hamer, D. M. A. E. Jonkers, A. Bast et al., "Butyrate modulates oxidative stress in the colonic mucosa of healthy humans," *Clinical Nutrition*, vol. 28, no. 1, pp. 88–93, 2009.

[27] L. Frémont, "Biological effects of resveratrol," *Life Sciences*, vol. 66, no. 8, pp. 663–673, 2000.

[28] J. A. Baur and D. A. Sinclair, "Therapeutic potential of resveratrol: the *in vivo* evidence," *Nature Reviews Drug Discovery*, vol. 5, no. 6, pp. 493–506, 2006.

[29] A. Malhotra, S. Bath, and F. Elbarbry, "An organ system approach to explore the antioxidative, anti-inflammatory, and cytoprotective actions of resveratrol," *Oxidative Medicine and Cellular Longevity*, vol. 2015, Article ID 803971, 15 pages, 2015.

[30] C. A. de La Lastra and I. Villegas, "Resveratrol as an antioxidant and pro-oxidant agent: mechanisms and clinical implications," *Biochemical Society Transactions*, vol. 35, no. 5, pp. 1156–1160, 2007.

[31] M. M.-Y. Chan, "Antimicrobial effect of resveratrol on dermatophytes and bacterial pathogens of the skin," *Biochemical Pharmacology*, vol. 63, no. 2, pp. 99–104, 2002.

[32] S. Y. Kim, Y. J. Jin, Y. S. Choi, and T. Park, "Resveratrol exerts anti-obesity effects via mechanisms involving down-regulation of adipogenic and inflammatory processes in mice," *Biochemical Pharmacology*, vol. 81, no. 11, pp. 1343–1351, 2011.

[33] L. Huminiecki and J. Horbańczuk, "The functional genomic studies of resveratrol in respect to its anti-cancer effects," *Biotechnology Advances*, vol. 36, no. 6, pp. 1699–1708, 2018.

[34] S. S. Leonard, C. Xia, B.-H. Jiang et al., "Resveratrol scavenges reactive oxygen species and effects radical-induced cellular responses," *Biochemical and Biophysical Research Communications*, vol. 309, no. 4, pp. 1017–1026, 2003.

[35] C. Manach, A. Scalbert, C. Morand, C. Rémésy, and L. Jiménez, "Polyphenols: food sources and bioavailability," *American Journal of Clinical Nutrition*, vol. 79, no. 5, pp. 727–747, 2004.

[36] T. Walle, F. Hsieh, M. H. DeLegge, J. E. Oatis Jr., and U. K. Walle, "High absorption but very low bioavailability of oral resveratrol in humans," *Drug Metabolism and Disposition*, vol. 32, no. 12, pp. 1377–1382, 2004.

[37] M. Azorín-Ortuño, M. J. Yañéz-Gascón, and F. J. Pallarés, "Pharmacokinetic study of trans-resveratrol in adult pigs," *Journal of Agricultural and Food Chemistry*, vol. 58, no. 20, pp. 11165–11171, 2010.

[38] A. Amri, J. C. Chaumeil, S. Sfar, and C. Charrueau, "Administration of resveratrol: what formulation solutions to bioavailability limitations?" *Journal of Controlled Release*, vol. 158, no. 2, pp. 182–193, 2012.

[39] X. Vitrac, A. Desmoulière, B. Brouillaud et al., "Distribution of [14C]-trans-resveratrol, a cancer chemopreventive polyphenol, in mouse tissues after oral administration," *Life Sciences*, vol. 72, no. 20, pp. 2219–2233, 2003.

[40] L. Zhao, Q. Zhang, W. Ma, F. Tian, H. Shen, and M. Zhou, "A combination of quercetin and resveratrol reduces obesity in high-fat diet-fed rats by modulation of gut microbiota," *Food & Function*, vol. 8, no. 12, pp. 4644–4656, 2017.

[41] Y. Qiao, J. Sun, S. Xia, X. Tang, Y. Shi, and G. Le, "Effects of resveratrol on gut microbiota and fat storage in a mouse model with high-fat-induced obesity," *Food & Function*, vol. 5, no. 6, pp. 1241–1249, 2014.

[42] J. C. Clemente, L. K. Ursell, L. W. Parfrey, and R. Knight, "The impact of the gut microbiota on human health: an integrative view," *Cell*, vol. 148, no. 6, pp. 1258–1270, 2012.

[43] K. Ikuma, A. W. Decho, and B. Lau, "The extracellular bastions of bacteria™ a biofilm way of life," *Nature Education Knowledge*, vol. 4, no. 2, pp. 2–19, 2013.

[44] S. A. Joyce and C. G. M. Gahan, "The gut microbiota and the metabolic health of the host," *Current Opinion in Gastroenterology*, vol. 30, no. 2, pp. 120–127, 2014.

[45] L. Weichselbaum and O. D. Klein, "The intestinal epithelial response to damage," *Science China Life Sciences*, pp. 1–7, 2018.

[46] R. M. Jones, L. Luo, C. S. Ardita et al., "Symbiotic lactobacilli stimulate gut epithelial proliferation via Nox-mediated generation of reactive oxygen species," *EMBO Journal*, vol. 32, no. 23, pp. 3017–3028, 2013.

[47] J. D. Lambeth, "NOX enzymes and the biology of reactive oxygen," *Nature Reviews Immunology*, vol. 4, no. 3, pp. 181–189, 2004.

[48] S. Voltan, D. Martines, M. Elli et al., "Lactobacillus crispatus M247-derived H2O2 acts as a signal transducing molecule activating peroxisome proliferator activated receptor-gamma in the intestinal mucosa," *Gastroenterology*, vol. 135, no. 4, pp. 1216–1227, 2008.

[49] I. Saxena, S. Srikanth, and Z. Chen, "Cross talk between H2O2and interacting signal molecules under plant stress response," *Frontiers in Plant Science*, vol. 7, no. 22, 2016.

[50] A. S. Neish, "Redox signaling mediated by the gut microbiota," *Free Radical Research*, vol. 47, no. 11, pp. 950–957, 2013.

[51] H. Bryan, *Molecular Investigation of Keap1-Dependent Regulation of the Nrf2 Cell Defence Pathwa*, University of Liverpool, 2014.

[52] M. Zaffagnini, M. Bedhomme, C. H. Marchand, S. Morisse, P. Trost, and S. D. Lemaire, "Redox regulation in photosynthetic organisms: focus on glutathionylation," *Antioxidants & Redox Signaling*, vol. 16, no. 6, pp. 567–586, 2012.

[53] M. Schieber and N. S. Chandel, "ROS function in redox signaling and oxidative stress," *Current Biology*, vol. 24, no. 10, pp. R453–R462, 2014.

[54] S. A. Ballal, P. Veiga, K. Fenn et al., "Host lysozyme-mediated lysis of Lactococcus lactis facilitates delivery of colitis-attenuating superoxide dismutase to inflamed colons," *Proceedings of the National Acadamy of Sciences of the United States of America*, vol. 112, no. 25, pp. 7803–7808, 2015.

[55] C. Reboul, J. Thireau, G. Meyer et al., "Free radical biology and medicine," *Free Radical Biology & Medicine*, vol. 35, no. 5, 2003.

[56] E. Balish and T. Warner, "Enterococcus faecalis induces inflammatory bowel disease in interleukin-10 knockout mice," *The American Journal of Pathology*, vol. 160, no. 6, pp. 2253–2257, 2002.

[57] K.-A. Lee, S.-H. Kim, E.-K. Kim et al., "Bacterial-derived uracil as a modulator of mucosal immunity and gut-microbe homeostasis in drosophila," *Cell*, vol. 153, no. 4, pp. 797–811, 2013.

[58] M. Aslan, Y. Nazligul, C. Bolukbas et al., "Peripheral lymphocyte DNA damage and oxidative stress in patients with ulcerative colitis," *Polskie Archiwum Medycyny Wewnętrznej*, vol. 121, no. 7-8, pp. 223–229, 2011.

[59] C. D. Packey and R. B. Sartor, "Commensal bacteria, traditional and opportunistic pathogens, dysbiosis and bacterial killing in inflammatory bowel diseases," *Current Opinion in Infectious Diseases*, vol. 22, no. 3, pp. 292–301, 2009.

[60] C. W. Png, S. K. Lindén, K. S. Gilshenan et al., "Mucolytic bacteria with increased prevalence in IBD mucosa augment in vitro utilization of mucin by other bacteria," *American Journal of Gastroenterology*, vol. 105, no. 11, pp. 2420–2428, 2010.

[61] V. Tremaroli and F. Bäckhed, "Functional interactions between the gut microbiota and host metabolism," *Nature*, vol. 489, no. 7415, pp. 242–249, 2012.

[62] D. Kelly, J. I. Campbell, T. P. King et al., "Commensal anaerobic gut bacteria attenuate inflammation by regulating nuclear-cytoplasmic shuttling of PPAR-γ and RelA," *Nature Immunology*, vol. 5, no. 1, pp. 104–112, 2004.

[63] M. A. R. Vinolo, G. J. Ferguson, S. Kulkarni et al., "SCFAs induce mouse neutrophil chemotaxis through the GPR43 receptor," *PLoS ONE*, vol. 6, no. 6, 2011.

[64] H. Tazoe, Y. Otomo, I. Kaji, R. Tanaka, S.-I. Karaki, and A. Kuwahara, "Roles of short-chain fatty acids receptors, GPR41 and GPR43 on colonic functions," *Journal of Physiology and Pharmacology*, vol. 59, no. 2, pp. 251–262, 2008.

[65] M. H. Kim, S. G. Kang, J. H. Park, M. Yanagisawa, and C. H. Kim, "Short-chain fatty acids activate GPR41 and GPR43 on intestinal epithelial cells to promote inflammatory responses in mice," *Gastroenterology*, vol. 145, no. 2, pp. 396.e10–406.e10, 2013.

[66] W.-J. Lee and K. Hase, "Gut microbiota-generated metabolites in animal health and disease," *Nature Chemical Biology*, vol. 10, no. 6, pp. 416–424, 2014.

[67] R. Masui, M. Sasaki, Y. Funaki et al., "G protein-coupled receptor 43 moderates gut inflammation through cytokine regulation from mononuclear cells," *Inflammatory Bowel Diseases*, vol. 19, no. 13, pp. 2848–2856, 2013.

[68] T. Hudcovic, R. Štěpánková, J. Cebra, and H. Tlaskalová-Hogenová, "The role of microflora in the development of intestinal inflammation: acute and chronic colitis induced by dextran sulfate in germ-free and conventionally reared immunocompetent and immunodeficient mice," *Folia Microbiologica*, vol. 46, no. 6, pp. 565–572, 2001.

[69] N. Huda-Faujan, A. S. Abdulamir, A. B. Fatimah et al., "The impact of the level of the intestinal short chain Fatty acids in inflammatory bowel disease patients versus healthy subjects," *The Open Biochemistry Journal*, vol. 4, pp. 53–58, 2010.

[70] J. Sauer, K. K. Richter, and B. L. Pool-Zobel, "Physiological concentrations of butyrate favorably modulate genes of oxidative and metabolic stress in primary human colon cells," *The Journal of Nutritional Biochemistry*, vol. 18, no. 11, pp. 736–745, 2007.

[71] Y. Litvak, M. X. Byndloss, and A. J. Bäumler, "Colonocyte metabolism shapes the gut microbiota," *Science*, vol. 362, no. 6418, Article ID eaat9076, 2018.

[72] H. Lührs, T. Gerke, J. G. Müller et al., "Butyrate inhibits NF-κB activation in lamina propria macrophages of patients with ulcerative colitis," *Scandinavian Journal of Gastroenterology*, vol. 37, no. 4, pp. 458–466, 2002.

[73] J. L. Anderson, R. J. Edney, and K. Whelan, "Systematic review: faecal microbiota transplantation in the management of inflammatory bowel disease," *Alimentary Pharmacology & Therapeutics*, vol. 36, no. 6, pp. 503–516, 2012.

[74] C. Staley, A. Khoruts, and M. J. Sadowsky, "Contemporary applications of fecal microbiota transplantation to treat intestinal diseases in humans," *Archives of Medical Research*, vol. 48, no. 8, Article ID S0188440917302357, pp. 766–773, 2017.

[75] M. Kitada, S. Kume, N. Imaizumi, and D. Koya, "Resveratrol improves oxidative stress and protects against diabetic nephropathy through normalization of Mn-SOD dysfunction in AMPK/SIRT1- independent pathway," *Diabetes*, vol. 60, no. 2, pp. 634–643, 2011.

[76] G. Yildiz, Y. Yildiz, P. A. Ulutas, A. Yaylali, and M. Ural, "Resveratrol pretreatment ameliorates TNBS colitis in rats," *Recent Patents on Endocrine Metabolic & Immune Drug Discovery*, vol. 9, no. 2, 2015.

[77] J. L. Barger, T. Kayo, J. M. Vann et al., "Correction: a low dose of dietary resveratrol partially mimics caloric restriction and retards aging parameters in mice," *PLoS ONE*, vol. 3, no. 6, Article ID e2264, 2008.

[78] Y. Shi, J. Zhou, B. Jiang, and M. Miao, "Resveratrol and inflammatory bowel disease," *Annals of the New York Academy of Sciences*, vol. 1403, no. 1, pp. 38–47, 2017.

[79] D. L. L. Ca and I. Villegas, "Resveratrol as an anti-inflammatory and anti-aging agent: mechanisms and clinical implications," *Molecular Nutrition & Food Research*, vol. 49, no. 5, 2010.

[80] J. Yang, C. Zhu, J. Ye et al., "Resveratrol protects porcine intestinal epithelial cells from deoxynivalenol induced damage via the Nrf2 signaling pathway," *Journal of Agricultural and Food Chemistry*, 2018.

[81] J. Yao, J.-Y. Wang, L. Liu et al., "Anti-oxidant effects of resveratrol on mice with DSS-induced ulcerative colitis," *Archives of Medical Research*, vol. 41, no. 4, pp. 288–294, 2010.

[82] A. Mattarei, M. Carraro, M. Azzolini, C. Paradisi, M. Zoratti, and L. Biasutto, "New water-soluble carbamate ester derivatives of resveratrol," *Molecules*, vol. 19, no. 10, pp. 15900–15917, 2014.

[83] I. M. Kapetanovic, M. Muzzio, Z. Huang, T. N. Thompson, and D. L. McCormick, "Pharmacokinetics, oral bioavailability, and metabolic profile of resveratrol and its dimethylether analog, pterostilbene, in rats," *Cancer Chemotherapy and Pharmacology*, vol. 68, no. 3, pp. 593–601, 2011.

[84] M. Larrosa, M. J. Yañéz-Gascón, M. V. Selma et al., "Effect of a low dose of dietary resveratrol on colon microbiota, inflammation and tissue damage in a DSS-induced colitis rat mode," *Journal of Agricultural and Food Chemistry*, vol. 57, no. 6, pp. 2211–2220, 2009.

[85] M. Rotches-Ribalta, M. Urpi-Sarda, R. Llorach et al., "Gut and microbial resveratrol metabolite profiling after moderate long-term consumption of red wine versus dealcoholized red wine in humans by an optimized ultra-high-pressure liquid chromatography tandem mass spectrometry method," *Journal of Chromatography A*, vol. 1265, pp. 105–113, 2012.

[86] H. Colom, I. Alfaras, M. Maijó, M. E. Juan, and J. M. Planas, "Population pharmacokinetic modeling of trans-resveratrol and its glucuronide and sulfate conjugates after oral and intravenous administration in rats," *Pharmaceutical Research*, vol. 28, no. 7, pp. 1606–1621, 2011.

[87] M. Muzzio, Z. Huang, S. C. Hu, W. D. Johnson, D. L. Mccormick, and I. M. Kapetanovic, "Determination of resveratrol and its sulfate and glucuronide metabolites in plasma by LC-MS/MS and their pharmacokinetics in dogs," *Journal of Pharmaceutical Biomedical Analysis*, vol. 59, no. 59, pp. 201–208, 2012.

[88] G. E. S. Faust, D. J. Boocock, K. R. Patel et al., "Oral administration of resveratrol in humans: Evaluation of plasma and urine levels," *Cancer Research*, vol. 65, 2005.

[89] F. Cardona, C. Andrés-Lacueva, S. Tulipani, F. J. Tinahones, and M. I. Queipo-Ortuño, "Benefits of polyphenols on gut microbiota and implications in human health," *The Journal of Nutritional Biochemistry*, vol. 24, no. 8, pp. 1415–1422, 2013.

[90] U. Etxeberria, N. Arias, N. Boqué et al., "Reshaping faecal gut microbiota composition by the intake of trans-resveratrol and quercetin in high-fat sucrose diet-fed rats," *The Journal of Nutritional Biochemistry*, vol. 26, no. 6, pp. 651–660, 2015.

[91] C. Yang, Q. Deng, J. Xu et al., "Sinapic acid and resveratrol alleviate oxidative stress with modulation of gut microbiota in high-fat diet-fed rats," *Food Research International*, vol. 116, pp. 1202–1211, 2019.

[92] M. Li, Y. Wu, Y. Hu, L. Zhao, and C. Zhang, "Initial gut microbiota structure affects sensitivity to DSS-induced colitis in a mouse model," *Science China Life Sciences*, pp. 1–8, 2017.

[93] M.-L. Chen, L. Yi, Y. Zhang et al., "Resveratrol attenuates trimethylamine-N-oxide (TMAO)-induced atherosclerosis by regulating TMAO synthesis and bile acid metabolism via

remodeling of the gut microbiota," *MBio*, vol. 7, no. 2, pp. 02210–02215, 2016.

[94] W. Fang, *Effect of High Fat Diet and Oxidated Protein on Small Mice Gut Flora and Redox State*, JiangNan University, China, 2012.

[95] P. del Valle, M. R. García-Armesto, D. de Arriaga, C. González-Donquiles, P. Rodríquez-Fernández, and J. Rúa, "Antimicrobial activity of kaempferol and resveratrol in binary combinations with parabens or propyl gallate against Enterococcus faecalis," *Food Control*, vol. 61, pp. 213–220, 2016.

[96] A. S. Wellman, M. R. Metukuri, N. Kazgan et al., "Intestinal epithelial sirtuin 1 regulates intestinal inflammation during aging in mice by altering the intestinal microbiota," *Gastroenterology*, vol. 153, no. 3, pp. 772–786, 2017.

[97] M. Lagouge, C. Argmann, Z. Gerhart-Hines et al., "Resveratrol improves mitochondrial function and protects against metabolicdisease by activating SIRT1 and PGC-1α," *Cell*, vol. 127, no. 6, pp. 1109–1122, 2006.

[98] N. L. Price, A. P. Gomes, A. J. Y. Ling et al., "SIRT1 is required for AMPK activation and the beneficial effects of resveratrol on mitochondrial function," *Cell Metabolism*, vol. 15, no. 5, pp. 675–690, 2012.

[99] G. Torres Santiago, J. I. Serrano Contreras, M. E. Meléndez Camargo, and L. G. Zepeda Vallejo, "NMR-based metabonomic approach reveals changes in the urinary and fecal metabolome caused by resveratrol," *Journal of Pharmaceutical and Biomedical Analysis*, vol. 162, pp. 234–241, 2019.

[100] L. M. Bode, D. Bunzel, M. Huch et al., "In vivo and in vitro metabolism of trans-resveratrol by human gut microbiota," *American Journal of Clinical Nutrition*, vol. 97, no. 2, pp. 295–309, 2013.

[101] C. M. Jung, T. M. Heinze, L. K. Schnackenberg et al., "Interaction of dietary resveratrol with animal-associated bacteria," *FEMS Microbiology Letters*, vol. 297, no. 2, pp. 266–273, 2009.

[102] D. Lin, F. Dai, L.-D. Sun, and B. Zhou, "Toward an understanding of the role of a catechol moiety in cancer chemoprevention: the case of copper- and o-quinone-dependent Nrf2 activation by a catechol-type resveratrol analog," *Molecular Nutrition & Food Research*, vol. 59, no. 12, pp. 2395–2406, 2015.

[103] S. W. Tsang, Y.-F. Guan, J. Wang, Z.-X. Bian, and H.-J. Zhang, "Inhibition of pancreatic oxidative damage by stilbene derivative dihydro-resveratrol: implication for treatment of acute pancreatitis," *Scientific Reports*, vol. 6, no. 22859, Article ID 22859, 2016.

[104] S. Fabris, F. Momo, G. Ravagnan, and R. Stevanato, "Antioxidant properties of resveratrol and piceid on lipid peroxidation in micelles and monolamellar liposomes," *Biophysical Chemistry*, vol. 135, no. 1–3, pp. 76–83, 2008.

[105] Y. Chen, D.-Q. Zhang, Z. Liao et al., "Anti-oxidant polydatin (piceid) protects against substantia nigral motor degeneration in multiple rodent models of Parkinson's disease," *Molecular Neurodegeneration*, vol. 10, no. 1, 2015.

[106] K. Driscoll, A. Deshpande, A. Chapp, K. Li, R. Datta, and W. Ramakrishna, "Anti-inflammatory and immune-modulating effects of rice callus suspension culture (RCSC) and bioactive fractions in an in vitro inflammatory bowel disease model," *Phytomedicine*, vol. 57, pp. 364–376, 2019.

[107] Y. Zhu, W.-H. Pan, C. F. Ku, H.-J. Zhang, and S. W. Tsang, "Design, synthesis and evaluation of novel dihydrostilbene derivatives as potential anti-melanogenic skin-protecting agents," *European Journal of Medicinal Chemistry*, vol. 143, pp. 1254–1260, 2018.

[108] Z.-S. Lin, C. F. Ku, Y.-F. Guan et al., "Dihydro-resveratrol ameliorates lung injury in rats with cerulein-induced acute pancreatitis," *Phytotherapy Research*, vol. 30, no. 4, pp. 663–670, 2016.

[109] T. T. Kim, N. Parajuli, M. M. Sung et al., "Fecal transplant from resveratrol-fed donors improves glycaemia and cardiovascular features of the metabolic syndrome in mice," *American Journal of Physiology-Endocrinology and Metabolism*, vol. 315, no. 4, pp. E511–E519, 2018.

[110] M. M. Sung, T. T. Kim, E. Denou et al., "Improved glucose homeostasis in obese mice treated with resveratrol is associated with alterations in the gut microbiome," *Diabetes*, vol. 66, no. 2, pp. 418–425, 2017.

Hindawi
BioMed Research International
Volume 2019, Article ID 4081253, 10 pages
https://doi.org/10.1155/2019/4081253

Research Article

Dittrichia viscosa L. Ethanolic Extract Based Ointment with Antiradical, Antioxidant, and Healing Wound Activities

Wafa Rhimi [1,2], **Raoudha Hlel** [1,2], **Issam Ben Salem** [2], **Abdennacer Boulila** [3], **Ahmed Rejeb** [4], and **Mouldi Saidi** [2]

[1] *Faculté des Sciences de Bizerte, Zarzouna, Université de Carthage, 7021, Tunisia*
[2] *Laboratory of Biotechnology and Nuclear Technology, National Centre of Nuclear Science and Technology (CNSTN), Sidi Thabet Technopark, 2020 Ariana, Tunisia*
[3] *Laboratory of Natural Substances LR10INRAP02, National Institute of Research and Physicochemical Analysis, Biotechpole of Sidi Thabet, Ariana 2020, Tunisia*
[4] *Laboratory of Anatomy Pathology, University of Manouba, National School of Veterinary Medicine, Tunisia*

Correspondence should be addressed to Wafa Rhimi; wafa_rhimi@hotmail.com

Received 18 January 2019; Revised 30 March 2019; Accepted 8 April 2019; Published 22 April 2019

Academic Editor: Gang Liu

Copyright © 2019 Wafa Rhimi et al. This is an open access article distributed under the Creative Commons Attribution License, which permits unrestricted use, distribution, and reproduction in any medium, provided the original work is properly cited.

Dittrichia viscosa which belongs to the *Asteraceae* family is frequently used to treat hematomas and skin disorders in Mediterranean herbal medicine. This study aims to validate its antioxidant effects and its potential on healing wounds. The ethanolic extract of *D. viscosa* leaves was formulated as 2.5% and 5% (w/w) in ointment bases on the beeswax and sesame oil. During this study, the ethanolic *D. viscosa* extract, ointments containing 2.5% and 5% of *D. viscosa* extract, and the vehiculum were assessed for their total phenol content (TPC), caffeoylquinic acid content (CQC), and antioxidant activities using complementary methods (TAC, the DPPH, ABTS, FRAP, and the BCB). The effects on wound healing of obtained ointments were evaluated by excision of the wound in a mice model for 12 days. Subsequently, the excised wound areas were measured at the 3rd, 9th, and 12th days. The skin tissues were isolated for histological studies. The ointments containing *D. viscosa* extract (2.5%, 5%) possessed a considerable TPC, CQC, radical scavenging potential, and antioxidant activities compared to the vehiculum. Treated animals with ointments containing *D. viscosa* extract at 2.5% and 5% showed almost and totally healed wounds compared to the vehiculum and control groups, evidenced by good skin regeneration and reepithelialization. The present work showed the role of *D. viscosa* antioxidants exerted by its polyphenolic compounds, in particular, caffeoylquinic acids, in enhancing wound healing.

1. Introduction

The research to ensure a good quality of wound closure and scarless healing remains a health preoccupation until today [1, 2]. Recent investigation in wound healing mechanisms has evidenced that reactive oxygen species (i.e., hydroxyl OH^-, peroxyl radicals ROO^-, and superoxide anion O_2^-) act as mediator molecules between lymphoid cells and the wound sites as well as defensive molecules against pathogenic microorganisms in the wound area [3, 4]. In fact, basal level of reactive oxygen species (ROS) is necessary to regularize the inflammatory response, construction, and relaxation of blood vessels around wound areas [3, 4]. However, an excess of ROS level causes an imbalance between cellular production of free radicals (oxidants), and antioxidant defenses mechanisms, augmentation in inflammatory response, and inhibition of the wound repair [5, 6].

Indeed, antioxidants are scavengers molecules which are indispensable for neutralization of free radicals and for remediation of ROS damage during healing process [3, 6]. In this sense, plants extracts are emerging as a rich source of active compounds (i.e., triterpenes, flavonoids, polyphenolic, and tannins) for their pertinent properties to prevent from (i) accumulation of free radicals, (ii) oxidation of lipid, and (iii) inhibition of inflammatory disease. The use of several medicinal plants was strongly associated to their antioxidant properties. In particular, *Asteraceae* species plants were frequently used in wound healing treatment due to their high amount of phenolic compounds [7].

Among them, *Dittrichia viscosa* belonging to the genus of *Dittrichia* produced typical secondary metabolites such as phenolic compounds with antioxidant properties [7–10]. The *D. viscosa* was investigated against some free radicals (i.e., DPPH and ABTS). Then, some isolated flavonoids from this plant (i.e., sakuranetin, 7-O-methylaromadendrin, and 3-acetyl-7-O-methylaromadendrin) have been studied for their anti-inflammatory properties by subcutaneous injection of phospholipase A2 (PLA2) into mouse paws. However, to the best of our knowledge, the data about the antioxidant activities of crude extracts is scanty and there are no previous studies about the wound healing activity of *D. viscosa* ethanolic extract. The high use of this plant in traditional medicine in Mediterranean area explains our interest to suggest the usefulness of the extract of *D. viscosa* as wound healing ointment. The aims of the present study are to investigate in vitro the antiradical and antioxidant properties of ointments based on ethanolic *D. viscosa* extract and then to evaluate the potential of these ointments in wound healing in *vivo*.

2. Materials and Methods

2.1. Plant Extraction and Identification of Major Constituents. Fresh leaves of *D. viscosa* were collected from a remote area in Sidi Thabet, province of Ariana, North West of Tunisia. The plant was botanically identified in the Laboratory of Botany and Ornamental Plants, National Institute of Agronomic Research of Tunis. Leaves were air dried and then ground (0.5 mm) using blender mill. The powdered leaf was macerated in ethanol (10:100, w/v (g/ml)) during 48 h. After filtration, the solvent of extract was removed in rotary evaporator (Schwabach, Germany). The dried ethanolic extract was used for all experiments. The constituents of *Dittrichia viscosa* extract were identified using HPLC-DAD-ESI/MS as previously reported [11], and 20 μL of extract at the concentration of 5 mg/mL was used for high performance liquid chromatography analysis (HPLC) using a chromatograph Alliance e2695 (waters, Bedford, MA, USA) equipped with photodiode array detector (PDA), interfaced with a triple quadruple mass spectrometer (MSD 3100, Waters) and an ESI ion source. The separation was carried out on an RP-xTerra MS column (150 × 4.6 mm. i.d., 3.5 μm particles sizes). The phase mobile composed of water (A) and acetonitrile (B), both containing formic acid 0.1% with flow rate of 0.5 mL/min. The following gradient elution was used as follows: 0-40 min, 86 A%; 40-60 min, 85% A; 60-75 min, 100% A; 75-80 min, 86 % A. The mass spectra were acquired over m/z 100-1000 amu. The PDA acquisition wavelength was set in 200-800 nm, and the ionization conditions were performed as follows: electrospray voltage on negative mode of the ion source 25 V and a capillary temperature of 380°C. Mass Lynx v.4.1 software was used for data acquisition and processing. Identification of the constituents was based on their retention times, UV absorption spectra, and mass spectra data, as well as by comparison with authentic standards if available or literature data.

2.2. Ointment Preparation

2.2.1. Formulation of Topical Preparation. Two concentrations of *D. viscosa* ethanolic extract (2.5% and 5% (w:w)) were used to formulate ointments according to the method of Alkafafy et al. [12] with a slight modification. Black sesame oil was heated to 100°C and ethanolic extract was added and homogenized for 3 min using an Ultra-Turrax homogenizer (T25, IKA Works, Wilmington, NC). Then, the liquefied beewax (10% of ointment) was added into the mixture and dispersed for 2 min using Ultra-Turrax homogenizer. Finally, obtained ointments were transferred to cool in ambient temperature and stored for all subsequent studies.

In order to evaluate the total phenol content, the caffeoylquinic acid content, and the antiradical and antioxidant potential of samples, ethanolic extract of *D. viscosa* was solubilized in methanol at a concentration of 1 mg/mL, while ointments containing *D. viscosa* (2.5% and 5%) and ointment base (vehiculum) were solubilized in dimethyl sulfoxide (DMSO) at concentration of 10 mg/mL.

2.2.2. Total Phenol Content (TPC). The TPC was determined using the Folin-Ciocalteu assay according to the method of Meda et al. [13]. Briefly, 500 μL of each dissolved sample (extract, or ointment) was added to 2.5 mL of 10-fold diluted Folin-Ciocalteu reagent. Then, the 2 mL of saturated sodium carbonate (Na_2CO_3) solution (7.5%) was added to the mixture. The reaction mixtures were kept in the dark for 2 h. After the incubation, the samples absorbance was measured at 760 nm against the blank (methanol for extract and DMSO for ointments). All assays were conducted in triplicate and the results were averaged. The gallic acid (GAE) was used as the standard and the results were expressed as milligrams of gallic acid equivalent per gram of sample (extract or ointment) (mg GAE/g sample).

2.2.3. Caffeoylquinic Acid Content (CQC). The CQC in all samples was determined with the molybdate colorimetric assay according to the method of Chan et al. [14]. Briefly, 0.3 mL of appropriate sample solution was added to 2.7 mL of the molybdate reagent (1.65 g sodium molybdate, 0.8 g dipotassium hydrogen phosphate, and 0.79 g potassium dihydrogen phosphate in 100 mL of deionized water). The reaction mixture was incubated for 10 min, and its absorbance was measured at 370 nm against a blank sample. The chlorogenic acid (ChlA) was used as the standard and the results were expressed as milligram of ChlA equivalent per gram of sample (extract or ointment) (mg ChlA/g sample).

2.3. Antiradical and Antioxidant Properties

2.3.1. Total Antioxidant Capacity (TAC) Method. The total antioxidant capacities of extract and ointments were evaluated using the phosphomolybdenum method described by Prieto et al. [15] with slight modifications. An aliquot of 0.25 mL sample solution (with concentration that ranged from 0.01 to 1mg/mL for extract and from 1mg to 10 mg/mL for ointments and vehiculum) was mixed with 0.75 mL of reagent solution (2.4 M of sulfuric acid, 112 mM of sodium phosphate, and 16 mM of ammonium molybdate). Methanol was used as blank. The tubes were capped and incubated in a boiling water bath at 95°C for 90 min. After the samples had cooled in room temperature, the absorbance of each sample was measured in spectrophotometer (Milton Roy, New York, USA) at 695 nm. Total antioxidant capacity was expressed as equivalents of ascorbic acid per gram of sample (extract or ointment) (mg AAE/g of sample).

2.3.2. Diphenyl-1-Picrylhydrazyl (DPPH•) Method. The radical scavenging activity of the extracts against DPPH• free radical was determined by the method of Molyneux et al. [16] with some adjustments. 1 mL of sample solution (with concentration that ranged from 0.01 to 1mg/mL for extract and from 1mg to 10 mg/mL for ointments and vehiculum) was combined with methanol DPPH• solution (0.1 mM). The obtained samples were mixed vigorously and kept in the dark for 60 min.

Subsequently, the absorbance of each sample was measured at 517 nm. The scavenging activity was measured as the decrease in absorbance of the samples versus DPPH• standard solution. BHT synthetic antioxidant was used as positive control. Results were expressed as radical scavenging activity percentage (%) of the DPPH• according to the following equation:

$$\%\ \text{DPPH radical scavenging} = \frac{(\text{Abs}_0 - \text{Abs}_s)}{\text{Abs}_0)} * 100 \quad (1)$$

where Abs_0 represents absorbance value of the control and Abs_s represents absorbance value of sample.

The DPPH radical scavenging activity is shown as EC_{50} (μg sample/mL) which is the concentration necessary to 50% reduction of DPPH• radical.

2.3.3. 2-Azino-Bis-3-Ethylbenzothiazoline-6-Sulfonic Acid (ABTS) Method. The ABTS method is used according to Thaipong et al. [17] for investigating the radical scavenging capacity of each extract. The ABTS• solution was prepared by the dissolving of 7 mM ABTS• in deionized water with potassium persulfate (2.45 mM). The mixture was stranded in the dark at room temperature for 12-16 hours before use. The ABTS• solution was diluted in methanol to an absorbance of 0.7 at 734 nm. For each analysis, a 0.15 mL aliquot of sample solution (with concentration that ranged from 0.01 to 1 mg/mL for extract and from 1mg to 10 mg/mL for ointments and vehiculum) was added to 2.875 mL of ABTS• solution. The samples mixed were incubated for 15 min in the dark, and the absorbance was measured at 734 nm. BHT was used as standard.

Results were expressed in terms of EC_{50} (μg sample/mL), which is the concentration necessary to 50% reduction of ABTS• radical.

2.3.4. Ferric Reducing Antioxidant Power (FRAP) Method. The FRAP assay was performed as described by the method of Gouveia et al. [18]. The stock solutions included 300 mM of acetate buffer (3.1 g of $C_2H_3NaO_23H_2O$ and 16 mL of $C_2H_4O_2$, at pH 3.6, 10 mM of 2, 4, 6-tripyridyl-s-triazine (TPTZ) solution in 10 mM HCl, and 20 mM $FeCl_3$ $6H_2O$ solution). The FRAP solution was prepared by mixing acetate buffer, TPTZ solution, and $FeCl_3$ $6H_2O$ (10:1:1), and it was then warmed at 37°C before using. For each analysis, 0.15 mL of sample solution with concentration that ranged from 0.01 to 1mg/mL for extract and from 1mg to 10 mg/mL for ointments and vehiculum was added to 2,85 mL of the FRAP solution. The absorbance of the reaction mixture was measured at 593 nm after 30 min against methanol as blank. Results were expressed as micromole of Trolox equivalent per gram of sample (μmol TE/g of sample).

2.3.5. ß-Carotene Linoleic Acid (BCB) Method. The ß-carotene bleaching test was determined according to the method described by Velioglu et al. [19]. This assay based on the measure of the discoloration of ß-carotene during the oxidation of linoleic acid at 50°C of temperature. 0.2 mg of ß-carotene, 20 mg of linoleic acid, and 200 mg of tween 40 were dissolved in 0.5 mL of chloroform. After removing chloroform, 100 mL of oxygenated water was added to the final mixture and mixed until homogenization of the emulsion.

4 mL of the prepared mixture was added to 0.2 mL of sample solution (at concentration of 1mg/mL for extract and 10 mg/mL for ointments and vehicle) incubated for 2 h at 50°C in water bath. The BHT was used as a standard. The absorbance of all samples was measured at 470 nm at two times (t = 0 h and t = 2 h). The antioxidant power of sample was evaluated in terms of bleaching of ß-carotene using the following equation:

$$\begin{aligned} &\%\ \text{inhibition of the ß-carotene bleaching radical} \\ &= 100 * \left[1 - \frac{(\text{Abs}_0 - \text{Abs}_t)}{(\text{Abs}_0\,(t=0) - \text{Abs}_t\,(t=0))}\right] \end{aligned} \quad (2)$$

where Abs_0 (t=0) represents absorbance value of control at zero time, Abs_0 represents absorbance value of control after 2 h of incubation, Abs_t (t=0) represents absorbance value of sample at zero time, and Abs_t represents absorbance value of sample after 2 h of incubation.

2.4. Wound Healing Experimental Design. Forty Swiss Webster mice weighing about 20-25g were purchased from the Pasteur Institute of Tunis, Tunisia. Animals were fed with standard pellet diet and were maintained under the following conditions: temperature (25 ± 3°C), humidity (60 ± 5%), and 24-h light/dark cycle. All experiments were performed with respect to the Institutional Animal Ethical Committee. Hair was shaved on the dorsal back of mice and disinfected with ethanol (70 %). Skin wounds of 10 mm diameter circular full-thickness were made on back of mice using a skin biopsy punch. Animals were randomly allocated into four groups (n=10 each): Group 1: negative control; the group had not received any healing creams/ointments. Group 2: the wounded area was treated with the ointment base (vehiculum). Group 3: the wounded area was treated with ointment of *D. viscosa* extract 2.5%. Group 4: the wounded area was treated with ointment of *D. viscosa* extract 5%. Ointments and vehiculum were applied daily during 12 post-wounding days [12]. At 3, 9, and 12 days of wound healing period, the wound area was measured and the percentage wound contraction was calculated according to the following equation:

$$\begin{aligned}&\%\ \text{Wound contraction}\\&=\left(\frac{(\text{Wound area on day"0"} - \text{Wound area on day"n"})}{\text{Wound area on day"0"}}\right)\\&\times 100\end{aligned} \qquad (3)$$

2.5. Histological Studies. On the 3rd, 9th, and 12th days, three mice were randomly taken from each group for the histological examination. The isolated wound tissues from mice skin were formalin fixed and paraffin blocked. Then, 5 μm thick transverse incisions were made by means of a microtome fixed blade. Finally, sections were stained with hematoxylin and eosin (HE) and examined by light microscope (Olympus BX51) and photomicrographed using light microscope (Olympus BX51).

2.6. Statistical Analysis. Results were statistically analysed by using one way analysis of variance (ANOVA) test. Significant differences were set at $p<0.05$. The IBM SPSS 22 was used to perform statistical analysis.

3. Results and Discussion

3.1. HPLC-DAD-MS Analysis of D. viscosa Ethanolic Extract. Based on mass spectrum, UV spectra, and retention time of each peak of HPLC-PDA-ESI-MS/MS data, 29 phenolics were identified in ethanol extract of *D. viscosa* (Table 1).

The dicaffeoylquinic isomers (i.e., chlorogenic acid, 1, 3-O-dicaffeoylquinic acid, 3, 4 dicaffeoylquinic acid, 3, 5-dicaffeoylquinic acid, 1, 5-Di-caffeoylquinic acid, and 4, 5-dicaffeoylquinic acid) and quercetin derivatives (i.e., quercetin-galactosylrhamnoside, rutin-O-pentoside, quercetin-3-O-glucoside, rutin, and dihydroquercetin) were the major phenolic compounds. Others minor compounds (i.e., isoorientin, apigenin-glucoside, myricetin, and isorhamnetin-O-glucuronopyranoside) were also found.

To the best of our knowledge the triterpenoid ganoderic acids were identified for the first time in *D. viscosa* ethanolic extract. In this context, the comparison of our finding with previous results evidenced that the main representative compounds were unchangeable contrary to other minor compounds which are dependent on environmental factors (i.e., territory, temperature, and period of plant collection) and methods of extraction (materials, solvent, and extraction time) [11, 30].

3.2. Contents of Total Phenolics and Caffeoylquinic Acid. The TPC and CQC of *D. viscosa* ethanolic extract leaves, ointment base, and ointments containing 5% and 2.5% of extract have been reported in Table 2.

The TPC and CQC of *D. viscosa* ethanolic extract leaves were comparable to leaves of *Asteraceae* family plant (i.e., *Cynara scolymus L.* and *Cynara cardunculus*) [31–33]. The TPC and CQC values of ointment containing 2.5% and 5% of *D. viscosa* ethanolic extract showed that there is no considerable loss in amount of both phenolic and caffeoylquinic acid compounds during the formulation of ointments. In this sense, it has been reported that the CQC are slightly modifiable after heating at temperature of 100°C for 5 min [34].

3.3. Antiradical and Antioxidant Properties. The TAC, The DPPH, ABTS, FRAP, and the BCB of *D. viscosa* ethanolic extract, ointment base, and ointment containing 5% and 2.5% of extract have been represented in Table 3.

The results of antiradical and antioxidants screening of *D. viscosa* leaves showed that our findings were comparable to other plants of *Asteraceae* family. In fact, the TAC, EC_{50} (DPPH), EC_{50} (ABTS), FRAP, and BCB values were in the range of other *Asteraceae* plants from different country where the TAC ranged from 110.03 to 194.64 mg AAE/g extract [35, 36], and EC_{50} (DPPH) values ranged from 100 to 250 μg/mL [37]. EC_{50} (ABTS) ranged from 180 to 200 μg/mL. FRAP values were ranging from 12.083 to 626.783 mg TE/g extract [38] and BCB percentage ranged from 34.8 to 75.20% [36, 39].

To the best of our knowledge there is no data on FRAP and BCB method of *D. viscosa* extracts. However, the TAC, EC_{50} (DPPH), and EC_{50} (ABTS) are in good agreement with those of Morocco *D. viscosa* leaves extracts [40]. Based on those findings the ethanolic *D. viscosa* exhibited a strong antioxidant activity explained by the high phenolic content, particularly by the highest caffeoylquinic acid content as indicated in Table 2. Previous investigation on plant of *Asteraceae* family was in relation to the role of polyphenols such as hydroxycinnamic acids (ferulic acid, p-coumaric acid, chlorogenic acid, and caffeic acid) on the antioxidant activity [41, 42]. Other studies confirmed the implication of dicaffeoylquinic derivatives in antioxidant activity and other biological activities [41, 43, 44].

In particular, the high contribution of caffeoyl derivatives in the antioxidant activities of *D. viscosa* was confirmed by Danino et al. [45] who proved that the isolated compound 1, 3-diCQA from *D. viscosa* has the greatest scavenging activity DPPH (EC_{50}=40μM) and ABTS (EC_{50} =12±0.4 μM) than the trolox standard.

As shown in Table 3, 10 mg of ointments based on *D. viscosa* extract (2.5 and 5%) that exhibited excellent antiradical and antioxidant capacity values was comparable to 1 mg of BHT. The antioxidants, ointment samples showed dependence on to the concentration used. The ointment of *D. viscosa* extract (5%) possessed the high and the total antioxidant capacity comparing to ointment of *D. viscosa* extract (2.5%) and the base ointment, evidenced by its strongest radical scavenging activities, ferric reducing as well as BCB inhibition. These findings suggested that the formulation at temperature of 100°C did not affect significantly the phenolic composition and did not significantly change *the antioxidant activities*. Our findings were in agreement with previous

Table 1: Retention time, UV and mass spectral data, and tentative identification of the phenolic components in ethanolic leaves extractof *D. viscosa*.

Peak n	Tr (min)	λ max max	$[M-H]^-$ (m/z)	Fragments ions (m/z)	Tentative of identification	Ref/std
1	7.969	325	353	191 (100)-161(10)	Chlorogenic acid	std
2	8.231	260-324	375	375(20)-191(100)	3-o-Caffeoylquinic acid	std
3	9.153	293-324-	543	387(50)-191(100)	1,3-O-Dicaffeoylquinic acid	std
4	11.405	260	599	467(100)	Ganoderic acid C_6	[20]
5	11.694	260	599	467(100)	Ganoderic acid C_6	[20]
6	12.243	280	583	467(100)-329(50)	Ganoderic acid D	[20]
7	18.712	284sh	609	429(60)-341(20)-301(100)-151(60)	Quercetin-galactosylrhamnoside	[21]
8	19.609	260-284sh	741	509(50)- 301(100)- 241(60)	Rutin-O-pentoside	[22]
9	20.751	260-331	463	301(100)-179(20)-151(30)	Quercetin-3-O-glucoside	[23]
10	21.158	260-332	591	301(100)-179(20)-151(30)	Rutin	std
11	22.791	326 sh	741	301(100)-241(20)-151(30)	Quercetin-7-O-xyloside-3-O-rutinoside	[23]
12	23.350	327	515	315(70)-191(40)-179(100)	3,4-Dicaffeoylquinic acid	std
13	25.543	327	515	353 (33)-191 (100)- 179(30)	3,5-Dicaffeoylquinic acid	std
14	26.253	327	677	515(15)-353(15)-191(100)-179(40)-135(20)	Dicaffeoylquinic acid glucoside	[24]
15	27.015	326	653	515(15)-353(15)-191(100)-179(40)-135(20	3, 4,5-Tricaffeoylquinic acid	std
16	28.901	327	515	353(30)-191(50)-179(100)-135(40)	1,5-Dicaffeoylquinic acid	std
17	29.180	327	515	353(30)-191(50)-179(100)-135(40)	3,5-Dicaffeoylquinic acid	std
18	30.525	324	591	509(30)-191(70)-179(100)	4,5-Dicaffeoylquinic acid	std
19	32.022	326	790	591- 405(80)-241(100)-191(60)	Dehydrodimers of caffeic acid	[25]
20	33.291	260-327	489	241(100)	Isoorientin	[26]
21	35.414	281-327	489	241(100)	Isoorientin	[26]
22	36.108	292-323	303	241(60), 151(100)	Dihydroquercetin	[21]
23	39.280	280-328	567	413(100)	Apigenin-glucoside	[26]
24	41.792	288	493	493(100)	Myricetin-O-glucuronide	[27]
25	44.651	332-288	495	493(100)	Dihydromyricetin-O-glucuronide	[28]
26	46.004	260-297-330	493	493(75)-315(100)-300 (50)-271 (80)	Isorhamnetin-O-glucuronopyranoside	[29]
27	47.815	260-290-331	533	515(100), 353 (80)	Dicaffeoylquinic derivatives	std
28	51.130	260-327	757	553(25), 323 (20), 203(100), 165 (50), 133 (30)	Caffeoyl-N-tryptophan	[26]
29	52.061	260-330	553	265(70), 203(100), 163(40)	Caffeoyl-N-tryptophan-rhamnoside	[26]

Table 2: Total phenol content (TPC), caffeoylquinic acid content (CQC) of *D. viscosa* ethanolic extract, ointment base, and ointment containing 5% and 2.5% of extract.

	Ethanolic extract [11]	Ointment containing 2.5% of extract	Ointment containing 5% of extract	Ointment base (vehiculum)
TPC (mg GAE/g of sample)	117.58 ± 1.29	4.70 ± 0.19	11.27 ± 0.121	0.94 ± 0.05
CQC (mg ChlA/g of sample)	71.85 ± 0.35	1.85 ± 0.06	4.77 ± 0.02	0.00±0.00

Table 3: Total antioxidant capacity, free radical scavenging (DPPH; ABTS), ferric reducing power, linoleic acid inhibition of *D. viscosa* ethanolic extract, ointment base, and ointment containing 5% and 2.5% of extract.

	TAC (mg AAE/g of sample)	*EC_{50} DPPH* (μg/ml)	*EC_{50} ABTS* (μg/ml)	*FRAP* (mg TE/g of sample)	*ß-carotene linoleic acid*
Ethanolic extract	133.02 ± 3.1	56.25 ± 1.2	147.26 ± 1.5	296.425 ± 3.3	54.01± 1.4 (%I for 1 mg/mL)
Ointment base (Vehiculum)	1.61± 0.1	7977.00 ± 225.0	12550 ± 132	4.37 ±0.3	10.85 ± 1.1 (%I for 10 mg/mL)
Ointment containing 2.5% of extract	3.41 ±0.2	3073.70±138.8	6290± 183.9	11.69 ± 0.2	36.22 ± 0.9 (%I for 10 mg/mL)
Ointment containing 5% of extract	7.46 ± 0.7	1360.50±90.6	3473.7± 217.5	19.85 ± 0.4	48.05± 1.8 (%I for 10 mg/mL)
BHT	-	26.92 ± 1.22	42.64 ± 0.12	-	62.18 ± 1.6 (% I for 1 mg/mL)

Values expressed are means ± S.D.

studies that proved that phenolic acids (i.e., gallic, gentisic, protocatechuic, and caffeic acids) in pork lard showed a significant antioxidant activity at 150°C [46]. In another study, the addition of antioxidant (i.e., caffeic acid and tyrosol) into refined camellia oil before heating at temperature up to 120°C has been protecting the oil from oxidation and molecular changing [47].

3.4. Wound Contraction Ratio. Comparing the three animal groups treated with ointments to the negative control, the wound area decreased significantly ($p<0.05$) by the twelfth day. The wound contraction ratio depends on the concentration of extract present in the ointment. In particular, on the 3, 9, and 12 days, the ointment containing *D. viscosa* 5% presented the highest wound contraction ratio to animals (Figures 1 and 2).

After 12 days, mice treated with ointments containing *D. viscosa* at 2.5% and 5% were totally healed while the vehicle showed a 57 % healing rate (Figure 2). A correlation between the antioxidant activities and wound contraction ratio of animals was observed. Thus, we suggest that antioxidant properties of *D. viscosa* enhanced the wound healing.

3.5. Histological Study. Over 3 days, the tissue sections of all mice groups showed incomplete healing in wound site without significant difference between the groups; this was manifested by the large area of scab tissue. The inflammatory cells and fibrin were accumulated in granulation tissue and fibroblasts were dispersed (Figure 3: C3, V3, O (2.5%) a, and O (5%) a).

After 9 days, the tissue sections showed obvious difference between groups, though the number of inflammation cells decreased in all groups. Scab area tissue was observed only in the control group and vehicle group. On the other hand, there was great epithelial and collagen fibers organization, remarkable reduction in inflammation cell, and high distribution of fibroplasias. Groups treated with ointments containing *D. viscosa* (5%, 2.5%) showed greater healing quality compared with other groups manifested by tissue remodeling, the deposition of collagen in the wound and vessels regression, and mostly restored and keratinized epidermis after 9 days (Figure 3: O (5%) b and O (2.5%) b). With 5 % of *D. viscosa* extract, proliferation of collagens fibers was observed and inflammatory infiltrate was more important than those observed in group treated with 2.5% of *D. viscosa* extract (Figure 3: O (5%) b).

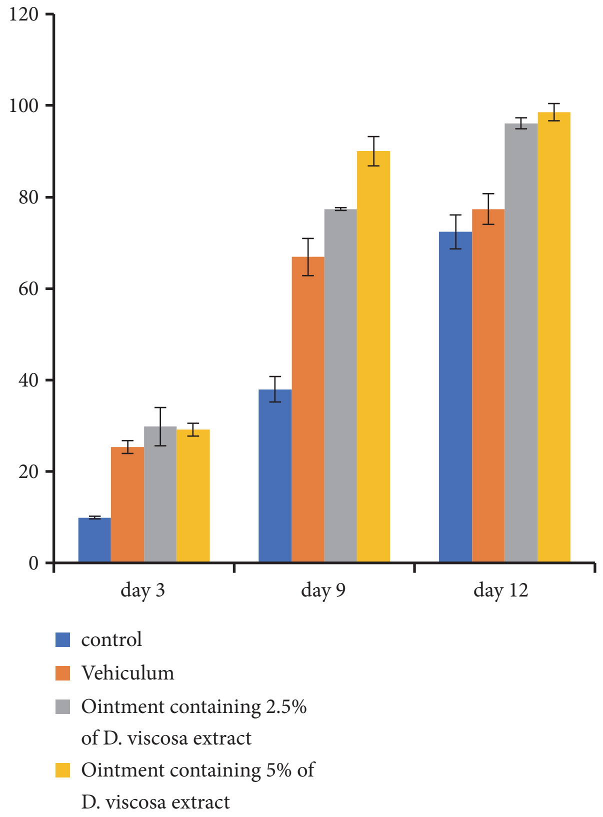

Figure 1: Percentage of wound contraction rate of mice treated with *D. viscosa* (2.5%, 5%) ointments, positive control (vehicle) and negative control on in vivo wound model.

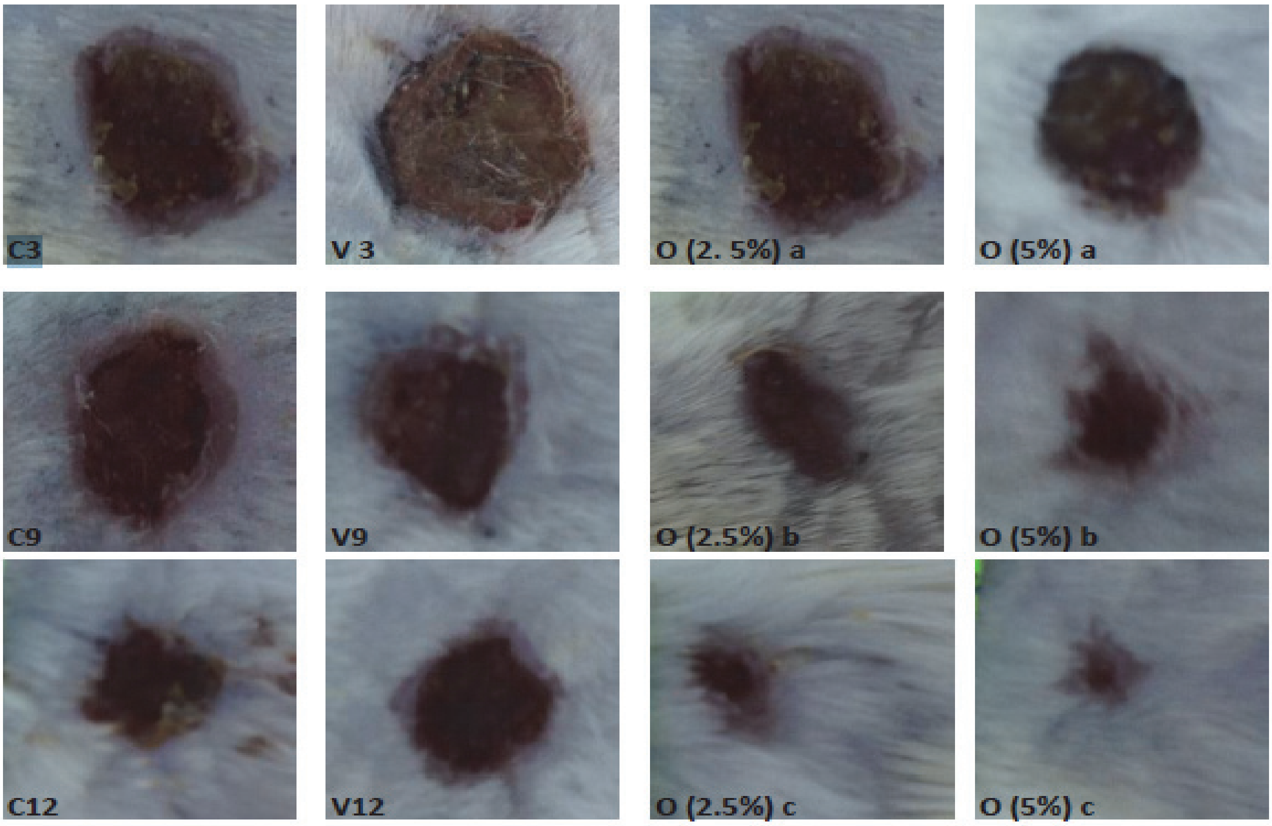

Figure 2: Morphological representation on wound contraction of different groups after 3, 9, and 12 days of topical application: ∗C3: control day 3; ∗C9: control day 9; ∗C12: control day 12; ∗V3: control day 3; ∗V9: control day 9; ∗V12: control day 12; O (2.5%) a: ointment containing *D. viscosa* (2.5%) day 3; O (2.5%) b: ointment containing *D. viscosa* (2.5%) day 9; O (2.5%) a: ointment containing *D. viscosa* (2.5%) day 12; O (2.5%) a: ointment containing *D. viscosa* (5%) day 3; O (2.5%) b: ointment containing *D. viscosa* (5%) day 9; O (2.5%) a: ointment containing *D. viscosa* (5%) day 12.

On day 12, the tissue section showed difference between untreated group (negative control, vehicle) and treated ones with ointments containing *D. viscosa*. Untreated group showed incomplete healing skin (Figure 3: C9, C12, V9, and V12), while group treated with ointment containing 2.5% revealed quasi-complete healing with maturated granulation tissue and hair follicles as well as highly organized collagen and high distribution of fibroblast cells (Figure 3: O (2.5%) c). Concerning the group treated with ointment containing 5% it showed complete healing and full reepithelialization where the numbers of cells and blood vessels were decreased significantly and the collagen fibers had been cross linked (Figure 3: O (5%) c).

In general, our findings are in agreement with previous observations that natural antioxidants promote the wound healing [12, 48, 49]. The wound healing is a dynamic interaction between epidermal and dermal cells and extracellular cells, which occurs in three successive phases: inflammation, proliferation, and maturation. In fact, during the inflammatory process the antioxidant altered the migration of the neutrophil to wound area and modulated neutrophil and macrophages influx (i.e., hydrolytic enzymes, reactive oxygen species, and reactive nitrogen species) [50], thus scavenging free radicals and preventing them from damage during proliferation and maturation process. The antioxidants stimulate synthesis of collagen, enhance cell proliferation and the angiogenesis, and promote the reepithelization of the wound [51]. In this context, some individual phenolic compounds (i.e., protocatechuic acid and caffeic acid) have a potential role in cytokines release in wound site, i.e., vascular endothelial growth factor (VEGF) and transforming growth factor beta (TGF-b) which are involved in remodeling the damaged tissue and accelerate the reepithelization [51, 52].

4. Conclusions

Our findings suggest that Tunisian *D. viscosa* could be a consistent source of antioxidant compounds particularly the caffeoylquinic, being able to scavenge free radicals and to prevent from oxidative damage. Subsequently, the investigation on properties of ointment containing *D. viscosa* leaves showed the potential antioxidant and wound healing effect. Thus, we suggest the role of phenolic compounds in antioxidant and healing wound activities. Hence, this study scientifically opens the perspective to the usefulness of *D. viscosa* as new pharmaceuticals product for oxidative stress

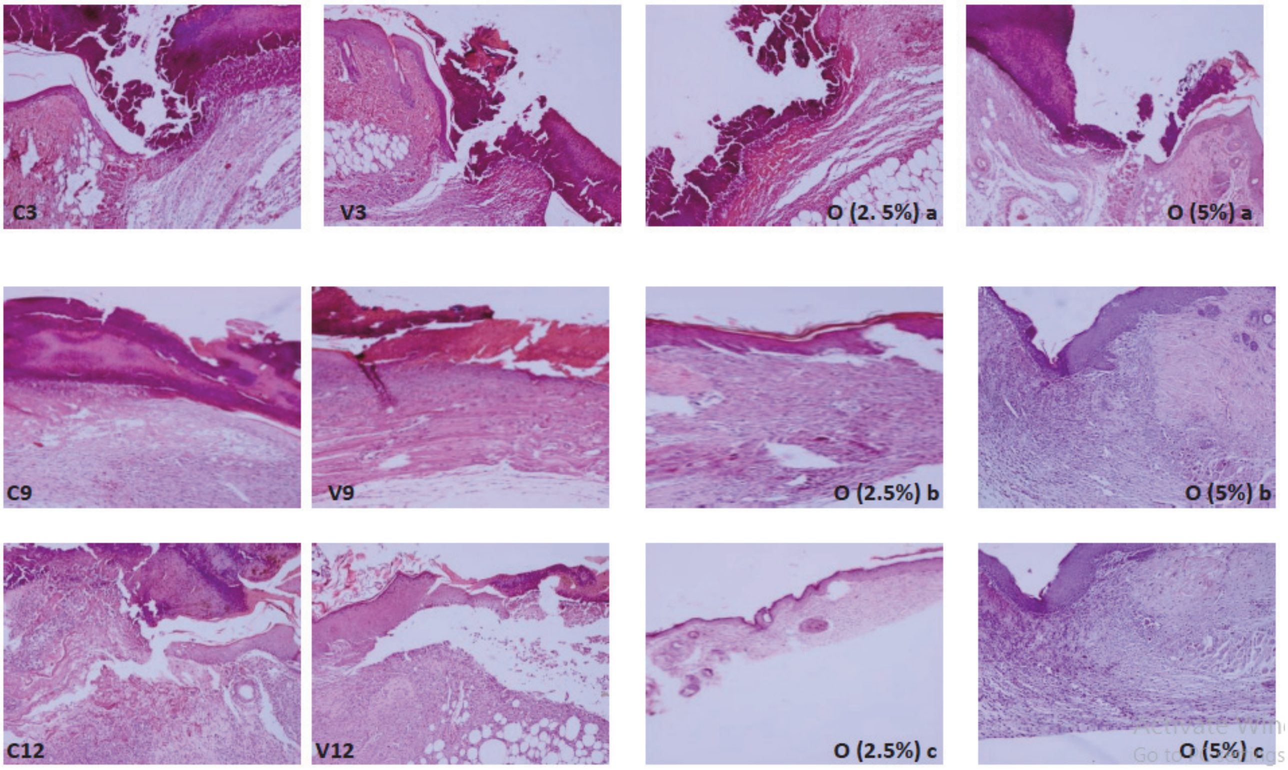

Figure 3: Histological sections of mice of different groups after 3, 9, and 12 days of topical application C3, V3, O (2.5%) a, and O (5%) a: complete destruction acute of epiderm, presence of inflammatory cells, and fibrin. C9, C12, V9, and V12: acute inflammation and destruction of epiderm. O (2.5%) b: proliferation of collagens fibers, inflammatory discreet infiltrate, and reepithelization. O (5%) b: proliferation of collagens fibers and inflammatory discreet infiltrate more important than those observed in O (2.5%) b. O (2.5%) c: Complete reepithelization. O (5%) c: reepithelization and crosslinking of collagen fibers.

and wound healing. However, further in *vivo* tests should be carried out.

Data Availability

The data used to support the findings of this study are available from the corresponding author upon request.

Conflicts of Interest

The authors declare that there are no conflicts of interest regarding the publication of this paper.

Acknowledgments

This research was funded by the Tunisian Ministry of High Education and Scientific Research.

Supplementary Materials

Graphic summary description: the ethanolic extract of *D. viscosa* leaves was leaves chemically characterized with HPLC-DAD-MS and it was used to formulate ointments (5% and 2.5% (w/w)) for healing wound test. Then, the antioxidants and the healing activities of those ointments were evaluated. The results obtained from this study revealed the excellent antioxidant potential of ointments base on ethanolic extract of *D. viscosa* and evidence their role in improving the rate and the quality of wound contraction samples. *(Supplementary Materials)*

References

[1] M. Takeo, W. Lee, and M. Ito, “Wound healing and skin regeneration,” *Cold Spring Harbor Perspectives in Medicine*, vol. 5, no. 1, 2015.

[2] C. C. Yates, P. Hebda, and A. Wells, “Skin wound healing and scarring: fetal wounds and regenerative restitution,” *Birth Defects Research Part C - Embryo Today: Reviews*, vol. 96, no. 4, pp. 325–333, 2012.

[3] C. Dunnill, T. Patton, J. Brennan et al., “Reactive oxygen species (ROS) and wound healing: the functional role of ROS and emerging ROS-modulating technologies for augmentation of the healing process,” *International Wound Journal*, vol. 12, no. 6, pp. 1–8, 2015.

[4] M. Mittal, M. R. Siddiqui, K. Tran, S. P. Reddy, and A. B. Malik, “Reactive oxygen species in inflammation and tissue injury,” *Antioxidants & Redox Signaling*, vol. 20, no. 7, pp. 1126–1167, 2014.

[5] A. Rahal, A. Kumar, V. Singh et al., “Oxidative stress, prooxidants, and antioxidants: the interplay,” *BioMed Research International*, vol. 2014, Article ID 761264, 19 pages, 2014.

[6] L. A. Pham-Huy, H. He, and C. Pham-Huy, “Free radicals, antioxidants in disease and health,” *International Journal of Biomedical Science*, vol. 4, no. 2, pp. 89–96, 2008.

[7] S. M. F. Bessada, J. C. M. Barreira, and M. B. P. P. Oliveira, “Asteraceae species with most prominent bioactivity and their potential applications: a review,” *Industrial Crops and Products*, vol. 76, pp. 604–615, 2015.

[8] E. Castells, P. P. J. Mulder, and M. Pérez-Trujillo, “Diversity of pyrrolizidine alkaloids in native and invasive Senecio pterophorus (Asteraceae): implications for toxicity,” *Phytochemistry*, vol. 108, pp. 137–146, 2014.

[9] I. Jallali, Y. Zaouali, I. Missaoui, A. Smeoui, C. Abdelly, and R. Ksouri, “Variability of antioxidant and antibacterial effects of essential oils and acetonic extracts of two edible halophytes: Crithmum maritimum L. and Inula crithmoïdes L.,” *Food Chemistry*, vol. 145, pp. 1031–1038, 2014.

[10] C. Zidorn, “Altitudinal variation of secondary metabolites in flowering heads of the Asteraceae: trends and causes,” *Phytochemistry Reviews*, vol. 9, no. 2, pp. 197–203, 2010.

[11] W. Rhimi, I. Ben Salem, D. Immediato, M. Saidi, A. Boulila, and C. Cafarchia, “Chemical composition, antibacterial and antifungal activities of crude Dittrichia viscosa (L.) greuter leaf extracts,” *Molecules*, vol. 22, no. 7, article 942, 2017.

[12] M. Alkafafy, M. Montaser, S. A. El-Shazly, S. Bazid, and M. M. Ahmed, “Ethanolic extract of sharah, Plectranthus aegyptiacus, enhances healing of skin wound in rats,” *Acta Histochemica*, vol. 116, no. 4, pp. 627–638, 2014.

[13] A. Meda, C. E. Lamien, M. Romito, J. Millogo, and O. G. Nacoulma, “Determination of the total phenolic, flavonoid and proline contents in Burkina Fasan honey, as well as their radical scavenging activity,” *Food Chemistry*, vol. 91, no. 3, pp. 571–577, 2005.

[14] E. W. C. Chan, Y. Y. Lim, S. K. Ling, S. P. Tan, K. K. Lim, and M. G. H. Khoo, “Caffeoylquinic acids from leaves of Etlingera species (Zingiberaceae),” *LWT- Food Science and Technology*, vol. 42, no. 5, pp. 1026–1030, 2009.

[15] P. Prieto, M. Pineda, and M. Aguilar, “Spectrophotometric quantitation of antioxidant capacity through the formation of a phosphomolybdenum complex: specific application to the determination of vitamin E,” *Analytical Biochemistry*, vol. 269, no. 2, pp. 337–341, 1999.

[16] P. Molyneux, “The use of the stable radical diphenylpicrylhydrazyl (DPPH) for estimating antioxidant activity,” *Songklanakarin Journal of Science and Technology*, vol. 26, no. 2, pp. 211–219, 2004.

[17] K. Thaipong, U. Boonprakob, K. Crosby, L. Cisneros-Zevallos, and B. D. Hawkins, “Comparison of ABTS, DPPH, FRAP, and ORAC assays for estimating antioxidant activity from guava fruit extracts,” *Journal of Food Composition and Analysis*, vol. 19, no. 6-7, pp. 669–675, 2006.

[18] S. Gouveia, J. Gonçalves, and P. C. Castilho, “Characterization of phenolic compounds and antioxidant activity of ethanolic extracts from flowers of Andryala glandulosa ssp. varia (Lowe ex DC.) R.Fern., an endemic species of Macaronesia region,” *Industrial Crops and Products*, vol. 42, no. 1, pp. 573–582, 2013.

[19] Y. S. Velioglu, G. Mazza, L. Gao, and B. D. Oomah, “Antioxidant activity and total phenolics in selected fruits, vegetables, and grain products,” *Journal of Agricultural and Food Chemistry*, vol. 46, no. 10, pp. 4113–4117, 1998.

[20] C. S. Yang, J. D. Lambert, J. Ju, G. Lu, and S. Sang, “Tea and cancer prevention: Molecular mechanisms and human relevance,” *Toxicology and Applied Pharmacology*, vol. 224, no. 3, pp. 265–273, 2007.

[21] W. Mullen, T. Yokota, M. E. J. Lean, and A. Crozier, “Analysis of ellagitannins and conjugates of ellagic acid and quercetin in raspberry fruits by LC-MSn,” *Phytochemistry*, vol. 64, no. 2, pp. 617–624, 2003.

[22] A. Vallverdú-Queralt, O. Jáuregui, G. Di Lecce, C. Andrés-Lacueva, and R. M. Lamuela-Raventós, “Screening of the polyphenol content of tomato-based products through accurate-mass spectrometry (HPLC-ESI-QTOF),” *Food Chemistry*, vol. 129, no. 3, pp. 877–883, 2011.

[23] M. J. Simirgiotis, J. Benites, C. Areche, and B. Sepu, “Antioxidant capacities and analysis of phenolic compounds in three endemic nolana species by HPLC-PDA-ESI-MS,” *Molecules*, vol. 20, no. 6, pp. 11490–11507, 2015.

[24] L.-Z. Lin and J. M. Harnly, “Identification of the phenolic components of chrysanthemum flower (*Chrysanthemum morifolium* Ramat),” *Food Chemistry*, vol. 120, no. 1, pp. 319–326, 2010.

[25] J.-G. Yang and T. Uchiyama, “Dehydrodimers of caffeic acid in the cell walls of suspension-cultured mentha,” *Bioscience, Biotechnology, and Biochemistry*, vol. 64, no. 4, pp. 862–864, 2000.

[26] E. J. Llorent-Martínez, V. Spínola, S. Gouveia, and P. C. Castilho, “HPLC-ESI-MSn characterization of phenolic compounds, terpenoid saponins, and other minor compounds in Bituminaria bituminosa,” *Industrial Crops and Products*, vol. 69, pp. 80–90, 2015.

[27] A. Stalmach, C. A. Edwards, J. D. Wightman, and A. Crozier, “Identification of (Poly)phenolic compounds in concord grape juice and their metabolites in human plasma and urine after juice consumption,” *Journal of Agricultural and Food Chemistry*, vol. 59, no. 17, pp. 9512–9522, 2011.

[28] L. Barros, E. Pereira, R. C. Calhelha et al., “Bioactivity and chemical characterization in hydrophilic and lipophilic compounds of *Chenopodium ambrosioides* L,” *Journal of Functional Foods*, vol. 5, no. 4, pp. 1732–1740, 2013.

[29] Ł. Marczak, P. Znajdek-Awizeń, and W. Bylka, “The use of mass spectrometric techniques to differentiate isobaric and isomeric flavonoid conjugates from Axyris amaranthoides,” *Molecules*, vol. 21, no. 9, p. 1229, 2016.

[30] I. Trimech, E. K. Weiss, V. S. Chedea et al., “Evaluation of antioxidant and acetylcholinesterase activity and identification of polyphenolics of the invasive weed dittrichia viscosa,” *Phytochemical Analysis*, vol. 25, no. 5, pp. 421–428, 2014.

[31] E. Kollia, P. Markaki, P. Zoumpoulakis, and C. Proestos, “Antioxidant activity of Cynara scolymus L. and Cynara cardunculus L. extracts obtained by different extraction techniques,” *Natural Product Research (Formerly Natural Product Letters)*, vol. 31, no. 10, pp. 1163–1167, 2017.

[32] P. Pinelli, F. Agostini, C. Comino, S. Lanteri, E. Portis, and A. Romani, “Simultaneous quantification of caffeoyl esters and flavonoids in wild and cultivated cardoon leaves,” *Food Chemistry*, vol. 105, no. 4, pp. 1695–1701, 2007.

[33] M. Wang, J. E. Simon, I. F. Aviles, K. He, Q.-Y. Zheng, and Y. Tadmor, “Analysis of antioxidative phenolic compounds in artichoke (Cynara scolymus L.),” *Journal of Agricultural and Food Chemistry*, vol. 51, no. 3, pp. 601–608, 2003.

[34] A. L. Dawidowicz and R. Typek, “Thermal stability of 5-o-caffeoylquinic acid in aqueous solutions at different heating

conditions," *Journal of Agricultural and Food Chemistry*, vol. 58, no. 24, pp. 12578–12584, 2010.

[35] S. Albayrak, A. Aksoy, O. Sagdic, and E. Hamzaoglu, "Compositions, antioxidant and antimicrobial activities of Helichrysum (Asteraceae) species collected from Turkey," *Food Chemistry*, vol. 119, no. 1, pp. 114–122, 2010.

[36] S. Albayrak, A. Aksoy, S. Albayrak, and O. Sagdic, "In vitro antioxidant and antimicrobial activity of some Lamiaceae species," *Iranian Journal of Science & Technology*, vol. 37, no. 1, pp. 1–9, 2013.

[37] U. Özgen, A. Mavi, Z. Terzi, M. Coflkun, and Y. Ali, "Antioxidant activities and total phenolic compounds amount of some asteraceae species," *Turkish Journal of Pharmaceutical Sciences*, vol. 1, pp. 203–216, 2004.

[38] O. Kenny, T. J. Smyth, D. Walsh, C. T. Kelleher, C. M. Hewage, and N. P. Brunton, "Investigating the potential of under-utilised plants from the Asteraceae family as a source of natural antimicrobial and antioxidant extracts," *Food Chemistry*, vol. 161, pp. 79–86, 2014.

[39] A. Akrout, L. A. Gonzalez, H. El Jani, and P. C. Madrid, "Antioxidant and antitumor activities of *Artemisia campestris* and *Thymelaea hirsuta* from southern Tunisia," *Food and Chemical Toxicology*, vol. 49, no. 2, pp. 342–347, 2011.

[40] N. Chahmi, J. Anissi, S. Jennan, A. Farah, K. Sendide, and M. El Hassouni, "Antioxidant activities and total phenol content of *Inula viscosa* extracts selected from three regions of Morocco," *Asian Pacific Journal of Tropical Biomedicine*, vol. 5, no. 3, pp. 228–233, 2015.

[41] R. Jaiswal, J. Kiprotich, and N. Kuhnert, "Determination of the hydroxycinnamate profile of 12 members of the Asteraceae family," *Phytochemistry*, vol. 72, no. 8, pp. 781–790, 2011.

[42] D. B. Silva, L. T. Okano, N. P. Lopes, and D. C. R. De Oliveira, "Flavanone glycosides from Bidens gardneri Bak. (Asteraceae)," *Phytochemistry*, vol. 96, pp. 418–422, 2013.

[43] D. Fraisse, C. Felgines, O. Texier, and L. J. Lamaison, "Caffeoyl derivatives: major antioxidant compounds of some wild herbs of the *Asteraceae* family," *Journal of Food and Nutrition Sciences*, vol. 2, no. 3, pp. 181–192, 2011.

[44] C. Zidorn, E. P. Ellmerer, S. Sturm, and H. Stuppner, "Tyrolobibenzyls E and F from *Scorzonera humilis* and distribution of caffeic acid derivatives, lignans and tyrolobibenzyls in European taxa of the subtribe Scorzonerinae (Lactuceae, Asteraceae)," *Phytochemistry*, vol. 63, no. 1, pp. 61–67, 2003.

[45] O. Danino, H. E. Gottlieb, S. Grossman, and M. Bergman, "Antioxidant activity of 1,3-dicaffeoylquinic acid isolated from Inula viscosa," *Food Research International*, vol. 42, no. 9, pp. 1273–1280, 2009.

[46] Z. Réblová, "Effect of temperature on the antioxidant activity of phenolic acids," *Czech Journal of Food Sciences*, vol. 30, no. 2, pp. 171–177, 2012.

[47] Z. Haiyan, D. R. Bedgood Jr., A. G. Bishop, P. D. Prenzler, and K. Robards, "Effect of added caffeic acid and tyrosol on the fatty acid and volatile profiles of camellia oil following heating," *Journal of Agricultural and Food Chemistry*, vol. 54, no. 25, pp. 9551–9558, 2006.

[48] S. Rawat, R. Singh, P. Thakur, S. Kaur, and A. Semwal, "Wound healing agents from medicinal plants: a review," *Asian Pacific Journal of Tropical Biomedicine*, vol. 2, no. 3, pp. S1910–S1917, 2012.

[49] Y. Song, R. Zeng, L. Hu, K. G. Maffucci, X. Ren, and Y. Qu, "In vivo wound healing and in vitro antioxidant activities of Bletilla striata phenolic extracts," *Biomedicine & Pharmacotherapy*, vol. 93, pp. 451–461, 2017.

[50] J. Infante, P. L. Rosalen, J. G. Lazarini, M. Franchin, and S. M. De Alencar, "Antioxidant and anti-inflammatory activities of unexplored Brazilian native fruits," *PLoS ONE*, vol. 11, no. 4, article e0152974, 2016.

[51] O. T. Agar, M. Dikmen, N. Ozturk, M. A. Yilmaz, H. Temel, and F. P. Turkmenoglu, "Comparative studies on phenolic composition, antioxidant, wound healing and cytotoxic activities of selected achillea L. species growing in Turkey," *Molecules*, vol. 20, no. 10, pp. 17976–18000, 2015.

[52] A. A. Geronikaki and A. M. Gavalas, "Antioxidants and inflammatory disease: synthetic and natural antioxidants with anti-inflammatory activity," *Combinatorial Chemistry & High Throughput Screening*, vol. 9, no. 6, pp. 425–442, 2006.

Hindawi
BioMed Research International
Volume 2019, Article ID 2585743, 8 pages
https://doi.org/10.1155/2019/2585743

Research Article

The Nutritional Cytokine Leptin Promotes NSCLC by Activating the PI3K/AKT and MAPK/ERK Pathways in NSCLC Cells in a Paracrine Manner

Fengzhou Li,[1,2] **Shilei Zhao**,[1,2] **Tao Guo**,[1,2] **Jinxiu Li**,[2] **and Chundong Gu**[1,2]

[1] *Department of Thoracic Surgery, The First Affiliated Hospital of Dalian Medical University, Dalian, Liaoning 116011, China*
[2] *Lung Cancer Diagnosis and Treatment Center, Dalian 116011, Liaoning, China*

Correspondence should be addressed to Jinxiu Li; lijinxiu@dmu.edu.cn and Chundong Gu; guchundong@dmu.edu.cn

Received 28 January 2019; Revised 26 March 2019; Accepted 8 April 2019; Published 18 April 2019

Guest Editor: Hengjia Ni

Copyright © 2019 Fengzhou Li et al. This is an open access article distributed under the Creative Commons Attribution License, which permits unrestricted use, distribution, and reproduction in any medium, provided the original work is properly cited.

Purpose. Leptin is a nutritional cytokine encoded by the obesity gene whose concentration in the tumor microenvironment is closely related to the occurrence and progression of cancer. However, previous evidence has suggested that there is no clear relationship between serum leptin concentrations and lung cancer progression. Cancer-associated fibroblasts (CAFs), the most abundant component of the tumor microenvironment in a variety of solid tumors, were recently reported to produce leptin. Therefore, it was inferred that leptin is most likely to affect non-small-cell lung cancer (NSCLC) through an autocrine and paracrine mechanism. In the current study, we investigated the paracrine effect and mechanism of leptin produced by CAFs on NSCLC by establishing a novel in vitro cell coculture system. *Methods.* A noncontact coculture device was designed and made by 3D printing. CAFs and paired normal lung fibroblasts (NLFs) from 5 patients were successfully isolated and cocultured with two NSCLC cell lines in a coculture system. The background expression of leptin was detected by western blot. The in situ expression of leptin and its receptor (Ob-R) in NSCLC tissues and paired normal lung tissues was analyzed by immunohistochemistry. Furthermore, we downregulated the expression of leptin in CAFs and assessed changes in its promotion on NSCLC cells in the coculture system. Finally, changes in the phosphorylation of ERK1/2 and AKT were examined to investigate the molecular mechanisms responsible for the paracrine promotion of NSCLC cells by leptin. *Results.* Leptin was overexpressed in nearly all five primary CAF lines compared with its expression in paired NLFs. IHC staining showed that the expression of leptin was high in NSCLC cells, slightly lower in CAF, and negative in normal lung tissue. Ob-R was strongly expressed in NSCLC cells. The ability of A549 and H1299 cells to proliferate and migrate was enhanced by high leptin levels in both the cocultured fibroblasts and the culture medium. Furthermore, western blot assays suggested that the MAPK/ERK1/2 and PI3K/AKT signaling pathways were activated by leptin produced by CAFs, which demonstrated that the functions of paracrine leptin in NSCLC are as those of the serum leptin to other cancers. *Conclusion.* Leptin produced by CAF promotes proliferation and migration of NSCLC cells probably via PI3K/AKT and MAPK/ERK1/2 signaling pathways in a paracrine manner.

1. Introduction

Lung cancer is the most common malignancy worldwide [1]. Non-small-cell lung cancer (NSCLC) accounts for approximately 85% of all lung cancers [2], and is usually diagnosed at an advanced stage, often with metastases [3]. Therefore, the elucidation of the mechanisms involved in occurrence and progress of NSCLC could lead to novel diagnostic and therapeutic approaches [4].

Obesity is considered to be a growing health problem worldwide [5]. Leptin, a 16 kDa peptide hormone encoded by LEP gene (an obesity gene) and a nutritional cytokine, is closely related to cancer [6]. The main function of leptin is to regulate energy metabolism and fat synthesis in the body, and it also amplifies inflammation and immunity signals [7]. Leptin exerts its effects through a specific transmembrane receptor on the surface of its target cells, the obesity receptor (Ob-R), which is assigned to the class I cytokine receptor family [8]. The binding of leptin to its receptor activates multiple downstream signaling pathways such as those involving JAK2-STAT3, mitogen-activated protein kinase (MAPK), and phosphatidylinositol 3-kinase/protein kinase B (PI3K/AKT) [9]. Therefore, leptin-mediated signaling pathways play an important role in cancer cell proliferation, invasion, and metastasis [10].

In recent years, crosstalk between the tumor microenvironment and cancer cells has received increasing attention [11]. The tumor microenvironment is the internal environment in which cancer cells intergrow and interact with the “nontumoral” components [12]. Cancer-associated fibroblasts (CAFs), the most abundant component of the tumor microenvironment of NSCLC, account for 70% of the total number of cells in solid tumors [13] and are most often identified by the expression of myofibroblastic biomarkers such as α-smooth muscle actin (α-SMA) [14]. Besides, fibroblast activating protein (FAP) and vimentin are also used as auxiliary markers to identify CAF [15]. CAFs can promote tumor progression through the secretion of various cytokines.

In addition to its synthesis by adipocytes, leptin can also be synthesized by epithelial cells or fibroblasts. Leptin is usually absent in nonneoplastic tissue; however, recent studies demonstrated that, leptin was also secreted by CAFs in breast cancer [16]. Thus, we inferred that CAF in NSCLC tissues can also produce leptin and affect the function of NSCLC in a paracrine manner. This hypothesis is supported by several recent pieces of evidence, as the increase of leptin concentration in the microenvironment was related to the occurrence and metastasis of several types of cancer [17–19]. On the other hand, a recent meta-analysis [20] suggested that there may be no clear relationship between the serum leptin concentration and lung cancer progression. This may be due to the special histological characteristics of alveoli and bronchi. Therefore, leptin is most likely to affect NSCLC through autocrine and paracrine effects. In the current study, we investigated the protumorigenic effect of leptin produced by CAFs on NSCLC by establishing a novel in vitro cell coculture system.

2. Methods

2.1. Cell Lines. Human embryonic lung fibroblasts (HLF) and the human NSCLC cell lines A549 and H1299 were obtained from the American type culture collection (ATCC), and all cell lines were cultured in DMEM (Gibco) supplemented with 10% fetal bovine serum (FBS, Gibco) and penicillin/streptomycin at 37°C in 5% CO_2.

2.2. Culture of Primary Fibroblasts. Tissue samples from 5 patients who had a definitive pathological diagnosis of stage IIIA NSCLC were resected by thoracoscopic lobectomy in the 1st Hospital of Dalian Medical University in April 2018. The tissues were soaked in DMEM at 0°C and digested within 2 h of resection. Tumor tissues and their paired normal lung tissues (4~5 cm away from the incisal margin) were homogenized and digested for 2.5~4 h at 37°C in DMEM containing 0.1 mg/mL DNase I (Roche, Switzerland) and 1 mg/mL collagenase (Roche, Switzerland). The cells were filtered with a 75 μm filter and then resuspended and plated with DMEM containing 1% penicillin/streptomycin and 15% FBS. The cultures were maintained at 37°C in 5% CO_2. After 5 passages, fibroblast purity was tested by RT-qPCR. Then, CAFs were immortalized with SV40-large T antigen (EX-SV40T-Lv105, GeneCopoeia, USA) following the recommended protocol.

2.3. Noncontact Coculture System. A noncontact coculture device was designed (already in the patent examination and approval process in China) and made by 3D printing (Wanwan 3D, Dongguan, China) with highly transparent nontoxic resin to simulate the internal environment. The device was a vessel consisting of two culture wells and a precipitation well (Figure 1(a)). The culture wells and the precipitation well were separated by two 2 mm-high partitions. During cell seeding, the level of the liquid in both culture wells should be kept below the height of the partition. Fibroblasts and NSCLC cells were seeded into the two culture wells, at a 2:1 ratio. After cell adherence, DMEM containing 10% FBS was added to the vessel until the level was above the partition. Based on the design of the coculture device, floating cells do not go directly into the contralateral culture well but are deposited into the precipitation well. Before anything was done to the cells, the medium in the precipitation well was drained in case any floating cells entered their contralateral culture well. Then, the two cell lines were isolated again, and 0.5% trypsin was used for separate passage/collection of the two cell lines.

2.4. Conditioned Medium. Fibroblasts were cultured in DMEM with 10% FBS and routine antibiotics. Then, the medium was changed to FBS-free medium when the cells had grown to 80% confluence. After 48 h, the supernatant was extracted and centrifuged at 1600×g for 10 min. The conditioned medium (CM) was stored at –79°C and used for the colony formation assay.

2.5. Reagents and Antibodies. Recombinant human leptin was purchased from Pepro Tech (Rocky Hill, USA). A primary antibody against α-SMA was purchased from Abcam (Cambridge, UK). Primary antibodies against Ob-R were purchased from Wanleibio (Shenyang, China). A leptin antibody was obtained from Bioss (Beijing, China). Other primary antibodies against AKT, p-AKT, ERK, and p-ERK were obtained from Cell Signaling Technology (Massachusetts, USA). And other chemicals were purchased from Sigma (St. Louis, USA) and Vetec (St. Louis, USA).

2.6. Plasmids and Lentivirus. pLK0.1-PXR-shRNA targeting the LEP gene was acquired from the Institute of Cancer Stem Cell at Dalian Medical University and was packaged with the pMD2.G lentivirus packing system (GeneCopoeia, USA). Viral packaging was conducted based on the recommended protocols and previous articles.

2.7. RNA Extraction and Real-Time RT-PCR. Total RNA was extracted from CAFs and the NLFs using the TRIzol method according to previous articles [21]. TransScript One-step gDNA Removal and cDNA Synthesis Supermix (Transgene, Beijing, China) was used to synthesize first strand cDNA. SYBR Premix Ex Taq II (RR820A, Takara, Japan) was used

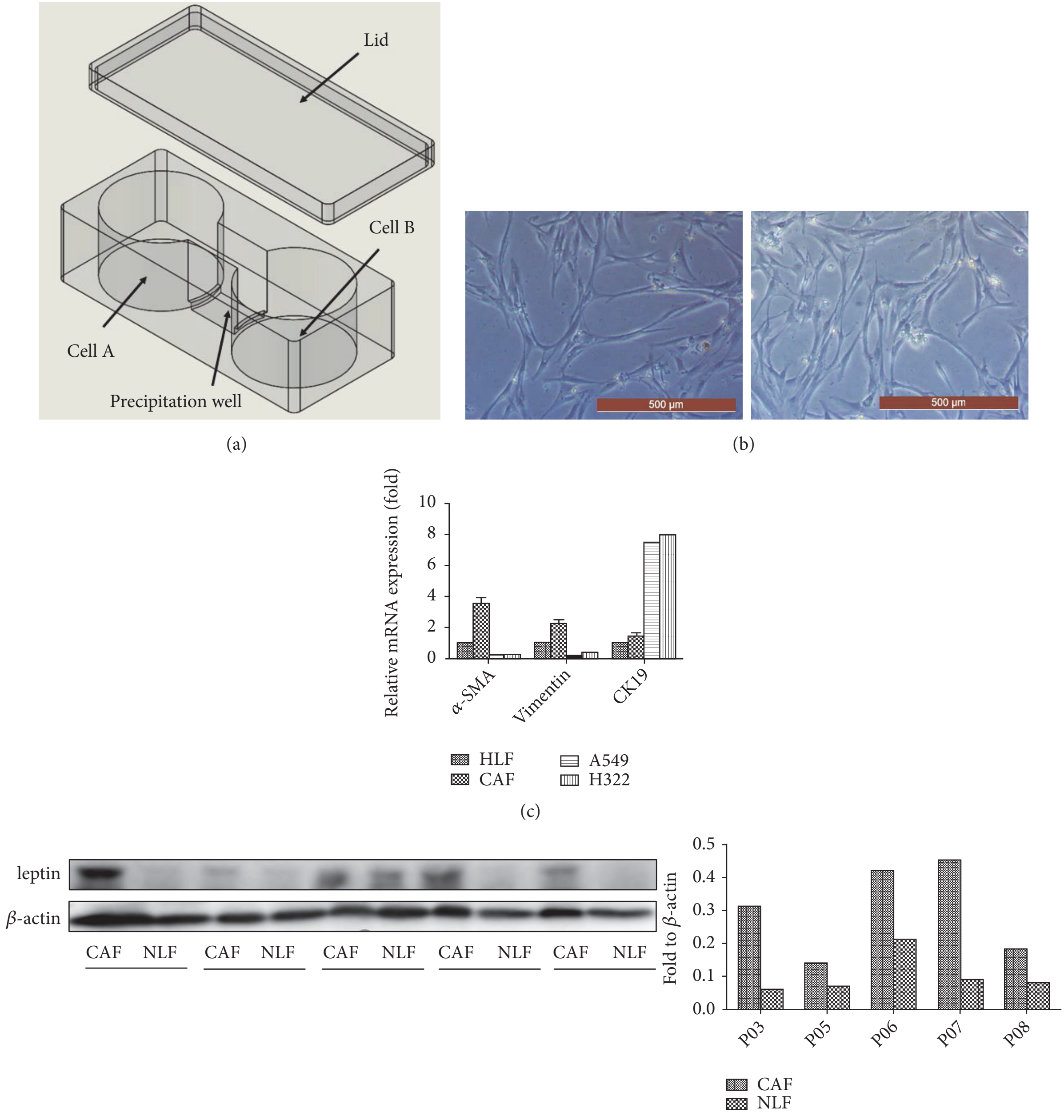

(a)

(b)

(c)

(d)

Figure 1: *Isolation and characterization of CAFs and NLFs.* (a) Three-dimensional model of the novel noncontact coculture device. (b) Morphology of primary fibroblasts under a microscope. Left: CAF, right: NLF. Scale bar = 500 μm. (c) The purity of the primary cells was verified by RT-qPCR to determine the levels of α-SMA, vimentin, and CK19. (d) Leptin expression in primary CAF and NLF cell lines was detected with western blot. The quantification of leptin is shown in the bar chart.

for quantitative polymerase chain reaction according to the manufacturer's instructions. The primer sequences used were as follows: α-SMA:5'- ATTGCCGACCGAATGCAGA -3',5'- ATGGAGCCACCGATCCAGAC-3'; vimentin: 5'- TGC-CGTTGAAGCTGCTAACTA -3', 5'- CCAGAGGGAGTG-AATCCAGATTA -3'; CK-19: 5'- ACCAAGTTTGAGACG-GAACAG -3', 5'- CCCTCAGCGTACTGATTTCCT -3'. The comparative Ct method was used to calculate relative changes in gene expression.

2.8. Immunohistochemistry Staining. IHC staining of leptin, Ob-R and α-SMA was performed according to the manufacturer's instructions. A streptavidin-peroxidase staining kit was purchased from ZSGB BIO (Beijing, China). The paraffin-embedded tissues were prepared by a pathology specialist, and dewaxed, and rehydrated in the lab. The experimental steps were carried out according to the instructions of the SP kit. The tissues were incubated with primary antibodies diluted to the recommended concentration overnight

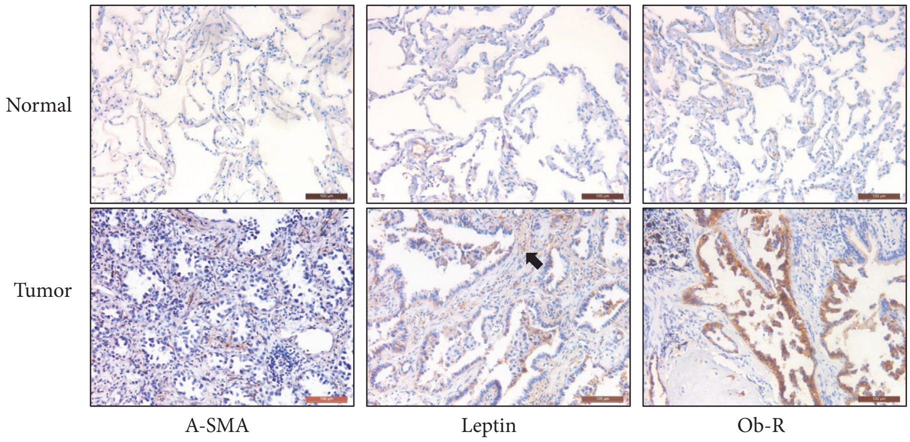

Figure 2: *Immunohistochemical analyses of α-SMA, leptin and Ob-R in NSCLC.* The expression of α-SMA, leptin, and Ob-R in the tumor and paired normal lung tissues of a 54-year-old male patient with acinar growth predominant lung adenocarcinoma was detected by IHC assay. The leptin overexpressed in the tumor stroma is marked with a black arrow in the corresponding position. Scale bar = 100 μm.

at 4°C with antibodies that was dilute to the recommended concentration. Then 3,3′-diaminobenzidine (DAB) staining was performed, and the results were observed under a microscope.

2.9. Western Blot Analysis. Total protein was collected according to the methods in our previous article [22]. The protein concentration of the cell lysis solution was assessed using a Thermo Fisher BCA kit. Then 30 μg of total protein was run on 10% SDS-PAGE and transferred to a PVDF membrane. Samples were incubated with primary antibodies diluted to the recommended concentration overnight at 4°C. The samples were incubated with HRP-conjugated secondary antibody at room temperature for 2 h and protein bands were detected with a chemiluminescence device.

2.10. Colony Formation Assay. Briefly, A549 cells or H1299 cells were seeded into six-well plates (2×10^3 per well) and incubated in complete DMEM for 24 h. Then, the medium was replaced by the abovementioned CM with 10% FBS, and the cells were cultured in a 37°C incubator with 5% CO2 for 2 weeks until they grew into macroscopic colonies. Finally, the medium was removed, and the cell colonies were stained with 0.1% crystal violet and counted.

2.11. Cell Migration Assay. Cell migration assays were performed in Transwell chambers with an 8.0μm pore size (Corning, US). The cells were starved in FBS-free DMEM overnight before they were collected and resuspended. A total of 1×10^5 A549 or H1299 cells were resuspended in 250 μL DMEM with 10% FBS and injected into the upper chamber. A total of 3×10^5 CAF cells were resuspended in 500 μL DMEM with 10% FBS and injected into the lower chamber. After 24 h, the upper chamber was washed with PBS, the nonpenetrated cells were removed with a cotton swab, and the Transwell chamber was dried at RT. The migrated cells at the back side of the Transwell membrane were stained with 0.1% crystal violet and then observed under a microscope.

3. Results

3.1. Isolation and Characterization of CAFs and NLFs. CAFs and paired normal lung fibroblasts (NLFs) from 5 patients were successfully established, their cell morphology was first observed under an inverted microscope (Figure 1(b)), and no significant difference was observed between the two cell lines. The purity of the primary cells was verified by biomarkers using RT-qPCR. α-SMA, vimentin, and FAP were more strongly expressed, while CK19 and E-cadherin were more weakly expressed in the 5 CAF lines compared with their expression in the respective paired normal fibroblasts (Figure 1(c)). Leptin was overexpressed in almost all five primary CAF lines compared to its expression in paired corresponding NLFs (Figure 1(d)).

3.2. A Noncontact Coculture Model Was Successfully Established. One of the five CAF cell lines (CAF03), whose leptin background expression level was the highest, was selected for further study. Since it was difficult to stably culture NLFs in vitro, HLF cells were used as an alternative to the NLFs in the coculture system. In the coculture device, CAFs and HLF were successfully cocultured with A549 and H1299 cells through 5 consecutive passages.

3.3. Leptin Produced by CAFs Promotes the Proliferation of NSCLC. The original tumor tissue of the CAF03 cell line (from a 54-year-old female patient with stage IIIA acinar growth predominant lung adenocarcinoma) and its adjacent normal lung tissue were stained by immunohistochemistry, and α-SMA clearly marked the location of the stroma. IHC staining showed that leptin was highly expressed in epithelial cells and expressed at a slightly lower level in the cytoplasm of tumor stromal cells (mainly CAF). In contrast, both α-SMA and leptin were not expressed in normal lung tissues (Figure 2). Ob-R was strongly expressed in NSCLC cells and was expressed at low levels in both tumor stroma and normal tissues. Subsequently, the LEP gene in CAFs was stably downregulated by lentivirus transfection (sh4) with

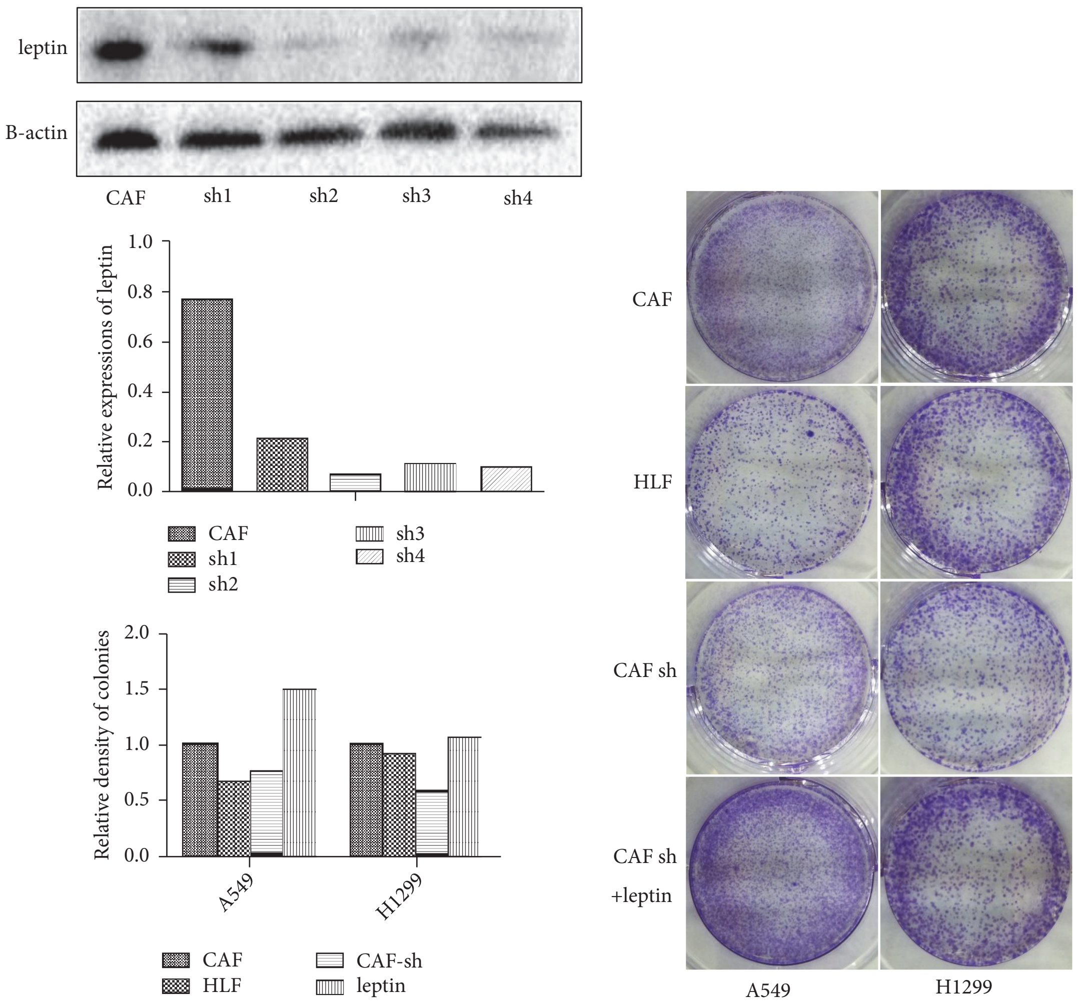

(a) (b)

Figure 3: *The proliferation of NSCLC cells was inhibited by the downregulation of leptin in CAFs.* (a) The efficiency of gene intervention by four different shRNA fragments was verified by western blot. (b) The proliferation of NSCLC cell lines treated with the CM of different fibroblasts was assessed with a colony formation assay. The quantification of cell colonies is shown in the bar chart.

shRNA (Figure 3(a)). The ability of A549 and H1299 cells cultured with CAF-CM to form colonies was greater than that of cells cultured with HLF-CM. However, A549 and H1299 cells cultured with shLEP-CAF-CM showed inhibited proliferation, while this decrease in the ability to form colonies was reversed by the addition of 50 ng/ml recombinant leptin into the CM (Figure 3(b)).

3.4. Leptin Produced by CAFs Promotes Migration of NSCLC. Similar to the results of the cloning assay, the migration of A549 and H1299 cells cocultured with CAFs was enhanced compared with that of cells cocultured with HLF cells. While the expression of leptin was downregulated by shLEP in CAFs, the cocultured A549 and H1299 cells showed inhibited migration. However, this decrease in migration was reversed by the addition of 50 ng/ml recombinant into the medium (Figure 4).

3.5. Leptin Produced by CAFs Mediates the Activation of Inflammatory Cytokine-Related Pathways in NSCLC. A549 cells grown with HLF, CAFs, CAF-shLEP, and CAF-shLEP+leptin were continuously cultured to four passages in the coculture system. Then the total proteins of the A549 cells were analyzed by western blot (Figure 5). The expression of Ob-Rb was no different in the four groups. Furthermore, changes in the phosphorylation of ERK1/2 and AKT were examined to investigate the molecular mechanisms responsible for the paracrine promotion of NSCLC cells by leptin. Similarly, leptin significantly increased the phosphorylation of ERK1/2 and AKT. This result suggested that these two pathways, which are closely related to the internal inflammatory malignant environment, were activated under conditions of high paracrine leptin secretion.

4. Discussion

CAFs act on NSCLC cells by secreting a variety of cytokines, thereby affecting the proliferation, migration, invasion, and other biological functions of NSCLC cells. At the same time, cancer cells have positive feedback on the activation and

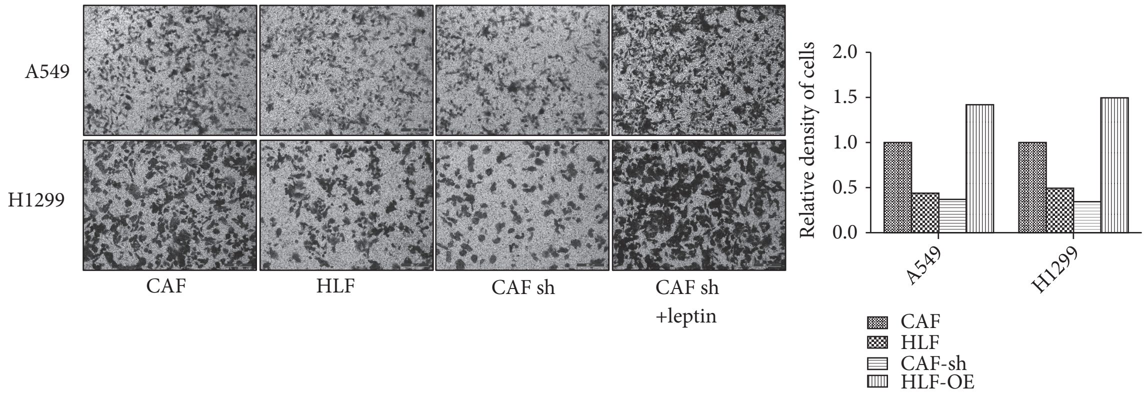

Figure 4: *The migration of NSCLC cells was inhibited by the downregulation of leptin in CAFs.* The migration of NSCLC cell lines cocultured with different fibroblasts was assessed by Transwell migration assay. The quantification of the migrated cells is shown in the bar chart.

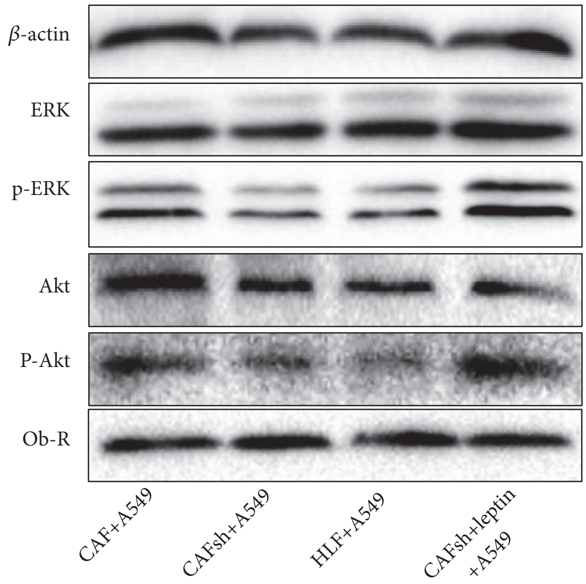

Figure 5: *The phosphorylation of ERK1/2 and AKT depends on paracrine leptin.* (a) Leptin significantly increased the phosphorylation of ERK1/2 and AKT. Three independent experiments were performed, and representative protein bands from one of the three tests are shown. Leptin treatment: 50 ng/ml, 1 hour.

maintenance of the cancer-associated properties of CAFs [23]. Researchers have tried many methods to simulate tumor microenvironment in both in vivo and in vitro experiments, especially to revive the interaction between CAFs and tumor cells. Classic models include conditioned medium, the Transwell system [24], the Boyden chamber system [25], and xenoanimal coinjection models [26]. In recent years, microfluidic chip technology [27] and the patient-derived xenograft mouse model [28] (PDX) have also become common research tools. In the current study, we introduced a novel noncontact coculture device, that solves the limitations of previous models in terms of cell quantity and passages, and its practicality was experimentally verified.

Leptin is a cytokine and hormone first shown to be secreted by adipose tissue [29]. Leptin is also produced and secreted by many nonadipose tissues, including gastric mucosal [30], breast [31], muscle [32], placenta [33], and lung tissues [34]. Studies have suggested that a leptin-enriched microenvironment promotes tumor cells [17–19, 35]. In the current study, we confirmed that leptin was overexpressed in NSCLC and was produced not only from epithelial cells, but also from CAFs. Furthermore, we found that the receptor of leptin, Ob-Rb, was only overexpressed in NSCLC cells, and was not expressed in CAFs. As previous studies have shown that serum leptin has no significant effect on lung cancer, we hypothesized that leptin most likely affects NSCLC through autocrine and paracrine mechanisms.

Furthermore, we observed the effect of paracrine leptin on NSCLC, and found that CAF-produced leptin reversibly promoted colony formation and migration of NSCLC cells. On this basis we found that the function of paracrine leptin was similar to that of the addition of recombinant leptin directly into the medium. Nevertheless, the downregulation of leptin produced by CAFs can offset this effect. This result confirmed that paracrine leptin promotes the proliferation and migration of NSCLC cells. However, given that NSCLC cells themselves also produce large amounts of leptin, whether autocrine leptin has an effect on NSCLC still needs to be explored in future studies.

The function of leptin depends on a specific receptor (leptin receptor, OB- Rb) on the surface of its target cells [36]. Ob-R is expressed at very low levels in epithelial cells from normal human mammary glands, but it is overexpressed in cancer cells [37]. A variety of inflammatory cytokines and inflammatory-mediating pathways are downstream of the leptin-OB-Rb signaling pathway, such as the PI3K/AKT, MAPK/ERK1/2, JAK2/STAT3, and insulin receptor substance (IRS) pathways [38]. In the current study, we investigated changes in key molecules from several signaling pathways in NSCLC cells cocultured with CAFs and found that the MAPK/ERK1/2 and PI3K/AKT signaling pathways were activated by leptin produced by CAFs, which demonstrated that the functions of paracrine leptin in NSCLC were similar to those in the same pattern with that of the serum leptin to in other cancers. Thus, it was concluded that leptin produced by CAFs promotes the proliferation and migration of NSCLC cells probably via the PI3K/AKT and MAPK/ERK1/2 signaling pathways in a paracrine manner.

Data Availability

The experimental data used to support the findings of this study are included within the article. The 3D printing drawing data are available from the corresponding author upon request. Detailed data of the patients involved in the study are restricted by the Ethics Committee of the 1st Hospital of Dalian Medical University. Data are available from Dr. Gu (guchundong@dmu.edu.cn) for researchers who meet the criteria for access to confidential data.

Conflicts of Interest

The author reports no conflicts of interest in this work.

Authors' Contributions

All authors contributed to the design of the study and the preparation and critical revision of the manuscript and agreed to be accountable for all aspects of the study. The manuscript is approved by all authors for publication. Fengzhou Li and Shilei Zhao contributed equally to this study.

Acknowledgments

This work was supported by grants from the National Natural Science Foundation of China (81173453, 81774078, and 81803886) and Natural Science Foundation of Liaoning Province, China (201602227).

References

[1] R. L. Siegel, K. D. Miller, and A. Jemal, "Cancer statistics," *CA: A Cancer Journal for Clinicians*, vol. 68, no. 1, pp. 7–30, 2018.

[2] F. Li, S. Zhang, Q. Zhang, J. Li, S. Zhao, and C. Gu, "CYP1B1 G199T polymorphism affects prognosis of NSCLC patients with the potential to be an indicator and target for precise drug intervention," *BioMed Research International*, vol. 2017, Article ID 1529564, 2017.

[3] T. Yu, Z. Guo, H. Fan et al., "Cancer-associated fibroblasts promote non-small cell lung cancer cell invasion by upregulation of glucose-regulated protein 78 (GRP78) expression in an integrated bionic microfluidic device," *Oncotarget*, vol. 7, no. 18, pp. 25593–25603, 2016.

[4] M. Shafiee, E. Mohammadzadeh, S. Shahidsales et al., "Current status and perspectives regarding the therapeutic potential of targeting EGFR pathway by curcumin in lung cancer," *Current Pharmaceutical Design*, vol. 23, no. 13, pp. 2002–2008, 2017.

[5] X. Zhou, L. He, S. Zuo et al., "Serine prevented high-fat diet-induced oxidative stress by activating AMPK and epigenetically modulating the expression of glutathione synthesis-related genes," *Biochimica et Biophysica Acta (BBA) - Molecular Basis of Disease*, vol. 1864, no. 2, pp. 488–498, 2018.

[6] X. Gui, H. Chen, H. Cai, L. Sun, and L. Gu, "Leptin promotes pulmonary fibrosis development by inhibiting autophagy via PI3K/Akt/mTOR pathway," *Biochemical and Biophysical Research Communications*, vol. 498, no. 3, pp. 660–666, 2018.

[7] Y. Zhang, R. Proenca, M. Maffei, M. Barone, L. Leopold, and J. M. Friedman, "Positional cloning of the mouse obese gene and its human homologue," *Nature*, vol. 372, no. 6505, pp. 425–432, 1994.

[8] S. Uddin, R. Bu, M. Ahmed et al., "Leptin receptor expression and its association with PI3K/AKT signaling pathway in diffuse large B-cell lymphoma," *Leukemia & Lymphoma*, vol. 51, no. 7, pp. 1305–1314, 2010.

[9] C. Giordano, F. Chemi, S. Panza et al., "Leptin as a mediator of tumor-stromal interactions promotes breast cancer stem cell activity," *Oncotarget* , vol. 7, no. 2, pp. 1262–1275, 2016.

[10] L. Zabeau, D. Lavens, F. Peelman, S. Eyckerman, J. Vandekerckhove, and J. Tavernier, "The ins and outs of leptin receptor activation," *FEBS Letters*, vol. 546, no. 1, pp. 45–50, 2003.

[11] Y. Huang, D. Lin, and C. M. Taniguchi, "Hypoxia inducible factor (HIF) in the tumor microenvironment: friend or foe?" *Science China Life Sciences*, vol. 60, no. 10, pp. 1114–1124, 2017.

[12] M. Berdiel-Acer, R. Sanz-Pamplona, A. Calon et al., "Differences between CAFs and their paired NCF from adjacent colonic mucosa reveal functional heterogeneity of CAFs, providing prognostic information," *Molecular Oncology*, vol. 8, no. 7, pp. 1290–1305, 2014.

[13] S. Vicent, L. C. Sayles, D. Vaka et al., "Cross-species functional analysis of cancer-associated fibroblasts identifies a critical role for CLCF1 and IL-6 in non-small cell lung cancer in vivo," *Cancer Research*, vol. 72, no. 22, pp. 5744–5756, 2012.

[14] S. M. Goicoechea, R. García-Mata, J. Staub et al., "Palladin promotes invasion of pancreatic cancer cells by enhancing invadopodia formation in cancer-associated fibroblasts," *Oncogene*, vol. 33, no. 10, pp. 1265–1273, 2014.

[15] Z. Liao, Z. W. Tan, P. Zhu, and N. S. Tan, "Cancer-associated fibroblasts in tumor microenvironment - Accomplices in tumor malignancy," *Cellular Immunology*, 2018.

[16] I. Barone, S. Catalano, L. Gelsomino et al., "Leptin mediates tumor-stromal interactions that promote the invasive growth of breast cancer cells," *Cancer Research*, vol. 72, no. 6, pp. 1416–1427, 2012.

[17] A. Calgani, S. Delle Monache, P. Cesare, C. Vicentini, M. Bologna, and A. Angelucci, "Leptin contributes to long-term stabilization of HIF-1α in cancer cells subjected to oxygen limiting conditions," *Cancer Letters*, vol. 376, no. 1, pp. 1–9, 2016.

[18] K. Li, L. Wei, Y. Huang et al., "Leptin promotes breast cancer cell migration and invasion via IL-18 expression and secretion," *International Journal of Oncology*, vol. 48, no. 6, pp. 2479–2487, 2016.

[19] A. I. Yousef, O. S. El-Masry, and E. H. Yassin, "The anti-oncogenic influence of ellagic acid on colon cancer cells in leptin-enriched microenvironment," *Tumor Biology*, vol. 37, no. 10, pp. 13345–13353, 2016.

[20] X. Tong, Y. Ma, Q. Zhou et al., "Serum and tissue leptin in lung cancer: A meta-analysis," *Oncotarget* , vol. 8, no. 12, pp. 19699–19711, 2017.

[21] D. C. Rio, M. Ares Jr., G. J. Hannon, and T. W. Nilsen, "Purification of RNA using TRIzol (TRI Reagent)," *Cold Spring Harbor Protocols*, vol. 2010, no. 6, 2010.

[22] S. Zhao, W. Guo, J. Li et al., "High expression of Y-box-binding protein 1 correlates with poor prognosis and early recurrence in patients with small invasive lung adenocarcinoma," *OncoTargets and Therapy*, vol. 9, pp. 2683–2692, 2016.

[23] W. J. Chen, C. C. Ho, and Y. L. Chang, "Cancer-associated fibroblasts regulate the plasticity of lung cancer stemness via paracrine signalling," *Nature Communications*, vol. 5, article 3472, 2014.

[24] G. Lv, Y. Tan, H. Lv et al., "MXR7 facilitates liver cancer metastasis via epithelial-mesenchymal transition," *Science China Life Sciences*, vol. 60, no. 11, pp. 1203–1213, 2017.

[25] I. Hebeiss, R. Truckenmüller, S. Giselbrecht, and U. Schepers, "Novel three-dimensional Boyden chamber system for studying transendothelial transport," *Lab on a Chip* , vol. 12, no. 4, pp. 829–834, 2012.

[26] A. F. Olumi, G. D. Grossfeld, S. W. Hayward, P. R. Carroll, T. D. Tlsty, and G. R. Cunha, "Carcinoma-associated fibroblasts direct tumor progression of initiated human prostatic epithelium," *Cancer Research*, vol. 59, no. 19, pp. 5002–5011, 1999.

[27] Q. Zhang, T. Liu, and J. Qin, "A microfluidic-based device for study of transendothelial invasion of tumor aggregates in realtime," *Lab on a Chip* , vol. 12, no. 16, pp. 2837–2842, 2012.

[28] K. Igarashi, T. Murakami, K. Kawaguchi et al., "A patient-derived orthotopic xenograft (PDOX) mouse model of a cisplatinum-resistant osteosarcoma lung metastasis that was sensitive to temozolomide and trabectedin: Implications for precision oncology," *Oncotarget* , vol. 8, no. 37, pp. 62111–62119, 2017.

[29] A. De Vincentis, C. Pedone, U. Vespasiani-Gentilucci et al., "Effect of sibutramine on plasma C-reactive protein, leptin and adipon ectin concentrations: a systematic review and meta-analysis of randomized contr olled trials," *Current Pharmaceutical Design*, vol. 23, no. 6, pp. 870–878, 2017.

[30] C. R. González, J. E. Caminos, R. Gallego et al., "Adiponectin receptor 2 is regulated by nutritional status, leptin and pregnancy in a tissue-specific manner," *Physiology & Behavior*, vol. 99, no. 1, pp. 91–99, 2010.

[31] A. MacCiò, C. Madeddu, G. Gramignano et al., "Correlation of body mass index and leptin with tumor size and stage of disease in hormone-dependent postmenopausal breast cancer: Preliminary results and therapeutic implications," *Journal of Molecular Medicine*, vol. 88, no. 7, pp. 677–686, 2010.

[32] J. Wang, R. Liu, M. Hawkins, N. Barzilial, and L. Rossetti, "A nutrient-sensing pathway regulates leptin gene expression in muscle and fat," *Nature*, vol. 393, no. 6686, pp. 684–688, 1998.

[33] S. Basak and A. K. Duttaroy, "Leptin induces tube formation in first-trimester extravillous trophoblast cells," *European Journal of Obstetrics & Gynecology and Reproductive Biology*, vol. 164, no. 1, pp. 24–29, 2012.

[34] X.-J. Zheng, Z.-X. Yang, Y.-J. Dong et al., "Downregulation of leptin inhibits growth and induces apoptosis of lung cancer cells via the Notch and JAK/STAT3 signaling pathways," *Biology Open*, vol. 5, no. 6, pp. 794–800, 2016.

[35] E. M. Bullwinkle, M. D. Parker, N. F. Bonan, L. G. Falkenberg, S. P. Davison, and K. L. DeCicco-Skinner, "Adipocytes contribute to the growth and progression of multiple myeloma: Unraveling obesity related differences in adipocyte signaling," *Cancer Letters*, vol. 380, no. 1, pp. 114–121, 2016.

[36] Y. Chen, W. Lu, N. Gao et al., "Generation of obese rat model by transcription activator-like effector nucleases targeting the leptin receptor gene," *Science China Life Sciences*, vol. 60, no. 2, pp. 152–157, 2017.

[37] G. Newman and R. R. Gonzalez-Perez, "Leptin-cytokine crosstalk in breast cancer," *Molecular and Cellular Endocrinology*, vol. 382, no. 1, pp. 570–582, 2014.

[38] W. Song, Z. Wang, X. Zhang, and Y. Li, "Ethanol extract from Ulva prolifera prevents high-fat diet-induced insulin resistance, oxidative stress, and inflammation response in mice," *BioMed Research International*, vol. 2018, Article ID 1374565, 9 pages, 2018.

Hindawi
BioMed Research International
Volume 2019, Article ID 2015978, 15 pages
https://doi.org/10.1155/2019/2015978

Review Article

Quorum Sensing: A Prospective Therapeutic Target for Bacterial Diseases

Qian Jiang,[1,2,3] **Jiashun Chen**,[1] **Chengbo Yang**,[3] **Yulong Yin**,[1] **and Kang Yao**[1]

[1] *Laboratory of Animal Nutritional Physiology and Metabolic Process, Institute of Subtropical Agriculture, Chinese Academy of Sciences, China*
[2] *University of Chinese Academy of Sciences, Beijing 100043, China*
[3] *Department of Animal Science, University of Manitoba, Winnipeg, MB, Canada R3T 2N2*

Correspondence should be addressed to Kang Yao; yaokang@isa.ac.cn

Received 29 January 2019; Accepted 20 March 2019; Published 4 April 2019

Guest Editor: Deguang Song

Copyright © 2019 Qian Jiang et al. This is an open access article distributed under the Creative Commons Attribution License, which permits unrestricted use, distribution, and reproduction in any medium, provided the original work is properly cited.

Bacterial quorum sensing (QS) is a cell-to-cell communication in which specific signals are activated to coordinate pathogenic behaviors and help bacteria acclimatize to the disadvantages. The QS signals in the bacteria mainly consist of acyl-homoserine lactone, autoinducing peptide, and autoinducer-2. QS signaling activation and biofilm formation lead to the antimicrobial resistance of the pathogens, thus increasing the therapy difficulty of bacterial diseases. Anti-QS agents can abolish the QS signaling and prevent the biofilm formation, therefore reducing bacterial virulence without causing drug-resistant to the pathogens, suggesting that anti-QS agents are potential alternatives for antibiotics. This review focuses on the anti-QS agents and their mediated signals in the pathogens and conveys the potential of QS targeted therapy for bacterial diseases.

1. Introduction

Antibiotics have been commonly used to prevent bacterial infection and diseases for many decades since their discovery at the beginning of the 20th century. However, emerging evidence [1–6] indicates that traditional antibiotic treatments tend to be ineffective for the patients, due to the emergence of drug-resistant pathogens resulting from antibiotics overuse [7, 8]. The fact that bacterial infection annually deprives about 16 million human lives prompts us to develop novel approaches fighting against the drug-resistant pathogens and related diseases [9].

Bacterial quorum sensing (QS) signaling can be activated by the self-produced extracellular chemical signals in the milieu. The QS signals mainly consist of acyl-homoserine lactones (AHLs), autoinducing peptides (AIPs) and autoinducer-2 (AI-2), all of which play key roles in the regulation of bacterial pathogenesis. For instance, studies [10–12] reported that QS signals participate in the synthesis of virulence factors such as lectin, exotoxin A, pyocyanin, and elastase in the *Pseudomonas aeruginosa* during bacterial growth and infection. The synthesis and secretion of hemolysins, protein A, enterotoxins, lipases, and fibronectin protein are regulated by the QS signals in the *Staphylococcus aureus* [13, 14]. These virulence factors regulated by QS help bacteria evade the host immune and obtain nutrition from the hosts.

The anti-QS agents, which are considered as alternatives to antibiotics due to its capacity in reducing bacterial virulence and promoting clearance of pathogens in different animal model, have been verified to prevent the bacterial infection. The clinical application of anti-QS agents is still not mature. This review builds on the increasing discoveries and applications of the anti-QS agents from the studies in the past two decades. Our goal is to illustrate the potential of exploiting the QS signals-based drugs and methods for preventing the bacterial infection without resulting in any drug-resistance of pathogens.

2. Quorum Sensing Signals

The bacterial QS signals mainly consist of acyl-homoserine lactones (AHLs), autoinducing peptides (AIPs), and autoinducer-2 (AI-2) and participate in the various physiological processes of bacteria including biofilm formation, plasmid conjugation, motility, and antibiotic resistance by which bacteria can adapt to and survive from disadvantages [15]. The Gram-negative and Gram-positive bacteria have different QS signals for cell-to-cell communications. The AHL signaling molecules are mainly produced by Gram-negative bacteria [16], and AIP signaling molecules are produced by the Gram-positive bacteria [17]. Both Gram-negative and Gram-positive bacteria produce and sense the AI-2 signals [18]. These three families of QS signals are gaining more and more attention due to their regulatory roles in bacterial growth and infection.

Lux-I type AHL synthase circuit has been considered as the QS signals producer in the Gram-negative bacteria [19]. Once the AHLs accumulate in the extracellular environment and exceed the threshold level, these signal molecules will diffuse across the cell membrane [20] and then bind to specific QS transcriptional regulators, thereby promoting target gene expression [21]. The signal molecules AIPs are synthesized in Gram-positive bacteria and secreted by membrane transporters [17]. When an environmental concentration of AIPs exceeds the threshold, these AIPs bind to a bicomponent histidine kinase sensor, whose phosphorylation, in turn, alters target gene expression and triggers related physiological process [22]. For instance, QS signals in *Staphylococcus aureus* are strictly regulated by the accessory gene regulator (ARG) which associated with AIPs secretion [23, 24]. ARG genes are involved in the production of many toxins and degradable exoenzymes [25], which are mainly controlled by P2 and P3 promoters [26, 27]. The AGR genes also participate in the encoding of AIPs and the signaling transduction of histidine kinase [28]. Bacteria can sense and translate the signals from other strains in the environment known as AI-2 interspecific signals. AI-2 signaling in most bacterial strains is catalyzed by LuxS synthase [29, 30]. LuxS is involved not only in the regulation of the AI-2 signals but also in the activated methyl cycle and has been revealed to control the expressions of 400 more genes associated with the bacterial processes of surface adhesion, movement, and toxin production [31].

3. Biofilm Formation and Virulence Factors

Bacteria widely exist in the natural environment, on the surface of hospital devices, and in the pathological tissues [32]. Biofilm formation is one of the necessary requirements for bacterial adhesion and growth [33]. The biofilm formation is accompanied by the production of extracellular polymer and adhesion matrix [34, 35] and leads to fundamental changes in the bacterial growth and gene expression [36]. The formation of biofilm significantly reduces the sensitivity of bacteria to antibacterial agents [37, 38] and radiations [39] and seriously affects public health. Some formidable infections are associated with the formation of bacterial biofilms on the pathological tissues, and most infections induced by hospital-acquired bloodstream and urinary tract are caused by biofilms-coated pathogens on hospital medical devices. A large number of studies [33, 40, 41] have shown that bacterial quorum sensing (QS) signaling plays important roles in biofilm formation. Specific QS signaling blockage is considered an effective means to prevent the biofilms formation of most pathogens, thereby increasing the sensitivity of pathogens to antibacterial agents and improving the bactericidal effect of antibiotics [42, 43].

The production of virulence factors, which could help bacteria evade the host's immune response and cause pathological damage, is crucial for the pathogenesis of infections [44–46]. The virulence factors produced by different strains are different. For example, Gram-negative *Pseudomonas aeruginosa* produces virulence factors, such as pyocyanin, elastase, lectin, and exotoxin A [47, 48], and Gram-positive *Staphylococcus aureus* produces virulence factors such as fibronectin binding protein, hemolysin, protein A, lipase, and enterotoxin [49, 50]. Studies have shown that the production of these virulence factors is regulated by the bacterial QS signaling systems [51, 52]. Disruption of QS to control the production of virulence factors seems to be an attractive broad-spectrum therapeutic strategy.

4. Strategies for QS Disruption

The fact pathogens colonized in the host must active the QS signaling to form biofilm and produce virulence factors suggests that breaking this bacterial ”conversation” by anti-QS agents makes pathogens more susceptible to host immune responses and antibiotics. In this section, we discuss the QS disruption strategies including receptor inactivation, signals synthesis inhibition, signals degradation, signaling blockage by antibody, and combining use with antibiotics and convey the potential of QS as the therapeutic target for bacterial diseases.

4.1. QS Receptor Inactivation. Inactivation of receptors in QS signaling is an effective strategy for reducing bacterial virulence and infection (Table 1). Studies [53] have demonstrated that flavonoids can bind to QS receptors and significantly reduce the virulence gene expression in *Pseudomonas aeruginosa*. N-decanoyl-L-homoserine benzyl ester, a structural analog of AHL signals, has been revealed to reduce the production of virulence factors, such as elastase and rhamnolipid, by blocking the homologous receptors in *Pseudomonas aeruginosa* [54, 55]. Receptor antagonists have been revealed to enhance the antibacterial activity of various antibiotics and minimize the therapeutic dose of antibiotics for *Pseudomonas aeruginosa* infection [56]. The meta-bromo-thiolactone was reported to prevent *Pseudomonas aeruginosa* infection by decreasing the pyocyanin production and inhibiting the biofilm formation [57]. Geske et al. have developed AHLs analogs that can bind with the LuxR, TraR, and LasR receptors in *Vibrio fischeri, Agrobacterium tumefaciens, and Pseudomonas aeruginosa*, respectively [58]. However, the application of receptor inhibitors for treating bacterial diseases is lagging behind due to the properties of instability and degradability within alkaline conditions. Further studies are warranted to improve the stability of these effective anti-QS agents.

Table 1: Studies demonstrating the quorum sensing (QS) signaling disruption by receptor inactivation. Abbreviations: 3-oxo-C12, N-3-oxododecanoyl-C12; AHL, N-acyl-homoserine lactones; AI, autoinducer; C4-LHL, butenyl homoserine lactones; C6-LHL, hexanoyl homoserine lactones; HSL, L-homoserine lactone; PHL, propionyl homoserine lactones.

Models	Strains	Anti-QS agents	Target	Effects	Ref
In-vitro	*Pseudomonas aeruginosa*	Flavonoids	Allosteric inhibition of AI-binding receptors, LasR and RhlR	Altered transcription of QS-controlled target promoters and suppresses virulence factor production	[53]
In-vitro	*Pseudomonas aeruginosa* PAO1	N-decanoyl-L-homoserine benzyl ester	Activating quorum sensing control repressor	Attenuated the activity of protease and elastase, swarming motility and biofilm formation	[54, 55]
In-vitro, *C. elegans*, A549 cells,	*Pseudomonas aeruginosa* PA14	Meta-bromo-thiolactone	Inhibition of LasR and RhlR	Inhibited both the production of the virulence factor pyocyanin and biofilm formation	[57]
In-vitro	*Pseudomonas aeruginosa*	AHL ligands A4, 4-bromophenyl-PHL B7, 4-iodo PHL C10, and 3-nitro PHL C14	Binding to TraR, LasR, and LuxR	Strongly inhibited virulence factor production	[58]
In-vitro, Mice	*Aeromonas hydrophila*	C4- and C6-HSLs, 3-oxo-C12-HSL	Regulating the host immune receptor	Increased survivability of infected mice	[59]

4.2. QS Signals Synthesis Inhibition. The acyl-homoserine lactone molecules (AHLs) not only participate in bacterial communication but also play roles in conversations with eukaryotic cells. AHLs can regulate the signaling pathways in epithelial cells and affect the behavior of innate immune cells [59, 60]. Inhibiting the synthesis of AHLs is a direct strategy to reduce AHL-mediated virulence factors and prevent pathological damage (Table 2). For example, studies have revealed that the sinefungin, butyryl-SAM, and S-adenosylhomocysteine can attenuate the secretion of QS-mediated virulence factors and prevent the bacterial infection by inhibiting the AHLs synthesis in *Pseudomonas aeruginosa* [61–63]. Singh et al. reported that immucillin A and its derivatives can reduce the AHLs synthesis by inhibiting the 5-MTAN/S-adenosylhomocysteine nucleosidase [64]. The triclosan has been verified to reduce AHL synthesis by inhibiting the production of enoyl-ACP reductase precursors [65, 66]. However, these agents for AHLs synthesis inhibition also block the metabolism of amino acid and fatty acid that play key roles in bacterial basic nutrition [67]. The fact that triclosan increased the antibiotic-resistance of *Pseudomonas aeruginosa* implies selective pressure on bacteria were triggered by the blocking effects of triclosan on the metabolism of amino acid and fatty acid in the bacteria [68]. The triclosan is considered as bioindicator pollution due to its potential in causing the drug-resistance of the pathogens and increasing human health risks [69]. Thus, the drugs specifically targeting AHLs synthesis inhibition without blocking nutritional metabolisms of bacteria should be developed and identified by sufficient *in vitro* experiments before their clinical application.

4.3. QS Signals Degradation. Degradation of QS signals by enzymes can effectively disrupt the "communication" among the bacteria without causing any selective pressure to the bacteria. The enzymes consist of lactonase, acylase, oxidoreductases, and 3-Hydroxy-2-methyl-4(1H)-quinolone 2, 4-dioxygenase, all of which are derived from different bacterial strains and have been applied for QS signals degradation (Tables 3 and 4).

The AHL lactonase, a member of Metallo-β-lactamase superfamily, was able to prevent bacterial infection by degrading AHLs with different length of side chain [70, 71]. The AHL lactonases were reported to increase bacterial sensitivity to antibiotics without affecting the growth of *Pseudomonas aeruginosa* [72, 73] and *Acinetobacter baumannii* [74]. The AHL lactonase also has been applied to block the biofilm formation of *Pseudomonas aeruginosa* [75–77]. The AHL lactonase AiiK produced by the engineered *Escherichia coli* was revealed to inhibit extracellular proteolytic activity and pyocyanin production of *Pseudomonas aeruginosa* PAO1 [78]. In addition, synergistic action of AHL lactonase and antibiotics was observed in the mice model infected with *Pseudomonas aeruginosa*; that is, the drugs containing AHL lactonase can effectively inhibit the spread of skin pathogens while minimizing the effective dose of antibiotics. The AHL lactonase has also been applied in the fishery industry, for instance, Liu et al. reported the lactonase AIO6 supplemented to tilapia was able to prevent the *Aeromonas hydrophila* infection [79]. Studies reported the lactonase AiiA can decrease the virulence and inhibit biofilm formation of *Vibrio parahaemolyticus* in shrimps [80, 81].

The acylase, which was initially found in *Variovorax paradoxus* and *Ralstonia,* can block the QS signaling by hydrolyzing the amide bond of AHLs [82–84]. The acylase was revealed to decrease the growth of *Pseudomonas aeruginosa* ATCC 10145 and PAO1 by 60% [85, 86] and has been widely applied in human health care; for example, the acylase-coated device showed a well antibacterial property due to the QS signaling disruption by the acylase [87]. The acylase is also chemically immobilized on some nanomaterials to act as an antifouling agent [88]. Undoubtedly, these applications of acylase will greatly reduce the health care cost caused by the spread and colonization of pathogenic bacteria on medical devices.

Oxidoreductases are enzymes that can affect the AHLs specificity of homologous intracellular receptors by modifying acyl side chains, thus interfering with the expression of QS related virulence genes [89]. Previous studies have demonstrated the secretion of oxidoreductases by bacteria as a protective mechanism instead of a pathogenic signaling [90]. The BpiB09 oxidoreductase was reported to inhibit the activation of N-3-oxo-dodecanoyl homoserine lactone (3-oxo-C12-HSL) in the *Pseudomonas aeruginosa* PAO1 and decrease bacterial motility, biofilms formation, and pyocyanin secretion [91]. Immobilization of oxidoreductases on the glass surface can inhibit the bacterial biofilm formation and decrease the growth rate of *Klebsiella oxytoca* and *Klebsiella pneumoniae* [92, 93].

The dioxygenase has been revealed to block the quinolone signals in the QS system of *Pseudomonas aeruginosa* [94]. Dioxygenase can degrade 2-heptyl-3-hydroxy-4 (1H)-quinolone mediated signals and decreases signaling molecules accumulation in the bacterial milieu, therefore reducing the secretion of pyocyanin, rhamnolipid, and lectin A toxin, which protects the host from infective damage [95, 96].

Together, the anti-QS signaling enzymes are promising alternatives to antibiotics that can be used not only to control bacterial infection but also to minimize the risk of causing antibiotic-resistant strains. However, the stability of enzymes *in vivo* is the most difficult problem for their biomedical applications. It is of great significance to study and develop the stability of the anti-QS signaling enzymes *in vivo*. QS degradation by nonpathogenic bacteria is an effective strategy for QS disruption. *Pectobacterium carotovorum* subsp. *carotovorum* is a preferred and commonly used bacterial strain for QS degradation [97]. This biological strategy for QS signal degradation has been applied to prevent plant diseases [98] but has not been applied for human diseases treatment. By exploring novel QS-degradation strains, it might be possible to cure the chronic diseases caused by the antibiotic-resistant pathogens.

4.4. Target Antibodies for QS Blockage. The activation of AHL and AI-2 signaling can induce programmed cell death by affecting the host's immune system [59, 99]. Kaufmann et

Table 2: Studies demonstrating the QS disruption by signals synthesis inhibition. Abbreviations: AI, autoinducer; enoyl-ACP, enoyl-acyl carrier protein; HSL, L-homoserine lactone; PHL, propionyl homoserine lactones.

Models	Strains	Anti-QS agents	Target	Effects	Ref
In-vitro, Rats	*Streptococcus pneumoniae* D-39	Sinefungin	Inhibition of AI-2 synthesis via downregulating luxS, pfs, and speE expression	Inhibited pneumococcal biofilm growth in vitro and middle ear colonization in vivo	[62]
In-vitro	*Pseudomonas aeruginosa*	Sinefungin, butyryl-SAM, and S-adenosylhomocysteine	Inhibiting acyl-HSL signals	Inhibited formation of a covalent acyl–enzyme	[61]
In-vitro	*Escherichia coli*	Methylthio-DADMe-immucillin-A	Downregulating 5′-methylthioadenosine, S-adenosyl-homocysteine nucleosidase hydrolyzes	Disrupted key bacterial pathways of methylation, polyamine synthesis, methionine salvage, and quorum sensing	[64]
Mouse	*Plasmodium falciparum*	Triclosan	Inhibiting enoyl-ACP reductase	Protected against blood stages of malaria, enhanced elastic strength	[66]

Table 3: Studies demonstrating QS disruption by signals degradation.

Models	Strains	Anti-QS agents	Target	Effects	Ref
In-vitro	*Pseudomonas aeruginosa*	Lactonase SsoPox	Degradation of the acyl-homoserine lactones	Inhibited the virulence of 51 clinical P. aeruginosa isolated from diabetic foot ulcers by decreasing the secretion of proteases and pyocyanin, and biofilm formation	[72]
In-vitro, rats	*Pseudomonas aeruginosa* PAO1	Lactonase SsoPox-1	Degradation of the acyl-homoserine lactones	Decreased lasB virulence gene activity, pyocyanin synthesis, proteolytic activity, and biofilm formation. Reduced the mortality of rats with acute pneumonia from 75% to 20%. Attenuated lung damage of the rat model	[73]
In-vitro	A.baumannii S1,S2,S3	Engineered lactonase	Degradation of the acyl-homoserine lactones	Reduced the biomass of A. baumannii associated biofilms	[74]
In-vitro	*Pseudomonas aeruginosa*	Lactonase Aii810	Degradation of the acyl-homoserine lactones	Attenuated Virulence Factors and Biofilm Formation. Degraded N-butyryl-L-homoserine lactone and N-(3-oxododecanoyl)-L-homoserine lactone, by 72.3 and 100%	[75]
In-vitro	*Pseudomonas aeruginosa*	Overexpression of lactonase enzyme AHL-1	Degradation of the acyl-homoserine lactones	Reduced the protease, pyocyanin, rhamnolipids. Inhibited the activities on the swarming motility and biofilm formation	[76]
In-vitro	*Pseudomonas aeruginosa*	Novel Lactonase cloned by bpiB01, bpiB04	Degradation of the N-(3-oxooctanoyl)-L-homoserine lactone	Inhibited motility and biofilm formation	[77]
In-vitro	*Pseudomonas aeruginosa* PAO1	Lactonase AiiK	Degradation of the acyl-homoserine lactones	Inhibited the biofilm formation and attenuates extracellular proteolytic activity and pyocyanin production	[78]
In-vitro	*Pseudomonas aeruginosa* PAO1	N-Acyl-Homoserine Lactone Acylase PA2385	Degradation of 3-oxo-C12-HSL and 2-heptyl-3-hydroxy-4(1H)-quinolone	Reduced production of the virulence factors elastase and pyocyanin	[85]
In-vitro, *C. elegans*	*Pseudomonas aeruginosa* PAO1	NADP-dependent short-chain dehydrogenase/reductase (bpiB09)	Inactivation of N-(3-oxo-dodecanoyl)-L-homoserine lactone (3-oxo-C12-HSL)	Reduced pyocyanin production, decreased motility, poor biofilm formation and absent paralysis of *C. elegans*	[91]
In-vitro, plant	*Pseudomonas aeruginosa* PAO1	3-hydroxy-2-methyl-4(1H)-quinolone	Catalyzing the conversion of PQS to N-octanoylanthranilic acid and carbon monoxide	Reduced expression of the PQS biosynthetic gene pqsA, expression of the PQS-regulated virulence determinants lectin A, pyocyanin, and rhamnolipids, and virulence in plant	[94]

Table 4: Applications involving with AHLs degradation by anti-QS agents. 3-oxo-C12, N-3-oxododecanoyl-HSL; AHL, N-acyl-homoserine lactones; C4-LHL, butenyl homoserine lactones; C6-LHL, hexanoyl homoserine lactones.

Objectives	Strains	Anti-QS agents	Target	Effects	Ref
Tilapia	*Aeromonas hydrophila*	AHL lactonase AIO6	Degradation of the acyl-homoserine lactones	Maintained the microvilli length in the foregut of tilapia, but significantly lower than those of the control.	[79]
Shrimp and clam	*Vibrionaceae strains*	Deletion of AHLs genes in 34 marine *Vibrionaceae* strains	Acyl-homoserine lactones inactivation	Reduced virulence and mortality of the mutant strains in brine shrimp and Manila clam.	[80]
Shrimp	*Vibrio parahaemolyticus*	AHL-lactonase (AiiA)	Degradation of the acyl-homoserine lactones	Inhibited vibrio biofilm development and attenuated infection and mortality. Reduce vibrio viable counts and biofilm development in the intestine.	[81]
Enzyme multilayer coatings	*Chromobacterium violaceum* CECT 5999, *Pseudomonas aeruginosa* ATCC 10145	Acylase from *Aspergillus melleus*	Degradation of C6-LHL	Inhibited 50% violacein production by *Chromobacterium violaceum* CECT 5999; Reduces the *Pseudomonas aeruginosa* ATCC 10145 biofilm formation under static and dynamic conditions.	[86]
Acylase-containing polyurethane coatings	*Pseudomonas aeruginosa* ATCC 10145 and PAO1	Acylase from *Aspergillus melleus*	Degradation of C4-LHL, C6-LHL, and 3-oxo-C12-LHL	Immobilization of acylase led to an approximately 60% reduction in biofilm formation, reduce the secretion of pyocyanin.	[87]
Immobilization on Nanofibers	*Pseudomonas aeruginosa* PAO1	Acylase (EC.3.5.1.14)	Degradation of AHL inducers	Reduced the biofilm/biofouling formation under static and continuous flow conditions.	[88]

Table 5: Studies demonstrating QS disruption by antibodies targeting.

Models	Strains	Anti-QS agents	Target	Effects	Ref
In-vitro and RAW 264.7 cells	*Pseudomonas aeruginosa*	Antibody RS2-1G9 generated against a 3-oxo-dodecanoyl homoserine lactone analog hapten	Targeting the bacterial N-3-oxo-dodecanoyl homoserine lactone molecules	Protect murine bone marrow-derived macrophages from the cytotoxic effects and also prevented the activation of the mitogen-activated protein kinase p38.	[100]
In-vitro	*Pseudomonas aeruginosa*	Antibody XYD-11G2	Hydrolyzing N-3-(oxododecanoyl)-L-homoserine lactone	Suppressed QS signaling.	[101]
In-vitro and mouse model	*Staphylococcus aureus*	Antibody AP4-24H11 elicited against a rationally designed hapten	Sequestration of the autoinducing peptide-4	Suppressed S. aureus pathogenicity in an abscess formation mouse model *in vivo* and provided complete protection against a lethal *Staphylococcus aureus* challenge.	[103]

Table 6: Studies demonstrating the synergistic effects of anti-QS agents and antibiotics.

Models	Strains	Anti-QS agents	Target	Effects	Ref
Mice	*Pseudomonas aeruginosa*	Furanone C-30, ajoene or horseradish juice extract in	QS inhibition enhance the sensitivity of pathogen to antibiotics	Resulted in an increased clearance of *Pseudomonas aeruginosa* in a foreign-body infection model.	[107]
In-vitro	*Pseudomonas aeruginosa*	Combination curcumin with tobramycin, gentamicin and azithromycin	Induced concentrations of C12- homoserine lactone and C4- homoserine lactone	Curcumin showed synergistic effects with azithromycin and gentamicin. Combination use reduced QS-related virulence factors. Downregulated QS-related genes.	[112]
In-vitro	*Staphylococci*	Epigallocatechin-3-gallate with Tetracycline	Inhibition of the activity of Tet(K) pumps efflux pumps of a different class Tet(B)	Enhanced the bactericidal effect of Tetracycline on *Staphylococci.*	[113]
In-vitro	*Pseudomonas aeruginosa*	N-(2-pyrimidyl) butanamide, C11	Downregulation of rhl, rhlA and lasB genes	Increased the susceptibility to antibiotics and attenuated the pathogenicity of the bacterium.	[115]
In-vitro	*Staphylococcus aureus* (methicillin-resistant *S. aureus*)	Farnesol with β-lactam antibiotics	Inhibition of lipase activity and disruption of the cytoplasmic membrane through the leakage of potassium ions	Attenuated the rate of growth of bacteria, and countering ubiquitous β-lactam resistance in bacteria.	[116, 117]
In-vitro, *C. elegans*, *Galleria mellonella*, mice	*Burkholderia cenocepacia*, *Staphylococcus aureus*, *Escherichia coli*	Baicalin hydrate, cinnamaldehyde, hamamelitannin with Tobramycin, vancomycin, and clindamycin;	Inhibition of biofilm formation. QS inhibition enhance the sensitivity of pathogen to antibiotics	Combining the use of antibody and anti-QS agents increased susceptibility of the bacteria to the antibiotic, and increased host survival rate after infection	[118]

al. found in their study [100] that the antibody RS2-1G9 can bind to 3-oxo-C12-HSL in the extracellular environment of *Pseudomonas aeruginosa*, thereby attenuating the inflammatory response of the host. XYD-11G2 antibody has been shown to catalyze the hydrolysis of 3-oxo-C12-HSL signaling, thus inhibiting the pyocyanin production by Gram-negative bacteria [101, 102]. The monoclonal antibody AP4-24H11 was found to block the QS signal of Gram-positive *Staphylococcus aureus* by interfering with AIP IV [103]. Another *in vivo* study showed that the antibody AP4-24H11 could significantly attenuate the tissue necrosis in the infected model [104]. Although these monoclonal antibodies have been identified to block the QS signaling of pathogenic bacteria (Table 5), their applications for treating bacterial diseases are still in the initial stage.

4.5. Combinations of Anti-QS Agents and Antibiotics. Combining use of antibiotic with an anti-QS agent is the most effective clinical strategy for the treatment of bacterial diseases at present [105, 106]. Many studies have confirmed the synergistic effect of antibiotics and anti-QS agents (Table 6). Ajoene, furanone c-30, and horseradish extract have been revealed to reduce the expression of virulence factors in *Pseudomonas aeruginosa* and make *Pseudomonas aeruginosa* easier to be cleared by tobramycin [107–111]. Another study has confirmed the synergistic effects of curcumin, gentamicin, and azithromycin on *Pseudomonas aeruginosa*; that is, the expressions of virulence genes were significantly downregulated by the combining use of curcumin together with gentamicin or azithromycin, and the therapeutic doses of gentamicin and azithromycin were minimized by curcumin supplementation [112]. The anti-QS compounds, such as gallocatechin 3-gallate and caffeic acid, enhanced therapeutic effects on *Mycoplasma pneumoniae* infection by combining use with tetracycline, ciprofloxacin, or gentamicin [113, 114]. N-(2-pyrimidyl) butylamine was confirmed to enhance the antibacterial effect of tobramycin, colistin, and ciprofloxacin on *Pseudomonas aeruginosa* [115]. Recent studies [116, 117] have shown that both farnesol and hamamelitannin can reduce the virulence of *Staphylococcus aureus* and increase the sensitivity of *Staphylococcus aureus* to β-lactam antibiotics. Synergistic effects of hamamelitannin, baicalin, hydrate, cinnamaldehyde, and antibiotics have been demonstrated in different infection models [118, 119]. These findings imply that combining use of antibiotics with ant-QS agents has great therapeutic potential for bacterial diseases.

5. Conclusions

Regulating bacterial QS signaling by QS-targeted agents is an effective strategy to control the production of bacterial virulence factors and the formation of biofilm. This novel nonantibiotic therapy can inhibit the expression of pathogenic genes, prevent infection, and reduce the risk of drug resistance of bacterial cells and has been widely exploited in recent years. A large number of studies have identified many anti-QS agents to control the pathogenic phenotypes of most bacteria and to attenuate the pathological damage in various animal infection models. However, most anti-QS agents are still in the preclinical phase and more human clinical trials are warranted to test their practical feasibility. The results of several existing clinical studies [120–122] on anti-QS agents show that, compared with antibiotics, the anti-QS compounds may have potential toxicity and their therapeutic effect is not as stable as that of antibiotics, which limited their extensive application. Combining use of anti-QS agents with conventional antibiotics can significantly improve the efficacy of therapeutic drugs and decrease the cost of human healthcare and is likely to be the main application method of anti-QS agents for bacterial diseases treatment in the future.

Conflicts of Interest

The authors declare that there are no conflicts of interest regarding the publication of this paper.

Acknowledgments

The authors are thankful to the China Scholarship Council (CSC) for both financial support and scholarships. The authors appreciate Dr. Ruiqiang Yang at the Nanjing Agriculture University for his help on this review. This work was supported by the National Natural Science Foundation of China (31472107); the Youth Science Fund Project of the National Natural Science Foundation of China (31702126); the Chinese Academy of Sciences ‘Hundred Talent’ award, the National Science Foundation for Distinguished Young Scholars of Hunan Province (2016JJ1015); the Postgraduate Research and Innovation Project of Hunan Province (CX2017B348); the Hunan Province “Hunan Young Science and Technology Innovation Talent” Project (2015RS4053); the Hunan Agricultural University Provincial Outstanding Doctoral Dissertation Cultivating Fund (YB2017002); and the Open Foundation of Key Laboratory of Agro-ecological Processes in Subtropical Region, Institute of Subtropical Agriculture, Chinese Academy of Sciences (ISA2016101).

References

[1] M. Etminan, B. Carleton, J. A. C. Delaney, and R. Padwal, “Antibiotics ineffective for prevention of recurrent MI,” *Journal of Family Practice*, vol. 53, no. 7, p. 525, 2004.

[2] F. E. Akram, T. El-Tayeb, K. Abou-Aisha, and M. El-Azizi, “A combination of silver nanoparticles and visible blue light enhances the antibacterial efficacy of ineffective antibiotics against methicillin-resistant Staphylococcus aureus (MRSA),” *Annals of Clinical Microbiology and Antimicrobials*, vol. 15, no. 1, p. 48, 2016.

[3] L. A. Barton and M. W. Simon, “Prophylactic antibiotics: Ineffective or inefficacious,” *Clinical Pediatrics*, vol. 53, no. 8, p. 813, 2014.

[4] J. Neumaier, “Antibiotics are up to 90% ineffective: what really helps in common colds,” *MMW—Fortschritte der Medizin*, vol. 153, no. 3, pp. 18-19, 2011.

[5] B. Schlemmer, “Better prescribing of antibiotics. Preventing the risk of ineffective treatment in current infection,” *La Revue du praticien*, vol. 53, no. 14, pp. 1525-1526, 2003.

[6] P. Stiefelhagen, “Suspected severe pneumonia. Antibiotics are ineffective - what now?” *MMW—Fortschritte der Medizin*, vol. 157, no. 17, p. 28, 2015.

[7] Z. Li and M. Knetsch, “Antibacterial strategies for wound dressing: preventing infection and stimulating healing,” *Current Pharmaceutical Design*, vol. 24, no. 8, pp. 936–951, 2018.

[8] W. Xu, S. Dong, Y. Han, S. Li, and Y. Liu, “Hydrogels as antibacterial biomaterials,” *Current Pharmaceutical Design*, vol. 24, no. 8, pp. 843–854, 2018.

[9] “Microbiology by numbers,” *Nature Reviews Microbiology*, vol. 9, no. 9, p. 628, 2011.

[10] J. P. Pearson, E. C. Pesci, and B. H. Iglewski, “Roles of Pseudomonas aeruginosa las and rhl quorum-sensing systems in control of elastase and rhamnolipid biosynthesis genes,” *Journal of Bacteriology*, vol. 179, no. 18, pp. 5756–5767, 1997.

[11] C. Van Delden, E. C. Pesci, J. P. Pearson, and B. H. Iglewski, “Starvation selection restores elastase and rhamnolipid production in a Pseudomonas aeruginosa quorum-sensing mutant,” *Infection and Immunity*, vol. 66, no. 9, pp. 4499–4502, 1998.

[12] L. E. Dietrich, A. Price-Whelan, A. Petersen, M. Whiteley, and D. K. Newman, “The phenazine pyocyanin is a terminal signalling factor in the quorum sensing network of Pseudomonas aeruginosa,” *Molecular Microbiology*, vol. 61, no. 5, pp. 1308–1321, 2006.

[13] E. C. Carnes, D. M. Lopez, N. P. Donegan et al., “Confinement-induced quorum sensing of individual Staphylococcus aureus bacteria,” *Nature Chemical Biology*, vol. 6, no. 1, pp. 41–45, 2010.

[14] J. M. Yarwood, D. J. Bartels, E. M. Volper, and E. P. Greenberg, “Quorum sensing in staphylococcus aureus biofilms,” *Journal of Bacteriology*, vol. 186, no. 6, pp. 1838–1850, 2004.

[15] M. J. Eickhoff and B. L. Bassler, “SnapShot: bacterial quorum sensing,” *Cell*, vol. 174, no. 5, p. 1328.e1321, 2018.

[16] M. Schuster, D. Joseph Sexton, S. P. Diggle, and E. Peter Greenberg, “Acyl-homoserine lactone quorum sensing: from evolution to application,” *Annual Review of Microbiology*, vol. 67, pp. 43–63, 2013.

[17] M. H. Sturme, M. Kleerebezem, J. Nakayama, A. D. Akkermans, E. E. Vaugha, and W. M. De Vos, “Cell to cell communication by autoinducing peptides in gram-positive bacteria,” *Antonie Van Leeuwenhoek*, vol. 81, no. 1–4, pp. 233–243, 2002.

[18] C. S. Pereira, J. A. Thompson, and K. B. Xavier, “AI-2-mediated signalling in bacteria,” *FEMS Microbiology Reviews*, vol. 37, no. 2, pp. 156–181, 2013.

[19] M. Yang, K. Sun, L. Zhou, R. Yang, Z. Zhong, and J. Zhu, “ Functional analysis of three AHL autoinducer synthase genes in *Mesorhizobium loti* reveals the important role of quorum sensing in symbiotic nodulation ,” *Canadian Journal of Microbiology*, vol. 55, no. 2, pp. 210–214, 2009.

[20] A. Ivanova, K. Ivanova, and T. Tzanov, “Inhibition of Quorum-Sensing: A New Paradigm in Controlling Bacterial Virulence and Biofilm Formation,” in *Biotechnological Applications of Quorum Sensing Inhibitors*, V. C. Kalia, Ed., pp. 5–10, 2018.

[21] Y. Zeng, Y. Wang, Z. Yu, and Y. Huang, “Hypersensitive response of plasmid-encoded AHL synthase gene to lifestyle and nutrient by Ensifer adhaerens X097,” *Frontiers in Microbiology*, vol. 8, p. 1160, 2017.

[22] A. O. Shpakov, “Bacterial autoinducing peptides,” *Mikrobiologiia*, vol. 78, no. 3, pp. 291–303, 2009.

[23] G. J. Lyon, J. S. Wright, T. W. Muir, and R. P. Novick, “Key determinants of receptor activation in the agr autoinducing peptides of Staphylococcus aureus,” *Biochemistry*, vol. 41, no. 31, pp. 10095–10104, 2002.

[24] E. J. Murray and P. Williams, “Detection of agr-type autoinducing peptides produced by staphylococcus aureus,” *Methods in Molecular Biology*, vol. 1673, pp. 89–96, 2018.

[25] M. J. Martin, S. Clare, D. Goulding et al., “The agr locus regulates virulence and colonization genes in clostridium difficile 027,” *Journal of Bacteriology*, vol. 195, no. 16, pp. 3672–3681, 2013.

[26] S. Cheraghi, L. Pourgholi, M. Shafaati et al., “Analysis of virulence genes and accessory gene regulator (agr) types among methicillin-resistant Staphylococcus aureus strains in Iran,” *Journal of Global Antimicrobial Resistance*, vol. 10, pp. 315–320, 2017.

[27] P. Gilot, G. Lina, T. Cochard, and B. Poutrel, “Analysis of the genetic variability of genes encoding the RNA III-activating components Agr and TRAP in a population of *Staphylococcus aureus* strains isolated from cows with mastitis,” *Journal of Clinical Microbiology*, vol. 40, no. 11, pp. 4060–4067, 2002.

[28] G. Lina, S. Jarraud, G. Ji et al., “Transmembrane topology and histidine protein kinase activity of AgrC, the agr signal receptor in Staphylococcus aureus,” *Molecular Microbiology*, vol. 28, no. 3, pp. 655–662, 1998.

[29] M. Guo, S. Gamby, Y. Zheng, and H. Sintim, “Small molecule inhibitors of AI-2 signaling in bacteria: state-of-the-art and future perspectives for anti-quorum sensing agents,” *International Journal of Molecular Sciences*, vol. 14, no. 9, pp. 17694–17728, 2013.

[30] J. Thompson, R. Oliveira, A. Djukovic, C. Ubeda, and K. Xavier, “Manipulation of the quorum sensing signal AI-2 affects the antibiotic-treated gut microbiota,” *Cell Reports*, vol. 10, no. 11, pp. 1861–1871, 2015.

[31] K. R. Hardie, “Autoinducer 2 activity in Escherichia coli culture supernatants can be actively reduced despite maintenance of an active synthase, LuxS,” *Microbiology*, vol. 149, no. 3, pp. 715–728, 2003.

[32] J. Wang, F. Li, and Z. Tian, “Role of microbiota on lung homeostasis and diseases,” *Science China Life Sciences*, vol. 60, no. 12, pp. 1407–1415, 2017.

[33] K. Riedel, A. Gotschlich, M. Givskov et al., “The cep quorum-sensing system of Burkholderia cepacia H111 controls biofilm formation and swarming motility,” *Microbiology*, vol. 147, no. 9, pp. 2517–2528, 2001.

[34] J. C. Linnes, H. Ma, and J. D. Bryers, “Giant extracellular matrix binding protein expression in staphylococcus epidermidis is regulated by biofilm formation and osmotic pressure,” *Current Microbiology*, vol. 66, no. 6, pp. 627–633, 2013.

[35] A. M. Romaní, K. Fund, J. Artigas, T. Schwartz, S. Sabater, and U. Obst, “Relevance of polymeric matrix enzymes during biofilm formation,” *Microbial Ecology*, vol. 56, no. 3, pp. 427–436, 2008.

[36] I. Kanwar, A. K. Sah, and P. K. Suresh, “Biofilm-mediated antibiotic-resistant oral bacterial infections: mechanism and combat strategies,” *Current Pharmaceutical Design*, vol. 23, no. 14, pp. 2084–2095, 2017.

[37] S. Keelara, S. Thakur, and J. Patel, “Biofilm formation by environmental isolates of *Salmonella* and their sensitivity to natural antimicrobials,” *Foodborne Pathogens and Disease*, vol. 13, no. 9, pp. 509–516, 2016.

[38] F. Sepandj, H. Ceri, A. Gibb, R. Read, and M. Olson, “Minimum inhibitory concentration versus minimum biofilm eliminating

concentration in evaluation of antibiotic sensitivity of enterococci causing peritonitis," *Peritoneal Dialysis International*, vol. 27, no. 4, pp. 464-465, 2007.

[39] B. A. Niemira and E. B. Solomon, "Sensitivity of planktonic and biofilm-associated salmonella spp. to ionizing radiation," *Applied and Environmental Microbiology*, vol. 71, no. 5, pp. 2732–2736, 2005.

[40] A. M. Gamage, G. Shui, M. R. Wenk, and K. L. Chua, "N-Octanoylhomoserine lactone signalling mediated by the BpsI-BpsR quorum sensing system plays a major role in biofilm formation of Burkholderia pseudomallei," *Microbiology*, vol. 157, no. 4, pp. 1176–1186, 2011.

[41] S. H. Hong, M. Hegde, J. Kim, X. Wang, A. Jayaraman, and T. K. Wood, "Synthetic quorum-sensing circuit to control consortial biofilm formation and dispersal in a microfluidic device," *Nature Communications*, vol. 3, p. 613, 2012.

[42] P. Sankar Ganesh and V. Ravishankar Rai, "Attenuation of quorum-sensing-dependent virulence factors and biofilm formation by medicinal plants against antibiotic resistant Pseudomonas aeruginosa," *Journal of Traditional and Complementary Medicine*, vol. 8, no. 1, pp. 170–177, 2018.

[43] P. Shih, "Effects of quorum-sensing deficiency on Pseudomonas aeruginosa biofilm formation and antibiotic resistance," *Journal of Antimicrobial Chemotherapy*, vol. 49, no. 2, pp. 309–314.

[44] M. I. Chernukha, I. A. Shaginian, I. M. Romanova, G. V. Maleev, and A. L. Gintsburg, "The role of "quorum sensing" regulation system in symbiotic interaction of bacteria Burkholderia cepacia and Pseudomonas aeruginosa during mixed infection," *Zhurnal Mikrobiologii, Epidemiologii, Immunobiologii*, no. 4, pp. 32–37, 2006.

[45] F. M. Husain, I. Ahmad, A. S. Al-Thubiani, H. H. Abulreesh, I. M. AlHazza, and F. Aqil, "Leaf extracts of Mangifera indica L. inhibit quorum sensing - Regulated production of virulence factors and biofilm in test bacteria," *Frontiers in Microbiology*, vol. 8, p. 727, 2017.

[46] D. G. Renter, J. G. Morris, J. M. Sargeant et al., "Prevalence, risk factors, O serogroups, and virulence profiles of shiga toxin–producing bacteria from cattle production environments," *Journal of Food Protection*, vol. 68, no. 8, pp. 1556–1565, 2005.

[47] A. R. Hauser, "Pseudomonas aeruginosa: So many virulence factors, so little time*," *Critical Care Medicine*, vol. 39, no. 9, pp. 2193-2194, 2011.

[48] R. Le Berre, S. Nguyen, E. Nowak et al., "Relative contribution of three main virulence factors in Pseudomonas aeruginosa pneumonia*," *Critical Care Medicine*, vol. 39, no. 9, pp. 2113–2120, 2011.

[49] M. M. Gallardo-Garcia, G. Sanchez-Espin, R. Ivanova-Georgieva et al., "Relationship between pathogenic, clinical, and virulence factors of Staphylococcus aureus in infective endocarditis versus uncomplicated bacteremia: a case-control study," *European Journal of Clinical Microbiology & Infectious Diseases*, vol. 35, no. 5, pp. 821–828, 2016.

[50] F. Sabouni, S. Mahmoudi, A. Bahador et al., "Virulence factors of staphylococcus aureus isolates in an iranian referral children's hospital," *Osong Public Health and Research Perspectives*, vol. 5, no. 2, pp. 96–100, 2014.

[51] H. M. Aboushleib, H. M. Omar, R. Abozahra, A. Elsheredy, and K. Baraka, "Correlation of quorum sensing and virulence factors in Pseudomonas aeruginosa isolates in Egypt," *The Journal of Infection in Developing Countries*, vol. 9, no. 10, pp. 1091–1099, 2015.

[52] R. T. Sturbelle, L. F. Avila, T. B. Roos et al., "The role of quorum sensing in Escherichia coli (ETEC) virulence factors," *Veterinary Microbiology*, vol. 180, no. 3-4, pp. 245–252, 2015.

[53] J. E. Paczkowski, S. Mukherjee, A. R. McCready et al., "Flavonoids suppress *Pseudomonas aeruginosa* Virulence through allosteric inhibition of quorum-sensing receptors," *The Journal of Biological Chemistry*, vol. 292, no. 10, pp. 4064–4076, 2017.

[54] L. Weng, Y. Yang, Y. Zhang, and L. Wang, "A new synthetic ligand that activates QscR and blocks antibiotic-tolerant biofilm formation in Pseudomonas aeruginosa," *Applied Microbiology and Biotechnology*, vol. 98, no. 6, pp. 2565–2572, 2014.

[55] Y.-X. Yang, Z.-H. Xu, Y.-Q. Zhang, J. Tian, L.-X. Weng, and L.-H. Wang, "A new quorum-sensing inhibitor attenuates virulence and decreases antibiotic resistance in *Pseudomonas aeruginosa*," *Journal of Microbiology*, vol. 50, no. 6, pp. 987–993, 2012.

[56] J. N. Capilato, S. V. Philippi, T. Reardon et al., "Development of a novel series of non-natural triaryl agonists and antagonists of the Pseudomonas aeruginosa LasR quorum sensing receptor," *Bioorganic & Medicinal Chemistry*, vol. 25, no. 1, pp. 153–165, 2017.

[57] C. T. O'Loughlin, L. C. Miller, A. Siryaporn, K. Drescher, M. F. Semmelhack, and B. L. Bassler, "A quorum-sensing inhibitor blocks Pseudomonas aeruginosa virulence and biofilm formation," *Proceedings of the National Acadamy of Sciences of the United States of America*, vol. 110, no. 44, pp. 17981–17986, 2013.

[58] G. D. Geske, J. C. O'Neill, D. M. Miller, M. E. Mattmann, and H. E. Blackwell, "Modulation of bacterial quorum sensing with synthetic ligands: systematic evaluation of N-acylated homoserine lactones in multiple species and new insights into their mechanisms of action," *Journal of the American Chemical Society*, vol. 129, no. 44, pp. 13613–13625, 2007.

[59] B. K. Khajanchi, M. L. Kirtley, S. M. Brackman, A. K. Chopra, and B. A. McCormick, "Immunomodulatory and protective roles of quorum-sensing signaling molecules *N*-acyl homoserine lactones during infection of mice with aeromonas hydrophila," *Infection and Immunity*, vol. 79, no. 7, pp. 2646–2657, 2011.

[60] H. Tomioka, C. Sano, and Y. Tatano, "Host-directed therapeutics against mycobacterial infections," *Current Pharmaceutical Design*, vol. 23, no. 18, pp. 2644–2656, 2017.

[61] M. R. Parsek, D. L. Val, B. L. Hanzelka, J. E. Cronan Jr., and E. P. Greenberg, "Acyl homoserine-lactone quorum-sensing signal generation," *Proceedings of the National Acadamy of Sciences of the United States of America*, vol. 96, no. 8, pp. 4360–4365, 1999.

[62] M. K. Yadav, S. W. Park, S. W. Chae, and J. J. Song, "Sinefungin, a natural nucleoside analogue of S-adenosylmethionine, inhibits Streptococcus pneumoniae biofilm growth," *BioMed Research International*, vol. 2014, Article ID 156987, 10 pages, 2014.

[63] M. Hentzer and M. Givskov, "Pharmacological inhibition of quorum sensing for the treatment of chronic bacterial infections," *The Journal of Clinical Investigation*, vol. 112, no. 9, pp. 1300–1307, 2003.

[64] V. Singh, G. B. Evans, D. H. Lenz et al., "Femtomolar transition state analogue inhibitors of 5'-methylthioadenosine/S-adenosylhomocysteine nucleosidase from Escherichia coli," *The Journal of Biological Chemistry*, vol. 280, no. 18, pp. 18265–18273, 2005.

[65] A. Priyadarshi, E. E. Kim, and K. Y. Hwang, " Structural insights into *Staphylococcus aureus* enoyl-ACP reductase (FabI),

in complex with NADP and triclosan ," *Proteins: Structure, Function, and Bioinformatics*, vol. 78, no. 2, pp. 480–486, 2010.

[66] N. Surolia and A. Surolia, "Triclosan offers protection against blood stages of malaria by inhibiting enoyl-ACP reductase of Plasmodium falciparum," *Nature Medicine*, vol. 7, no. 2, pp. 167–173, 2001.

[67] E. Krol and A. Becker, "Rhizobial homologs of the fatty acid transporter FadL facilitate perception of long-chain acyl-homoserine lactone signals," *Proceedings of the National Acadamy of Sciences of the United States of America*, vol. 111, no. 29, pp. 10702–10707, 2014.

[68] J. L. Copitch, R. N. Whitehead, and M. A. Webber, "Prevalence of decreased susceptibility to triclosan in Salmonella enterica isolates from animals and humans and association with multiple drug resistance," *International Journal of Antimicrobial Agents*, vol. 36, no. 3, pp. 247–251, 2010.

[69] S. Lu, N. Wang, S. Ma, X. Hu, L. Kang, and Y. Yu, "Parabens and triclosan in shellfish from Shenzhen coastal waters: bioindication of pollution and human health risks," *Environmental Pollution*, vol. 246, pp. 257–263, 2018.

[70] N. Huma, P. Shankar, J. Kushwah et al., "Diversity and polymorphism in AHL-Lactonase gene (aiiA) of *Bacillus*," *Journal of Microbiology and Biotechnology*, vol. 21, no. 10, pp. 1001–1011, 2011.

[71] S. Y. Park, B. J. Hwang, M. Shin, J. Kim, H. Kim, and J. Lee, "N-acylhomoserine lactonase-producing *Rhodococcus spp.* with different AHL-degrading activities," *FEMS Microbiology Letters*, vol. 261, no. 1, pp. 102–108, 2006.

[72] A. Guendouze, L. Plener, J. Bzdrenga et al., "Effect of quorum quenching lactonase in clinical isolates of pseudomonas aeruginosa and comparison with quorum sensing inhibitors," *Frontiers in Microbiology*, vol. 8, p. 227, 2017.

[73] S. Hraiech, J. Hiblot, J. Lafleur et al., "Inhaled lactonase reduces pseudomonas aeruginosa quorum sensing and mortality in rat pneumonia," *PLoS ONE*, vol. 9, no. 10, Article ID e107125, 2014.

[74] J. Y. Chow, Y. Yang, S. B. Tay, K. L. Chua, and W. S. Yew, "Disruption of biofilm formation by the human pathogen acinetobacter baumannii using engineered quorum-quenching lactonases," *Antimicrobial Agents and Chemotherapy*, vol. 58, no. 3, pp. 1802–1805, 2014.

[75] X. Fan, M. Liang, L. Wang, R. Chen, H. Li, and X. Liu, "Aii810, a novel cold-adapted N-acylhomoserine lactonase discovered in a metagenome, can strongly attenuate Pseudomonas aeruginosa virulence factors and biofilm formation," *Frontiers in Microbiology*, vol. 8, p. 1950, 2017.

[76] M. M. Sakr, K. M. Aboshanab, W. F. Elkhatib, M. A. Yassien, and N. A. Hassouna, "Overexpressed recombinant quorum quenching lactonase reduces the virulence, motility and biofilm formation of multidrug-resistant Pseudomonas aeruginosa clinical isolates," *Appl Microbiol Biotechnol*, vol. 102, no. 24, pp. 10613–10622, 2018.

[77] C. Schipper, C. Hornung, P. Bijtenhoorn, M. Quitschau, S. Grond, and W. R. Streit, "Metagenome-derived clones encoding two novel lactonase family proteins involved in biofilm inhibition in pseudomonas aeruginosa," *Applied and Environmental Microbiology*, vol. 75, no. 1, pp. 224–233, 2008.

[78] W. Dong, J. Zhu, X. Guo et al., "Characterization of AiiK, an AHL lactonase, from Kurthia huakui LAM0618T and its application in quorum quenching on Pseudomonas aeruginosa PAO1," *Scientific Reports*, vol. 8, no. 1, p. 6013, 2018.

[79] W. Liu, C. Ran, Z. Liu et al., "Effects of dietary Lactobacillus plantarum and AHL lactonase on the control of Aeromonas hydrophila infection in tilapia," *Microbiologyopen*, vol. 5, no. 4, pp. 687–699, 2016.

[80] M. Torres, J. C. Reina, J. C. Fuentes-Monteverde et al., "AHL-lactonase expression in three marine emerging pathogenic Vibrio spp. reduces virulence and mortality in brine shrimp (Artemia salina) and Manila clam (Venerupis philippinarum)," *PLoS ONE*, vol. 13, no. 4, Article ID e0195176, 2018.

[81] G. Vinoj, B. Vaseeharan, S. Thomas, A. J. Spiers, and S. Shanthi, "Quorum-quenching activity of the AHL-lactonase from bacillus licheniformis DAHB1 inhibits vibrio biofilm formation in vitro and reduces shrimp intestinal colonisation and mortality," *Marine Biotechnology*, vol. 16, no. 6, pp. 707–715, 2014.

[82] V. C. Kalia, "In search of versatile organisms for quorum-sensing inhibitors: acyl homoserine lactones (AHL)-acylase and AHL-lactonase," *FEMS Microbiology Letters*, vol. 359, no. 2, p. 143, 2014.

[83] V. B. Maisuria and A. S. Nerurkar, "Interference of quorum sensing by Delftia sp. VM4 depends on the activity of a novel n-acylhomoserine lactone-acylase," *PLoS ONE*, vol. 10, no. 9, Article ID e0138034, 2015.

[84] R. Mukherji, N. K. Varshney, P. Panigrahi, C. Suresh, and A. Prabhune, "A new role for penicillin acylases: degradation of acyl homoserine lactone quorum sensing signals by Kluyvera citrophila penicillin G acylase," *Enzyme and Microbial Technology*, vol. 56, pp. 1–7, 2014.

[85] C. F. Sio, L. G. Otten, R. H. Cool et al., "Quorum quenching by an *N*-acyl-homoserine lactone acylase from *Pseudomonas aeruginosa* PAO1," *Infection and Immunity*, vol. 74, no. 3, pp. 1673–1682, 2006.

[86] K. Ivanova, M. M. Fernandes, E. Mendoza, and T. Tzanov, "Enzyme multilayer coatings inhibit Pseudomonas aeruginosa biofilm formation on urinary catheters," *Applied Microbiology and Biotechnology*, vol. 99, no. 10, pp. 4373–4385, 2015.

[87] N. Grover, J. G. Plaks, S. R. Summers, G. R. Chado, M. J. Schurr, and J. L. Kaar, "Acylase-containing polyurethane coatings with anti-biofilm activity," *Biotechnology and Bioengineering*, vol. 113, no. 12, pp. 2535–2543, 2016.

[88] J. Lee, I. Lee, J. Nam, D. S. Hwang, K.-M. Yeon, and J. Kim, "Immobilization and stabilization of acylase on carboxylated polyaniline nanofibers for highly effective antifouling application via quorum quenching," *ACS Applied Materials & Interfaces*, vol. 9, no. 18, pp. 15424–15432, 2017.

[89] S. Uroz, S. R. Chhabra, M. Cámara, P. Williams, P. Oger, and Y. Dessaux, "*N*-acylhomoserine lactone quorum-sensing molecules are modified and degraded by *Rhodococcus erythropolis* W2 by both amidolytic and novel oxidoreductase activities," *Microbiology*, vol. 151, no. 10, pp. 3313–3322, 2005.

[90] B. Eva and S. Maria, "Microbial secondary metabolites as inhibitors of pharmaceutically important transferases and oxidoreductases," *Ceska Slov Farm*, vol. 61, no. 3, pp. 107–114, 2012.

[91] P. Bijtenhoorn, H. Mayerhofer, J. Müller-Dieckmann et al., "A novel metagenomic Short-Chain dehydrogenase/reductase attenuates pseudomonas Aeruginosa biofilm formation and virulence on Caenorhabditis elegans," *PLoS ONE*, vol. 6, no. 10, Article ID e26278, 2011.

[92] J. D. Wildschut, R. M. Lang, J. K. Voordouw, and G. Voordouw, "Rubredoxin: oxygen oxidoreductase enhances survival of desulfovibrio vulgaris hildenborough under microaerophilic conditions," *Journal of Bacteriology*, vol. 188, no. 17, pp. 6253–6260, 2006.

[93] X. Zhang, S. Ou-yang, J. Wang, L. Liao, R. Wu, and J. Wei, "Construction of antibacterial surface via layer-by-layer method," *Current Pharmaceutical Design*, vol. 24, no. 8, pp. 926–935, 2018.

[94] C. Pustelny, A. Albers, K. Büldt-Karentzopoulos et al., "Dioxygenase-mediated quenching of quinolone-dependent quorum sensing in pseudomonas aeruginosa," *Chemistry & Biology*, vol. 16, no. 12, pp. 1259–1267, 2009.

[95] J. T. Hodgkinson, W. R. Galloway, M. Welch, and D. R. Spring, "Microwave-assisted preparation of the quorum-sensing molecule 2-heptyl-3-hydroxy-4(1H)-quinolone and structurally related analogs," *Nature Protocols*, vol. 7, no. 6, pp. 1184–1192, 2012.

[96] F. Witzgall, T. Depke, M. Hoffmann et al., "The alkylquinolone repertoire of *Pseudomonas aeruginosa* is linked to structural flexibility of the fabh-like 2-heptyl-3-hydroxy-4(1*H*)-quinolone (PQS) biosynthesis enzyme PqsBC," *ChemBioChem*, vol. 19, no. 14, pp. 1531–1544, 2018.

[97] L. Andresen, E. Sala, V. Koiv, and A. Mae, "A role for the Rcs phosphorelay in regulating expression of plant cell wall degrading enzymes in Pectobacterium carotovorum subsp. carotovorum," *Microbiology*, vol. 156, no. 5, pp. 1323–1334, 2010.

[98] L. Andresen, V. Kõiv, T. Alamäe, and A. Mäe, "The Rcs phosphorelay modulates the expression of plant cell wall degrading enzymes and virulence in Pectobacterium carotovorum ssp. carotovorum," *FEMS Microbiology Letters*, vol. 273, no. 2, pp. 229–238, 2007.

[99] R. K. Gupta, S. Chhibber, and K. Harjai, "Acyl homoserine lactones from culture supernatants of pseudomonas aeruginosa accelerate host immunomodulation," *PLoS ONE*, vol. 6, no. 6, Article ID e20860, 2011.

[100] G. F. Kaufmann, J. Park, J. M. Mee, R. J. Ulevitch, and K. D. Janda, "The quorum quenching antibody RS2-1G9 protects macrophages from the cytotoxic effects of the Pseudomonas aeruginosa quorum sensing signalling molecule N-3-oxo-dodecanoyl-homoserine lactone," *Molecular Immunology*, vol. 45, no. 9, pp. 2710–2714, 2008.

[101] S. Koul, J. Prakash, A. Mishra, and V. C. Kalia, "Potential emergence of multi-quorum sensing inhibitor resistant (MQSIR) bacteria," *Indian Journal of Microbiology*, vol. 56, no. 1, pp. 1–18, 2016.

[102] T. Praneenararat, A. G. Palmer, and H. E. Blackwell, "Chemical methods to interrogate bacterial quorum sensing pathways," *Organic & Biomolecular Chemistry*, vol. 10, no. 41, pp. 8189–8199, 2012.

[103] J. Park, R. Jagasia, G. F. Kaufmann et al., "Infection control by antibody disruption of bacterial quorum sensing signaling," *Chemistry & Biology*, vol. 14, no. 10, pp. 1119–1127, 2007.

[104] C. Grandclément, M. Tannières, S. Moréra, Y. Dessaux, D. Faure, and M. Camara, "Quorum quenching: role in nature and applied developments," *FEMS Microbiology Reviews*, vol. 40, no. 1, pp. 86–116, 2016.

[105] M. Han, J. Gu, G. F. Gao, and W. J. Liu, "China in action: national strategies to combat against emerging infectious diseases," *Science China Life Sciences*, vol. 60, no. 12, pp. 1383–1385, 2017.

[106] J. Liu, H. Yu, Y. Huang et al., "Complete genome sequence of a novel bacteriophage infecting Bradyrhizobium diazoefficiens USDA110," *Science China Life Sciences*, vol. 61, no. 1, pp. 118–121, 2018.

[107] L. D. Christensen, M. van Gennip, T. H. Jakobsen et al., "Synergistic antibacterial efficacy of early combination treatment with tobramycin and quorum-sensing inhibitors against Pseudomonas aeruginosa in an intraperitoneal foreign-body infection mouse model," *Journal of Antimicrobial Chemotherapy*, vol. 67, no. 5, pp. 1198–1206, 2012.

[108] J. Fong, M. Yuan, T. H. Jakobsen et al., "Disulfide bond-containing ajoene analogues as novel quorum sensing inhibitors of *Pseudomonas aeruginosa*," *Journal of Medicinal Chemistry*, vol. 60, no. 1, pp. 215–227, 2017.

[109] R. García-Contreras, M. Martínez-Vázquez, N. Velázquez Guadarrama et al., " Resistance to the quorum-quenching compounds brominated furanone C-30 and 5-fluorouracil in *Pseudomonas aeruginosa* clinical isolates ," *Pathogens and Disease*, vol. 68, no. 1, pp. 8–11, 2013.

[110] T. H. Jakobsen, S. K. Bragason, R. K. Phipps et al., "Food as a source for quorum sensing inhibitors: iberin from horseradish revealed as a quorum sensing inhibitor of pseudomonas aeruginosa," *Applied and Environmental Microbiology*, vol. 78, no. 7, pp. 2410–2421, 2012.

[111] A. Vadekeetil, H. Saini, S. Chhibber, and K. Harjai, " Exploiting the antivirulence efficacy of an ajoene-ciprofloxacin combination against *Pseudomonas aeruginosa* biofilm associated murine acute pyelonephritis ," *Biofouling*, vol. 32, no. 4, pp. 371–382, 2016.

[112] S. Bahari, H. Zeighami, H. Mirshahabi, S. Roudashti, and F. Haghi, "Inhibition of pseudomonas aeruginosa quorum sensing by subinhibitory concentrations of curcumin with gentamicin and azithromycin," *Journal of Global Antimicrobial Resistance*, vol. 10, pp. 21–28, 2017.

[113] A. S. Roccaro, A. R. Blanco, F. Giuliano, D. Rusciano, and V. Enea, "Epigallocatechin-gallate enhances the activity of tetracycline in staphylococci by inhibiting its efflux from bacterial cells," *Antimicrobial Agents and Chemotherapy*, vol. 48, no. 6, pp. 1968–1973, 2004.

[114] C. Chu, J. Deng, Y. Man, and Y. Qu, "Green tea extracts epigallocatechin-3-gallate for different treatments," *BioMed Research International*, vol. 2017, Article ID 5615647, 9 pages, 2017.

[115] A. Furiga, B. Lajoie, S. El Hage, G. Baziard, and C. Roques, "Impairment of pseudomonas aeruginosa biofilm resistance to antibiotics by combining the drugs with a new quorum-sensing inhibitor," *Antimicrobial Agents and Chemotherapy*, vol. 60, no. 3, pp. 1676–1686, 2016.

[116] Y. Inoue, N. Togashi, and H. Hamashima, "Farnesol-induced disruption of the staphylococcus aureus cytoplasmic membrane," *Biological and Pharmaceutical Bulletin*, vol. 39, no. 5, pp. 653–656, 2016.

[117] C. Kim, D. Hesek, M. Lee, and S. Mobashery, "Potentiation of the activity of beta-lactam antibiotics by farnesol and its derivatives," *Bioorganic & Medicinal Chemistry Letters*, vol. 28, no. 4, pp. 642–645, 2018.

[118] G. Brackman, P. Cos, L. Maes, H. J. Nelis, and T. Coenye, "Quorum sensing inhibitors increase the susceptibility of bacterial biofilms to antibiotics in vitro and in vivo," *Antimicrobial Agents and Chemotherapy*, vol. 55, no. 6, pp. 2655–2661, 2011.

[119] G. Brackman, K. Breyne, R. De Rycke et al., "The quorum sensing inhibitor hamamelitannin increases antibiotic susceptibility of staphylococcus aureus biofilms by affecting peptidoglycan biosynthesis and eDNA release," *Scientific Reports*, vol. 6, Article ID 20321, 2016.

[120] J. M. Walz, R. L. Avelar, K. J. Longtine, K. L. Carter, L. A. Mermel, and S. O. Heard, "Anti-infective external coating of central venous catheters: A randomized, noninferiority trial comparing

5-fluorouracil with chlorhexidine/silver sulfadiazine in preventing catheter colonization*," *Critical Care Medicine*, vol. 38, no. 11, pp. 2095–2102, 2010.

[121] C. van Delden, T. Köhler, F. Brunner-Ferber, B. François, J. Carlet, and J. Pechère, "Azithromycin to prevent Pseudomonas aeruginosa ventilator-associated pneumonia by inhibition of quorum sensing: a randomized controlled trial," *Intensive Care Medicine*, vol. 38, no. 7, pp. 1118–1125, 2012.

[122] A. R. Smyth, P. M. Cifelli, C. A. Ortori et al., "Garlic as an inhibitor of Pseudomonas aeruginosa quorum sensing in cystic fibrosis–a pilot randomized controlled trial," *Pediatric Pulmonology*, vol. 45, no. 4, pp. 356–362, 2010.

Hindawi
BioMed Research International
Volume 2019, Article ID 3746326, 13 pages
https://doi.org/10.1155/2019/3746326

Research Article

Microarray Based Functional Analysis of Myricetin and Proteomic Study on Its Anti-Inflammatory Property

Tao Li,[1] Jihe Zhu,[1] Fangming Deng,[1] Weiguo Wu,[1] Zhibing Zheng,[1] Chenghao Lv,[1] Yong Li,[1] Wei Xiang,[2] Xiangyang Lu,[1,2] and Si Qin[1,2,3]

[1] *Core Research Program 1515, Key Laboratory for Food Science and Biotechnology of Hunan Province, College of Food Science and Technology, Hunan Agricultural University, Changsha 410128, China*
[2] *Hunan Co-Innovation Center for Utilization of Botanical Functional Ingredients, College of Bioscience and Biotechnology, Hunan Agricultural University, Changsha 410128, China*
[3] *The United Graduate School of Agricultural Sciences, Faculty of Agriculture, Kagoshima University, Korimoto 1-21-24, Kagoshima 890-0065, Japan*

Correspondence should be addressed to Xiangyang Lu; xiangyangcn@163.com and Si Qin; qinsiman@hunau.edu.cn

Received 13 November 2018; Accepted 11 February 2019; Published 7 March 2019

Guest Editor: Deguang Song

Copyright © 2019 Tao Li et al. This is an open access article distributed under the Creative Commons Attribution License, which permits unrestricted use, distribution, and reproduction in any medium, provided the original work is properly cited.

Myricetin has been reported as a promising chemopreventive compound with multiple biofunctions. To evaluate its influence on gene expressions in genome-wide set and further investigate its anti-inflammatory property, the present study performed Gene Ontology and Ingenuity Pathway Analysis (IPA) to describe the basic gene expression characteristics by myricetin treatment in HepG2 cells, confirmed its multi-biofunction by real-time fluorescent quantitative PCR (RT-qPCR), and further verified its anti-inflammatory property by Western blotting and bio-plex-based cytokines assay. The IPA data showed that 337 gene expressions (48% of the top molecules) are disturbed over 2-fold, and the most possible biofunctions of myricetin are the effect on "cardiovascular disease, metabolic disease, and lipid metabolism," via regulation of 28 molecules with statistic score of 46. RT-qPCR data confirmed the accuracy of microarray data, and cytokines assay results indicated that 6 of the total 27 inflammatory cytokine secretions were significantly inhibited by myricetin pretreatment, including TNF-α, IFN-γ, IL-1α, IL-1β, IL-2, and IL-6. The present study is the first time to elucidate the multi-function of myricetin in genome-wide set by IPA analysis and verify its anti-inflammatory property by proteomics of cytokines assay. Therefore, these results enrich the comprehensive bioactivities of myricetin and reveal that myricetin has powerful anti-inflammatory property, which provides encouragement for *in vivo* studies to verify its possible health benefits.

1. Introduction

Myricetin is a well-defined natural flavonoid with hydroxyl groups at the positions of 3, 5, 7, 3', 4', and 5', which is widely existed in vegetables, fruits, and teas, as well as medicinal herbs [1]. Myricetin has been proved to be the most potent and promising chemopreventive compound for its multiple biofunctions, such as antioxidation, anti-inflammation, antitumor, anti-diabetes, and anti-mutation effects [2, 3]. For the antioxidant property, myricetin was reported to attenuate the deleterious effect of oxidative stress in human red blood cells [4], prevent against I/R-induced myocardial injury in rats [5], and exhibit a significant hepatoprotective activity to reduce hepatic oxidative stress in mice [6], by the induction of antioxidant genes or proteins. For the anti-inflammatory property, overexpression of tumor necrosis factor-alpha (TNF-α) and cyclooxygenase-2 (COX-2) in mouse liver was found to be reduced by myricetin treatment [6], and the production of proinflammatory mediators was inhibited by myricetin via inhibition of NF-κB and STAT1 pathways and induction of Nrf2-HO-1 pathway in LPS-stimulated RAW264.7 macrophages [7]. For the anticancer property, myricetin was recognized to be able to induce apoptosis of Human T24 bladder cancer cells via modulation of Bcl-2 family proteins and caspase-3, significantly inhibit the tumor growth on T24 bladder cancer xenografts model [8], and promote apoptosis through regulation of apoptotic protein Bax, Bad, and Bcl-2 in HepG2 cells [9].

The recent arising concept of nutrigenomics is defined to investigate the omics-wide influences of classical nutrients or other dietary bioactive components in food. Nutrients or dietary bioactive components are mediators that can be detected by the cellular sensor systems and influence gene expressions, protein synthesis, and metabolite production [10]. Nutrigenomics is designed to investigate the dietary components in distinguished cells, tissues, and organisms and to elucidate how they influence the redox balance and homeostasis of the cells, which plays crucial role on human health maintenance and disease prevention [10, 11]. However, limited researches were performed to study the functional effects of flavonoids and elucidate the underlying mechanism by using methods of nutrigenomics. For instance, by using quantitative proteomics approach, EGCG was reported to exert its effect on alleviation to vanadium stress in laying hens through regulation of metal-binding mediation, cell proliferation, and immune function-related proteins [12]. Grape polyphenols were found to improve cellular parameters and reduce the amount of lipogenesis and glycolysis enzymes, enhance fatty acid oxidation and stimulate insulin signaling, and ameliorate protein oxidation or endoplasmic reticulum stress [13]. By using transcriptomics expression analysis, cocoa polyphenols were reported to possess antiobesity effects in high fat diet induced obese rats by regulation of lipid metabolism genes and reduce adiposity in adipose tissue [14]. Recently, a comprehensive review had summarized the data in the last decade and found that dietary polyphenols may function as ideal modulators of the mammalian gene expressions by histone deacetylation, histone acetylation, and DNA methylation in experimental models [15, 16]. Another interesting review further provides the reliable scientific data to reveal the importance of polyphenols to fight against carcinogenesis epigenetically and focuses on the effects of dietary polyphenols to mitigate carcinogenesis [17]. Our previous study had applied microarray to analyze the effects of myricetin on genome-wide set; however, the analysis of the data remains scarce and shallow [18]. Therefore, further analysis on the microarray data of myricetin and other attached new omics tools should be performed, such as proteomics assay.

The studies on the biofunction of polyphenols mainly focus on the regulation of redox signaling pathways and related genes or proteins linked to human health, especially on the inhibition of inflammation [19]. Inflammation is defined by the increased acute phase reactants or other mediators, the activation of inflammatory signal pathways, and abnormal cytokine or inflammatory marker expressions [20]. Cytokines are important inflammatory signaling proteins to mediate a wide range of physiological responses and a spectrum of related diseases, such as tumor growth, infections, and Parkinson's disease. Cytokines are generally detected by either immunoassay or bioassay [21, 22]. Recently, the newly discovered Bio-Plex suspension array instrument from Bio-Rad Company can simultaneously detect up to 100 cytokines in a single well of a 96-well microplate by application of novel technology with color-coded beads. Therefore, bio-plex based technology is of great significance to understand the whole inflammatory process. To elucidate the more detail about the multiple biofunctions of myricetin, comprehensive analysis of microarray data in genome-wide set by advanced software and specific verification of the anti-inflammatory property by proteomic tool were performed in the present study.

2. Materials and Methods

2.1. Materials and Antibodies. Myricetin (≥99%, purified by HPLC) was purchased from Extrasynthese (Lyon Nord, France). Human hepatoblastoma (HepG2) cells were donated by the Cancer Cell Repository (Tohoku University, Japan). Fetal bovine serum (FBS) and Dulbecco's modified Eagle's medium (DMEM) were purchased from Hyclone (Logan, USA). Lipopolysaccharide (LPS) and other general reagents used in the chemical analysis were purchased from Sigma-Aldrich (Shanghai, China). The antibodies for COX-2, iNOS, α-tubulin, and others were purchased from Santa Cruz Biotechnology (Santa Cruz, USA) and Cell Signaling Technology (Beverly, USA).

2.2. Reverse Transcription and Real-Time qPCR. HepG2 cells were planted in dishes for 24 h and then treated with 20 μM of myricetin in 0.1% DMSO or alone for additional 9 h. Total RNA was extracted with RNA extraction kit (Nippon Gene Co., Japan) as described accordingly. The primers used in the present study were designed by PRIMER3 and synthesized by company as follows: *AKR1C1*, forward (5'- ATC CCT CCG AGA AGA ACC AT-3') and reverse (5'- ACA CCT GCA CGT TCT GTC TG-3'); *AKR1C2*, forward (5'- GAT CCC ATC GAG AAG AAC CA-3') and reverse (5'-ACA CCT GCA CGT TCT GTC TG-3'); *GCLC*, forward (5'- GAG CTG GGA GGA AAC CAA G -3') and reverse (5'- TGG TTT GGG TTT GTC CTT TC-3'); *SERPINE*, forward (5'-GTG CTG GTG AAT GCC CTC T-3') and reverse (5'- GCA GTT CCA GGA TGT CGT -3'); *IL11*, forward (5'-GCG GAC AGG GAA GGG TTA AAG-3') and reverse (5'- GGG CGA CAG CTG TAT CTG G -3'); *IGFBP1*, forward (5'- ATG ATG GCT CGA AGG CTC TC-3') and reverse (5'-ATG TCT CAC ACT GTC TGC TGT-3'). Reverse transcription and real-time qPCR were performed with RT-qPCR Kit (Finnzymes Oy., Espoo, Finland) accordingly. Briefly, 200 ng of RNA was reverse-transcribed to cDNA at 37°C for 30 min, and the reaction was then terminated at 85∘C for 5 min, and other reaction conditions or procedures were described previously [18]. The results were presented as the relative expression levels normalized with that in control cells.

2.3. Microarray Data Analysis and Network Generation. Microarray results were classified by Gene Ontology ID (http://www.geneontology.org/) and analyzed by general method and then were imported into Ingenuity Pathway Analysis (IPA) System (http://www.ingenuity.com) for further analysis. The gene ontology classification and analysis are primary bioinformatics to standardize their presentation of gene and gene product attributes from different species and databases. The Ingenuity Knowledge Base is built by the huge data extracted from the millions of full text literatures with weekly update, which is the leader of its kind to analyze the results originated from microarray. [23]. The original microarray data was imported into the IPA system according to gene accession numbers and the fold change upon myricetin treatment versus control and other necessary data. P<0.002 was set as the cutoff point of the IPA system, and the genes were classified according to the molecular functions. The canonical pathways analysis was performed to identify the most possible disturbed pathways from the IPA system with the most significance in the dataset [24, 25].

The network analysis was carried out to identify series of genes belonging to certain genetic networks associated with functions or diseases in the IPA system and were ranked by the score that represents the possibility that a class of genes were disturbed. The genetic network analysis was also based on the information or findings originated from millions of literatures focused on the study of functional relationships between genes. A network pathway contains a class of genes or gene products, which are represented as nodes, and the biological relationship between 2 nodes is represented as an edge (line). This kind of network is a graphical representation of the molecular relationships between genes or gene products. All the correlations or links are supported by at least one reference stored in the Ingenuity Pathways Knowledge Base, including literature, textbook, and canonical information. The intensity of the node color indicates the degree of regulation: the red represents up and the green represents down. The various shapes of nodes and labels of edges describe different functional gene product and the nature of the relationship between the nodes, respectively.

2.4. Immunoblots of Inflammatory Proteins. HepG2 cells were precultured in dishes for 24 h first and then starved by adding serum-free medium for additional 2.5 h. The cells were divided into 4 groups, which were a control group without treatment; a negative control group treated with 1 μg/ml of LPS alone; two groups were treated with 20μM of myricetin before exposure to LPS, or not. Every group were treated for 30 min. Cellular lysates were boiled for 5 min, equal amounts of which (40 μg) were run on SDS-PAGE gel (10%) and transferred to PVDF membrane (Amersham Pharmacia Biotech). The membrane was incubated with specific primary antibody overnight at 4°C and incubated with respective secondary antibodies for 1 h. Immunoblot binds were detected by ECL system with the Image Quant LAS 4000 mini (GE Healthcare, Chicago, US). The relative amount of detected proteins was quantified by ImageQuant TL software.

2.5. Bio-Plex-Based Assays of Inflammatory Cytokine. HepG2 cells were precultured and starved accordingly to eliminate the effect of FBS. The cells were then treated with 10-20 μM of myricetin for half hour before exposure to 1 μg/mL LPS for additional 12 h. The 27 cytokines detection, including TNF-α, G-CSF, IFN-γ, IL-1α, IL-1β, IL-2, IL-4, IL-5, IL-6, IL-7, IL-8, IL-9, IL-10, IL-12(p70), IL-13, IL-15, IL-17, RANTES, Eotaxin, PDGF-BB, FGF basic, IP-10, MCP-1(MCAF), MIP-1α, MIP-1β, GM-CSF, and VEGF were performed by using Bio-Plex Pro Human Cytokine 27-Plex Panel kit (Bio-Rad Laboratories) and Bio-Plex cytokines assay system (Bio-Plex 200, Bio-Rad) according to the manufacturer's instructions and the results were analyzed by the Bio-Plex manager software (version 4.0).

2.6. Statistical Analysis. All the experimental data in the present study were repeated at least three or four times. Significances or differences of treated versus control were analyzed by the Student's t-test, and $p<0.05$ was considered significant.

3. Results

3.1. Gene Expression Profiling of Myricetin-Treated HepG2 Cells by GO Analysis. According to our previous study, we have performed basic analysis to the huge microarray data. Among the total 44K gene probes, 20μM of myricetin upregulated the expressions of 143 genes (0.33% of total probes) and downregulated the expressions of 476 genes (1.08% of total probes) by greater than or equal to twofolds in HepG2 cells [18]. However, the comprehensive analysis of the data is scarce. Thus, we further utilize the free available tool, Gene Ontology, to analyze the basic characteristic of gene expressions in HepG2 cells by myricetin treatment. As shown in Table 1, three basic classes, including biological process, molecular function, and cellular component, were list out. In each class, we further list out the gene function subclasses with the ratio of significant regulated genes greater than 2% of the total, which includes 3, 5, and 16 subclasses, respectively.

Among biological process, signal transduction, metabolism, and lipid metabolism have been largely disturbed by myricetin treatment, with significantly regulated gene ratio of 7.27%, 4.68%, and 2.26%, respectively, which implies that myricetin has the potency on the regulation of signaling transduction and cellular metabolism, especially lipid metabolism. For instance, in signal transduction, expressions of *F2RL2, IGFBP1, ARHGAP26, PDE11A, ADM, SOS1, NF1, F2RL1, IL8, VDR,* and *TXNRD1* were identified to be linked to the biofunction of myricetin (Table S1). In cellular component, one of the notable affected subclasses is nucleus, containing the largest gene ratio of 19.22%. It involves several response element promoters of signaling pathways, such as ARE, NF-κB, XRE, or AP-1, which are associated with oxidative stress response, inflammation, or xenobiotic metabolism. There are several gene expressions were remarkably altered in cellular component, including *BHLHB2, DIDO1, NDRG1, EID3, SORBS2, WDHD1, KIAA1429, SORBS2, JUN,* and *SLC2A4RG*, as shown in Table S2. Another important subclass is mitochondrion, with the differential gene ratio of 4.2%. Mitochondrion is critical in endothelial physiology and pathophysiology, and plays a prominent role on production of ATP, energy currency of the cell, through respiration, and then regulates the cellular metabolism [26, 27]. Myricetin was found to exert a crucial role on mitochondria function and keep the redox balance, which was evidenced by the differentially expressed genes after myricetin medication, such as *HSPA1A, GLS,*

Table 1: Gene expression profiling by GO analysis.

Class	Subclass	Ratio [%]
Biological process	Signal transduction	7.27
	Metabolism	4.68
	Lipid metabolism	2.26
Cellular component	Nucleus	19.22
	Extracellular	7.27
	Plasma membrane	6.79
	Cytosol	3.72
	Mitochondrion	4.20
Molecular function	Protein binding	27.30
	DNA binding	10.02
	Binding	7.59
	Kinase	3.39
	Protein kinase activity	2.26
	calcium ion binding	3.88
	nucleic acid binding	6.46
	transcription factor activity	4.36
	RNA binding	3.55
	nucleotide binding	9.69
	actin binding	3.55
	catalytic activity	5.33
	structural molecule activity	2.26
	protein kinase activity	2.26
	hydrolase	5.98
	Receptor activity	5.65

Table 2: Gene expression profiling of myricetin-treated HepG2 cells by IPA analysis.

Fold of Change		IPA data	
	Total	Numbers	Regulation
>4	15	8	up
		7	down
3<~<4	36	16	up
		20	down
2<~<3	286	56	up
		230	down
Total	337	80	up
		257	down

PDK1, ABAT, SYNE2, ATP5S, and *ETFDH* (Table S3). The significantly activated molecular functions were generally related to protein binding, DNA binding, kinase, and protein kinase activity, with the corresponding proportion of 27.3%, 10.02%, 3.39%, and 2.26%, respectively. Almost all the features of cells on their surfaces and interiors are based on diversity protein carrier in terms of tool-like receptor, facilitated glucose transporter, thioredoxin reductase 1, etc. Before that, many signal pathways associated to molecular function rely on DNA linking, the deliverance of genetic information, and the period is usually activated by protein kinases [28]. As shown in Table S3, a series of typical genes belonging to the above 4 subclasses disturbed by myricetin have been listed out, such as *SLC2A4RG, SLC22A3, SERPINE1, MAP3K13, ACVR1B, MAP3K8, ARHGAP26, BHLHB2, DMXL1, NCF2, HSPA1A/B, HMOX1,* FGFR3, *ATR, FGFR3, ACVR1B, WDHD1, HELLS, SOS1,* and *JUN*. These results indicated that myricetin has the potential to regulate molecular function, via regulation of gene expression pathways and modulation of signal transduction.

3.2. Gene Expression Profiling of Myricetin-Treated HepG2 Cells by IPA Analysis.

Next, to further analyze the microarray data, we input the data into IPA system, and the gene expression profiling of myricetin-treated HepG2 cells has changed a little. As shown in Table 2, comparing the signals of myricetin-treated group with the control, the result revealed that the expressions of 15 genes were disturbed significantly by equal or greater than 4-fold, with upregulation of 8 genes and downregulation of 7 genes; the expressions of 36 genes were disturbed between 3-fold to 4-fold, with upregulation of 16 genes and downregulation of 20 genes; the expressions of 286 genes were disturbed between 2-fold to 3-fold, with upregulation of 56 genes and downregulation of 230 genes. Taken together, 337 gene expressions of the total 702 molecules (48%) exported by IPA were disturbed with fold changes over 2-fold.

3.3. Top Function and Canonical Pathway Analysis of Myricetin-Treated HepG2 Cells by IPA.

To obtain a further investigation for the elucidation of the effects and underlying molecular mechanism of myricetin in HepG2 cells, the advanced analysis tool of IPA system was performed. In brief, IPA constructed the connection and relationship of the above significantly regulated genes, which also output the top 10 cellular functions and diseases altered by myricetin treatment in HepG2 cells with a p-value less than 0.05, as shown in Table 3. The most possible cellular function/disease of myricetin is the regulation of "cardiovascular disease, metabolic disease, and lipid metabolism," which consists of 28 molecules with the score of 46. The secondary top cellular function/disease, "connective tssue development and function, skeletal and muscular system development and function, and tissue morphology" was significantly influenced by myricetin treatment as well, with 22 molecules and the score of 33. Besides, other cellular functions/diseases, such as "endocrine system disorders," "cardiovascular system development and function," "cellular assembly and organization," "cellular movement," "cancer," "cell death," and "hepatic system disease," were also identified to be significantly disturbed by myricetin treatment. However, "cancer" was found to be the most frequently influenced disease with the occurrence of 4 times in top 10 functions, and "cell death" and "metabolism disease" were both mentioned 3 times there. The above result indicates that myricetin may exert its biofunction by the regulation of chronic disease related biomarkers and the representative signaling pathways. For instance, *MAP3K8*, *MAP3K13*, *NCF2*, *NF-κB (family)*, *NFATC2*, *NF-κB (complex),* and *NR2F2* were significantly disturbed by myricetin treatment, which are belonging to cancer related MAPK/NF-κB inflammatory signaling pathway.

Table 3: Top 10 cellular functions and diseases altered by myricetin treatment in HepG2 cells.

	Molecules in Network	Score	Focus Molecules
Cardiovascular Disease, Metabolic Disease, Lipid Metabolism	ACVR1B, C14ORF139, CD3, CD36, DDX58, DYX1C1, E2f, EFHC1, EPPK1, FST, GPAM, HAMP, HSPA1A, IFN Beta, IKK, INHBE, INSIG2, KLF3, MAP3K8, MAP3K13, NCF2, NF-κB (family), NFATC2, NFκB (complex), NR2F2, Rab11, RAB11B, RAB11FIP4, RGS3, SLC2A2, SQSTM1, TFRC, TMEM126B, TXNRD1, VSNL1	46	28
Connective Tissue Development and Function, Skeletal and Muscular System Development and Function, Tissue Morphology	ADM, AGPAT9, Akt, BHLHB2, DCBLD2, HELLS, HSPG2 (includes EG:3339), Ige, IGF2, IGF2BP2, IL11, INPP5D, JAG1, Laminin, LCAT, Mek, NEXN, p70 S6k, PALLD, Pdgf, PDGF BB, PP2A, Ptk, RORA, Shc, SKAP2, SLC2A3, SLC6A4, SLC6A6, SORBS2, Sos, STAT, Tgf beta, TINAG, XRN1	33	22
Endocrine System Disorders, Hematological Disease, Metabolic Disease	Adaptor protein 2, AKR1B10, Ap1, AP2A1, BNIP3L, C5ORF34, CBR1, Ck2, Creb, DENND4A, hCG, HIP1, Histone h3, HMOX1, Igfbp, IGFBP1, IGFBP3, JUN, KLF5, LDL, MAFF, MAZ, Mmp, NRP1, P38 MAPK, PFKFB3, SMC4, SPP1, SULT2A1, SYNE2, tyrosine kinase, VDR, Vegf, VitaminD3-VDR-RXR, VRK1	32	22
Cardiovascular System Development and Function, Tissue Morphology, Amino Acid Metabolism	A1CF, AKR1C1, AKR1C2, AKR1C3, Angiotensin II receptor type 1, EGR1, ERK, ETS, F2RL1, FGFR3, Fibrin, FOS, G-Actin, GCLC, GCLM, GDF15, GNRH, JUN/JUNB/JUND, KLB, KLF4, LIMA1, NF1, NGF, NTN4, PLAUR, Rar, RASGRF2, Rxr, SCLT1, SERPINE1, SWI-SNF, T3-TR-RXR, Thyroid hormone receptor, TRA2A, Trans-1,2-dihydrobenzene-1,2-diol dehydrogenase	30	21
Cellular Assembly and Organization, Cellular Function and Maintenance, Nervous System Development and Function	14-3-3, ACTA1, ALB, ARHGAP26, ARHGDIA, ATP6V0A1, ATYPICAL PROTEIN KINASE C, CCAR1, CPLX1, F Actin, F2RL2, FGD4, GABBR1, Gsk3, Insulin, Jnk, MAP2K1/2, MARCKS (includes EG:4082), NEDD4L, Nfat, PARD3, PCYT1B, Pkc(s), Pld, PRLR, Rac, Raf, Ras, Ras homolog, RGNEF, SH3BP2, SOS1, TCR, TNS1, VAMP2	26	20
Cellular Movement, Dermatological Diseases and Conditions, Organismal Injury and Abnormalities	ADCY, AIM1 (includes EG:202), ALP, ARFGEF1, ARID1A, Calmodulin, Calpain, Cyclin A, Cyclin E, CYP1A1, ERK1/2, G alphai, Hdac, Histone h4, IL8, IL12, Interferon alpha, ITPR2, KNG1 (includes EG:3827), Mapk, MED13, MYLK, NDRG1, NRD1, PDZK1, Pka, Pkg, PRKAR1A, PTRF, Rb, RBL1, RNA polymerase II, SMARCA4, SUV420H1, THRB	24	18
Cancer, Cell Death, Reproductive System Disease	AASS, ANXA3, APPBP2, beta-estradiol, BICD1, BUB1, CCAR1, CHM, CORO2A, DIMT1L, EID3, FCGRT, geranylgeranyl pyrophosphate, GJB2, GRM3, HELLS, HRAS, IGFBP1, IREB2, KIAA2018, KLHDC2, MIRN29B2, MYC, NME5, NR3C1, PDK1, PTP4A2, RAB6A, RABGGTB, RASA4 (includes EG:10156), RPN2, SARDH, SELENBP1, SGK3, TXN	23	17
Cancer, Cell Cycle, Cell Death	ABAT, ADM, ALDH5A1, BMP15, CDKN2B, CEACAM5 (includes EG:1048), CENPE, CENPF, CMAS, CRK, FOXG1, FSH, FST, GCLC, GPRC5A, GRLF1, HNRPDL, INHA, KCNA5, KLF10, LACTB, LYVE1, MST1R, MTMR10, PCF11, PGRMC1, RB1, SEMA6B, SMAD5, SPAG4, TGFB1, THOC1, THOC2, thyroid hormone, TRIP11	21	16
Cell Death, Cancer, Cell Cycle	ACAP1, ADAM12, BBS7, C10ORF88, C16ORF57, C3ORF63, CALR, CD59, CLTC, CMIP, CUGBP1, DCP1A, F2RL2, KIAA1219, KIAA1429, KRT18, METTL7A, MME, PDIA2, PDIA3, PHACTR2, PPP1CA, PRLR, SH3BP4, SLC6A8, SMAD4, SRC, SSB, TFE3, TNS1, TOM1, TOM1L1, TUSC3, YWHAZ, ZFYVE16	21	16
Cancer, Hepatic System Disease, Liver Hyperplasia/Hyperproliferation	ATP5S, C3, CTBP1, CYP4B1, CYP4F11, EDA2R, ELK3, FGD4, FRY, GDF15, GPRC5A, LEFTY2, LRBA, MAP3K13, MAPK8, MAPK9, MINK1, MSLN, PEX1, PKP2, PRAM1, RAE1, RCOR3 (includes EG:55758), retinoic acid, RGL4, SH3BP5, SH3RF2, SMOX, SPAG9, SSBP3, STMN3, TAL1, TFF2, YWHAG, ZNF217	21	16

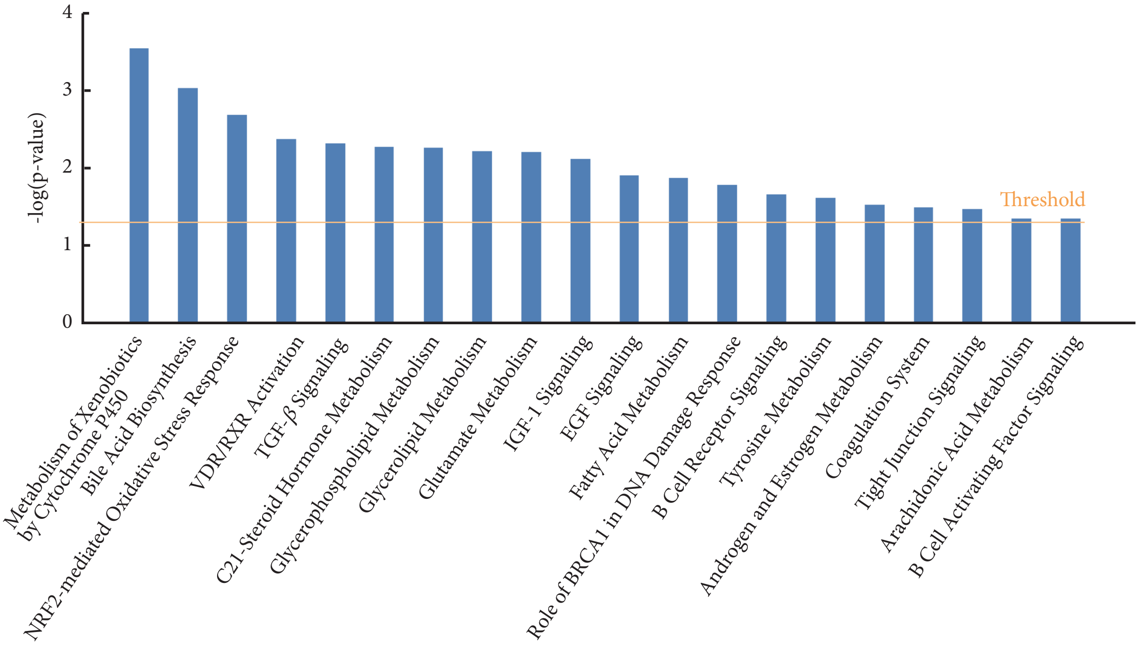

Figure 1: Top canonical pathway analysis of myricetin-treated HepG2 cells by IPA.

In addition to cellular function and disease, IPA system also listed out the significantly disturbed genes by distinct canonical pathways based on IPKB. As shown in Figure 1, IPA system outputs all the significantly affected signaling pathways by myricetin treatment with a p-value less than 0.05. Among the total 20 canonical pathways, Nrf-2-mediated oxidative stress response, TGF-β signaling, and B cell receptor signaling are strongly associated to chronic inflammation; metabolism of xenobiotics by cytochrome P450, bile acid biosynthesis, C21-steroid hormone metabolism, glycerophospholipid metabolism, glycerolipid metabolism, glutamate metabolism, IGF-1 signaling, and fatty acid metabolism are closely linked to metabolic disease, especially glucolipid metabolism dysfunction.

3.4. Network Analysis of Myricetin-Treated HepG2 Cells by IPA. Furthermore, IPA further built gene networks to connect key genes and enrich categories of diseases and functions, via the construction of the correlation between the significantly disturbed genes by myricetin treatment. We have listed out the top 1 network to further elucidate the cellular functions vividly and distinctly, corresponding to the top 1 cellular function and disease, as shown in Table 3.

As shown in Figure 2, top 1 network is related to cardiovascular disease, metabolic disease, and lipid metabolism. It consists of 35 genes, 28 of which are expressed differentially. It is worth noting that the cellular function of oxidative stress and inflammation response were vastly involved in this network. Among these genes, *SLC2A2* (*solute carrier family 2 member 2*), also called *GLUT2*, is the most downregulated gene, with the reduction of 4.89-fold by myricetin treatment, and its expression is indirectly adjusted by *NF-κB* family. The reduction of *SLC2A2* expression suggested the inhibition of glucose absorption, which has a strong correlation to the glucose and lipid metabolic pathways [29]. Clinical data shows that *SLC2A2 (GLUT2)* mutations are the cause for Fanconi-Bickel syndrome, a rare autosomal recessive disease about carbohydrate metabolism dysfunction, and the tested patients showed typical characteristics such as glycogen storage disorders and proximal renal tubular nephropathy [30]. The most upregulated gene is *NCF2* (*solute carrier family 2 member 2*), with the induction of 4.27-fold by myricetin treatment, and it is also indirectly adjusted by *NF-κB* family. NCF2 is reported to be associated with chronic disease, especially inflammatory chronic granulomatous disease [31]. Besides, multiple protein kinase genes related to inflammation are directly regulated by myricetin via modulation of inflammatory transcription factors. For instance, *MAP3K13* and *MAP3K8*, the upstream protein kinases of NF-κB pathway, displayed the decreasing expression folds of 2.06 and 2.33, respectively, where the expression of *MAP3K8* was indirectly affected by *NF-κB*. Thus, we may speculate that inflammatory signal molecular and the upstream protein kinase would interact with each other.

What is more, *NF-κB* is the core of this network and monitors the activities of a series of inflammatory factors and the expressions of several typical antioxidant genes. Inflammatory genes *CD36* (3.25-fold), *KLF3* (2.57-fold), *NFATC2* (2.36-fold), and *ACVR1B* (2.15-fold) were downregulated indirectly by myricetin treatment via *NF-κB* pathway, while antioxidant genes *TXNRD1* (2.04-fold), *SQSTM1* (2.45-fold), *TMEM126B* (2.26-fold), and *HSPA1A* (3.35-fold) were upregulated. All the above changes imply that myricetin could inhibit inflammation and activate the antioxidant chemoprevention to play a critical role in the cellular redox equilibrium. Two typical signaling pathways

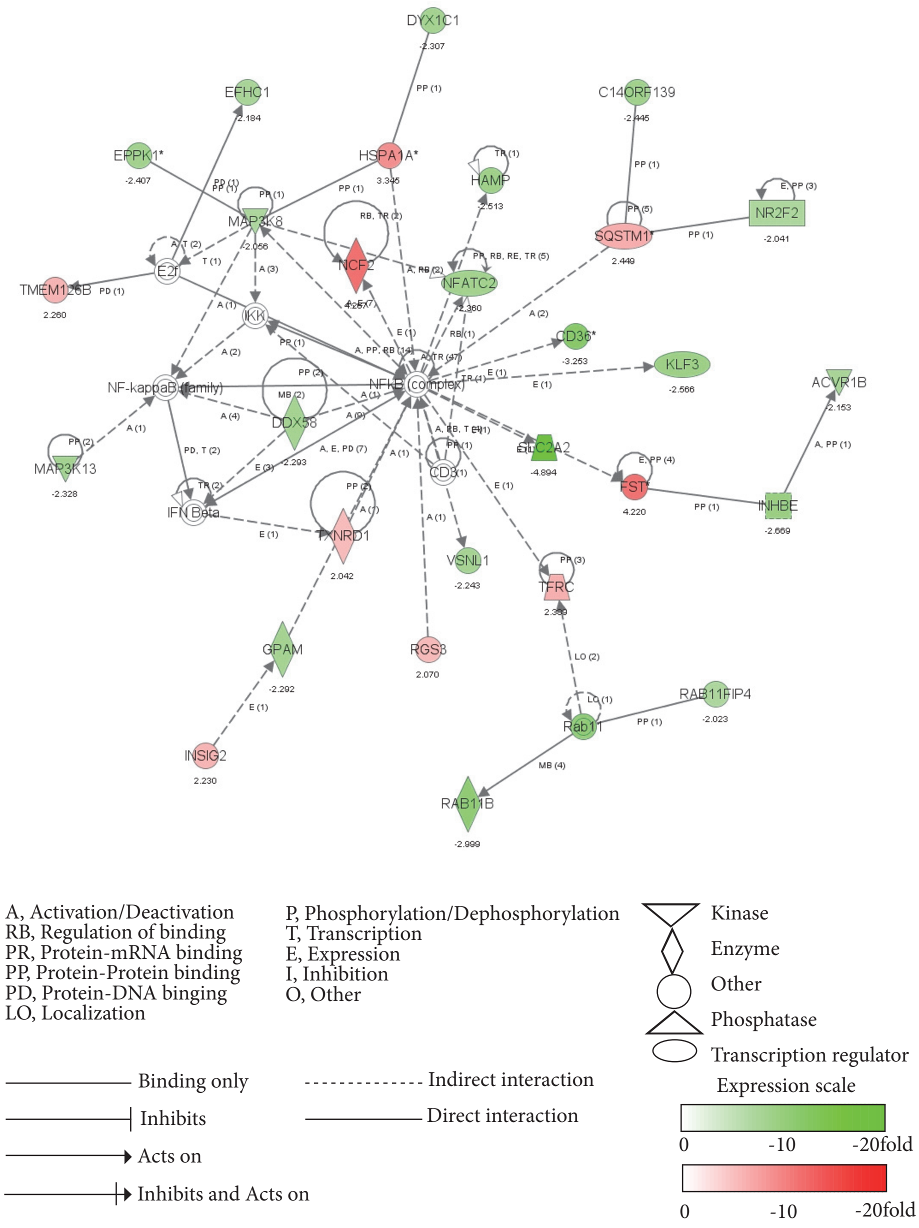
DYX1C1
-2.307
EFHC1
2.184
C14ORF139
-2.445
EPPK1*
-2.407
HSPA1A*
3.345
HAMP
-2.513
NR2F2
-2.041
MAP3K8
-2.056
SQSTM1*
2.449
NCF2
4.257
NFATC2
-2.360
TMEM126B
2.260
E2f
IKK
CD36*
-3.253
KLF3
-2.566
ACVR1B
2.153
NF-kappaB (family)
NFkB (complex)
DDX58
-2.293
SLC2A2
-4.894
MAP3K13
-2.328
FST
4.220
INHBE
-2.669
CD3
IFN Beta
TXNRD1
2.042
VSNL1
-2.243
TFRC
2.389
GPAM
-2.292
RGS3
2.070
RAB11FIP4
-2.023
Rab11
INSIG2
2.230
RAB11B
-2.999
A, Activation/Deactivation
RB, Regulation of binding
PR, Protein-mRNA binding
PP, Protein-Protein binding
PD, Protein-DNA binging
LO, Localization
P, Phosphorylation/Dephosphorylation
T, Transcription
E, Expression
I, Inhibition
O, Other
Kinase
Enzyme
Other
Phosphatase
Transcription regulator
Binding only
Inhibits
Acts on
Inhibits and Acts on
Indirect interaction
Direct interaction
Expression scale
0
-10
-20fold
0
-10
-20fold

Figure 2: Top network analysis of myricetin-treated HepG2 cells by IPA. The dataset was analyzed by Ingenuity Pathway Analysis software. The node color indicates the expression level of the genes. Nodes and edges are displayed with various shapes and labels that present the functional class of genes and the nature of the relationship between the nodes, respectively.

are found to be involved in the top 1 network, including B cell receptor signaling and Nrf2-mediated antioxidant pathway. B cell receptor signaling was reported to activate NF-κB by PKC/TAK1 pathway [32]. *NFATC2*, *MAP3K13,* and *MAP3K8* are belonging to B cell receptor signaling, and their downregulation reveals that myricetin can exert its anti-inflammatory effect via inhibition of B cell receptor signaling. Similarly, the upregulation of *SQSTM1* and *TXNRD1* in Nrf2-mediated antioxidant pathway indicates that myricetin can also inhibit inflammation via activation of Nrf2-mediated antioxidant pathway.

3.5. Real-Time qPCR Verification of the Specific Functional Genes. To verify the microarray data and the above biofunction caused by myricetin in HepG2 cells, we performed RT-qPCR and compared the result of selective top 20 altered molecules in IPA to the raw gene chip data. As shown in Figure 3(a), we have selected typical significantly disturbed genes with their respective change fold from microarray data by myricetin treatment, including antioxidant genes *GCLC*, *AKR1C1/2/3* and *NCF2*, inflammatory genes *SERPINE*, *ARHGAP26*, *FST* and *IL11*, and metabolic genes *IGFBP1*, *F2RL2*, *SLC2A2/6A6*, and *HSPA1A*, which are all

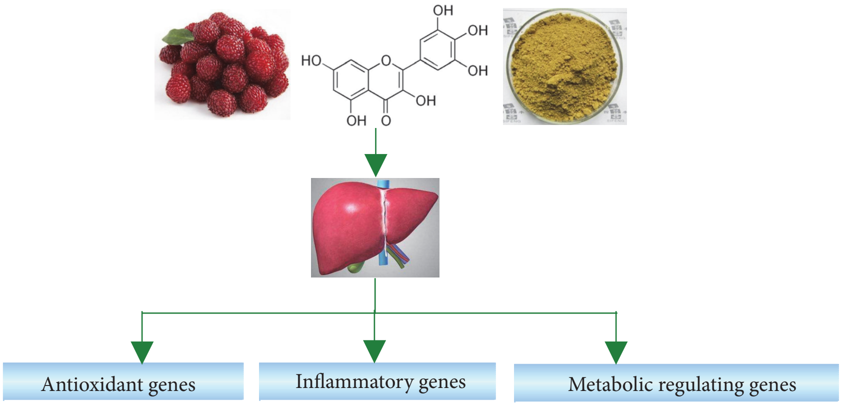

AKR1C1	↑ 4.87	*SERPINE*	↑ 6.00	*F2RL2*	↑ 7.65
AKR1C2	↑ 2.85	ARHGAP26	↓ 4.58	IGFBP1	↑ 5.06
AKR1C3	↑ 2.07	FST	↑ 4.22	SLC2A2	↓ 4.89
NCF2	↑ 4.27	IL11	↑ 3.33	SLC6A6	↑ 3.27
GCLC	↑ 3.50			HSPA1A	↑ 3.35

(a)

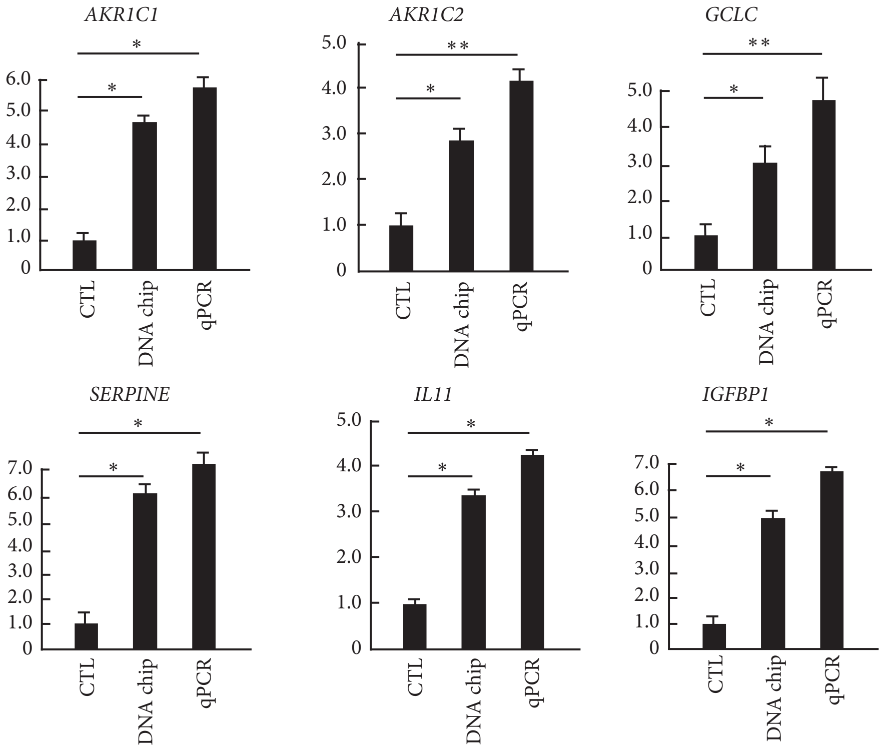

(b)

Figure 3: Real-time quantitative PCR verification of the specific functional genes identified by DNA microarray and IPA. (a) Three basic biofunction related genes filtrated by IPA. After DNA microarray, the whole data were input into ingenuity pathway analysis system. The genes classified to antioxidant genes, inflammatory genes, and metabolic regulating genes are displayed with more than twofold expression change by myricetin. (b) Real-time PCR verification data versus microarray data. HepG2 cells were pretreated with or without myricetin for 9 h. RNA extract and real-time PCR were described in Material and Methods. The result was expressed as the relative expression level. Each value represents the mean ± SD of three separate experiments, $*p < 0.05$; $**p < 0.01$ versus control, respectively. CTL, control; AKR1C, aldo-keto reductase family 1, member C; GCLC, glutamate cysteine ligase, catalytic subunit; SERPINE, serpin peptidase inhibitor clade; IL, interleukin; IGFBP1, insulin -like growth factor-binding protein 1.

regulated by Nrf2 or NF-κB signaling pathways. Then, we further verify the gene chip results of several selected key genes by RT-qPCR and make a comparison. As shown in Figure 3(b), RT-qPCR results have confirmed the accuracy of the gene chip results, and their changes are even bigger. These results indicate that myricetin can stimulate the expressions of antioxidant genes, inhibit that of inflammatory genes, and induce the expressions of metabolic regulating genes in HepG2 cells.

3.6. Bio-Plex Based Inflammatory Cytokines Assay by Myricetin Treatment in HepG2 Cells Induced by LPS. The above IPA analysis results reveal that inflammation is the main interface targeted by myricetin. However, these results just stay in mRNA level. To investigate whether myricetin indeed works on inflammation inhibition, and we conducted Western blotting and bio-plex inflammatory cytokine assay in HepG2 cells, which is a more suitable inflammation model. Cytokines are important in cell signaling and play a significant role in inflammation [33].

Before starting, we firstly performed Western blotting of typical biomarkers of inflammation, iNOS and COX-2, to confirm the anti-inflammatory efficiency and the toxicity of myricetin. The results showed that iNOS and COX-2 expressions are both significantly decreased dose-dependently (Figure 4(a)) and 20 μM of myricetin had no cytotoxicity on HepG2 cells, which is similar to our previous study[18]. Then, we applied 10-20 μM of myricetin in bio-plex cytokines assay. As shown in Figure 4(b), 27 kinds of cytokines were detected by bio-plex system, just 9 of which were significantly inhibited by myricetin pretreatment, including TNF-α, IFN-γ, IL-1α, IL-1β, IL-2, and IL-6.

4. Discussion

In the present study, we conducted microarray and bioinformatic analysis to comprehensively describe the biofunction of myricetin in HepG2 cells, GO, and IPA analysis results provided some hints for the anti-inflammation, antioxidation, and intervention on metabolism of myricetin, which were partly verified by RT-qPCR. The function and canonical pathway analysis by IPA further confirmed that myricetin plays a crucial role on the regulation of redox signaling pathways and metabolic process, especially the inhibition on inflammation. Thus, we finally performed the proteomic analysis by the application of bio-plex cytokines assay, and the results indicated that myricetin does exert potent anti-inflammatory effect by secretion inhibitions of IL-1α, IL-1β, IL-2, IL-6, IFN-γ, and TNF-α.

Top molecules generated by IPA help us to focus on the most impossible biofunction rapidly. For example, top metabolic gene *SLC2A2* plays a key role in HIF-1-α signaling, which acts as the central system on regulation of metabolism. The concentration of HIF-1-α (and its subsequent activity) is regulated by NF-κB-dependent regulation [34]. HIF-1 is overexpressed in many human cancers, and its overexpression promotes tumour growth and metastasis through its initial angiogenesis and regulation of cell metabolism to overcome hypoxia [35]. Thus, an inference can be made from the phenomenon that *SLC2A2* was involved in the HIF-1-α signaling, and its decreased expression by myricetin treatment implies that myricetin has the potency on the regulation of metabolic process, which is evidenced by the canonical pathway analysis of IPA. As shown in Figure 1, several metabolic pathways have been found to be associated with the metabolic regulation property of myricetin, including "metabolism of xenobiotics by cytochrome P450, bile acid biosynthesis, C21-steroid hormone metabolism, glycerophospholipid metabolism, glycerolipid metabolism, glutamate metabolism, IGF-1 signaling, and fatty acid metabolism." These metabolic pathways were all significantly disturbed by myricetin treatment, indicating that myricetin possesses the ability of regulating glucolipid metabolism dysfunction.

In addition to the top 1 network associated with cellular function and disease, top 2 and top 3 networks are also found to be related to inflammation. As shown in Table 3, the top 2 and top 3 cellular functions and diseases are "connective tissue development and function, skeletal and muscular system development and function, and tissue morphology" (with a score of 33 and focus molecules of 22) and "endocrine system disorders, haematological disease, and metabolic disease" (with a score of 32 and focus molecules of 22). The cores of their networks are TGF-β and AP-1 (data not shown here), and their respective key molecules include *IL11*, *STAT*, *SORBS2*, *Sos*, *NEXN*, *SLC6A4*, *XRN1*, etc. Most of the inflammatory genes were significantly downregulated by myricetin treatment; however, a series of antioxidant genes, such as *SQSTM1*, *TXNRD1*, *HMOX1,* and *SLC family*, were found to be upregulated significantly, which reveals that myricetin plays a complex role on the balance between inflammation and antioxidation, the redox interface in HepG2 cells. Moreover, glucolipid metabolism was also found to be related to the redox status, for the disturbed expressions of *IGF2*, *IGF2BP2*, *IGFBP1,* and *IGFBP3*.

Our study is the first time to apply the inflammatory proteomic tool of bio-plex cytokines assay to investigate the inflammatory property of myricetin in HepG2 cells. In the total typical 27 cytokines, the secretions of IL-1α, IL-1β, IL-2, IL-6, IFN-γ, and TNF-α have been found to be inhibited by myricetin treatment. TNF-α, acting as a major member of tumour necrosis factor, is an important proinflammatory cytokine in the inflammatory response model. TNF-α, by means of binding to its receptor, can regulate NF-κB expression by modulation of TRAF2 and RIP [36]. Therefore, the significant decrease of TNF-α expression indicates that the remission of inflammatory response is caused by myricetin treatment through the inhibition of NF-κB activity, which is evidenced by other studies [37]. IL-6 and IL-1 are also important proinflammatory cytokines, and they were found to be inhibited remarkably by myricetin treatment in the present study. As reported, LPS can activate NF-κB by stimulating monocyte MAPK signaling pathway and then promote the expression of IL-1 gene; besides, IL-1 can induce activation of p38 to promote the expression of NF-κB in turn [38]. IL-6 is closely correlated with STAT3, and STAT3 plays a key role in cell proliferation and differentiation, so IL-6 can not only promote the development of inflammation but

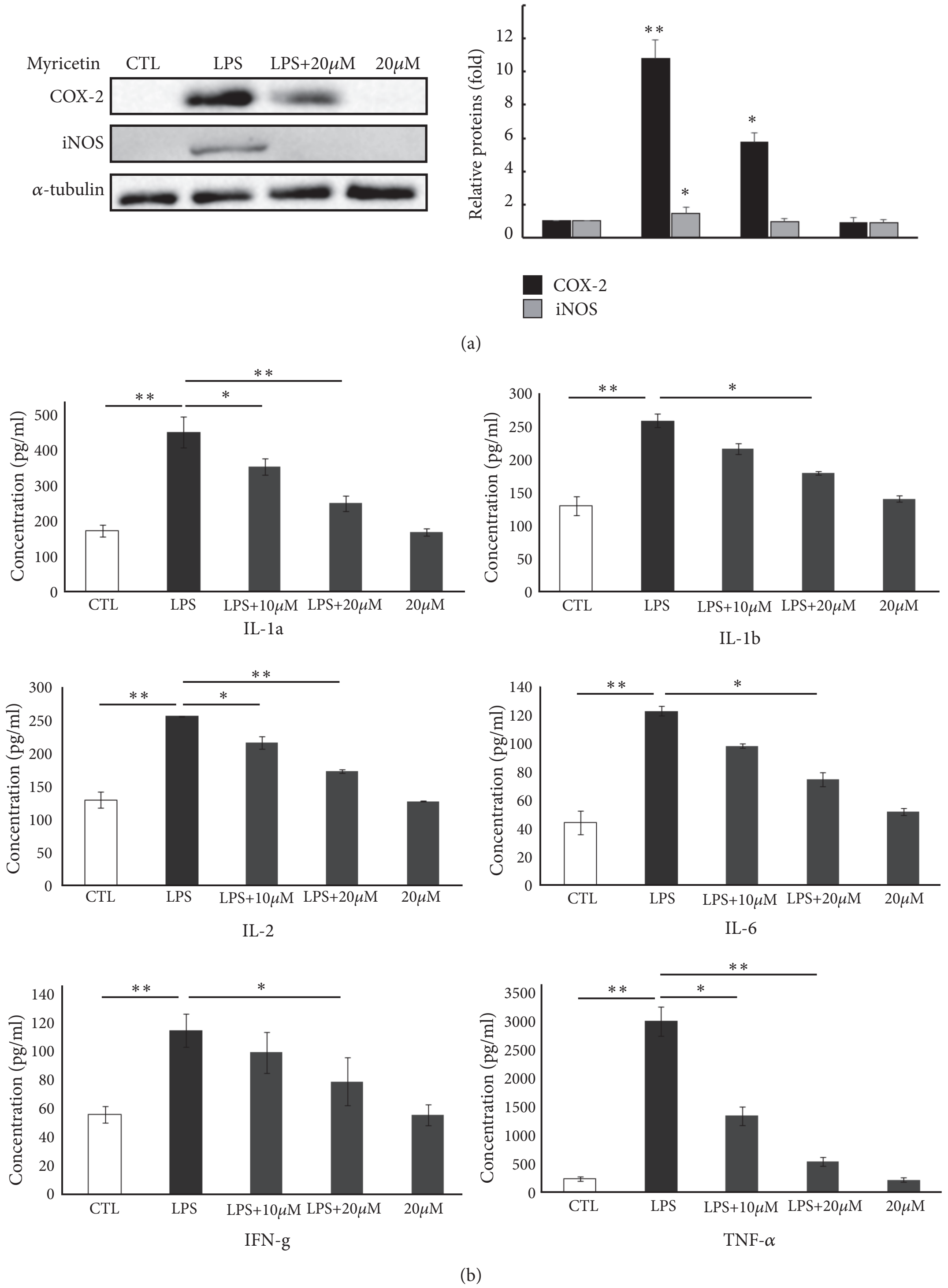

Figure 4: Influence of myricetin on the production of inflammatory proteins and cytokines. (a) Influence of myricetin on the production of iNOS and COX-2 protein. HepG2 cells (1×106 cells) were precultured for 24 h and starved in serum-free medium for 2.5 h. The cells were then treated with the indicated concentrations of myricetin for 30 min and then exposed to 1 μg/mL LPS for 12 h. The proteins of iNOS, COX-2, and α-tubulin were detected by Western blotting with their antibodies, respectively. (b) Myricetin decreased the levels of multiple inflammatory cytokines in HepG2 cells. The levels of 27 kinds of cytokines were measured by multiplex technology and bio-plex assay and arranged in an order from high to low change in the experimental inflammatory HepG2 cells. The data represent mean ± SD of four mice. $*p < 0.05$ and $**p < 0.01$. CTL, control; IL, interleukin; IFN-γ, interferon-gamma; TNF-α, tumor necrosis factor.

also accelerate the proliferation of normal cells and tumour cells [39]. Hence, NF-κB signaling in the HepG2 cells was inhibited by myricetin because of the decrease of IL-6 and IL-1 productions. According to the result of proteomic assay of cytokines, spontaneously, the speculation that myricetin has a powerful effect on the inhibition of inflammation is obtained, which encourages *in vivo* studies to verify its possible health benefits.

5. Conclusions

Obviously, by the combined application of genomic microarray and proteomic cytokine assay, we not only comprehensively understand the multiple functions of myricetin, in the form of regulation on redox signaling pathways and metabolic process at mRNA level, but also verify its crucial and potent anti-inflammatory property at protein level. Therefore, myricetin exerts potent multiple biofunctions linked to redox balance and metabolic regulation, especially its remarkable anti-inflammatory activity. The present study could promote the application of nutritional intervention by myricetin in the research and development of functional food or special medical use food.

Abbreviations

AP-1:	Activator protein 1
GF:	Growth factor
GO:	Gene Ontology
IκB:	Inhibitory protein of NF-κB
IRF3:	Interferon regulatory factor 3
IL:	Interleukin
IFN:	Interferon
IPA:	Ingenuity pathways analysis
LPS:	Lipopolysaccharides
MAPK:	Mitogen-activated protein kinase
NF-κB:	Nuclear factor-kappa B
Nrf2:	Nuclear factor-erythroid 2 p45-related factor 2
NCF2:	Neutrophil cytosolic factor 2 (65kDa, chronic granulomatous disease, autosomal 2)
RT-PCR:	Real-time quantity polymerase chain reaction
SLC2A2:	Solute carrier family 2 (facilitated glucose transporter), member 2
TGF-β:	Transforming growth factor beta
TNF:	Tumour necrosis factor.

Data Availability

The data used to support the findings of this study are available from the corresponding author upon request.

Disclosure

We have just submitted the abstract and give an oral presentation with some of the content in this manuscript in the 3rd International Conference on Agriculture and Agro-Industry 2018 (ICAAI2018), but without publishing this manuscript. Tao Li and Jihe Zhu are joint first authors.

Conflicts of Interest

The authors declare that there are no conflicts of interest regarding the publication of this paper.

Authors' Contributions

Tao Li and Jihe Zhu contributed equally to the work.

Acknowledgments

This work was partially supported by Natural Science Foundation of China and Hunan Province, Key Scientific Research Fund of Hunan Provincial Science and Technology Department (2017NK2093), Core Research Program 1515 and double first-class construction project of Hunan Agricultural University (No. SYL201802025) to Si Qin. The authors would like to thank Key Laboratory for Food Science and Biotechnology of Hunan Province, College of Food Science and Technology, Hunan Agricultural University for providing the facilities to carry out this study.

Supplementary Materials

Supplementary Table 1: the disturbed genes involved in signal transduction. Supplementary Table 2: the disturbed genes involved in nucleus and mitochondrion. Supplementary Table 3: the disturbed genes involved in DNA binding, protein binding, kinase, and protein kinase activity. *(Supplementary Materials)*

References

[1] J. M. Harnly, R. F. Doherty, G. R. Beecher et al., "Flavonoid content of U.S. fruits, vegetables, and nuts," *Journal of Agricultural and Food Chemistry*, vol. 54, no. 26, pp. 9966–9977, 2006.

[2] K. C. Ong and H. E. Khoo, "Biological effects of myricetin," *General Pharmacology: The Vascular System*, vol. 29, no. 2, pp. 121–126, 1997.

[3] K. W. Lee, N. J. Kang, E. A. Rogozin et al., "Myricetin is a novel natural inhibitor of neoplastic cell transformation and MEK1," *Carcinogenesis*, vol. 28, no. 9, pp. 1918–1927, 2007.

[4] P. K. Maurya, P. Kumar, S. Nagotu, S. Chand, and P. Chandra, "Multi-target detection of oxidative stress biomarkers in quercetin and myricetin treated human red blood cells," *RSC Advances*, vol. 6, no. 58, pp. 53195–53202, 2016.

[5] Y. Qiu, N. Cong, M. Liang, Y. Wang, and J. Wang, "Systems pharmacology dissection of the protective effect of myricetin against acute ischemia/reperfusion-induced myocardial injury in isolated rat heart," *Cardiovascular Toxicology*, vol. 17, no. 3, pp. 277–286, 2017.

[6] R. Domitrović, K. Rashed, O. Cvijanović, S. Vladimir-Knežević, M. Škoda, and A. Višnić, "Myricitrin exhibits antioxidant, anti-inflammatory and antifibrotic activity in carbon tetrachloride-intoxicated mice," *Chemico-Biological Interactions*, vol. 230, pp. 21–29, 2015.

[7] B. O. Cho, H. H. Yin, S. H. Park, E. B. Byun, H. Y. Ha, and S. I. Jang, "Anti-inflammatory activity of myricetin from diospyros lotus through suppression of nf-κb and stat1 activation and nrf2-mediated ho-1 induction in lipopolysaccharide-stimulated raw264.7 macrophages," *Bioscience, Biotechnology, and Biochemistry*, vol. 80, no. 8, pp. 1520–1530, 2016.

[8] F. Sun, X. Y. Zheng, J. Ye, T. T. Wu, J. L. Wang, and W. Chen, "Potential anticancer activity of myricetin in human T24 bladder cancer cells both in vitro and in vivo," *Nutrition and Cancer*, vol. 64, no. 4, pp. 599–606, 2012.

[9] X.-H. Zhang, S.-Y. Chen, L. Tang et al., "Myricetin induces apoptosis in HepG2 cells through Akt/p70s6K/Bad signaling and mitochondrial apoptotic pathway," *Anti-Cancer Agents in Medicinal Chemistry*, vol. 13, no. 10, pp. 1575–1581, 2013.

[10] M. Müller and S. Kersten, "Nutrigenomics: goals and strategies," *Nature Reviews Genetics*, vol. 4, no. 4, pp. 315–322, 2003.

[11] K. R. Martin, "Using nutrigenomics to evaluate apoptosis as a preemptive target in cancer prevention," *Current Cancer Drug Targets*, vol. 7, no. 5, pp. 438–446, 2007.

[12] J. Wang, X. Bai, X. Ding et al., "Quantitative proteomic analysis reveals the role of tea polyphenol EGCG in egg whites in response to vanadium stress," *Nutrition Journal* , vol. 39-40, pp. 20–29, 2017.

[13] L. Méndez, S. Ciordia, M. S. Fernández et al., "Changes in liver proteins of rats fed standard and high-fat and sucrose diets induced by fish omega-3 PUFAs and their combination with grape polyphenols according to quantitative proteomics," *The Journal of Nutritional Biochemistry*, vol. 41, pp. 84–97, 2017.

[14] F. Ali, A. Ismail, N. M. Esa, and C. P. Pei, "Transcriptomics expression analysis to unveil the molecular mechanisms underlying the cocoa polyphenol treatment in diet-induced obesity rats," *Genomics*, vol. 105, no. 1, pp. 23–30, 2015.

[15] S. Malireddy, S. R. Kotha, J. D. Secor et al., "Phytochemical antioxidants modulate mammalian cellular epigenome: implications in health and disease," *Antioxidants & Redox Signaling*, vol. 17, no. 2, pp. 327–339, 2012.

[16] W. Zam and A. Khadour, "Impact of phytochemicals and dietary patterns on epigenome and cancer," *Nutrition and Cancer*, vol. 69, no. 2, pp. 184–200, 2017.

[17] J.-C. Wu, C.-S. Lai, P.-S. Lee et al., "Anti-cancer efficacy of dietary polyphenols is mediated through epigenetic modifications," *Current Opinion in Food Science*, vol. 8, pp. 1–7, 2016.

[18] S. Qin, J. Chen, S. Tanigawa, and D.-X. Hou, "Microarray and pathway analysis highlight Nrf2/ARE-mediated expression profiling by polyphenolic myricetin," *Molecular Nutrition & Food Research*, vol. 57, no. 3, pp. 435–446, 2013.

[19] B. Kloesch, T. Becker, E. Dietersdorfer, H. Kiener, and G. Steiner, "Anti-inflammatory and apoptotic effects of the polyphenol curcumin on human fibroblast-like synoviocytes," *International Immunopharmacology*, vol. 15, no. 2, pp. 400–405, 2013.

[20] J. Chen, T. Uto, S. Tanigawa, T. Kumamoto, M. Fujii, and D.-X. Hou, "Expression profiling of genes targeted by bilberry (*Vaccinium myrtillus*) in macrophages through DNA microarray," *Nutrition and Cancer*, vol. 60, no. 1, pp. 43–50, 2008.

[21] M. F. Neurath, "Cytokines in inflammatory bowel disease," *Nature Reviews Immunology*, vol. 14, no. 5, pp. 329–342, 2014.

[22] J. M. Rubio-Perez and J. M. Morillas-Ruiz, "A review: inflammatory process in alzheimer's disease, role of cytokines," *The Scientific World Journal*, vol. 2012, Article ID 756357, 15 pages, 2012.

[23] J. Helleman, M. Smid, M. P. H. M. Jansen, M. E. L. van der Burg, and E. M. J. J. Berns, "Pathway analysis of gene lists associated with platinum-based chemotherapy resistance in ovarian cancer: the big picture," *Gynecologic Oncology*, vol. 117, no. 2, pp. 170–176, 2010.

[24] C.-J. Li, R. W. Li, Y.-H. Wang, and T. H. Elsasser, "Pathway analysis identifies perturbation of genetic networks induced by butyrate in a bovine kidney epithelial cell line," *Functional & Integrative Genomics*, vol. 7, no. 3, pp. 193–205, 2007.

[25] N. K. Sethy, M. Singh, R. Kumar, G. Ilavazhagan, and K. Bhargava, "Upregulation of transcription factor NRF2-mediated oxidative stress response pathway in rat brain under short-term chronic hypobaric hypoxia," *Functional & Integrative Genomics*, vol. 11, no. 1, pp. 119–137, 2011.

[26] M. A. Kluge, J. L. Fetterman, and J. A. Vita, "Mitochondria and endothelial function," *Circulation Research*, vol. 112, pp. 1171–1188, 2013.

[27] D. Voet, J. G. Voet, and C. W. Pratt, "Cancer cytogenetics: chromosomal and molecular genetic aberrations of tumour cells," in *Journal of General Plant Pathology*, vol. 70, pp. 278–283, 4th edition, 2015.

[28] D. A. Walsh and C. D. Ashby, "Protein kinases: aspects of their regulation and diversity," *Recent Progress in Hormone Research*, vol. 29, pp. 329–359, 1973.

[29] A. R. Saltiel and C. R. Kahn, "Insulin signalling and the regulation of glucose and lipid metabolism," *Nature*, vol. 414, no. 6865, pp. 799–806, 2001.

[30] W. Wang, M. Wei, H. M. Song et al., "SLC2A2 gene analysis in three Chinese children with Fanconi-Bickel syndrome," *Zhongguo Dang Dai Er Ke Za Zhi*, vol. 17, pp. 362–366, 2015.

[31] M. Gentsch, A. Kaczmarczyk, K. Van Leeuwen et al., "Alu-repeat-induced deletions within the NCF2 gene causing p67-phox-deficient chronic granulomatous Disease (CGD)," *Human Mutation*, vol. 31, no. 2, pp. 151–158, 2010.

[32] Y. Herishanu, P. Pérez-Galán, D. Liu et al., "The lymph node microenvironment promotes B-cell receptor signaling, NF-κB activation, and tumor proliferation in chronic lymphocytic leukemia," *Blood*, vol. 117, no. 2, pp. 563–574, 2011.

[33] G. Landskron, M. De la Fuente, P. Thuwajit, C. Thuwajit, and M. A. Hermoso, "Chronic Inflammation and Cytokines in the Tumor Microenvironment," *Journal of Immunology Research*, vol. 2014, Article ID 149185, 19 pages, 2014.

[34] G. Li, Y. Zhang, Y. Qian et al., "Interleukin-17A promotes rheumatoid arthritis synoviocytes migration and invasion under hypoxia by increasing MMP2 and MMP9 expression through NF-κB/HIF-1α pathway," *Molecular Immunology*, vol. 53, no. 3, pp. 227–236, 2013.

[35] G. L. Semenza, "HIF-1 mediates metabolic responses to intratumoral hypoxia and oncogenic mutations," *The Journal of Clinical Investigation*, vol. 123, no. 9, pp. 3664–3671, 2013.

[36] H. Zelová and J. Hošek, "TNF-α signalling and inflammation: interactions between old acquaintances," *Inflammation Research*, vol. 62, no. 7, pp. 641–651, 2013.

[37] C. Xie, J. Kang, Z. Li et al., "The açaí flavonoid velutin is a potent anti-inflammatory agent: Blockade of LPS-mediated TNF-α and IL-6 production through inhibiting NF-κB activation and MAPK pathway," *The Journal of Nutritional Biochemistry*, vol. 23, no. 9, pp. 1184–1191, 2012.

[38] B.-P. Huang, C.-H. Lin, H.-M. Chen, J.-T. Lin, Y.-F. Cheng, and S.-H. Kao, "AMPK activation inhibits expression of proinflammatory mediators through downregulation of PI3K/p38 MAPK

and NF-κB signaling in murine macrophages," *DNA and Cell Biology*, vol. 34, no. 2, pp. 133–141, 2015.

[39] B. Tu, L. Du, Q.-M. Fan, Z. Tang, and T.-T. Tang, "STAT3 activation by IL-6 from mesenchymal stem cells promotes the proliferation and metastasis of osteosarcoma," *Cancer Letters*, vol. 325, no. 1, pp. 80–88, 2012.

Hindawi
BioMed Research International
Volume 2019, Article ID 3904923, 11 pages
https://doi.org/10.1155/2019/3904923

Research Article

MicroRNA-15a-5p Regulates the Development of Osteoarthritis by Targeting PTHrP in Chondrocytes

Zhi-xi Duan,[1] **Peng Huang**,[2] **Chao Tu**,[1] **Qing Liu**,[1] **Shuang-qing Li**,[1]
Ze-ling Long,[1] **and Zhi-hong Li**[1]

[1] *Department of Orthopedics, The Second Xiangya Hospital, Central South University, 139 Renmin Road, Changsha 410011, China*
[2] *Department of General Surgery, Xiangya Hospital, Central South University, No. 87 Xiangya Road, Changsha 410008, China*

Correspondence should be addressed to Zhi-hong Li; lizhihong@csu.edu.cn

Received 30 January 2019; Accepted 20 February 2019; Published 5 March 2019

Guest Editor: Hengjia Ni

Copyright © 2019 Zhi-xi Duan et al. This is an open access article distributed under the Creative Commons Attribution License, which permits unrestricted use, distribution, and reproduction in any medium, provided the original work is properly cited.

Background and Aims. A growing body of research has demonstrated that the degeneration of chondrocytes is the primary cause of osteoarthritis (OA). Parathyroid hormone-related protein (PTHrP) can alleviate the degeneration of chondrocytes via promotion of chondrocyte proliferation and inhibition of terminal differentiation, but the underlying mechanism remains unknown. This study aimed to identify the microRNAs (miRNAs) that may target PTHrP and regulate the proliferation and terminal differentiation of chondrocytes. *Methods*. Bioinformatic analysis was used to predict which miRNAs target PTHrP. We collected human knee cartilage specimens to acquire the primary chondrocytes, which we then used to test the expression and function of the targeted miRNAs. To explore the effects of miR-15a-5p on the putative binding sites, specific mimics or inhibitors were transfected into the chondrocytes. Furthermore, a dual-luciferase reporter gene assay and chondrocyte degeneration-related factors were used to verify the possible mechanism. *Results*. The expression of PTHrP was upregulated in the OA chondrocytes, whilst miR-15a-5p was downregulated in the OA chondrocytes. A negative correlation was observed between PTHrP and miR-15a-5p. The knockdown of miR-15a-5p promoted the growth of chondrocytes and inhibited calcium deposition, whilst overexpression of miR-15a-5p reversed this trend. The effect of miR-15a-5p overexpression was neutralised by PTHrP. Dual-luciferase reporter assays revealed that PTHrP can be used as a novel targeting molecule for miR-15a-5p. *Conclusions*. miR-15a-5p promotes the degeneration of chondrocytes by targeting PTHrP and, in addition to helping us understand the development of OA, may be a potential biomarker of OA.

1. Introduction

Osteoarthritis (OA), a degenerative joint condition, is the most common disease in adults and, in addition to leading to high medical expenses, is one of the most frequent causes of pain, loss of function, and psychological disability [1, 2]. Several treatment options are available for relief of OA symptoms, but because the pathogenesis of OA remains unclear, few practical ways of stopping the progressive degradation of the articular cartilage have been found [3, 4].

Deterioration of the smoothness of the articular cartilage is the chief characteristic of OA, and chondrocytes are the only type of cells in the articular cartilage, so dysregulation of cell proliferation and differentiation in chondrocytes contributes directly to OA [5–7]. The primary function of chondrocytes is to maintain the balance of the extracellular matrix, which consists mainly of collagen and proteoglycans. However, the pattern of gene expression and the related mechanisms involved in chondrocyte action remain unclear.

Parathyroid hormone-related protein (PTHrP, also known as PTHLH) is a widely occurring protein produced by most tissues in the body [8, 9] and is an essential factor in many of the physiological and pathological processes involved in OA [10]. Numerous reports have confirmed that PTHrP contributes to chondrocyte proliferation and inhibits terminal differentiation [8, 11–13]. However, the regulation of PTHrP in OA is still poorly understood.

MicroRNAs (miRNAs), about 23 nt of endogenous small noncoding RNA, are involved in the regulation of target protein-encoding genes via translational inhibition and/or degradation of the target mRNA [14–16]. The expression of various small RNAs in OA changes in relation to that in normal cartilage, which suggests that the expression of small RNA may affect cartilage homeostasis [17]. The significance of miR-15a-5p for the survival and metastasis of tumours, especially during the process of cell proliferation or differentiation, has attracted much attention [18, 19]. The function of miR-15a-5p in regulating the degradation of the cartilage matrix has also been investigated [20]. Unfortunately, the underlying mechanism of the involvement of miR-15a-5p in the progress of OA remains unclear. In this study, we found that PTHrP served as the target of miR-15a-5p and clarified the effects of miR-15a-5p on the proliferation and differentiation of chondrocytes.

2. Materials and Methods

2.1. Human Specimens. In this study, rheumatoid arthritis and septic arthritis were excluded, and samples of human articular cartilage were obtained from 16 patients with OA (OA Grade III–IV) who underwent total knee arthroplasty. Eight patients with osteosarcoma who were undergoing segmental resection and artificial knee prosthesis replacement or amputation were also recruited to allow collection of normal articular cartilage specimens. Table 1 lists the corresponding information. Our work was approved by the ethics committee of Second Xiangya Hospital, Central South University (Changsha, Hunan, China).

2.2. Isolation and Culture of Chondrocytes. The cartilage specimens were collected immediately after surgery, placed in Petri dishes, and wetted with phosphate-buffered saline solution (PBS). The cartilage samples were cut into 1–3 mm^3 pieces with two sterile scalpels. The PBS was removed, and the diced tissues were placed in Dulbecco's modified Eagle's medium (DMEM; Sangon, Shanghai, China) with 2.0 mg/mL collagenase type II (Worthington, USA). The tube was capped, covered with Parafilm, and then placed on an orbital shaker at 200 rpm for 10–12 h at 37°C. The next day, the suspension was filtered through a 40-μm mesh into a sterile 50-ml centrifuge tube. The digestate was centrifuged at 1200 rpm for 10 min. The supernatant was removed, and the pellet was gently resuspended in 10 mL of DMEM. The specific protocol of the primary chondrocyte culture is based on the literature [21, 22]. The cells were centrifuged, washed, and resuspended in the medium, placed in a T-25 flask, and cultured in DMEM plus 10% FBS at 37°C, 5% CO_2. The chondrocytes in the second passage were used in all of the experiments.

2.3. Cartilage Tissue and Chondrocyte Staining. The excised cartilage tissues were fixed in 4% paraformaldehyde (PFA), briefly decalcified in 10% ethylenediaminetetraacetic acid (EDTA) for 4 weeks, and sectioned into 4–5 mm thick slices with a scalpel blade. Each slice was embedded in paraffin and sectioned at 6 μm. Serial sections from each slice were stained routinely with Safranin O/Fast Green. The cell-attached slides were washed using PBS and stained using Toluidine blue for 15 min. The cells were rewashed with PBS, and the morphology of the cartilage tissues and cells was assessed.

2.4. Immunohistochemical Analysis. After being seeded into special chamber slides, the human primary chondrocytes were fixed with 4% PFA for 10 min, permeabilised with 0.1% Triton X-100 for 15 min, and treated with 1% bovine serum albumin for 30 min. Next, the cells were incubated with PTHrP antibody for 1 h, and the anti-goat IgG antibody conjugated with peroxidase was then incubated for 30 min. Finally, the nuclei were counterstained with haematoxylin. All of the procedures were performed at room temperature.

2.5. Calcium Deposition Assay. To evaluate the extent of the calcification or calcium deposition in the intervention and control groups of the cultured primary chondrocytes, we used Alizarin Red S staining, which is one of the most commonly used methods. The cells were fixed at room temperature with 4% PFA for 10 min and exposed to Alizarin Red S for 15 min. The cells were then washed with PBS and then photographed under a microscope.

2.6. Western Blotting Analysis. The total protein was extracted from each intervention group by lysing the cells in a radioimmunoprecipitation assay buffer (Beyotime, Shanghai, China). Quantitative analysis of the protein concentrations was performed with a special analytical kit (Beyotime, Shanghai, China). The same amount of proteins was obtained by 10% sodium dodecyl sulphate-polyacrylamide gel electrophoresis and electrotransferred onto polyvinylidene fluoride (PVDF) membranes. The PVDF membranes were then blocked with 5% skimmed milk powder in TBST (Tris-buffered saline solution containing 0.1% Tween 20) and cultured with primary and secondary antibodies. The specific protocol of the western blotting is based on the literature [23]. After washing, the staining was visualised with an enhanced chemiluminescence kit (Beyotime, Shanghai, China), and the specific strip was measured with the MicroChemi 4.2 system (DNR Bio-Imaging Systems, Jerusalem, Israel).

2.7. Cell Transfection and Cell Proliferation Analysis. OA chondrocytes in logarithmic phase were seeded into six-well plates and cultured for 24 h. The cells were then allotted to several groups: the siPTHrP group, the negative control (NC) group, the miR-15a-5p mimics group, the NC inhibitors group, and the miR-15a-5p inhibitors group. The plasmids were purchased from GenePharma Co Ltd (Shanghai, China). The cells were transiently transfected with plasmids using the Lipofectamine 2000 reagent (Thermo Fisher Scientific) as previously reported [24]. The corresponding sequences are listed in Table 2. A Cell Counting Kit-8 (CCK-8, Beyotime Biotechnology, China) was used to test cell proliferation after the cells had been incubated for various periods of time. The OD values at 450 nm were measured by spectrophotometry.

2.8. Luciferase Reporter Assay. We constructed wild-type and mutant plasmids for PTHrP to explore the targeting link between miR-15a-5p and PTHrP. Table 2 lists the sequences

Table 1: Patients information.

Group	Diagnosis (K-L Grade)	Gender		Age
		Female	Male	
OA	OA (III)	2	0	72.5 ± 3.7
	OA (IV)	8	6	
Normal	Osteosarcoma	3	5	17.6 ± 4.0

Grading standards based on Kellgren and Lawrence system (K-L Grade).

used. We verified the recombinant plasmids via restriction enzyme digestion and DNA sequencing.

HEK293T cells were added into a 12-well plate to confirm the direct interaction between miR-15a-5p and PTHrP mRNA. The cells were transfected with miR-15a-5p mimics and PTHrP wild-type or PTHrP mutants using the Lipofectamine 2000 reagent after 24 hours. The samples were then cotransfected with a pRL-TK plasmid that expresses Renilla luciferase. About 48 hours after the transfection, the cells were lysed and the Firefly and Renilla luciferase activities were detected with a dual luciferase reporter assay system (Biotek, Winooski, VT). The transfection was performed in triplicate.

2.9. Quantitative Real-Time PCR (qRT-PCR). The total RNA was separated by Trizol Reagent (Thermo Fisher Science), reverse transcribed into cDNA, and used for the qRT-PCR analysis, as previously reported [25]. The ABI Prism VIIA7 system was used to quantify the gene expression by qRT-PCR (ABI Prism ViiA7, Applied Biosystems, CA). The level of PTHrP was analysed using qRT-PCR and normalised to actin. The miR-15a-5p was normalised to U6. The primer design of miR-15a-5p was acquired from Sangon (Shanghai, China). The corresponding primer sequences are listed in Table 2.

2.10. Statistical Analysis. The statistical analysis was performed using GraphPad Prism Software (Version 7.0). The results are expressed as mean ± standard deviation (SD). Student's t-test was used to detect the differences between the two groups. A P value of less than 0.05 was considered to indicate significant variation between groups.

3. Results

3.1. Upregulation of PTHrP in Chondrocytes from Human Knee OA. The general morphology of the normal and OA articular cartilage samples was examined after Safranin O/Fast Green staining, which revealed differences in the surface of the tibial plateaus. The normal articular cartilage was smooth, whilst the OA articular cartilage showed extensive wear (Figure 1(a)). To better understand the related mechanism, the expression of PTHrP was detected by RT-PCR in 8 normal chondrocytes and 16 OA chondrocytes. The results showed a significant increase in the expression of PTHrP in the OA chondrocytes (Figure 1(b)). Furthermore, we cultured chondrocytes from the articular cartilage and observed the cell morphology after Toluidine blue staining (Figure 1(c)). A previous study showed that the level of PTHrP was higher in OA than in normal human knee articular cartilage [26]. Similarly, in this study, immunohistochemical analysis revealed a significantly higher level of PTHrP in the OA chondrocytes than in the normal chondrocytes ($p<0.01$) (Figure 1(c)). Analysis of the PTHrP protein expression in the chondrocytes by western blotting confirmed significant upregulation of PTHrP in the OA chondrocytes ($p<0.05$) (Figure 1(d)).

3.2. PTHrP Prevents Terminal Differentiation and Promotes Proliferation in Human OA Chondrocytes. To determine the role played by PTHrP in promoting proliferation and preventing terminal differentiation in human knee OA chondrocytes, cells were cultured with siPTHrP, the corresponding controls, or recombinant human PTHrP (rhPTHrP). As shown in Figure 2(a), a CCK8 experiment showed that the growth rate of primary cultured chondrocytes transfected with siPTHrP was slower than that of the control group, whilst rhPTHrP caused a significant increase in growth ($p<0.05$). qRT-PCR was performed to further test the effect of PTHrP on the chondrocytes. Biomarkers of proliferation and terminal differentiation, including collagen II, aggrecan, and MMP-13, were investigated. MMP13 is a major enzyme that targets cartilage and leads to the degradation of collagen II and proteoglycan. Aggrecan, a proteoglycan, and collagen II are critical components of the cartilage structure and function of chondrocytes [27]. As shown in Figure 2(b), a significant increase of MMP-13 was observed in the siPTHrP group relative to the control group ($p<0.01$), whilst the level of MMP-13 was lower in the rhPTHrP group than in the control group ($p<0.05$). In contrast, the level of collagen II increased in the rhPTHrP group ($p<0.05$, versus the NC group) and decreased in the siPTHrP group in comparison with the NC group ($p<0.05$). The level of aggrecan was also higher in the rhPTHrP group than in the NC group ($p<0.05$) and lower in the siPTHrP group than in the NC group ($p<0.05$).

Alizarin Red S staining demonstrated the presence of calcium deposits in the OA chondrocytes. As shown in Figure 2(c), the extracellular and intracellular areas were both stained with Alizarin Red S at 12 days. Higher levels of calcium deposition were induced by siPTHrP than in the other groups, whilst those in the rhPTHrP group were lower.

3.3. PTHrP Is a Direct Target of miR-15a-5p and Is Negatively Correlated with Its Expression in Human Primary Cultured Chondrocytes. PTHrP $3'$UTR contains miR-15a-5p binding sites (Figure 3(a)). To confirm that miR-15a-5p targets PTHrP, a dual-luciferase analysis was performed 48 h

Table 2: Primer sequences used in this study.

Name	5′-3′ sequence
PTHrP plasmid	F:CTAGCATTTTGTAAATGTATCTTGGTGCTGCTGAATTTCTATATTTTTTGTAACATAATGCACTTTAGATATACATATCAAGT
	R:CTAGACTTGATATGTATATCTAAAGTGCATTATGTTACAAAAAATATAGAAATTCAGCAGCACCAAGATACATTTACAAAATG
PTHrP mutant plasmid	F:CTAGCATTTTGTAAATGTATCTTGGACGACGAGAATTTCTATATTTTTTGTAACATAATGCACTTTAGATATACATATCAAGT
	R:CTAGACTTGATATGTATATCTAAAGTGCATTATGTTACAAAAAATATAGAAATTCTCGTCGTCCAAGATACATTTACAAAATG
siPTHrP	F: GGUGGAGACGUACAAAGAGTT
	R: CUCUUUGUACGUCUCCACCTT
miR-15a-5p (mimics)	F: UAGCAGCACAUAAUGGUUUGUG
	R: CAAACCAUUAUGUGCUGCUAUU
miR-15a-5p (control)	F: UUCUCCGAACGUGUCACGUTT
	R: ACGUGACACGUUCGGAGAATT
miR-15a-5p (inhibitors)	F: CACAAACCAUUAUGUGCUGCUA
β-Actin	F: CACCCAGCACAATGAAGATCAAGAT
	R: CCAGTTTTTAAATCCTGAGTCAAGC
PTHrP	F: CTGGTTCAGCAGTGGAGCGT
	R: AAGGAAGAATCGTCGCCGTA
U6	F: CTCGCTTCGGCAGCACA
miR-15a-5p	F: GCGTAGCAGCACATAATGGTTTGTG
Collagen II	F: CAGGACCAAAGGGACAGAAAGG
	R: GCAAAGTTTCCACCAAGACCAG
Aggrecan	F: AGCTCTGGGGAGGAATCTGG
	R: GCAGTTCACCAACCGTAGGAGT
MMP-13	F: GCCTTCAAAGTTTGGTCCGATG
	R: TGGTCAAGACCTAAGGAGTGGC

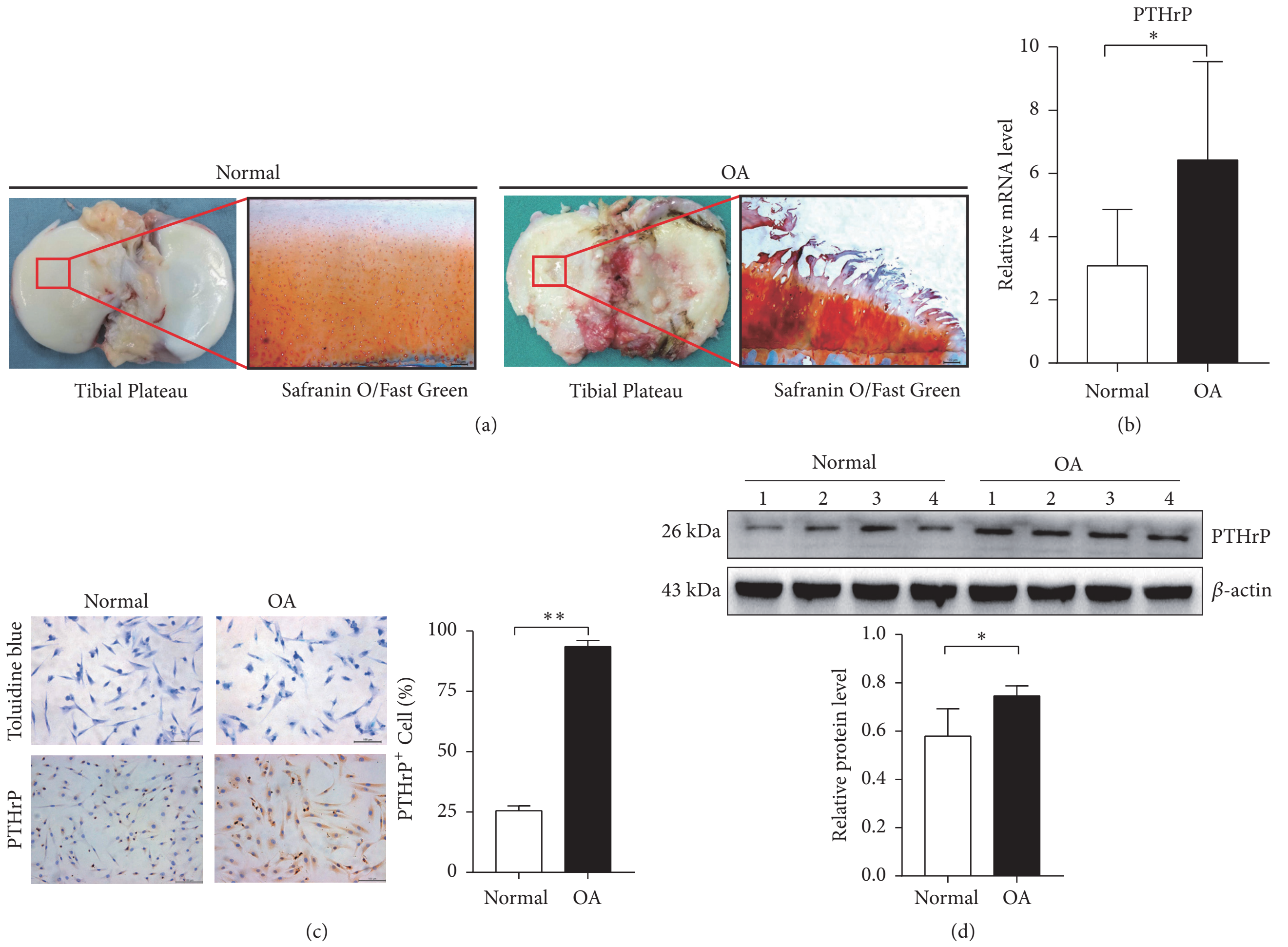

Figure 1: *Expression of PTHrP in human normal and OA chondrocytes*. Human knee articular cartilage was taken from subjects after total knee arthroplasty or amputation surgery. (a) Tissue morphology and Safranin O/Fast Green staining of normal and OA articular cartilage (scale bars, 100 μm). (b) RT-PCR was used to detect the relative levels of PTHrP in normal and OA chondrocytes, $*p<0.05$, n(normal) = 8, and n(OA) = 16. (c) Toluidine blue staining and immunohistochemical staining of chondrocytes (scale bars, 100 μm). The number of PTHrP (+) cells after IHC is presented as mean ± SD in the lower panels ($**p<0.01$, n = 6). (d) Western blot analysis shows the relative expression of PTHrP in chondrocytes. The quantitative results are presented as mean ± SD in the lower panels ($*p<0.05$, n = 4).

after transfection of the HEK293 cells with pmir-PTHrP-wt or pmir-PTHrP-mut reporter vectors. As shown in Figure 3(b), cells cotransfected with miR-15a-5p and the pmiR-PTHrP-wt vector showed a significant decrease in luciferase activity in comparison with the NC group, indicating that miR-15a-5p directly targets PTHrP ($p<0.01$, versus the NC group). Furthermore, the protein levels of PTHrP were analysed by western blotting, which confirmed that miR-15a-5p mimics downregulated the PTHrP protein level (Figure 3(c)). These results confirm that miR-15a-5p can directly bind to the PTHrP mRNA 3$'$UTR region and regulate the PTHrP protein level, thus indicating that PTHrP is the target for miR-15a-5p.

We used qRT-PCR to measure the levels of miR-15a-5p in normal and OA chondrocytes to determine the expression of miR-15a-5p in human OA chondrocytes. The expression of miR-15a-5p was significantly lower in the OA chondrocytes than in the normal chondrocytes (Figure 3(d)), whilst the expression of PTHrP was statistically higher in the OA chondrocytes than in the normal chondrocytes ($p<0.05$) (Figure 3(e)). A close relationship was observed between miR-15a-5p and PTHrP ($p<0.01$) (Figure 3(f)).

3.4. PTHrP Suppresses the Influence of miR-15a-5p on Chondrocyte Proliferation and Terminal Differentiation.

To understand whether miR-15a-5p has a negative effect on chondrocytes, as shown in Figure 4(a), the CCK8 assay was used to evaluate cell proliferation. The growth rate of primary cultured chondrocytes transfected with miR-15a-5p mimics was slower than that seen in the control group, whilst the growth rate of the miR-15a-5p inhibitors increased slightly.

qRT-PCR was performed to further detect the effects of miR-15a-5p mimics on the proliferation and terminal differentiation of chondrocytes. Chondrocytes were transfected with miR-15a-5p mimics and the inhibitors, and the markers of proliferation and terminal differentiation were

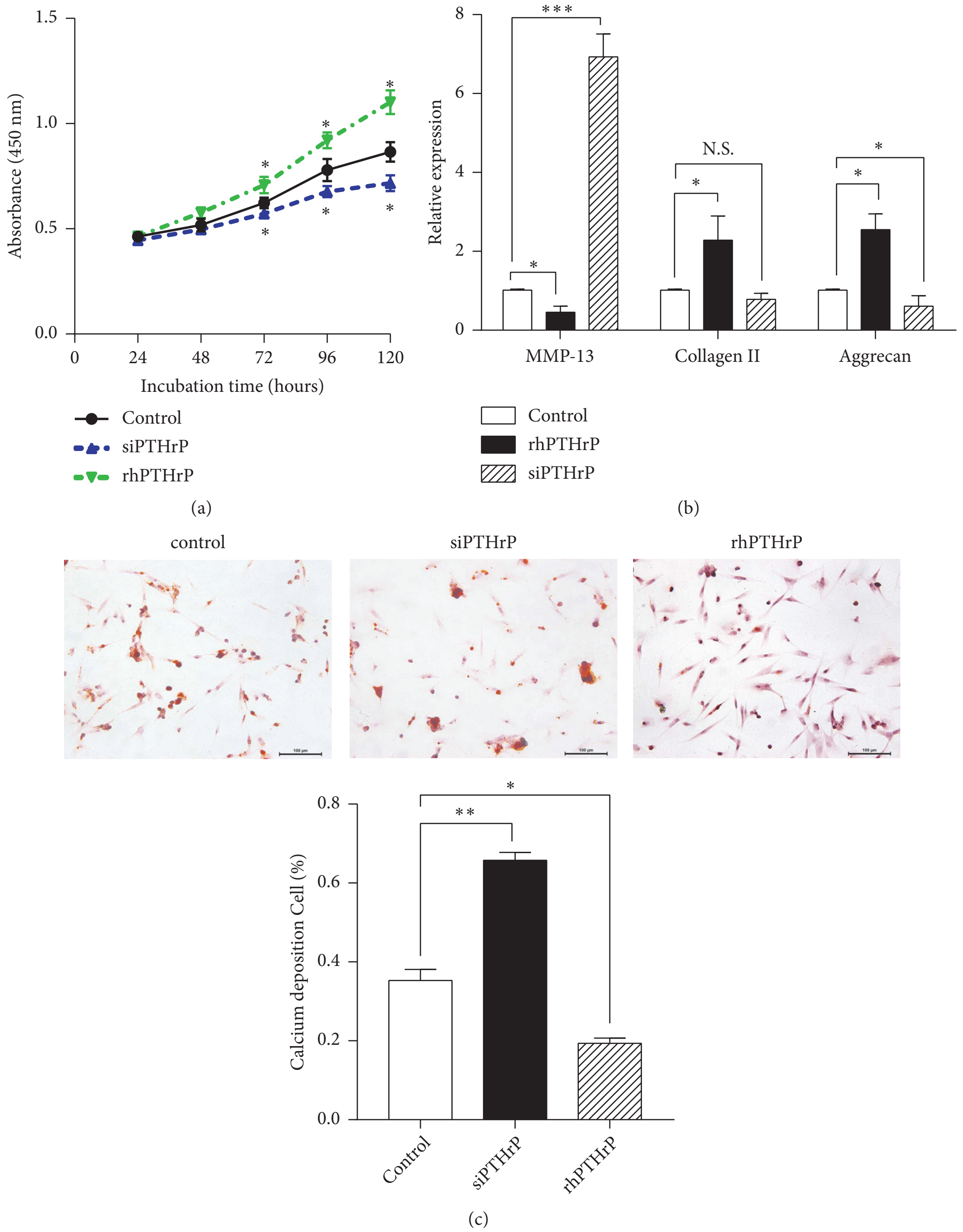

(a)

(b)

(c)

Figure 2: *Effect of PTHrP on chondrocyte proliferation and differentiation.* OA chondrocytes were transfected with siPTHrP or a control plasmid or treated with rhPTHrP. (a) Cell viability was tested with a CCK8 kit after 24, 48, 72, 96, and 120 h. (b) qRT-PCR was performed to examine the MMP-13, collagen II, and aggrecan expression in the chondrocytes ($*p<0.05$, $***p<0.001$ in comparison to the control, n = 6). (c) Calcium deposition was visualised by Alizarin Red S staining (scale bars, 100 μm). Calcium deposition (+) cells are presented as mean ± SD in the lower panels ($*p<0.05$, $**p<0.01$, and n = 6).

investigated, including type II collagen, aggrecan, and MMP-13. Transfection with the miR-15a-5p mimics led to decreases in the expression of collagen II and aggrecan ($p<0.05$) (Figure 4(b)). At the same time, the level of MMP-13 was substantially higher after treatment with the miR-15a-5p mimics than in the control group ($p<0.01$).

Alizarin Red S (ARS) staining at 12 days was also used to identify calcium deposits in the chondrocytes. As

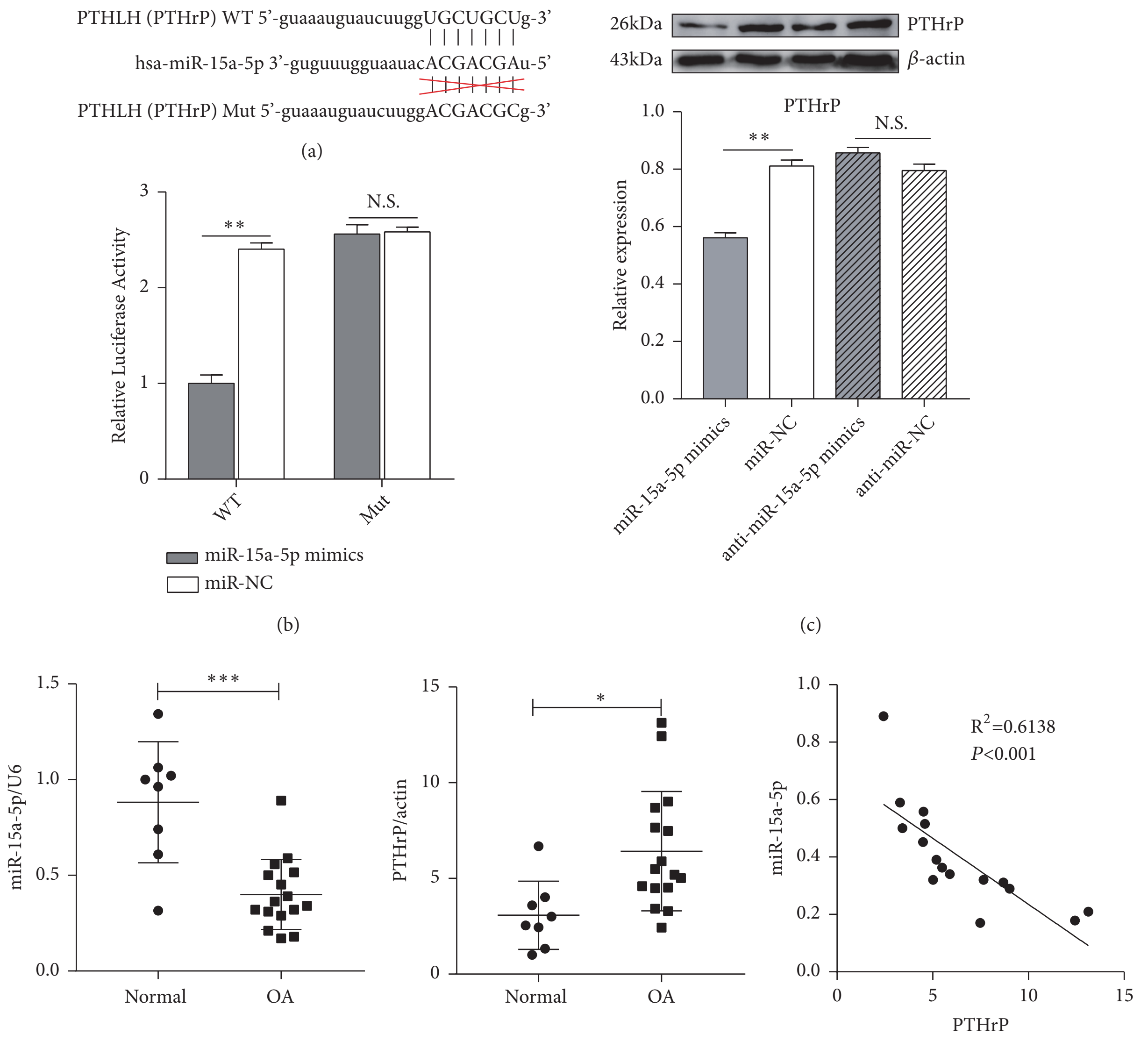

(d) (e) (f)

Figure 3: *PTHrP is a direct target of miR-15a-5p.* (a) Sequences of miR-15a-5p and potential miR-15a-5p-binding sites in the 3′UTR of PTHrP. (b) Luciferase activity assay for pGL3-PTHrP-wt or pGL3-PTHrP-mut versus the activity of Renilla luciferase in HEK293T cells after transient transfection with miR-NC or miR-15a-5p mimics ($**p<0.001$). (c) Level of PTHrP in OA chondrocytes treated with miR-15a-5p-mimics or anti-miR-15a-5p by western blot ($**p<0.001$). (d, e) RT-PCR analysis of the relative expression of miR-15a-5p or PTHrP ($*p<0.05$, $**p<0.001$, n(normal) = 8, and n(OA) = 16). (f) Correlation between miR-15a-5p and PTHrP in OA chondrocytes.

shown in Figure 4(c), both the extracellular and intracellular areas of Alizarin Red S staining were observed. The calcium deposition in the miR-15a-5p mimics group was higher than in the other groups, whilst that in the anti-miR-15a-5p group was lower (Figure 4(d)). The level of PTHrP in the chondrocytes increased significantly when endogenous miR-15a-5p was used as a knockdown and, at the same time, the expression of PTHrP decreased when endogenous miR-15a-5p was upregulated via transfection with specific miR-15a-5p mimics or inhibitors. Moreover, the role of miR-15a-5p in regulating the level of PTHrP in the chondrocytes was rescued by the addition of exogenous PTHrP (rhPTHrP) to the cell culture medium (Figure 4(e)).

4. Discussion

This study reveals a new mechanism of action of PTHrP in the development of OA. We found that PTHrP was upregulated in OA chondrocytes, which is in agreement with several studies in which the expression of PTHrP in OA cartilage was shown to be higher than in normal human articular cartilage [26, 28]. Several reports also suggested that PTHrP is a vital tumour prognostic factor [29, 30], and a recent study found that PTHrP protected chondrocytes from degeneration [31]. Our function verification analysis also revealed that upregulated PTHrP promoted the proliferation of chondrocytes, whilst the forced downregulation of PTHrP can reduce this effect, which confirms the protective role

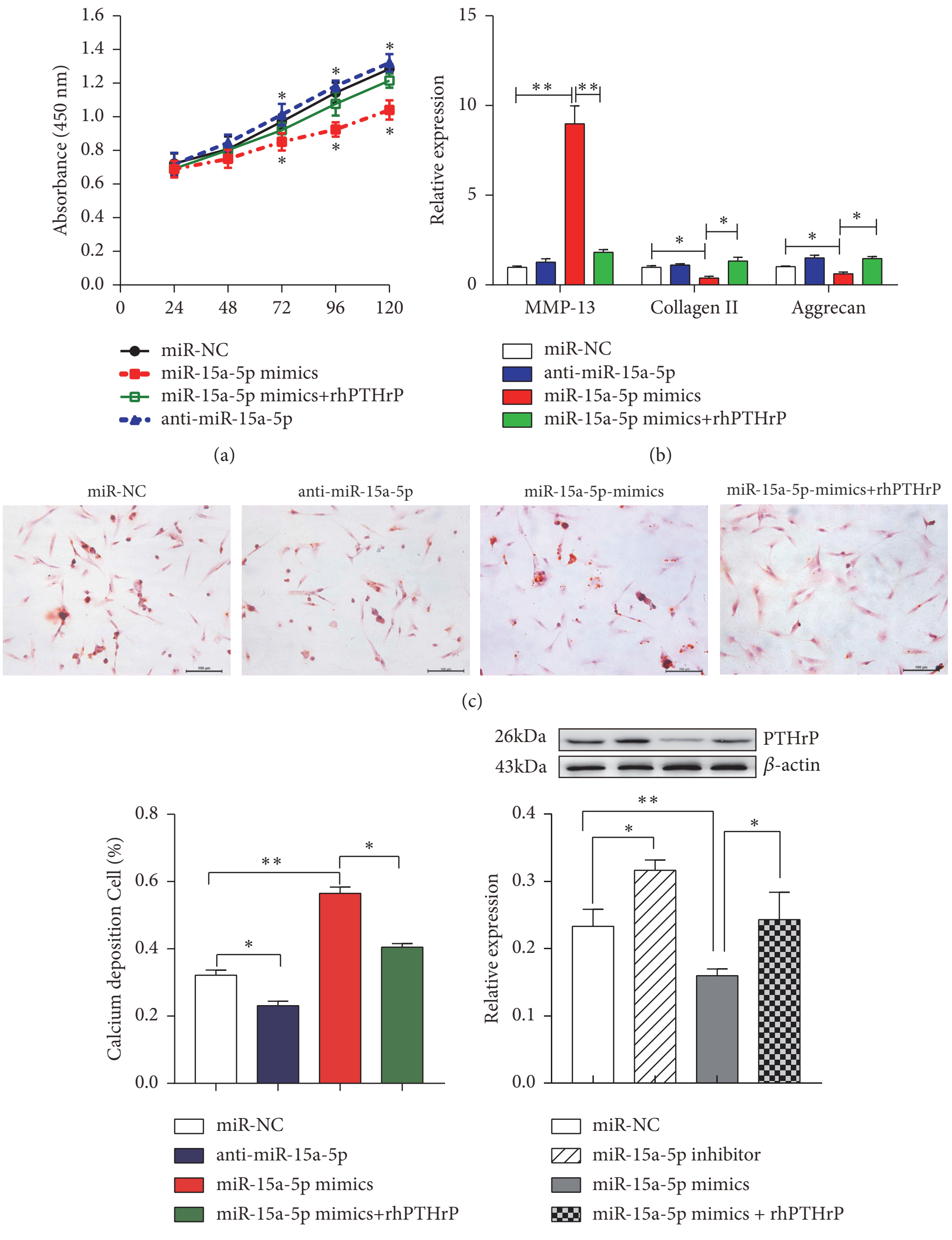

(a) (b)

(c)

(d) (e)

FIGURE 4: *miR-15a-5p regulates chondrocyte proliferation and differentiation by targeting PTHrP*. OA chondrocytes were treated with miR-15a-5p mimics, miR-15a-5p inhibitors, miR-15a-5p mimics + rhPTHrP, or negative controls. (a) Cell viability was tested with a CCK-8 kit after 24, 48, 72, 96, and 120 h ($*p<0.05$). (b) RT-PCR was used to analyse the relative expression of collagen II, aggrecan, and MMP-13 in the chondrocytes ($*p<0.05$, $**p<0.01$). (c) Calcium deposition was visualised by Alizarin Red S staining (scale bars, 100 μm). (d) Calcium deposition-positive cells from Alizarin Red S staining are presented as mean ± SD in the lower panels ($*p<0.05$, $**p<0.001$). (e) Western blotting analysis of PTHrP expression in transfected cells treated with miR-15a-5p mimics, miR-15a-5p inhibitors, miR-15a-5p mimics + rhPTHrP, or negative controls ($**p<0.001$, $*p<0.05$, and n = 6).

of PTHrP in suppressing the terminal differentiation of chondrocytes.

Although miRNAs play an important role in the regulation and maintenance of normal physiological conditions, in pathological situations, their levels may change due to dysfunction [14, 32–34]. Consequently, findings regarding the function of miRNAs in OA have varied depending on their expression and the genes targeted [17, 35]. PTHrP has been reported to be a direct target of miR-126-5p in giant cell tumours and of miR-33a in lung cancer [36, 37]. We found that PTHrP was also a potential target of miR-15a-5p in OA. MiR-15a-5p is a member of the miR-15 family, and the expression of miR-15a-5p has been found to be associated with tumour progression, especially in terms of cell proliferation and differentiation [18, 19]. We observed that the expression of miR-15a-5p was downregulated in human OA chondrocytes and was negatively related to the expression of PTHrP. Furthermore, in OA chondrocytes, we found that miR-15a-5p regulated the expression and function of PTHrP.

The levels of collagen II, aggrecan, and MMP-13 in chondrocytes have been found to be dysregulated in degenerative joint diseases including OA, and these abnormal expression patterns can therefore be regarded as biomarkers of chondrocyte function [27, 38]. MMP-13 is reportedly overexpressed in OA, whilst the expression of collagen II and aggrecan is reduced [39]. Aggrecan and collagen II are critical components of cartilage structure and are important for joint function. Consequently, the synthesis and degradation of aggregated proteoglycan and collagen II can reveal their roles in cartilage degradation during joint injury, disease, and aging [40, 41]. In this study, we discovered that the overexpression of miR-15a-5p significantly increased the MMP-13 levels and reduced the levels of type II collagen and aggrecan. This is contrary to the effect of PTHrP. Wang et al. found that PTHrP inhibited the expression of MMP-13 in antler chondrocytes [42], whilst other studies observed that the application of PTHrP significantly increased the expression of type II collagen and aggrecan [31].

Calcium deposition is a marker of chondrocyte terminal differentiation and pathological calcification in osteoarthritic joints [43, 44]. The two most common pathologically relevant calcium crystals deposited in particular tissues are calcium pyrophosphate dihydrate and basic calcium phosphate [45]. Calcium deposition was reported to be closely related to chondrocyte differentiation. In our study, we found that PTHrP reduces calcium deposition. In addition, we found that miR-15a-5p promotes calcium deposition by targeting PTHrP. Our study also showed that miR-15a-5p overexpression may facilitate OA. However, these findings were only observed *in vitro* and will be validated in an animal model in subsequent experiments.

5. Conclusions

We demonstrated that miR-15a-5p is downregulated in OA chondrocytes in relation to the upregulated expression of PTHrP. MiR-15a-5p promotes the degeneration of chondrocytes by targeting PTHrP. Our findings provide new evidence that may be useful for future research on targeting miR-15a-5p in the treatment of OA.

Data Availability

The data used to support the findings of this study are available from the corresponding author upon request.

Conflicts of Interest

All authors declare no conflicts of interest.

Acknowledgments

This work was supported by the Central South University Innovation Foundation for Postgraduate Studies (No. 2017zzts231), the National Natural Science Foundation of China (No. 81372180), the Key Research and Development Program of Hunan Province Science & Technology Department (Nos. 2017DK2013, 2018JJ3716), and Hunan Science and Technology Project (No. 2016JC2056).

References

[1] J. Racine and R. K. Aaron, "Pathogenesis and epidemiology of osteoarthritis," *Rhode Island Medical Journal*, vol. 96, no. 3, pp. 19–22, 2013.

[2] A. Litwic, M. H. Edwards, E. M. Dennison, and C. Cooper, "Epidemiology and burden of osteoarthritis," *British Medical Bulletin*, vol. 105, no. 1, pp. 185–199, 2013.

[3] S. Glyn-Jones, A. J. Palmer, R. Agricola et al., "Osteoarthritis," *The Lancet*, vol. 386, no. 9991, pp. 376–387, 2015.

[4] Y.-S. Li, W.-F. Xiao, and W. Luo, "Cellular aging towards osteoarthritis," *Mechanisms of Ageing and Development*, vol. 162, pp. 80–84, 2017.

[5] R. F. Loeser, S. R. Goldring, C. R. Scanzello, and M. B. Goldring, "Osteoarthritis: a disease of the joint as an organ," *Arthritis & Rheumatism*, vol. 64, no. 6, pp. 1697–1707, 2012.

[6] M. B. Goldring, "Chondrogenesis, chondrocyte differentiation, and articular cartilage metabolism in health and osteoarthritis," *Therapeutic Advances in Musculoskeletal Disease*, vol. 4, no. 4, pp. 269–285, 2012.

[7] X. Yuan, H. Liu, L. Li et al., "The roles of endoplasmic reticulum stress in the pathophysiological development of cartilage and chondrocytes," *Current Pharmaceutical Design*, vol. 23, no. 11, pp. 1693–1704, 2017.

[8] G. J. Strewler, "The physiology of parathyroid hormone-related protein," *The New England Journal of Medicine*, vol. 342, no. 3, pp. 177–185, 2000.

[9] T. John Martin, "Parathyroid hormone-related protein, its regulation of cartilage and bone development, and role in treating bone diseases," *Physiological Reviews*, vol. 96, no. 3, pp. 831–871, 2016.

[10] H. Zhang, H. Wang, C. Zeng et al., "mTORC1 activation downregulates FGFR3 and PTH/PTHrP receptor in articular chondrocytes to initiate osteoarthritis," *Osteoarthritis and Cartilage*, vol. 25, no. 6, pp. 952–963, 2017.

[11] W. Kafienah, S. Mistry, S. C. Dickinson, T. J. Sims, I. Learmonth, and A. P. Hollander, "Three-dimensional cartilage tissue engineering using adult stem cells from osteoarthritis patients," *Arthritis & Rheumatology*, vol. 56, no. 1, pp. 177–187, 2007.

[12] M. Petersson, E. Bucht, B. Granberg, and A. Stark, "Effects of arginine-vasopressin and parathyroid hormone-related protein (1-34) on cell proliferation and production of YKL-40 in cultured chondrocytes from patients with rheumatoid arthritis and osteoarthritis," *Osteoarthritis and Cartilage*, vol. 14, no. 7, pp. 652–659, 2006.

[13] Y.-J. Kim, H.-J. Kim, and G.-I. Im, “PTHrP promotes chondrogenesis and suppresses hypertrophy from both bone marrow-derived and adipose tissue-derived MSCs,” *Biochemical and Biophysical Research Communications*, vol. 373, pp. 104–108, 2008.

[14] D. P. Bartel, “MicroRNAs: target recognition and regulatory functions,” *Cell*, vol. 136, no. 2, pp. 215–233, 2009.

[15] P. Huang, L.-F. Mao, Z.-P. Zhang et al., “Down-regulated miR-125a-5p promotes the reprogramming of glucose metabolism and cell malignancy by increasing levels of CD147 in thyroid cancer,” *Thyroid*, vol. 28, no. 5, pp. 613–623, 2018.

[16] N. Lv, S. Hao, C. Luo et al., “miR-137 inhibits melanoma cell proliferation through downregulation of GLO1,” *Science China Life Sciences*, vol. 61, no. 5, pp. 541–549, 2018.

[17] M. Zhang, K. Lygrissea, and J. Wanga, “Role of MicroRNA in osteoarthritis,” *Journal of Arthritis*, vol. 6, 2017.

[18] D. Chen, D. Wu, K. Shao, B. Ye, J. Huang, and Y. Gao, “MiR-15a-5p negatively regulates cell survival and metastasis by targeting CXCL10 in chronic myeloid leukemia,” *American Journal of Translational Research*, vol. 9, no. 9, pp. 4308–4316, 2017.

[19] C. K. Kontos, P. Tsiakanikas, M. Avgeris, I. N. Papadopoulos, and A. Scorilas, “miR-15a-5p, a novel prognostic biomarker, predicting recurrent colorectal adenocarcinoma,” *Molecular Diagnosis and Therapy*, vol. 21, no. 4, pp. 453–464, 2017.

[20] X. Lu, J. Lin, J. Jin, W. Qian, and X. Weng, “Hsa-miR-15a exerts protective effects against osteoarthritis by targeting aggrecanase-2 (ADAMTS5) in human chondrocytes,” *International Journal of Molecular Medicine*, vol. 37, no. 2, pp. 509–516, 2016.

[21] H. S. Hwang, S. J. Park, M. H. Lee, and H. A. Kim, “MicroRNA-365 regulates IL-1beta-induced catabolic factor expression by targeting HIF-2alpha in primary chondrocytes,” *Scientific Reports*, vol. 7, article 17889, 2017.

[22] M. Schnabel, S. Marlovits, G. Eckhoff et al., “Dedifferentiation-associated changes in morphology and gene expression in primary human articular chondrocytes in cell culture,” *Osteoarthritis and Cartilage*, vol. 10, no. 1, pp. 62–70, 2002.

[23] X. Zhou, L. He, S. Zuo et al., “Serine prevented high-fat diet-induced oxidative stress by activating AMPK and epigenetically modulating the expression of glutathione synthesis-related genes,” *Biochimica et Biophysica Acta (BBA) - Molecular Basis of Disease*, vol. 1864, no. 2, pp. 488–498, 2018.

[24] P. Huang, S. Chang, X. Jiang et al., “RNA interference targeting CD147 inhibits the proliferation, invasiveness, and metastatic activity of thyroid carcinoma cells by down-regulating glycolysis,” *International Journal of Clinical and Experimental Pathology*, vol. 8, pp. 309–318, 2015.

[25] P. Huang, B. Kaluba, X.-L. Jiang et al., “Liver X receptor inverse agonist SR9243 suppresses nonalcoholic steatohepatitis intrahepatic inflammation and fibrosis,” *BioMed Research International*, vol. 2018, Article ID 8071093, 7 pages, 2018.

[26] R. Terkeltaub, M. Lotz, K. Johnson et al., “Parathyroid hormone-related protein is abundant in osteoarthritic cartilage, and the parathyroid hormone-related protein 1-173 isoform is selectively induced by transforming growth factor β in articular chondrocytes and suppresses generation of extracellular inorganic pyrophosphate,” *Arthritis & Rheumatology*, vol. 41, no. 12, pp. 2152–2164, 1998.

[27] E. Nummenmaa, M. Hämäläinen, T. Moilanen, K. Vuolteenaho, and E. Moilanen, “Effects of FGF-2 and FGF receptor antagonists on MMP enzymes, aggrecan, and type II collagen in primary human OA chondrocytes,” *Scandinavian Journal of Rheumatology*, vol. 44, no. 4, pp. 321–330, 2015.

[28] K. Okano, T. Tsukazaki, A. Ohtsuru et al., “Expression of parathyroid hormone-related peptide in human osteoarthritis,” *Journal of Orthopaedic Research*, vol. 15, no. 2, pp. 175–180, 1997.

[29] S. Sen, P. Dasgupta, G. Kamath, and H. S. Srikanth, “Parатharmone related protein (peptide): a novel prognostic, diagnostic and therapeutic marker in Head and Neck cancer,” *Journal of Stomatology, Oral and Maxillofacial Surgery*, vol. 119, pp. 33–36, 2018.

[30] K. Kamp, R. A. Feelders, R. C. S. Van Adrichem et al., “Parathyroid hormone-related peptide (PTHrP) secretion by gastroenteropancreatic neuroendocrine tumors (GEP-NETs): clinical features, diagnosis, management, and follow-up,” *The Journal of Clinical Endocrinology & Metabolism*, vol. 99, no. 9, pp. 3060–3069, 2014.

[31] J. Fischer, A. Aulmann, V. Dexheimer, T. Grossner, and W. Richter, “Intermittent PTHrP(1–34) exposure augments chondrogenesis and reduces hypertrophy of mesenchymal stromal cells,” *Stem Cells and Development*, vol. 23, no. 20, pp. 2513–2523, 2014.

[32] T. Chang, J. Xie, H. Li, D. Li, P. Liu, and Y. Hu, “MicroRNA-30a promotes extracellular matrix degradation in articular cartilage via downregulation of Sox9,” *Cell Proliferation*, vol. 49, no. 2, pp. 207–218, 2016.

[33] X. Du, J. Zhang, J. Wang, X. Lin, and F. Ding, “Role of miRNA in lung cancer-potential biomarkers and therapies,” *Current Pharmaceutical Design*, vol. 23, no. 39, pp. 5997–6010, 2017.

[34] X. Gong, R. Chao, P. Wang et al., “Interplay of transcription factors and microRNAs during embryonic hematopoiesis,” *Science China Life Sciences*, vol. 60, no. 2, pp. 168–177, 2017.

[35] C. Yu, W.-P. Chen, and X.-H. Wang, “MicroRNA in osteoarthritis,” *Journal of International Medical Research*, vol. 39, no. 1, pp. 1–9, 2011.

[36] W. Zhou, H. Yin, T. Wang et al., “MiR-126-5p regulates osteolysis formation and stromal cell proliferation in giant cell tumor through inhibition of PTHrP,” *Bone*, vol. 66, pp. 267–276, 2014.

[37] P. L. Kuo, S. Liao, J. Hung, M. Huang, and Y. Hsu, “MicroRNA-33a functions as a bone metastasis suppressor in lung cancer by targeting parathyroid hormone related protein,” *Biochimica et Biophysica Acta (BBA) - General Subjects*, vol. 1830, no. 6, pp. 3756–3766, 2013.

[38] S. Settle, L. Vickery, O. Nemirovskiy et al., “Cartilage degradation biomarkers predict efficacy of a novel, highly selective matrix metalloproteinase 13 inhibitor in a dog model of osteoarthritis: confirmation by multivariate analysis that modulation of type II collagen and aggrecan degradation peptides parallels pathologic changes,” *Arthritis and Rheumatology*, vol. 62, no. 10, pp. 3006–3015, 2010.

[39] C. J. Brew, P. D. Clegg, R. P. Boot-Handford, J. G. Andrew, and T. Hardingham, “Gene expression in human chondrocytes in late osteoarthritis is changed in both fibrillated and intact cartilage without evidence of generalised chondrocyte hypertrophy,” *Annals of the Rheumatic Diseases*, vol. 69, no. 1, pp. 234–240, 2010.

[40] C. Kiani, L. Chen, Y. J. Wu, A. J. Yee, and B. B. Yang, “Structure and function of aggrecan,” *Cell Research*, vol. 12, no. 1, pp. 19–32, 2002.

[41] S. S. Sivan, E. Wachtel, and P. Roughley, “Structure, function, aging and turnover of aggrecan in the intervertebral disc,” *Biochimica et Biophysica Acta (BBA) - General Subjects*, vol. 1840, no. 10, pp. 3181–3189, 2014.

[42] S.-T. Wang, Y.-J. Gao, C.-C. Duan et al., “Effects of PTHrP on expression of MMP9 and MMP13 in sika deer antler chondrocytes,” *Cell Biology International*, vol. 37, no. 12, pp. 1300–1307, 2013.

[43] R. Dreier, “Hypertrophic differentiation of chondrocytes in osteoarthritis: the developmental aspect of degenerative joint disorders,” *Arthritis Research and Therapy*, vol. 12, article 216, 2010.

[44] C. Thouverey, G. Bechkoff, S. Pikula, and R. Buchet, “Inorganic pyrophosphate as a regulator of hydroxyapatite or calcium pyrophosphate dihydrate mineral deposition by matrix vesicles,” *Osteoarthritis and Cartilage*, vol. 17, no. 1, pp. 64–72, 2009.

[45] A. K. Rosenthal, “Calcium crystal deposition and osteoarthritis,” *Rheumatic Disease Clinics of North America*, vol. 32, no. 2, pp. 401–412, 2006.

Hindawi
BioMed Research International
Volume 2019, Article ID 1613820, 8 pages
https://doi.org/10.1155/2019/1613820

Research Article

Leukemia Inhibitory Factor Receptor Is Involved in Apoptosis in Rat Astrocytes Exposed to Oxygen-Glucose Deprivation

Liang Huo , Yuying Fan , and Hua Wang

Department of Pediatrics, Shengjing Hospital of China Medical University, Shenyang, China

Correspondence should be addressed to Hua Wang; wangh1@sj-hospital.org

Received 12 January 2019; Accepted 12 February 2019; Published 27 February 2019

Guest Editor: Hengjia Ni

Copyright © 2019 Liang Huo et al. This is an open access article distributed under the Creative Commons Attribution License, which permits unrestricted use, distribution, and reproduction in any medium, provided the original work is properly cited.

Leukemia inhibitory factor (LIF) and leukemia inhibitory factor receptor (Lifr) protect CNS cells, specifically neurons and myelin-sheath oligodendrocytes, in conditions of oxygen-glucose deprivation (OGD). In the case of astrocyte apoptosis resulting from reperfusion injury following hypoxia, the function of the Lifr remains to be fully elucidated. This study established models of *in vivo* ischemia/reperfusion (I/R) using an *in vitro* model of OGD to investigate the direct impact of silencing the Lifr on astrocyte apoptosis. Astrocytes harvested from newborn Wistar rats were exposed to OGD. Cell viability and apoptosis levels were determined by the MTT (3-(4,5-dimethylthiazol-2-yl)-2,5-diphenyltetrazolium bromide) assay and annexin V/propidium iodide (PI) staining assays, respectively. Apoptosis was further investigated by the TdT-mediated dUTP nick-end labelling (TUNEL) assay. A standard western blotting protocol was applied to determine levels of the protein markers Bcl2, Bax, p-Akt/Akt, p-Stat3/Stat3, and p-Erk/Erk. The cell viability assay (MTT) showed that astrocyte viability decreased in response to OGD. Furthermore, blocking RNA to silence the Lifr further reduces astrocyte viability and increases levels of apoptosis as detected by annexin V/PI double staining. Likewise, western blotting after Lifr silencing demonstrated increased levels of the apoptosis-related proteins Bax and p-Erk/Erk and correspondingly lower levels of Bcl2, p-Akt/Akt, and p-Stat/Stat3. The data gathered in these analyses indicate that the Lifr plays a pivotal role in the astrocyte apoptosis induced by hypoxic/low-glucose environments. Further investigation of the relationship between apoptosis and the Lifr may provide a potential therapeutic target for the treatment of neurological injuries.

1. Introduction

Hypoxic-ischemic encephalopathy (HIE) is known to be a major cause of child mortality and disability, but the processes that lead to neuronal apoptosis in HIE are as yet undefined. Previous research has focused on blood flow and vasculature and the effects on neurons [1, 2]; however, interest has grown in the pathophysiology of astrocytes and their role in HIE-related conditions [3]. Astrocytes are the glial cell type present in the greatest numbers within the brain; they repair and maintain brain tissues and provide trophic, structural, and metabolic support to neurons and facilitate formation of neuronal synapses [4–6]. Given the pivotal role of astrocytes in CNS metabolism and glutamate balance, their death or disruption results in damage to the CNS and neuronal cell death [7, 8]. It is recognised that astrocytes are involved in many events resulting from cerebral ischemia and hypoxia-ischemia (HI) [9, 10]. Specifically, early astrocyte death due to hypoxia and ischemia leads to an interruption in key mechanisms, generating greater neuronal apoptosis, which causes larger lesions and disrupts synaptogenesis [11, 12]. In light of their critical role, it is clear that astrocytes offer a robust therapeutic target to minimise damage resulting from cerebral HI.

Leukemia inhibitory factor (LIF) belongs to an interleukin 6 (IL-6) class and is recognised as a neuroprotector with anti-inflammatory properties [13, 14]. Furthermore, acting on macrophages and T-helper cells, LIF induces an anti-inflammatory phenotype [15]. Production of LIF is stimulated by the proinflammatory cytokines IL-6 and tumor necrosis factor-α. The beneficial functions of LIF are demonstrable both histologically and functionally, depending on the maturity and the cell type upon which it acts. Activation of the LIF receptor (Lifr), a 190-kD type 1 cytokine receptor located in the nuclei of neuronal cells until injury occurs, initiates upon binding of LIF [16–18]. Protein-receptor binding forms a high-affinity complex that starts the LIF signal through several cellular pathways, including Janus kinase- (JAK-) signal transducer and activator of transcription (STAT), mitogen-activated protein kinase (MAPK), and extracellular signal-regulated kinase (ERK), preserving stroke-damaged brain cells [19]. Additionally, LIF/Lifr binding drives phenotypic alterations in T cells and macrophages to switch to an anti-inflammatory response from the immediate inflammatory response to brain injury, which leads to neurodegeneration [20, 21]. The signal-transducing role of the Lifr is widely recognised, but its molecular and cellular functions remain to be elucidated.

This research aimed to define the role of Lifr in OGD and the mechanism by which it affects hypoxic-ischemic astrocytes. To accomplish this goal, the impact of RNA disruption of Lifr on apoptosis levels in primary rat astrocyte cultures was assessed. To gain deeper insight into the function of the Lifr in astrocytes deprived of oxygen and glucose, expression levels of a range of apoptosis-related proteins were determined. The proteins assessed included Lifr, B-cell lymphoma 2 (Bcl2), Bax, p-Akt/Akt, p-Stat3/Stat3, and p-Erk/Erk.

2. Materials and Methods

2.1. Primary Culture of Astrocytes. The Local Animal Ethics Committee of China Medical University approved the protocols and procedures for care and use of animals in this research. Primary astrocyte cultures were derived from newborn Wistar rats. Briefly, the cerebral cortices were harvested following hypothermic anaesthetisation and decapitation. After excision of the meninges, the cortical tissue was cut into small pieces and added to culture medium. The tissue suspension was mixed by vortexing and then filtred through nylon mesh filtres, firstly of pore size 80 μm and then 10 μm. The resulting filtrate was further diluted in Dulbecco's minimal essential medium (DMEM) with 7.5 mM glucose and 20% horse serum. The cultures were placed in a humidified incubator at 37°C / 5% CO_2. Cultures were maintained by exchanging medium with 10% serum on day 3 and thereafter every 3-4 days. Rotary shaking of the culture flasks at 260 rpm facilitated the removal of other cell types. Primary astrocytes were passaged a maximum of three times in culture and used in assays when 80 – 90% confluent. The astrocyte cultures showed a near-uniform immunoreactivity (greater than 95%) to glial fibrillary acidic protein.

2.2. Hypoxia and Glucose Deprivation Experiments. Briefly, following a wash with glucose-free culture medium, primary astrocyte cultures were supplied with fresh glucose-free medium in the absence of serum. For the hypoxic conditions, the cells were placed in a humidified Tri-gas incubator (Thermo Scientific, Waltham, MA) for 24 hours, with conditions of 94% N_2/5% CO_2/1% O_2. Following the 24-hour incubation, the cells were returned to standard incubator conditions (see Section 2.1) for an additional 24 hours. Control cells, used in all assays, were maintained in normal incubator conditions and fed with glucose-containing DMEM.

2.3. RNA Interference. Transient transfection of small interfering RNAs (SiRNAs; Jima Medicine, Shanghai, China) was conducted using lipofectamine reagent (Invitrogen, Grand Island, NY) on 70% confluent primary astrocytes in six-well plates in accordance with the manufacturer's instructions. The sequences of the SiRNAs used to interrupt expression of Lifr were as follows: sense 5′ GGUGAUCACGAAGUAACAATT-3′ and antisense 5′ UUGUUACUUCGUGAUCACCTT-3′. Western blotting was used to demonstrate effective downregulation of Lifr expression.

2.4. Cell Viability and Apoptosis Assays. MTT assays were conducted using a kit purchased from Sigma (USA) to determine cell viability. To determine levels of apoptosis, cells were double-stained with annexin V/PI in accordance with manufacturer's protocols, and cells stained positively were enumerated by flow cytometry (FACSCalibur™, Becton Dickinson, San Jose, CA). Data were analysed by CellQuest™ software (BD Biosciences). To summarise, the apoptosis protocol was conducted on astrocytes harvested in ice-cold PBS and pelleted by centrifugation. Thereafter, cells were rinsed in staining buffer and exposed to 100 μl of buffer containing 5 μl of annexin V-FITC and 5 μg/ml of PI, for 30 minutes at 4°C in darkness. Following incubation, the cells were washed and resuspended in 250 μl of staining buffer prior to flow cytometry analysis using both forward- and side-scatter light. CellQuest software was used to assess the output from 10,000 events. Apoptotic cells are those that exhibit positive annexin V-FITC staining in combination with negative PI staining.

2.5. TdT-Mediated dUTP Nick-End Labelling (TUNEL) Assay. The cells were stained with the *In Situ* Cell Death Detection Kit (Cat. No. 11684817910, Roche), in accordance with the manufacturer's recommended protocol. Cell nuclei were stained with 4′,6-diamidino-2-phenylindole (DAPI, Roche), and the cells were visualised by fluorescent microscopy (Olympus iX70). Levels of apoptosis were calculated as a percentage of positive cells per 1000 DAPI-stained nuclei.

2.6. Western Blotting. Astrocyte cultures were prepared for western blotting as described by others [22], with 30 μg of protein (unless otherwise noted) being separated by 10% SDS-PAGE. The gel-separated proteins were then electroblotted to transfer to a polyvinylidene difluoride membrane. The transferred proteins were probed with the following primary antibodies: Anti-LIFR antibody (ab202847, Abcam, 1:1000), Beta Actin Mouse Monoclonal antibody (66009-1-ig, Proteintech, 1:5000), Phospho-AKT (Ser473) (D9E)XP Rabbit mAb (Cell Signaling Technology, 1:2000), AKT (pan) (C67E7) Rabbit mAb (Cell Signaling Technology, 1:1000), Phospho-Stat3 (Tyr705) (D3A7) XP Rabbit mAb (Cell Signaling Technology, 1:2000), Stat3 (D3Z2G) Rabbit mAb (Cell Signaling Technology, 1:1000), Anti-Bcl2 Rabbit mAb (ab196495, Abcam, 1:1000), Anti-Bax Rabbit mAb (ab32509, Abcam, 1:2000), Phospho-p44/42 MAPK (Erk1/2) (Thr202/Tyr204) (D13.14.4E) XP® Rabbit mAb (Cell Signaling Technology, 1:2000), and p44/42 MAPK (Erk1/2) (137F5) Rabbit mAb (Cell Signaling Technology, 1:1000). The membrane was washed and then incubated with the secondary antibodies HRP-conjugated Affinipure Goat Anti-Rabbit IgG(H+L) (SA00001-2, Proteintech, 1:2000) and HRP-conjugated Affinipure Mouse Anti-Rabbit IgG(H+L) (SA00001-1, Proteintech, 1:2000). After another wash, the detection substrate Immobilon™ Western Chemiluminescent HRP Substrate (Millipore) was applied.

2.7. Statistical Analysis. Statistical analysis (t-test) was conducted using GraphPad Prism V.7.0, from mean data (± SEM) derived from three independent tests. Statistical significance was determined as $P < 0.05$.

3. Results

The efficacy of the Lifr knockdown was measured by western blotting of the LIFR expressed protein. The levels of LIFR were significantly lower ($P < 0.05$) in both the ORNA-silenced groups (N+SiRNA) and oxygen-glucose deprivation (OGD) plus SiRNA (OGD+SiRNA) groups than in either control (normal control, N) or ODG treatment group (Figure 1). Furthermore, the levels of LIFR protein in the OGD treatment group were significantly higher than in the normal control (N) group ($P < 0.05$) (Figure 1).

Astrocyte cell viability was determined by the MTT assay (Figure 2). OGD-treated cells had significantly lower ($P < 0.01$) levels of cell viability, showing a 23% reduction in comparison with the N controls. Silencing of the Lifr in otherwise normal cells led to a slight reduction in cell viability. However, silencing of the Lifr in OGD-treated cells revealed a significant ($P < 0.05$) decrease in viability compared with OGD-treated cells. These data indicate that under OGD conditions, silencing of the Lifr significantly decreased cell viability and stimulated cell damage.

Next, we determined the effect of Lifr silencing on apoptosis levels of OGD-treated astrocytes, using the annexin V/PI double-staining method (Figure 3). The results show a significant increase ($P < 0.01$) in apoptosis levels in both OGD-treated and SiRNA+OGD-treated groups in comparison with N and N+SiRNA, respectively. Furthermore, apoptosis increased significantly ($P < 0.05$) in both the silenced (N+SiRNA) group in comparison with the N group and the OGD+SiRNA group in comparison with the OGD group.

Levels of apoptosis were further elucidated by testing each group with the TUNEL assay (Figure 4). N and N+SiRNA astrocytes demonstrated low numbers of apoptotic cells, whereas both OGD and OGD-SiRNA astrocytes exhibited large numbers of apoptotic cells. Silencing of both the N cells (N+SiRNA) and OGD-treated cells (OGD+SiRNA) led to a significant increase in apoptotic cells compared with N and OGD cells, respectively ($P < 0.05$ and $P < 0.001$, respectively). These data suggest that suppression of Lifr further stimulates OGD-induced apoptosis in primary astrocytes.

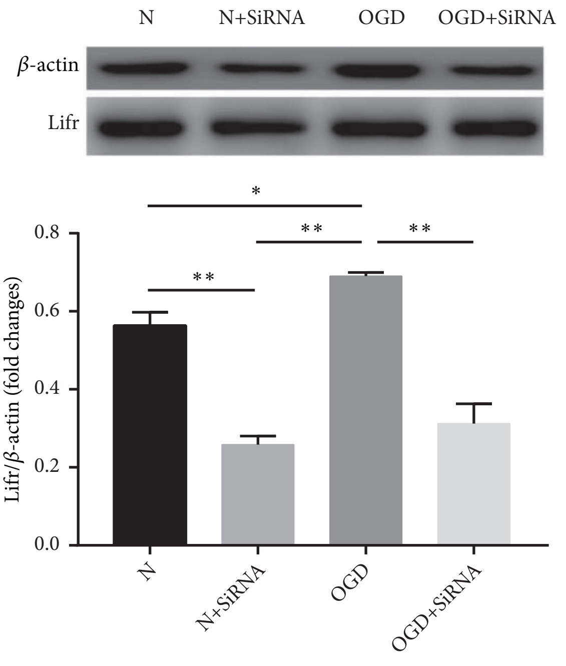

Figure 1: LIFR levels in response to SiRNA treatment in comparison with untreated control and OGD-treated cells. Error bars represent mean ± SEM ($*P < 0.05$; $**\ P < 0.01$).

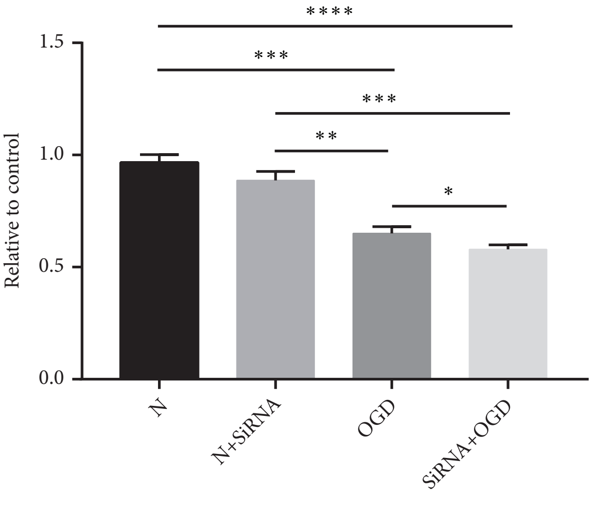

Figure 2: Comparison of cell viability in normal, normal-silenced, OGD-treated, and OGD-treated and silenced astrocytes as determined by MTT assay. Error bars represent mean ± SEM ($*P < 0.05$; $**\ P < 0.01$; $*\ *\ *\ P < 0.001$).

Levels of proteins in astrocytes that are associated with apoptosis (i.e., B-cell lymphoma 2 (Bcl2), BAX, p-Akt/Akt, p-Stat3/Stat3, and p-Erk/Erk) were assessed by western blotting (Figure 5). OGD treatment led to a significant reduction ($P < 0.01$) in levels of Bcl2 in comparison with the N group, whereas silencing of OGD-treated cells further rescued these

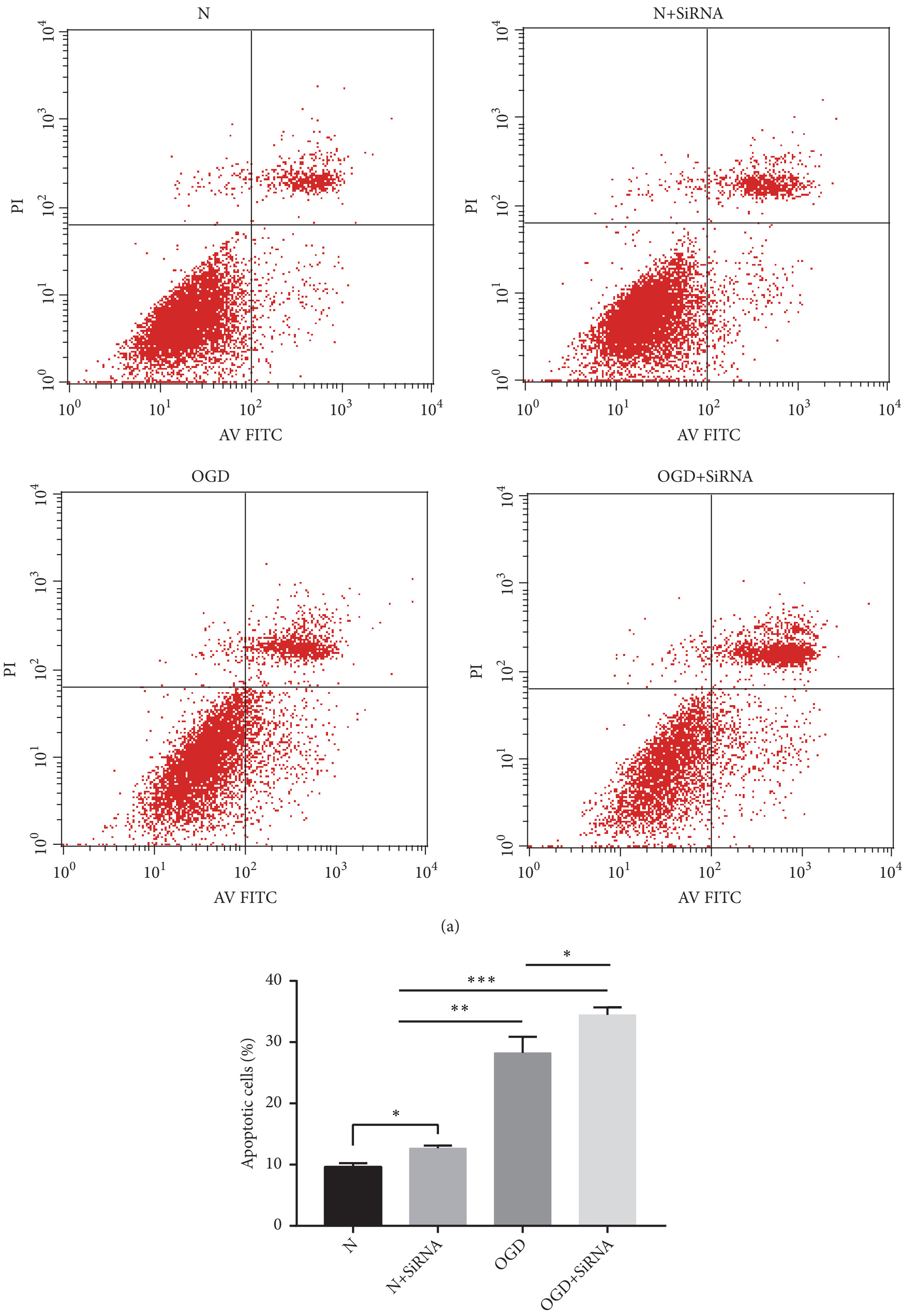

(a)

(b)

Figure 3: Comparison of apoptosis levels in normal, normal-silenced, OGD-treated, and OGD-treated and silenced astrocytes using annexin V/PI double staining ($* P < 0.05$; $** P < 0.01$; $*** P < 0.001$).

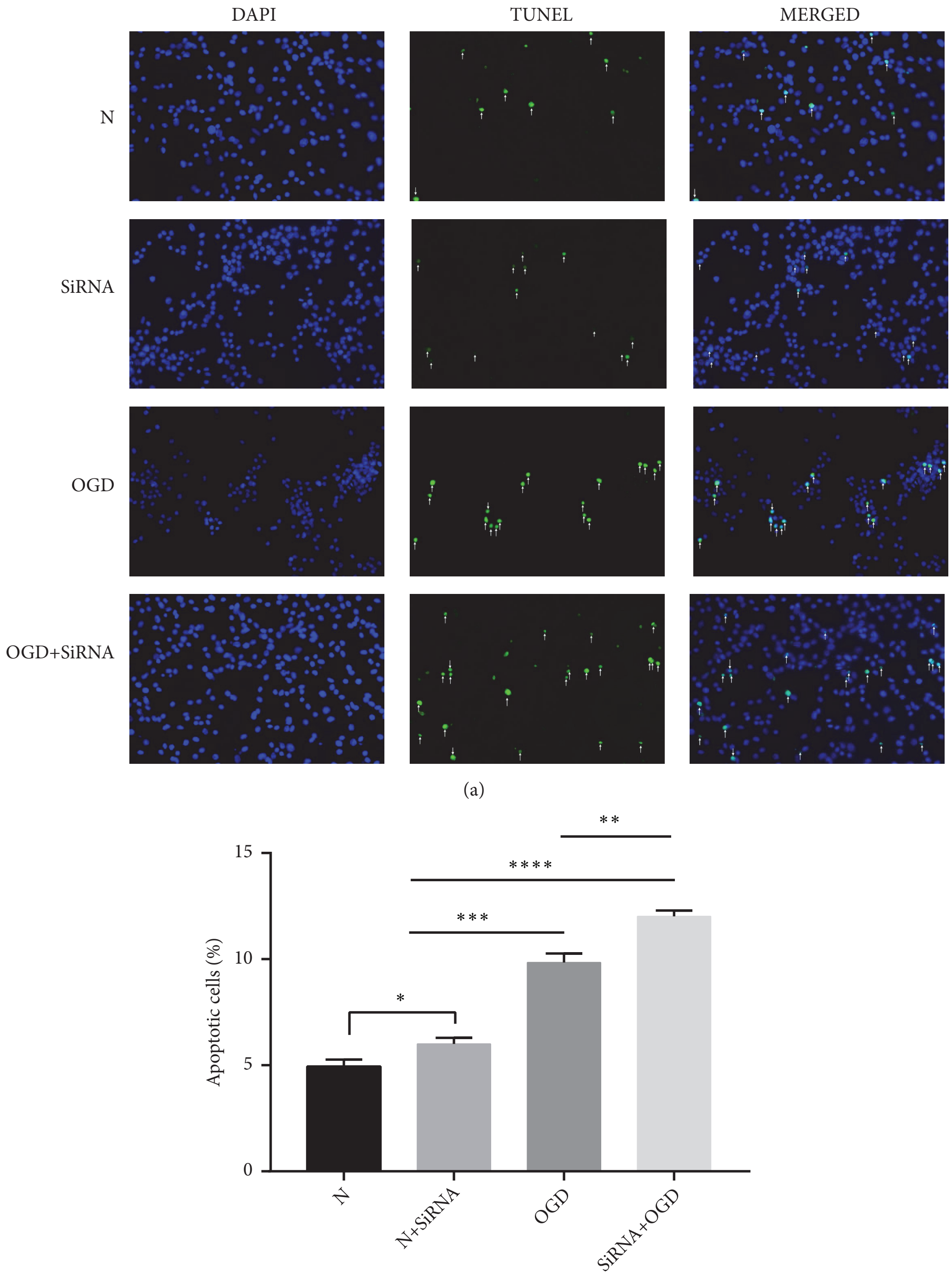

(a)

(b)

Figure 4: Apoptosis rates in normal, normal-silenced, OGD-treated, and OGD-treated and silenced astrocytes using the TUNEL assay (×200 magnification). Error bars represent mean ± SEM ($* P < 0.05$; $** P < 0.01$; $* * * P < 0.001$).

levels ($P < 0.01$) in comparison with OGD treatment ($P < 0.01$). Correspondingly, levels of BAX were significantly higher in the OGD group than the N group ($P < 0.01$) and in the OGD-SiRNA group than in the OGD group ($P < 0.05$).

The ratios of the proteins p-Akt/Akt and p-Stat3/Stat3 were significantly lower in the OGD group compared with the N group ($P < 0.05$) and in the OGD-SiRNA group compared with the OGD group ($P < 0.05$). Conversely, ratios of p-Erk/Erk increased significantly in both OGD ($P < 0.05$) and OGD+SiRNA ($P < 0.01$), compared with the N and OGD groups, respectively. In combination, these data indicate a critical role for these pathways in OGD-induced apoptosis, and silencing Lifr may regulate these proteins in a manner that further promotes apoptosis in OGD-treated cells.

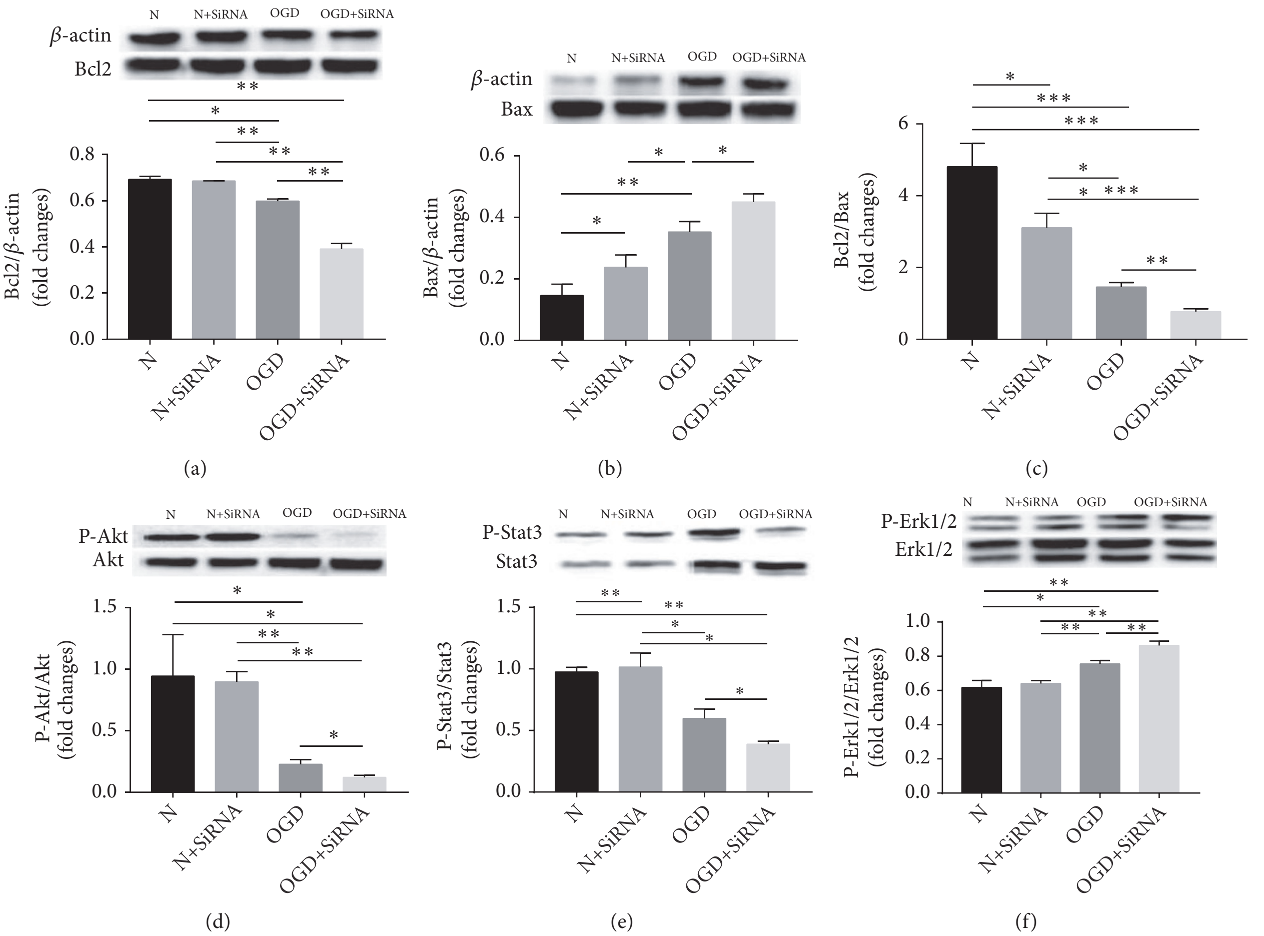

Figure 5: Signaling pathway in OGD-induced apoptosis of astrocytes was detected by western blotting ($* P < 0.05$; $** P < 0.01$).

4. Discussion

The link between brain injury resulting from ischemia and astrocyte damage is widely recognised [23, 24], and it is proposed here that protecting astrocytes in this environment from further apoptotic damage and death may be pivotal in partially protecting brain tissue from ischemic injury and thus improving postischemic functionality. OGD was used *in vitro* to induce apoptosis in astrocytes through two mechanisms: endoplasmic reticulum stress and mitochondrial disruption [25, 26]. Our data show that cell viability, assessed by MMT, is reduced in OGD-treated astrocytes compared with normal (untreated) controls. Furthermore, silencing of the LIF receptor (Lifr) further decreases cell viability and increases apoptosis, as measured using the annexin V/PI method, in comparison with OGD-treated cells. Investigation of apoptosis pathways through western blotting analysis revealed significantly increased levels of BAX and p-ERK/ERK ratios, and a corresponding significant decrease in Bcl2 levels and in p-Akt/Akt and p-Stat3/Stat3 ratios in OGD+SiRNA-treated cells when compared with OGD-treated cells. These data indicate that Lifr control of apoptosis-signaling pathways is important in OGD-stimulated astrocyte apoptosis.

The ratios of Bcl-2 to Bax are intrinsically linked to the balance of apoptosis [27], as Bcl-2 is known as an anti-apoptotic protein, the action of which is to prevent cellular apoptosis, whereas Bax is an apoptosis-stimulating protein [27, 28]. A stable ratio of Bcl-2 to Bax has been demonstrated to inhibit H_2O_2-induced apoptosis of cultured astrocytes. In apoptotic conditions, the action of Bax after translocation to the mitochondria enables the extracellular release of proapoptotic proteins and operates through permeabilisation of the cell membrane [28].

The protective effects of an increased Bcl-2/Bax ratio, through upregulation of Bcl-2 and corresponding downregulation of Bax, was successfully demonstrated in a coculture of IL-6-producing mesenchymal stem cells and oxygen-glucose deprived astrocytes, wherein the mesenchymal cells successfully inhibited apoptosis [29]. In our study, after OGD treatment, expression of Bcl-2 was decreased in comparison with controls and Bax was correspondingly increased, indicating an increased level of apoptosis. In OGD-treated astrocytes that were also exposed to silencing of Lifr, the ratio of Bcl-2 to Bax further decreased, indicating that, following OGD, suppression of Lifr expression further reduces the Bcl-2/Bax ratio and stimulates apoptosis.

Resulting from cell damage caused by several factors, apoptosis is a widely known cell death mechanism that is initiated by the upregulation of apoptotic protein production [27, 30–32]. Researchers have found that increased levels of Bax expression may lead to apoptosis via activation of procaspase-3 [32, 33], whereas others define the pivotal actions of Bcl-2, p-Akt, and p-ERK1/2 on balancing cell survival and death [34, 35]. Suppression of Akt activity within the CNS is linked to post-HI injury-induced neuronal death, demonstrating the importance of the phosphoinositide 3-kinase (PI3K)/Akt pathway as an antiapoptotic mechanism to protect neurons [36]. The activity of Akt is increased by phosphorylation of serine-473 (Ser473) [37, 38]. We found in this study that p-Akt levels significantly decreased in response to I/R damage, with no effect on levels of unphosphorylated Akt. This response was further enhanced by silencing Lifr, whereby lower levels of p-Akt, corresponding to lower activity of Akt, were found. These data indicate that there is a role for Lifr in apoptosis regulation that may be managed via PI3K/Akt signaling.

Contributing to existing evidence of a neuroprotective role for Lifr, our data elucidate the impact of Lifr silencing on OGD-induced apoptosis. Furthermore, these data enhance our current knowledge of the biological function of Lifr and initiate a pathway for continued research from a clinical perspective to the applicability of Lifr in treating stroke and neurological damage. However, our work investigating the role of Lifr in neurological damage requires further investigation and expansion.

Data Availability

All the data are available from the correspondence author upon request.

Conflicts of Interest

The authors declare that there are no conflicts of interest regarding the publication of this article.

Authors' Contributions

Liang Huo and Yuying Fan contributed equally to this manuscript.

Acknowledgments

This work was supported by National Natural Science Foundation of China (81501299).

References

[1] F. Zhao, Y. Qu, H. Wang et al., "The effect of miR-30d on apoptosis and autophagy in cultured astrocytes under oxygen-glucose deprivation," *Brain Research*, vol. 1671, pp. 67–76, 2017.

[2] B. J. Dixon, C. Reis, W. M. Ho, J. Tang, and J. H. Zhang, "Neuroprotective strategies after neonatal hypoxic ischemic encephalopathy," *International Journal of Molecular Sciences*, vol. 16, no. 9, pp. 22368–22401, 2015.

[3] D. Kasprowska, G. Machnik, A. Kost, and B. Gabryel, "Time-dependent changes in apoptosis upon autophagy inhibition in astrocytes exposed to oxygen and glucose deprivation," *Cellular and Molecular Neurobiology*, vol. 37, no. 2, pp. 223–234, 2017.

[4] C. Farina, F. Aloisi, and E. Meinl, "Astrocytes are active players in cerebral innate immunity," *Trends in Immunology*, vol. 28, no. 3, pp. 138–145, 2007.

[5] C. Lambert, P. Cisternas, and N. C. Inestrosa, "Role of Wnt signaling in central nervous system injury," *Molecular Neurobiology*, vol. 53, no. 4, pp. 2297–2311, 2016.

[6] S. A. Liddelow, K. A. Guttenplan, L. E. Clarke et al., "Neurotoxic reactive astrocytes are induced by activated microglia," *Nature*, vol. 541, no. 7638, pp. 481–487, 2017.

[7] T. Chitnis and H. L. Weiner, "CNS inflammation and neurodegeneration," *The Journal of Clinical Investigation*, vol. 127, no. 10, pp. 3577–3587, 2017.

[8] A. Almad and N. J. Maragakis, "A stocked toolbox for understanding the role of astrocytes in disease," *Nature Reviews Neurology*, vol. 14, no. 6, pp. 351–362, 2018.

[9] Z. W. Liu and M. Chopp, "Astrocytes, therapeutic targets for neuroprotection and neurorestoration in ischemic stroke," *Progress in Neurobiology*, vol. 144, pp. 103–120, 2016.

[10] Y. Jin, S. Chen, N. Li et al., "Defect-related luminescent bur-like hydroxyapatite microspheres induced apoptosis of MC3T3-E1 cells by lysosomal and mitochondrial pathways," *SCIENCE CHINA Life Sciences*, vol. 61, no. 4, pp. 464–475, 2018.

[11] E. Ramos, P. Patiño, R. J. Reiter et al., "Ischemic brain injury: new insights on the protective role of melatonin," *Free Radical Biology & Medicine*, vol. 104, pp. 32–53, 2017.

[12] E. Rocha-Ferreira and M. Hristova, "Plasticity in the neonatal brain following hypoxic-ischaemic injury," *Neural Plasticity*, vol. 2016, Article ID 4901014, 16 pages, 2016.

[13] S. M. Davis, L. A. Collier, C. C. Leonardo, H. A. Seifert, C. T. Ajmo Jr., and K. R. Pennypacker, "Leukemia inhibitory factor protects neurons from ischemic damage via upregulation of superoxide dismutase 3," *Molecular Neurobiology*, vol. 54, no. 1, pp. 608–622, 2017.

[14] D. D. Rowe, C. C. Leonardo, A. A. Hall et al., "Cord blood administration induces oligodendrocyte survival through alterations in gene expression," *Brain Research*, vol. 1366, pp. 172–188, 2010.

[15] K. Janssens, C. Van den Haute, V. Baekelandt et al., "Leukemia inhibitory factor tips the immune balance towards regulatory T cells in multiple sclerosis," *Brain, Behavior, and Immunity*, vol. 45, pp. 180–188, 2015.

[16] N. J. Gardiner, W. B. J. Cafferty, S. E. Slack, and S. W. N. Thompson, "Expression of gp130 and leukaemia inhibitory factor receptor subunits in adult rat sensory neurones: regulation by nerve injury," *Journal of Neurochemistry*, vol. 83, no. 1, pp. 100–109, 2002.

[17] S. M. Davis, L. A. Collier, S. Goodwin, D. E. Lukins, D. K. Powell, and K. R. Pennypacker, "Efficacy of leukemia inhibitory factor as a therapeutic for permanent large vessel stroke differs among aged male and female rats," *Brain Research*, vol. 1707, pp. 62–73, 2019.

[18] J.-W. Zhao, S. C. Dyson, C. Kriegel et al., "Modelling of a targeted nanotherapeutic 'stroma' to deliver the cytokine LIF,

or XAV939, a potent inhibitor of Wnt-β-catenin signalling, for use in human fetal dopaminergic grafts in Parkinson's disease," *Disease Models & Mechanisms*, vol. 7, no. 10, pp. 1193–1203, 2014.

[19] D. D. Rowe, C. C. Leonardo, J. A. Recio, L. A. Collier, A. E. Willing, and K. R. Pennypacker, "Human umbilical cord blood cells protect oligodendrocytes from brain ischemia through Akt signal transduction," *The Journal of Biological Chemistry*, vol. 287, no. 6, pp. 4177–4187, 2012.

[20] A. H. Miller and C. L. Raison, "The role of inflammation in depression: from evolutionary imperative to modern treatment target," *Nature Reviews Immunology*, vol. 16, no. 1, pp. 22–34, 2016.

[21] M. V. Russo and D. B. McGavern, "Immune surveillance of the CNS following infection and injury," *Trends in Immunology*, vol. 36, no. 10, pp. 637–650, 2015.

[22] B. Gabryel, A. Kost, D. Kasprowska et al., "AMP-activated protein kinase is involved in induction of protective autophagy in astrocytes exposed to oxygen-glucose deprivation," *Cell Biology International*, vol. 38, no. 10, pp. 1086–1097, 2014.

[23] N. Sun, J.-R. Hao, X.-Y. Li et al., "GluR6-FasL-Trx2 mediates denitrosylation and activation of procaspase-3 in cerebral ischemia/reperfusion in rats," *Cell Death & Disease*, vol. 4, article e771, 2013.

[24] K. Zhu, Q. He, L. Li, Y. Zhao, and J. Zhao, "Silencing thioredoxin1 exacerbates damage of astrocytes exposed to OGD/R by aggravating apoptosis through the Actin–Ras2–cAMP–PKA pathway," *International Journal of Neuroscience*, vol. 128, no. 6, pp. 512–519, 2018.

[25] G. Faraco, S. Fossati, M. E. Bianchi et al., "High mobility group box 1 protein is released by neural cells upon different stresses and worsens ischemic neurodegeneration in vitro and in vivo," *Journal of Neurochemistry*, vol. 103, no. 2, pp. 590–603, 2007.

[26] Y. Y. Fan, J. M. Zhang, H. Wang, X. Y. Liu, and F. H. Yang, "Leukemia inhibitory factor inhibits the proliferation of primary rat astrocytes induced by oxygen-glucose deprivation," *Acta Neurobiologiae Experimentalis*, vol. 73, no. 4, pp. 485–494, 2013.

[27] L. Grosse, C. A. Wurm, C. Brüser, D. Neumann, D. C. Jans, and S. Jakobs, "Bax assembles into large ring-like structures remodeling the mitochondrial outer membrane in apoptosis," *EMBO Journal*, vol. 35, no. 4, pp. 402–413, 2016.

[28] Y. Liu, X. Zeng, Y. Hui et al., "Activation of α7 nicotinic acetylcholine receptors protects astrocytes against oxidative stress-induced apoptosis: implications for Parkinson's disease," *Neuropharmacology*, vol. 91, pp. 87–96, 2015.

[29] L. Yaidikar and S. Thakur, " Punicalagin attenuated cerebral ischemia–reperfusion insult via inhibition of proinflammatory cytokines, up-regulation of Bcl-2, down-regulation of Bax, and caspase-3," *Molecular and Cellular Biochemistry*, vol. 402, no. 1-2, pp. 141–148, 2015.

[30] Q. Jiang, J. Chen, S. Liu, G. Liu, K. Yao, and Y. Yin, "l-Glutamine attenuates apoptosis induced by endoplasmic reticulum stress by activating the IRE1α-XBP1 axis in IPEC-J2: a novel mechanism of l-glutamine in promoting intestinal health," *International Journal of Molecular Sciences*, vol. 18, no. 12, 2017.

[31] X. Ying, A. Huang, Y. Xing, L. Lan, Z. Yi, and P. He, "Lycorine inhibits breast cancer growth and metastasis via inducing apoptosis and blocking Src/FAK-involved pathway," *Science China Life Sciences*, vol. 60, no. 4, pp. 417–428, 2017.

[32] D. Wan, Q. Wu, W. Qu, G. Liu, and X. Wang, "Pyrrolidine dithiocarbamate (PDTC) inhibits DON-induced mitochondrial dysfunction and apoptosis via the NF-kappaB/iNOS pathway," *Oxidative Medicine and Cellular Longevity*, vol. 2018, Article ID 1324173, 8 pages, 2018.

[33] J. W. Shin, S. B. Kwon, Y. Bak, S. K. Lee, and D. Y. Yoon, "BCI induces apoptosis via generation of reactive oxygen species and activation of intrinsic mitochondrial pathway in H1299 lung cancer cells," *Science China Life Sciences*, vol. 61, no. 10, pp. 1243–1253, 2018.

[34] E. Abdelwahid, A. Stulpinas, and A. Kalvelyte, "Effective agents targeting the mitochondria and apoptosis to protect the heart," *Current Pharmaceutical Design*, vol. 23, no. 8, pp. 1153–1166, 2017.

[35] V. Vijayan, K. Shalini, V. Yugesvaran, T. H. Yee, S. Balakrishnan, and V. R. Palanimuthu, "Effect of paclitaxel-loaded PLGA nanoparticles on MDA-MB type cell lines: apoptosis and cytotoxicity studies," *Current Pharmaceutical Design*, vol. 24, no. 28, pp. 3366–3375, 2018.

[36] D. Heras-Sandoval, J. M. Pérez-Rojas, J. Hernández-Damián, and J. Pedraza-Chaverri, "The role of PI3K/AKT/mTOR pathway in the modulation of autophagy and the clearance of protein aggregates in neurodegeneration," *Cellular Signalling*, vol. 26, no. 12, pp. 2694–2701, 2014.

[37] D. D. Sarbassov, D. A. Guertin, S. M. Ali, and D. M. Sabatini, "Phosphorylation and regulation of Akt/PKB by the rictor-mTOR complex," *Science*, vol. 307, no. 5712, pp. 1098–1101, 2005.

[38] N. Chu, A. L. Salguero, A. Z. Liu et al., "Akt kinase activation mechanisms revealed using protein semisynthesis," *Cell*, vol. 174, no. 4, pp. 897.e14–907.e14, 2018.

Hindawi
BioMed Research International
Volume 2019, Article ID 5721585, 6 pages
https://doi.org/10.1155/2019/5721585

Review Article

Benzoic Acid Used as Food and Feed Additives Can Regulate Gut Functions

Xiangbing Mao,[1,2] **Qing Yang**,[3] **Daiwen Chen**,[1,2] **Bing Yu**,[1,2] **and Jun He**[1,2]

[1] *Animal Nutrition Institute, Sichuan Agricultural University, No. 211, Gongpinghuimin Road, Wenjiang District, Chengdu 611130, China*
[2] *Key Laboratory of Animal Disease-Resistance Nutrition, Chinese Ministry of Education, Chengdu 611130, China*
[3] *Department of Animal Science, Oklahoma State University, Stillwater, OK 74078, USA*

Correspondence should be addressed to Xiangbing Mao; acatmxb2003@163.com

Received 22 December 2018; Revised 27 January 2019; Accepted 6 February 2019; Published 26 February 2019

Academic Editor: Gang Liu

Copyright © 2019 Xiangbing Mao et al. This is an open access article distributed under the Creative Commons Attribution License, which permits unrestricted use, distribution, and reproduction in any medium, provided the original work is properly cited.

As a kind of antibacterial and antifungal preservative, benzoic acid is widely used in foods and feeds. Recently, many studies showed that it could improve the growth and health, which should, at least partially, be derived from the promotion of gut functions, including digestion, absorption, and barrier. Based on the similarity of gut physiology between human and pigs, many relative studies in which piglets and porcine intestinal epithelial cells were used as the models have been done. And the results showed that using appropriate benzoic acid levels might improve gut functions via regulating enzyme activity, redox status, immunity, and microbiota, but excess administration would lead to the damage of gut health through redox status. However, the further mechanisms that some intestinal physiological functions might be regulated are not well understood. The present review will, in detail, summarize the effect of benzoic acid on gut functions.

1. Introduction

The gut is a highly proliferative and secretary organ, which plays important functions in the growth and health of the whole body [1]. On the one hand, the intestine is a main organ of nutrient digestion and absorption. On the other hand, it also has the barrier function. This will protect the whole body against pathogens and toxins as the first defense. The gut barrier function is composed of nonspecific barrier mechanisms (including mucosal-epithelial regenerating capacity, intercellular junctions between the epithelial cells, and the mucus gel layer), specific immunological responses, and microbiota [2–8]. Therefore, the gut is important for health of humans and animals, which is associated with nutrient supply and defense from harmful factors.

Because of hypoplasia digestive tract in young children and animals, the production of gastric acid is not enough for the digestion of nutrients (especially protein). This will be not beneficial of growth. And the utilization of acidifiers, including inorganic acidifier, organic acidifier, and complex acidifier, can decrease the pH value in foods and feeds [9]. This can not only increase the nutrient digestibility but also inhibit the harmful microorganisms (such as *E. coli*) in diets and digestive tract [10]. Therefore, the acidifiers have already been considered as a kind of gut health products in humans and animals.

As a kind of organic acidifier, benzoic acid ($C_7H_6O_2$, BA) is the colorless crystalline solid, which is the simplest aromatic carboxylic acid [11]. It is mainly absorbed and transported in small intestines via the monocarboxylic acid transporter 1 [12]. And the absorption rate for the jejunum is higher than those for the duodenum and ileum, which is consistent with the distribution of monocarboxylic acid transporter 1 [12]. After orally administered [^{14}C]BA in man and 20 other species of animal, Bridges et al. (1970) found that, in human, BA would be entirely metabolized to hippuric acid and then be excreted through urine [13].

BA can inhibit pathogenic microorganisms, which makes it a preservative in food and feed industry [14, 15]. It may also increase growth and health and inhibit the diarrhea induced by *E. coli* challenge [16–26]. This can be due to the fact that BA improves the gut functions. Many studies (including the researches in our lab) about the physiological functions of BA mainly involve pigs and porcine cells. However, there is the resemblance between humans and pigs (including gut function and immunity) [27]. Pigs are usually considered as a research model for humans. In addition, intestinal porcine epithelial cell-1 (IPEC-1) is an appropriate model for being directly comparable to the trial animal that is used as an *in vivo* model for humans [28]. Therefore, BA has potential to be used as an additive of improving health in foods.

2. Benzoic Acid and Digestion and Absorption in Gut

Dietary BA supplementation can increase the digestibility of nutrients. In recent studies, dietary 0.5% BA supplementation increased the digestibility of total nitrogen, energy, and amino acids in weaned and growing pigs [17, 29–31], and we also found that 0.5% BA administration in diets could increase dry matter, crude protein, ether extract, energy, crush ash, and Ca and P digestibility in weaned piglets (about 1.39-22.38%) and growing pigs (about 2.66-10.38%) [22, 25]. In addition, in lactating sows, the digestibility of organic matter, protein, fat, and fibre is also enhanced by 5.05%, 3.44%, 7.04%, and 34.02% by dietary 2% BA supplementation, respectively [32]. Moreover, Papadomichelakis et al. (2011) showed that the digestibility of organic matter, dry matter, crude protein, energy, and cellulose was increased by dietary 0.5% and 2% BA administration in weaned rabbits [19].

Besides improvement of nutrient digestibility, supplementing BA in diets may decrease the ammonia nitrogen (N) of distal intestinal digesta and faeces. Halas et al. (2010) and Galassi et al. (2011) found that the ammonia-N levels of faeces were reduced 20.17-25.57% by dietary BA supplementation in weaned piglets and finishing pigs [33, 34]. Our recent study in which piglets were utilized as the trial subject also found that BA administration in diets could decrease the ammonia-N concentration (about 49.10-57.32%) in the cecal digesta [23].

These results illustrated that BA improves the utilization of nutrients. And it is possible that BA's function should be due to the effect of BA on production and activation of digestive enzymes, and absorption of nutrients in the intestine (Figure 1).

2.1. The Effect of BA on Digestive Enzymes. BA administration can promote the production and activation of digestive enzymes. On the one hand, BA increases the digestive enzyme production. Our recent study in which piglets were utilized as the model indicated that the trypsin, lipase, and amylopsin concentrations in the pancreas were increased 74.02%, 67.05%, and 90.44% by BA administration, respectively [35]. On the other hand, BA can activate the digestive enzymes via decreasing the pH value in the proximal gastrointestinal tract. The pH value is important to maintain or increase the activity of enzymes in the gut. In our studies in which pigs were utilized as the trial subject, compared with the control, BA (0.2-0.5%) administration in different-type diets could significantly decrease the pH value of digesta in stomachs (pH 4.14-4.38 vs pH 3.39-3.79) and jejunums (pH 6.15-6.45 vs pH 5.69-6.18) [20, 21, 25, 36]. And the trypsin, lipase, amylase, maltase, sucrose, and lactase activities of digesta were enhanced about 30.02-141.34% by BA treatment in jejunum of piglets, and this effect would be decreased with age [22, 25].

However, Dierick et al. (2004) reported that supplementing 1.0% benzoic acid in the barley-wheat type diet did not significantly affect the pH value in stomach and jejunum of pigs [37]. Therefore, it is possible that the effect of BA on pH value and enzymes' activities in the proximal gastrointestinal tract is associated with dietary type and BA doses.

2.2. The Effect of BA on Nutrient Absorption. As the above description, the increasing nutrient digestibility is associated with the improvement of digestive ability. Moreover, the enhancement of nutrient digestibility can also be relative to the absorption capacity. The capacity of absorption mainly depends on the absorbing regions of intestinal mucosa. Thus, the enhancement of surface area in mucosa is beneficial to the substances' transfer from lumen to vascular system [38]. The surface area is mainly associated with gut mucosal structure, such as villi and crypts [38]. Halas et al. (2010) reported that dietary BA supplementation could increase mucosal villus height of ileum in weaned piglets [31]. Our recent studies also showed that BA administration in different-type diets might enhance the villus height and/or decrease the mucosal crypt depth in duodenum, jejunum, and/or ileum of piglets [23, 35, 36]. These results indirectly demonstrate that BA treatment can improve the absorption capacity of the gut.

In addition, it is well known that pH value plays an important role in the mineral absorption. Some studies have shown that BA treatment significantly increases the digestibility of minerals [22, 25, 30], which could be due to the fact that BA administration decreases the pH value of digesta in the gastrointestinal tract.

Therefore, BA has the ability to promote nutrient digestion and absorption in gut, which will lead to the increasing nutrient digestibility in diets. However, some studies also showed that supplementing BA in diets did not promote the nutrient digestibility [16, 34, 39]. Based on the difference among these results, we analyzed and compared the trial design of these researches. And we found that BA improving nutrient digestibility could be influenced by some factors, such as age, dietary type and composition, and environment.

3. Benzoic Acid and Gut Barrier Functions

BA administration in diets can decrease the serum levels of diamine oxidase and D-lactic acid and alleviate the diarrhea induced by *E. coli* challenge [26, 36], which is possible that BA can increase the barrier functions of intestine. And many studies also further found that BA treatment could indeed improve gut barrier function, including nonspecific barrier mechanisms, specific immunological responses, and microbiota (Figure 2).

3.1. The Effect of BA on Nonspecific Barrier Mechanisms in Gut. The mucosal-epithelial integrity is a part of nonspecific

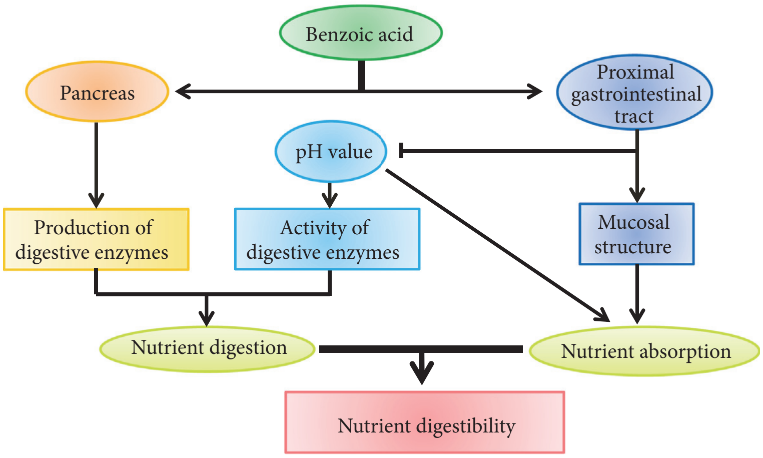
Benzoic acid
Pancreas
Proximal gastrointestinal tract
pH value
Production of digestive enzymes
Activity of digestive enzymes
Mucosal structure
Nutrient digestion
Nutrient absorption
Nutrient digestibility

FIGURE 1: The effect of benzoic acid on nutrient digestibility. Benzoic acid treatment can increase nutrient digestibility in humans and animals via improving nutrient digestion and absorption. This is associated with the improvement of mucosal structure, pH value of digesta, and production and activity of digestive enzymes in intestines.

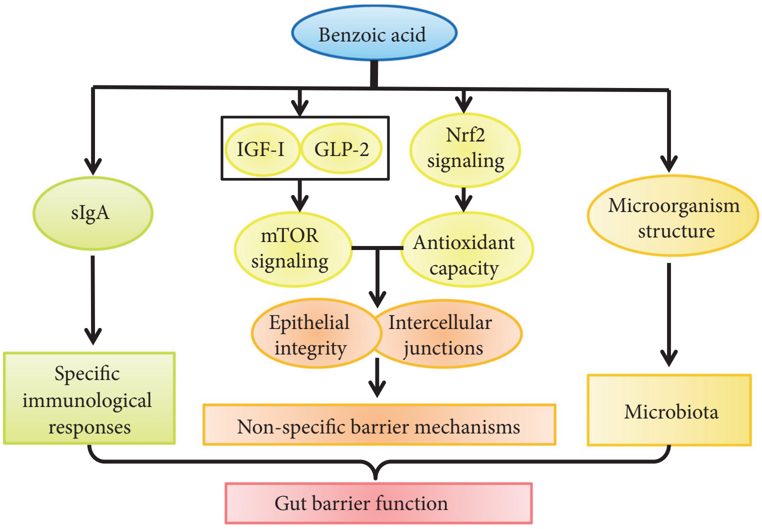
Benzoic acid
IGF-I
GLP-2
Nrf2 signaling
sIgA
mTOR signaling
Antioxidant capacity
Microorganism structure
Epithelial integrity
Intercellular junctions
Specific immunological responses
Non-specific barrier mechanisms
Microbiota
Gut barrier function

FIGURE 2: The effect of benzoic acid on gut barrier function. Benzoic acid administration can improve specific immunological responses, nonspecific barrier mechanisms, and microbiota. IGF-I, insulin-like growth factor I. GLP-2, glucagon like peptide 2. Nrf2, nuclear factor-E2-related factor 2. sIgA, secretory immunoglobulin A. mTOR, mammalian target of rapamycin.

barrier mechanisms, which is usually evaluated through morphology analysis [2]. As mentioned above, compared with control, dietary BA supplementation can increase the relative weight (intestinal weight: intestinal length) of small intestine (0.067 vs 0.077), and BA treatment also improves the morphology of the proximal gastrointestinal tract [31], which is similar to our results [23, 35, 36].

The gut can produce many hormones, which will ensure that the gut epithelium has the high ability of regeneration and restitution [40]. The further *in vivo* and *in vitro* experiments in our lab showed that BA treatment could stimulate the expressions of IGF-1 and GLP-2, which regulated some signaling pathways (i.e., mTOR), in small intestine of piglets and IPEC-1 cells [25, 35, 36]. And our *in vivo* and *in vitro* experiments also found that BA treatment improved the redox status in small intestine of piglets and IPEC-1 cells via Nrf2 signaling pathway [35]. These should be the possible reasons that BA improves gut-epithelial integrity.

The intercellular junctions between the epithelial cells also play a critical role for maintaining the gut barrier functions [2]. And the intercellular junctions between the gut epithelial cells are formed mainly via some transmembrane and nonmembrane proteins, including ZO-1 and occludin [41]. The study in which pigs were utilized as the model showed that dietary BA supplementation could stimulate the expressions of ZO-1 and occludin in the jejunal mucosa [36].

These results suggest that BA administration can improve nonspecific barrier mechanisms in the gut. However, it is unknown whether BA treatment can affect the mucus gel layer, as a part of nonspecific barrier mechanisms, in the intestinal mucosa, which needs further researches.

3.2. The Effect of BA on Specific Immunological Responses in Gut. There is little study about the effect of BA on gut specific immunological responses. Only a study in which piglets were utilized as the trial subject found that supplementing BA in diets tended to increase the sIgA concentration of duodenum but did not affect that of jejunum and ileum [35]. Except this finding, it is totally unknown whether BA is able to influence cellular immunity and innate immunity (such as host defense peptides) in intestines.

3.3. The Effect of BA on Microbiota in Gut. Recently, the critical role of gut microbiota in health, especially gut health, has been gradually recognized [5, 6, 42, 43]. It has been considered as a part of intestinal barrier functions. Torrallardona et al. (2007) and Halas et al. (2010) reported that supplementing BA in diets could increase the diversity of intestinal microbiota in piglets [18, 31]. And 0.5% BA administration can increase population of effective microorganisms (e.g., *Lactobacillus*, *Bifidobacterium*) and/or decrease population of harmful microorganisms (e.g., *E. coli*) in the intestine, especially distal intestine [16, 17, 31]. Our recent studies in which piglets were utilized as the model have similar results [21, 23, 24, 36]. However, dietary 0.85% and 1% BA supplementation also decreased the population of *Lactobacillus* while it reduced the population of *E. coli* in the intestinal digesta of pigs [16, 44], and supplementing 0.25-0.75% BA in diets did not affect the gastrointestinal microbiota in broilers [45]. These findings demonstrate that appropriate BA treatment may improve the gut microbiota, and the effect of BA on microbiota is associated with the species of trial subject.

4. Excess of Benzoic Acid Administration Impairs the Gut Health

Excessive intake of BA will induce acute or chronic toxicity symptoms, which seriously impairs the health and growth of humans and animals [46–49]. Our recent studies in which piglets were utilized as the model have also shown that excess of dietary BA supplementation leads to the dysfunction and damage of liver, spleen, and lung and may impair the mucosal morphology of duodenum, jejunum, and ileum [50, 51]. In an *in vitro* experiment, excess of BA treatment inhibited the proliferation of IPEC-1 cells, which could be related to the impairment of redox status regulated by Nrf2 pathway [35].

5. Conclusion and Future Perspectives

In summary, benzoic acid administration can improve gut functions, including digestion, absorption, and barrier, which is an important reason that benzoic acid can improve the growth and health in the studies that used the animals as models. This is due to the fact that it can regulate enzyme activity, redox status, immunity, and microbiota. Via analysis of results in these studies, we can further ensure that benzoic acid may be used as a kind of gut health products in humans and animals. And it has potential to be used as an additive of improving health in foods, especially to some patients in convalescence. The supplementing dose of BA should be 0.2-0.5% in feeds. However, as gut health products in humans, the using dose of benzoic acid in foods also needs to be further determined. In addition, for further comprehension and utilization, some further researches should be focused on the effect of benzoic acid on gut functions, especially the relative mechanisms.

Conflicts of Interest

There are no conflicts related to the manuscript.

Acknowledgments

This work was supported by the grant from the China Agriculture Research System (CARS-35), the fund from Science and Technology Support Project of Sichuan Province (2016NYZ0052), and the fund from the research program of "Sheng Yang" students' association (B2016010). Special thanks are due to Professor De Wu of Sichuan Agricultural University for revising this manuscript.

References

[1] J. R. Turner, "Intestinal mucosal barrier function in health and disease," *Nature Reviews Immunology*, vol. 9, no. 11, pp. 799–809, 2009.

[2] X. Mao, X. Zeng, S. Qiao, G. Wu, and D. Li, "Specific roles of threonine in intestinal mucosal integrity and barrier function," *Frontiers in Bioscience*, vol. E3, no. 4, pp. 1192–1200, 2011.

[3] F. He, C. Wu, P. Li et al., "Functions and signaling pathways of amino acids in intestinal inflammation," *BioMed Research International*, Article ID 9171905, 2018.

[4] S. Wang and Y.-G. Chen, "BMP signaling in homeostasis, transformation and inflammatory response of intestinal epithelium," *SCIENCE CHINA Life Sciences*, vol. 61, no. 7, pp. 800–807, 2018.

[5] D. Zhu, Y. Ma, S. Ding, H. Jiang, and J. Fang, "Effects of melatonin on intestinal microbiota and oxidative stress in colitis mice," *BioMed Research International*, Article ID 2607679, 2018.

[6] F. Chen, J. Jiang, D. Tian et al., "Targeting obesity for the prevention of chronic cardiovascular disease through gut microbiota-herb interactions: An opportunity for traditional herbs," *Current Pharmaceutical Design*, vol. 23, no. 8, pp. 1142–1152, 2017.

[7] R. Eri, R. Vemuri, and R. Gundamaraju, "Editorial: novel interventional targets for gastrointestinal and metabolic disorders," *Current Pharmaceutical Design*, vol. 23, no. 16, pp. 2287-2288, 2017.

[8] L. Weichselbaum and O. D. Klein, "The intestinal epithelial response to damage," *Science China Life Sciences*, vol. 61, no. 10, pp. 1205–1211, 2018.

[9] H. Diao, *Effects of Benzoic Acid and Thymol on Growth Performance and Gut Health in Piglets*, Sichuan Agricultural University, 2013.

[10] S. Qin, H. Zhang, X. Tang, and Y. Wang, "The physiology function of acidifier and how to select acid from different acids," *Chinese Journal of Animal Nutrition*, vol. 19, pp. 515–520, 2007.

[11] G. A. Sim, J. M. Robertson, and T. H. Goodwin, "The crystal and molecular structure of benzoic acid," *Acta Crystallographica*, vol. 8, no. 3, pp. 157–164, 1955.

[12] D. Cong, A. K. Y. Fong, R. Lee, and K. S. Pang, "Absorption of benzoic acid in segmental regions of the vascularly perfused rat small intestine preparation," *Drug Metabolism and Disposition*, vol. 29, no. 12, pp. 1539–1547, 2001.

[13] J. W. Bridges, M. R. French, R. L. Smith, and R. T. Williams, "The fate of benzoic acid in various species.," *Biochemical Journal*, vol. 118, no. 1, pp. 47–51, 1970.

[14] A. del Olmo, J. Calzada, and M. Nuñez, "Benzoic acid and its derivatives as naturally occurring compounds in foods and as additives: Uses, exposure, and controversy," *Critical Reviews in Food Science and Nutrition*, vol. 57, no. 14, pp. 3084–3103, 2015.

[15] A. Knarreborg, N. Miquel, T. Granli, and B. B. Jensen, "Establishment and application of an in vitro methodology to study the effects of organic acids on coliform and lactic acid bacteria in the proximal part of the gastrointestinal tract of piglets," *Animal Feed Science and Technology*, vol. 99, no. 1-4, pp. 131–140, 2002.

[16] H. Kluge, J. Broz, and K. Eder, "Effect of benzoic acid on growth performance, nutrient digestibility, nitrogen balance, gastrointestinal microflora and parameters of microbial metabolism in piglets," *Journal of Animal Physiology and Animal Nutrition*, vol. 90, no. 7-8, pp. 316–324, 2006.

[17] P. Guggenbuhl, A. Séon, A. P. Quintana, and C. S. Nunes, "Effects of dietary supplementation with benzoic acid (VevoVitall®) on the zootechnical performance, the gastrointestinal microflora and the ileal digestibility of the young pig," *Livestock Science*, vol. 108, no. 1-3, pp. 218–221, 2007.

[18] D. Torrallardona, I. Badiola, and J. Broz, "Effects of benzoic acid on performance and ecology of gastrointestinal microbiota in weanling piglets," *Livestock Science*, vol. 108, no. 1-3, pp. 210–213, 2007.

[19] G. Papadomichelakis, K. C. Mountzouris, E. Zoidis, and K. Fegeros, "Influence of dietary benzoic acid addition on nutrient digestibility and selected biochemical parameters in fattening rabbits," *Animal Feed Science and Technology*, vol. 163, no. 2-4, pp. 207–213, 2011.

[20] J. Chen, D. Chen, B. Yu et al., "Effects of benzoic acid on growth performance, organ indexes and gastrointestinal content pH of weaned piglets," *Chinese Journal of Animal Nutrition*, vol. 27, pp. 238–246, 2015.

[21] Z. Gao, B. Yu, P. Zheng et al., "Effects of Benzoic acid on intestinal microflora and metabolites of piglets," *Chinese Journal of Animal Nutrition*, vol. 26, pp. 1044–1054, 2014.

[22] H. Diao, P. Zheng, B. Yu et al., "Effects of benzoic acid on growth performance, serum biochemical parameters, nutrient digestibility and digestive enzyme activities of jejunal digesta in weaner piglets," *Chinese Journal of Animal Nutrition*, vol. 25, pp. 768–777, 2013.

[23] H. Diao, P. Zheng, B. Yu et al., "Effects of dietary supplementation with benzoic acid on intestinal morphological structure and microflora in weaned piglets," *Livestock Science*, vol. 167, no. 1, pp. 249–256, 2014.

[24] H. Diao, P. Zheng, B. Yu et al., "Effects of benzoic acid and thymol on growth performance and gut characteristics of weaned piglets," *Asian-Australasian Journal of Animal Sciences*, vol. 28, no. 6, pp. 827–839, 2015.

[25] H. Diao, Z. Gao, B. Yu et al., "Effects of benzoic acid (VevoVitall®) on the performance and jejunal digestive physiology in young pigs," *Journal of Animal Science and Biotechnology*, vol. 7, no. 1, 2016.

[26] D. Halas, C. F. Hansen, D. J. Hampson, B. P. Mullan, R. H. Wilson, and J. R. Pluske, "Effect of dietary supplementation with inulin and/or benzoic acid on the incidence and severity of post-weaning diarrhoea in weaner pigs after experimental challenge with enterotoxigenic Escherichia coli," *Archives of Animal Nutrition*, vol. 63, no. 4, pp. 267–280, 2009.

[27] X. Mao, C. Gu, M. Ren et al., "l-Isoleucine Administration Alleviates Rotavirus Infection and Immune Response in the Weaned Piglet Model," *Frontiers in Immunology*, vol. 9, 2018.

[28] K. Verhoeckx, P. Cotter, I. López-Expósito et al., *The Impact of Food Bioactives on Health*, Springer International Publishing, 2015.

[29] K. Bühler, B. Bucher, C. Wenk, and J. Broz, "Influence of benzoic acid in high fibre diets on nutrient digestibility and VFA production in growing/finishing pigs," *Archives of Animal Nutrition*, vol. 63, no. 2, pp. 127–136, 2009.

[30] W. Sauer, M. Cervantes, J. Yanez et al., "Effect of dietary inclusion of benzoic acid on mineral balance in growing pigs," *Livestock Science*, vol. 122, no. 2-3, pp. 162–168, 2009.

[31] D. Halas, C. F. Hansen, D. J. Hampson et al., "Dietary supplementation with benzoic acid improves apparent ileal digestibility of total nitrogen and increases villous height and caecal microbial diversity in weaner pigs," *Animal Feed Science and Technology*, vol. 160, pp. 137–147, 2011.

[32] H. Kluge, J. Broz, and K. Eder, "Effects of dietary benzoic acid on urinary pH and nutrient digestibility in lactating sows," *Livestock Science*, vol. 134, no. 1-3, pp. 119–121, 2010.

[33] D. Halas, C. F. Hansen, D. J. Hampson et al., "Effects of benzoic acid and inulin on ammonia-nitrogen excretion, plasma urea levels, and the pH in faeces and urine of weaner pigs," *Livestock Science*, vol. 134, no. 1-3, pp. 243–245, 2010.

[34] G. Galassi, L. Malagutti, S. Colombini, L. Rapetti, and G. Matteo Crovetto, "Effects of benzoic acid on nitrogen, phosphorus and energy balance and on ammonia emission from slurries in the heavy pig," *Italian Journal of Animal Science*, vol. 10, no. 3, pp. 200–204, 2011.

[35] Z. Gao, *Regulatory Effects of Benzoic Acid on Digestive Physiology and Nutritional Metabolism of Young Pigs*, Sichuan Agricultural University, 2013.

[36] J. Chen, *Effects of Benzoic Acid on Growth Performance and Intestinal Function and the Optimum Dietary Dose in Weaning Piglets*, Sichuan Agricultural University, 2015.

[37] N. Dierick, J. Michiels, and C. Van Nevel, "Effect of medium chain fatty acids and benzoic acid, as alternatives for antibiotics, on growth and some gut parameters in piglets," *Communications in Agricultural and Applied Biological Sciences*, vol. 69, pp. 187–190, 2004.

[38] J. M. DeSesso and C. F. Jacobson, "Anatomical and physiological parameters affecting gastrointestinal absorption in humans and rats," *Food and Chemical Toxicology*, vol. 39, no. 3, pp. 209–228, 2001.

[39] K. Bühler, B. Bucher, and C. Wenk, "Apparent nutrient and mineral digestibility in growing-finishing pigs fed phosphorus reduced diets supplemented with benzoic acid and phytase," *Livestock Science*, vol. 134, no. 1-3, pp. 103–105, 2010.

[40] A. U. Dignass, "Mechanisms and modulation of intestinal epithelial repair," *Inflammatory Bowel Diseases*, vol. 7, no. 1, pp. 68–77, 2001.

[41] M. G. Laukoetter, M. Bruewer, and A. Nusrat, "Regulation of the intestinal epithelial barrier by the apical junctional complex," *Current Opinion in Gastroenterology*, vol. 22, no. 2, pp. 85–89, 2006.

[42] H. Diao, H. L. Yan, Y. Xiao et al., "Erratum to: Intestinal microbiota could transfer host Gut characteristics from pigs to mice," *BMC Microbiology*, vol. 16, no. 1, 2016.

[43] H. Yan, H. Diao, Y. Xiao et al., "Gut microbiota can transfer fiber characteristics and lipid metabolic profiles of skeletal muscle from pigs to germ-free mice," *Scientific Reports*, vol. 6, no. 1, 2016.

[44] M. Øverland, N. P. Kjos, M. Borg, and H. Sørum, "Organic acids in diets for entire male pigs," *Livestock Science*, vol. 109, no. 1-3, pp. 170–173, 2007.

[45] D. Józefiak, S. Kaczmarek, M. Bochenek, and A. Rutkowski, "A note on effect of benzoic acid supplementation on the performance and microbiota population of broiler chickens," *Journal of Animal and Feed Sciences*, vol. 16, no. 2, pp. 252–256, 2007.

[46] N. Amaechi and C. Anueyiagu, "The effect of dietary benzoic acid supplementation on growth performance and intestinal wall morphology of broilers," *Online Journal of Animal and Feed Research*, vol. 2, pp. 401–404, 2012.

[47] P. G. Bedford and E. G. Clarke, "Experimental benzoic acid poisoning in the cat.," *Veterinary Record*, vol. 90, no. 3, pp. 53–58, 1972.

[48] P. qi, H. Hong, X. Liang, and D. Liu, "Assessment of benzoic acid levels in milk in China," *Food Control*, vol. 20, no. 4, pp. 414–418, 2009.

[49] F. A. Andersen, "Final report on the safety assessment of Benzyl Alcohol, Benzoic Acid, and Sodium Benzoate," *International Journal of Toxicology*, vol. 20, no. 3, pp. 23–50, 2001.

[50] Y. Shu, B. Yu, J. He et al., "Excess of dietary benzoic acid supplementation leads to growth retardation, hematological abnormality and organ injury of piglets," *Livestock Science*, vol. 190, pp. 94–103, 2016.

[51] Y. Shu, *Safety Evaluation of Benzoic Acid in Piglets*, Sichuan Agricultural University, 2016.

Hindawi
BioMed Research International
Volume 2019, Article ID 3801639, 8 pages
https://doi.org/10.1155/2019/3801639

Research Article

Comparison of Chromium and Iron Distribution in Serum and Urine among Healthy People and Prediabetes and Diabetes Patients

Qi Zhou,[1] Wenjia Guo,[2] Yanan Jia,[2] and Jiancheng Xu[2]

[1] *Department of Pediatrics, First Hospital of Jilin University, Changchun 130021, China*
[2] *Department of Laboratory Medicine, First Hospital of Jilin University, Changchun 130021, China*

Correspondence should be addressed to Jiancheng Xu; jianchengxu@yeah.net

Received 19 December 2018; Accepted 10 February 2019; Published 24 February 2019

Guest Editor: Filipa S. Reis

Copyright © 2019 Qi Zhou et al. This is an open access article distributed under the Creative Commons Attribution License, which permits unrestricted use, distribution, and reproduction in any medium, provided the original work is properly cited.

The effect of chromium (Cr) and iron (Fe) on prevalence of diabetes has received great attention. This study investigated serum and urinary Cr and Fe levels among patients with impaired fasting glucose (IFG), impaired glucose tolerance (IGT), type 1 diabetes (T1D), and type 2 diabetes (T2D) in the Northeast Chinese population. From January 2010 to October 2011, patients with IFG (n=12), IGT (n=15), T1D (n=25), T2D (n=137) and healthy controls (n=50) were enrolled in the First Hospital of Jilin University. Trace elements were detected using an inductively coupled plasma spectrometer. Serum Cr levels decreased in T2D without complications, diabetic retinopathy (DR), diabetic peripheral neuropathy (DPN), and diabetic nephropathy (DN) ($P<0.05$). The urinary Cr level in T1D was the highest of all, which significantly exceeded those of the T2D groups with and without complications. No significant differences of serum Fe levels were found among all groups. The urinary Fe level of T1D was significantly increased ($P<0.05$). The correlation between serum Cr and serum Fe in T2D was obviously positive ($P<0.05$). One month of simvastatin therapy exerted no effects on serum or urinary Cr and Fe levels. These results suggest the potential role of Cr and Fe in diabetes should receive attention.

1. Introduction

Incidence of diabetes mellitus (DM) has been remaining high worldwide. The chronic disease has caused 1.6 million people to die in 2015 [1] and WHO predicts the number of patients would be over 592 million people in 2035 [2]. As the 4th-fatal illness of the noncommunicable diseases [1], it worsens patients' health and quality of life severely. Previous studies have shown increasing prevalence of diabetes in China, which is the world's largest diabetes epidemic now.

Among the Chinese adult population in 2013, the estimated standardized prevalence of total diagnosed and undiagnosed diabetes is 10.9%; that of diagnosed diabetes, 4.0%; and that of prediabetes, 35.7% [3]. Diet plus physical activity may reduce the incidence of type 2 diabetes (T2D) in people with impaired glucose tolerance (IGT).

Basic and clinical studies reveal that transportation, distribution, excretion, and accumulation of various kinds of trace elements under diabetic condition changed differently [4–6] and influence development of diabetes and complication progression dissimilarly [7]. Considering the nosogenesis mechanism, chromium (Cr) and iron (Fe) promote diabetes through insulin resistance solely [8, 9]. Some scholars believe Cr benefits the human body [10]. Cr promotes glycolysis in muscle cells and fat cells, acts as an inhibitor of glycogen decomposition in myocytes, and is able to regulate glucose according to a variety of animal models and clinical trials. It is classified as a "hypoglycemic metal element" in the review of Adrian et al. [11], which is involved in carbohydrate, lipid, and protein metabolism primarily by increasing insulin efficiency [12]. Chromium-containing compounds enhance insulin activity, and what is approved is that insulin-responsiveness is improved in diabetic patients after supplementation with chromium-based compounds [13]. Its mechanism may be increasing the concentration of the insulin receptor RNA messenger; complex formation with insulin enhancing its activity; and increasing islet β cell sensitivity by reducing concentration of TNF-α, resistin, and interleukin-6 [14]. Many clinical studies have confirmed the decrease of serum Cr in patients with T1D and T2D [15, 16] with a drastic increase of Cr in urine [17]. Plasma Cr is negatively correlated with glucose in patients with T2D [18].

Fe is an essential element of organisms, a constituent of various proteins and enzymes. There has been no experiment so far proving that Fe directly increases glucose, while evidence shows it damages the pancreas and induces diabetes [11]. It is currently believed that Fe overload strongly associates with insulin resistance, hyperglycemia, and high risk of T2D [19]. For example, ferritin, the index for Fe storage, is correlated with diabetes [20]. Some researchers believe that Fe induces diabetes through oxidative stress and direct damage towards pancreatic β cells [21]. In addition, the other side is that frequent blood donation (≥2 times per year) is considered to be a protective factor for diabetes, which reduces Fe reserve, increases insulin sensitivity, and weakens postprandial hyperinsulinemia [22].

The function of each element is different and their relationships appear to be complex, as calcium, magnesium, titanium, zinc, vanadium, and Fe reduce Cr absorption [23]. Therefore many investigators now turn to "pack" them to analyze the changes and roles of several more related ones. We have done so as with magnesium and calcium, copper, and zinc [5, 6]. Because both Cr and Fe function as an insulin resistant, we conduct this comparative study on the distribution and correlation of Cr and Fe among healthy, prediabetic, and diabetic populations and try to explore the interaction of the two. By exploring their levels in the serum and urine of subjects, respectively, we also intend to track metabolic changes and disease-relevant information subsequently.

2. Materials and Methods

2.1. Ethical Statements. This retrospective study was approved by the Ethics Committee of the First Hospital of Jilin University. All patients provided signed informed consent. Data were obtained from electronic medical records of the hospital, and the information was anonymous.

2.2. Subjects. To ensure academic integrity and rigor, subject selection of this study is the same as those of our previous researches [5, 6], which can be described briefly as 189 definitively diagnosed patients enrolled from January 2010 to October 2011 in the First Hospital of Jilin University and grouped based on medical certification as follows: impaired fasting glucose (IFG, n=12 people), impaired glucose tolerance (IGT, n=15), type 1 diabetes (T1D, n=25), type 2 diabetes without complications (T2D, n=29), diabetic nephropathy (DN, n=24), diabetic retinopathy (DR, n=34), and diabetic peripheral neuropathy (DPN, n=50). The control group (CON, n=50) was enrolled according to the age and sex proportion from physical examination group at the same standard meantime, noting that subjects had not received any element supplement due to official approval of effectiveness. The subjects' basic information as age, sex, and BMI will not be detailed here to avoid redundancy and duplication [5].

2.3. Element Measurement. The elements' measurements were the same as previous studies of our research project [5, 6], using ICP-MS. The quality control of all analyzed samples was performed by using standard reference materials from the China Standard Material Center. Limits of detection (LOD) were 1.0 μg/L for Cr and Fe. The recovery of standard trace elements (accuracy) ranged from 93.3% to 98.9%.

2.4. Statistics. Statistical description was performed as median (interquartile range); the Kruskal-Wallis test was used for evaluation among multigroups, and the comparison between groups was assessed applying the Mann-Whitney test with correction by the Bonferroni method of α; correlation was analyzed with Spearman's method. The P value reported was two-sided and statistically significant at $P < 0.05$. All analysis was conducted using SPSS 24.0.

3. Results and Discussion

3.1. Trace Elements Levels in Prediabetes and Diabetes. Serum glucose and HbA1c were tested to support the enrollment standard. Table 1 showed that, compared with the control group, serum Cr levels decreased in the T2DCON, DR, DPN, and DN groups (P<0.05); though no statistical significance (P>0.05) was shown, a downward trend appeared in IFG, IGT, and T1D. On the other hand, the urinary Cr level in T1D was the highest of all (Figure 1(a)), which significantly exceeded those of the T2D groups with and without complications. Surprisingly, we barely found significant difference of serum Fe levels among all groups. The urinary Fe level of T1D was significantly increased (P<0.05) and reached the peak (Figure 1(b)), while that of T2D was lower (P<0.05).

3.2. Correlation Analysis of Trace Elements. As presented in Table 2, the correlation between serum Cr and serum Fe in T2D was positive obviously (P<0.05); meanwhile these relations in IFG, IGT, and T1D were not statistically significant (P>0.05).

3.3. Effect of Simvastatin Treatment on Trace Elements in T2D Patients. Statin treatment was often used to lower lipid in the patients with T2D. Therefore the effect of simvastatin therapy for one month on serum or urinary Cr and Fe levels was detected in the patients with T2D. As presented in Table 3, one month of simvastatin therapy had no effects on serum or urinary Cr and Fe levels.

4. Discussion

4.1. Comparison of Serum and Urinary Cr. It is currently believed that diabetic patients are under a state of trace elements disorder, such as insulin promoting discrepancy of distribution of multiple ions in the bloodstream [4]. More than 80% of the Cr in the human body is excreted in urine [24], and the amount of urinary Cr in T1D patients is considered to be more than twice that of the control group [17]. Some scientists attributed this to its increased loss plus decreased absorption [25]. Therefore, we believe the

TABLE 1: Comparison of indexes among groups [$M(P_{25} \sim P_{75})$].

	CON (*n*=50)	IFG (*n*=12)	IGT (*n*=15)	T1D (*n*=25)	T2DCON (*n*=29)	DN (*n*=24)	DR (*n*=34)	DPN (*n*=50)
Glu (mmol/L)	4.8 (4.1-5.6)	6.4^{1} (6.3-6.7)	5.9^{1,2} (5.6-6.1)	11.9^{1,2,3} (8.5-14.8)	9.8^{1,2,3} (8.3-12.8)	8.2^{1,2,3} (7.5-9.5)	9.2^{1,2,3} (7.7-11.4)	8.8^{1,2,3} (7.6-11.1)
HbA1c (%)	5.1 (4.2-6.0)	6.1^{1} (5.9-6.2)	5.5^{2} (5.4-5.7)	11.3^{1,2,3} (10.3-12.8)	8.5^{1,2,3,4} (7.7-8.9)	8.5^{1,2,3,4} (8.0-8.8)	8.6^{1,2,3,4} (8.0-8.9)	8.2^{1,2,3,4} (7.2-8.7)
Cr (mg/L)	0.185 (0.136-0.221)	0.164 (0.098-0.214)	0.172 (0.128-0.202)	0.151 (0.104-0.191)	0.131^{1} (0.107-0.168)	0.096^{1} (0.062-0.149)	0.083^{1,3,4} (0.064-0.149)	0.135^{1} (0.073-0.173)
UCr (mg/L)	0.034 (0.024-0.041)	0.038 (0.027-0.039)	0.023 (0.015-0.034)	0.120^{1,2,3} (0.094-0.141)	0.050^{1,3,4} (0.028-0.082)	0.040^{4} (0.023-0.050)	0.035^{4} (0.020-0.057)	0.044^{1,3,4} (0.026-0.063)
Cr/UCr	5.329 (3.810-8.852)	5.511 (3.292-6.165)	7.353 (5.577-10.227)	1.270^{1,2,3} (0.980-1.576)	2.750^{1,3,4} (1.415-4.800)	2.525^{1,3,4} (1.445-5.265)	3.232^{1,3,4} (1.386-4.636)	3.168^{1,3,4} (1.973-4.300)
Fe (mg/L)	1.697 (1.402-2.185)	2.087 (1.554-2.303)	2.116 (1.454-2.650)	1.857 (1.172-2.341)	2.014 (1.587-2.410)	1.447 (1.027-2.025)	1.539 (1.025-2.350)	1.841 (1.147-2.409)
UFe (mg/L)	0.335 (0.199-0.585)	0.466 (0.301-0.538)	0.279 (0.216-0.425)	1.140^{1,2,3} (0.595-1.465)	0.450^{4} (0.310-0.700)	0.410^{4} (0.108-0.908)	0.290^{4} (0.159-0.553)	0.385^{4} (0.279-0.803)
Fe/UFe	4.784 (3.023-7.879)	4.382 (3.394-6.389)	7.343 (3.421-10.727)	1.803^{1,2,3} (1.061-3.445)	3.744^{4} (2.498-6.997)	5.077 (1.662-10.395)	6.092 (1.595-9.896)	4.120^{4} (2.679-7.522)

UCr refers to urinary Cr; UFe refers to urinary Fe. ^{1}Compared with the CON group, there is significant difference. ^{2}Compared with the IFG group, there is significant difference. ^{3}Compared with the IGT group, there is significant difference. ^{4}Compared with the T1D group, there is significant difference. ^{5}Compared with the T2DCON group, there is significant difference. ^{6}Compared with the DN group, there is significant difference.

Table 2: Correlation between Cr, Fe, and other indicators in serum and urine within each group.

		CON (*n*=50)	*P*	IFG (*n*=12)	*P*	IGT (*n*=15)	*P*	T1D (*n*=25)	*P*	T2D CON (*n*=29)	*P*	DN (*n*=24)	*P*	DR (*n*=34)	*P*	DPN (*n*=50)	*P*
Glu (mmol/L)	*r*1	-0.170	0.239	-0.220	0.491	0.065	0.819	0.137	0.515	-0.061	0.754	-0.023	0.914	0.030	0.866	0.115	0.427
	*r*2	-0.482	<0.001∗	-0.004	0.991	-0.079	0.780	-0.389	0.055	-0.262	0.170	-0.279	0.186	-0.207	0.241	-0.159	0.269
	*r*3	-0.063	0.663	0.068	0.834	0.387	0.154	0.332	0.105	0.231	0.228	-0.081	0.706	-0.179	0.310	0.139	0.335
	*r*4	-0.109	0.453	-0.011	0.974	0.335	0.222	-0.171	0.413	0.003	0.986	-0.155	0.468	-0.086	0.629	-0.001	0.994
HbA1c (%)	*r*1	-0.233	0.104	0.095	0.768	0.265	0.340	0.093	0.658	0.258	0.177	0.122	0.570	0.098	0.580	0.095	0.511
	*r*2	-0.409	0.003∗	-0.212	0.507	0.032	0.909	0.139	0.507	-0.100	0.606	0.104	0.629	-0.055	0.759	0.175	0.224
	*r*3	-0.060	0.681	0.050	0.877	0.518	0.048∗	0.254	0.221	0.091	0.638	0.043	0.843	0.047	0.791	0.180	0.211
	*r*4	-0.089	0.539	-0.007	0.983	0.483	0.068	0.289	0.161	0.138	0.476	0.222	0.298	-0.128	0.469	0.110	0.448
Cr (mg/L)	*r*2	0.419	0.002∗	-0.154	0.634	0.464	0.081	0.283	0.170	0.557	0.002∗	0.774	<0.001∗	0.470	0.006∗	0.500	<0.001∗
	*r*3	0.096	0.505	0.121	0.707	0.216	0.438	0.390	0.054	0.022	0.910	0.228	0.284	0.143	0.419	0.149	0.302
	*r*4	0.366	0.009∗	-0.655	0.021∗	0.082	0.771	-0.169	0.421	-0.037	0.849	-0.157	0.463	0.112	0.528	-0.106	0.465
UCr (mg/L)	*r*2	-0.116	0.421	-0.409	0.186	-0.041	0.884	0.096	0.647	-0.153	0.428	0.217	0.308	0.068	0.704	0.127	0.379
	*r*4	0.665	<0.001∗	-0.032	0.921	0.623	0.013∗	0.186	0.375	0.010	0.957	0.298	0.157	0.374	0.030∗	0.255	0.074
Fe (mg/L)	*r*4	-0.020	0.892	-0.102	0.753	-0.243	0.383	0.174	0.406	0.097	0.616	-0.063	0.771	0.021	0.905	0.092	0.525

*r*1 means the correlation coefficient between serum Cr and other indicators; *r*2 is the correlation coefficient between serum Fe and other indicators; *r*3 is the correlation coefficient between urinary Cr and other indicators; *r*4 is the correlation coefficient between urinary Fe and other indicators.∗$P<0.05$ means significant difference.

TABLE 3: Serum parameters in T2D patients treated with simvastatin.

	Simvastatin (n=24)		
	Pretreatment	Posttreatment	P
Cr	0.165(0.087-0.241)	0.178(0.067-0.234)	0.695
UCr	0.048(0.020-0.064)	0.034(0.021-0.057)	0.837
Fe	2.235(1.461-2.742)	2.147(1.685-2.852)	0.680
UFe	0.370(0.173-0.735)	0.320(0.213-0.770)	0.724

Data presentation and abbreviations' spelt-out forms are the same as the description for Table 1.

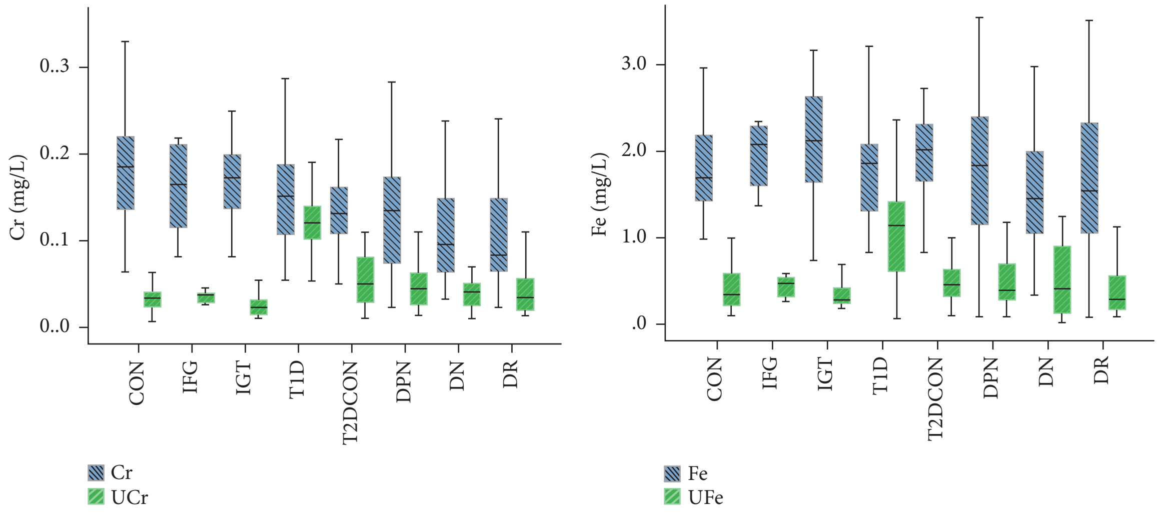

(a)

(b)

FIGURE 1: Levels of Cr and Fe in the healthy control, IFG, IGT, T1D, T2D without complications, DPN, DN, and DR groups. Boxplots display the extreme, the upper and lower quartiles, and the median of the maximum difference in the healthy control, IFG, IGT, T1D, T2D without complications, DPN, DN, and DR groups. The median for each dataset is indicated by the centerline, and the first and third quartiles are presented by the edges of the area, which is known as the interquartile range (IQR). (a) Serum Cr levels decreased in the T2DCON, DR, DPN, and DN group (P<0.05) and urinary Cr level in T1D was the highest; (b) urinary Fe level of T1D was significantly increased (P<0.05).

simultaneous study of both serum and urine trace element levels may provide better overview of the state and degree. We confirmed serum Cr levels were lower in the T2DCON, DR, DPN, and DN population than that of the control, which is consistent with findings of other investigators [7, 26, 27]; IFG and IGT had lower serum Cr levels than the control even with no statistical significance, which is similar to the conclusion of Chen [27]; the comparison of serum Cr between T1D and the control showed no significant difference and was consistent with Lin's study [28] of T1D children, adults, and healthy people.

As for urinary Cr, the sum that T2D patients have higher levels of urinary Cr was the same as the proposition of Kazi et al. [7] who proved no statistically significant difference as well but deemed the tendency existed; it elevated visibly in T1D; considering the severity of illness and thus selection being incomprehensive, prediabetes showed no significant difference comparing with the control group on urinary Cr level; the Cr/UCr in diabetic groups was lower than those of the prediabetic and control group, indicating diabetic patients were all under low Cr state. It is already proved in a research launching in Indian rural areas that elevated urinary Cr is strongly correlated to diabetes [29]; our experiment adopted a random urine specimen, which might have varied greatly due to physical and chemical factors; thus the statistical difference could not be that obvious. Besides, it is noticeable that the excretion rate of Cr and Fe changed mildly in DN patients, which was opposite to our expectation that severe renal function damaged influenced elements in urine.

Combined with serum Cr information, it was stated in our experiment that T2D patients lied in low Cr condition, the same as findings of relatively low Cr content in T2D patients' hair [7] and nails [30]. That explained what Cefalu WT [31] purposed in which low Cr induced upward fasting glucose and glycosuria. T1D patients exhibited a negative Cr balance [32], which was in consistency with the results of no significant change of serum Cr and overt increase of urinary Cr in our study. It is stated that the T1D metabolic control system required additional Cr whereas the absorbed element was not utilized and discharged in urine [17].

Besides, Cr/UCr results also revealed that diabetic patients were losing Cr. Morris [18] found diabetic patients had a 33% reduction of plasma Cr and 100% increase of urinary Cr. Our experiment could not find stationary correlation between Cr and lipid indicators which was testified in a lot of animal and clinical studies [4, 31, 33, 34], possibly resulting from therapeutic regimens and medications.

As an enhancer for insulin function, Cr participates in carbohydrate, lipid, and protein metabolism by improving insulin efficiency, and its deficiency seriously affects glucose tolerance and lipid homeostasis [12]. The concrete mechanism remains unknown [12], whereas studies confirmed Cr regulated glucose in a variety of pathways. For example, Cr is involved in hyperinsulinemia and insulin resistance [35]; Vincent et al. [36] demonstrated that chromodulin was able to activate insulin receptor kinase; Pattar et al. [37] believed Cr altered membrane fluidity and regulated glucose uptake consequently by changing cholesterol content; it might impact structure of lipid bilayer [38] and the like. Both animal experiments [39] and clinical studies [40–42] have affirmed that Cr supplementation reduced glucose; therefore experts suggested [43] that that be applied as T2D complementary therapy.

However, healthy people did not benefit from that tentative plan [44]. Therefore, Lewicki S [12] thought this treatment was probably only valid to a population with metabolic disorders, which should be supplemented as appropriate.

4.2. Comparison of Serum and Urinary Fe. Surprisingly, there was no significant difference of serum Fe levels among the groups in our study, which was contrary with others' [45, 46]. Most current views were that diabetic patients are being Fe overloaded; evidence stood as diabetes associating with elevated ferritin [47]. Yet some data turned out that serum Fe level was not distinctive between diabetic patients and healthy people [15, 47–49]. Duan et al. [47] considered hyperglycemia led to enhancing oxidative stress that reduced free iron in circulation, with elevated hepcidin inhibiting the intestine absorbing Fe and release of Fe by the reticuloendothelial system; the correlation between serum Cr and serum Fe in IFG and IGT was not significant, but we still found the tendency existed. Therefore it might be ascribed to small sample size or case selection. Urinary Fe in T1D increased significantly and was much higher than that of T2D and the control. Additionally, Fe/UFe in T1D was apparently lower than other groups', indicating more Fe excretion. In the present study, serum Fe of DPN was not very disparate from that of CON and DN; the DPN and DR group encountered the same situation, which might result in no significant discrepancy. In the present study, one month of simvastatin therapy had no effects on serum or urinary Fe levels.

4.3. Correlation of Cr and Fe. Because of wide variety and complex mechanism of trace elements in the body, their mutual correlation and influence are still inconclusive in this emerging field. We have observed a significant correlation between serum Cr and serum Fe, in accordance with previous findings from supplement experiments [50, 51], possibly due to the cotransport mechanism of Cr and Fe resulting competition for binding sites of transferrin. *In vivo* and *in vitro* studies in rats have shown that approximately 80% of the Cr in the blood is associated with transferrin [52]. After being absorbed from the intestinal tract, Cr combines with proteins related to Fe metabolism, forming a complex transported into cells. The efficiency of the compound passing through the membrane depends on insulin concentration [53]. The bioavailability of Fe in rats treated with Cr intraperitoneally was reduced, and the animal even developed symptoms of anemia [54].

Our experiment concluded that patients with T2D were in low Cr state. The levels of urinary Cr and Fe in T1D patients were higher than those of T2D patients. It is suspected that loss and degree of disorder of trace elements in T1D patients are more severe. We assumed that diabetes affected absorption, transportation, and utilization of Cr and Fe. The limitations of this experiment are that the number of enrolled cases was not enough and the prediabetic group consisted of outpatients; therefore it would be difficult to follow up; there is no more detailed research, such as disease-staging patients; in a way, a 24 h urine sample may be better than a random urine specimen, which reflects cumulative exposure, exposure approaches, and different forms of elements [29]; metabolism, lifestyle, or drugs may not be excluded from impact of exposure, absorption, or excretion of certain elements.

We have not found any significant difference after simvastatin treatment. However, the data presented that serum Cr elevated and serum Fe and urinary Cr and Fe decreased after treatment. The efficacy might be obvious and statistically significant if the duration was set longer.

5. Conclusions

Trace elements and diabetes affect each other mutually. Research is now clinically focused on supplement effectiveness [55, 56] and control glucose as a result [47, 48]. For the reason that it has not yet accessibly arrived at an evidence-based aspect, there is no final conclusion concerning safety and availability [56]. What remains a current and difficult point in future research is to accurately extract and analyze the relationship and mechanism of synergy and antagonism through ingenious experimental design and research.

Data Availability

The data used to support the findings of this study are available from the corresponding author upon request.

Conflicts of Interest

The authors declare that there are no conflicts of interest regarding the publication of this paper.

Acknowledgments

We are thankful for Suyan Tian and Zhifang Jia for providing statistical advice. The data cited from the laboratories of the authors were supported in part by grants from the National Science Foundation of China (no. 81501839, to Dr. Qi Zhou), Scientific and Technological "13th Five-Year

Plan" Project of Jilin Provincial Department of Education (no. JJKH20180214KJ, to Dr. Qi Zhou), Jilin Province Health and Technology Innovation Development Program (no. 2017J071, to Dr. Jiancheng Xu), the Jilin Science and Technology Development Program (no. 20170623092TC-09, to Dr. Jiancheng Xu; no. 20160101091JC, to Dr. Jiancheng Xu; no. 20150414039GH, to Dr. Jiancheng Xu; no. 20190304110YY, to Dr. Jiancheng Xu), the First Hospital Translational Funding for Scientific & Technological Achievements (no. JDYYZH-1902002, to Dr. Jiancheng Xu), and Norman Bethune Program of Jilin University (no. 2012223, to Dr. Jiancheng Xu).

References

[1] World Health Organization, "World health statistics," 2017.

[2] World Health Organization, "Global report on diabetes," WHO, 2016.

[3] L. Wang, P. Gao, M. Zhang et al., "Prevalence and ethnic pattern of diabetes and prediabetes in china in 2013," *Journal of the American Medical Association*, vol. 317, no. 24, pp. 2515–2523, 2017.

[4] H. Staniek, N. R. Rhodes, K. R. Di Bona et al., "Comparison of tissue metal concentrations in zucker lean, zucker obese, and zucker diabetic fatty rats and the effects of chromium supplementation on tissue metal concentrations," *Biological Trace Element Research*, vol. 151, no. 3, pp. 373–383, 2013.

[5] J. Xu, Q. Zhou, G. Liu, Y. Tan, and L. Cai, "Analysis of serum and urinal copper and zinc in chinese northeast population with the prediabetes or diabetes with and without complications," *Oxidative Medicine and Cellular Longevity*, vol. 2013, Article ID 635214, 11 pages, 2013.

[6] Q. Zhou, W. Guo, Y. Jia, and J. Xu, "Effect of 4-phenylbutyric acid and tauroursodeoxycholic acid on magnesium and calcium metabolism in streptozocin-induced type 1 diabetic mice," *Biological Trace Element Research*, pp. 1–10, 2018.

[7] T. G. Kazi, H. I. Afridi, N. Kazi et al., "Copper, chromium, manganese, iron, nickel, and zinc levels in biological samples of diabetes mellitus patients," *Biological Trace Element Research*, vol. 122, no. 1, pp. 1–18, 2008.

[8] S. Fargion, P. Dongiovanni, A. Guzzo, S. Colombo, L. Valenti, and A. L. Fracanzani, "Iron and insulin resistance," *Alimentary Pharmacology and Therapeutics, Supplement*, vol. 22, Suppl 2, pp. 61–63, 2005.

[9] Y. Hua, S. Clark, J. Ren, and N. Sreejayan, "Molecular mechanisms of chromium in alleviating insulin resistance," *The Journal of Nutritional Biochemistry*, vol. 23, no. 4, pp. 313–319, 2012.

[10] S. Weksler-Zangen, T. Mizrahi, I. Raz, and N. Mirsky, "Glucose tolerance factor extracted from yeast: oral insulin-mimetic and insulin-potentiating agent: in vivo and in vitro studies," *British Journal of Nutrition*, vol. 108, no. 05, pp. 875–882, 2012.

[11] A. González-Villalva, L. Colín-Barenque, P. Bizarro-Nevares et al., "Pollution by metals: Is there a relationship in glycemic control?" *Environmental Toxicology and Pharmacology*, vol. 46, pp. 337–343, 2016.

[12] S. Lewicki, R. Zdanowski, M. Krzyzowska et al., "The role of chromium III in the organism and its possible use in diabetes and obesity treatment," *Annals of Agricultural and Environmental Medicine*, vol. 21, no. 2, pp. 331–335, 2014.

[13] M. Lai, "Antioxidant Effects and Insulin Resistance Improvement of Chromium Combined with Vitamin C and E Supplementation for Type 2 Diabetes Mellitus," *Journal of Clinical Biochemistry and Nutrition*, vol. 43, no. 3, pp. 191–198, 2008.

[14] S. K. Jain and K. Kannan, "Chromium chloride inhibits oxidative stress and TNF-α secretion caused by exposure to high glucose in cultured U937 monocytes," *Biochemical and Biophysical Research Communications*, vol. 289, no. 3, pp. 687–691, 2001.

[15] G. Forte, B. Bocca, A. Peruzzu et al., "Blood metals concentration in type 1 and type 2 diabetics," *Biological Trace Element Research*, vol. 156, no. 1-3, pp. 79–90, 2013.

[16] C. R. Flores, M. P. Puga, K. Wrobel, M. E. G. Sevilla, and K. Wrobel, "Trace elements status in diabetes mellitus type 2: possible role of the interaction between molybdenum and copper in the progress of typical complications," *Diabetes Research and Clinical Practice*, vol. 91, no. 3, pp. 333–341, 2011.

[17] A. C. Nsonwu, C. A. O. Usoro, M. H. Etukudo, and I. N. Usoro, "Glycemic control and serum and urine levels of zinc and magnesium in diabetics in Calabar, Nigeria," *Pakistan Journal of Nutrition*, vol. 5, no. 1, pp. 75–78, 2006.

[18] B. Morris, S. MacNeil, C. Hardisty, S. Heller, C. Burgin, and T. Gray, "Chromium homeostasis in patients with type II (NIDDM) diabetes," *Journal of Trace Elements in Medicine and Biology*, vol. 13, no. 1-2, pp. 57–61, 1999.

[19] J. M. Fernández-Real, A. López-Bermejo, and W. Ricart, "Cross-talk between iron metabolism and diabetes," *Diabetes*, vol. 51, no. 8, pp. 2348–2354, 2002.

[20] Y. Wang, W. Koh, J. Yuan, and A. Pan, "Plasma ferritin, C-reactive protein, and risk of incident type 2 diabetes in Singapore Chinese men and women," *Diabetes Research and Clinical Practice*, vol. 128, pp. 109–118, 2017.

[21] M. Hatunic, F. M. Finucane, A. M. Brennan, S. Norris, G. Pacini, and J. J. Nolan, "Effect of iron overload on glucose metabolism in patients with hereditary hemochromatosis," *Metabolism*, vol. 59, no. 3, pp. 380–384, 2010.

[22] J. M. Fernández-Real, A. López-Bermejo, and W. Ricart, "Iron stores, blood donation, and insulin sensitivity and secretion," *Clinical Chemistry*, vol. 51, no. 7, pp. 1201–1205, 2005.

[23] N. S. Chen, A. Tsai, and I. A. Dyer, "Effect of chelating agents on chromium absorption in rats," *Journal of Nutrition*, vol. 103, no. 8, pp. 1182–1186, 1973.

[24] V. Ducros, "Chromium metabolism - A literature review," *Biological Trace Element Research*, vol. 32, no. 1-3, pp. 65–77, 1992.

[25] J. J. Cunningham, "Micronutrients as nutriceutical interventions in diabetes mellitus," *Journal of the American College of Nutrition*, vol. 17, no. 1, pp. 7–10, 1998.

[26] G. Sridhar, V. Sujatha, V. Anita, and P. Sundararaman, "Serum chromium levels in gestational diabetes mellitus," *Indian Journal of Endocrinology and Metabolism*, vol. 16, no. 7, pp. S70–S73, 2012.

[27] S. Chen, X. Jin, Z. Shan et al., "Inverse association of plasma chromium levels with newly diagnosed type 2 diabetes: a case-control study," *Nutrients*, vol. 9, no. 3, 2017.

[28] C. Lin, G. Tsweng, C. Lee, B. Chen, and Y. Huang, "Magnesium, zinc, and chromium levels in children, adolescents, and young adults with type 1 diabetes," *Clinical Nutrition*, vol. 35, no. 4, pp. 880–884, 2016.

[29] G. Velmurugan, K. Swaminathan, G. Veerasekar et al., "Metals in urine in relation to the prevalence of pre-diabetes, diabetes

and atherosclerosis in rural India," *Occupational and Environmental Medicine*, vol. 75, no. 9, pp. 661–667, 2018.

[30] M. Khamaisi, I. D. Wexler, J. Skrha et al., "Cardiovascular disease in type 2 diabetics: epidemiology,risk factors and therapeutic modalities," *The Israel Medical Association Journal (IMAJ)*, vol. 5, pp. 801–806, 2003.

[31] W. T. Cefalu, Z. Q. Wang, X. H. Zhang, L. C. Baldor, and J. C. Russell, "Oral Chromium Picolinate Improves Carbohydrate and Lipid Metabolism and Enhances Skeletal Muscle Glut-4 Translocation in Obese, Hyperinsulinemic (JCR-LA Corpulent) Rats," *Journal of Nutrition*, vol. 132, no. 6, pp. 1107–1114, 2002.

[32] B. S. Karagun, F. Temiz, G. Ozer et al., "Chromium levels in healthy and newly diagnosed type 1 diabetic children," *Pediatrics International*, vol. 54, no. 6, pp. 780–785, 2012.

[33] R. Bennett, B. Adams, A. French, Y. Neggers, and J. B. Vincent, "High-dose chromium(iii) supplementation has no effects on body mass and composition while altering plasma hormone and triglycerides concentrations," *Biological Trace Element Research*, vol. 113, no. 1, pp. 53–66, 2006.

[34] M. H. Lai, Y. Y. Chen, and H. H. Cheng, "Chromium yeast supplementation improves fasting plasma glucose and ldl-cholesterol in streptozotocin-induced diabetic rats," *International Journal for Vitamin and Nutrition Research*, vol. 76, no. 6, pp. 391–397, 2006.

[35] M. P. Longnecker and J. L. Daniels, "Environmental contaminants as etiologic factors for diabetes.," *Environmental Health Perspectives*, vol. 109, no. suppl 6, pp. 871–876, 2001.

[36] J. B. Vincent, "Mechanisms of chromium action: low-molecular-weight chromium-binding substance," *Journal of the American College of Nutrition*, vol. 18, no. 1, pp. 6–12, 1999.

[37] G. R. Pattar, L. Tackett, P. Liu, and J. S. Elmendorf, "Chromium picolinate positively influences the glucose transporter system via affecting cholesterol homeostasis in adipocytes cultured under hyperglycemic diabetic conditions," *Mutation Research - Genetic Toxicology and Environmental Mutagenesis*, vol. 610, no. 1-2, pp. 93–100, 2006.

[38] N. S. Raja, K. Sankaranarayanan, A. Dhathathreyan, and B. U. Nair, "Interaction of chromium(III) complexes with model lipid bilayers: Implications on cellular uptake," *Biochimica et Biophysica Acta (BBA) - Biomembranes*, vol. 1808, no. 1, pp. 332–340, 2011.

[39] J. R. Komorowski, M. Tuzcu, N. Sahin et al., "Chromium picolinate modulates serotonergic properties and carbohydrate metabolism in a rat model of diabetes," *Biological Trace Element Research*, vol. 149, no. 1, pp. 50–56, 2012.

[40] S. Sharma, R. P. Agrawal, M. Choudhary, S. Jain, S. Goyal, and V. Agarwal, "Beneficial effect of chromium supplementation on glucose, HbA1C and lipid variables in individuals with newly onset type-2 diabetes," *Journal of Trace Elements in Medicine and Biology*, vol. 25, no. 3, pp. 149–153, 2011.

[41] T. Drake, K. Rudser, E. Seaquist, and A. Saeed, "Chromium infusion in hospitalized patients with severe insulin resistance: a retrospective analysis," *Endocrine Practice*, vol. 18, no. 3, pp. 394–398, 2012.

[42] S. R. Surani, "Severe insulin resistance treatment with intravenous chromium in septic shock patient," *World Journal of Diabetes*, vol. 3, no. 9, pp. 170–173, 2012.

[43] S. K. Jain, G. Kahlon, L. Morehead et al., "Effect of chromium dinicocysteinate supplementation on circulating levels of insulin, TNF-α, oxidative stress, and insulin resistance in type 2 diabetic subjects: Randomized, double-blind, placebo-controlled study," *Molecular Nutrition & Food Research*, vol. 56, no. 8, pp. 1333–1341, 2012.

[44] U. Masharani, C. Gjerde, S. McCoy et al., "Chromium supplementation in non-obese non-diabetic subjects is associated with a decline in insulin sensitivity," *BMC Endocrine Disorders*, vol. 12, p. 31, 2012.

[45] A. D. Wolide, B. Zawdie, T. Alemayehu Nigatu, and S. Tadesse, "Evaluation of serum ferritin and some metal elements in type 2 diabetes mellitus patients: comparative cross-sectional study," *Diabetes, Metabolic Syndrome and Obesity: Targets and Therapy*, vol. Volume 9, pp. 417–424, 2016.

[46] F. A. Khan, N. Al Jameil, S. Arjumand et al., "Comparative Study of Serum Copper, Iron, Magnesium, and Zinc in Type 2 Diabetes-Associated Proteinuria," *Biological Trace Element Research*, vol. 168, no. 2, pp. 321–329, 2015.

[47] F. Duan, Y. Li, F. Yang, and Y. Wang, "Study on iron metabolism in type 2 diabetes patients," *Journal of Modern Laboratory Medcine*, vol. 30, pp. 151-152, 2015.

[48] Q. Ling, R. Xu, S. Wang et al., "Correlation of serum levels of trace elements withglycometabolic parameters in patients with type 2 diabetes," *Chinese Journal of Multiple Organ Diseases in the Elderly*, vol. 14, pp. 440–443, 2015.

[49] M. Basaki, M. Saeb, S. Nazifi, and H. A. Shamsaei, "Zinc, copper, iron, and chromium concentrations in young patients with type 2 diabetes mellitus," *Biological Trace Element Research*, vol. 148, no. 2, pp. 161–164, 2012.

[50] A. Dogukan, N. Sahin, M. Tuzcu et al., "The effects of chromium histidinate on mineral status of serum and tissue in fat-fed and streptozotocin-treated type II diabetic rats," *Biological Trace Element Research*, vol. 131, no. 2, pp. 124–132, 2009.

[51] H. Staniek and Z. Krejpcio, "The effects of supplementary Cr3 (chromium(III) propionate complex) on the mineral status in healthy female rats," *Biological Trace Element Research*, vol. 180, no. 1, pp. 90–99, 2017.

[52] W. Feng, B. Li, J. Liu et al., "Study of chromium-containing proteins in subcellular fractions of rat liver by enriched stable isotopic tracer technique and gel filtration chromatography," *Analytical and Bioanalytical Chemistry*, vol. 375, no. 3, pp. 363–368, 2003.

[53] B. J. Clodfelder and J. B. Vincent, "The time-dependent transport of chromium in adult rats from the bloodstream to the urine," *JBIC Journal of Biological Inorganic Chemistry*, vol. 10, no. 4, pp. 383–393, 2005.

[54] M. Ani and A. A. Moshtaghie, "The effect of chromium on parameters related to iron metabolism," *Biological Trace Element Research*, vol. 32, no. 1-3, pp. 57–64, 1992.

[55] B. Sundaram, K. Singhal, and R. Sandhir, "Ameliorating effect of chromium administration on hepatic glucose metabolism in streptozotocin-induced experimental diabetes," *BioFactors*, vol. 38, no. 1, pp. 59–68, 2012.

[56] J. B. Vincent, "Chromium: is it essential, pharmacologically relevant, or toxic?" *Metal Ions in Life Sciences*, vol. 13, pp. 171–198, 2013.

Hindawi
BioMed Research International
Volume 2019, Article ID 3921315, 10 pages
https://doi.org/10.1155/2019/3921315

Research Article

The Impact of *Lactobacillus plantarum* on the Gut Microbiota of Mice with DSS-Induced Colitis

Fei Zhang,[1,2] **Yue Li**,[1,2] **Xiliang Wang**,[1,2] **Shengping Wang**,[3] **and Dingren Bi**[1,2]

[1] *State Key Laboratory of Agricultural Microbiology, College of Veterinary Medicine, Huazhong Agricultural University, Wuhan, China*
[2] *Key Laboratory of Preventive Veterinary Medicine in Hubei Province, College of Veterinary Medicine, Huazhong Agricultural University, Wuhan, China*
[3] *Hunan Institute of Microbiology, Changsha, Hunan, China*

Correspondence should be addressed to Xiliang Wang; wxl070@mail.hzau.edu.cn

Received 12 December 2018; Revised 29 January 2019; Accepted 7 February 2019; Published 20 February 2019

Guest Editor: Deguang Song

Copyright © 2019 Fei Zhang et al. This is an open access article distributed under the Creative Commons Attribution License, which permits unrestricted use, distribution, and reproduction in any medium, provided the original work is properly cited.

The pathogenesis of inflammatory bowel disease (IBD) is due in part to a loss of equilibrium among the gut microbiota, epithelial cells, and resident immune cells. The gut microbiota contains a large proportion of probiotic commensal *Lactobacillus* species; some natural microbiota and probiotics confer protection against IBD. In this study, mice with colitis triggered by dextran sodium sulphate (DSS) were given *Lactobacillus plantarum* orally. We assessed the damage caused by DSS and the therapeutic activity of *L. plantarum*. The colitis triggered by DSS was less severe in the mice that received the *L. plantarum* treatment, which also diversified the microbe species in the colon, enhanced the ratio of Firmicutes to Bacteroidetes, and diminished the relative abundance of *Lactobacillus*. The taxonomic units of greatest diversity in the DSS and *L. plantarum* groups were identified using a linear discriminant and effect size (LEfSe) analysis. *Aliihoeflea* was established to be the genus of bacteria that was affected in the *L. plantarum* group most extensively. In conclusion, gut health was promoted by *L. plantarum*, as it diversified the microbes in the colon and restricted the activity of pathogenic bacteria in the intestine. Moreover, according to the LEfSe analysis, the DSS group was impacted more significantly by gut microorganisms than the *L. plantarum* group, suggesting that *L. plantarum* improved the stability of the intestinal tract.

1. Introduction

Crohn's disease (CD) and ulcerative colitis (UC) are collectively known as inflammatory bowel disease (IBD), which manifests itself as a chronic inflammatory relapse of the gastrointestinal tract caused by a range of genetic and environmental factors [1]. A previous report suggested subjects with a genetic predisposition to IBD exhibit abnormal and ongoing inflammatory reactions to the commensal gut microbiome [2]. Research in animal models has also suggested intestinal inflammation is critically dependent on bacterial colonization of the gut, which highlights the importance of the gut microbiota in IBD [3]. A wide range of drug-based treatments are available for IBD, but their effectiveness is moderate and can be accompanied by secondary effects such as toxicity and an increased likelihood of infectious complications [4, 5]. Thus, it is necessary to develop alternative treatments for IBD. Exactly how IBD develops remains uncertain, but there is consensus that the imbalance of homeostasis between the gut microbiota and the mucosal immune system is a major contributor to the disease [6, 7].

Many studies suggest different benefits of probiotics, and IBD could potentially be treated with probiotic supplements [8, 9]. Nevertheless, knowledge about the exact manner in which probiotics protect against IBD remains incomplete. The gut microflora contain an abundance of commensal *Lactobacillus* species, which can rehabilitate homeostasis in intestinal disorders and hence could protect against IBD [10]. As live microorganisms, probiotics have the ability to regulate the composition of the gut microbiota and correct abnormal responses of the mucosal immune system to chronic gut inflammation. Probiotics can also strengthen the gut barrier function by influencing the production of cytokines, stimulating the release of regulatory T cells, and aiding the survival of intestinal cells [11]. Probiotics are advantageous not only from a health perspective, but also from a cost and safety perspective. The only drawback of this strategy is that a comprehensive understanding of how probiotics exert their health effects has not yet been achieved [12].

We conducted an experiment in mice with colitis induced by dextran sodium sulphate (DSS) to determine the impact of *Lactobacillus plantarum* on gut inflammation and whether the effects of this bacterium were correlated with the immune response and gut microbiota.

2. Materials and Methods

2.1. Animals. The animal experiments were approved by the Medical Ethics Committee of Huazhong Agricultural University, and we complied with their guidelines while conducting the experiments. The Hubei Province Centre for Disease Control and Prevention (Wuhan, China) provided 20 specific pathogen free (SPF) ICR mice of female sex. The mice were 8-10 weeks of age and weighed 20±2.1 g. The conditions under which the mice were kept included an SPF environment with alternating 12 h of light and 12 h of darkness. There were no restrictions on water or food. The mice were allowed to become accustomed to the laboratory conditions for 7 d prior to the experiments.

2.2. Colitis Induced by DSS and the Structure of the Experiments. The mice were separated into two groups according to a completely randomized design. The groups were a DSS group and an LPZ group, which were, respectively, given a basal diet [13] and a basal diet enriched with 2 x 10^{10} CFU/kg *L. plantarum* for one week. Colitis was triggered by giving all the mice 5% DSS (MW 36-50 kDa, Kayon Biological Technology Co. Ltd.) in the drinking water on day 8 [13, 14]. The substitution of DSS was conducted daily for one week. Upon completion of the experiments, the average weight gain per day was determined by weighing the mice on the morning of day 15; the mice were anesthetized intraperitoneally and then killed. The measurement of colon length and weight was conducted in line with an earlier study [13]. During the experiment process, the modifications in body weight and disease activity index (DAI) were measured every day to determine how severe the colitis was according to a previously published method [13, 14]. Briefly, the mice were also subjected to evaluation in terms of body weight loss (score: 0 = none; 1 = 0-5%; 2 = 6-10%; 3 = 11-15%; 4 = 16-20%; 5 = 21-25%; and 6 = 26-30%), stool consistency (score: 0 = normal stool; 1 = soft stool; and 2 = liquid stool), and rectal bleeding (score: 0 = negative fecal occult blood; 1 = positive fecal occult blood; and 2 = visible rectal bleeding).

2.3. Histopathological Analysis. The procedures of extraction and fixation in 10% formalin of the terminal colon were conducted. Hematoxylin and eosin were used for preparation and staining of the sections embedded in paraffin for a subsequent histology-based assessment and scoring of epithelial loss (0 = no loss; 1 = 0-5% loss; 2 = 5-10% loss; and 4 = more than 10% loss), crypt damage (0 = no damage; 1 = 0-10% damage; 2 = 10-20% damage; and 3 = more than 20% damage), reduction in the number of goblet cells (0 = none; 1 = mild; 2 = moderate; and 3 = severe), and inflammatory cell infiltration (0 = none; 1 = mild; 2 = moderate; and 3 = severe). These scores were summed to obtain the overall score.

2.4. Enzyme-Linked Immunosorbent Assay. Sandwich enzyme-linked immunosorbent assays (ELISA Ready-SET-GO, eBioscience, CA, USA) were conducted for the purpose of measuring TNF-α, IL-1β, IL-6, IL-10, and IL-17A levels in the colon tissues. Color development was achieved with horseradish peroxidase-avidin. An ELISA microplate reader (Molecular Devices, Sunnyvale, CA, USA) permitted the measurement of the absorbance at 405 nm.

2.5. DNA Purification and Amplification. Prior to conducting the process of extracting DNA, the samples were kept in storage at a temperature of -80°C. The QIAamp DNA Stool Mini Kit (QIAGEN, Hilden, Germany) was used in keeping with the manufacturer's guidelines to extract the DNA from the 200 mg samples. The samples were run on a 1.0% agarose gel to verify how concentrated and pure the DNA was. The general bacterial primers 515F $5'$-GTGCCAGCMGCCGCGGTAA-$3'$ and 926R $5'$-CCGTCAATTCMTTTGAGTTT-$3'$ were used to amplify 16S rRNA genes by carrying out a polymerase chain reaction (PCR). According to the manufacturer's guidelines regarding overhang sequences, the two primers included the primer of the Illumina $5'$ overhang sequence and dual barcodes for the two-step construction of the amplicon library. The reaction volumes (25 μL) comprising 1-2 μL DNA template, 250 mM dNTPs, 0.25 mM of each primer, 1X reaction buffer, and 0.5 U Phusion DNA Polymerase (New England Biolabs, USA) were used to undertake the first PCR reactions. The PCR conditions involved an initial 2 min denaturation at 94°C, followed by 30 cycles of 30 s denaturation at 94°C, 30 s annealing at 56°C, and a 30 s extension at 72°C. These conditions were followed by a final 5 min extension at 72°C. The adaptors and 8 base barcodes were added to either end of the 16S amplicons via eight-cycle PCR reactions of the second-step PCR. The cycling conditions involved an initial 2 min denaturation at 94°C, followed by 30 cycles of 30 sec denaturation at 94°C, 30 sec annealing at 56°C, and a 30 sec extension at 72°C. These conditions were followed by a final 5 min extension at 72°C. A DNA gel extraction kit (Axygen, China) and FTC -3000 TM real-time PCR were, respectively, used for purification and quantification of the barcoded PCR products before library pooling.

2.6. DNA Sequencing and Bioinformatic Analysis. A HiSeq Rapid SBS Kit v2 (Illumina; Tiny Gene Bio-Tech (Shanghai) Co., Ltd) was used for the sequencing of the libraries based on 2∗250 bp paired-end sequencing on the HiSeq platform. The barcode enabled the demultiplexing of the raw fastq files, and base pairs of poor quality were eliminated by running PE reads for every sample via Trimmomatic (version 0.35) and using the parameters SLIDINGWINDOW:

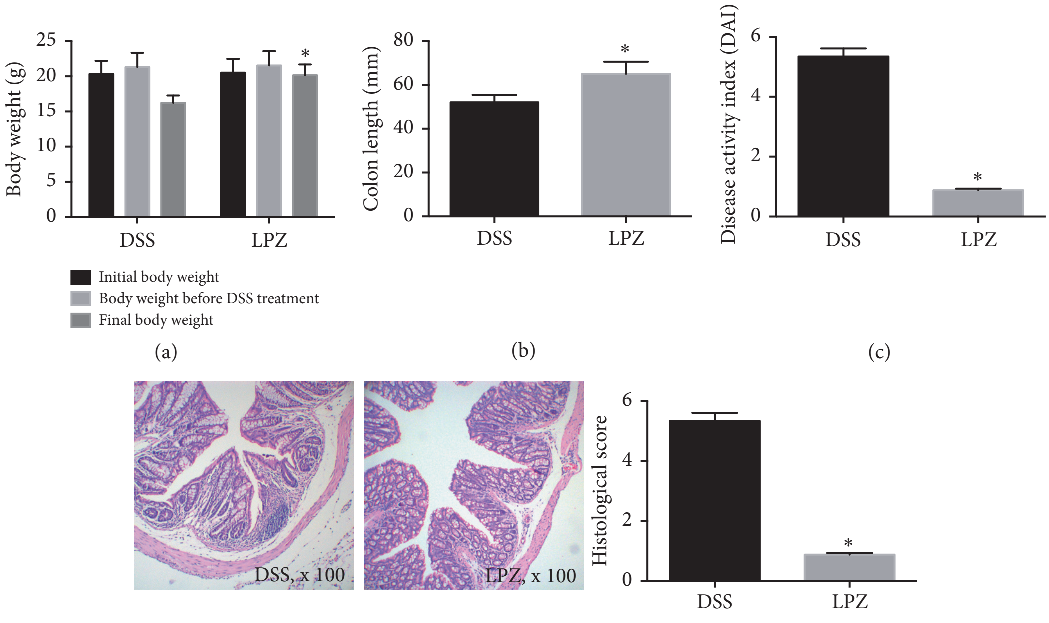

(a)

(b)

(c)

(d)

Figure 1: Effects of *L. plantarum* on (a) the body weight, (b) colon length, (c) disease activity index, and (d) histological score. n=10. ∗ indicated $P < 0.05$ for comparison of the LPZ and DSS groups.

50:20 and MINLEN: 50. The Flash program (version 1.2.11) was subsequently used with default parameters to further integrate the trimmed reads. The screen.seqs command was applied alongside the filtering parameters maxambig=0, minlength=200, maxlength=580, and maxhomop=8 to eliminate contigs of poor quality. The software packages mothur (version 1.33.3), UPARSE (usearch version v8.1.1756, http://drive5.com/uparse/), and R (version 3.2.3) were all used for the purposes of analysis of the 16S sequences. Meanwhile, the UPARSE pipeline (http://drive5.com/usearch/manual/uparse_pipeline.html) permitted the grouping of demultiplexed reads at 97% sequence identity into operational taxonomic units (OTUs). The classify.seqs command in mothur enabled the allocation for taxonomy of the OTU representative sequences against the Silva 119 database with a confidence score equal to or greater than 0.8. NCBI helped to determine OTUs, from phylum to species. mothur permitted the determination of the Shannon, Simpson, Chao, and ACE indices and rarefaction curves for the alpha-diversity analysis, while R was used for plotting those curves. Moreover, mothur also enabled the determination of the weighted and unweighted UniFrac distance matrix for the beta-diversity metrics and principal coordinate analysis (PCoA) and a tree by R facilitated visualization. R was used for both determination and visualization of the Bray-Curtis metrics.

2.7. Statistical Analysis. GraphPad Prism (V.6.0 for Windows; GraphPad Software) based on the Student's *t*-test was used for every statistical analysis. The experimental values are expressed as mean ± standard error of the mean (SEM). Statistical significance is given by a P value of less than 0.05.

3. Results

To determine the impact of *L. plantarum* on the manner in which colitis developed and how severe it became, the weight and colon length of mice from both experimental groups were measured (Figures 1(a) and 1(b)). The LPZ group had a significantly higher body weight and a longer colon length than the DSS group ($P < 0.05$). Meanwhile, the LPZ group had a significantly lower DAI (Figure 1(c)) and histological score (Figure 1(d)) than the DSS group ($P < 0.05$).

An ELISA was used to evaluate the protection conferred by *L. plantarum* against colitis through modulation of inflammatory cytokines (Figure 2). In comparison to the DSS group, the levels of IL-1β, IL-6, IL-17, and TNF-α were decreased in the LPZ group. The level of IL-10 was elevated in the experimental group administered *L. plantarum* ($P < 0.05$).

The v3-v4 regions of 16S rRNA obtained from the fecal samples of the colon were sequenced. The rarefaction curves of the numbers of observed OTUs per sample indicated the mean numbers of observed OTUs were approximately 28,000 sequence reads (Figure 3(a)). Out of the 580 bacterial species-level OTUs found in this study, only 365 (63%) were shared (Figure 3(b)). Nonmetric multidimensional scales (NMDS) were used to detect the relationship among colonic eco-communities to determine whether OTUs identified using the Kruskal-Wallis (KW) filters differentiated between the DSS and LPZ mice. The identified taxa successfully divided the mice into two different groups, and only 1 of the 8 mice in the DSS group clustered with the LPZ group (Figure 3(c)).

The colonic microbial diversity was measured by ACE diversity (Figure 4(a)), Chao diversity (Figure 4(b)), Simpson diversity (Figure 4(c)), and Shannon diversity (Figure 4(d))

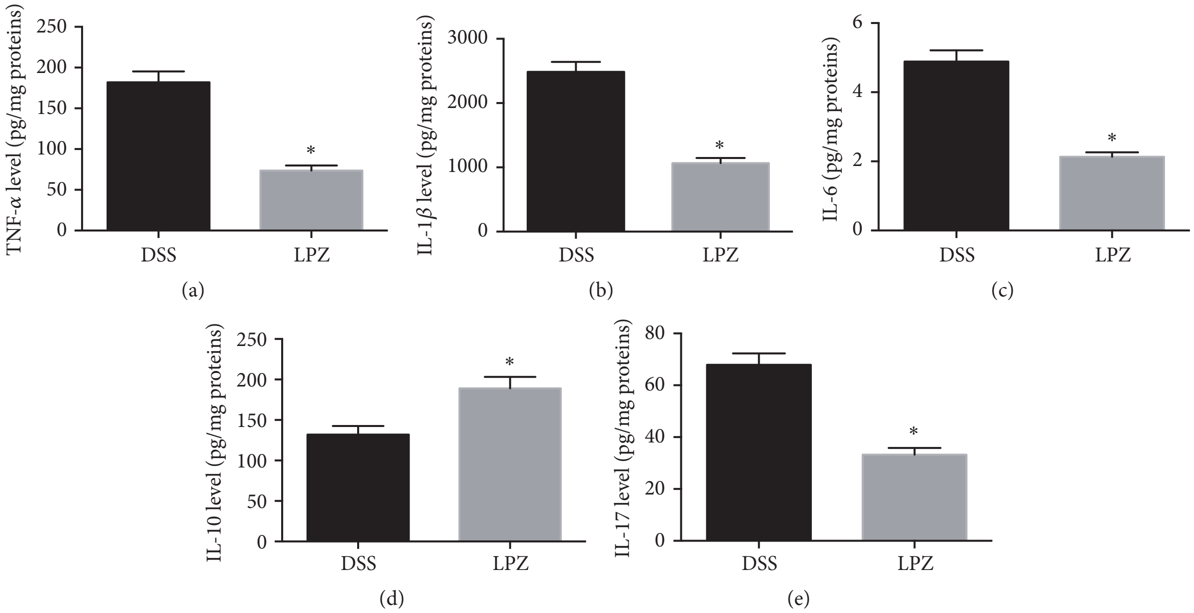

FIGURE 2: Effects of *L. plantarum* on the (a) TNF-α, (b) IL-1β, (c) IL-6, (d) IL-10, and (e) IL-17 of the colonic tissues. N=8, $*$ indicated $P < 0.05$ for comparison of the LPZ and DSS groups.

between the DSS and LPZ groups. *L. plantarum* increased the Simpson index in relation to the mice in the DSS group ($P < 0.05$), but there were no significant effects on the other indices.

The bacteria of the Bacteroidetes, Firmicutes, Verrucomicrobia, and Proteobacteria were predominant at the phylum level, accounting for more than 97% of the total microbial composition (Figure 5(a)). In the DSS and LPZ groups the respective proportions of Bacteroidetes were 41.09% and 50.36%, and for Firmicutes the proportions were 31.78% and 24.09%. The ratio of Firmicutes to Bacteroidetes was increased in LPZ group compared to the DSS group ($P<0.05$) (Figure 5(b)).

Figure 6 shows the top 10 generic-level microbes of relative abundance in the DSS and LPZ groups. The top five genera in the control group were *Akkermansia* (16.45%), *Bacteroides* (12.05%), *Lactobacillus* (10.89%), *Parasutterella* (3.67%), and *Desulfovibrio* (1.25%); in the LPZ group the top five strains were *Akkermansia* (19.02%), *Bacteroides* (17.23%), *Lactobacillus* (2.84%), *Parasutterella* (2.45%), and *Desulfovibrio* (1.06%). The LPZ treatment had a negative effect on the relative abundance of *Lactobacillus* in comparison to the DSS group, with an 8.05% reduction ($P<0.05$).

To identify the specific bacteria in the DSS and LPZ groups, the colonic microbial differential species were analyzed using the linear discriminant analysis (LDA) effect size (LEfSe) based on a nonparametric factorial KW and rank test. Figure 7 shows the species with significant differences, indicated by an LDA score greater than 2.0, which reflects the degree of influence of a species with a significant difference between the groups. A pairwise comparison between the gut microbiota of the DSS and LPZ groups revealed that, at the genus level, the DSS treatment increased the abundance of *Aliihoeflea* and increased *Clostridium methylpentosum* and *Bacteroides intestinalis*; uncultured *Aliihoeflea sp* and *Clostridium sp ASF356* were increased at the species level. Compared to the DSS treatment, there were more diverse changes in the structure of the colonic microbiota. At the phylum level, the oral administration of *L. plantarum* enriched the amount of Firmicutes and increased Erysipelotrichia and Bacilli at the class level. In addition, *L. plantarum* treatment significantly increased the abundance of *Turicibacter* and *Lactobacillus* at the genus level and *Staphylococcus xylosus*, *Bifidobacterium animalis*, *Lactobacillus intestinalis*, *Lactobacillus murinus*, *Gemmobacter intermedius*, and *Lactobacillus prophage Lj928* at the species level.

4. Discussion

IBD manifests as mucosal and systemic inflammation occurring primarily in the large intestine, as in the case of UC, or at any site within the gastrointestinal tract as in the case of CD. The reason for the occurrence of such an inflammatory response is mucosal immune intolerance and especially the disruption of the equilibrium between the anti-inflammatory cytokine IL-10 and other cytokines.

A wide range of IBD treatments exist, but treatment unresponsiveness and occurrence of side-effects continue to be experienced by some patients [15]. Among the latest promising IBD treatments is therapy involving the oral administration of lactic acid bacteria [16, 17]. However, it is still unclear exactly how particular action mechanisms and the therapeutic roles of bacteria are correlated, so the clinical feasibility of this therapy is under debate [18, 19]. We used a mouse model of colitis triggered by DSS to investigate the use of the most popular probiotic, *L. plantarum*, in

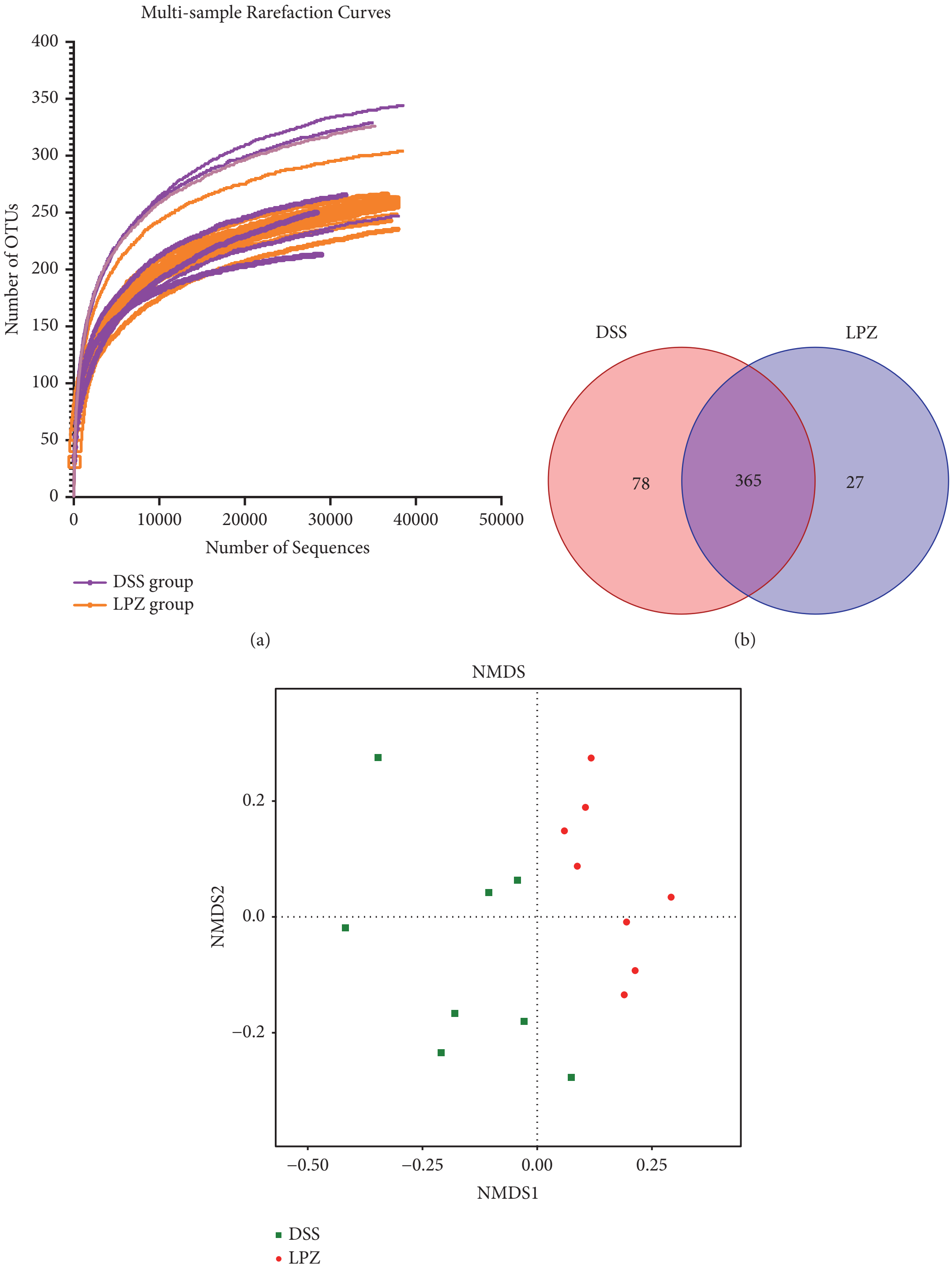

(a)

(b)

(c)

Figure 3: Comparison of the colonic microbial sequences and NMDS analysis between the DSS and LPZ groups. (a) Rarefaction curves show the numbers of unique OTU for each sample. (b) The Venn diagram depicts OTUs that were unique to the 8 mice in the DSS and LPZ groups. (c) The NMDS analysis of the differences between the DSS and LPZ groups. The samples are separated into different parts of the plot, indicating differences between groups or within groups. N=8.

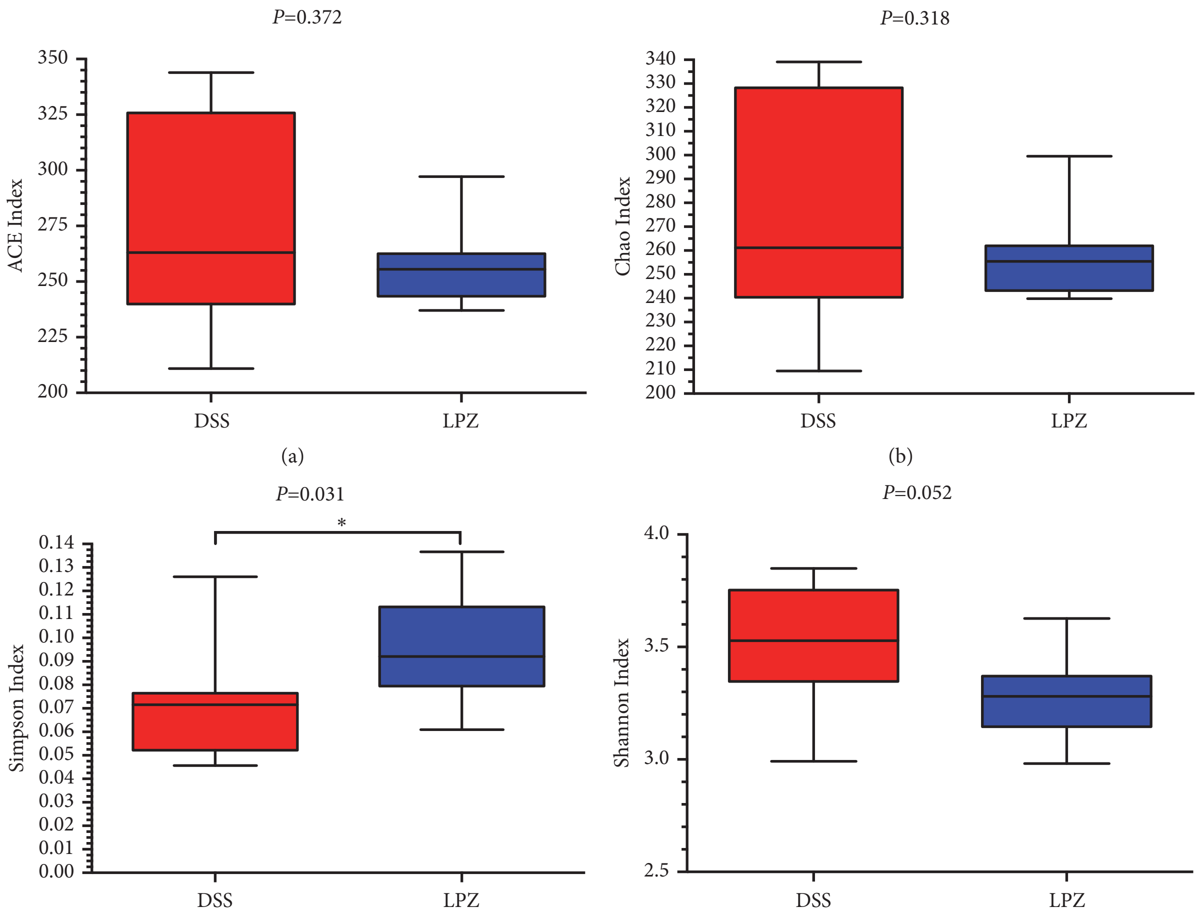

(a) (b) (c) (d)

Figure 4: Phylogenetic diversity of colonic microbiota between the DSS and LPZ groups. Box plots indicate microbiome diversity differences of (a) ACE diversity, (b) Chao diversity, (c) Simpson diversity, and (d) Shannon diversity between the DSS and LPZ groups. N=8, ∗ indicates $P < 0.05$.

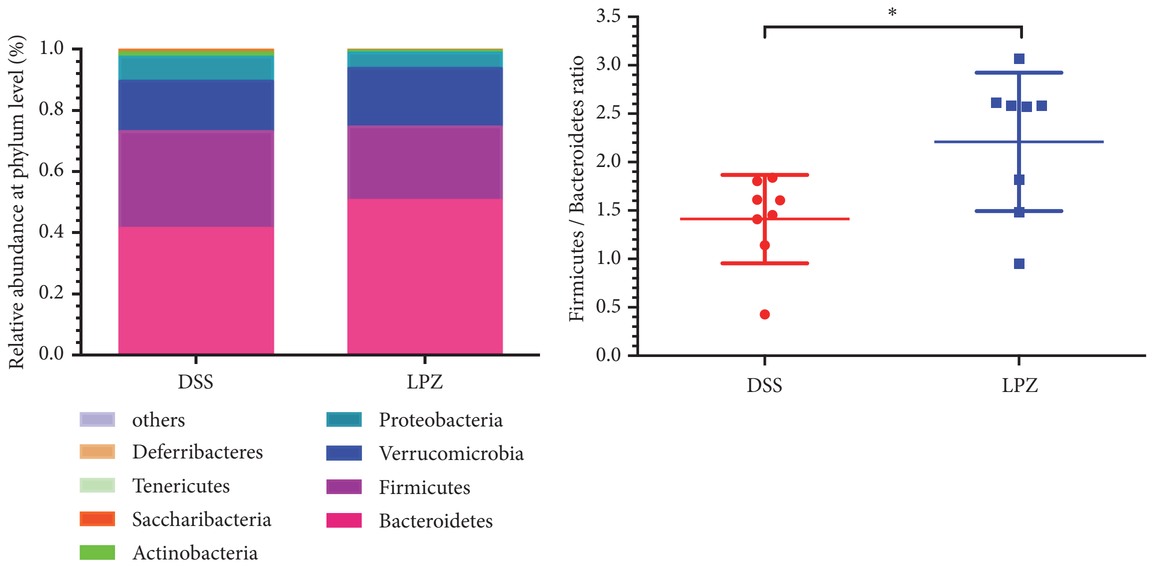

(a) (b)

Figure 5: Analysis of microbial composition at the phylum level. (a) Phylum level microbial changes in the colon in the DSS and LPZ groups. (b) Ratio of Bacteroidetes to Firmicutes in the colon of mice from the two groups. N=8, ∗ indicates $P < 0.05$.

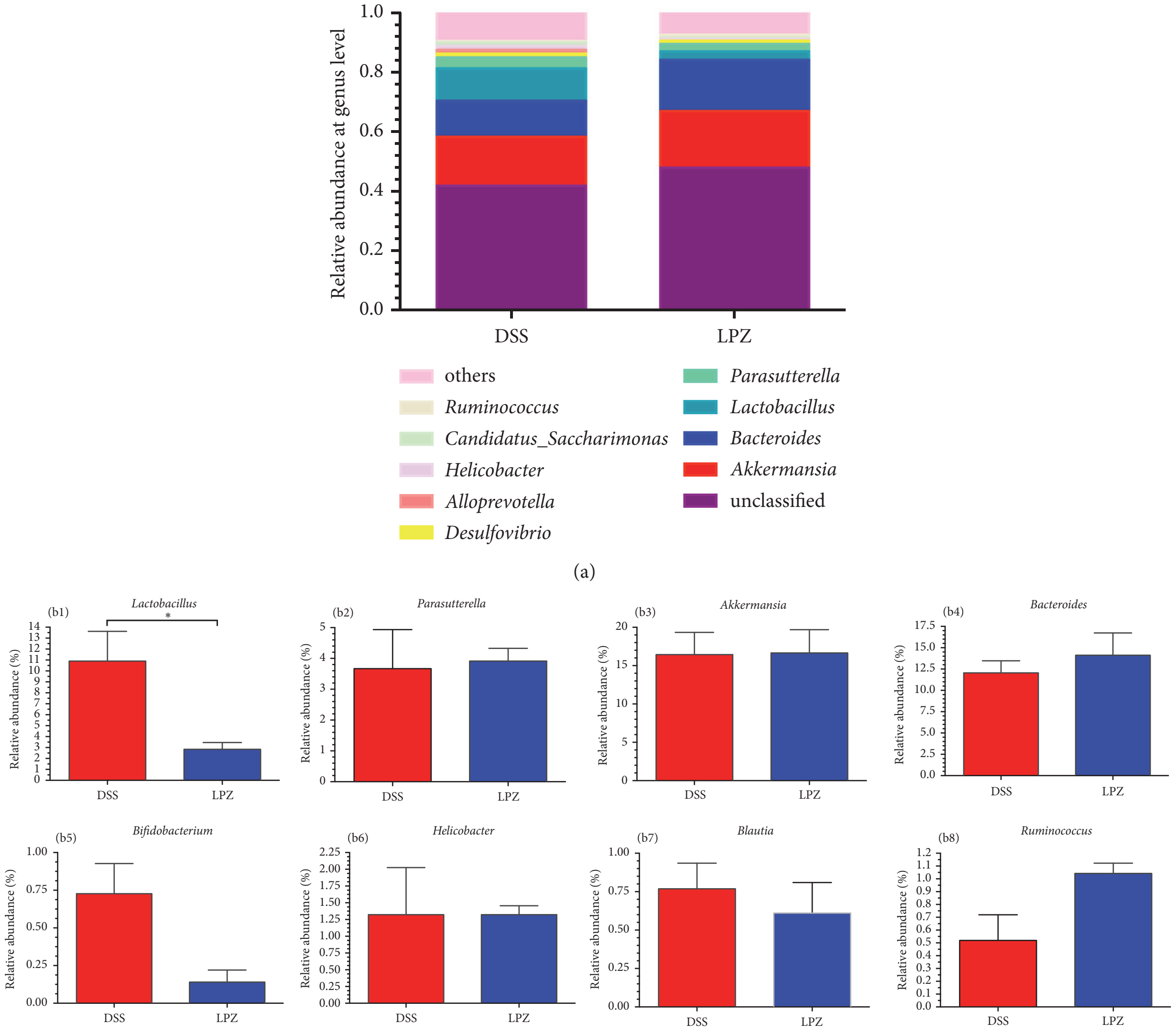

(a)

(b)

Figure 6: Analysis of the microbial composition at the genus level. (a) Genus-level microbial changes in the colon of the DSS and LPZ groups. (b) Comparison of genus-level microbiota in the DSS and LPZ groups: (b1) *Lactobacillus*; (b2) *Parasutterella*; (b3) *Akkermansia*; (b4) *Bacteroides*; (b5) *Bifidobacterium*; (b6) *Helicobacter*; (b7) *Blautia*; and (b8) *Ruminococcus*. N=8, ∗ indicates $P < 0.05$.

IBD treatment. The mice treated with *L. plantarum* did not lose weight or exhibit a reduced colon length. Furthermore, in comparison to the DSS group, the *L. plantarum* group exhibited less pronounced DAI and histological alterations.

IL-10 production was also stimulated by *L. plantarum* directly, but the IL-17 production was inhibited. Recent evidence points to the involvement of IL-17A in the fibrosis of the lungs, liver, and heart [20–22]. Conversely, inflammatory models with suppression of IL-17 revealed the amelioration of fibrosis, while pulmonary fibrosis models showed that cardiac fibroblasts were encouraged by IL-17A to proliferate and migrate [23]. Such findings highlight the fact that fibrosis depends on IL-17 and Th17 cells. In addition to providing protection from the key proinflammatory cytokine TNF-α [24], IL-10 also regulates chronic intestinal inflammation, so colitis of high severity occurs when low IL-10 levels are associated with intestinal endoplasmic reticulum (ER) stress [24, 25]. Meanwhile, evidence has been put forth that IL-10 production in colitis can be stimulated by certain probiotics [26, 27]. Some support exists for the idea that colitis attenuation can be achieved by certain *Lactobacillus* strains through an increase of regulatory T cells (Tregs) in colonic tissues [28]. Nevertheless, the mechanism of the impact of probiotics and IL-10 on ER stress remains unknown, and more research needs to be conducted to determine precisely how *L. plantarum* exerts its effects. Our results imply *L. plantarum* has potential for use as an effective immunomodulator in IBD and could make a notable contribution to IBD treatment.

The value of probiotics for preventing and treating gastrointestinal disorders is gaining recognition [8]. As live microorganisms, probiotics can be beneficial to host health, provided they are administrated in suitable concentrations.

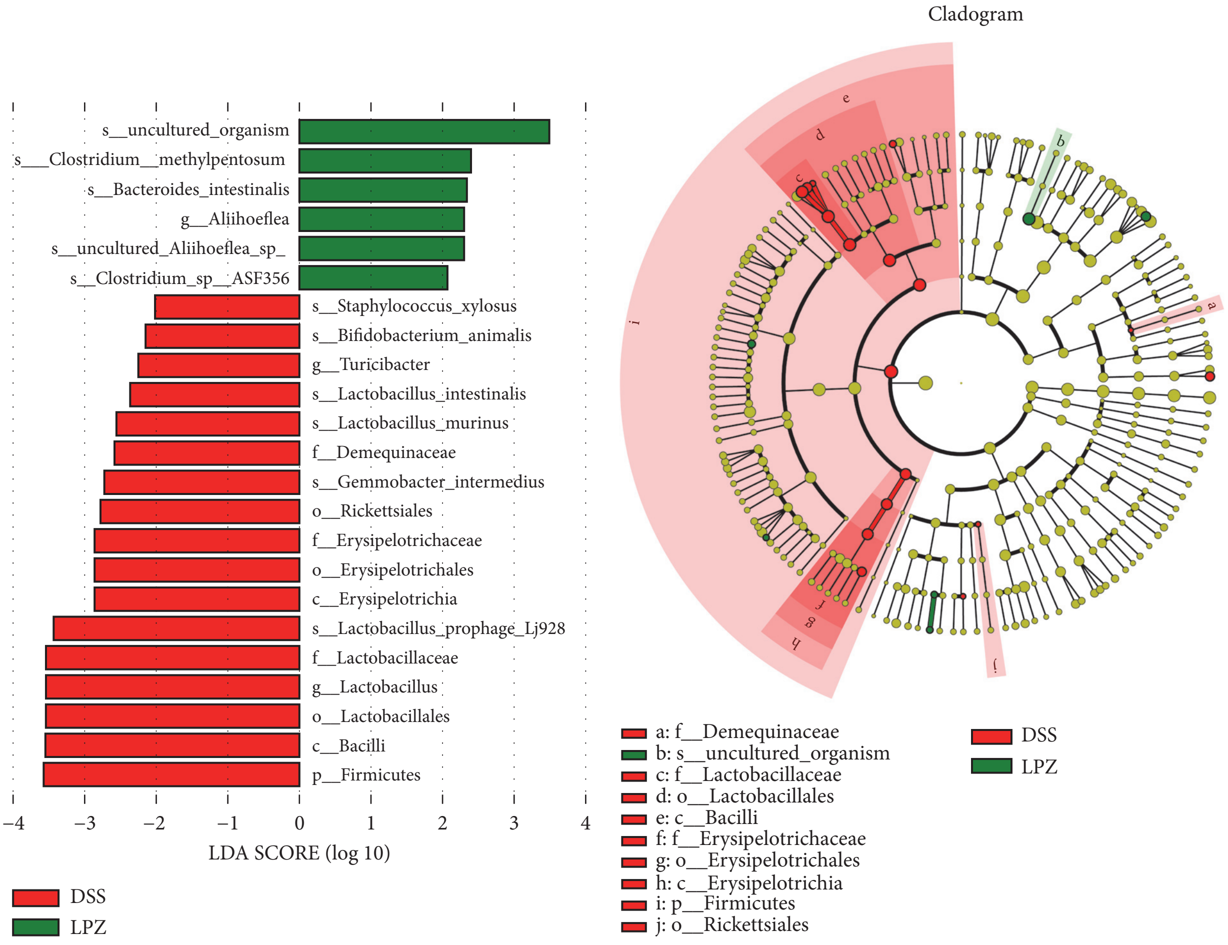

(a)

(b)

Figure 7: LEfSe and LDA analyses based on OTUs characterized the microbiomes of the DSS and LPZ groups. (a) LDA scores show the significant bacterial differences between the LCT and HT (log LDA >2.0; n = 8). (b) Cladogram using the LEfSe method shows the phylogenetic distribution of the colonic microbes associated with the mice administrated DSS (green) and the mice treated with *L. plantarum* (red).

They modulate the proinflammatory and anti-inflammatory cytokines produced by the immunocytes in the gut and thus contribute to the maintenance of homeostasis in the gut microbiota [29, 30]. There are a number of probiotic strains that could be beneficial for IBD, but the clinical use of probiotics has produced incongruous outcomes [31]. Studies examining how probiotics acted against inflammation found NF-κB activation and the expression of inflammatory cytokines in mice with colitis were both hindered by probiotics [32, 33].

Health and wellbeing are dependent on beneficial symbionts and commensals having a mutualistic relation; otherwise dysbiosis and, eventually, disease occur [34]. There is a high degree of complexity to such a “symbiotic ecosystem,” and the lumen and external mucosal layer of the colon contain the greatest aggregation of microorganisms. We investigated the effects of *Lactobacillus plantarum* on colonic microorganisms in a DSS-induced colitis mouse model. The *L. plantarum* treatment increased the colonic microbial diversity and Firmicutes/Bacteroidetes ratio but reduced the relative abundance of *Lactobacillus*. The LEfSe and LDA analyses were used to determine the most diverse taxonomic units in the DSS and the LPZ groups. The bacterium with the greatest influence on the LPZ group at the genus level was *Aliihoeflea*. The bacteria affecting the DSS group were diverse and distributed in various taxon units, such as Firmicutes at the phylum level and *Turicibacter* and *Lactobacillus* at the genus level. The gut microbiota is made more resilient by microbial diversity, contributing significantly to health and wellbeing [35]. The condition of the human gut microbiota has been demonstrated to be reflected in the ratio of Firmicutes to Bacteroidetes [36]. This ratio was decreased in mice with diabetes [37] and in some CD and UC patients, alongside a relative proliferation of proteobacteria [38]. A greater diversity in microbial species results in a more diverse functional response, defined as the level of sensitivity variation to ecosystem modifications exhibited by a species in a community contributing to the same ecosystem function. For instance, when an environmental disruption impacts an abundant species, a less abundant species fulfilling a similar function can take on the role of the abundant species when functional response is suitably diverse [39, 40]. To maintain gut health, beneficial bacteria must be promoted, and pathogenic bacteria must be minimized in the gut microbiota.

There are also some shortcomings of this study. The findings indicate *L. plantarum* reduced the expression of proinflammatory cytokines, thus having a positive impact on colitis. The mechanisms of the inflammation regulation remain unknown. The study also focused solely on the preventive action of *L. plantarum* and not on its therapeutic action. Future research should address these issues and the mechanisms through which the progress of colitis is slowed.

To summarize, *L. plantarum* significantly contributed to the suppression of the inherent production of proinflammatory cytokines during the development of colitis and is likely to ameliorate the pathophysiology of colitis triggered by DSS. *L. plantarum* improved the intestinal tract stability as the impact of intestinal microorganisms was less extensive in the *L. plantarum* group than the DSS group. In conclusion, *L. plantarum* might be effective for managing colitis symptoms and have potential as an effective IBD therapeutic agent.

Data Availability

The data used to support the findings of this study are available from the corresponding author upon request.

Conflicts of Interest

The authors declare that there are no conflicts of interest regarding the publication of this article.

Acknowledgments

This work was supported by the National Key Research and Development Program of China (2017YFD0501000).

References

[1] A. D. Kostic, R. J. Xavier, and D. Gevers, "The microbiome in inflammatory bowel disease: current status and the future ahead," *Gastroenterology*, vol. 146, no. 6, pp. 1489–1499, 2014.

[2] A. Spor, O. Koren, and R. Ley, "Unravelling the effects of the environment and host genotype on the gut microbiome," *Nature Reviews Microbiology*, vol. 9, no. 4, pp. 279–290, 2011.

[3] S. J. Robertson, A. Goethel, S. E. Girardin, and D. J. Philpott, "Innate immune influences on the gut microbiome: lessons from mouse models," *Trends in Immunology*, vol. 39, no. 12, pp. 992–1004, 2018.

[4] S. Ramiro, A. Sepriano, K. Chatzidionysiou et al., "Safety of synthetic and biological DMARDs: a systematic literature review informing the 2016 update of the EULAR recommendations for management of rheumatoid arthritis," *Annals of the Rheumatic Diseases*, vol. 76, no. 6, pp. 1101–1136, 2017.

[5] M. R. Grever, O. Abdel-Wahab, L. A. Andritsos et al., "Consensus guidelines for the diagnosis and management of patients with classic hairy cell leukemia," *Blood*, vol. 129, no. 5, pp. 553–560, 2017.

[6] H. S. P. De Souza, C. Fiocchi, and D. Iliopoulos, "The IBD interactome: an integrated view of aetiology, pathogenesis and therapy," *Nature Reviews Gastroenterology & Hepatology*, vol. 14, no. 12, pp. 739–749, 2017.

[7] Y.-Z. Zhang and Y.-Y. Li, "Inflammatory bowel disease: pathogenesis," *World Journal of Gastroenterology*, vol. 20, no. 1, pp. 91–99, 2014.

[8] G. R. Gibson, R. Hutkins, M. E. Sanders et al., "Expert consensus document: the international scientific association for probiotics and prebiotics (ISAPP) consensus statement on the definition and scope of prebiotics," *Nature Reviews Gastroenterology & Hepatology*, vol. 14, no. 8, pp. 491–502, 2017.

[9] L. E. Hudson, S. E. Anderson, A. H. Corbett, and T. J. Lamb, "Gleaning insights from fecal microbiota transplantation and probiotic studies for the rational design of combination microbial therapies," *Clinical Microbiology Reviews*, vol. 30, no. 1, pp. 191–231, 2017.

[10] L. Chen, Y. Zou, J. Peng et al., "Lactobacillus acidophilus suppresses colitis-associated activation of the IL-23/Th17 axis," *Journal of Immunology Research*, vol. 2015, Article ID 909514, 10 pages, 2015.

[11] Y. A. Ghouri, D. M. Richards, E. F. Rahimi, J. T. Krill, K. A. Jelinek, and A. W. DuPont, "Systematic review of randomized controlled trials of probiotics, prebiotics, and synbiotics in infammatory bowel disease," *Clinical and Experimental Gastroenterology*, vol. 7, pp. 473–487, 2014.

[12] D. Jonkers, J. Penders, A. Masclee, and M. Pierik, "Probiotics in the management of inflammatory bowel disease: a systematic review of intervention studies in adult patients," *Drugs*, vol. 72, no. 6, pp. 803–823, 2012.

[13] W. Ren, J. Yin, M. Wu et al., "Serum amino acids profile and the beneficial effects of L-arginine or L-glutamine supplementation in dextran sulfate sodium colitis," *PLoS ONE*, vol. 9, no. 2, article e88335, 2014.

[14] G. Liu, L. Yu, J. Fang et al., "Methionine restriction on oxidative stress and immune response in dss-induced colitis mice," *Oncotarget* , vol. 8, no. 27, pp. 44511–44520, 2017.

[15] D. C. Baumgart and W. J. Sandborn, "Inflammatory bowel disease: clinical aspects and established and evolving therapies," *The Lancet*, vol. 369, no. 9573, pp. 1641–1657, 2007.

[16] S. Kosler, B. Štrukelj, and A. Berlec, "Lactic acid bacteria with concomitant IL-17, IL-23 and TNFα-binding ability for the treatment of inflammatory bowel disease," *Current Pharmaceutical Biotechnology*, vol. 18, no. 4, pp. 318–326, 2017.

[17] A. de Moreno de LeBlanc, R. Levit, G. Savoy de Giori, and J. G. LeBlanc, "Vitamin producing lactic acid bacteria as complementary treatments for intestinal inflammation," *Anti-Inflammatory & Anti-Allergy Agents in Medicinal Chemistry*, vol. 17, no. 1, pp. 50–56, 2018.

[18] M. Li, Y. Wu, Y. Hu, L. Zhao, and C. Zhang, "Initial gut microbiota structure affects sensitivity to DSS-induced colitis in a mouse model," *Science China Life Sciences*, vol. 61, no. 7, pp. 762–769, 2018.

[19] C. Qin, H. Zhang, L. Zhao et al., "Microbiota transplantation reveals beneficial impact of berberine on hepatotoxicity by improving gut homeostasis," *Science China Life Sciences*, pp. 1–8, 2017.

[20] G. Liu, Q. Jiang, S. Chen et al., "Melatonin alters amino acid metabolism and inflammatory responses in colitis mice," *Amino Acids*, vol. 49, no. 12, pp. 2065–2071, 2017.

[21] Y. Liu, H. Zhu, Z. Su et al., "Il-17 contributes to cardiac fibrosis following experimental autoimmune myocarditis by

a PKCβ/Erk1/2/NF-κB-dependent signaling pathway," *International Immunology*, vol. 24, no. 10, pp. 605–612, 2012.

[22] Y. Lu, H. Lin, K. Zhai, X. Wang, Q. Zhou, and H. Shi, "Interleukin-17 inhibits development of malignant pleural effusion via interleukin-9-dependent mechanism," *Science China Life Sciences*, vol. 59, no. 12, pp. 1297–1304, 2016.

[23] Y. Okamoto, M. Hasegawa, T. Matsushita et al., "Potential roles of interleukin-17A in the development of skin fibrosis in mice," *Arthritis & Rheumatology*, vol. 64, no. 11, pp. 3726–3735, 2012.

[24] S. Z. Hasnain, S. Tauro, I. Das et al., "IL-10 promotes production of intestinal mucus by suppressing protein misfolding and endoplasmic reticulum stress in goblet cells," *Gastroenterology*, vol. 144, no. 2, pp. 357.e9–368.e9, 2013.

[25] J. Liu, J. Wang, H. Luo et al., "Screening cytokine/chemokine profiles in serum and organs from an endotoxic shock mouse model by LiquiChip," *Science China Life Sciences*, vol. 60, no. 11, pp. 1242–1250, 2017.

[26] M. Gad, P. Ravn, D. A. Soborg, K. Lund-Jensen, A. C. Ouwehand, and S. S. Jensen, "Regulation of the IL-10/IL-12 axis in human dendritic cells with probiotic bacteria," *FEMS Immunology & Medical Microbiology*, vol. 63, no. 1, pp. 93–107, 2011.

[27] S. Latvala, M. Miettinen, R. A. Kekkonen, R. Korpela, and I. Julkunen, "Lactobacillus rhamnosus GG and Streptococcus thermophilus induce suppressor of cytokine signalling 3 (SOCS3) gene expression directly and indirectly via interleukin-10 in human primary macrophages," *Clinical and Experimental Immunology*, vol. 165, no. 1, pp. 94–103, 2011.

[28] H.-K. Kwon, C.-G. Lee, J.-S. So et al., "Generation of regulatory dendritic cells and $CD4^{+}Foxp3^{+}$ T cells by probiotics administration suppresses immune disorders," *Proceedings of the National Acadamy of Sciences of the United States of America*, vol. 107, no. 5, pp. 2159–2164, 2010.

[29] M. A. Azad, M. Sarker, and D. Wan, "Immunomodulatory effects of probiotics on cytokine profiles," *BioMed Research International*, vol. 2018, Article ID 8063647, 10 pages, 2018.

[30] M. J. Saez-Lara, C. Gomez-Llorente, J. Plaza-Diaz, and A. Gil, "The role of probiotic lactic acid bacteria and bifidobacteria in the prevention and treatment of inflammatory bowel disease and other related diseases: a systematic review of randomized human clinical trials," *BioMed Research International*, vol. 2015, Article ID 505878, 15 pages, 2015.

[31] P. Marteau, M. Lémann, P. Seksik et al., "Ineffectiveness of Lactobacillus johnsonii LA1 for prophylaxis of postoperative recurrence in Crohn's disease: a randomised, double blind, placebo controlled GETAID trial," *Gut*, vol. 55, no. 6, pp. 842–847, 2006.

[32] Z.-H. Shen, C.-X. Zhu, Y.-S. Quan et al., "Relationship between intestinal microbiota and ulcerative colitis: mechanisms and clinical application of probiotics and fecal microbiota transplantation," *World Journal of Gastroenterology*, vol. 24, no. 1, pp. 5–14, 2018.

[33] S. W. Kim, H. M. Kim, K. M. Yang et al., "Bifidobacterium lactis inhibits NF-κB in intestinal epithelial cells and prevents acute colitis and colitis-associated colon cancer in mice," *Inflammatory Bowel Diseases*, vol. 16, no. 9, pp. 1514–1525, 2010.

[34] J. L. Round and S. K. Mazmanian, "The gut microbiota shapes intestinal immune responses during health and disease," *Nature Reviews Immunology*, vol. 9, no. 5, pp. 313–323, 2009.

[35] H. B. Kim and R. E. Isaacson, "The pig gut microbial diversity: Understanding the pig gut microbial ecology through the next generation high throughput sequencing," *Veterinary Microbiology*, vol. 177, no. 3-4, pp. 242–251, 2015.

[36] R. E. Ley, P. J. Turnbaugh, S. Klein, and J. I. Gordon, "Microbial ecology: human gut microbes associated with obesity," *Nature*, vol. 444, no. 7122, pp. 1022-1023, 2006.

[37] L. Wen, R. E. Ley, P. Y. Volchkov et al., "Innate immunity and intestinal microbiota in the development of Type 1 diabetes," *Nature*, vol. 455, no. 7216, pp. 1109–1113, 2008.

[38] D. N. Frank, A. L. S. Amand, R. A. Feldman, E. C. Boedeker, N. Harpaz, and N. R. Pace, "Molecular-phylogenetic characterization of microbial community imbalances in human inflammatory bowel diseases," *Proceedings of the National Acadamy of Sciences of the United States of America*, vol. 104, no. 34, pp. 13780–13785, 2007.

[39] E. E. Hansen, C. A. Lozupone, F. E. Rey et al., "Pan-genome of the dominant human gut-associated archaeon, Methanobrevibacter smithii, studied in twins," *Proceedings of the National Acadamy of Sciences of the United States of America*, vol. 108, no. 1, pp. 4599–4606, 2011.

[40] C. A. Lozupone, J. I. Stombaugh, J. I. Gordon, J. K. Jansson, and R. Knight, "Diversity, stability and resilience of the human gut microbiota," *Nature*, vol. 489, no. 7415, pp. 220–230, 2012.

Hindawi
BioMed Research International
Volume 2019, Article ID 9461960, 9 pages
https://doi.org/10.1155/2019/9461960

Research Article

Orostachys japonicus A. Berger Extracts Induce Immunity-Enhancing Effects on Cyclophosphamide-Treated Immunosuppressed Rats

Hak Yong Lee,[1] Young Mi Park,[1] Jeong Kim,[2] Hong Geun Oh,[3] Kang Sung Kim,[4] Hee Joo Kang,[5] Ri Rang Kim,[5] Min Jung Kim,[5] Sang Hee Kim,[5] Hye Jeong Yang,[5] and Jisun Oh[6]

[1] *INVIVO Co. Ltd., Iksan, Jeollabuk-do 54538, Republic of Korea*
[2] *Namwon Herb Agricultural Corp., Namwon, Jeollabuk-do 55770, Republic of Korea*
[3] *Huvet Co. Ltd., Iksan, Jeollabuk-do 54630, Republic of Korea*
[4] *Department of Food Science and Nutrition, Yong In University, Yongin, Gyeonggi-do 17092, Republic of Korea*
[5] *Korea Food Research Institute, Wanju, Jeollabuk-do 55365, Republic of Korea*
[6] *School of Food Science and Biotechnology (BK21 Plus), Kyungpook National University, Daegu 41566, Republic of Korea*

Correspondence should be addressed to Jisun Oh; j.oh@knu.ac.kr

Received 26 September 2018; Revised 21 November 2018; Accepted 29 November 2018; Published 6 January 2019

Guest Editor: Hengjia Ni

Copyright © 2019 Hak Yong Lee et al. This is an open access article distributed under the Creative Commons Attribution License, which permits unrestricted use, distribution, and reproduction in any medium, provided the original work is properly cited.

In this study, we evaluated the immunity-enhancing effects of *Orostachys japonicus* A. Berger (OJ). To examine the immune protective effect in vitro, primary mouse splenocytes were treated with water or ethanol extracts of OJ in the absence or presence of cyclophosphamide (CY), which is a cytotoxic, immunosuppressive agent. The extracts increased the propagation of splenocytes and inhibited CY-induced cytotoxicity. Further, to examine the immunostimulatory effects *in vivo*, adult Wistar rats were orally administered OJ extracts with or without CY treatment. With the administration of OJ extracts, CY-treated immunosuppressed rats showed improved physical endurance, as assessed by the forced swim test. In addition, extract administration increased not only the number of immunity-related cells but also the levels of plasma cytokines. OJ extracts also recovered splenic histology in CY-treated rats. These findings suggest that an OJ regimen can enhance immunity by increasing immune cell propagation and specific plasma cytokine levels.

1. Introduction

Cyclophosphamide (CY) is known to possess antitumor and immunomodulatory properties [1, 2]. CY is a cytotoxic agent that disrupts DNA replication and inhibits cell propagation [3, 4] and thus widely used as a chemotherapeutic drug for various types of cancer [2, 5]. In addition, CY can suppress an immune response by modulating lymphocytes [5–8]. Since CY-induced immunosuppression increases vulnerability to pathogen infections and incidence of morbidity and mortality [9–11], adjuvant alternatives in alleviating immunotoxicity and enhancing host immunity are of great interest in cancer therapy [12]. For this reason, the immune-modulating properties of natural plants and their components have been explored for the development of functional foods [9, 13, 14].

Orostachys japonicus A. Berger (OJ), known as rock pine (or "Wa-song" in Korean), is a perennial herb belonging to the family Crassulaceae [15] that contains various bioactive compounds such as flavonoids, triterpenoid, and gallic acid [16–22]. OJ is used as a folk remedy, with antioxidant [22–25], anti-inflammatory, and anticancer effects [26–31]. Recently, the immunostimulatory activity of OJ water extract has been studied in RAW264.7 murine macrophage cell line [20]. However, data to support its physiological function are still required.

In this study, we evaluated the immunity-enhancing effect of OJ water and ethanol extracts *in vitro* and *in vivo* using isolated splenocytes and immunosuppressed rats. In particular, the immunomodulatory effects of OJ extracts *in vivo* were assessed by measuring the number of immunity-related cells and the levels of plasma cytokines with or without OJ extract treatment in CY-treated rats.

2. Materials and Methods

2.1. Preparation of O. japonicus Extracts. Dried OJ (harvested in September 2013; sun-dried) was obtained from the Namwon County Office, Jeollabuk-do, S. Korea. After grinding the dried OJ, including its leaves, stems, and flowers, 100 g of OJ powder was suspended in 1 L of distilled water or 70% ethanol. OJ was extracted from the water or ethanol suspensions by stirring and indirect heating at 100°C or 80°C, respectively, for 3 h. After centrifugation (Beckman, Sanford, ME, USA), at 8000 *g* for 30 min each supernatant was filtered through a filter paper (8-μm pore size; Whatman, Little Chalfont, UK), vacuum-evaporated (rotary evaporator RV 10 control, IKA®; Baden-Württemberg, Germany), and freeze-dried (lyophilizer; Il Shin, Seoul, S. Korea) for use in later experiments.

2.2. Cell Culture. To obtain splenocytes, spleens were aseptically dissected from 8-week-old Balb/c mice. The tissues were teased apart gently with forceps and then forced through a 70-μm cell strainer (SPL Life Sciences, Pocheon-si, Gyeonggi-do, S. Korea). The resulting cell suspension was washed three times in RPMI-1640 (Invitrogen, Carlsbad, CA, USA) by centrifugation (1,000 g, 5 min, 4°C) and treated with red blood cell lysis buffer (Sigma-Aldrich, St. Louis, MO, USA). The isolated splenocytes were maintained in RPMI-1640-based culture medium supplemented with 10% fetal bovine serum (FBS) and 1% penicillin-streptomycin (all from Invitrogen) in a culture incubator (37°C, 5% CO_2, humidified).

2.3. Cell Viability Assay. To test cell viability after administration of the OJ extracts, Cell Counting Kit-8 (CCK-8; Dojindo Laboratories, Kumamoto, Japan) was used as described previously [32]. Briefly, the cultured splenocytes were harvested, suspended in maintenance medium, and dispensed into a 96-well plate at a density of 2×10^5 in 100 μL per well. After the cells were incubated for 24 h, various concentrations of each extract were applied to the cells in the absence or presence of 1.6 mg/mL of CY (Sigma-Aldrich). After 48 h of cultivation, the CCK-8 assay was performed as instructed by the manufacturer. The absorbance (*Abs*), which is proportional to the number of living cells in each well, was measured at 450 nm using a microplate reader (Infinite 200 PRO, Tecan Group Ltd., Männedorf, Switzerland). Cell viability was calculated with the following equation: Cell viability (%) = $(Abs_{\text{sample}} - Abs_{\text{blank}})/(Abs_{\text{control}} - Abs_{\text{blank}}) \times 100$.

2.4. Experimental Animals. All animal studies were conducted according to the guidelines of the Committee on Care and Use of Laboratory Animals of the Wonkwang University (approval number: WKU15-99). Five-week-old male Wistar rats weighing 120–130 g were purchased from Samtako Inc. (Osan-si, Gyunggi-do, S. Korea). After adaptation for 1 week to a 12-h light/12-h dark regimen (temperature, 23 ± 1°C; humidity, 50 ± 5%; illumination, 150–300 lux), with access to food and water *ad libitum*, 6-week-old rats (150 ± 4 g) were used in this study.

2.5. Sample Treatment. Sixty Wistar rats were randomly assigned to six groups (10 rats per group): Untreated (normal), CY-treated (without administration of OJ extract), OJ water extract (OJWE)-low (OJWE administered at 100 mg/kg body weight (BW) with CY treatment), OJWE-high (OJWE administered at 1,000 mg/kg BW with CY treatment), OJ ethanol extract (OJEE)-low (OJEE administered at 100 mg/kg BW with CY treatment), or OJEE-high (OJEE administered at 1,000 mg/kg BW with CY treatment). The OJ extracts were orally administered for 4 weeks using a gastric sonde attached to a syringe on a daily basis. CY was prepared in normal saline and was administered concomitantly with the OJ extracts. To determine the optimal concentration of CY for use in treatments [33], a preliminary *in vivo* experimental study was performed using three different concentrations of CY (5 mg/kg BW, 10 mg/kg BW, and 20 mg/kg BW) in comparison with a control (0 mg/kg BW). Five milligrams of CY/kg BW was determined to be optimal concentration to reduce immunity with minimal effects on body and organ weights and hematology [33, 34] (data not shown).

2.6. Forced Swim Test. To assess physiological changes, the forced swim test was performed as described previously [35]. The test was conducted 1 h after the final sample treatment in a Plexiglass cylinder. Prior to the swimming challenge, each animal was weighed, and a weight of about 10% of the animal's BW was placed on its tail. Swimming duration was measured from the time the animal entered the apparatus to 10 sec after the animal stopped moving.

2.7. Hematological Assay and Enzyme-Linked Immunosorbent Assays (ELISA). After the final administration of OJ extracts, the animals were anesthetized with diethyl ether. Whole blood was collected through the abdominal vena cava in ethylenediaminetetraacetic acid (EDTA) microtubes. White blood cell counts for lymphocytes, monocytes/macrophage, and granulocytes (including neutrophils, eosinophils, and basophils) were analyzed using a Hemavet 950 counter (Drew Scientific Group, Dallas, TX, USA). Plasma cytokines, TNF-α, IFN-γ, and IL-2, were quantified by ELISA kits (R&D Systems, Minneapolis, MN, USA).

2.8. Histological Analysis. After each animal was sacrificed, and the organs (liver, kidney, thymus, and spleen) were removed, weighed, and then fixed in 10% neutral buffered formalin. Fixed organs were processed, embedded in paraffin, and cut into 4–7 μm-thick sections using a microtome (Thermo Scientific, Waltham, MA, USA). The sectioned tissues were then stained with hematoxylin and eosin. Tissue damage was observed under an optical microscope (Olympus, Fukuoka, Japan).

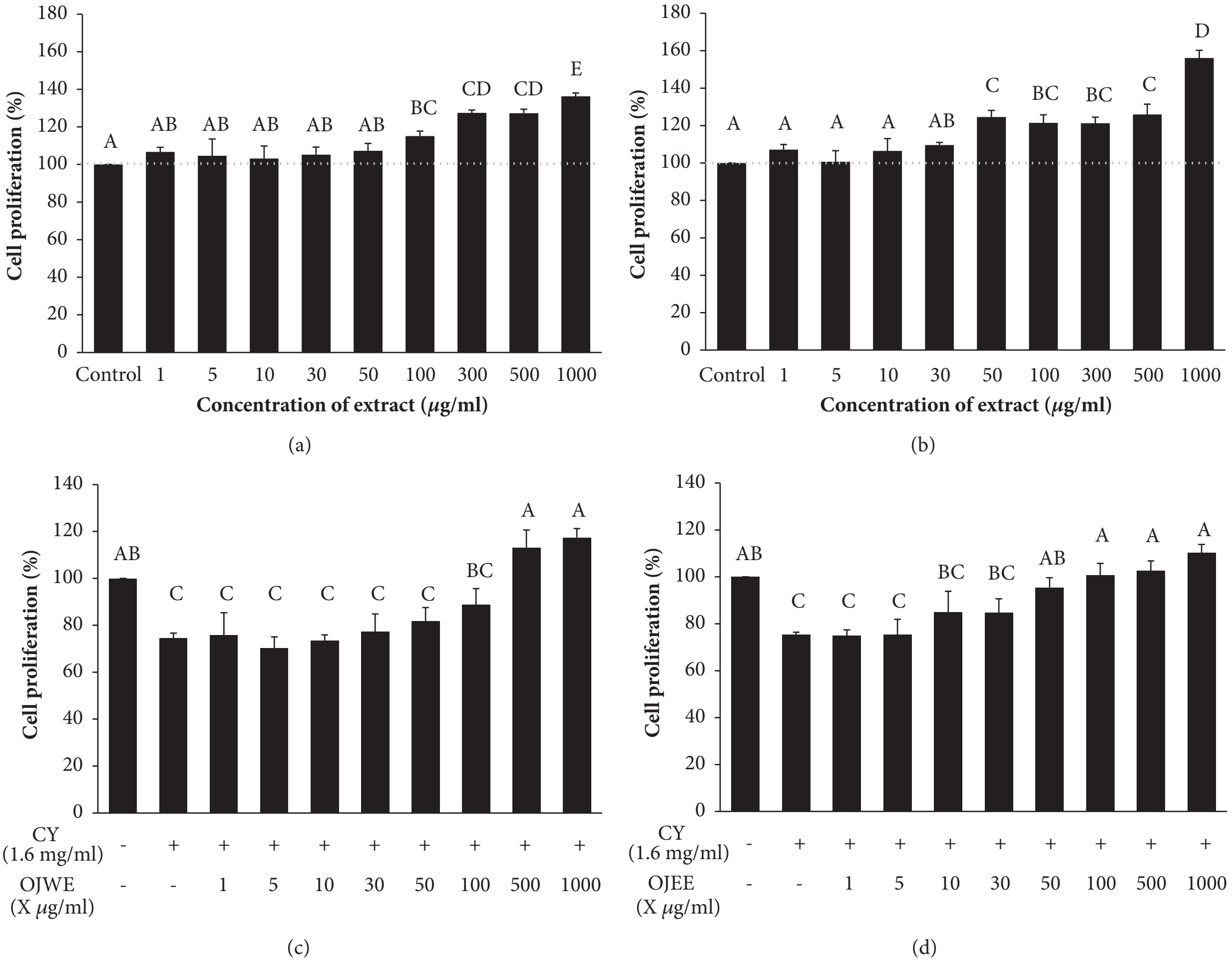

(a)

(b)

(c)

(d)

Figure 1: **OJ extracts increased splenocyte proliferation and protected against CY-induced splenocyte damage**. (a–b) The number of isolated splenocytes was augmented with OJWE (a) or OJEE (b) treatment. (c–d) CY-induced splenocyte cytotoxicity was abolished by OJWE (c) or OJEE (d) treatment. Values represent mean ± standard error of the mean (SEM) from three independent experimental sessions (N = 3). Bars not sharing common letter represent statistically significant difference from each other ($p < 0.05$).

2.9. Statistical Analysis. The data were analyzed by one-way analysis of variance (ANOVA) and Duncan's multiple range test (SAS software; SAS Institute Inc., USA). *P*-values less than an α of 0.05 were considered significantly different. Statistical differences are indicated by letters.

3. Results

3.1. OJ Extracts Stimulate Splenocyte Proliferation and Protect Splenocytes from CY-Induced Damage. To examine the cytotoxicity and cell proliferating effects of both OJWE and OJEE, the isolated splenocytes were treated with various concentrations of the OJ extracts (0, 1, 5, 10, 30, 50, 100, 300, 500, and 1000 μg/mL) for 48 h followed by cell viability testing (Figure 1(a) for OJWE and Figure 1(b) for OJEE). The portion of splenocytes viable increased in a dose-dependent fashion with OJ extract treatment. At 1000 μg/mL of OJWE or OJEE, cell viability was 136.3 ± 1.8% or 156.2 ± 4.1%, respectively, compared to the control (0 μg/mL of OJ extract).

To further examine the cytoprotective effect of OJ extracts against CY-induced damage [4], splenocytes were cultured with the OJ extracts in the absence or presence of CY (Figure 1(c) for OJWE and Figure 1(d) for OJEE). The percent of splenocytes that were viable decreased to about 75% with CY treatment, compared to the control (no treatment). However, cell viability was recovered to the level of the control with treatments of ≥ 500 μg/mL of OJWE or ≥ 50 μg/mL of OJEE.

3.2. OJ Extracts Protect the Thymus and Spleen from Weight Loss Resulting from CY Treatment. To evaluate the effects of a 4-week regimen of OJ extract feeding *in vivo*, 6-week-old Wistar rats were orally administered two different concentrations (100 mg/kg BW or 1,000 mg/kg BW) of OJWE or OJEE. Weekly changes in body weight, water intake, and food intake were monitored for each animal and compared among the groups (Supplementary Figure S1A). There were no significant differences observed among the six groups in any of these measures.

After the animals were sacrificed, the weights of the liver, kidney, thymus, and spleen of each animal were measured and then averaged across the group (Supplementary Figure

S1B–E). No significant differences in kidney weight were observed among the groups. The liver weight in the group that received CY and/or a high-dose of OJEE was slightly higher than that of the other groups. Interestingly, the weights of the immune-related organs (the thymus and spleen) were similar to those of the control group when OJEE was administered.

3.3. OJ Extracts Increase the Swimming Duration and White Blood Cell Counts in Immunosuppressed Rats. To evaluate the effect of OJ extracts on resistance against physical stress, the forced swim test was performed. After being fed OJ extracts without or with CY for 4 weeks, rats were allowed to swim, and then the swimming duration of each rat was measured and averaged across the group (Figure 2(a)). We observed that CY treatment decreased the swimming time, while OJ extract treatment tended to increase the time. In particular, a high-dose of OJEE significantly increased the time.

At the end of the OJ extract regimen, a number of WBCs in the blood collected from the sacrificed animals was determined (Figure 2(b)). Total WBC counts were reduced by CY treatment. However, OJ extract treatment caused the counts to rebound in a dose-dependent manner. This phenomenon was observed for the numbers of lymphocytes, granulocytes, and monocytes as well (Figures 2(c)–2(e)).

3.4. OJ Extracts Increase the Plasma Levels of Immune-Related Cytokines in Immunosuppressed Rats. To test *in vivo* the effect of OJ extracts on the levels of plasma cytokines related to immunity, the concentrations of TNF-α, IFN-γ, and IL-2 were measured in the blood collected from animals in all experimental groups (Figures 3(a)–3(c)). The levels of these cytokines in the CY-treated animals were not significantly different from those of the control (no CY treatment). However, the cytokine levels in the OJ extract-fed groups were all higher than those of the groups that were not fed OJ extracts. More specifically, the IFN-γ and IL-2 levels were significantly higher in the groups fed OJEE than in those fed OJWE.

Furthermore, spleens were sectioned and histologically analyzed (Figure 3(d)). We found in the normal tissue (i) the white pulp surrounded the central vein and (ii) the marginal zone was observed in between the white pulp and red pulp. In the tissues from the CY-treated group, the marginal zone was obscure, and irregular cell condensates were observed in the red pulp area. However, in the tissues from the groups fed OJ extracts, especially those fed a high concentration of extracts, a clear marginal zone between the white and red pulp was present, and cell condensates were rarely observed. This result indicates that administration of OJ extracts ameliorated CY-induced spleen damage.

4. Discussion

In this study, we investigated the activity of OJ water and ethanol extracts on immune enhancement. Both OJ water and ethanol extracts facilitated splenocyte proliferation in a concentration-dependent manner, and the extracts protected splenocytes from CY-induced cytotoxicity. Administration of OJ extracts to CY-treated immunosuppressed rats increased physical endurance, as assessed by the forced swim test. Furthermore, extract administration increased not only WBC counts but also the immunity-related plasma cytokines, TNF-α, IFN-γ, and IL-2 and recovered normal splenic histology.

CY is an alkylating cytotoxic agent that disrupts DNA replication by crosslinking DNA strands, inhibiting cell propagation and inducing apoptosis [3, 4]. CY is metabolized by cytochrome P450 enzymes, which results in the production of 4-hydroxycyclophosphamide that decomposes into the toxic compound phosphoramide mustard [36, 37]. CY is also known to suppress immune responses by modulating lymphocytes [6, 7]. Thus, CY and its metabolites are commonly used as antineoplastic and immunosuppressive drugs [38]. To generate the immunosuppressed animal model in the present study, we used CY to treat isolated splenocytes as well as Wistar rats. *In vitro* results indicated that OJ extracts could recover splenocyte viability after CY treatment. *In vivo* results showed that administration of OJ extracts could at least in part restore immunity affected by CY treatment, suggesting immune recuperation as a result of extract administration.

There have been many reports of immune disturbances associated with behavioral symptoms in the context of depression [39–41]. The CY-immunosuppressed rats may have been more vulnerable to swim stress than the normal rats [42]. Our data from the blood test showed that treatment with CY, an immunosuppressive agent, reduced the number of WBCs, including lymphocytes, granulocytes, and monocytes/macrophages. However, the reduced WBC counts significantly increased in the high-dose OJ extract-administered individuals. In addition, the duration of forced swimming was reduced by CY treatment but increased in the high-dose OJEE-fed groups. These results suggest that OJ extracts, especially a high-dose of OJEE, may impart resilience against stress by stimulating innate and adaptive immunity.

Consistent with the results that suggest an immunostimulatory function of OJ extracts, the plasma levels of the immunity-related cytokines TNF-α, IFN-γ, and IL-2 were augmented in CY-treated animals following the administration of OJ extract. In particular, OJEE significantly increased those cytokines compared to OJWE. Cytokines are generally produced by various immune cells and modulate immune responses, such as immune cell survival and differentiation, inflammation, and host defense against bacterial infection [43–45]. In particular, TNF-α regulates inflammation and host defense in response to bacterial infection [46] and is suppressed by acute stress [47]. INF-γ and IL-2 are produced primarily by T-helper cells [48]. INF-γ is a mediator of innate immunity that activates monocytes/macrophages and upregulates major histocompatibility complex (MHC) molecules [49]. IL-2 is a major growth factor for T cells [50] that enhances T cell responses by regulating homeostasis and differentiation of T-regulatory lymphocytes [51]. Thus, the blood test results support the hypothesis that administration of OJ extracts may stimulate innate and adaptive immunity by facilitating the production of immunity-related cytokines.

According to the existing literature, OJ extracts that showed biologically beneficial effects *in vitro* and *in vivo*

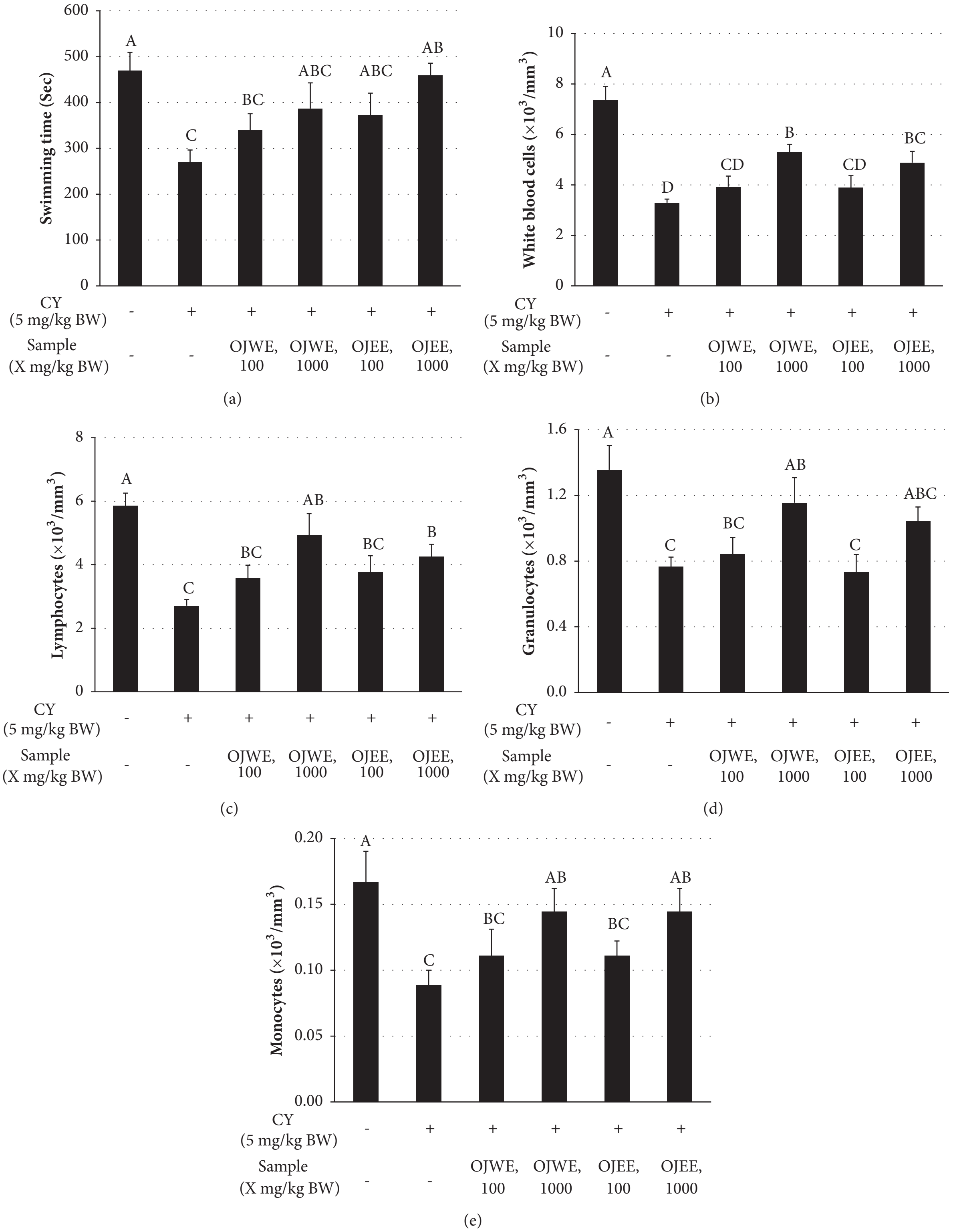

Figure 2: **OJ extracts increased white blood cell counts in immunosuppressed rats**. (a) Swimming duration in the forced swim test. (b–e) White blood cell (WBC) counts: (b) total number of WBCs, (c) lymphocyte counts, (d) granulocyte counts, and (e) monocyte counts. The data obtained from individual animal samples per group were averaged (n = 8); values represent mean ± standard deviation (SD). Bars not sharing common letter represent statistically significant difference from each other ($p < 0.05$).

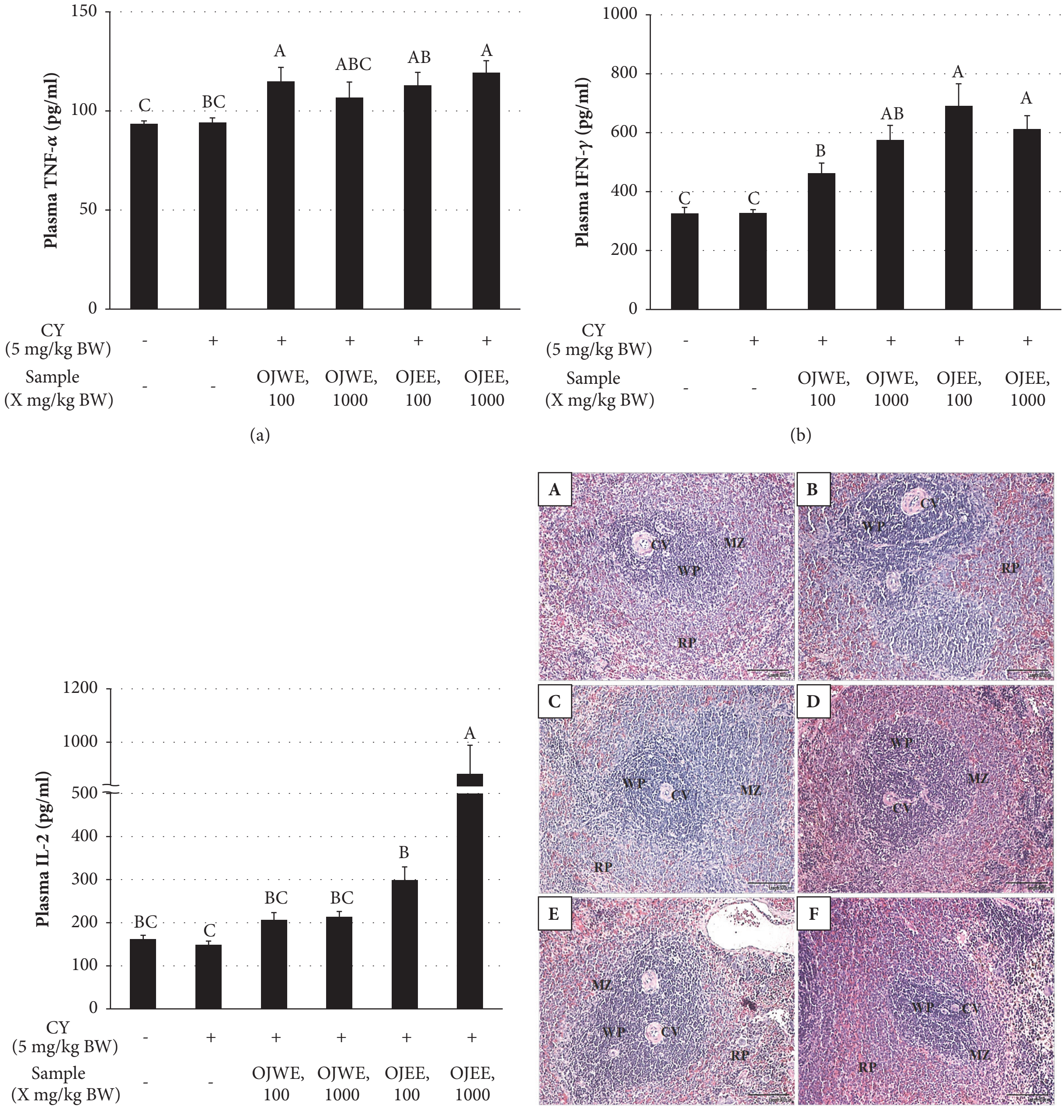

(a)

(b)

(c)

(d)

Figure 3: **OJ extracts increased immunity-associated plasma cytokine levels.** (a) Plasma TNF-α level. (b) Plasma IFN-γ level. (c) Plasma IL-2 level. Values represent mean ± SD (n = 8). Bars not sharing common letter represent statistically significant difference from each other ($p < 0.05$). (d) Representative images of sectioned spleens: (A) normal (no treatment), (B) only CY-treated, (C) OJWE-low, OJWE administered at 100 mg/kg with CY treatment; (D) OJWE-high, OJWE administered at 1,000 mg/kg with CY treatment; (E) OJEE-low, OJEE administered at 100 mg/kg with CY treatment; and (F) OJEE-high, OJEE administered at 1,000 mg/kg with CY treatment. Scale bar in A, 100 μm, applicable to B–F. CV, central vein; MZ, marginal zone; RP, red pulp; WP, white pulp.

exerted strong antioxidant activity and contained a plenty of total phenolics and flavonoids [20–22, 25, 26]. Consistently, both OJWE and OJEE were highly capable of scavenging free radicals (data not shown) and rich in flavonoids (Supplementary Table S1). In particular, OJWE and OJEE highly contained gallic acid, catechins, and glycosides of kaempferol and quercetin. However, identification of bioactive components in the extracts that are responsible for immune enhancement awaits further study.

Taken together, our findings from *in vitro* and *in vivo* studies suggest that OJ extracts, especially in ethanol, have immunity-enhancing and host defense effects by increasing the number of immune-related cells and specific cytokines following immunosuppression.

Data Availability

The datasets generated during and/or analyzed during the current study are available from the corresponding author upon reasonable request.

Additional Points

Practical Application. The activity of water and ethanol extracts of *Orostachys japonicus* A. Berger was investigated on immune enhancement. Our findings indicate that both water and ethanol extracts of *Orostachys japonicus* A. Berger have immunity-enhancing and host defense effects by increasing the number of immune-related cells and specific cytokines following immunosuppression. It would have implications for development of nutraceuticals or functional foods which could aid immunologically vulnerable individuals.

Conflicts of Interest

The authors declare that they have no conflicts of interest.

Authors' Contributions

Hak Yong Lee contributed to experimental design, data collection, analysis, and interpretation; Young Mi Park contributed to collection and assembly of *in vivo* experimental data; Jeong Kim contributed to study conception and financial support; Hong Geun Oh contributed to study conception and supervision of animal studies; Kang Sung Kim contributed to study conception and data interpretation; Min Jung Kim contributed to sample preparation, cell culture, and *in vitro* data collection; Sang Hee Kim contributed to sample preparation, cell culture, and *in vitro* assays; Hye Jeong Yang contributed to project management and supervision of *in vivo* evaluation; Jisun Oh contributed to data interpretation and manuscript writing and is corresponding author.

Acknowledgments

This work was supported by the "Food Functionality Evaluation Program" funded by the Ministry of Agriculture, Food and Rural Affairs and partly by the Korea Food Research Institute (E0150302-02), Republic of Korea.

Supplementary Materials

Supplementary Figure S1: OJ extracts increased the weights of the thymus and spleen in immunosuppressed animals. (A) Weekly changes in the body weights, water intake, and food intake of Wistar rats treated or untreated with OJ extracts. Normal, no treatment; Control, only CY-treated; OJWE-low, OJWE administered at 100 mg/kg with CY treatment; OJWE-high, OJWE administered at 1,000 mg/kg with CY treatment; OJEE-low, OJEE administered at 100 mg/kg with CY treatment; OJEE-high, OJEE administered at 1,000 mg/kg with CY treatment. (B–E) Organ weights of OJ extract-treated rats after termination of the 4-week regimen: (B) percent liver weight over BW, (C) percent kidney weight over BW, (D) percent thymus weight over BW, and (E) percent spleen weight over BW. Values represent mean ± SD (n = 8). Bars not sharing common letter represent statistically significant difference from each other ($p < 0.05$). **Supplementary Table S1**: flavonoid contents in the power or extracts of *O. japonica*. *(Supplementary Materials)*

References

[1] A. Sistigu, S. Viaud, N. Chaput, L. Bracci, E. Proietti, and L. Zitvogel, "Immunomodulatory effects of cyclophosphamide and implementations for vaccine design.," *Seminars in Immunopathology*, vol. 33, no. 4, pp. 369–383, 2011.

[2] M. Ahlmann and G. Hempel, "The effect of cyclophosphamide on the immune system: implications for clinical cancer therapy," *Cancer Chemotherapy and Pharmacology*, vol. 78, no. 4, pp. 661–671, 2016.

[3] S. Brode and A. Cooke, "Immune-potentiating effects of the chemotherapeutic drug cyclophosphamide," *Critical Reviews in Immunology*, vol. 28, no. 2, pp. 109–126, 2008.

[4] O. M. Colvin, "An overview of cyclophosphamide development and clinical applications," *Current Pharmaceutical Design*, vol. 5, no. 8, pp. 555–560, 1999.

[5] L. Galluzzi, A. Buqué, O. Kepp, L. Zitvogel, and G. Kroemer, "Immunological Effects of Conventional Chemotherapy and Targeted Anticancer Agents," *Cancer Cell*, vol. 28, no. 6, pp. 690–714, 2015.

[6] G. Strauss, W. Osen, and K.-M. Debatin, "Induction of apoptosis and modulation of activation and effector function in T cells by immunosuppressive drugs," *Clinical & Experimental Immunology*, vol. 128, no. 2, pp. 255–266, 2002.

[7] L. Bracci, G. Schiavoni, A. Sistigu, and F. Belardelli, "Immune-based mechanisms of cytotoxic chemotherapy: implications for the design of novel and rationale-based combined treatments against cancer," *Cell Death & Differentiation*, vol. 21, no. 1, pp. 15–25, 2014.

[8] X.-H. Huyan, Y.-P. Lin, T. Gao, R.-Y. Chen, and Y.-M. Fan, "Immunosuppressive effect of cyclophosphamide on white blood cells and lymphocyte subpopulations from peripheral blood of Balb/c mice," *International Immunopharmacology*, vol. 11, no. 9, pp. 1293–1297, 2011.

[9] K. Shirani, F. V. Hassani, K. Razavi-Azarkhiavi, S. Heidari, B. R. Zanjani, and G. Karimi, "Phytotrapy of cyclophosphamide-induced immunosuppression," *Environmental Toxicology and Pharmacology*, vol. 39, no. 3, pp. 1262–1275, 2015.

[10] S. Wang, S. Huang, Q. Ye et al., "Prevention of Cyclophosphamide-Induced Immunosuppression in Mice with the Antimicrobial Peptide Sublancin," *Journal of Immunology Research*, vol. 2018, Article ID 4353580, 11 pages, 2018.

[11] A. C. Wiseman, "Immunosuppressive medications," *Clinical Journal of the American Society of Nephrology*, vol. 11, no. 2, pp. 332–343, 2016.

[12] S. I. Grivennikov, F. R. Greten, and M. Karin, "Immunity, Inflammation, and Cancer," *Cell*, vol. 140, no. 6, pp. 883–899, 2010.

[13] S. Chirumbolo, "Plant phytochemicals as new potential drugs for immune disorders and cancer therapy: Really a promising path?" *Journal of the Science of Food and Agriculture*, vol. 92, no. 8, pp. 1573–1577, 2012.

[14] C. I. Abuajah, A. C. Ogbonna, and C. M. Osuji, "Functional components and medicinal properties of food: a review," *Journal of Food Science and Technology*, vol. 52, no. 5, pp. 2522–2529, 2015.

[15] D.-S. Ryu, H.-S. Lee, G.-S. Lee, and D.-S. Lee, "Effects of the ethylacetate extract of Orostachys japonicus on induction of apoptosis through the p53-mediated signaling pathway in human gastric cancer cells," *Biological & Pharmaceutical Bulletin*, vol. 35, no. 5, pp. 660–665, 2012.

[16] H.-J. Jung, J. Choi, J.-H. Nam, and H.-J. Park, "Anti-ulcerogenic effects of the flavonoid-rich fraction from the extract of Orostachys japonicus in mice," *Journal of Medicinal Food*, vol. 10, no. 4, pp. 702–706, 2007.

[17] C. J. Ma, W. J. Jung, K. Y. Lee, Y. C. Kim, and S. H. Sung, "Calpain inhibitory flavonoids isolated from *Orostachys japonicus*," *Journal of Enzyme Inhibition and Medicinal Chemistry*, vol. 24, no. 3, pp. 676–679, 2009.

[18] H. J. Kim, J. Y. Lee, S. M. Kim et al., "A new epicatechin gallate and calpain inhibitory activity from Orostachys japonicus," *Fitoterapia*, vol. 80, no. 1, pp. 73–76, 2009.

[19] S. H. Sung, W. J. Jung, and Y. C. Kim, "A novel flavonol lyxoside of Orostachys japonicus herb," *Natural Product Research (Formerly Natural Product Letters)*, vol. 16, no. 1, pp. 29–32, 2002.

[20] H.-J. Park, H. J. Yang, K. H. Kim, and S. H. Kim, "Aqueous extract of Orostachys japonicus A. Berger exerts immunostimulatory activity in RAW 264.7 macrophages," *Journal of Ethnopharmacology*, vol. 170, pp. 210–217, 2015.

[21] D. Y. Shin, W. S. Lee, J. H. Jung et al., "Flavonoids from orostachys japonicus A. berger inhibit the invasion of LnCaP prostate carcinoma cells by inactivating Akt and modulating tight junctions," *International Journal of Molecular Sciences*, vol. 14, no. 9, pp. 18407–18420, 2013.

[22] S. J. Lee, G. F. Zhang, and N. J. Sung, "Hypolipidemic and hypoglycemic effects of orostachys japonicus A. Berger extracts in streptozotocin-induced diabetic rats," *Nutrition Research and Practice*, vol. 5, no. 4, pp. 301–307, 2011.

[23] J. H. Lee, S. J. Lee, S. Park et al., "Characterisation of flavonoids in *Orostachys japonicus* A. Berger using HPLC-MS/MS: contribution to the overall antioxidant effect," *Food Chemistry*, vol. 124, no. 4, pp. 1627–1633, 2011.

[24] J. C. Park, W. D. Han, J. R. Park, S. H. Choi, and J. W. Choi, "Changes in hepatic drug metabolizing enzymes and lipid peroxidation by methanol extract and major compound of Orostachys japonicus," *Journal of Ethnopharmacology*, vol. 102, no. 3, pp. 313–318, 2005.

[25] S.-J. Lee, E.-J. Song, S.-Y. Lee et al., "Antioxidant activity of leaf, stem and root extracts from orostachys japonicus and their heat and pH stabilities," *Journal of the Korean Society of Food Science and Nutrition*, vol. 38, no. 11, pp. 1571–1579, 2009.

[26] Y. I. Kim, S.-W. Park, Y.-K. Yoon et al., "Orostachys japonicus inhibits the expression of MMP-2 and MMP-9 mRNA and modulates the expression of iNOS and COX-2 genes in human PMA-differentiated THP-1 cellsvia inhibition of NF-κB and MAPK activation," *Molecular Medicine Reports*, vol. 12, no. 1, pp. 657–662, 2015.

[27] G.-S. Lee, H.-S. Lee, S.-H. Kim, D.-H. Suk, D.-S. Ryu, and D.-S. Lee, "Anti-cancer activity of the ethylacetate fraction from Orostachys japonicus for modulation of the signaling pathway in HepG2 human hepatoma cells," *Food Science and Biotechnology*, vol. 23, no. 1, pp. 269–275, 2014.

[28] H.-S. Lee, D. Bilehal, G.-S. Lee et al., "Anti-inflammatory effect of the hexane fraction from Orostachys japonicus in RAW 264.7 cells by suppression of NF-κB and PI3K-Akt signaling," *Journal of Functional Foods*, vol. 5, no. 3, pp. 1217–1225, 2013.

[29] H.-S. Lee, D.-S. Ryu, G.-S. Lee, and D.-S. Lee, "Anti-inflammatory effects of dichloromethane fraction from *Orostachys japonicus* in RAW 264.7 cells: suppression of NF-κB activation and MAPK signaling," *Journal of Ethnopharmacology*, vol. 140, no. 2, pp. 271–276, 2012.

[30] J.-H. Jeong, D.-S. Ryu, D.-H. Suk, and D.-S. Lee, "Anti-inflammatory effects of ethanol extract from *Orostachys japonicus* on modulation of signal pathways in LPS-stimulated RAW 264.7 cells," *BMB Reports*, vol. 44, no. 6, pp. 399–404, 2011.

[31] D. S. Ryu, S. H. Kim, J. H. Kwon, and D. S. Lee, "Anti-proliferative effect of ethylacetate fraction from Orostachys japonicus on modulation of MAPK signaling pathways in human gastric cancer cells," *FASEB Journal*, vol. 27, 2013.

[32] J. Oh, S. B. Jeon, Y. Lee et al., "Fermented red ginseng extract inhibits cancer cell proliferation and viability," *Journal of Medicinal Food*, vol. 18, no. 4, pp. 421–428, 2015.

[33] F. X. Hou, H. F. Yang, T. Yu, and W. Chen, "The immunosuppressive effects of 10 mg/kg cyclophosphamide in Wistar rats," *Environmental Toxicology and Pharmacology*, vol. 24, no. 1, pp. 30–36, 2007.

[34] M. E. De Jonge, A. D. R. Huitema, S. Rodenhuis, and J. H. Beijnen, "Clinical pharmacokinetics of cyclophosphamide," *Clinical Pharmacokinetics*, vol. 44, no. 11, pp. 1135–1164, 2005.

[35] J.-H. Kim, E.-H. Shin, H.-Y. Lee et al., "Immunostimulating effects of extract of Acanthopanax sessiliflorus," *Journal of Experimental Animal Science*, vol. 62, no. 3, pp. 247–253, 2013.

[36] K. M. Huttunen, H. Raunio, and J. Rautio, "Prodrugs-from serendipity to rational design," *Pharmacological Reviews*, vol. 63, no. 3, pp. 750–771, 2011.

[37] S. M. Ludeman, "The chemistry of the metabolites of cyclophosphamide," *Current Pharmaceutical Design*, vol. 5, no. 8, pp. 627–643, 1999.

[38] S. T. Matalon, A. Ornoy, and M. Lishner, "Review of the potential effects of three commonly used antineoplastic and immunosuppressive drugs (cyclophosphamide, azathioprine, doxorubicin on the embryo and placenta)," *Reproductive Toxicology*, vol. 18, no. 2, pp. 219–230, 2004.

[39] C. L. Raison and A. H. Miller, "The neuroimmunology of stress and depression.," *Seminars in Clinical Neuropsychiatry*, vol. 6, no. 4, pp. 277–294, 2001.

[40] L. H. Price and S. A. Rasmussen, "Stress and depression: Is neuroimmunology the missing link?" *Harvard Review of Psychiatry*, vol. 5, no. 2, pp. 108–112, 1997.

[41] J. Blume, S. D. Douglas, and D. L. Evans, "Immune suppression and immune activation in depression," *Brain, Behavior, and Immunity*, vol. 25, no. 2, pp. 221–229, 2011.

[42] E. A. Levay, A. Govic, A. Hazi et al., "Endocrine and immunological correlates of behaviorally identified swim stress resilient and vulnerable rats," *Brain, Behavior, and Immunity*, vol. 20, no. 5, pp. 488–497, 2006.

[43] B. B. Aggarwal, "Signalling pathways of the TNF superfamily: a double-edged sword," *Nature Reviews Immunology*, vol. 3, no. 9, pp. 745–756, 2003.

[44] F. Belardelli and M. Ferrantini, "Cytokines as a link between innate and adaptive antitumor immunity," *Trends in Immunology*, vol. 23, no. 4, pp. 201–208, 2002.

[45] F. Annunziato, C. Romagnani, and S. Romagnani, "The 3 major types of innate and adaptive cell-mediated effector immunity," *The Journal of Allergy and Clinical Immunology*, vol. 135, no. 3, pp. 626–635, 2015.

[46] C. Giai, C. Gonzalez, C. Ledo et al., "Shedding of tumor necrosis factor receptor 1 induced by protein A decreases tumor necrosis factor alpha availability and inflammation during systemic *Staphylococcus aureus* infection," *Infection and Immunity*, vol. 81, no. 11, pp. 4200–4207, 2013.

[47] T. J. Connor, C. Brewer, J. P. Kelly, and A. Harkin, "Acute stress suppresses pro-inflammatory cytokines TNF-α and IL-1β independent of a catecholamine-driven increase in IL-10 production," *Journal of Neuroimmunology*, vol. 159, no. 1-2, pp. 119–128, 2005.

[48] G. E. Kaiko, J. C. Horvat, K. W. Beagley, and P. M. Hansbro, "Immunological decision-making: how does the immune system decide to mount a helper T-cell response?" *The Journal of Immunology*, vol. 123, no. 3, pp. 326–338, 2008.

[49] K. Schroder, P. J. Hertzog, T. Ravasi, and D. A. Hume, "Interferon-γ: an overview of signals, mechanisms and functions," *Journal of Leukocyte Biology*, vol. 75, no. 2, pp. 163–189, 2004.

[50] B. H. Nelson, "IL-2, regulatory T cells, and tolerance," *The Journal of Immunology*, vol. 172, no. 7, pp. 3983–3988, 2004.

[51] P. Zhang, S.-K. Tey, M. Koyama et al., "Induced regulatory T cells promote tolerance when stabilized by rapamycin and IL-2 in vivo," *The Journal of Immunology*, vol. 191, no. 10, pp. 5291–5303, 2013.

Hindawi
BioMed Research International
Volume 2019, Article ID 5756189, 12 pages
https://doi.org/10.1155/2019/5756189

Research Article

Splenectomy Promotes Macrophage Polarization in a Mouse Model of Concanavalin A- (ConA-) Induced Liver Fibrosis

Yongjuan Wang,[1,2] **Xiaopei Guo**,[1] **Guohui Jiao**,[1] **Lili Luo**,[3] **Lu Zhou**,[1] **Jie Zhang**,[1] **and Bangmao Wang**[1]

[1] *Department of Gastroenterology and Hepatology, Tianjin Medical University, General Hospital, Tianjin, China*
[2] *Department of Gastroenterology and Hepatology, The Second Affiliated Hospital of Hebei Medical University, Hebei, China*
[3] *Department of Geriatric Medicine, Tianjin Medical University, General Hospital, Tianjin, China*

Correspondence should be addressed to Lu Zhou; lzhou01@tmu.edu.cn and Jie Zhang; zhangjie_xhk@tmu.edu.cn

Received 2 November 2018; Accepted 24 December 2018; Published 6 January 2019

Guest Editor: Hengjia Ni

Copyright © 2019 Yongjuan Wang et al. This is an open access article distributed under the Creative Commons Attribution License, which permits unrestricted use, distribution, and reproduction in any medium, provided the original work is properly cited.

Background. Splenectomy can improve liver function and survival in patients with autoimmune hepatitis (AIH) and liver cirrhosis. We investigated the underlying mechanism in a mouse model of concanavalin A- (ConA-) induced liver fibrosis. *Methods.* We used ConA to induce immune liver fibrosis in BALB/c mice. Splenectomy was performed alone or with the administration of dexamethasone (DEX). Changes in blood and liver tissues were evaluated. *Results.* Mice treated with ConA for 7 weeks developed advanced liver fibrosis, while splenectomy suppressed liver fibrosis. Although the populations of macrophages/monocytes and M1 macrophages decreased after splenectomy, the inflammatory factors associated with M2 macrophages increased after splenectomy. Furthermore, the population of circulating $CD11b^{+}Ly6C^{high}$ myeloid-derived suppressor cells (MDSCs) increased after splenectomy. After ConA treatment, elevated levels of activated and total NF-kBp65/p50 combined with DNA were observed in hepatic tissues. In contrast, the levels of NF-κB p65/p50 decreased after splenectomy. *Conclusions.* Splenectomy may promote the polarization of $CD11b^{+}Ly6C^{high}$ MDSCs and the differentiation of M2 macrophages while restricting the level of NF-κB p65-p50 heterodimers. These factors may suppress the progression of liver fibrosis.

1. Introduction

Autoimmune hepatitis (AIH) is characterized by the infiltration of mononuclear cells into the liver which, together with elevated levels of gamma globulins and autoantibodies, can induce fibrosis and cirrhosis [1]. Liver cirrhosis frequently causes portal hypertension and splenomegaly and eventually liver failure. Recent studies in various clinical settings have indicated that splenectomy can lead to improvements in both liver function parameters and thrombocytopenia [2, 3]. Moreover, a study by Maruoka et al. demonstrated that splenectomy could treat corticosteroid insufficiency in mice and increased the duration of positive effects from dexamethasone (DEX) [4]. Nonetheless, the mechanism behind this phenomenon remained unknown.

Kupffer cells (KCs) are a subset of highly heterogeneous macrophages that can be stratified into types M1 and M2 [5, 6]. Bacterial lipopolysaccharide (LPS) can stimulate the differentiation of macrophages to the M1 type, which produce the inflammatory factors tumor necrosis factor- (TNF-) α, interleukin- (IL-) 12, IL-23, and inducible nitric oxide synthase (iNOS). In contrast, IL-4, IL-13, IL-10, and glucocorticoids can induce macrophage polarization to the M2 type, which produce cytokines such as IL-4, IL-5, and IL-10, which can inhibit inflammation while promoting blood and lymphatic vessel formation, digestion, and extracellular matrix repair [7, 8]. Therefore, macrophages and macrophage-related factors might play an essential role in the development and pathogenesis of hepatic lesions and fibrosis [9–11]. However, the polarization of M1/M2 macrophages in AIH remains unclear.

Myeloid-derived suppressor cells (MDSCs) comprise a heterogeneous population of cells that inhibit the proliferation and regular functions of T cells, suppress the cytotoxicity of NK cells, and accelerate the polarization of regulatory T cells (Tregs) in tumor-bearing hosts, all of which play key regulatory roles in tumor-related diseases [12, 13]. In mice, MDSCs are $CD11b^{+}Gr1^{+}$ myeloid cells, which can be subdivided into $CD11b^{+}Gr1^{+}Ly6G^{high}$ $Ly6C^{low}$ and $CD11b^{+}Gr1^{+}Ly6G^{low}Ly6C^{high}$ MDSCs. Although many reports have discussed the immunosuppressive function of MDSCs in various cancer-related diseases, the specific regulatory mechanisms of these cells in immunological liver disease remained unclear [13, 14]. Zhang et al. established a model of acute immunological liver injury by injecting BALB/c mice with concanavalin A (ConA) and found that rapamycin could promote the proliferation of $CD11b^{+}Gr1Ly6C^{high}$MDSCs, which protected against immunological hepatic injury in this model [15]. This led us to wonder whether splenectomy could inhibit liver fibrosis by promoting the polarization of MDSCs.

NF-κB, a key transcription factor, is found in cell types throughout the body. This factor is a homo- or heterodimer comprising the p50 and p65 (RelA) subunits [16]. The regulation of NF-κB signaling may lead to macrophage-driven inflammation in both autoimmune and hematological diseases [17, 18]. Furthermore, NF-κB p50 can regulate M2 polarization in the context of LPS-induced inflammation [19]. However, the correlation between macrophage infiltration and underlying NF-κB function in immune-related liver fibrosis remained unclear.

Con A-induced hepatitis is a widely accepted and successful mouse model of AIH that resembles advanced immune-related liver fibrosis in humans [20, 21]. In this study, we investigated the effects of splenectomy in a mouse model of ConA-induced liver fibrosis and determined whether MDSCs and NF-κB were necessary to the protective effects of splenectomy against liver cirrhosis in these animals.

2. Methods

2.1. Animal Models. The study was approved by the Medical Ethics Committee of the General Hospital of Tianjin Medical University. All animals used experimentally were treated humanely, and all procedures were conducted according to the guidelines set forth by the Animal Care Committee of the General Hospital of Tianjin Medical University. Specific pathogen-free female BALB/c mice (7 weeks of age) were acquired from Beijing, China. A total of 24 mice were used for the experiments. The mice were randomly assigned to four groups: the control group, ConA model group, splenectomy group, and splenectomy combined with dexamethasone (DEX) group. Except mice in the control group, all mice received a weekly dose of 12.5 mg/kg body weight of ConA via tail vein injection. Splenectomy was conducted 1 day after the sixth injection. Mice in the splenectomy combined with DEX group also received an intraperitoneal injection of DEX at 1 mg/kg body weight every second day. To mimic the presence of immune damage *in vivo*, ConA treatment was maintained until death. All mice were sacrificed after 7 weeks, and blood and liver tissue samples were collected. The liver tissues were embedded in paraffin and subjected to hematoxylin and eosin (H&E) staining and Masson's trichrome staining.

2.2. Splenectomy. For splenectomy, the abdominal wall of the mouse was opened by making a left subcostal minimal incision under chloral hydrate. The splenic arteries and veins were ligated at the splenic hilum with a 3–0 silk suture and divided. All surgical procedures were conducted under completely sterile conditions.

2.3. Histological Analysis. The histological analysis procedures have already been outlined according to previous reports [22, 23]. Liver tissues were fixed in 10% buffered formalin and embedded in paraffin. Subsequently, the samples were stained with H&E and Masson's trichrome (to assess fibrosis) and evaluated under a light microscope.

2.4. Immunohistochemical Staining. Samples were also subjected to immunohistochemistry. A goat monoclonal antibody (mAb) specific for human CD68 (Santa Cruz Biotechnology, Dallas, TX, USA) and mouse mAb specific for human CD206 (Santa Cruz Biotechnology) were used to label macrophages and M2 macrophages. A goat mAb specific for mouse α-smooth muscle actin (SMA, Santa Cruz Biotechnology) was used to label α-SMA. The labeled sections were further incubated with a biotin-free secondary antibody. Horseradish peroxidase (Santa Cruz Biotechnology) was then applied, and the labeled tissues were developed using diaminobenzidine (Sigma, St Louis, MO, USA) followed by hematoxylin counterstaining.

2.5. Immunofluorescence Staining. A goat mAb specific for human CD68 and mouse mAb specific for human CD206 (both Santa Cruz Biotechnology) were used to immunofluorescently label macrophages and M2 macrophages. Goat mAbs specific for mouse F4/80 and mouse iNOS (both Abcam, Cambridge, MA, USA) were used to immunofluorescently label macrophages and M1 macrophages. The following reagents were used in all immunofluorescence experiments: Alexa 488-labeled donkey anti-rat, Alexa 647-labeled donkey anti-rabbit antibodies (Molecular Probes, Eugene, OR, USA), Alexa Fluor 568-labeled donkey anti-mouse, and Alexa Fluor 488-labeled rabbit anti-goat. DAPI was used for nuclear counterstaining.

2.6. Quantitative RT-PCR (Real-Time PCR). The RT-PCR analysis was conducted as previously described [24, 25]. Table 1 lists the primers used in this experiment. The data were analyzed using SDS 2.1 software. For all target genes, the expression is represented as a "fold change" relative to the control sample ($2\text{-}^{\triangle\triangle}$comparative threshold).

2.7. MAbs and Flow Cytometry. MAbs specific for CD11b (M1/70), F4/80 (BM8), and Ly6C were obtained from BioLegend (San Diego, CA, USA). The cells were suspended in buffer and incubated with the above antibody for 30 minutes. Subsequently, the cells were analyzed on a FACSCalibur flow cytometer (Becton Dickinson, San Jose, CA, USA) or Beckman Coulter Epics XL bench-top flow cytometer (Beckman Coulter, Brea, CA, USA). Data were analyzed using FlowJo software (TreeStar, Ashland, OR, USA). The number

Table 1: Oligo sequences for RT-PCR used in this study.

genes	Forward	Reverse
β-actin	5′-TGTGTCCGTCGTGGATCTGA-3′	5′-CCTGCTTCACCACCTTCTTGA-3′
IL-10	5′-TGGACAACATACTGCTAACCG-3′	5′-GGATCATTTCCGATAAGGCT-3′
ARG-1	5′-TGGCTTGCGAGACGTAGAC-3′	5′-GCTCAGGTGAATCGGCCTTTT-3′
IL-4	5′-CACCAGCTATGCATTGGAGA-3′	5′-TTTGGCGGTCAATGTATTTCT-3′

of cells in several different populations was calculated by multiplying the percentages of the counted targeted cells by the number of total cells.

2.8. Western Blotting. Polyvinylidene fluoride (PVDF) membranes were incubated overnight at 4°C with antibodies specific for NF-κB p50 and NF-κB p65 (Santa Cruz Biotechnology). Samples were then washed in Tris-buffered saline with Tween-20 and labeled further with a goat anti-mouse secondary antibody (LI-COR Biotechnology, Lincoln, NE, USA). Labeled protein bands were detected using an Odyssey infrared imaging system (LI-COR). Glyceraldehyde 3-phosphate dehydrogenase (GAPDH) was used as an internal reference control.

2.9. Electrophoretic Mobility Shift Assay (EMSA). PCR primers were labeled with [-33P]-ATP (Perkin Elmer, Waltham, MA, USA) using T4 DNA polynucleotide kinase (New England Biolabs, Ipswich, MA, USA). Subsequently, DNA probes were created by labeling the forward primers and unlabeling the reverse primers via PCR. Two micrograms of nuclear protein were incubated with a biotin-labeled NF-κB p65 binding-site DNA probe (5′-AGTTGAGGGGACTTTCCCAGGC-3′; Sigma Genosys) in buffer for 30 minutes on ice. Gels were placed on Whatman paper, vacuum-dried, and exposed to a phosphoscreen for 12 hours. Subsequently, the screen was scanned using a storm 860 PhosphorImager, and the data were analyzed using ImageQuant software (Molecular Dynamics/GE Healthcare, Amersham, UK).

2.10. Statistical Analysis. All numeric values are expressed as means ± standard deviations (SD). Students' t-test or the Mann–Whitney U test was used to detect the statistical significance of differences between groups. Multiple group comparisons were assessed using a one-way analysis of variance (ANOVA) combined with Bonferroni's post hoc test. A P value<0.05 was considered the statistical significance threshold.

3. Results

3.1. Effects of Splenectomy in a Mouse Liver Fibrosis Model. Clear increases in splenic volume were observed after a 5-week course of intravenous ConA injection, and the resulting immune hepatic injury was characterized by hepatocellular necrosis, portal inflammation, mononuclear cell infiltration into the parenchyma, and sinusoidal hyperemia (Figures 1(a), 1(b), and 1(c)). These tissue changes were concomitant with significant increases in the serum levels of aspartate aminotransferase (AST) and alanine aminotransferase (ALT ($P<0.05$) (Figure 1(d)). Most importantly, immunohistochemical staining of α-SMA revealed a marked and significant increase in the number of activated hepatic stellate cells ($P<0.05$) (Figure 1(e)).

3.2. Splenectomy Attenuated ConA-Induced Liver Fibrosis. In the ConA model group, the hepatic surfaces were dark red and granular, whereas mice were subjected to splenectomy had smooth hepatic surfaces (Figure 2(a)). Notably, splenectomy was associated with significant decreases in serum ALT and AST levels ($P<0.05$) (Figure 2(b)). An analysis of liver tissue from the splenectomy group revealed a decrease in interface hepatitis (Figure 2(c)) and significant attenuation of liver fibrosis, as indicated by a semiquantitative analysis of α-SMA-positive areas ($P<0.05$) (Figures 2(d) and 2(e)), Masson-stained areas (Figure 2(f)), and Ishak scores ($P<0.05$) (Figure 2(g)). The Ishak score was lower in the DEX group relative to the splenectomy group ($P<0.05$).

3.3. Percentages of Macrophages/Monocytes and M2 Macrophages. We used flow cytometry, immunofluorescence staining, and RT-PCR to detect changes in the numbers of monocytes in peripheral blood and liver macrophage populations. Notably, the ratio of F4/80-positive monocytes in the peripheral blood increased significantly in the ConA model group but decreased in the splenectomy group ($P<0.05$) (Figure 3). Immunofluorescence staining (Figure 4(a)) revealed increases in the percentages of F4/80-positive macrophages and M1 (F4/80$^+$iNOS$^+$) macrophages after ConA treatment, as well as decreases in both populations after splenectomy ($P<0.05$) (Figure 4(b)). Furthermore, RT-PCR revealed the increased expression of mRNAs encoding M2 macrophage-associated factors, such as IL-10, ARG-1, and IL-4, after splenectomy ($P<0.05$) (Figure 4(c)).

3.4. Splenectomy Promoted the Differentiation of CD11b$^+$Ly6C^{high} MDSCs in the Peripheral Blood. To evaluate the potential involvement of MDSCs in ConA-induced immune liver fibrosis, we used flow cytometry to analyze peripheral MDSCs. Notably, the proportion of CD11b$^+$Ly6C$^+$ MDSCs decreased after ConA treatment but increased significantly after splenectomy ($P<0.05$) (Figures 5(a) and 5(b)). We also used flow cytometry to analyze changes in the percentage of CD11b$^+$Ly6C^{high} MDSCs in the peripheral blood. Here, the percentage of CD11b$^+$Ly6C^{high}

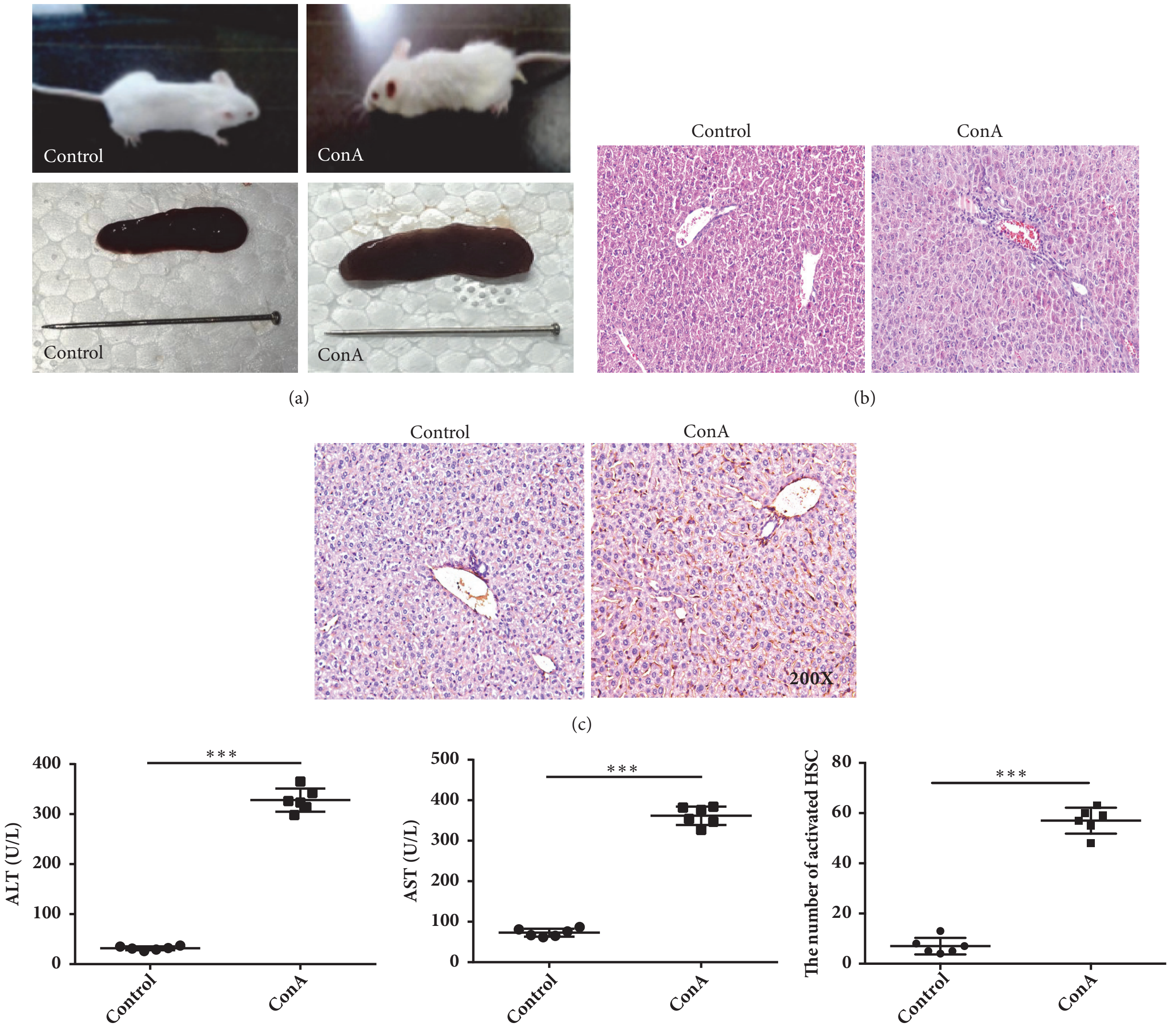

(a) (b)

(c)

(d) (e)

Figure 1: Morphological and immunohistochemical analysis of liver tissues in control and concanavalin A- (ConA-) treated mice. (a) Mice and liver in the control and ConA-treated groups. (b) Hematoxylin and eosin staining showing inflammatory cell infiltration in the portal area. (c) Immunohistochemical analysis of α-smooth muscle actin (SMA) expression in liver tissues (immunohistochemical stain, magnification ×200). (d) Alanine (ALT) and aspartate aminotransferase (AST) levels detected using an enzyme-linked immunosorbent assay. (e) The numbers of activated hepatic stellate cells (HSC). $***$ indicates $P < 0.001$.

MDSCs decreased after ConA treatment but increased significantly after splenectomy (P<0.05) (Figures 5(a) and 5(b)).

3.5. Splenectomy Inhibited NF-κB Signaling in Immune Hepatic Fibrosis. We next used Western blotting to analyze the levels of NF-κB p65 and NF-κB p50 proteins in the liver. The level of p65 decreased dramatically after splenectomy (P<0.05), whereas the expression of p50 was increased after splenectomy (P<0.05) (Figure 5(c)).

Finally, to analyze the DNA-binding capacity of nuclear p65, we used EMSA to measure the amounts of the NF-κB p50/p65 heterodimer and p50/p50 homodimer that had bound to a specific site using a ^{32}P-labeled probe containing the −178 site. A band larger than the p50 homodimer band was extracted from cells cotransfected with p50 and p65 and indicated that p50/p65 could bind to the specific site, suggesting that the levels of both p50/p65 and p50/p50 increased significantly after ConA treatment (P<0.05). In contrast, the level of the p50/p65 heterodimer decreased significantly after splenectomy (P<0.05). Furthermore, the levels of both p50/p65 and p50/p50 were significantly decreased in the DEX group (P<0.05) (Figure 5(d)).

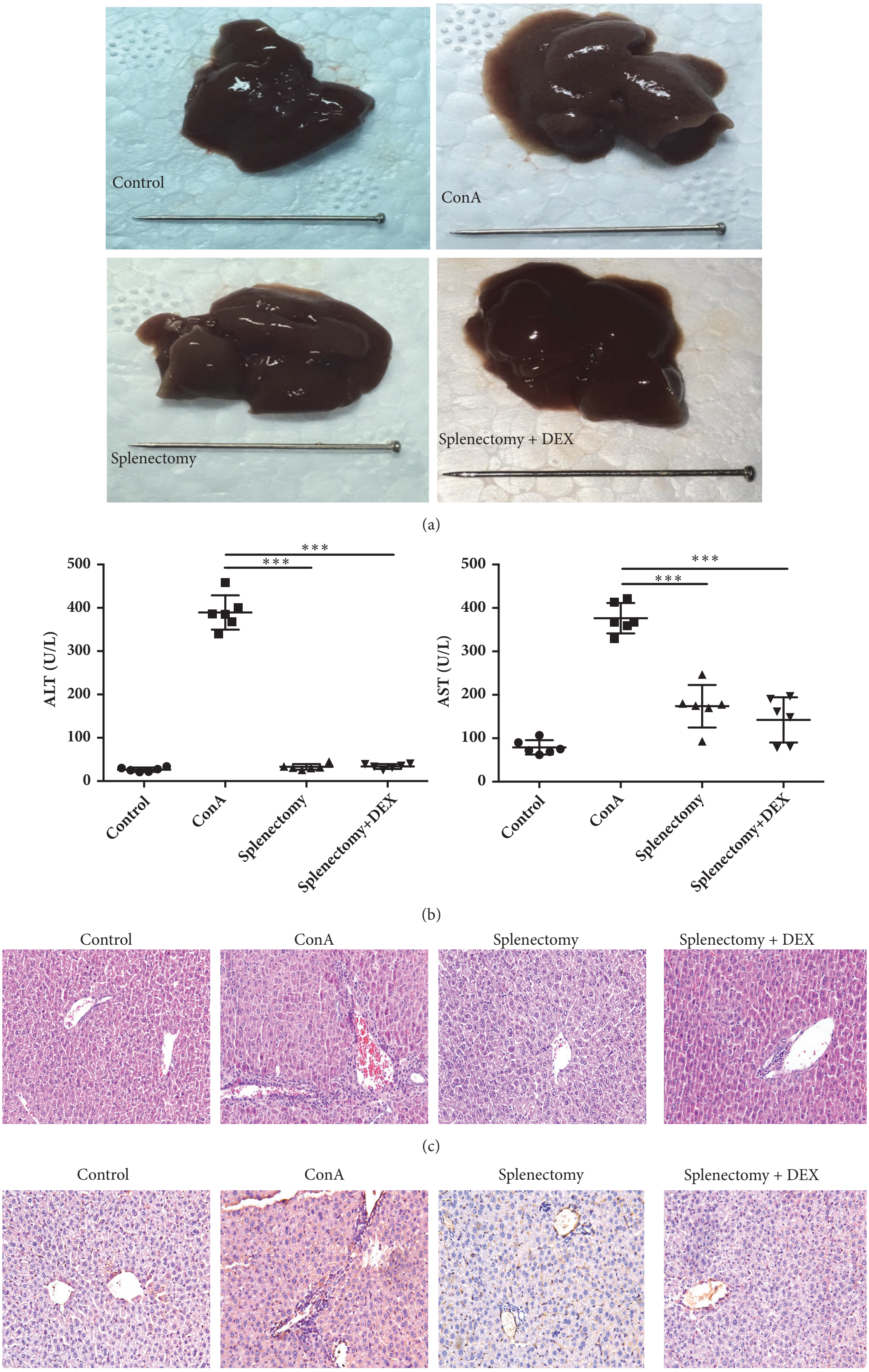
Control
ConA
Splenectomy
Splenectomy + DEX
(a)
ALT (U/L)
500
400
300
200
100
0
***
***
Control
ConA
Splenectomy
Splenectomy+DEX
AST (U/L)
500
400
300
200
100
0
***
***
Control
ConA
Splenectomy
Splenectomy+DEX
(b)
Control
ConA
Splenectomy
Splenectomy + DEX
(c)
Control
ConA
Splenectomy
Splenectomy + DEX
(d)

Figure 2: Continued.

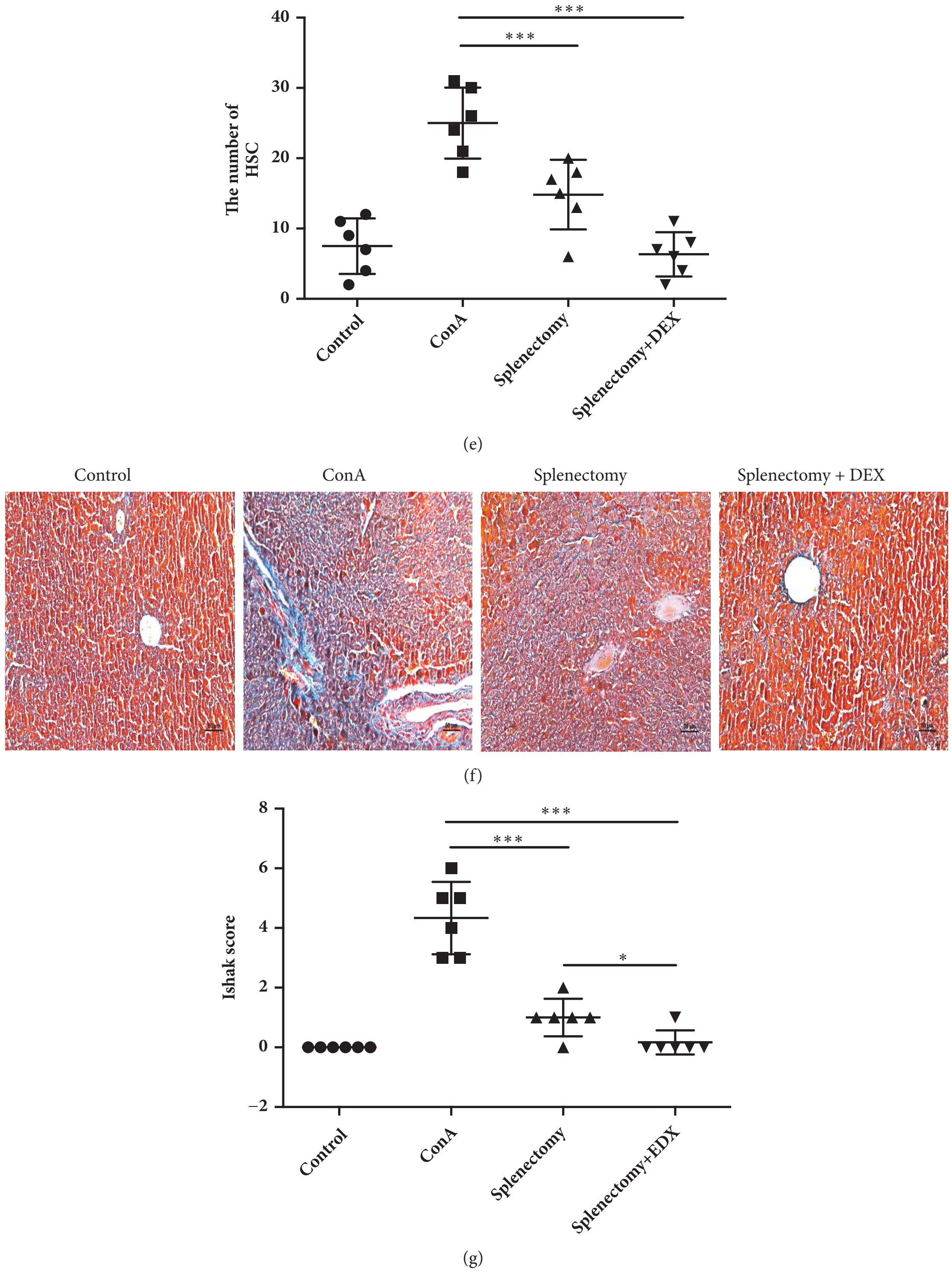

Figure 2: Morphologic features, histological and immunohistochemical staining (magnification ×200), and alanine (ALT) and aspartate aminotransferase (AST) levels in liver tissues from mice in four treatment groups. (a) Gross liver tissues. (b) The levels of ALT and AST detected by enzyme-linked immunosorbent assay. (c) Hematoxylin and eosin (HE) revealing inflammatory cell infiltration in the portal area. (d) Immunohistochemistry used to detect α-smooth muscle actin (SMA) expression in liver tissues. (e) Numbers of activated hepatic stellate cells (HSC) evaluated (immunohistochemical stain). (f) Masson trichrome stain. Blue areas indicate collagen fiber deposition in the liver tissues. (g) Ishak scores. $*$ indicates $P < 0.05$; $* * *$ indicates $P < 0.001$.

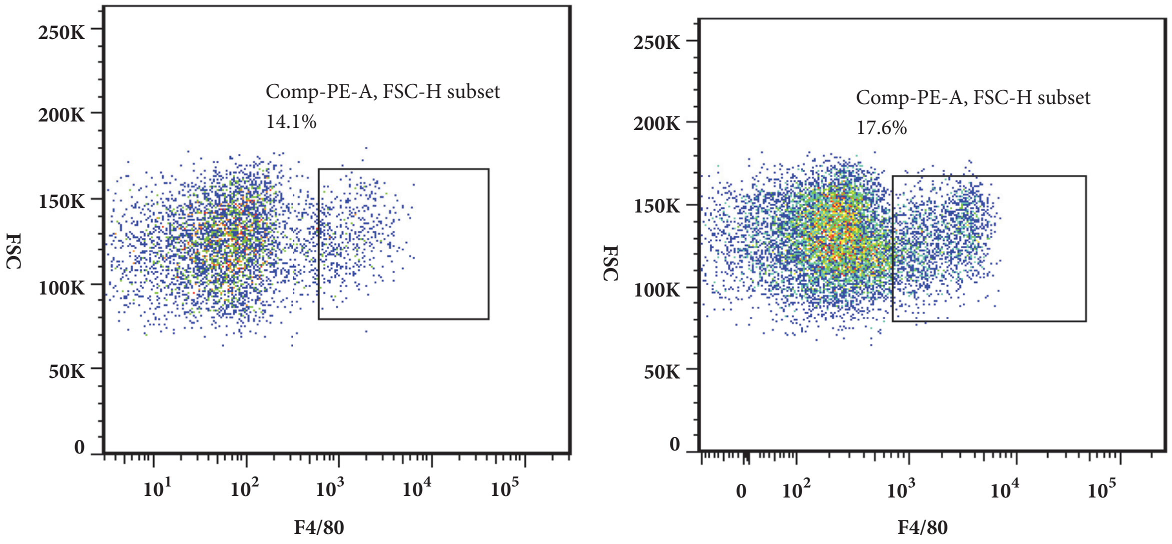

(a) Control (b) ConA

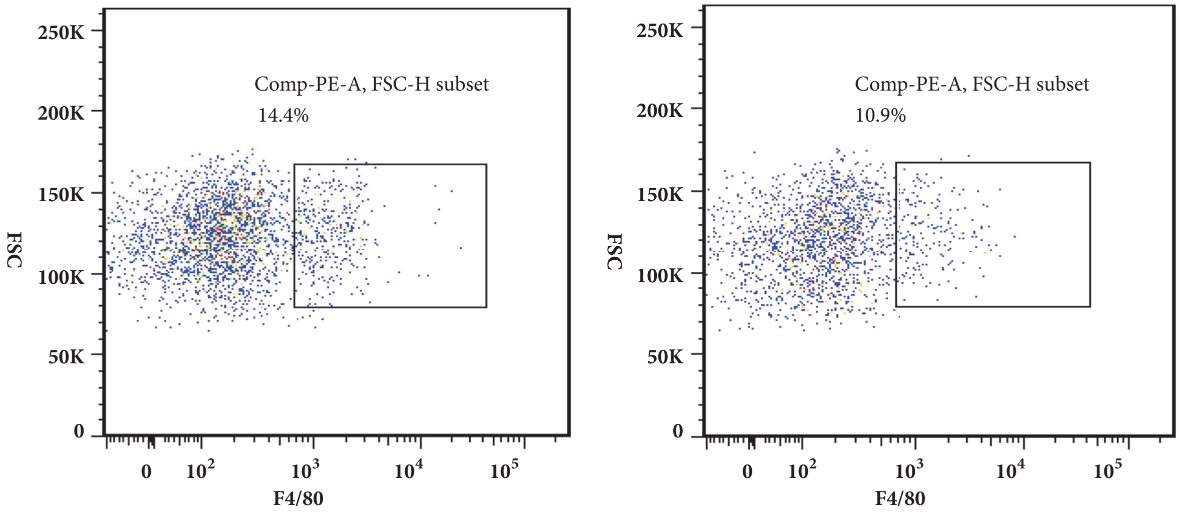

(c) Splenectomy (d) Splenectomy + DEX

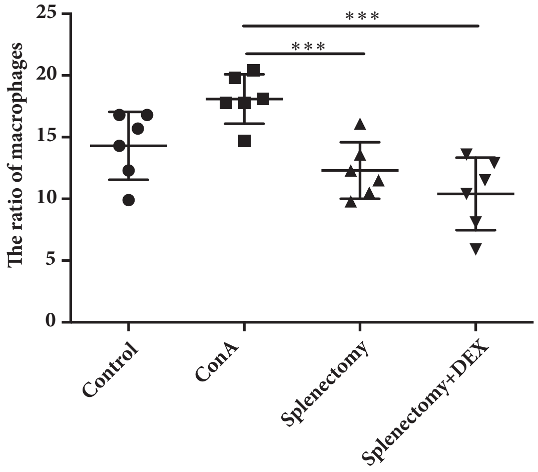

(e)

Figure 3: Flow cytometric analysis of monocytes from mice in (a) control, (b) ConA-treated, (c) splenectomy, and (d) splenectomy+DEX groups, and (e) the ratios of F4/80 monocytes. $***$ indicates $P < 0.001$.

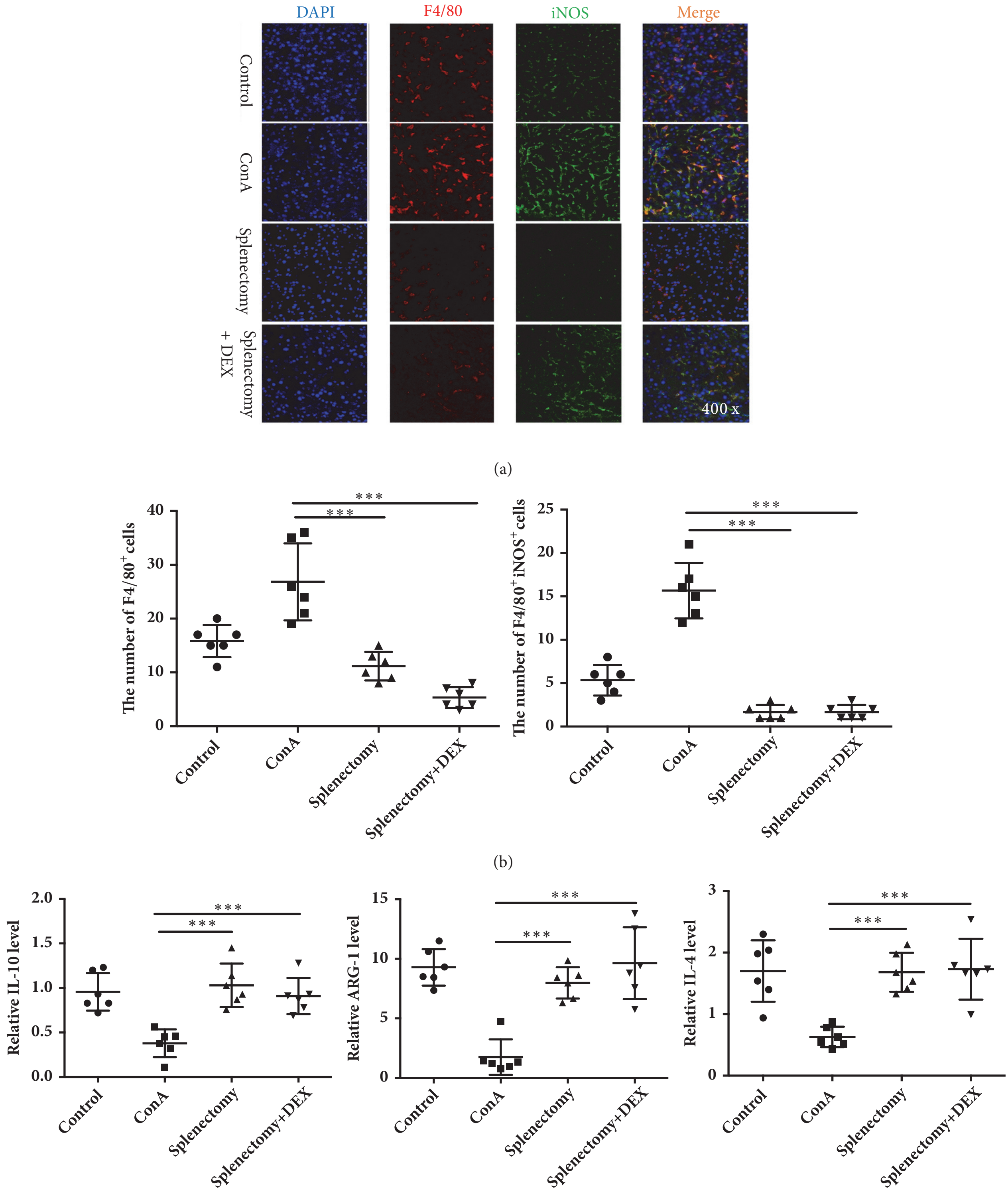

(a)

(b)

(c)

Figure 4: F4/80$^+$ macrophages and F4/80$^+$ inducible nitric oxide synthase (NOS)$^+$ macrophages were detected by (a) immunofluorescent staining and (b) the ratios were calculated. The M2 macrophage-related cytokines (c) interleukin- (IL-) 10, arginase- (ARG-) 1, and IL-4 were detected by RT-PCR. ConA, concanavalin A; DEX, dexamethasone. $***$ indicates $P < 0.001$.

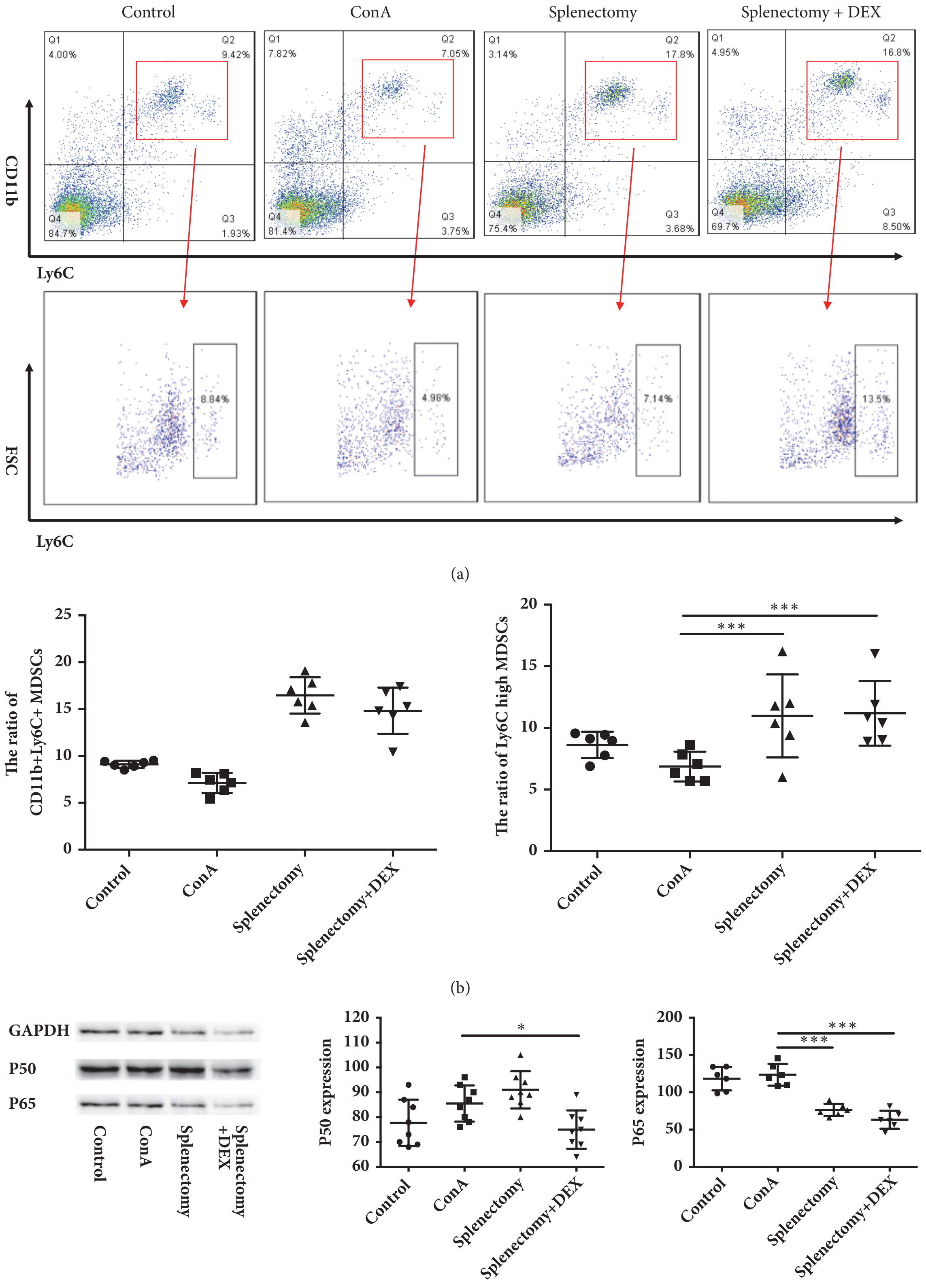

(a)

(b)

(c)

Figure 5: Continued.

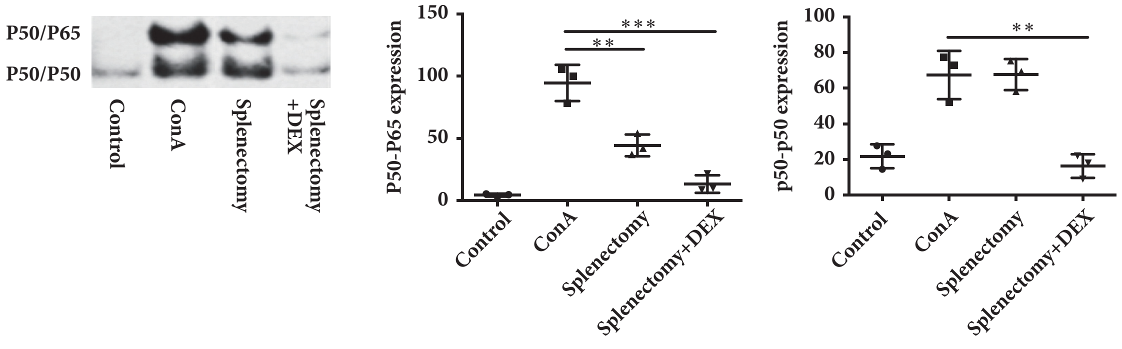

(d)

Figure 5: The ratios of CD11b$^+$Ly6C and CD11b$^+$Ly6C^{high} myeloid-derived suppressor cells (MDSCs) were detected by flow cytometry. (a) Flow cytometry analysis, (b) the ratios of CD11b$^+$Ly6C and CD11b$^+$Ly6C^{high} MDSCs, (c) the levels of p65 and p50, and (d) ratios of p65/p50 and p50/p50 in treatment different groups of mice. ConA, concanavalin A; DEX, dexamethasone. $*$ indicates $P < 0.005$, $**$ indicates $P < 0.01$, and $***$ indicates $P < 0.001$.

4. Discussion

Liver cirrhosis greatly limits the use of immunosuppressants in patients with AIH [1]. Several studies have reported the potential protective effects of splenectomy liver function parameters in this patient population [2, 4]. For example, in a series of 12 patients with end-stage AIH who underwent liver transplantation, Xu et al. found that splenectomy could prevent the posttransplantation recurrence of AIH [3]. In previous studies, ConA has always been used at a dose of 15–20mg/kg body weight to induce acute liver injury in mice [26]. However, we successfully established a mouse model of immune liver fibrosis using a ConA dose of 12.5 mg/kg body weight for up to 5 weeks. In our ConA model, we observed significant increases in serum ALT and AST levels, the spleen/body weight ratio, and the tissue level of α-SMA. We also found that splenectomy could significantly reduce these signs of ConA-induced liver fibrosis.

Macrophages and macrophage-related factors have been reported to play an essential role in the pathogenesis of hepatic lesions and fibrosis [9–11]. Jindal et al. observed a significant increase in F4/80-positive macrophages in NASH mice and significant decreases in the expression of M1 macrophage-related markers, such as IL-10 and CXCL10 [27]. However, the polarization of M1/M2 macrophages in the context of AIH remained unclear. Interestingly, we found that the total and M1 macrophage populations were increased in AIH patients, whereas the M2 macrophage population had decreased. In our ConA-induced mouse model of liver fibrosis, we similarly observed increases in macrophages and M1 macrophages and a decrease in M2 macrophages, consistent findings in AIH patients. After splenectomy, the numbers of macrophages and M1 macrophages in our model mice decreased, while the expression of M2 macrophage-related cytokines increased. These findings suggest that M2 macrophages play an important role in suppressing liver fibrosis in AIH.

Umemura et al. reported that MDSCs exhibit pleiotropic characteristics of both M1 and M2 monocytes/macrophages [28]. In recent years, MDSCs have been identified in the context of various inflammatory and immune responses, including parasitic infections and autoimmune reactions [29, 30]. However, few studies have evaluated MDSCs in patients with AIH. In a BALB/c mouse model of ConA-induced acute immunological liver injury, Zhang et al. found that rapamycin promoted the proliferation of CD11b$^+$Gr1Ly6C^{high}MDSCs, which protected against immunological hepatic injury [15]. In this study, we observed a significant decrease in the frequency of CD11b$^+$Ly6C^{high}MDSCs after ConA treatment but a significant increase in this population after splenectomy. Therefore, we suggest that CD11b$^+$Ly6C^{high}MDSCs may be key inhibitors of liver inflammation in AIH. We also suggest that CD11b$^+$Ly6C^{high}MDSCs could potentially transform into M2 macrophages.

MDSCs can differentiate into M1 and M2 macrophages in a process that is mainly regulated by STAT1 and NF-κB [31]. The NF-κB signaling pathway is known to regulate macrophage-driven inflammation in autoimmune diseases, and the NF-κBp50/50 homodimer is a regulator of M2 polarization[19]. Using Western blotting, we demonstrated significant increases in the protein levels of NF-κBp50 and P65 after treatment with ConA, as well as a significant decrease in the level of NF-κBp65 after splenectomy. As intracellular NF-κB can only exert transcriptional activity after binding to DNA, we also performed an EMSA and found that the expression of NF-κBp65/p50 and NF-κBp50/p50 both increased significantly after ConA treatment, whereas the expression of NF-κBp65/p50 decreased after splenectomy. Most interestingly, the expression of NF-κBp50/50 decreased significantly after splenectomy combined with DEX, whereas no significant change in this expression level was observed after splenectomy alone. We speculate that hormone therapy may inhibit NF-κB signaling pathway activity, whereas splenectomy only inhibits the formation of the NF-κBp65/p50 heterodimer.

Ryutaro Maruoka et al. reported that splenectomy could prolong the effects of corticosteroids in a mouse model of AIH [4]. Specifically, these authors suggested that although corticosteroid treatment protects against AIH, it allows

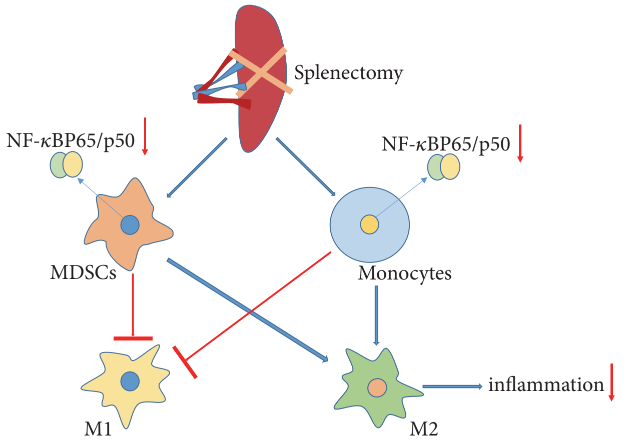

Figure 6: Proposed mechanisms by which splenectomy suppresses liver fibrosis in a mouse model.

residual splenic failed to regulate T_{FH} cells to remain after the treatment. Few previous reports have compared splenectomy with DEX therapy. In our study, we compared splenectomy alone or combined with DEX therapy. Our results indicate that splenectomy combined with DEX led to significantly reduced liver fibrosis scores, compared with the splenectomy alone. Moreover, the NF-κB signaling pathway was significantly inhibited after splenectomy combined with DEX. These results suggest that DEX and splenectomy have a synergistic effect in the treatment of ConA-induced liver fibrosis in mice. However, additional studies of the specific mechanism and long-term safety are needed.

This study provides basic information regarding the potential mechanism underlying the ability of splenectomy to inhibit liver inflammation. However, the exact mechanisms involving MDSCs, macrophages, and the NF-κB signaling pathway will require further study. Future research regarding therapeutic applications should aim to understand the mechanism underlying macrophage phenotype switches *in vivo*.

In summary, we have evaluated the role of splenectomy in the observed accumulation of $CD11b^{+}Ly6C^{high}$MDSCs in a mouse model of liver fibrosis. Notably, splenectomy induced the proliferation of M2 macrophages, possibly by inhibiting activation of the NF-κB signaling pathway (Figure 6). This finding suggests that MDSCs could be amplified *in vitro* and used therapeutically and indicates a new concept for the treatment of autoimmune diseases.

Data Availability

The data used to support the findings of this study are available from the corresponding author upon request.

Additional Points

Key Summary. Our research findings enabled us to newly clarify the molecular mechanism underlying the macrophage/monocyte activation and the inflammatory response in autoimmune hepatitis (AIH). We also newly detected the role of splenectomy in $CD11b^{+}Ly6C^{high}$MDSCs accumulation in a mouse model of liver fibrosis and demonstrated that splenectomy could induce the proliferation of M2 macrophages, possibly by inhibiting NF-κB signaling pathway activation.

Conflicts of Interest

The authors declare that there are no conflicts of interest regarding the publication of this article.

Authors' Contributions

Yongjuan Wang and Xiaopei Guo contributed equally to this manuscript.

Acknowledgments

This work was supported by Science and Technology Development Fund Project of Tianjin no. 17ZXMFSY00210 and the National Natural Science Foundation of China (81600509).

References

[1] European Association for the Study of the Liver, "EASL clinical practice guidelines: autoimmune hepatitis," *Journal of Hepatology*, vol. 63, no. 4, pp. 971–1004, 2015.
[2] K. Murata, K. Ito, K. Yoneda, K. Shiraki, H. Sakurai, and M. Ito, "Splenectomy improves liver function in patients with liver cirrhosis," *Hepatogastroenterology*, vol. 55, pp. 1407–1411, 2008.
[3] S. Yamada, Y. Morine, S. Imura et al., "Liver regeneration after splenectomy in patients with liver cirrhosis," *Hepatology Research*, vol. 46, no. 5, pp. 443–449, 2016.
[4] R. Maruoka, N. Aoki, M. Kido et al., "Splenectomy prolongs the effects of corticosteroids in mouse models of autoimmune hepatitis," *Gastroenterology*, vol. 145, no. 1, pp. 209–220, 2013.
[5] R. D. Stout, C. Jiang, B. Matta, I. Tietzel, S. K. Watkins, and J. Suttles, "Macrophages sequentially change their functional phenotype in response to changes in microenvironmental influences," *The Journal of Immunology*, vol. 175, pp. 342–349, 2005.
[6] I. M. J. Wolfs, M. M. P. C. Donners, and M. P. J. de Winther, "Differentiation factors and cytokines in the atherosclerotic plaque micro-environment as a trigger for macrophage polarisation," *Thrombosis and Haemostasis*, vol. 106, no. 5, pp. 763–771, 2011.
[7] A. Mantovani, A. Sica, S. Sozzani, P. Allavena, A. Vecchi, and M. Locati, "The chemokine system in diverse forms of macrophage activation and polarization," *Trends in Immunology*, vol. 25, no. 12, pp. 677–686, 2004.
[8] S. Gordon and F. O. Martinez, "Alternative activation of macrophages: mechanism and functions," *Immunity*, vol. 32, no. 5, pp. 593–604, 2010.
[9] K. K. Wijesundera, T. Izawa, A. H. Tennakoon et al., "M1- and M2-macrophage polarization in rat liver cirrhosis induced by thioacetamide (TAA), focusing on Iba1 and galectin-3," *Experimental and Molecular Pathology*, vol. 96, no. 3, pp. 382–392, 2014.
[10] Y. Sun, X. Li, X. Meng, C. Huang, L. Zhang, and J. Li, "Macrophage Phenotype in Liver Injury and Repair," *Scandinavian Journal of Immunology*, vol. 85, no. 3, pp. 166–174, 2017.

[11] H. Fukushima, S. Yamashina, A. Arakawa et al., "Formation of p62-positive inclusion body is associated with macrophage polarization in non-alcoholic fatty liver disease," *Hepatology Research*, vol. 48, no. 9, pp. 757–767, 2018.

[12] S. Ostrand-Rosenberg and P. Sinha, "Myeloid-derived suppressor cells: linking inflammation and cancer," *The Journal of Immunology*, vol. 182, no. 8, pp. 4499–4506, 2009.

[13] A. A. Al-Khami, P. C. Rodriguez, and A. C. Ochoa, "Metabolic reprogramming of myeloid-derived suppressor cells (MDSC) in cancer," *Oncoimmunology*, vol. 5, no. 8, Article ID e1200771, 2016.

[14] M. Shen, J. Wang, W. Yu et al., "A novel MDSC-induced PD-1(-)PD-L1(+) B-cell subset in breast tumor microenvironment possesses immuno-suppressive properties," *Oncoimmunology*, vol. 7, no. 4, Article ID e1413520, 2018.

[15] Y. Zhang, Y. Bi, H. Yang et al., "mTOR limits the recruitment of CD11b+Gr1+Ly6Chigh myeloid-derived suppressor cells in protecting against murine immunological hepatic injury," *Journal of Leukocyte Biology*, vol. 95, no. 6, pp. 961–970, 2014.

[16] M. S. Hayden and S. Ghosh, "Signaling to NF-kappaB," *Genes & Development*, vol. 18, no. 18, pp. 2195–2224, 2004.

[17] D. W. Kang, M. Park, H. Oh et al., "Phospholipase D1 has a pivotal role in interleukin-1beta-driven chronic autoimmune arthritis through regulation of NF-kappaB, hypoxia-inducible factor 1alpha, and FoxO3a," *Molecular and Cellular Biology*, vol. 33, no. 14, pp. 2760–2772, 2013.

[18] A. Valaperti, "Drugs targeting the canonical NF-kappaB pathway to treat viral and autoimmune myocarditis," *Current Pharmaceutical Design*, vol. 22, pp. 440–449, 2016.

[19] C. Porta, M. Rimoldi, G. Raes et al., "Tolerance and M2 (alternative) macrophage polarization are related processes orchestrated by p50 nuclear factor kappaB," *Proceedings of the National Acadamy of Sciences of the United States of America*, vol. 106, no. 35, pp. 14978–14983, 2009.

[20] J. Liang, B. Zhang, R.-W. Shen et al., "Preventive effect of halofuginone on concanavalin A-induced liver fibrosis," *PLoS ONE*, vol. 8, no. 12, Article ID e82232, 2013.

[21] J. Liang, B. Zhang, R. W. Shen et al., "The effect of antifibrotic drug halofugine on Th17 cells in concanavalin A-induced liver fibrosis," *Scandinavian Journal of Immunology*, vol. 79, no. 3, pp. 163–172, 2014.

[22] L. Chen, F. Lu, D. Chen et al., "BMSCs-derived miR-223-containing exosomes contribute to liver protection in experimental autoimmune hepatitis," *Molecular Immunology*, vol. 93, pp. 38–46, 2018.

[23] B. C. de Sousa, C. B. Miguel, W. F. Rodrigues et al., "Effects of short-term consumption of Morinda citrifolia (Noni) fruit juice on mice intestine, liver and kidney immune modulation," *Food and Agricultural Immunology*, vol. 28, no. 3, pp. 528–542, 2017.

[24] W. Ren, P. Wang, J. Yan et al., "Melatonin alleviates weanling stress in mice: Involvement of intestinal microbiota," *Journal of Pineal Research*, vol. 64, no. 2, Article ID e12448, 2018.

[25] J. Yin, J. Duan, Z. Cui, W. Ren, T. Li, and Y. Yin, "Hydrogen peroxide-induced oxidative stress activates NF-kappa B and Nrf2/Keap1 signals and triggers autophagy in piglets," *RSC Advances*, vol. 5, no. 20, pp. 15479–15486, 2015.

[26] M. I. Arshad, M. Rauch, A. L'Helgoualc'h et al., "NKT cells are required to induce high IL-33 expression in hepatocytes during ConA-induced acute hepatitis," *European Journal of Immunology*, vol. 41, no. 8, pp. 2341–2348, 2011.

[27] A. Jindal, S. Bruzzì, S. Sutti et al., "Fat-laden macrophages modulate lobular inflammation in nonalcoholic steatohepatitis (NASH)," *Experimental and Molecular Pathology*, vol. 99, no. 1, pp. 155–162, 2015.

[28] N. Umemura, M. Saio, T. Suwa et al., "Tumor-infiltrating myeloid-derived suppressor cells are pleiotropic-inflamed monocytes/macrophages that bear M1- and M2-type characteristics," *Journal of Leukocyte Biology*, vol. 83, no. 5, pp. 1136–1144, 2008.

[29] K. R. Crook, M. Jin, M. F. Weeks et al., "Myeloid-derived suppressor cells regulate T cell and B cell responses during autoimmune disease," *Journal of Leukocyte Biology*, vol. 97, no. 3, pp. 573–582, 2015.

[30] C. Guo, F. Hu, H. Yi et al., "Myeloid-derived suppressor cells have a proinflammatory role in the pathogenesis of autoimmune arthritis," *Annals of the Rheumatic Diseases*, vol. 75, no. 1, pp. 278–285, 2016.

[31] A. Lin, F. Liang, E. A. Thompson et al., "Rhesus Macaque Myeloid-Derived Suppressor Cells Demonstrate T Cell Inhibitory Functions and Are Transiently Increased after Vaccination," *The Journal of Immunology*, vol. 200, no. 1, pp. 286–294, 2018.

Hindawi
BioMed Research International
Volume 2019, Article ID 8676410, 7 pages
https://doi.org/10.1155/2019/8676410

Research Article

The Ovotransferrin-Derived Peptide IRW Attenuates Lipopolysaccharide-Induced Inflammatory Responses

Huanli Jiao, Qing Zhang, Yuanbang Lin, Ying Gao, and Peng Zhang

General Hospital of Tianjin Medical University, 154 Anshan Road, Heping District, Tianjin, 300052, China

Correspondence should be addressed to Peng Zhang; zhangpeng7812@tmu.edu.cn

Received 10 November 2018; Revised 12 December 2018; Accepted 18 December 2018; Published 2 January 2019

Guest Editor: Deguang Song

Copyright © 2019 Huanli Jiao et al. This is an open access article distributed under the Creative Commons Attribution License, which permits unrestricted use, distribution, and reproduction in any medium, provided the original work is properly cited.

IRW (Ile-Arg-Trp), a bioactive peptide isolated from egg ovotransferrin, has been shown to exert anti-inflammatory effects. In this study, the effects of IRW on inflammatory cytokines and microbiota were explored in human umbilical vein endothelial cells (HUVECs) and a lipopolysaccharide (LPS)-induced rat model of inflammatory peritonitis. Rats were injected intraperitoneally with LPS to establish peritonitis. HUVECs were exposed to IRW for 12 h before introducing LPS. Notably, IRW exerted beneficial effects against LPS-induced peritonitis, specifically, by reducing the serum levels of tumour necrosis factor (TNF)-α and interleukin (IL)-6 and myeloperoxidase (MPO) activity ($P<0.05$). A faecal microbiota analysis revealed that IRW significantly increased the Shannon and decreased the Simpson indices ($P<0.05$). Furthermore, IRW treatment significantly inhibited the LPS-induced enhancement of TNF-α, IL-8, intercellular cell adhesion molecule-1 (ICAM-1), and vascular cell adhesion molecule-1 (VCAM-1) expression in HUVECs ($P<0.05$). In conclusion, IRW supplementation inhibited the inflammatory mediator synthesis and LPS-induced inflammatory responses and influenced the gut microbiota.

1. Introduction

In several diseases, including atherosclerosis, cancer, diabetes mellitus, endotoxic shock, and thrombosis, the pathogenesis is modulated by endothelial cell inflammatory responses [1, 2]. Adhesion molecules and various cytokines, which are key stimulators of the innate immune response and endothelial dysfunction, are typically upregulated during the cellular inflammatory process [3]. Lipopolysaccharide (LPS) is a key membrane component in some Gram-negative bacteria and acts as an important pathogenic stimulus [4] that induces vascular inflammation when introduced into the blood [5]. Specifically, LPS stimulates Toll-like receptor 4 (TLR4) on the surfaces of immune cells to initiate a cascade of downstream signals in human vascular endothelial cells. This cascade leads to the uncontrolled production of cytokines, including tumour necrosis factor (TNF)-α, interleukin (IL)-6, and IL-8, as well as adhesion molecules such as intercellular cell adhesion molecule (ICAM) and vascular cell adhesion molecule (VCAM) [6, 7]. The overproduction of these cytokines induces vascular inflammation [8]. Accordingly, inhibiting either the synthesis or release of these inflammatory mediators may limit inflammatory disease.

The unavoidable side effects of synthetic drugs have increased interest in the identification of novel bioactive food components [9, 10]. Many compounds, such as bioactive peptides obtained from foods, are thought to harbour multiple bioactive qualities, including anticarcinogenic, antihypertensive, anti-inflammatory, antimicrobial, and antioxidant activities [11]. IRW (Ile-Arg-Trp), an ovotransferrin peptide isolated from egg white, has been reported to exhibit antioxidant and anti-inflammatory effects both *in vitro* and *in vivo* [12, 13]. However, the anti-inflammatory effects of IRW and the potential mechanisms of action have yet to be determined.

This study explored the anti-inflammatory effects of IRW in an LPS-induced rat model of peritonitis and human umbilical vein endothelial cells (HUVECs). Changes in the faecal microbiota were analysed and the underlying anti-inflammatory mechanisms were considered.

2. Materials and Methods

2.1. Reagents and Chemicals. Catalase, dithiothreitol (DTT), Dulbecco's phosphate-buffered saline (DPBS), M199 medium containing phenol red, porcine gelatine, and polyethylene glycol-conjugated superoxide dismutase (PEG-SOD) were purchased from Sigma (St. Louis, MO, USA). IRW was supplied by Ontores Co. Ltd. (Zhejiang, China), and its purity (>99%) was established using high-performance liquid chromatography-tandem mass spectrometry (HPLC-MS/MS). LPS (*Escherichia coli* 055:B5) was purchased from Sigma. Enzyme-linked immunosorbent assay (ELISA) kits for TNF-α, IL-6, and IL-8 were obtained from the Nanjing Jiancheng Bioengineering Institute (Nanjing, China). Primary antibodies specific for ICAM-1 (ab2213) and VCAM-1 (ab134047) and a horseradish peroxidase (HRP)-conjugated secondary antibody were purchased from Abcam China (Shanghai, China). All remaining reagents and chemicals were of analytical grade.

2.2. Animals and Experimental Protocols. This experiment was approved by the Animal Use and Care Committee of the General Hospital of Tianjin Medical University (Tianjin, China). Female adult Wistar–Hannover rats (body weights: 176–200 g) were purchased from the animal experimental centre of Tianjin Medical University. All rats were housed in a humidity- (40–80%) and temperature-controlled room (24°C ± 1°C) with access to food and water *ad libitum*. The rats were acclimatised to this environment for 1 week and maintained on a 12-hour:12-hour light:dark cycle. Thirty-two rats were randomly allotted to 4 groups: control, LPS, IRW, and IRW-LPS. Rats in the control and LPS groups continued to receive basic feed. Rats in the IRW and IRW-LPS groups received an IRW feed supplement (40 mg/kg feed) for 1 week. In the LPS group and IRW-LPS groups, peritonitis was induced by the intraperitoneal injection of LPS (10 mg/kg body weight). Faecal samples were collected from the different rat groups at 3 days after the injection. The rats were then sacrificed; blood was collected via cardiac puncture and divided into whole blood or plasma samples. The white blood cell (WBC) count was measured using a haematology analyser. ELISA kits from Invitrogen (Carlsbad, CA, USA) were used to detect the plasma levels of TNF-α (128 tests, catalogue # BMS607-2INST), IL-6 (96 tests, catalogue # KMC0061), and MPO (96 tests, catalogue # EMMPO) according to the manufacturer's instructions.

2.3. DNA Amplification and Sequencing. DNA was extracted from 1-g aliquots of faecal samples using the QIAamp DNA Stool Mini Kit (Qiagen, Hilden, Germany) in accordance with the manufacturer's instructions. A UV-vis spectrophotometer (Thermo Scientific, Waltham, MA, USA) was used to determine the final concentration and purity of the DNA. Next, the sample DNA was diluted to 40 ng/μl prior to use as PCR templates. The following primers were used for the PCR amplification of the V3–V4 region of 16S rRNA: 338F (5′-ACTCCTACGGGAGGCAGCAG-3′) and 806R (5′-GGACTACHVGGGTWTCTAAT-3′). The PCR amplification protocol was described in a previous report [14]. The samples were then sequenced by Novogene (Beijing, China) using an Illumina MiSeq platform (Illumina, Inc., San Diego, CA, USA) as described in a previous report [15].

2.4. Microbial Diversity Analysis. Trimmomatic was used to trim and quality-filter the raw FASTAQ files, which were subsequently merged using FLASH [15]. The following criteria were applied. (1) Reads were trimmed at any site where the average quality score was <20 over a 50-bp sliding window. (2) Primers were matched precisely to enable 2-nucleotide mismatching, and reads with indistinct bases were eliminated. (3) Sequences that overlapped by >10 bp were merged based upon their overlap sequence. Using UPARSE (version 7.1), operational taxonomic units (OTUs) were clustered using a homology cut-off of 97%. UCHIME was applied to detect and remove chimeric sequences. The taxonomy of each sequence was scrutinised using the RDP Classifier algorithm and evaluated against the Silva (SSU123) database [16]. The ACE, Chao1, and Shannon indices were used to determine the biodiversity of the samples [17, 18].

2.5. Cell Cultures. HUVEC cell lines were obtained from ATCC (Manassas, VA, USA). The cells were cultivated in a humidified atmosphere at 37°C with 5% CO_2/95% air. Cells were treated with various concentrations of IRW 12 hours prior to the LPS challenge (1 μg/ml).

2.6. Cell Viability and Cytokine Assays. To assess the effect of IRW on cell viability, a 3-(4,5-dimethylthiazol-2-yl)-2,5-biphenyl tetrazolium bromide (MTT) test was used to identify metabolically active viable cells. Briefly, HUVEC cells were cultured for 24 hours at 37°C and then treated with different concentrations of IRW for 2 hours. Subsequently, 1 μg/ml LPS was added to the cultures, which were incubated for 16 hours. Next, a 5 mg/ml MTT solution was added; the mixtures were incubated for 3 hours at 37°C and then stored overnight in sodium dodecyl sulphate (SDS) buffer (10%) containing 0.01 M HCl. A spectrophotometer (TECAN, Austria) was used to detect the absorbance in each well at 570 nm. These experiments were conducted in triplicate. Additionally, the levels of IL-8 and TNF-α in the culture medium were measured using ELISAs according to the user's manuals (Nanjing Jiancheng Bioengineering Institute, Nanjing, Jiangsu, China).

2.7. Detection of Adhesion Abilities. VCAM-1 and ICAM-1 levels were evaluated using Western blotting. Cells were collected and lysed in lysis buffer (50 mM Tris-HCl, pH 8.0; 5 mM EDTA; 150 mM NaCl; 1% NP-40; 1 mM PMSF; protease inhibitor cocktail and phosphatase inhibitor cocktail) on ice. The cell lysates were then heated to 95°C, held at this temperature for 15–20 min, and then centrifuged at 10,000 g for 12 min. The supernatants were drawn off, and 20 μg of total protein from each sample was separated using 12% SDS-polyacrylamide and transferred to a polyvinylidene fluoride membrane. The membrane was blocked for 1.5 hours with 5% nonfat milk (Bio-Rad) in Tris-buffered saline with 0.1% Tween-20 (TBST) and then incubated overnight with a primary antibody specific for VCAM-1 or ICAM-1 at 4°C. After 3 washes with TBST (8 min/wash), the membrane was incubated with the HRP-conjugated secondary antibody. GAPDH

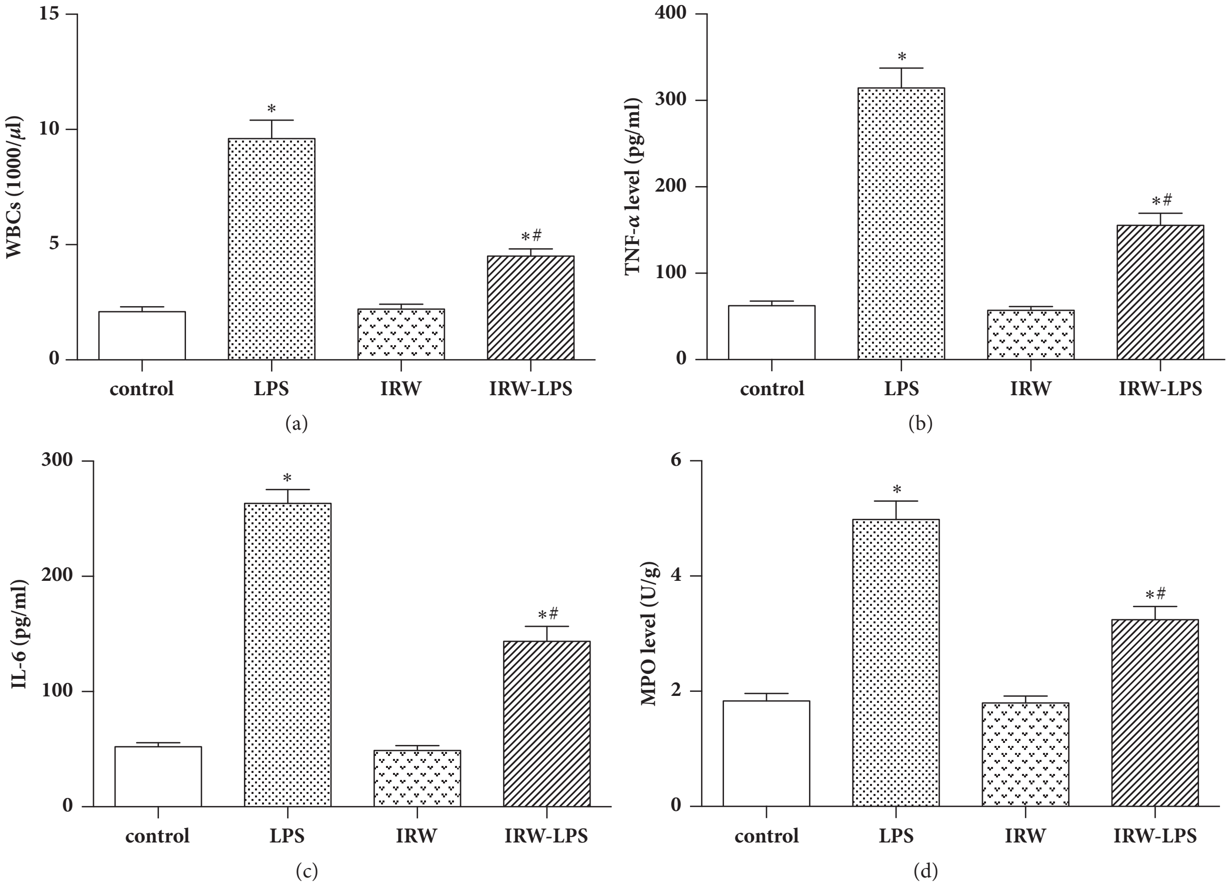

(a) (b) (c) (d)

Figure 1: Effects of IRW on (a) the number of WBCs, serum levels of (b) TNF-α and (c) IL-6, and (d) MPO activity in a rat model of peritonitis (N=8). $*$ P <0.05 versus the control group or IRW group. # P <0.05 versus the LPS group.

was also probed to confirm equal protein loading. A cell-cell adhesion assay was performed to detect the influences of various doses of IRW on the adhesion of neutrophils to endothelial cells. The neutrophils were fluorescently labelled as described in a previous report [19]. The following formula was used to calculate the percentage of leukocytes adhering to HUVECs: adherence (%) = (signal of adhesion/total signal) × 100.

2.8. Statistical Analysis. All data are shown as the means ± standard errors of the means. The statistical analyses were completed using SPSS software (V22.0) (IBM, New York, NY, USA). The data were analysed using Student's t-test or a 1-way analysis of variance, followed by Duncan's test. A P value <0.05 was considered to indicate statistical significance.

3. Results

The protective effects of IRW against LPS-induced peritonitis in a rat model were explored by examining the levels of WBCs, TNF-α, and IL-6. The results revealed significant reductions in the number of WBCs (P <0.05) and the levels of cytokines in LPS-challenged rats treated with IRW (P <0.05). Furthermore, IRW inhibited serum MPO activity in rats with peritonitis (P <0.05) (Figure 1).

An MTT assay was then performed to evaluate the cytotoxicity of IRW. Figure 2 depicts the cell viabilities at different concentrations of IRW. Consequently, IRW concentrations of 5, 10, and 15 μM were used in further studies.

ELISA was then used to determine the concentrations of TNF-α and IL-8 in HUVECs. Figure 3 shows that the levels of both proinflammatory cytokines were statistically higher in cells incubated with LPS (P <0.05). However, these increases were suppressed by IRW in a dose-dependent manner (P <0.05).

Western blotting was used to ascertain the impact of IRW on the expression of VCAM-1 and ICAM-1 on LPS-challenged HUVECs. Notably, the levels of both adhesion molecules were increased significantly in LPS-challenged HUVECs (P <0.05), while IRW inhibited these increases in a dose-dependent manner (Figures 4(a) and 4(b)). The effect of IRW on neutrophil adhesion rate was also assessed. Figure 4(c) shows that IRW suppresses the adhesion of neutrophils to HUVECs in a dose-dependent manner.

A high-throughput sequencing analysis of gut microbial diversity revealed significant differences in the observed diversities of the Shannon and Simpson indices between the LPS and IRW-LPS groups (Figure 5). Figure 6 depicts

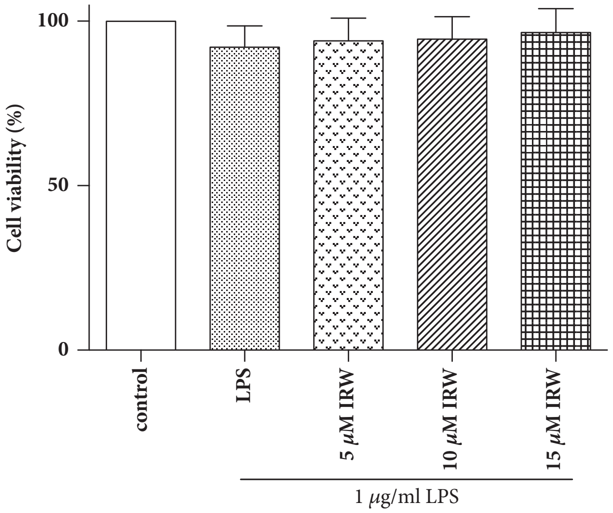

Figure 2: Effects of IRW on HUVEC viability. HUVECs were incubated for 24 hours with LPS and varying concentrations of IRW (5, 10, or 15 μM) (N=3).

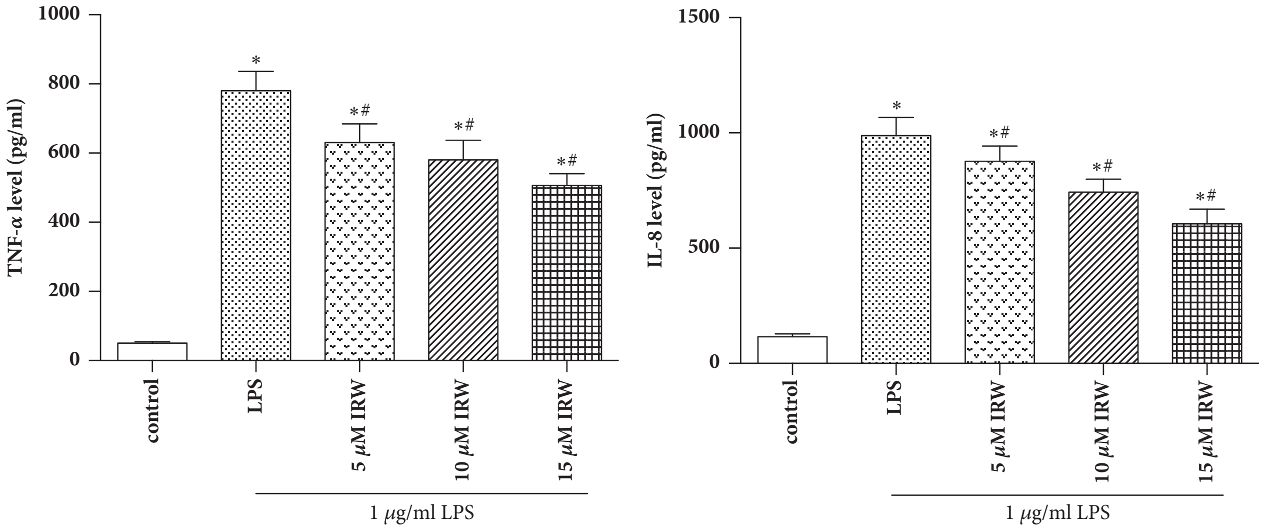

(a)

(b)

Figure 3: IRW suppressed the synthesis of TNF-α and IL-8 in LPS-challenged HUVECs (N=3). $*$ P <0.05 versus the control group. # P <0.05 versus the LPS group.

the microbiota composition and relative abundances at the phylum or order level. The faecal samples contained 8 phyla and 19 orders of bacteria. The most abundant phyla were Actinobacteria, Bacteroides, Firmicutes, and Proteobacteria. However, no between-group differences in the relative abundances were detected at the phylum level. The most abundant orders were Actinomycetales, Bacillales, Bacteroidales, Bifidobacteriales, and Coriobacteriales. Similarly, no between-group differences in these relative proportions were detected at the order level.

4. Discussion

Food-derived bioactive peptides could potentially be used to treat or even prevent chronic diseases such as diabetes, hypertension, and obesity [20, 21]. This study explored the anti-inflammatory effects of IRW, a tripeptide derived from ovotransferrin, on HUVEC cells and endothelial cells from rats with LPS-induced peritonitis. The study found that IRW exerted its anti-inflammatory and beneficial effects by altering microbial diversity and reducing the synthesis of inflammatory mediators.

The adhesion of monocytes to the endothelium, which is mediated by the interactions of monocytes with adhesion molecules such as VCAM-1 and ICAM-1, represents one of the earliest stages of atherogenesis [22]. These adhesion molecules are key initiators of inflammation and the recruitment of leukocytes to affected sites. Considerable evidence indicates that LPS or TNF-α can upregulate the expression of VCAM-1 and ICAM-1 [23]. As we have demonstrated in this

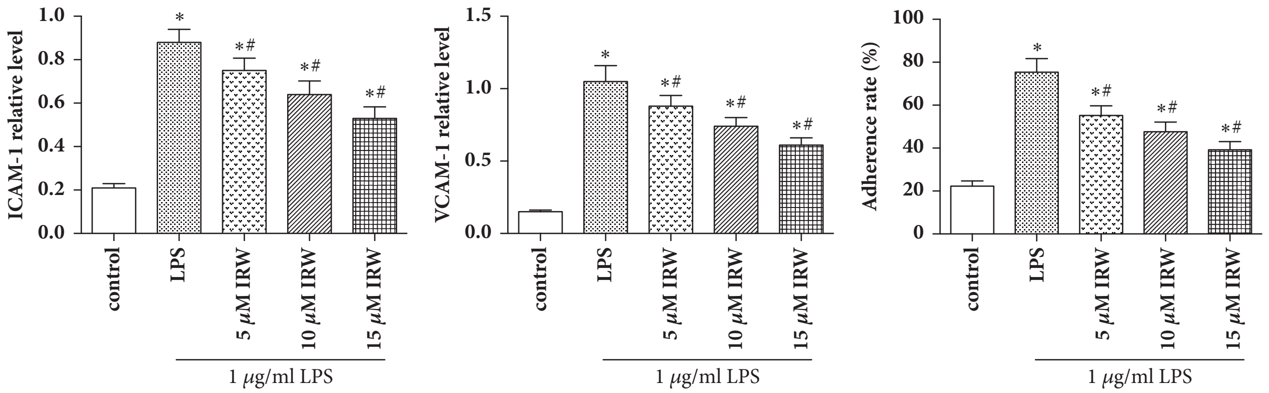

(a) (b) (c)

Figure 4: IRW inhibits the expression of (a) VCAM-1 and (b) ICAM-1 and (c) the adhesion of neutrophils to LPS-challenged HUVECs (N=3). $*$ $P < 0.05$ versus the control group. # $P < 0.05$ versus the LPS group.

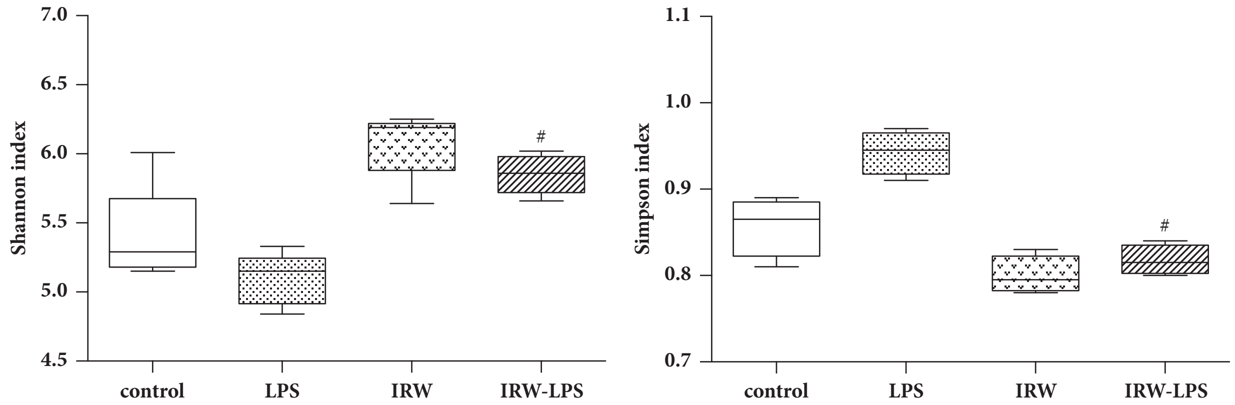

(a) (b)

Figure 5: Effect of IRW on the microbial diversity. (a) Shannon diversity index, (b) Simpson index (N=8). # $P < 0.05$ versus the LPS group.

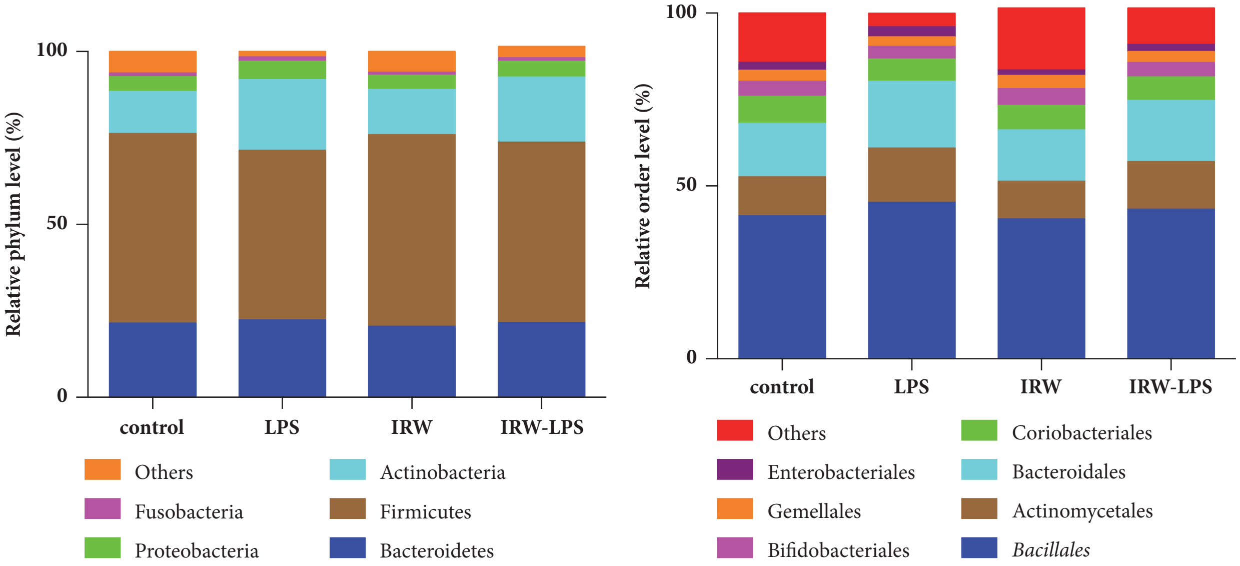

(a) (b)

Figure 6: Effect of IRW on faecal microbiota at the (a) phylum and (b) order levels (N=8).

study, the increased adhesion of neutrophils to HUVECs was reduced by IRW. Furthermore, the upregulation of VCAM-1 and ICAM-1 in LPS-challenged HUVECs was inhibited by IRW in a dose-dependent manner.

The results of this study reveal that LPS-induced peritonitis could be inhibited by IRW via the suppression of inflammatory cytokine synthesis. Furthermore, this study found that the synthesis of TNF-α and IL-8 by LPS-challenged HUVECs was inhibited by IRW in a dose-dependent manner. Research has demonstrated that the overexpression of cytokines is central to the development of inflammation. In particular instances, cytokine overproduction may result in shock, multiorgan failure, or even death [24]. Notably, LPS can upregulate the synthesis of IL-8 and TNF-α [25], which, respectively, recruit immune cells to sites of inflammation [26] and induce the synthesis of IL-6, VCAM-1, and ICAM-1 [27, 28]. Therefore, the pharmacological suppression of cytokine overproduction may represent an effective approach to controlling vascular inflammation [29, 30].

As demonstrated by the results of this study, the IRW-LPS group exhibited an increased Shannon index and decreased Simpson index compared with the LPS group. However, no significant differences in the prevalence of organisms were detected at either the phylum or order level. The mechanism by which IRW modifies microbial diversity remains to be established. The majority of studies evaluating the effects of bacteria on inflammatory responses have been constrained by technical challenges that limit the infection model to a single or few aetiologic agents. By contrast, real-world immune systems are exposed to a constant barrage of bacterial species, as well as their metabolites and products [31]. The relationships between immune systems and bacteria have evolved through natural selection over millennia. We therefore propose two potential mechanisms to first address the impact of metabolic modifications on gut microbiota and second explain the potential ability of IRW to improve the barrier function of the intestines. However, more research is needed to determine the mechanisms underlying these effects.

In conclusion, this study has shown that IRW can inhibit inflammatory responses in both HUVECs and a rat model of peritonitis. The observed beneficial effects might be attributable to the ability of IRW to modulate the gut microbiota. These results also support the application of bioactive peptides as functional anti-inflammatory ingredients.

Data Availability

The data used to support the findings of this study are available from the corresponding author upon request.

Conflicts of Interest

The authors declare that there are no conflicts of interest regarding the publication of this article.

Acknowledgments

The project was supported by Science and Technology Development Fund Project of Tianjin no. 20130138.

References

[1] U. Förstermann, N. Xia, and H. Li, "Roles of vascular oxidative stress and nitric oxide in the pathogenesis of atherosclerosis," *Circulation Research*, vol. 120, no. 4, pp. 713–735, 2017.

[2] H. Li, S. Horke, and U. Förstermann, "Vascular oxidative stress, nitric oxide and atherosclerosis," *Atherosclerosis*, vol. 237, no. 1, pp. 208–219, 2014.

[3] A. Cekici, A. Kantarci, H. Hasturk, and T. E. Van Dyke, "Inflammatory and immune pathways in the pathogenesis of periodontal disease," *Periodontology 2000*, vol. 64, no. 1, pp. 57–80, 2014.

[4] R. F. Maldonado, I. Sá-Correia, and M. A. Valvano, "Lipopolysaccharide modification in gram-negative bacteria during chronic infection," *FEMS Microbiology Reviews*, vol. 40, no. 4, pp. 480–493, 2016.

[5] L. Villacorta, L. Chang, S. R. Salvatore et al., "Electrophilic nitro-fatty acids inhibit vascular inflammation by disrupting LPS-dependent TLR4 signalling in lipid rafts," *Cardiovascular Research*, vol. 98, no. 1, pp. 116–124, 2013.

[6] Y. Wang, Y. Gao, W. Yu, Z. Jiang, J. Qu, and K. Li, "Lycopene protects against LPS-induced proinflammatory cytokine cascade in HUVECs," *Die Pharmazie*, vol. 68, no. 8, pp. 681–684, 2013.

[7] Q. Liang, F. Yu, X. Cui et al., "Sparstolonin B suppresses lipopolysaccharide-induced inflammation in human umbilical vein endothelial cells," *Archives of Pharmacal Research*, vol. 36, no. 7, pp. 890–896, 2013.

[8] X. Song, Y. Chen, Y. Sun et al., "Oroxylin A, a classical natural product, shows a novel inhibitory effect on angiogenesis induced by lipopolysaccharide," *Pharmacological Reports*, vol. 64, no. 5, pp. 1189–1199, 2012.

[9] H. González-Ponce, A. Rincón-Sánchez, F. Jaramillo-Juárez, and H. Moshage, "Natural dietary pigments: potential mediators against hepatic damage induced by over-the-counter nonsteroidal anti-inflammatory and analgesic drugs," *Nutrients*, vol. 10, no. 2, p. 117, 2018.

[10] M. A. Islam, F. Alam, M. I. Khalil, T. H. Sasongko, and S. H. Gan, "Natural products towards the discovery of potential future antithrombotic drugs," *Current Pharmaceutical Design*, vol. 22, no. 20, pp. 2926–2946, 2016.

[11] S. Chen, H. Jiang, H. Peng, X. Wu, and J. Fang, "The utility of ovotransferrin and ovotransferrin-derived peptides as possible candidates in the clinical treatment of cardiovascular diseases," *Oxidative Medicine and Cellular Longevity*, vol. 2017, 2017.

[12] W. Liao, S. Chakrabarti, S. T. Davidge, and J. Wu, "Modulatory effects of egg white ovotransferrin-derived tripeptide IRW (Ile-Arg-Trp) on vascular smooth muscle cells against angiotensin II stimulation," *Journal of Agricultural and Food Chemistry*, vol. 64, no. 39, pp. 7342–7347, 2016.

[13] W. Liao, H. Fan, and J. Wu, "Egg white-derived antihypertensive peptide IRW (Ile-Arg-Trp) inhibits angiotensin ii-stimulated migration of vascular smooth muscle cells via angiotensin type i receptor," *Journal of Agricultural and Food Chemistry*, vol. 66, no. 20, pp. 5133–5138, 2017.

[14] X.-F. Kong, Y.-J. Ji, H.-W. Li et al., "Colonic luminal microbiota and bacterial metabolite composition in pregnant Huanjiang mini-pigs: Effects of food composition at different times of pregnancy," *Scientific Reports*, vol. 6, 2016.

[15] T. Magoč and S. L. Salzberg, "FLASH: fast length adjustment of short reads to improve genome assemblies," *Bioinformatics*, vol. 27, no. 21, pp. 2957–2963, 2011.

[16] Q. Wang, G. M. Garrity, J. M. Tiedje, and J. R. Cole, "Naïve Bayesian classifier for rapid assignment of rRNA sequences into the new bacterial taxonomy," *Applied and Environmental Microbiology*, vol. 73, no. 16, pp. 5261–5267, 2007.

[17] P. D. Schloss, S. L. Westcott, T. Ryabin et al., "Introducing mothur: open-source, platform-independent, community-supported software for describing and comparing microbial communities," *Applied and Environmental Microbiology*, vol. 75, no. 23, pp. 7537–7541, 2009.

[18] C. Mu, Y. Yang, Y. Su, E. G. Zoetendal, and W. Zhu, "Differences in microbiota membership along the gastrointestinal tract of piglets and their differential alterations following an early-life antibiotic intervention," *Frontiers in Microbiology*, vol. 8, no. MAY, 2017.

[19] I. Kim, S.-O. Moon, S. H. Kim, H. J. Kim, Y. S. Koh, and G. Y. Koh, "Vascular endothelial growth factor expression of intercellular adhesion molecule 1 (ICAM-1), vascular cell adhesion molecule 1 (VCAM-1), and E-selectin through nuclear factor-kappa B activation in endothelial cells," *The Journal of Biological Chemistry*, vol. 276, no. 10, pp. 7614–7620, 2001.

[20] O. Power, A. B. Nongonierma, P. Jakeman, and R. J. Fitzgerald, "Food protein hydrolysates as a source of dipeptidyl peptidase IV inhibitory peptides for the management of type 2 diabetes," *Proceedings of the Nutrition Society*, vol. 73, no. 1, pp. 34–46, 2014.

[21] K. Erdmann, B. W. Y. Cheung, and H. Schröder, "The possible roles of food-derived bioactive peptides in reducing the risk of cardiovascular disease," *The Journal of Nutritional Biochemistry*, vol. 19, no. 10, pp. 643–654, 2008.

[22] E. J. Baker, M. H. Yusof, P. Yaqoob, E. A. Miles, and P. C. Calder, "Omega-3 fatty acids and leukocyte-endothelium adhesion: Novel anti-atherosclerotic actions," *Molecular Aspects of Medicine*, vol. 64, pp. 169–181, 2018.

[23] N. Sanadgol, A. Mostafaie, G. Bahrami, K. Mansouri, F. Ghanbari, and A. Bidmeshkipour, "Elaidic acid sustains LPS and TNF-α induced ICAM-1 and VCAM-I expression on human bone marrow endothelial cells (HBMEC)," *Clinical Biochemistry*, vol. 43, no. 12, pp. 968–972, 2010.

[24] A. Tedgui and Z. Mallat, "Cytokines in atherosclerosis: pathogenic and regulatory pathways," *Physiological Reviews*, vol. 86, no. 2, pp. 515–581, 2006.

[25] C.-X. Jian, M.-Z. Li, W.-Y. Zheng et al., "Tormentic acid inhibits LPS-induced inflammatory response in human gingival fibroblasts via inhibition of TLR4-mediated NF-κB and MAPK signalling pathway," *Archives of Oral Biolog*, vol. 60, no. 9, pp. 1327–1332, 2015.

[26] G. Landskron, M. de La Fuente, P. Thuwajit, C. Thuwajit, and M. A. Hermoso, "Chronic inflammation and cytokines in the tumor microenvironment," *Journal of Immunology Research*, vol. 2014, Article ID 149185, 19 pages, 2014.

[27] Y. Song, H. Zhao, J. Liu, C. Fang, and R. Miao, "Effects of Citral on Lipopolysaccharide-Induced Inflammation in Human Umbilical Vein Endothelial Cells," *Inflammation*, vol. 39, no. 2, pp. 663–671, 2016.

[28] J. Liu, J. Wang, H. Luo et al., "Screening cytokine/chemokine profiles in serum and organs from an endotoxic shock mouse model by LiquiChip," *SCIENCE CHINA Life Sciences*, vol. 60, no. 11, pp. 1242–1250, 2017.

[29] H.-Y. Wang, "Non-resolving inflammation and cancer," *SCIENCE CHINA Life Sciences*, vol. 60, no. 6, pp. 561-562, 2017.

[30] X. Wu and Z. Tian, "Gut-liver axis: gut microbiota in shaping hepatic innate immunity," *Science China Life Sciences*, vol. 60, no. 11, pp. 1191–1196, 2017.

[31] G. Liu, W. Yan, S. Ding et al., "Effects of IRW and IQW on Oxidative Stress and Gut Microbiota in Dextran Sodium Sulfate-Induced Colitis," *Cellular Physiology and Biochemistry*, vol. 51, no. 1, pp. 441–451, 2018.

Hindawi
BioMed Research International
Volume 2019, Article ID 2698570, 13 pages
https://doi.org/10.1155/2019/2698570

Research Article

Moringa peregrina Leaves Extracts Induce Apoptosis and Cell Cycle Arrest of Hepatocellular Carcinoma

Mohamed Mansour,[1,2] Magda F. Mohamed,[3] Abeer Elhalwagi,[2] Hanaiya A. El-Itriby,[2] Hossam H. Shawki,[2,4] and Ismail A. Abdelhamid[1]

[1] *Department of Chemistry, Faculty of Science, Cairo University, 12613 Giza, Egypt*
[2] *National Gene Bank of Egypt (NGB), Agricultural Research Center (ARC), Giza, Egypt*
[3] *Department of Chemistry (Biochemistry Branch), Faculty of Science, Cairo University, Giza, Egypt*
[4] *Department of Comparative and Experimental Medicine, Nagoya City University Graduate School of Medical Sciences, Nagoya, Japan*

Correspondence should be addressed to Hossam H. Shawki; shawkihh@med.nagoya-cu.ac.jp
and Ismail A. Abdelhamid; ismail_shafy@yahoo.com

Received 1 November 2018; Revised 6 December 2018; Accepted 17 December 2018; Published 1 January 2019

Guest Editor: Yan Huang

Copyright © 2019 Mohamed Mansour et al. This is an open access article distributed under the Creative Commons Attribution License, which permits unrestricted use, distribution, and reproduction in any medium, provided the original work is properly cited.

Moringa grows in the tropical and subtropical regions of the world. The genus *Moringa* belongs to family Moringaceae. It is found to possess various medicinal uses including hypoglycemic, analgesic, anti-inflammatory, hypolipidemic, and antioxidant activities. In this study, we investigated the antimicrobial and the anticancer activity of the *Moringa peregrina* as well as *Moringa oleifera* leaves extracts grown locally in Egypt. Results indicated that most of the extracts were found to possess high antimicrobial activity against gram-positive bacteria, gram-negative bacteria, and fungus. The survival rate of cancer cells was decreased in both hepatocellular carcinoma (HepG2) and breast carcinoma (MCF-7) cell lines when treated with *Moringa* leaves extracts. In addition, the cell cycle progression, apoptosis, and cancer-related genes confirmed its anticancer effect. The toxicity of each extract was also tested using the normal melanocytes cell line HFB4. The toxicity was low in both *Moringa peregrina* and *Moringa oleifera* leaves extracts. Furthermore, GC/MS analysis fractionized the phytochemicals content for each potential extract. In conclusion, results suggested that the *Moringa peregrina* and *Moringa oleifera* leaves extracts possess antimicrobial and anticancer properties which could be attributed to the bioactive phytochemical compounds present inside the extracts from this plant. These findings can be used to develop new drugs, especially for liver cancer chemotherapy.

1. Introduction

One of the richest sources of natural bioactive phytochemicals is the plant kingdom. The uses of plants in medicine are very old thought [1]. The lower toxicity and side effects of bioactive phytochemicals than the synthetic drugs made the uses of medicinal plants in treatment more desirable [2]. In addition, the presence of multiple phytochemicals molecules in a plant supports the participation in complex cellular pathways [1].

Moringa peregrina and *Moringa oleifera* belong to the family of Moringaceae. Moringa is a perennial and fast-growing tree that could reach a 7-12 m of maximum height with 20-40 cm of diameter with respect to chest level and grows naturally at up to 1000 m above sea level [3]. Moringa genus has 13 species spread around northeast Africa, southwest Africa, southwest Asia, and Madagascar [4]. Egyptians had used *Moringa* trees since old and middle kingdoms (3000-2000 B.C.) [5]. It was used traditionally to improve the overall body health. In addition, during wars the *Moringa oleifera* leaves were used by the Indian warriors to enhance their energy and reduce pain and stress [6].

Moringa trees possess high nutritional value because of the numerous essential phytochemical compounds presented in all its parts (leaves, pods, and/or seeds). Previous studies stated that *Moringa* leaves have vitamin C content more than oranges by 7 times, protein content more than yoghurt by 9 times, vitamin A content more than carrots by 10 times, potassium content more than bananas by 15 times, calcium content more than milk by 17 times, and iron content more than spinach by 25 times [1, 7]. Many studies on *Moringa oleifera* tree have discovered promising anticancer [8], anti-inflammatory [9], procoagulant [10], water purification [11], antifungal [12], and antibacterial [13] properties.

In this study, we focused on two *Moringa* species grown in Egypt (*Moring peregrina* and *Moringa oleifera*) to examine the effect of their leaves serial-extraction as an antimicrobial agent against gram-positive bacteria, gram-negative bacteria, and fungus as well as an anticancer agent against hepatocellular carcinoma (HepG2) and breast carcinoma (MCF-7) cell lines. In addition, cell survival, apoptosis, cell cycle progression, and cancer-related gene were examined to confirm the anticancer effect. Moreover, GC/MS analysis for each serial extract was done to rationalize this activity according to its leave extracts phytochemicals content.

2. Materials and Methods

2.1. Collection of Plants. Moringa peregrina and *Moringa oleifera* leaves were collected from trees in the Orman Garden, Ministry of Agriculture, Egypt. 2 kg of fresh leaves were collected for each species and air-dried in a shaded area, and the leaves were grinded into a coarse powder using a laboratory grinder.

2.2. Preparation of the Extracts. Serial extracts for *Moringa peregrina* and *Moringa oleifera* leaves were done using 5 solvents differing in polarity: Hexane, Diethyl ether, Ethyl acetate, Methanol, and Acetonitrile in series. The abbreviations used for each extract are explained in Table S1. Each of the coarsely powdered specimens was taken into a round bottom flask and 1000 ml of the hexane was added. The soluble constituents of the extract were dissolved in the solvent by overnight shaking. The soluble extracts were filtered and evaporated in a rotary evaporator (IKA, Germany; temp: 50°C; pressure 175 mbar) to yield semisolid residue. Supplemental Fig S1 shows the full extraction scheme. The remaining plant tissue from the hexane extraction was kept till using with the next solvent. The same is done until we finished the other 4 extraction solvents. Finally, the extract residues were collected and stored at 4°C until further uses.

2.3. Assay of Antimicrobial Activity. The antimicrobial activity of each *Moringa peregrina* and *Moringa oleifera* leaves extracts was determined using the agar well diffusion method [14]. Each extract was tested in vitro for its antibacterial activity against gram-positive bacteria (*Staphylococcus aureus* and *Streptococcus mutans*) and gram-negative bacteria (*Escherichia coli*, *Pseudomonas aeruginosa,* and *Klebsiella pneumonia*) and for its antifungal activity against *Candida albicans* using nutrient agar medium. Ampicillin, Gentamicin, and Nystatin were used as standard drugs for gram-positive and gram-negative bacteria and fungus, respectively. DMSO was used as the solvent control. The test was done at a concentration of 15 mg/ml from each extract against both bacterial and fungal strains. The sterilized media was poured onto the sterilized Petri dishes (20-25 ml, each petri dish) and allowed to solidify at room temperature. The microbial suspension was prepared in sterilized saline equivalent to McFarland 0.5 standard solution (1.5×10^5 CFU mL^{-1}) and its turbidity was adjusted to OD = 0.13 using spectrophotometer at 625 nm. Optimally, within 15 minutes after adjusting the turbidity of the inoculum suspension, a sterile cotton swab was dipped into the adjusted suspension and was flooded on the dried agar surface and then allowed to dry for 15 min with lid in place. Wells of 6 mm diameter were made in the solidified media with the help of sterile borer. 100 μL of the solution of each extract was added to each well with the help of micropipette. The plates were incubated at 37°C for 24 h. This experiment was carried out in triplicate and zones of inhibition were measured in mm scale.

2.4. Single Dose Measurement of the Cytotoxicity against Cell Lines Using SRB Assay. Potential of cytotoxicity of the 5 extract residues form each species was tested against two cancer cell lines (HepG2 and MCF-7) and the normal melanocytes cell line HFB4 using SRB assay method [15]. Each cell line was plated into 96-multiwell plate (10^4 cells/well) for 24 h before treatment to allow attachment of the cells to the plate wall. Then, a single dose of each extract (20 μg/ml) was added to each cell line. Monolayer triplicate wells were prepared for each individual dose. Monolayers cells were incubated with the extracts for 48 h at 37°C in an atmosphere of 5% CO_2. After 48 h, cells were fixed, washed, and stained with Sulfo-Rhodamine-B stain. Excess stain was washed with acetic acid and attached stain was recovered with Tris EDTA buffer. The color intensity was measured using an ELISA reader. Doxorubicin was used as a positive control for the HFB4 cell line.

2.5. MTT Assay. MTT assay is a sensitive, quantitative, and reliable colorimetric method that measures the viability of cells. The assay is based on the ability of mitochondrial lactate dehydrogenase enzymes (LDH) in living cells to convert the water-soluble substrate 3-(4,5-dimethylthiazol-2-yl)2,5diphenyl tetrazolium bromide (MTT) into a dark blue formazan which is water insoluble. A solubilization solution (dimethyl sulfoxide) is added to dissolve the insoluble purple formazan product into a colored solution. The absorbance of this colored solution can be quantified by measuring it using spectrophotometer at a wavelength usually between 500 and 600 nm [16]. The assay modification was done according to our previous work [17–19]. Different concentrations of each extract (0.5, 1, 2, 4, 6, 8, 16, 32, 62, 125, 250, 500, and 1000 mg/ml) were incubated with the HepG2 cell line. After 48 h of incubation at 37°C, the cells were incubated for 4 h at 37°C with MTT (0.8 mg/ml) and dissolved in serum-free mediums. Then the MTT was discarded and the cells were washed three times using 1 ml of PBS, followed by the addition of 1ml of DMSO. Then gentle shaking for 10 min was done until complete dissolution. 200 μl of the resulting solutions for each extract was transferred to 96-well plates. The optical densities (ODs) were measured at 570 nm using an ELISA plate reader. Viability percentage was calculated as

Table 1: The inhibition percentage of HepG2 and MCF-7 cell lines by each extract used.

M. Peregrina extracts	% inhibition		*M. Oleifera extracts*	% inhibition	
	HepG2	MCF7		HepG2	MCF7
P/H	62.8	73.6	O/H	73.5	61.3
P/DEE	77.3	79.4	O/DEE	72.2	80.3
P/EA	78	65.7	O/EA	80.7	63.5
P/MeOH	69	61.3	O/MeOH	76.7	61.3
P/ACN	76.7	59.7	O/ACN	79.7	52.8

follows: cell viability percentage = (OD of treated cells/OD of untreated cells) X 100. IC_{50} of the 4 extract residues was measured using Prism program (Graphpad Software incorporated, version 3).

2.6. Quantitative RT-PCR. The expression of *BAX*, *BCL2*, *P53*, *CASP3*, and *MMP1* genes was examined according to Ali et al. [20]. Total RNA was isolated from HepG2 cells treated with a concentration equal to the IC_{50} values of the most active extracts (O/DEE, O/EA, P/DEE, and P/EA). The RNA from untreated HepG2 cells was used as a control. The isolation and purification were done using Qiagen RNA extraction kit. The purity and the yield of extracted RNA were tested at 260 nm. SIGMA PCR kit was used for the synthesis of the cDNA strands and the real-time PCR test was done in a single tube using Rotor gene PCR system as a reader. The primers sequence for the tested genes (*BAX*, *BCL2*, *P53*, *CASP3,* and *MMP1*) and the reference housekeeping gene *GAPDH* are shown in Table S2. The recorded cycle threshold (Ct) values of the targeted genes were used to calculate the relative quantitation (RQ) by calculating the delta-delta Ct ($\Delta\Delta$Ct).

2.7. Flow Cytometry. The method was carried out as previously described [21]. Cell cycle distribution analysis by quantitative DNA content of HepG2 cells treated with the IC_{50} concentration of the Moringa extracts was performed using Propidium Iodide (PI) Flow Cytometry Kit for Cell Cycle Analysis (Abcam, Cat. # ab139418). The untreated HepG2 cells were used as a control. Briefly, cells were prepared at a density of $1x10^4$ per well, treated with the extracts for 24 h at 37°C, harvested in a single cell suspension, and fixed with 66% ethanol at 4°C. Cells were then stained by PI and cycle distribution was determined by using the FACS Calibur (BD Biosciences, San Jose, CA, USA). The analysis was done using BD CellQuest™ Pro Analysis software (BD Biosciences, San Jose, CA, USA). The percentage of apoptosis was recorded.

2.8. Gas Chromatography. The gas chromatographic analysis was carried out for the *Moringa* extracts using GC (Agilent Technologies 7890A) interfaced with a mass selective detector (MSD, Agilent 7000) equipped with a nonpolar Agilent HP-5ms ((5%-phenyl)-methylpolysiloxane) capillary column (30 m length X 0.25 mm inner diameter and 0.25 μm film thickness). The carrier gas was helium with the linear velocity of 1 ml/min. The injector and detector temperatures were 200 and 250°C, respectively. A volume of 1 μl of each extract was injected. The MS operating parameters were as follows: ionization potential 70 eV, interface temperature 250°C, and acquisition mass range 50-800 m/z. The identification of components was based on the comparison of their mass spectra and retention time with those of the authentic compounds and by computer matching with NIST and WILEY library as well as the comparison of the fragmentation pattern of the mass spectra data with those reported in the literature.

3. Results

3.1. Antimicrobial Activity of the Moringa Extracts. The antibacterial and antifungal activity of the *Moringa* extracts have been investigated using agar well diffusion method as explained in Materials and Methods. Each extract was tested for its antibacterial activity against gram-positive bacteria (*Staphylococcus aureus* and *Streptococcus mutans*) and gram-negative bacteria (*Escherichia coli*, *Pseudomonas aeruginosa,* and *Klebsiella pneumonia*) and for its anti-fungal activity against *Candida albicans* (Figure 1). Results in Figures 1(a) and 1(b) reveal that the extracts of P/EA, P/ACN, O/H, O/DEE, and O/EA had the ability to inhibit *Staphylococcus aureus*, while O/MeOH extract had the ability to inhibit the growth of *Streptococcus mutans* as compared to the positive control (Ampicillin). Moreover, O/ACN extract had the ability to inhibit growth of both the tested gram-positive bacteria: *Staphylococcus aureus* and *Streptococcus mutans.* Results of testing the extracts against gram-negative bacteria in Figures 1(c)–1(e) reveal that P/EA, P/ACN, O/EA, and O/ACN extracts had the ability to inhibit *Escherichia coli*, while P/H, P/EA, P/ACN, O/EA, and O/ACN extracts had the ability to inhibit the growth of *Klebsiella pneumoniae* as compared to the positive control (Gentamicin). Moreover, the diethyl ether extracts (O/DEE and P/DEE) had the ability to inhibit growth of the all tested gram-negative bacteria: *Escherichia coli*, *Pseudomonas aeruginosa, and Klebsiella pneumoniae*. On the other hand, extracts tested for their antifungal activity against *Candida albicans* in Figure 1(f) reveal that O/ACN was the only powerful extract effectively inhibiting the fungus with a high zone of inhibition 27.6 mm as compared to the positive control (Nystatin) which was 20 mm.

3.2. The Potential Cytotoxicity against Hepatocellular and Breast Carcinoma. Single dose cytotoxicity test was performed using sulforhodamine-B (SRB) assay to screen the anticancer activity of the *Moringa* leaves extracts. Table 1 shows the inhibition effect of all extracts against HepG2 and

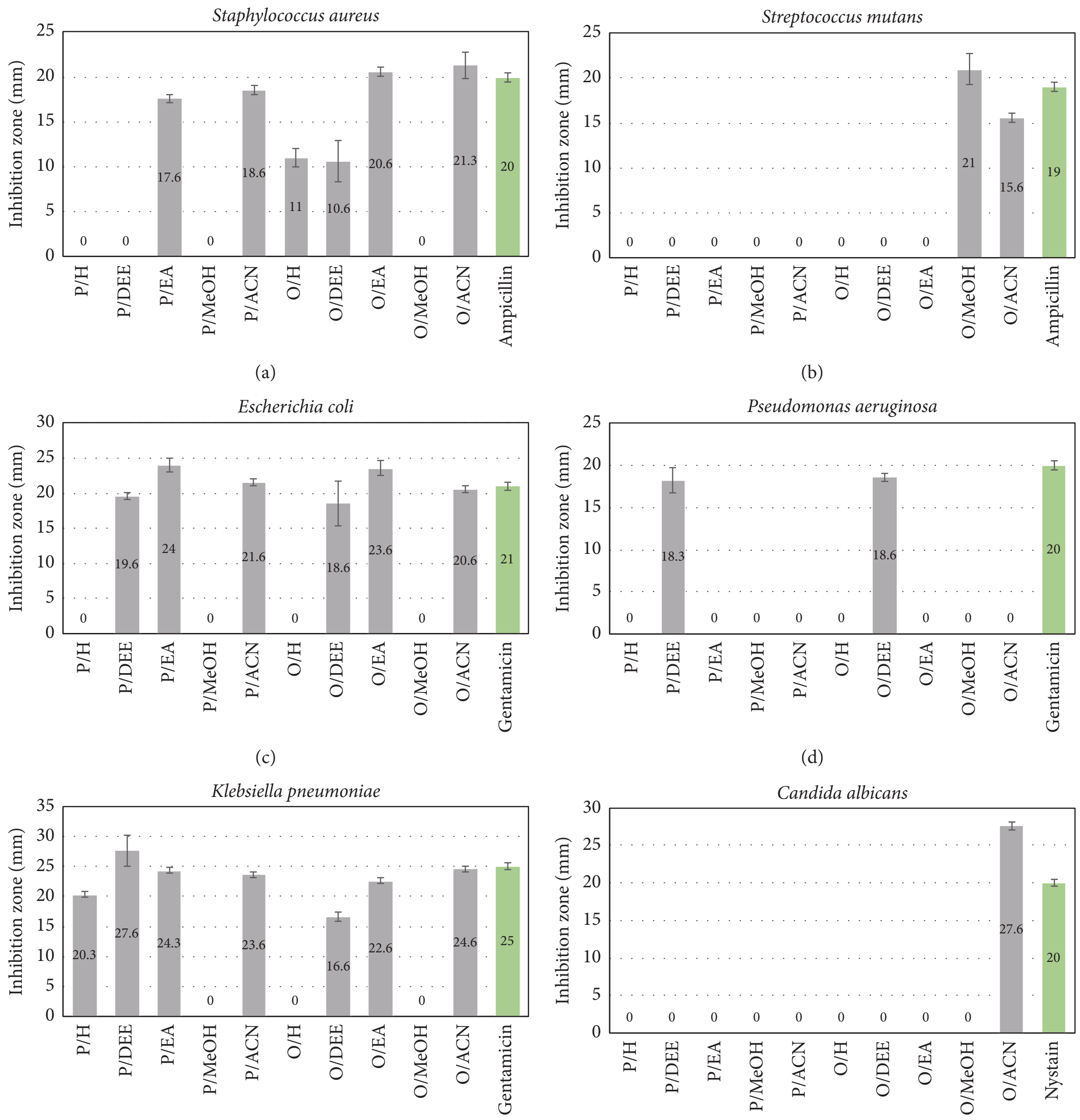

(a) (b) (c) (d) (e) (f)

Figure 1: **The antimicrobial activity of the *Moringa peregrina* and *Moringa oleifera* leaves extracts**. P/H, P/DEE, P/EA, P/MeOH, P/ACN, O/H, O/DEE, O/EA, O/MeOH, and O/ACN extracts were tested for their inhibition effect on (a) *Staphylococcus aureus,* (b) *Streptococcus mutans,* (c) *Escherichia coli,* (d) *Pseudomonas aeruginosa,* (e) *Klebsiella pneumonia,* and (f) *Candida albicans.* Ampicillin antibiotic was used as the positive control for gram-positive bacteria, Gentamicin for gram-negative bacteria, and Nystatin for fungus. Numbers above columns indicate the inhibition zones (mm).

MCF-7 cancer cell lines. The toxicity of the extracts against the normal melanocytes cell line HFB4 was done as shown in Table 2. *Moringa peregrina* and *Moringa oleifera* leaves ethyl acetate extracts (P/EA and O/EA) exhibited the highest inhibition activity against hepatocellular carcinoma HepG2 cell line (78% and 80.7% inhibition, respectively). In the same time, P/EA and O/EA show very low toxicity effect against the normal melanocytes cell line HFB4 (75% and 80% survival, respectively). *Moringa peregrina* and *Moringa oleifera* leaves diethyl ether extracts (P/DEE and O/DEE) were noted to be the most active extracts against breast carcinoma MCF-7 cell line with 79.4% and 80.3% inhibition, respectively. Both of P/DEE and O/DEE recorded the lowest toxicity effect on HFB4 cell line (87% survival) in comparison to the positive control Doxorubicin (21% survival). The rest of the extracts showed a moderate to a high response regarding their activity against HepG2 and MCF-7 cell lines. P/DEE, P/EA, O/DEE, and O/EA were the most selective and promising extracts with high anticancer activity and low toxicity.

Table 2: The survival percentage of HFB4 cell line incubated with each extract for 48 h.

Treatment	% survival	Treatment	% survival	Treatment	% survival
M. Peregrina		*M. Oleifera*		*Positive control*	
P/H	80	O/H	83	Doxorubicin	21
P/DEE	87	O/DEE	87		
P/EA	75	O/EA	80		
P/MeOH	77	O/MeOH	80		
P/ACN	81	O/ACN	82		

Table 3: Cell cycle phases and apoptosis of each extract compared to its control.

Sample Code	**%G0-G1**	**%S**	**%G2-M**	**%Apoptosis**
P/DEE	55.37	38.22	0.73	5.68
P/EA	61.8	20.28	9.58	8.34
O/DEE	57.44	16.17	14.82	11.57
O/EA	14.34	16.23	52.86	16.57
Control HepG2	73.11	21.69	4.36	0.84

3.3. IC50 Determination for Cell Inhibition. From the results above the most active extract residues were P/DEE, P/EA, O/DEE, and O/EA. Cytotoxicity against a model of study, HepG2 cell line, of the 4 most active *Moringa* leaves extracts was tested using MTT assay to find the IC_{50} values (concentrations that inhibited 50% of cell proliferation) of each (Figure 2). All of the 4 extracts exhibited high activity with low IC_{50} values relative to the positive control 5-fluorouracil (5-FU; IC_{50} 237 ± 1.153 μg/ml). The O/EA was the most active extract with lowest IC_{50} value (37.23 ± 0.645 μg/ml), followed by P/EA and O/DEE which recorded IC_{50} values of 40.72 ± 1.060 μg/ml and 42.56 ± 1.060 μg/ml, respectively. P/DEE lied at the end with IC_{50} value of 47.76 ± 2.485 μg/ml.

3.4. The Expression Level of Cancer-Related Genes. The 4 leaves extracts, P/DEE, P/EA, O/DEE, and O/EA, were selected for the molecular studies against hepatocellular carcinoma HepG2 as they exhibited best cytotoxicity and selectivity. The treated HepG2 cells and the untreated (control) were collected for genes expression analysis of the 5 following genes: *P53*, *BAX*, *CASP3*, *BCL2,* and *MMP1*. As shown in Figure 3(a), the 4 extracts induce the expression of the tumor suppressor gene *P53*. O/EA extract had the highest induction effect (17.59-fold) followed by O/DEE and P/DEE (14.78- and 5.81-fold, respectively). The lowest induction was P/EA (4.09-fold). The proapoptotic protein BAX (Figure 3(b)): O/EA had the highest effect on the expression level of *BAX* gene (150.992-fold increase) followed by O/DEE, P/EA, and P/DEE (98.40-, 47.38-, and 42.58-fold, respectively). At the same trend, the expression level of *CASP3* gene (an inducer of the execution phase of cell apoptosis) was highly increased by the treatment of the 4 extracts (Figure 3(c)). The fold change was 91.84-, 59.88-, 54.86-, and 36.31-fold for O/EA, O/DEE, P/DEE, and P/EA, respectively. On the other hand, the expression level of two antiapoptotic genes, *BCL2* and *MMP1*, was strongly decreased in HepG2 cells upon treatment with the 4 extracts (Figures 3(d) and 3(e)). As shown in Figure 3(d), the O/EA had the highest decrease of *BCL2* followed by P/DEE, O/DEE, and P/EA. Similarly, Figure 3(e) shows that O/EA had the highest decrease of *MMP1* followed by O/DEE, P/DEE, and P/EA.

3.5. Extract Effects on Cell Cycle Arrest and Apoptosis. The effects of the 4 *Moringa* leaves extracts, P/DEE, P/EA, O/DEE, and O/EA, on HepG2 cell cycle progression and apoptosis were examined. Results indicated that the P/DEE extract induced cell cycle arrest at S phase (Table 3 and Figure 4(a)), while cells treated with P/EA, O/DEE, and O/EA extracts were arrested at G2/M phase as shown in Table 3 and Figures 4(b), 4(c), and 4(d). Annexin V was used to detect the apoptotic cells of HepG2 after treatment with the different extracts. Results revealed that the percentage of apoptotic HepG2 cells increased with the stimulating effect of the 4 extracts as compared with the control (Table 3 and Figure 4). The O/EA extract stimulated the highest apoptotic induction effect 16.57 % followed by O/DEE, P/EA, and P/DEE (11.57%, 8.34%, and 5.68%, respectively), while the control group was 0.84 %.

3.6. Identification of Bioactive Compounds of Each Extract. GC/MS analyses of the 4 most active *Moringa* leaves extracts (P/DEE, P/EA, O/DEE, and O/EA) were done to identify any bioactive phytochemical compound. P/DEE showed 18 peaks on chromatogram, representing the phytochemical compound within this extract (Figure 5(a)). P/EA, O/DEE, and O/EA extracts showed 23, 34, and 14 peaks, respectively (Figures 5(b)–5(d)). The separated compounds from the 4 extracts were grouped as phenolics, hydrocarbons, long chain fatty acids, alcohols, and esters as summarized in Table 4. Several bioactive compounds were recognized in the leaves extracts of *Moringa peregrine* and *Moringa oleifera.* The chemical structures of some distinguished bioactive compounds identified and reported in literature including retinol, thymol, ascorbic acid, myristic acid, palmitic acid, and linoleic acid are illustrated in Figure 6.

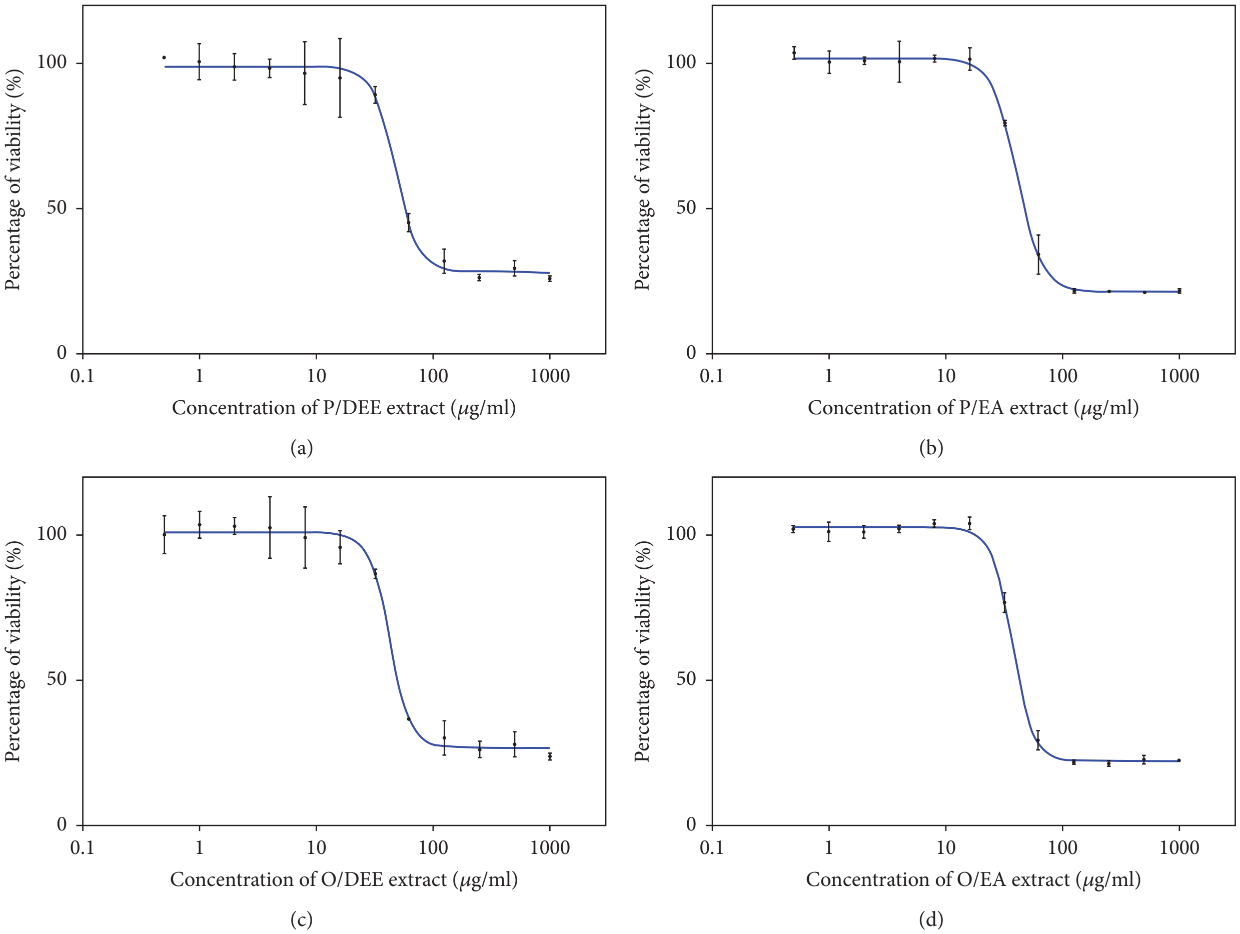

(a) (b) (c) (d)

Figure 2: **Cytotoxicity evaluations of the 4 most active *Moringa* leaves extracts against HepG2 cell line after 48 h of treatment**. (a) P/DEE extract. (b) P/EA extract. (c) O/DEE extract. (d) O/EA extract. The IC_{50} values were calculated using Prism software program (GraphPad software incorporated, version 3). The blue curve indicates the nonlinear regression.

4. Discussion

Over the last few years, plant phytochemicals, especially the ones possessing anticancer activity, gained extensive attention [22]. *Moringa* trees are one of the plants that have been adapted in several tropical and subtropical regions of the world [7]. Many bioactive phytochemical compounds with a high medicinal and nutritional value were reported for this plant [23]. Previous studies confirmed that *Moringa oleifera* leaves possess anticancer [8, 24], anti-inflammatory [9], procoagulant [10], antifungal [12], and antibacterial [13] properties. However, the medicinal properties for *Moringa peregrine* leaves were not well examined yet. In the current study, we used five serial extracts from *Moring peregrine* as well as *Moringa oleifera leaves* grown in Egypt, to examine their effectiveness as antimicrobial agent and anticancer agent against hepatocellular carcinoma (HepG2) and breast carcinoma (MCF-7) cell lines.

Moringa oleifera leaves were reported to possess antimicrobial activity against *Pseudomonas aeruginosa* and *Staphylococcus aureus* but not other gram-positive and gram-negative bacteria and fungus [25]. Our results indicated that leave extracts from *Moring peregrine* as well as *Moringa oleifera* locally growing in Egypt had antimicrobial activity against gram-positive and gram-negative bacteria and fungus. However, although most of the serial extracts have the antimicrobial activity, each of them has a specific activity against specific types of bacteria. We found that O/ACN was the most powerful extract to inhibit the growth of gram-positive bacteria, while O/DEE and P/DEE extracts were the most powerful to inhibit gram-negative bacteria. In addition, O/ACN was the only powerful extract effectively inhibiting the fungus. Therefore, these results could be attributed to the different bioactive compounds present within each extract.

The serial extracts of *Moringa peregrina* and *Moringa oleifera* leaves were then examined for their anticancer activity. The results revealed that *Moringa peregrine* leaves had anticancer activity the same as that previously reported for *Moringa oleifera* [24]. The bioactive compounds from the ethyl acetate extracts of both *Moringa* species (P/EA and O/EA) exhibited the highest inhibitory effect against hepatocellular carcinoma, while diethyl ether extracts (P/DEE and O/DEE) exhibited the highest inhibitory effect against breast carcinoma. Notably, these effects came from the

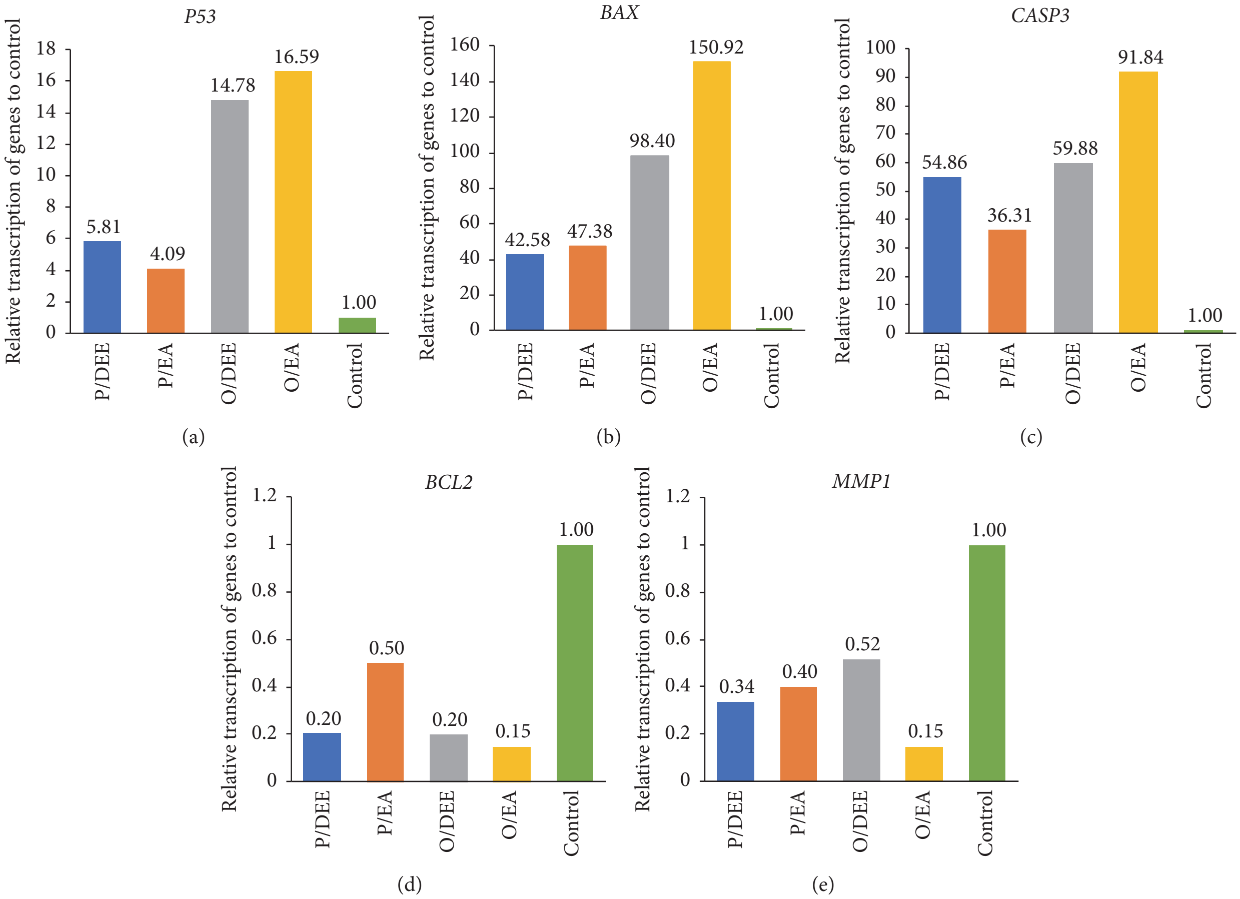

FIGURE 3: **The effect of *Moringa* leaves extracts on HepG2 mRNA transcription**. The relative transcription level of 5 cancer-related genes: (a) *P53*, (b) *BAX*, (c) *CASP3*, (d) *BCL2*, and (e) *MMP1* were determined by qRT-PCR from HepG2 cells treated for 48 h. Values above columns indicate the fold change compared to control. Gene expression levels were normalized to *GAPDH*.

extracts but not the solvent DMSO which were reported to have no biological effects at the final concentration of 0.1% [17, 26, 27]. Moreover, the active extracts (P/DEE, P/EA, O/DEE, and O/EA) had low toxicity effect against the normal melanocytes cell and low IC_{50} values. The effects of these four active extracts, P/DEE, P/EA, O/DEE, and O/EA, as an anticancer agent were confirmed by the expression level of cancer-related genes. Previous studies indicated that *p53* is a tumor suppressive [28], *BAX* is an apoptotic cell death inducer [29], and *CASP3* is a crucial mediator of apoptosis [30], while *BCL-2* is an antiapoptotic gene [31] and *MMP1* inducer of cancer cell proliferation [32]. Our data revealed that HepG2 cells treated with any of these 4 active extracts promote cell apoptosis by upregulation of *p53*, *BAX*, and *CASP3* and downregulation of *BCL-2* and *MMP1*. In this connection, *p53* is known to trigger apoptosis and cell cycle arrest at S phase and G2/M phase [33–36]. We similarly found that P/DEE extract induces cell arrest at S phase, along with P/EA, O/DEE, and O/EA extracts that induce cell cycle arrest at G2/M phase. Transcription factor p53 binds to the DNA-binding domain of the antiapoptotic BCL-2 protein which disrupts the BCL-2/BAX complex and that promotes the permeabilization of the mitochondrial membrane [37, 38]. Consequently, mitochondria permeabilization leads to activation of the caspase cascades and results in cell cycle arrest and apoptotic cell death. These events were totally matched with the observation of our gene expression analyses.

GC/MS of the 4 active *Moringa* leaves extracts were examined to detect bioactive compounds. Previously, it has been described that plants containing high phenolic contents have a considerable anticancer activity and are counted as anticancer potential source [39–42]. Moreover, extracts with long chain fatty acids and their derivatives are also considered as anticancer sources [43]. Our results were detected within the leaves extract: phenolic compounds (thymol and ascorbic acid), long chain fatty acids (myristic acid, palmitic acid, and linoleic acid), and retinol which is known as a cancer treatment [44]. Future studies are required to separate the bioactive compound from the leaves of *Moringa peregrina* and *Moringa oleifera* in order to identify the exact anticancer compounds. These results will contribute to developing anticancer drug for hepatocellular carcinoma from natural compounds.

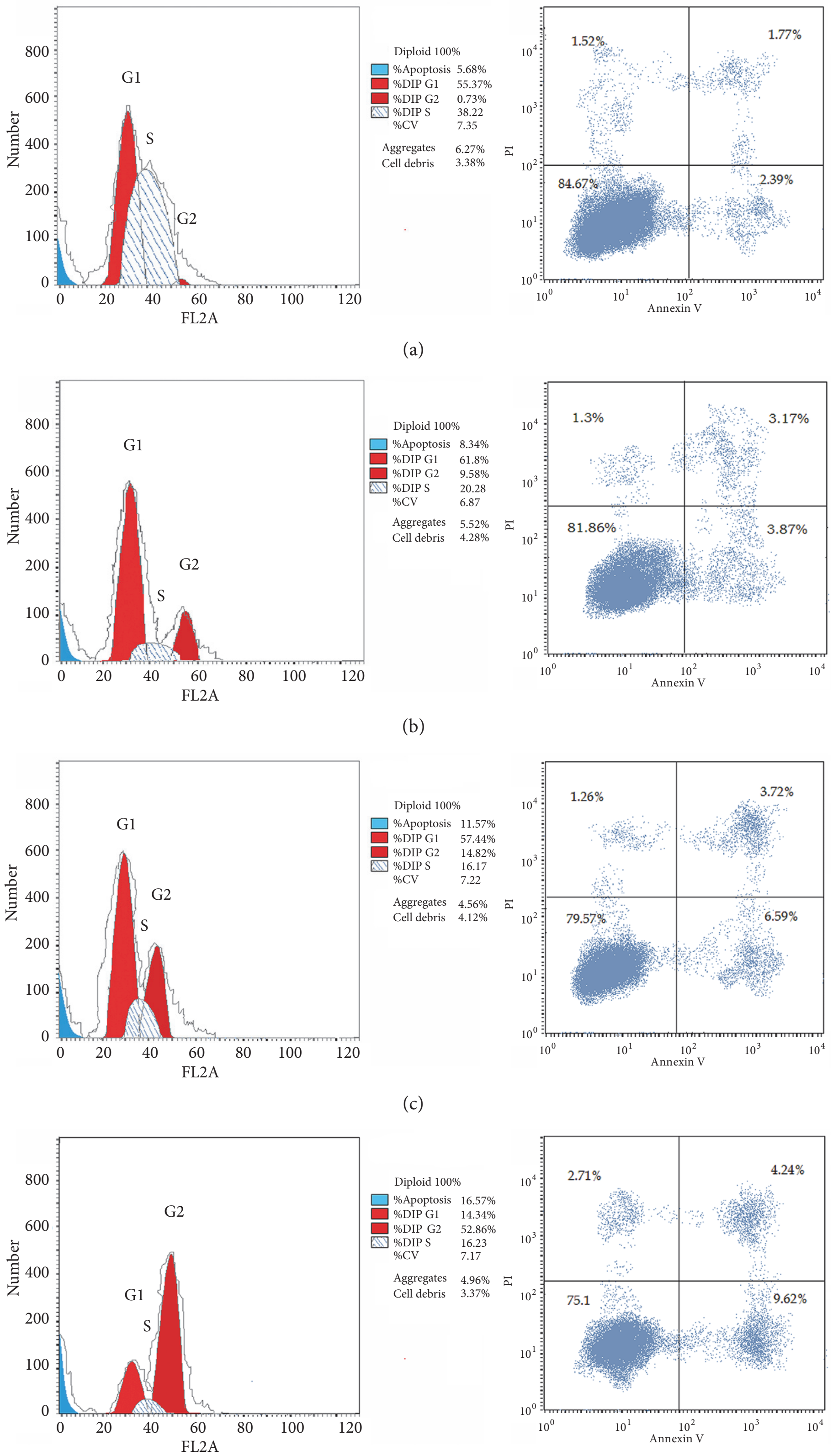

(a)

(b)

(c)

(d)

Figure 4: Continued.

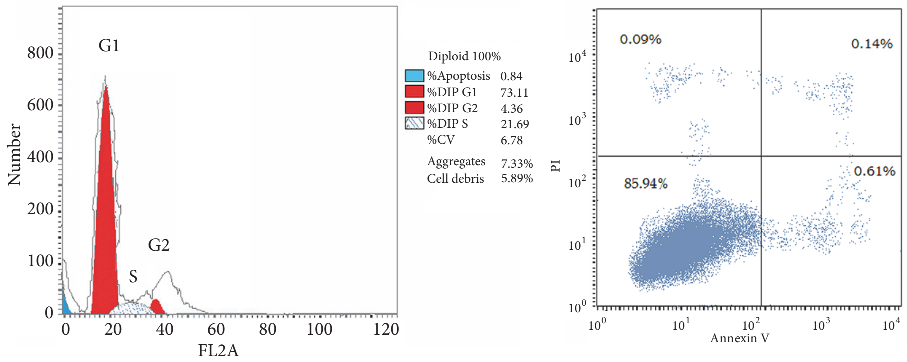

(e)

Figure 4: ***Moringa* leaves extracts induce cell cycle arrest and apoptosis in HepG2 cells**. Cells treated for 48 hours with 4 *Moringa* leaves extracts including (a) P/DEE, (b) P/EA, (c) O/DEE, (d) O/EA, and (e) untreated cells as controls. The cell cycle distribution was determined by propidium iodide staining (PI) and flow cytometry. Left panels show the distribution and the percentage of cells in phases of the cell cycle. Right panels show the distribution and the percentage of cells of apoptotic cells (Annexin$^+$). The cell cycle phases G1, S, and G2/M are indicated over the peaks. PI: cell survival marker; Annexin V: apoptotic marker.

Table 4: Compounds found in each extract using the GC/MS analysis.

Extract	(RT min) Compounds names
P/DEE	(9.065) Sorbitol, (10.809) Hexamethylbenzene, (11.502) Butylated Hydroxytoluene, (11.9) Oleic Acid, (13.374) 6-tert-Butyl-2,4-dimethylphenol, (13.971) Palmitaldehyde, (14.116) Levomenthol, (14.219) Isophytol, (14.83) Isopropyl palmitate, (16.084) Isopropyl linoleate, (16.225) Tetracosanoic acid, (17.668) Methyl tridecanoate, (18.245) Arachic acid, (20.25) Hexacosane, (20.865) L-Ascorbic acid, 6-octadecanoate, (21.41) Octacosane, (21.524) Erucic acid and (22.71) Triacontane
P/EA	(10.816) Hexamethylbenzene, (11.512) Butylated Hydroxytoluene, (11.902) Oleic Acid, (12.786) Phytol, (13.164) Methyl tetradecanoate, (13.377) 6-tert-Butyl-2,4-dimethylphenol, (13.974) Palmitaldehyde, (14.109) Levomenthol, (14.24) Isophytol, (14.36) Hexadecanoic acid & methyl ester, (14.884) Isopropyl palmitate, (15.407) Linolenic acid & methyl ester, (15.772) Methyl stearate, (16.085) Isopropyl linoleate, (16.277) Tetracosanoic acid, (17.569) 2-Hexadecoxyethanol, (17.668) Methyl tridecanoate, (18.23) Arachic acid, (18.779) Salsoline, (20.25) Hexacosane, (20.898) L-Ascorbic acid & 6-octadecanoate, (21.411) Octacosane and (22.715) Triacontane
O/DEE	(6.567) β-Hydroxydodecanoic acid, (7.038) Linoleic acid, (7.607) Hexadecenoic acid & Z-11, (7.699) 2-Hexadecanol, (8.014) Hexadecanedicarboxylic acid, (9.008) Erucic acid, (9.429) Benzyl laurate, (9.606) Thymol, (9.716) Cuminic alcohol, (9.853) Methyl phytanate, (10.38) Retinol, (10.809) Hexamethylbenzene, (11.502) Butylated Hydroxytoluene, (11.9) Oleic Acid, (12.729) Phytol, (13.16) Methyl tetradecanoate, (13.374) 6-tert-Butyl-2,4-dimethylphenol, (13.971) Palmitaldehyde, (14.116) Levomenthol, (14.24) Isophytol, (14.362) Hexadecanoic acid & methyl ester, (14.83) Isopropyl palmitate, (15.407) Linolenic acid & methyl ester, (15.77) Methyl stearate, (16.086) Isopropyl linoleate, (16.277) Tetracosanoic acid, (17.568) 2-Hexadecoxyethanol, (17.668) Methyl tridecanoate, (18.245) Arachic acid, (18.779) Salsoline, (20.25) Hexacosane, (20.865) L-Ascorbic acid & 6-octadecanoate, (21.41) Octacosane and (22.73) Triacontane.
O/EA	(10.38) Retinol, (11.502) Butylated Hydroxytoluene, (12.167) 1-Hexadecanol, (13.164) Methyl tetradecanoate, (13.943) Palmitaldehyde, (14.109) Levomenthol, (14.215) Isophytol, (14.399) Hexadecanoic acid & methyl ester, (14.832) Isopropyl palmitate, (15.407) Linolenic acid & methyl ester, (15.771) Methyl stearate, (16.083) Isopropyl linoleate, (20.25) Hexacosane and (22.718) Triacontane.

5. Conclusions

The serial leaves extract of *Moringa peregrina* as well as *Moringa oleifera* exhibited antimicrobial effects against gram-positive bacteria, gram-negative bacteria, and fungus. Extracts also exhibited cytotoxic effect against HepG2 and MCF-7 cell lines while exhibiting low toxicity on the normal melanocytes cell line. Diethyl ether and ethyl acetate extract methods were highly effective for anticancer activity by inducing cell cycle arrest and apoptosis of the HepG2 cells. GC/MS analysis showed that diethyl ether and ethyl acetate leaves extracts were rich in retinol, thymol, ascorbic acid, myristic acid, palmitic acid, and linoleic acid that would explain this activity.

Data Availability

All data used to support the findings of this study are included within the article and the supplementary information files.

Conflicts of Interest

The authors declare that they have no conflicts of interest.

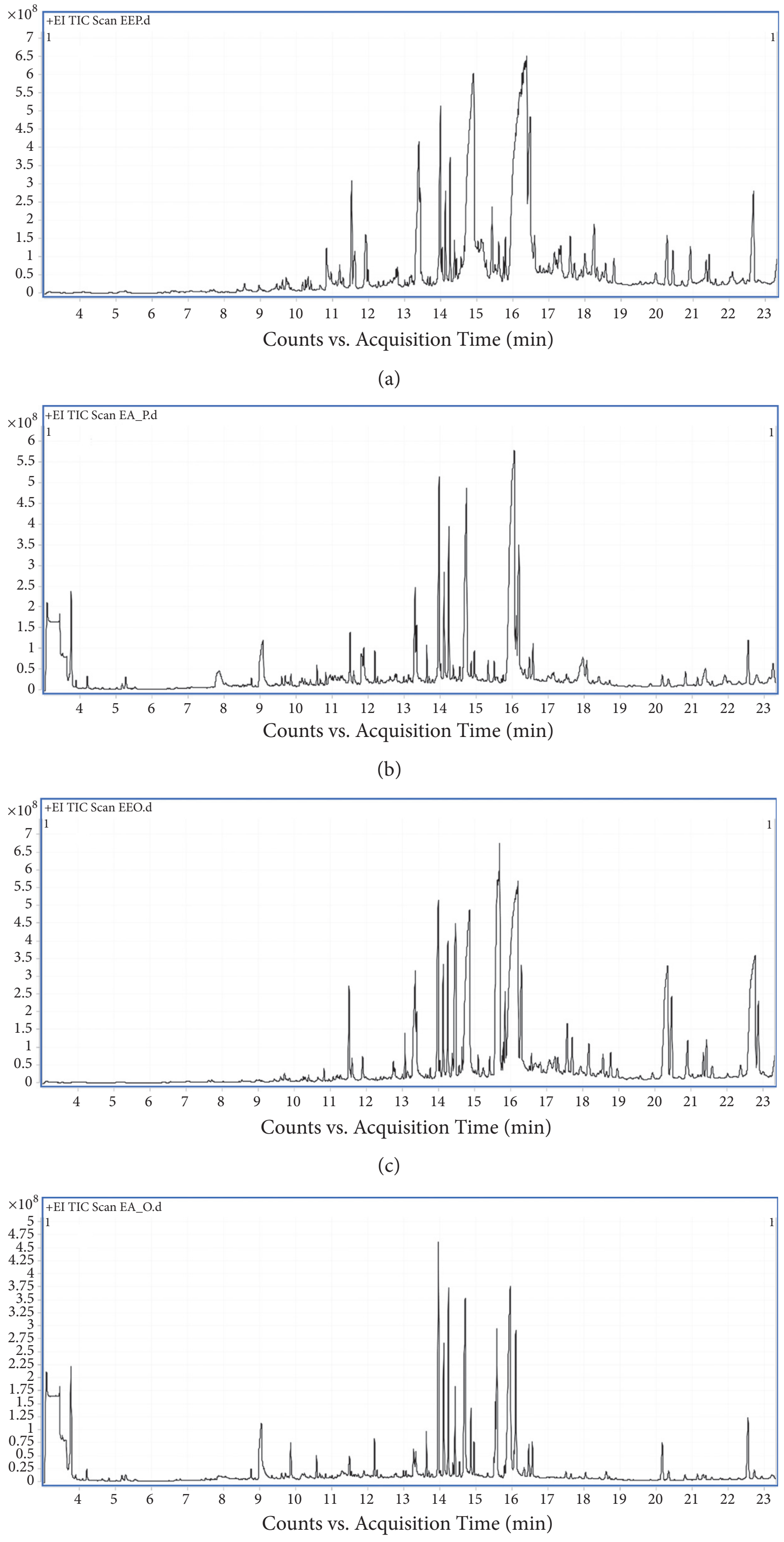

(a)

(b)

(c)

(d)

Figure 5: **GC/MS chromatograms of the active *Moringa* leaves extracts**. The chromatograms of (a) P/DEE, (b) P/EA, (c) O/DEE, and (d) O/EA extracts were analyzed using a GC (Agilent Technologies 7890A) interfaced with a mass selective detector (MSD, Agilent 7000) equipped with a nonpolar Agilent HP-5ms ((5%-phenyl)-methylpolysiloxane) capillary column. The carrier gas was helium with a linear velocity of 1 ml/min. The injector and detector temperatures were 200 and 250°C, respectively. A volume of 1 μl of each extract was injected. The MS operating parameters were as follows: Ionization potential 70 eV, interface temperature 250°C, and acquisition mass range 50-800 m/z.

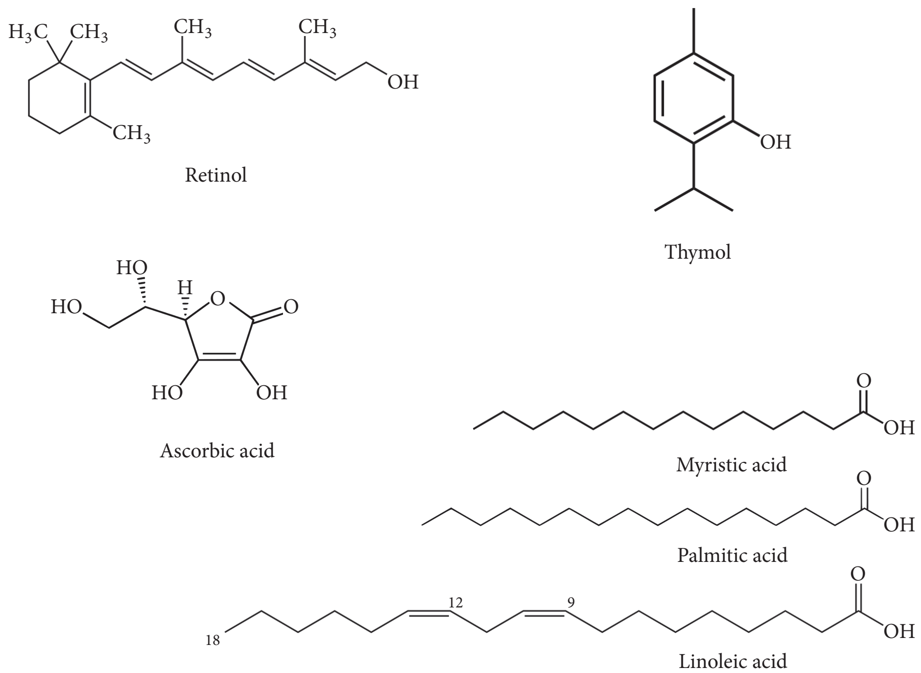

Figure 6: **Chemical structure of the bioactive compounds from *Moringa* extracts**. The major bioactive compounds were separated and identified from the 4 *Moringa* leaves extracts using the GC/MS. The name of each compound is indicated.

Acknowledgments

The authors express deep gratitude to Dr. Hisashi Oishi at Nagoya City University, Japan, Dr. Abdelfatteh El-Omri at King Abdulaziz University, Saudi Arabia, Dr. Mahmoud Ben Othman at University of Tsukuba, Japan, Dr. Ali M. Mahmoud at Institute of biomolecular Chemistry, Italy, and Dr. Emre Bektik at Case Western Reserve University, USA, for their valuable comments on this manuscript.

Supplementary Materials

Supplementary 1. Table S1: the abbreviation of each extract according to the *Moringa* species leaves and the solvents used (docx).

Supplementary 2. Table S2: primers sequence used for the tested genes (docx).

Supplementary 3. Fig S1: schematic diagram of the extraction procedures (TIF).

References

[1] H. A. H. Said-al Ahl, W. M. Hikal, and A. A. Mahmoud, “Biological Activity of Moringa peregrina: a Review,” *American Journal of Food Science and Health*, vol. 3, pp. 83–87, 2017.

[2] S. Verma and S. P. Singh, “Current and future status of herbal medicines,” *Veterinary World*, vol. 1, no. 11, pp. 347–350, 2008.

[3] H. E. Osman and A. A. Abohassan, “Morphological and analytical characterization of moringa peregrina populations in Western Saudi Arabia,” *International Journal of Theoretical and Applied Sciences*, vol. 4, pp. 174–184, 2012.

[4] N. Z. Abd Rani, K. Husain, and E. Kumolosasi, “Moringa genus: a review of phytochemistry and pharmacology,” *Frontiers in Pharmacology*, vol. 9, pp. 1–26, 2018.

[5] S. A. Elbatran, O. M. Abdel-Salam, K. A. Abdelshfeek, N. M. Nazif, S. I. Ismail, and F. M. Hammouda, “Phytochemical and pharmacological investigations on Moringa peregrina (Forssk) Fiori,” *Natural Product Sciences*, vol. 11, no. 4, pp. 199–206, 2005.

[6] K. T. Mahmood, T. Mugal, and I. U. Haq, “Moringa oleifera: A natural gift-a review,” *Journal of Pharmaceutical Sciences and Research*, vol. 2, no. 11, pp. 775–781, 2010.

[7] J. L. Rockwood, B. G. Anderson, and D. A. Casamatta, “Potential uses of Moringa oleifera and an examination of antibiotic efficacy conferred by M. oleifera seed and leaf extacts using crude extraction techniques available to underserved indigenous populations,” *International Journal of Phytotherapy Research*, vol. 3, pp. 61–71, 2013.

[8] A. K. Al-Asmari, S. M. Albalawi, M. T. Athar et al., “Moringa oleifera as an anti-cancer agent against breast and colorectal cancer cell lines,” *PLoS ONE*, vol. 10, pp. 1–14, 2015.

[9] I. C. Ezeamuzie, A. W. Ambakederemo, F. O. Shode, and S. C. Ekwebelem, “Antiinflammatory effects of Moringa oleifera root extract,” *Pharmaceutical Biology*, vol. 34, no. 3, pp. 207–212, 1996.

[10] T. Nkurunziza, J. B. Nduwayezu, E. N. Banadda, and I. Nhapi, “The effect of turbidity levels and Moringa oleifera concentration on the effectiveness of coagulation in water treatment,” *Water Science and Technology*, vol. 59, no. 8, pp. 1551–1558, 2009.

[11] J. Beltrán-Heredia and J. Sánchez-Martín, “ Improvement of water treatment pilot plant with ,” *Environmental Technology*, vol. 30, no. 6, pp. 525–534, 2009.

[12] P.-H. Chuang, C.-W. Lee, J.-Y. Chou, M. Murugan, B.-J. Shieh, and H.-M. Chen, “Anti-fungal activity of crude extracts and

essential oil of *Moringa oleifera* Lam," *Bioresource Technology*, vol. 98, no. 1, pp. 232–236, 2007.

[13] J. H. Doughari, M. S. Pukuma, and N. De, "Antibacterial effects of Balanites aegyptiaca L. Drel. and Moringa oleifera Lam. on Salmonella typhi," *African Journal of Biotechnology*, vol. 6, no. 19, pp. 2212–2215, 2007.

[14] A. C. Scott, "Laboratory control of antimicrobial therapy," in *Mackie and McCartney Practical Medical Microbiology*, J. G. Collee, J. P. Duguid, A. G. Fraser, and B. P. Marmion, Eds., pp. 161–181, 13th edition, 1989.

[15] P. Skehan, R. Storeng, D. Scudiero et al., "New colorimetric cytotoxicity assay for anticancer-drug screening," *Journal of the National Cancer Institute*, vol. 82, no. 13, pp. 1107–1112, 1990.

[16] A. H. Cory, T. C. Owen, J. A. Barltrop, and J. G. Cory, "Use of an aqueous soluble tetrazolium/formazan assay for cell growth assays in culture," *Cancer Communications*, vol. 3, no. 7, pp. 207–212, 1991.

[17] M. F. Mohamed, M. S. Mohamed, S. A. Shouman, M. M. Fathi, and I. A. Abdelhamid, "Synthesis and biological evaluation of a novel series of chalcones incorporated pyrazole moiety as anticancer and antimicrobial agents," *Applied Biochemistry and Biotechnology*, vol. 168, no. 5, pp. 1153–1162, 2012.

[18] S. K. Salama, M. F. Mohamed, A. F. Darweesh, A. H. Elwahy, and I. A. Abdelhamid, "Molecular docking simulation and anticancer assessment on human breast carcinoma cell line using novel bis(1,4-dihydropyrano[2,3-c]pyrazole-5-carbonitrile) and bis(1,4-dihydropyrazolo[4′,3′:5,6]pyrano[2,3-b]pyridine-6-carbonitrile) derivatives," *Bioorganic Chemistry*, vol. 71, pp. 19–29, 2017.

[19] M. F. Mohamed, H. M. Hassaneen, and I. A. Abdelhamid, "Cytotoxicity, molecular modeling, cell cycle arrest, and apoptotic induction induced by novel tetrahydro-[1,2,4]triazolo[3,4-a]isoquinoline chalcones," *European Journal of Medicinal Chemistry*, vol. 143, pp. 532–541, 2018.

[20] A. G. Ali, M. F. Mohamed, A. O. Abdelhamid, and M. S. Mohamed, "A novel adamantane thiadiazole derivative induces mitochondria-mediated apoptosis in lung carcinoma cell line," *Bioorganic & Medicinal Chemistry*, vol. 25, no. 1, pp. 241–253, 2017.

[21] K. K. Tiwari, C. Chu, X. Couroucli, B. Moorthy, and K. Lingappan, "Differential concentration-specific effects of caffeine on cell viability, oxidative stress, and cell cycle in pulmonary oxygen toxicity in vitro," *Biochemical and Biophysical Research Communications*, vol. 450, no. 4, pp. 1345–1350, 2014.

[22] T. Tesfaye and Y. D. Ravichadran, "Natural products chemistry and a review on anticancer activity of some plant-derived compounds and their mode of action," *Natural Products Chemistry and Research*, vol. 6, 2018.

[23] A. F. Abdull Razis, M. D. Ibrahim, and S. B. Kntayya, "Health benefits of Moringa oleifera," *Asian Pacific Journal of Cancer Prevention*, vol. 15, no. 20, pp. 8571–8576, 2014.

[24] M. Khalafalla and E. Abdellatef, "Active principle from Moringa oleifera Lam leaves effective against two leukemias and a hepatocarcinoma," *African Journal of Biotechnology*, vol. 9, pp. 8467–8471, 2010.

[25] A. Caceres, O. Cabrera, O. Morales, P. Mollinedo, and P. Mendia, "Pharmacological properties of Moringa oleifera. 1: preliminary screening for antimicrobial activity," *Journal of Ethnopharmacology*, vol. 33, no. 3, pp. 213–216, 1991.

[26] M. F. Mohameda, M. S. Mohameda, M. M. Fathib, S. A. Shoumanc, and I. A. Abdelhamid, "Chalcones incorporated pyrazole ring inhibit proliferation, cell cycle progression, angiogenesis and induce apoptosis of MCF7 cell line," *Anti-Cancer Agents in Medicinal Chemistry*, 2014.

[27] M. F. Mohamed, A. M. Abdelmoniem, A. H. Elwahy, and I. A. Abdelhamid, "DNA fragmentation, cell cycle arrest, and docking study of novel bis spiro-cyclic 2-oxindole of pyrimido[4,5-b]quinoline-4,6-dione derivatives against breast carcinoma," *Current Cancer Drug Targets*, vol. 18, no. 4, pp. 372–381, 2018.

[28] J. T. Zilfou and S. W. Lowe, "Tumor suppressive functions of p53," *Cold Spring Harbor Perspectives in Biology*, vol. 1, no. 5, 2009.

[29] J. Pawlowski and A. S. Kraft, "Bax-induced apoptotic cell death," *Proceedings of the National Acadamy of Sciences of the United States of America*, vol. 97, no. 2, pp. 529–531, 2000.

[30] A. G. Porter and R. U. Jänicke, "Emerging roles of caspase-3 in apoptosis," *Cell Death & Differentiation*, vol. 6, no. 2, pp. 99–104, 1999.

[31] C. Belka and W. Budach, "Anti-apoptotic Bcl-2 proteins: structure, function and relevance for radiation biology," *International Journal of Radiation Biology*, vol. 78, no. 8, pp. 643–658, 2009.

[32] I. Herrera, J. Cisneros, M. Maldonado et al., "Matrix metalloproteinase (MMP)-1 induces lung alveolar epithelial cell migration and proliferation, protects from apoptosis, and represses mitochondrial oxygen consumption," *The Journal of Biological Chemistry*, vol. 288, no. 36, pp. 25964–25975, 2013.

[33] Z. Tian, J. Shen, A. P. Moseman et al., "Dulxanthone A induces cell cycle arrest and apoptosisvia up-regulation of p53 through mitochondrial pathway in HepG2 cells," *International Journal of Cancer*, vol. 122, no. 1, pp. 31–38, 2008.

[34] M. L. Agarwal, A. Agarwal, W. R. Taylor, and G. R. Stark, "p53 controls both the G2/M and the G1 cell cycle checkpoints and mediates reversible growth arrest in human fibroblasts," *Proceedings of the National Acadamy of Sciences of the United States of America*, vol. 92, no. 18, pp. 8493–8497, 1995.

[35] X.-H. Zhang, Z.-Q. Zou, C.-W. Xu, Y.-Z. Shen, and D. Li, "Myricetin induces G2/M phase arrest in HepG2 cells by inhibiting the activity of the cyclin B/Cdc2 complex," *Molecular Medicine Reports*, vol. 4, no. 2, pp. 273–277, 2011.

[36] G. Wu, L. Xu, N. Lin, and B. Liu, "UCN-01 induces S and G2/M cell cycle arrest through the p53/p21waf1or CHK2/CDC25C pathways and can suppress invasion in human hepatoma cell lines," *BMC Cancer*, p. 167, 2013.

[37] S. Haupt, M. Berger, Z. Goldberg, and Y. Haupt, "Apoptosis—the p53 network," *Journal of Cell Science*, vol. 116, no. 20, pp. 4077–4085, 2003.

[38] X. Deng, F. Gao, T. Flagg, J. Anderson, and W. S. May, "Bcl2's Flexible Loop Domain Regulates p53 Binding and Survival," *Molecular and Cellular Biology*, vol. 26, no. 12, pp. 4421–4434, 2006.

[39] Y. Cai, Q. Luo, M. Sun, and H. Corke, "Antioxidant activity and phenolic compounds of 112 traditional Chinese medicinal plants associated with anticancer," *Life Sciences*, vol. 74, no. 17, pp. 2157–2184, 2004.

[40] R. W. Owen, A. Giacosa, W. E. Hull, R. Haubner, B. Spiegelhalder, and H. Bartsch, "The antioxidant/anticancer potential of phenolic compounds isolated from olive oil," *European Journal of Cancer*, vol. 36, no. 10, pp. 1235–1247, 2000.

[41] W.-Y. Huang, Y.-Z. Cai, and Y. Zhang, "Natural phenolic compounds from medicinal herbs and dietary plants: potential use for cancer prevention," *Nutrition and Cancer*, vol. 62, no. 1, pp. 1–20, 2010.

[42] S. Vuorela, K. Kreander, M. Karonen et al., “Preclinical evaluation of rapeseed, raspberry, and pine bark phenolics for health related effects,” *Journal of Agricultural and Food Chemistry*, vol. 53, no. 15, pp. 5922–5931, 2005.

[43] A. Intisar, L. Zhang, H. Luo, J. Boima Kiazolu, R. Zhang, and W. Zhang, “Anticancer constituents and cytotoxic activity of methanol-water extract of Polygonum Bistorta L,” *African Journal of Traditional, Complementary and Alternative Medicines*, vol. 10, pp. 53–59, 2013.

[44] E. Doldo, G. Costanza, S. Agostinelli et al., “Vitamin A, cancer treatment and prevention: the new role of cellular retinol binding proteins,” *BioMed Research International*, vol. 2015, Article ID 624627, 14 pages, 2015.

Hindawi
BioMed Research International
Volume 2018, Article ID 6057348, 9 pages
https://doi.org/10.1155/2018/6057348

Research Article

The Immunogenicity of the C Fragment of Tetanus Neurotoxin in Production of Tetanus Antitoxin

Rui Yu,[1] Chong Ji,[2,3] Junjie Xu,[1] Denghai Wang,[2] Ting Fang,[1] Yue Jing,[4,5] Clifton Kwang-Fu Shen,[4,5] and Wei Chen[1]

[1] *Beijing Institute of Biotechnology, 20 Dongdajie Street, Fengtai District, Beijing, China*
[2] *Gaotai Tianhong Biochemical Technology Development Co. Ltd., Gaotai, Gansu, China*
[3] *Jiangxi Institute of Biological Products, Jian, Jiangxi, China*
[4] *Shenzhen Qianhai Tianzheng (SQT) Biotechnology Ltd., Shenzhen, Guangdong, China*
[5] *Shenzhen JinRuiFeng (Golden Harvest) Biotechnology Ltd., Shenzhen, Guangdong, China*

Correspondence should be addressed to Yue Jing; yj443@nyu.edu, Clifton Kwang-Fu Shen; cliftonshen@gmail.com, and Wei Chen; cw0226@foxmail.com

Received 16 November 2018; Revised 10 December 2018; Accepted 16 December 2018; Published 31 December 2018

Guest Editor: Deguang Song

Copyright © 2018 Rui Yu et al. This is an open access article distributed under the Creative Commons Attribution License, which permits unrestricted use, distribution, and reproduction in any medium, provided the original work is properly cited.

The demand of tetanus antitoxin (TAT) as tetanus treatment in developing and underdeveloped countries is still great since it is relatively easy to achieve and affordable. However, there are still issues in the preparation of highly effective TAT with tetanus toxoid (TT) as the immunogen. The tetanus toxin native C-fragment (TeNT-Hc) retains many properties and it is a very promising candidate for the development of tetanus human vaccine. In this study, we tested the immunogenicity of TeNT-Hc in the preparation of tetanus antibodies, by TeNT-Hc alone or in different combinations with TT. The antibody titers and components in horse serum or plasma in different groups were analyzed and compared with those immunized by the conventional TT and it showed comparability with the results of traditional methods. The plasma efficacy and *in vivo* tetanus toxin neutralization were also tested. After two stages of immunizations, the average potency in plasma of all groups reached more than 1,000 IU / mL except that in group 4. In group 5, the first two basic immunizations with TT and the subsequent immunizations with TeNT-Hc, it showed slightly higher antibody titers and potency. This study demonstrated that TeNT-Hc is a safe, effective, and yet easy-to-produce low-cost immunogen and suitable for TT replacement in tetanus antitoxin production.

1. Introduction

Tetanus is an acute, lethal infectious disease and neurological disorder with fatality rate up to 40% [1]. Any injury or trauma has the possibility of getting *Clostridium tetani* (*C. tetani*) infection that causes tetanus toxin production [2]. Tetanus antibodies are the only effective intervention for preventing and treating tetanus on the first two-week period of infections [3, 4]. Tetanus antitoxin (TAT) and tetanus immunoglobulin (TIG) are currently available on the market [5, 6]. TIG, purified human tetanus antibodies, is manufactured from plasma of blood donors immunized with hepatitis B vaccine and then tetanus toxoid (TT) [7]. Due to its human origin, TIG can be applied directly without skin test. However, since it is a human blood product, potential risk of infecting human viruses, such as hepatitis C, AIDS, and other infectious diseases, still remains. In addition, due to source restrictions and unstable supplies, TIG products are generally rather expensive have hard-to-find and have only 20% or lower efficacy per vial compared to TAT, which requires multiple doses. Therefore, it is very difficult for developing and underdeveloped countries to afford TIG for the prevention and treatment of tetanus [8]. On the contrary, utilization of TAT as tetanus treatment in those countries is relatively easy to achieve and affordable. Thus, we can predict it will continue being in clinical applications in the near future [9].

TAT is made of toxin-neutralizing immunoglobulin fragments F $(ab')_2$, extracted, and purified from tetanus toxoid-immunized horse blood [10]. At present, there are still issues in the preparation of highly effective TAT: (1) due to its high toxicity, it is difficult to purify raw tetanus toxin and afford its high-purity form, even after formaldehyde inactivation/detoxification. During the initial immunization and subsequent hyperimmunization processes, interference of impurities within TT antigen results low-grade antibodies against tetanus toxin; (2) since TT still has residue toxicity, frequent and high dose injection of TT antigen into blood-harvesting horses induces the gradual hepatic degeneration and necrosis of their liver cells. This effect is generally quite visible after prolonged, repeated immunization cycle. During this time, the horse liver continues enlarging and deteriorating, and finally it ruptures and causes internal bleeding and the death of the horse; (3) the amount of TT used in horse immunization processes is considerably large and results in rather high cost. Therefore, antigen quality improvement, toxicity reduction, and lower production costs are all essential to achieve better TAT [11].

Tetanus toxin is an enormously potent neurotoxin secreted by the anaerobic bacterium *C. tetani*. After collecting culture supernatants and inactivating with formaldehyde, tetanus toxoid (TT) is simply harvested by filtration. Despite its good immunogenicity in horse, inactivated toxoid generally contaminates with residual formaldehyde which is still toxic. Additionally, *C. tetani* can form spores that resist heat and chemical treatment and post certain risks in TT production. Furthermore, inactivation step with formaldehyde sometimes could not guarantee complete detoxification of tetanus toxin that could be harmful to the horses [12].

The tetanus toxin native C-fragment (TeNT-Hc) retains many properties such as intact binding to gangliosides, immunogenic potency comparable to native toxin, low toxicity, and low allergenicity [13]. It is a very promising candidate for the development of tetanus subunit vaccines and genetic engineering vaccines, which have been used to in Phase I clinical trial as replacement of TT, vaccine conjugates with bacterial and viral vectors, mucosal vaccines and many more [14–17]. Our group has successfully developed a recombinant human tetanus vaccine with TeNT-Hc as an antigen in the past few years [18–20]. This study aimed at animal immunogenicity and toxicological pharmacology demonstrated that TeNT-Hc is a safe, effective, and yet easy-to-produce low-cost immunogen and suitable for TT replacement in tetanus antitoxin production.

In this study, we tested the immunogenicity of TeNT-Hc in the preparation of tetanus antitoxins, by TeNT-Hc alone or in different combinations with TT, to exploit its potential as a replacement immunogen of TT.

2. Materials and Methods

Animals: Adult male horses (4 to 10 years old, 250-400 kg body mass), without tetanus natural antibodies, were purchased from Datong area in Qinghai Province, China. ICR mice (17-19g, male and female) were purchased from Hunan SJA Laboratory Animal Co., Ltd. The horse and mice studies were carried out in accordance with the recommendations of SQT Biotech Antitoxin Production Council on Equine Welfare Guidelines (GS-P009-01 and GS-P001-01). The protocol was approved by the SQT Biotech Antitoxin Production Council (OS-P003-01 to OS-P008-01, GS-P006-01 and GS-P015-01). All animals used in this study were raised under humanitarian conditions with free access to food and water. All efforts were made to minimize suffering. After injection, mice were followed for the five days to check for any signs of paralysis or death. Loss of righting reflex was used as the humane end point of the experiment. Mice were monitored three times a day for their condition and for the occurrence of end point.

2.1. Materials

Incomplete Freund's Adjuvant. Liquid paraffin (Shanghai Zhongqin Chemical Reagent Co., Ltd.) and lanolin (Medical grade, China Huating Lanolin Plant) were mixed (volumetric ratio of 2: 1) to afford the adjuvant. *Antigen and Adjuvant*. TeNT-Hc (molecular weight 45 kD, prepared by the Department of vaccine and antibody engineering, Beijing Institute of Biotechnology) was mixed with incomplete Freund's adjuvant into a water-in-oil emulsion with protein content of 0.625 mg/mL. Tetanus toxoid (TT) purchased from Chengdu Olymvax Biopharmaceuticals, China, was mixed with incomplete Freund's adjuvant into a water-in-oil emulsion with a protein content of 0.625 mg/mL. A mixed antigen solution was prepared by mixing TeNT-Hc and TT with incomplete Freund's adjuvant with incomplete Freund's adjuvant into a water-in-oil emulsion with a protein content of 0.625 mg/mL. The SDS-PAGE electrophoresis analysis of TeNT-Hc and TT is shown in Figure 1. In comparison with TT, TeNT-Hc was shown as single component and has higher purity and smaller molecular weight. *Secondary Antibody*. HRP-conjugated anti-horse IgG and IgM as secondary antibodies was purchased from Abcam. *Standard*. Standard tetanus toxins and anti-tetanus serum were purchased from the China National Institutes of Food and Drug Control. *Borate Buffer*. The borate solution was made of 1L of water, 8.5g of NaCl, 4.5g of H_3BO_3, and 0.5g of $Na_2B_4O_7 \cdot 10H_2O$ and adjusted pH to 7.0-7.2.

2.2. Horse Grouping, Immunization Schedule, and Serum Plasma Separation.

Eighteen horses, with no natural antibodies against TeNT, were divided into 6 groups (3 horses each group) according to age, body weight, and health condition. Following the immunization schedule, different doses of TeNT-Hc, TT or mixed antigens (Mix Ag) were injected intramuscularly into the neck and back of horses. A three-stage immunization schedule was applied: (1) the first stage contains two basic immunization phases. The first phase is basic immunization with two shots and 7-day interval. Before the second phase, there is a rest of 56 days. The second phase is hyperimmunization with 7 shots and 7-day interval; (2) the second stage begins after a rest of 16 days with 3 shots and 7-day interval; (3) the third stage begins after a rest of 18 days with 3 shots and 7-day interval. The specific types of antigens and immunization dose administrated was summarized in Table 1. The schedule and the shots were summarized in

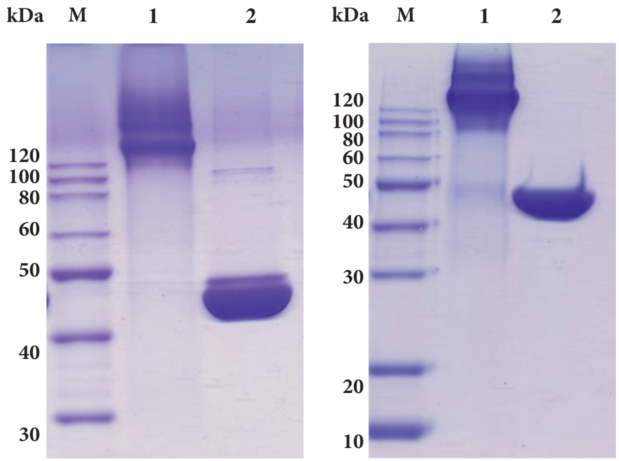

(a)

(b)

Figure 1: Nonreducing (a) and reducing (b) SDS–PAGE analysis of TT and TeNT-Hc. Lane M: molecular weight markers; lane 1: TT; lane 2: TeNT-Hc.

Table 1: Horse groups and immunization schedule and doses.

Schedule	Number of shots	Group 1 (mg)	Group 2 (mg)	Group 3 (mg)	Group 4 (mg)	Group 5 (mg)	Group 6 (mg)	Routine TT immunization (mg)
Stage 1 Phase 1 (Basic)	1	TeNT-Hc 0.625	TeNT-Hc 1.25	TeNT-Hc 0.625	TeNT-Hc 0.625	TT 0.625	Mix Ag 0.625	TT 0.625
	2	TeNT-Hc 1.875	TeNT-Hc 3.75	TeNT-Hc 1.875	TeNT-Hc 1.875	TT 1.875	Mix Ag 1.875	TT 1.875
Stage 1 Phase 2 (Hyperimmunization)	1	TeNT-Hc 1.25	TeNT-Hc 1.875	TT 1.25	TeNT-Hc 1.25	TeNT-Hc 1.25	Mix Ag 1.25	TT 1.25
	2	TeNT-Hc 2.5	TeNT-Hc 3.75	TT 2.5	TeNT-Hc 2.5	TeNT-Hc 2.5	Mix Ag 2.5	TT 2.5
	3	TeNT-Hc 3.75	TeNT-Hc 5.625	TT 3.75	TeNT-Hc 3.75	TeNT-Hc 3.75	Mix Ag 3.75	TT 3.75
	4	TeNT-Hc 5	TeNT-Hc 7.5	TeNT-Hc 5	TT 5	TeNT-Hc 5	Mix Ag 5	TT 5
	5	TeNT-Hc 5	TeNT-Hc 7.5	TeNT-Hc 5	TT 5	TeNT-Hc 5	Mix Ag 5	TT 5
	6	TeNT-Hc 7.5	TeNT-Hc 11.25	TeNT-Hc 7.5	TeNT-Hc 7.5	TeNT-Hc 7.5	Mix Ag 7.5	TT 7.5
	7	TeNT-Hc 10	TeNT-Hc 15	TeNT-Hc 10	TeNT-Hc 10	TeNT-Hc 10	Mix Ag 10	TT 10
Stage 2	1	TeNT-Hc 3.75	TeNT-Hc 3.75	TeNT-Hc 3.75	TeNT-Hc 3.75	TeNT-Hc 3.75	Mix Ag 3.75	TT 3.75
	2	TeNT-Hc 7.5	TeNT-Hc 7.5	TeNT-Hc 7.5	TeNT-Hc 7.5	TeNT-Hc 7.5	Mix Ag 7.5	TT 7.5
	3	TeNT-Hc 15	TeNT-Hc 15	TeNT-Hc 15	TeNT-Hc 15	TeNT-Hc 15	Mix Ag 15	TT 15
Stage 3	1	TeNT-Hc 3.75	TeNT-Hc 3.75	TeNT-Hc 3.75	TeNT-Hc 3.75	TeNT-Hc 3.75	Mix Ag 3.75	TT 3.75
	2	TeNT-Hc 7.5	TeNT-Hc 7.5	TeNT-Hc 7.5	TeNT-Hc 7.5	TeNT-Hc 7.5	Mix Ag 7.5	TT 7.5
	3	TeNT-Hc 15	TeNT-Hc 15	TeNT-Hc 15	TeNT-Hc 10	TeNT-Hc 15	Mix Ag 15	TT 15

Figure 2. In different stages/phases of immunization schedule, various samples of corresponding horse blood were collected and analyzed. Horse blood samples were collected from the jugular veins and the corresponding plasma was separated using a modified human blood apheresis machine. The corresponding serum was collected after the horse blood clotted and centrifugation.

2.3. SDS-PAGE Analysis of Plasma Antibodies. The plasma collected after the final immunization of the third stage from each group or collected after routine TT immunization was diluted 10 times with normal saline. After being added into 2 × loading buffer, the samples were detected by a 12% SDS-PAGE and the differences plasma components between different immune groups were analyzed.

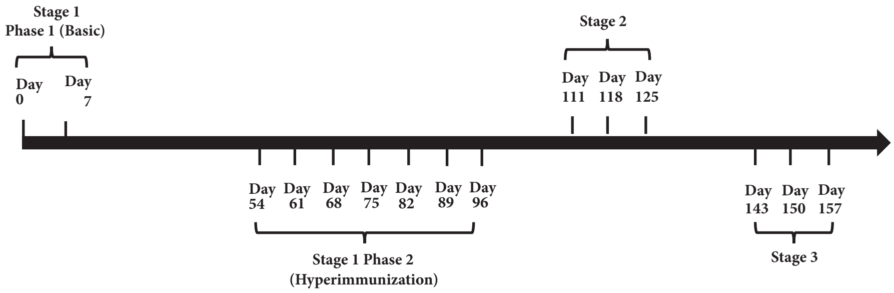

Figure 2: The summary of the immunization schedule and the shots.

2.4. Antibody Level Analysis. Horse serum and plasma were collected respectively at the end of the first stage (basic immunization, hyperimmunization), the second stage, and the third stage. The anti-TT and anti-TeNT-Hc antibody titers were determined by ELISA. The specific method was summarized as following: Each well on the 96-well ELISA plate (Costar) was coated with 2 μg / mL TT or TeNT-Hc at 4°C overnight, and washed 4 times with PBST (PBS + 0.1% Tween-20). Horse serum or plasma was diluted (1: 20000 v/v for IgG detection or 1: 500 for IgM detection), incubated at 37°C for 1 h, washed 4 times in PBST for 5 min, added 1: 100,000 dilution of HRP-anti horse IgG (1:100,000 dilution) or HRP-anti horse IgM (1: 20000 dilution), incubated at 37°C for 40 min, washed with PBST 4 times, and finally added chromogenic solution (TMB, Sigma). After color development, 2 M H_2SO_4 was applied to stop the reaction and the final readout was performed at 450 nm.

2.5. Agar Diffusion Test to Determine Plasma Antibody Titer. 2.25g of agarose was added 150 mL of purified water. It was heated to boil and poured into petri dishes. After cooling, 9 sample reservoirs were made by a hole puncher (one hole in the center with equal distance to the rest eight holes). To the center hole 100 μL of TeNT-Hc (0.17mg/mL) was added and, for the rest of holes, in the clockwise fashion, 100 μL of serial diluted immunized horse sera (v/v: 1/ 5, 1/10, 1/20, 1/40, 1/80, 1/160, 1/320, and 1/640) was added, respectively. The loaded petri dish was placed in a moisture control chamber and incubated at 37°C for 48 hours before recording the resulting precipitation lines.

2.6. Flocculation Method to Determine Plasma Efficacy. According to the method in Chinese Pharmacopoeia (2015 edition, Method 3506), different volumes (100 Lf/mL) of tetanus toxin standard solution were precisely-measured and added to the corresponding reaction tubes. Then diluted horse plasma (1 mL) was added quickly into those tubes and mixed thoroughly. The tubes were immersed in a water bath (45-50°C) and observed closely, and the volume of standard solution for first occurrence of flocculation was recorded. After repeating three times, the horse plasma efficacy (in flocculation unit (Lf/mL) = $V \times n \times 100$ [V is the volume of the tetanus toxin standard solution used in the first flocculation (mL); n is the dilution of the horse plasma]) can be determined.

2.7. In Vivo Tetanus Toxin Neutralization Test. According to the method in Chinese Pharmacopoeia (2015 edition, Method 3508), 0.2mL of the tetanus antitoxin standard (*ca* 0.5 IU/mL) and different concentrations of horse plasma (diluted by borate buffer) were mixed with 0.2mL of tetanus toxin standard, respectively. The mixtures were incubated at 37°C for 1 h and were then injected into mice intraperitoneally. There were three mice in each group and each group was observed at least twice a day for the first five days. The control group should all die within 72 to 120 hours. The efficacy of the horse serum was evaluated as the highest dilution which is most likely to die of the same symptoms as the control mice.

2.8. Statistical Analysis. Unpaired two-tailed Student's t-test was used to determine the significance of the differences in antibody titers and neutralizing potency between the groups. Probability (P) values <0.05 were considered to be significant and marked as $*$. P<0.01 was considered to be very significant and marked as $**$.

3. Results

3.1. Comparison of Plasma Composition after Different Immunization Methods. As shown in Figure 1, TeNT-Hc was shown as single component and has higher purity and smaller molecular weight in comparison with TT. However, SDS-PAGE (Figure 3) showed no significant difference between the main components (as well as antibodies) in the horse plasma prepared by different immunization methods (lanes 1-6) and those immunized by TT (lane 7). The molecular weight and proportion of the main components of each group are very similar.

3.2. Anti-Tetanus Toxin Antibody Levels Induced by TeNT-Hc. Serum titers of anti-TT, anti-TeNT-Hc IgG or IgM induced by TeNT-Hc alone or TeNT-Hc and TT co-immunization were tested. As shown in Figure 4, the titers of anti-TT IgG in serum of groups 5 and 6 were significantly higher than other groups one week post the basal immunization. However, further along the immunization schedule, there was no significant difference ($p \geq 0.05$) of anti-TT IgG antibody titers in serum among the groups except group 4 one week after the first, second, and third immunization. The lowest anti-TT IgG antibody titer in group 4 has significant difference with

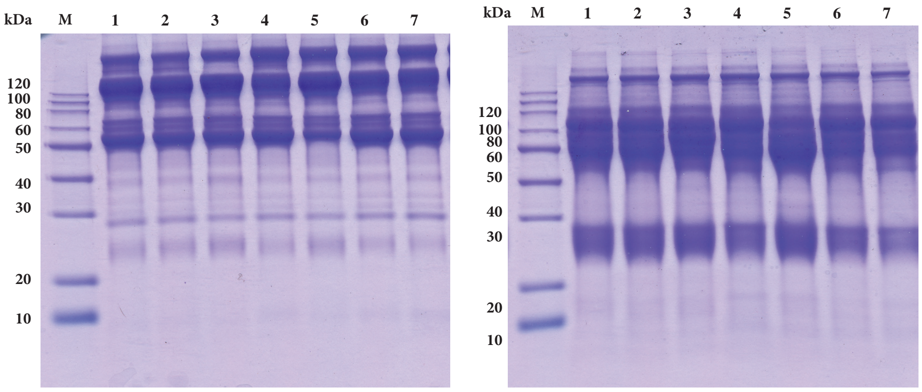

(a) (b)

Figure 3: Nonreducing (a) and reducing (b) SDS–PAGE analysis of horse plasmas. Lane M: molecular weight markers; lanes 1 to 6: plasma from horses in groups 1 to 6; lane 7: plasma from routine TT immunized horses.

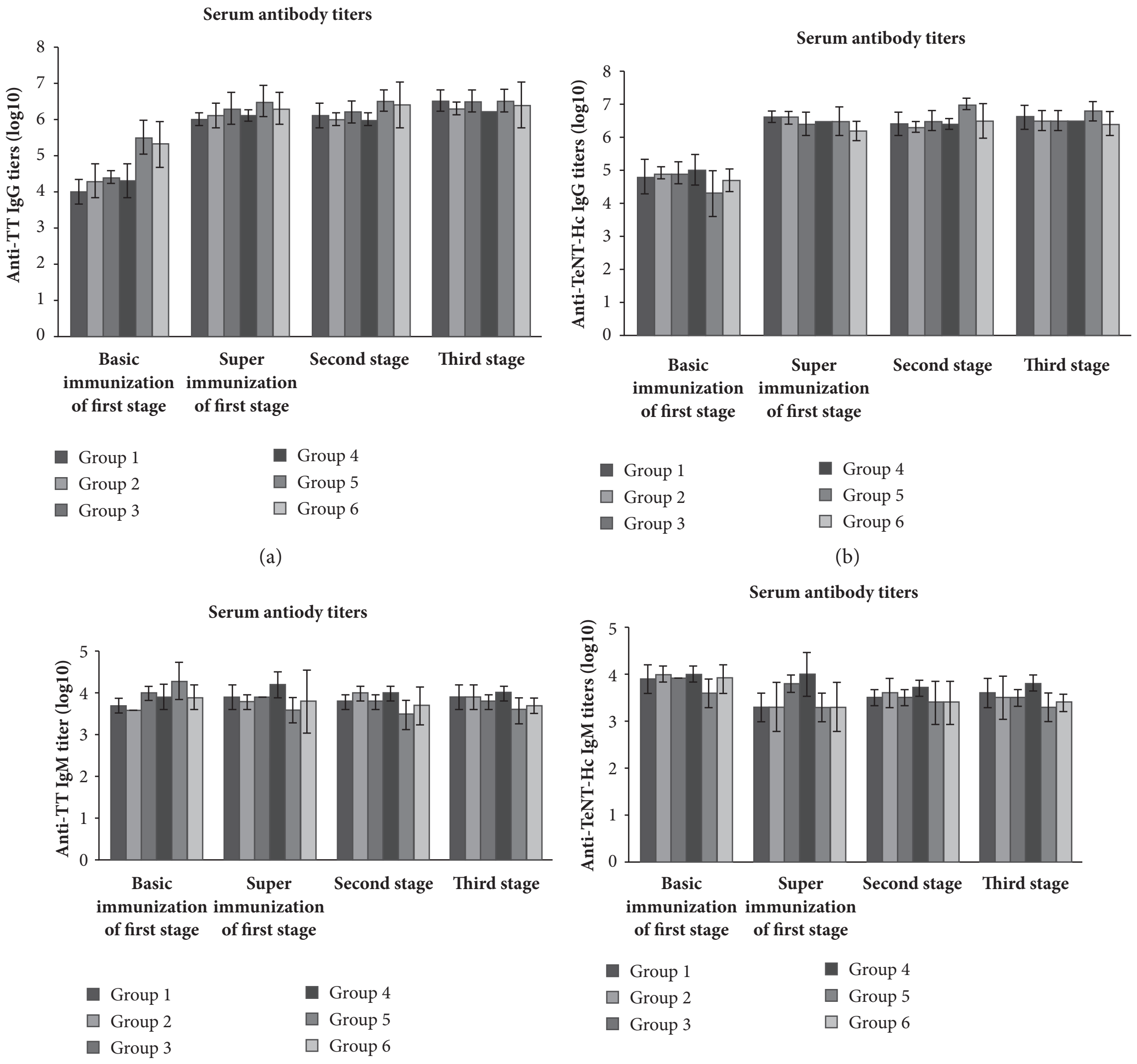

(a) (b)

(c) (d)

Figure 4: **Serum antibody titers after different immunization stages**. (a) Anti-TT IgG titers in serum; (b) anti-TeNT-Hc IgG titers in serum; (c) anti-TT IgM titers in serum; (d) anti-TeNT-Hc IgM titers in serum. Unpaired two-tailed Student's *t*-test was used to determine the significance of the differences in antibody titers between the groups. *P* values ≤ 0.05 were considered to be significant.

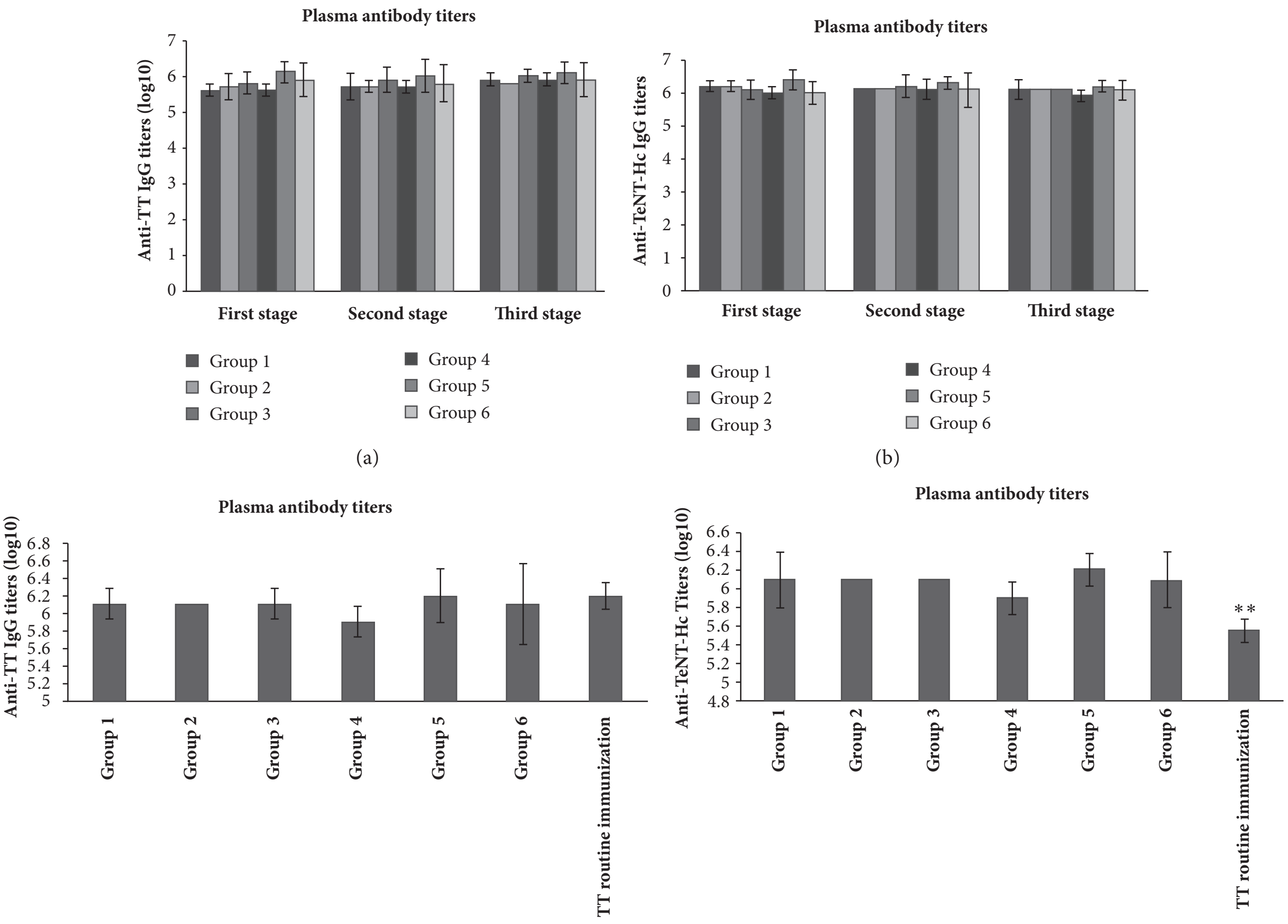

(a) (b) (c) (d)

Figure 5: **Plasma antibody titers after different immunization stages**. (a) Anti-TT IgG titers in plasma from group 1-6; (b) anti-TeNT-Hc IgG titers in plasma; (c) anti-TT IgG titers in plasma after three stages immunization and TT routine immunized plasma; (d) anti-TeNT-Hc IgG titers in plasma after three stages immunization and TT routine immunized plasma. Unpaired two-tailed Student's t-test was used to determine the significance of the differences in antibody titers between the groups. P values ≤ 0.05 were considered to be significant. $P<0.01$ was considered to be very significant and marked as $**$.

the highest antibody titer in group 5 ($p < 0.05$). Likewise, there were no significant difference in anti-TeNT-Hc IgG antibody titer, anti-TT, and TeNT-Hc IgM antibody titers between groups observed in immunization progress ($p > 0.05$). All immune methods can induce humoral immunity based on IgG antibody.

In addition to serum antibodies, antibody titers of anti-TT and anti-TeNT-Hc IgG in horse plasma one week after each stage of immunization were also studied (Figure 5). As the whole, the anti-TT IgG antibody titer in group 5 was generally higher than those in other groups and significantly higher than those in groups 1 and 4 after the first stage immunization ($p < 0.05$). However, there was no significant difference of anti-TT IgG titers among the groups after the second and the third stage immunization ($p \geq 0.05$). The titer of anti-TeNT-Hc IgG antibody in group 4 was slightly lower and significantly lower than those in group 5 after the first and third stage immunization ($p < 0.05$). No significant difference of anti-TeNT-Hc IgG titers was found among the other groups ($p \geq 0.05$). The anti-TT and anti-TeNT-Hc IgG titers in plasma after three stages of immunization with TeNT-Hc were compared with those collected after routine immunization with TT. The levels of anti-TT IgG antibodies among different groups had no significant difference ($p \geq 0.05$). However, the titers of anti-TeNT-Hc IgG antibody in the plasma of the TT conventional immunized group were significantly lower than those of the six groups of horse plasma immunized with TeNT-Hc ($p < 0.01$).

3.3. Specific Antibody Levels in Horse Plasma Tested by Agarose Diffusion. The titers of antitoxins specific binding to TeNT-Hc in different groups of horse plasma were evaluated of at different immunization stages by an agarose diffusion method. According to the result shown in Figure 6, the titers between group 3 and 4 had significant difference after the second immunization ($p < 0.05$). There was no significant difference in antibody titers among

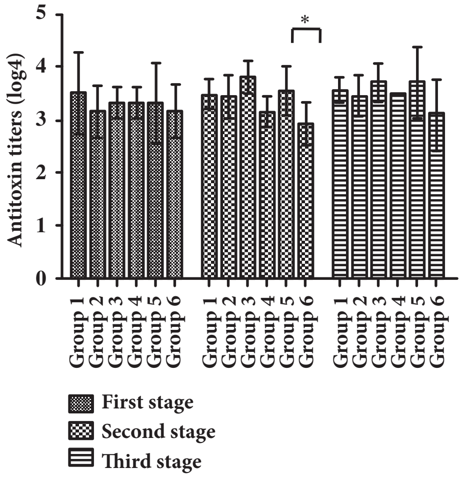

Figure 6: **Plasma antibody titers tested by agarose diffusion method**. Unpaired two-tailed Student's t-test was used to determine the significance of the differences in antibody titers between the groups. $P \leq 0.05$ was considered to be significant and marked as $*$.

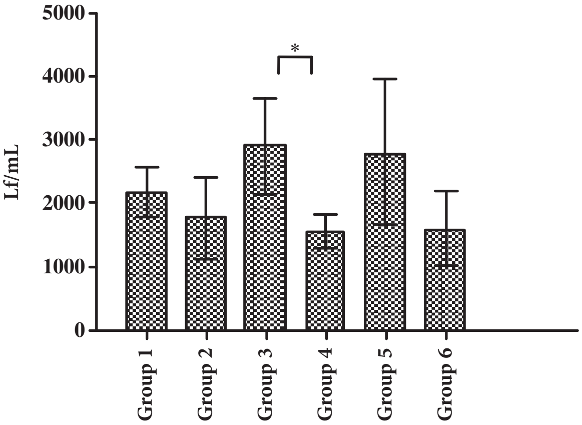

Figure 7: **Antitoxin titers in plasma measured by flocculation**. Unpaired two-tailed Student's t-test was used to determine the significance of the differences in antibody titers between the groups. $P \leq 0.05$ was considered to be significant and marked as $*$.

groups after the first and the third stage of immunization ($p \geq 0.05$).

3.4. Antitoxin Titers in Plasma Measured by Flocculation. In our preliminary experiments, the potency of TeNT-Hc with a protein concentration of 0.17 mg / mL was determined to be equivalent to the titer of tetanus toxoid (TT) of 100 Lf / mL. The potency of each group after three immunization stages was compared by using the TeNT-Hc (0.17 mg / mL) as the antigen. As shown in Figure 7, the antitoxin flocculent units in group 3 and group 5 were slightly higher than those in other groups. The flocculent units in group 4 were significantly lower than those in group 3 ($p < 0.05$). There was no significant difference among groups 1, 2, 3, 5, and 6 ($p \geq 0.05$).

3.5. In Vivo Neutralization of the Antitoxin in Mice. The *in vivo* neutralization test in mice was used to test the antitoxin potency of the plasma in each group one week after each stage of immunization. As shown in Figure 8, at one week after the first stage of immunization, the average titers of the plasma antitoxins in groups 2, 3, 5, and 6 were all higher than 1000 IU /mL, while the average titers of in groups 1 and 4 were less than 1000 IU /mL. One week after the second and third stage of immunization, the average antitoxin in each group was higher than 1000 IU/mL except that in group 4. According to statistical analysis, there was no significant difference among the antitoxin titers in groups 1, 2, 3, 5, and 6 ($p \geq 0.05$).

4. Discussion and Conclusion

As an effective immunogen, TT has played a critical role in the preparation of TAT. However, there were still inherent drawbacks of using TT: the production scale of toxin and bacterial strains were limited due to safety concern, the formaldehyde detoxification is generally incomplete, and the large-scale waste could cause environmental issues; the repeated immunization with considerable high-dose to the blood-harvesting horses will, sooner or later, induce the liver toxicity, resulting in reduced product quality and increased production costs. TeNT-Hc, the nontoxic fragment from TT and recombinant expressed in *E. coli*, has good immunogenicity, is low-cost, is easy to scale up, and is purified, not mention it is completely safe and nontoxic to both humans and horses. TeNT-Hc as a candidate for human tetanus vaccine is currently well underway and sued as a potential replacement of TT in TAT production. In this paper, using an established immunization procedures and doses, the *in vivo* immunogenicity of TeNT-Hc in horses was tested alone or in combination with TT antigen. The antibody titers in serum or plasma in different groups were compared with those immunized by the conventional TT and it showed very similar results from those using TT immunization. After additional two stages of immunization, the average potency in plasma of all groups reached more than 1,000 IU / mL except that in group 4. With refining the immunization methods and adjust the dosage, we have confidence that the results could easily exceed the potency required for tetanus antitoxin production. The purpose of this study is to evaluate the possibility of TeNT-Hc as an immunogen to replace TT in the tetanus antitoxin production. The difference in immune programs will affect the titers of antibodies and antitoxins. The immunization program used in this study is a routine and optimized procedure for the preparation of tetanus antitoxin by TT immunization. For TeNT-Hc, this program may be not the optimal program and it is necessary to further explore the best immunization program in the follow-up study.

As the experimental results show, there was no significant difference between the groups. In group 5, the first two basic immunizations with TT and the subsequent immunization with TeNT-Hc, it showed slightly higher antibody titers and potency. In group 4, which utilized the sequence of hyperimmunization with TT and the rest immunization with TeNT-Hc, it resulted in lower antibody titers and potency.

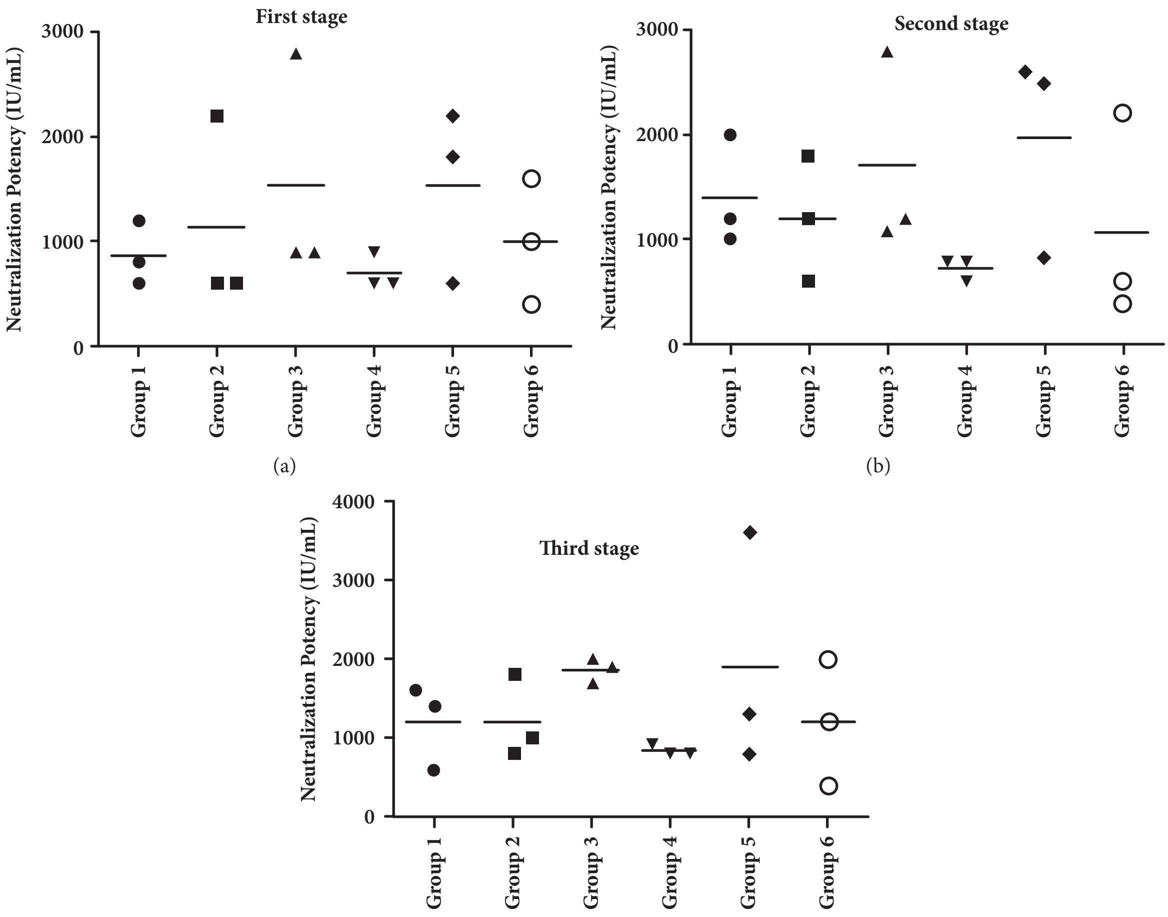

(a)

(b)

(c)

Figure 8: **Neutralizing potency of the corresponding antibodies in plasma from group 1-6**. (a) Plasma collected after the first immunization stage; (b) plasma collected after the second stage; (c) plasma collected after the third stage. Unpaired two-tailed Student's t-test was used to determine the significance of the differences in antibody titers between the groups.

The result that there was no significant difference in immunogenicity between the different dose groups and the different antigen combination groups may indicate that the lowest dose of TeNT-Hc used in the experiment was sufficient for the preparation of antitoxin. However, due to the small number of samples and large variations between the individual horses, a larger scale experiment is warranted to figure out the optimal immunization program. By optimizing the immunization schedule and the corresponding doses, TeNT-Hc may even show better immunogenicity.

Without the accumulated liver toxicity from TT immunization, TeNT-Hc positions itself as a completely nontoxic recombinant replacement while retaining all the effectiveness of TT, as a long-term safety study could easily reveal. In conclusion, this study further confirmed the validity of using TeNT-Hc to be replaced or used in conjugation with TT to produce TAT.

Data Availability

The data used to support the findings of this study are available from the corresponding author upon request.

Conflicts of Interest

Authors Chong Ji and Denghai Wang were employed by Gaotai Tianhong Biochemical Technology Development, Co., Ltd. Authors Yue Jing and Clifton Kwang-Fu Shen were employed by Shenzhen JinRuiFeng (Golden Harvest) Biotechnology, Ltd, which was a subsidiary of Shenzhen Qianhai Tianzheng (SQT) Biotechnology, Ltd. All other authors declare no conflicts of interest. The authors declare that they have no conflicts of interest with the contents of this article.

References

[1] I. H. Mallick and M. C. Winslet, "A review of the epidemiology, pathogenesis and management of tetanus," *International Journal of Surgery*, vol. 2, no. 2, pp. 109–112, 2004.

[2] L. Zibners, "Diphtheria, pertussis, and tetanus: evidence-based management of pediatric patients in the emergency department," *Pediatric Emergency Medicine Practice*, vol. 14, no. 2, pp. 1–24, 2017.

[3] I. Lukić, E. Marinković, A. Filipović et al., "Key protection factors against tetanus: Anti-tetanus toxin antibody affinity and its ability to prevent tetanus toxin - Ganglioside interaction," *Toxicon*, vol. 103, pp. 135–144, 2015.

[4] K. E. Vollman, N. M. Acquisto, and R. P. Bodkin, "Response to "protective effect of tetanus antibodies"," *The American Journal of Emergency Medicine*, vol. 32, no. 9, pp. 1128-1129, 2014.

[5] Y. Wu, Y. Gao, B. Zhu et al., "Antitoxins for diphtheria and tetanus decline more slowly after vaccination with DTwP than with DTaP: A study in a Chinese population," *Vaccine*, vol. 32, no. 22, pp. 2570–2573, 2014.

[6] S. Ghafourian, M. Raftari, N. Sadeghifard, and Z. Sekawi, "Toxin-antitoxin systems: Classification, biological function and application in biotechnology," *Current Issues in Molecular Biology*, vol. 16, no. 1, pp. 9–14, 2014.

[7] H. E. de Melker and E. W. Steyerberg, "Function of tetanus immunoglobulin in case of injury: administration often unnecessary," *Nederlands Tijdschrift voor Geneeskunde*, vol. 148, no. 9, pp. 429–433, 2004.

[8] S. Wendt, I. Eder, R. Wölfel, P. Braun, N. Lippmann, and A. Rodloff, "Botulism: Diagnosis and Therapy," *Deutsche Medizinische Wochenschrift*, vol. 142, no. 17, pp. 1304–1312, 2017.

[9] W. Xu, L. Ohanjanian, J. Sun et al., "A systematic review and meta-analysis of preclinical trials testing anti-toxin therapies for B. anthracis infection: A need for more robust study designs and results," *PLoS One*, vol. 12, no. 8, p. e0182879, 2017.

[10] I. Al-Abdulla, N. R. Casewell, and J. Landon, "Single-reagent one-step procedures for the purification of ovine IgG, F(ab′)2 and Fab antivenoms by caprylic acid," *Journal of Immunological Methods*, vol. 402, no. 1-2, pp. 15–22, 2014.

[11] S. Kodihalli, A. Emanuel, T. Takla et al., "Therapeutic efficacy of equine botulism antitoxin in Rhesus macaques," *PLoS ONE*, vol. 12, no. 11, 2017.

[12] F. Hirano, S. Imamura, Y. Sasaki et al., "Establishment of an equine tetanus antitoxin reference standard for veterinary use in Japan," *Biologicals*, vol. 44, no. 5, pp. 374–377, 2016.

[13] M. Yousefi, F. Tahmasebi, V. Younesi et al., "Characterization of neutralizing monoclonal antibodies directed against tetanus toxin fragment C," *Journal of Immunotoxicology*, vol. 11, no. 1, pp. 28–34, 2014.

[14] A. Rummel, S. Bade, J. Alves, H. Bigalke, and T. Binz, "Two carbohydrate binding sites in the HCC-domain of tetanus neurotoxin are required for toxicity," *Journal of Molecular Biology*, vol. 326, no. 3, pp. 835–847, 2003.

[15] J. L. Halpern and A. Loftus, "Characterization of the receptor-binding domain of tetanus toxin," *The Journal of Biological Chemistry*, vol. 268, no. 15, pp. 11188–11192, 1993.

[16] J. Herreros, G. Lalli, and G. Schiavo, "C-terminal half of tetanus toxin fragment C is sufficient for neuronal binding and interaction with a putative protein receptor," *Biochemical Journal*, vol. 347, no. 1, pp. 199–204, 2000.

[17] J. M. Wells, P. W. Wilson, P. M. Norton, M. J. Gasson, and R. W. F. Le Page, "*Lactococcus lactis*: high-level expression of tetanus toxin fragment C and protection against lethal challenge," *Molecular Microbiology*, vol. 8, no. 6, pp. 1155–1162, 1993.

[18] R. Yu, T. Fang, S. Liu et al., "Comparative Immunogenicity of the Tetanus Toxoid and Recombinant Tetanus Vaccines in Mice, Rats, and Cynomolgus Monkeys," *Toxins*, vol. 8, no. 7, p. 194, 2016.

[19] R. Yu, S. Yi, C. Yu et al., "A conformational change of C fragment of tetanus neurotoxin reduces its ganglioside-binding activity but does not destroy its immunogenicity," *Clinical and Vaccine Immunology*, vol. 18, no. 10, pp. 1668–1672, 2011.

[20] R. Yu, L. Hou, C. Yu et al., "Enhanced expression of soluble recombinant tetanus neurotoxin Hc in Escherichia coli as a tetanus vaccine candidate," *Immunobiology*, vol. 216, no. 4, pp. 485–490, 2011.

Hindawi
BioMed Research International
Volume 2018, Article ID 8594767, 14 pages
https://doi.org/10.1155/2018/8594767

Research Article

Chlorogenic Acid Functions as a Novel Agonist of PPARγ2 during the Differentiation of Mouse 3T3-L1 Preadipocytes

**Shu-guang Peng,[1,2,3] Yi-lin Pang,[1] Qi Zhu,[1] Jing-he Kang,[4]
Ming-xin Liu,[1] and Zheng Wang[1]**

[1] *College of Bioscience and Biotechnology, Hunan Agricultural University, 410128 Changsha, China*
[2] *Research Institute of Hunan Tobacco Science, Changsha 410007, China*
[3] *College of Plant Protection, Hunan Agricultural University, 410128 Changsha, China*
[4] *Key Laboratory of Agro-Ecological Processes in Subtropical, Institute of Subtropical Agriculture, Chinese Academy of Sciences, Hunan, Changsha 410125, China*

Correspondence should be addressed to Zheng Wang; zhengw@hunau.edu.cn

Received 12 September 2018; Accepted 19 November 2018; Published 3 December 2018

Guest Editor: Yan Huang

Copyright © 2018 Shu-guang Peng et al. This is an open access article distributed under the Creative Commons Attribution License, which permits unrestricted use, distribution, and reproduction in any medium, provided the original work is properly cited.

Rosiglitazone (RG) is a well-known activator of peroxisome proliferator-activated receptor-gamma (PPARγ) and used to treat hyperglycemia and type 2 diabetes; however, its clinical application has been confounded by adverse side effects. Here, we assessed the roles of chlorogenic acid (CGA), a phenolic secondary metabolite found in many fruits and vegetables, on the differentiation and lipolysis of mouse 3T3-L1 preadipocytes. The results showed that CGA promoted differentiation *in vitro* according to oil red O staining and quantitative polymerase chain reaction assays. As a potential molecular mechanism, CGA downregulated mRNA levels of the adipocyte differentiation-inhibitor gene *Pref1* and upregulated those of major adipogenic transcriptional factors (*Cebpb* and *Srebp1*). Additionally, CGA upregulated the expression of the differentiation-related transcriptional factor PPARγ2 at both the mRNA and protein levels. However, following CGA intervention, the accumulation of intracellular triacylglycerides following preadipocyte differentiation was significantly lower than that in the RG group. Consistent with this, our data indicated that CGA treatment significantly upregulated the expression of lipogenic pathway-related genes *Plin* and *Srebp1* during the differentiation stage, although the influence of CGA was weaker than that of RG. Notably, CGA upregulated the expression of the lipolysis-related gene *Hsl*, whereas it did not increase the expression of the lipid synthesis-related gene *Dgat1*. These results demonstrated that CGA might function as a potential PPARγ agonist similar to RG; however, the impact of CGA on lipolysis in 3T3-L1 preadipocytes differed from that of RG.

1. Introduction

Diabetes mellitus is a chronic degenerative metabolic disease that seriously affects human health and has reached epidemic proportions over the last 30 years [1]. Concomitant with the prevalence of obesity and increased lifespan in industrial countries, the incidence of type 2 diabetes has risen rapidly worldwide [2], with the number of people suffering from diabetes globally expected to rise to >600 million within the next 25 years [3]. Currently, China has the highest number of affected individuals, of whom 90% are afflicted with type 2 diabetes mellitus [4, 5]. A primary treatment strategy for type 2 diabetes relies upon improving insulin sensitivity, such as with the thiazolidinedione-class drug rosiglitazone (RG), a powerful insulin sensitizer. As a ligand of the nuclear receptor peroxisome proliferator-activated receptor-gamma (PPARγ), RG promotes the transcription of downstream genes of PPARγ [2]; however, long-term use of RG reportedly causes severe cardiovascular events and increased bone-fracture rates [6, 7]. Additionally, RG causes a significant weight increase in overweight subjects with type 1 diabetes [8]. Therefore, the safety of RG has been challenged. Accordingly, although RG is still utilized to treat patients suffering from type 2 diabetes in China [9, 10], it has been withdrawn from the European market [11]. To address this issue, researchers have focused on identifying new PPARγ agonists [11, 12] and insulin sensitizers as RG substitutes.

Many types of phenols have been advocated as natural remedies (*e.g.*, eugenol or capsaicins) or dietary supplements (*e.g.*, methoxypsoralen). The burden, metabolism, and biological effects of these dietary polyphenols are gradually gaining scientific and public attention and have been well studied, with results clarifying the margin of safety between a safe dose and the minimal dose necessary to produce significant adverse effects [13–15].

Epidemiological studies demonstrated that chlorogenic acid (CGA), a type of dietary polyphenol present in high quantities in plants and constituting the main active ingredient in many fruits, vegetables, and plants [16, 17], possesses numerous pharmacological activities, including those associated with antioxidative [18], anticancer [19–21], hypolipidemic [22], antihypertensive [23], anti-inflammatory [24], and hypoglycemic effects. Moreover, studies reported effects related to anti-insulin resistance and obesity [25], and protection against plant pathogenic fungi [26], as well as antimicrobial effects [27], inhibition of bile-duct ligation-induced liver injury [28], and attenuation of lipopolysaccharide-induced acute kidney injury [29]. Furthermore, CGA reportedly exhibits neuroprotective activity [30], and hypoxia-induced angiogenesis [31], and extends the lifespan of *Caenorhabditis elegans* [32]. Accumulating studies demonstrate that CGA exhibits antiobesity function by adjusting obesity-related adipokine levels, upregulating β-oxidation of fatty acids in the liver, and downregulating fatty acid and cholesterol biosynthesis in obese mice fed a high-fat diet (HFD) [16, 33]. Our previous study showed that CGA improved obesity-related metabolic disorders by upregulating *Pparg2* expression and inhibiting the nuclear factor (NF)-κB-signaling pathway in the adipose tissue of obese rats induced by a HFD [17]. Therefore, we hypothesized that CGA might function as a PPARγ agonist similar to RG, yet play a different regulatory role in preadipocyte differentiation to adipocytes.

Here, we used 3T3-L1 cells as an experimental model to explore the roles of CGA on lipogenesis. Specifically, we assessed the influence of CGA on 3T3-L1 cell proliferation and the expression of transcription factors [*Pparg2*, *CCAAT/enhancer binding protein beta* (*Cebpb*), and *sterol regulatory element-binding protein* (*Srebp*)1] and the key adipocyte-differentiation-related gene preadipocyte factor 1 (*Pref1*) during adipocyte differentiation. These results associated with CGA-mediated differentiation of mouse 3T3-L1 cells provide meaningful referential data for the rational use of CGA and the improvement of dietary structure.

2. Materials and Methods

2.1. Chemicals and Materials. Dulbecco's modified Eagle medium (DMEM), fetal bovine serum (FBS), streptomycin, and penicillin were acquired from Thermo Fisher Scientific (Waltham, MA, USA). CGA (⩾95% purity), rosiglitazone (RG; ⩾98% purity), and GW9662 (⩾99% purity) were purchased from Sigma-Aldrich (St. Louis, MO, USA), dissolved in dimethyl sulfoxide formulated as a 10 mM stock solution, and stored at -20°C. The rabbit monoclonal antibody against PPARγ (81B8) was purchased from Cell Signaling Technology (Danvers, MA, USA), and antibodies against β-actin, proliferating cell nuclear antigen (PCNA), horseradish peroxidase (HRP)-conjugated goat anti-mouse IgG, and HRP-conjugated goat anti-rabbit IgG were purchased from Proteintech (Rosemont, IL, USA).

2.2. Cell Culture. Undifferentiated mouse 3T3-L1 preadipocytes were purchased from the Cell Resource Center, Shanghai Institutes for Biological Sciences, Chinese Academy of Sciences (Shanghai, China), and cells were passaged 17 times. 3T3-L1 cells were cultured in high-glucose DMEM containing 10% FBS and 1% penicillin/streptomycin and incubated at 37°C in an atmosphere with 5% CO_2.

2.3. Cell-Viability Analysis. 3T3-L1 cells were seeded into 96-well plates at a density of 5×10^3 cells/well and incubated overnight. Cells were then incubated with different concentrations of CGA, and after 24 h, 48 h, and 72 h, cell viabilities were determined by counting living and dead cells using the trypan blue dye (0.05% solution)-exclusion method analyzed with a Bright-Line Hemacytometer (Sigma-Aldrich, USA) and cell counting kit (CCK)-8 (Dojindo, Kumamoto, Japan), respectively. After a 4 h incubation with 10 μL CCK-8 reagent, cell viability was calculated by measuring the optical density at 450 nm (Varioskan Flash; Thermo Fisher Scientific).

2.4. Induced Differentiation of Mouse 3T3-L1 Preadipocytes. 3T3-L1 cells were seeded into a 6-well plate at a concentration of 2×10^5 cells/well. Upon reaching ~90% confluence, the medium was replaced with fresh high-glucose DMEM containing 10% FBS and 1% penicillin/streptomycin, followed by incubation at 37°C in 5% CO_2 for 2 days and culture in cell-differentiation medium 1 (fresh high-glucose DMEM containing 10% FBS, 0.5 mM 3-isobutyl-1-methylxanthine, 1 μM dexamethasone, and 5 μg/mL insulin) containing 20 μM CGA, RG (positive control group), or GW9662 (negative control group). The differentiation time was calculated from the day at which the medium was changed. After 2 days, the medium was exchanged with cell-differentiation medium 2 (fresh high-glucose DMEM containing 10% FBS and 5 μg/mL insulin) containing the same combination of chemicals described. After another 2 days, cell-differentiation medium 2 was removed and replaced with cell-differentiation maintenance medium (CDMM) containing fresh high-glucose DMEM and 10% FBS. CDMM was changed every 2 days until the majority of the preadipocytes had differentiated into adipocytes and obvious lipid droplets were observed in the mature fat cells.

2.5. Oil Red O (ORO) Staining. The lipid accumulation in differentiated 3T3-L1 cells was observed by ORO staining on day (D)4, D6, D8, and D10 of differentiation. Cells were fixed with 4% formaldehyde for 30 min to 60 min after two washes with phosphate-buffered saline (PBS) and stained in ORO solution for 1 h after another two washes, followed by several rinses with 75% alcohol to remove excess dye. The

Table 1: Primer sequences used for real-time qPCR.

Gene	Primer sequence ($5'$–$3'$)
Pparg2	F:TCAAGGGTGCCAGTTTCG R:GGAGGCCAGCATCGTGT
Pref1	F:TCTCACGCACACTCACATCA R:CAACCTGGGGTCTCTCTCTG
Cebpb	F:GTTTCGGGACTTGATGCAAT R:AACCCCGCAGGAACATCT
Srebp1	F:AACCAGAAGCTCAAGCAGGA R:TCATGCCCTCCATAGACACA
Rxra	F:CCCAGCTCACCAAATGACCCT R:CTCGTTCCAGCCTGCCCGTA
Plin	F:TAGAGTTCCTCCTGCCACCA R:GTGCTGACCCTCCTCACAAG
Dgat1	F:TCCAGACAACCTGACCTACCGA R:CTCAAGAACTCGTCGTAGCAG
Hsl	F:AATCCCACGAGCCCTACCTCA R:CCTGCAAGGCATATCCGCTCT
Actb	F: CTTCTTTGCAGCTCCTTCG R: TTCTGACCCATTCCCACC

cells were then washed several times with ultrapure water, and photomicrographs were acquired at 200× magnification using a system incorporated in the DMI3000B inverted microscope (Leica, Wetzlar, Germany).

2.6. Triglyceride Assay. Intracellular triglycerides were evaluated using a triglyceride assay kit (GPO-POD; Applygen Technologies, Beijing, China) according to manufacturer protocol.

2.7. RNA Preparation and Quantitative Real-Time Polymerase Chain Reaction (qPCR). Total RNA was isolated from test cells using TRIzol reagent (Thermo Fisher Scientific), with 1 μg of each sample RNA used to generate cDNA using a reverse transcription reagent kit with gDNA Eraser (TaKaRa, Dalian, China) as a template for qPCR. Reactions were performed on a Step-One plus qPCR system (Applied Biosystems, Foster City, CA, USA) using SYBR Green qPCR master mix (TaKaRa). The sample was predenatured at 95°C for 30 s, followed by 40 cycles of denaturation at 95°C for 5 s and annealing at 60°C for 30 s. PCR efficiency for the primers ranged from 90% to 110%, and threshold cycle numbers (CT) were recorded for each reaction and normalized against that of *β-actin*. The primers were designed using Primer 5 software (Premier Biosoft, Palo Alto, CA, USA) and synthesized by Sangon Biotech Co., Ltd. (Shanghai, China) (Table 1).

2.8. Western Blot Analysis. On D0, D2, D4, D6, and D8 of 3T3-L1 cell differentiation, cells were lysed in radio immunoprecipitation assay lysis buffer (Applygen Technologies) supplemented with protease and phosphatase inhibitors on ice for 10 min after ice-cold PBS washes, followed by centrifugation at 12,000 *g* for 15 min at 4°C and supernatant collection. The nuclear fraction was extracted using a Nuc-Cyto-Mem preparation kit (Applygen Technologies), and protein concentrations were assayed using a BCA assay kit (Beyotime, Beijing, China). Each sample (50 μg protein) was separated by 10% gel electrophoresis before electrophoretic transfer onto polyvinylidene fluoride membranes (Bio-Rad, Hercules, CA, USA). Blots were blocked at room temperature for 2 h in blocking buffer [5% slim milk in Tris-buffered saline containing Tween20 (TBST)] and incubated with primary antibodies specific to PPARγ2 (1:1000), PCNA (1:5000), and β-actin (1:4000) overnight at 4°C. After three washes with TBST, the membrane was incubated with the secondary antibodies [HRP-conjugated anti-rabbit (1:6000) and anti-mouse (1:4000) IgG] at room temperature for 2 h with gentle agitation. Immunoreactive bands were visualized using an enhanced chemiluminescence reagent according to manufacturer instructions (Thermo Fisher Scientific). The optical density was quantified using Quantity One software (Bio-Rad).

2.9. Confocal Microscopy Analysis. On D0, D2, and D8 of 3T3-L1 cell differentiation, cells were rinsed with PBS twice for 5 min and fixed with 4% paraformaldehyde for 10 min, followed by three washes with PBS and permeabilization at room temperature for 30 min with 0.5% Triton X-100. Cells were then rinsed in PBS with Tween20 three times, followed by a blocking step with PBS containing 5% FBS at room temperature for 1 h. Samples were then incubated overnight at 4°C with a 1:100 dilution of anti-PPARγ2, followed by incubation with a secondary BODIPY conjugated goat anti-rabbit antibody (Cell Signaling Technology) at room temperature for 1.5 h. After incubation, cells were rinsed and stained with $4'$,6-diamidino-2-phenylindole (DAPI) for 6 min, followed by a series of 5-minute washes. The cells were sealed with an antifluorescence quencher; confocal images were captured using an LSM 7DUO confocal microscope (Carl Zeiss AG, Oberkochen, Germany) and processed using ZEN Lite software (Carl Zeiss AG).

2.10. Statistical Analysis. All values were expressed as the means ± standard error of the mean and analyzed with the SPSS package (v16.0; SPSS, Inc., Chicago, IL, USA). One-way analysis of variance, followed by least-significant difference tests, was used to evaluate significant differences between groups, with a $P < 0.05$ considered significant.

3. Results

3.1. Effect of CGA on Mouse 3T3-L1 Preadipocyte Proliferation. Cell-counting results showed that CGA influenced 3T3-L1 cell proliferation, with concentrations <50 μM resulting in no significant changes following incubation for 24 h and 48 h. However, increases in the incubation time to 72 h and CGA concentration $\geqslant 50$ μM resulted in significant inhibition of proliferation and a decrease in cell viability to 13.7% at 50 μM CGA (Figure 1). These results indicated that CGA displayed dose- and time-dependent effects on cell viability.

3.2. CGA Treatment Promotes Differentiation of 3T3-L1 Preadipocytes. CGA was tested to investigate its ability to

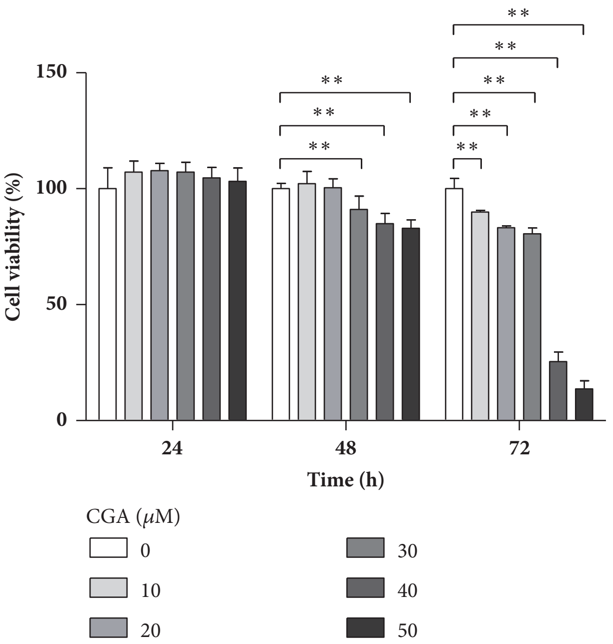

Figure 1: Chlorogenic acid (CGA) suppresses cell proliferation of mouse 3T3-L1 preadipocytes. 3T3-L1 preadipocytes were treated with control, 10, 20, 30, 40, and 50 μM CGA for 24, 48, and 72 h at 37°C, respectively. Experiments were performed in triplicate. Data are shown as the means ± SD (n = 3). $^{**}P < 0.01$.

promote 3T3-L1 preadipocyte differentiation. We observed the accumulation of lipid droplets in differentiated cells by microscopy on D10 of differentiation, after which morphological changes were detected in RG-treated 3T3-L1 cells, which changed from a predifferentiation spindle-like shape to a round shape following differentiation [Figure 2(A)(a, b)]. Additionally, microscopy analysis of ORO-stained lipid droplets within the cells revealed obvious lipid accumulation in RG- and CGA-treated cells relative to that observed in the control and GW9662-treated groups, although CGA treatment appeared less effective than RG treatment (Figure 2). Moreover, CGA-induced adipocyte morphology differed from that of the RG group (Figure 2).

To further evaluate the effect of CGA on 3T3-L1 preadipocyte differentiation, we determined the expression of genes involved in the protection of lipid droplets from lipolysis (*perilipin*; *Plin*) [34] and *de novo* lipogenesis (*Srebp1*) [35]. Compared with the positive and negative control (GW9662) groups, following CGA intervention, *Plin* and *Srebp1* mRNA levels were significantly upregulated during the differentiation process (Figures 2(B) and 2(C)); however, consistent with ORO-staining results, CGA treatment appeared less effective than RG treatment.

3.3. CGA Treatment Did Not Lead to Accumulation of Excess Intracellular Triacylglyceride (TAG). We determined TAG content to verify the influence of CGA on 3T3-L1 differentiation after D10. As shown in Figure 3, TAG content was significantly increased (about 2-fold) in 3T3-L1 cells treated with RG relative to that observed in the control group, whereas TAG content in CGA-treated 3T3-L1 cells was significantly decreased relative to that in the RG group ($P < 0.05$), although not significantly different from that in the control group. Additionally, treatment of differentiated cells with GW9662 (20 μM) decreased triglyceride levels by 42.9% as compared with the control group. These results were consistent with ORO-staining results, in that CGA treatment appeared less effective than RG treatment. These findings indicated that CGA effectively promoted adipocyte differentiation of 3T3-L1 cells, although the accumulation of intracellular TAG following preadipocyte differentiation was significantly lower than that in the RG-treated group.

To determine the mechanistic differences between CGA- and RG-induced 3T3-L1 differentiation, we analyzed the mRNA levels of genes involved in lipolysis (*hormone-sensitive lipase*; *Hsl*) and triglyceride biosynthesis (*diacylglycerol O-acyltransferase 1*; *Dgat1*). CGA treatment significantly increased *Hsl* expression by 30.9% to 58.1% during the prophase differentiation of 3T3-L1 cells (Figures 3(b) and 3(c)), whereas treatment with 20 μM CGA did not significantly alter *Dgat1* mRNA levels during the entire differentiation process relative to those observed in control and GW9662 groups. By contrast, RG treatment upregulated *Hsl* levels by 44.0% to 93.7% and *Dgat1* levels by 12.3% to 57.7% relative to those in control group. These results suggested that the reason CGA did not promote TAG accumulation might have been its upregulation of *Hsl* (lipolysis) and lack of effect on *Dgat1* (lipid synthesis) expression. These findings implied that the influence of CGA on preadipocytes differed from that of RG.

3.4. CGA Treatment Activates Key Genes Involved in Adipocyte Differentiation and the Transcription Factor PPARγ2. To quantify the role of CGA in the expression of key adipogenesis-related genes [*Pref1* and retinoid X receptor alpha (*Rxra*)] and major adipogenic transcription factors (*Pparg2* and *Cebpb*) during adipogenesis, preadipocytes were treated with 20 μM CGA during adipocyte differentiation on D2 to D10, and gene expression was analyzed by qPCR. Following CGA treatment, *Pparg2* and *Cebpb* mRNA levels increased relative to levels in control or GW9662-treated groups, whereas *Pref1* mRNA levels decreased during the differentiation process. However, no significant change in *Rxra* mRNA levels was observed between the CGA-treated and control groups. Also, it is worth noting that the effect of CGA on *Pref1*, *Cebpb,* and *Pparg2* mRNA levels appeared higher than that observed in the RG-treated group (Figure 4), suggesting that CGA treatment promoted 3T3-L1 cell differentiation to a level similar to that of RG treatment.

3.5. CGA Upregulates PPARγ2 Protein Levels during Adipocyte Differentiation. Western blot results showed that PPARγ2 levels increased significantly (by 18.42-76.92%) from D2 to D6 of differentiation following RG treatment as compared with levels in the control group (Figure 5). By contrast, CGA treatment resulted in significant increases in PPARγ2 levels in 3T3-L1 cells from D4 relative to those observed in control and GW9662-treated groups. However, on D8, the difference

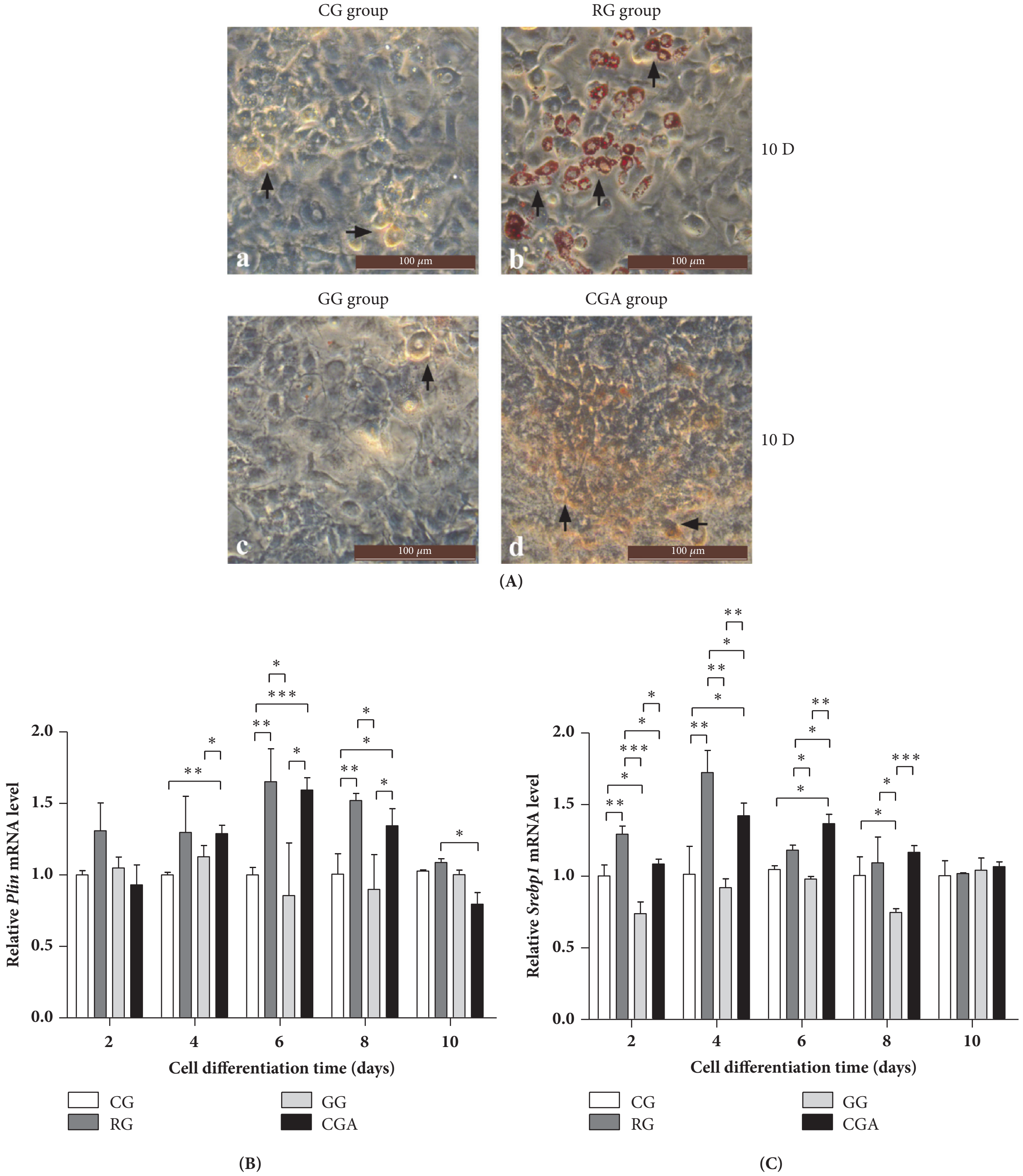

(A)

(B)

(C)

Figure 2: Comparative effect of chlorogenic acid (CGA) and rosiglitazone (RG) on the differentiation of mouse 3T3-L1 preadipocytes. (A) 3T3-L1 preadipocytes were cultured with or without CGA (20 μM) for 10 days; then cells were stained with ORO. RG was used as a positive control. GW9662 was used as a negative control group (GG). All images are shown at 200 × magnification. (a) Control group (CG); (b) RG group; (c) GG group; (d) CGA group; the arrows in a-d indicate the differentiation of preadipocytes; (B-C) effects of CGA on the expression of lipogenic pathway-related genes during the differentiation process of mouse 3T3-L1 preadipocytes. (B) *Plin*; (C) *Srebp1*. Data are shown as the means ± SD (n = 3). $^{*}P < 0.05$, $^{**}P < 0.01$, $^{***}P < 0.001$.

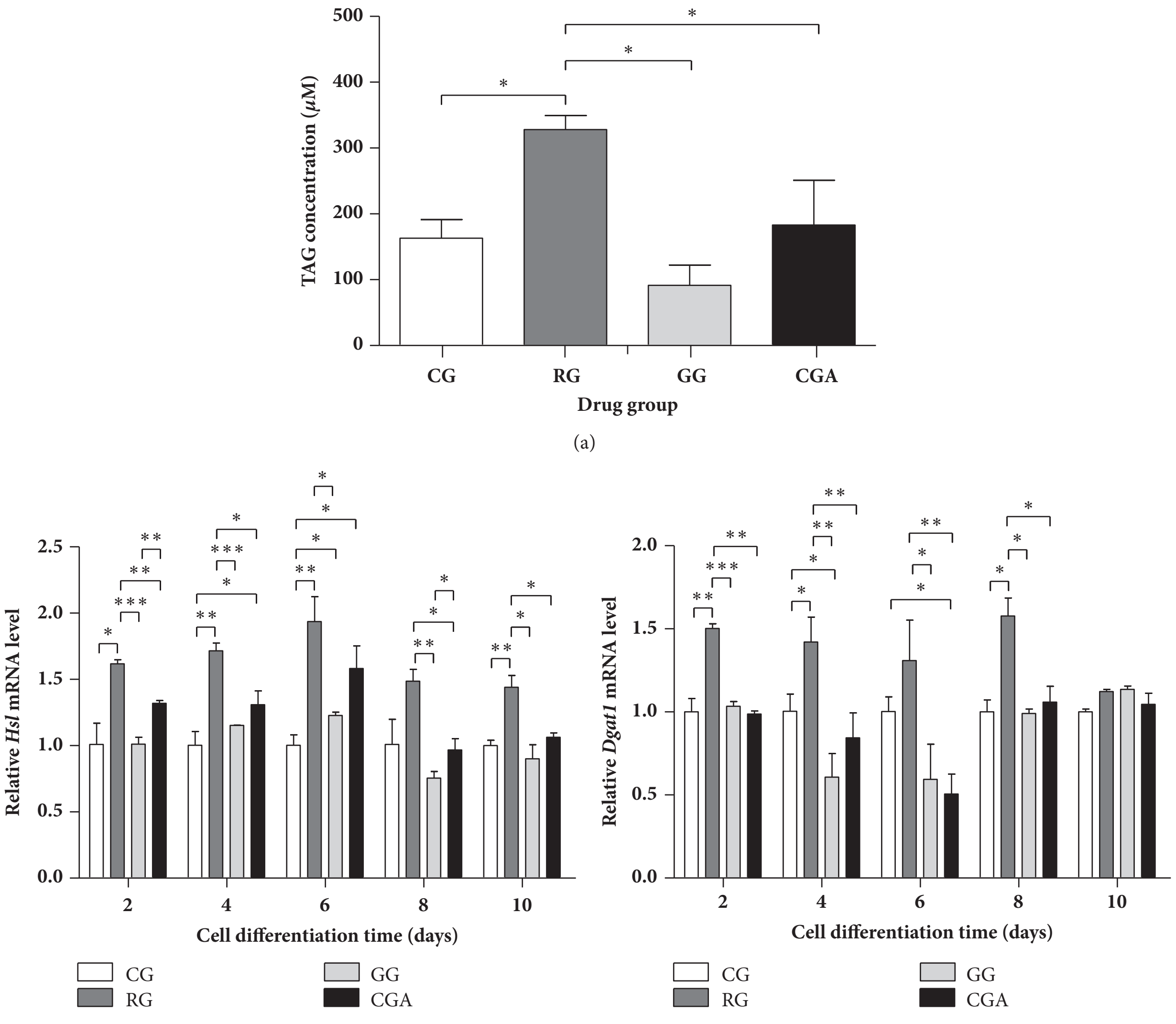

(a)

(b)

(c)

Figure 3: Chlorogenic acid (CGA) reduced triacylglyceride (TAG) accumulation in differentiated 3T3-L1 cells compared with the rosiglitazone group (RG). (a) Mouse 3T3-L1 preadipocytes were cultured without (control group, CG) or with CGA (20 μM) for 10 days; then the cellular TAG contents were measured using a TAG determination kit. (b-c) Effects of CGA on expression of the lipolysis-related gene *Hsl* (b) and triacylglycerol synthesis-related gene *Dgat1* (c) during the differentiation process of mouse 3T3-L1 preadipocytes. RG was used as a positive control. GW9662 was used as a negative control (GG). CG, control group. Data are shown as the means ± SD (n = 3). $^{*}P < 0.05$, $^{**}P < 0.01$, $^{***}P < 0.001$.

in these levels between the RG-treated and control groups was minimal, whereas those in the CGA group were >90% higher relative to PPARγ2 levels in the control ($P < 0.01$), GW9662-treated ($P < 0.01$), and RG-treated groups ($P < 0.05$), respectively.

In the nucleus of 3T3-L1 cells on D2 to D6, PPARγ2 levels in the CGA- and RG-treated groups increased relative to levels in the control and GW9662-treated groups. In particular, the highest PPARγ2 levels in the CGA-treated group appeared on D2 and were >2-fold higher than those in other treatment groups ($P < 0.01$). However, on D8, PPARγ2 levels in both the RG- and CGA-treated groups were significantly lower (~70%) than that in the control group ($P < 0.01$) and similar to that in the GW9662-treated group ($P > 0.05$). These results suggested that CGA treatment promoted adipocyte differentiation through upregulated PPARγ2 mRNA and protein levels.

3.6. CGA Affects the Subcellular Distribution of PPARγ2 during Adipocyte Differentiation. PPARγ2 is found specifically in adipose tissue [36]; however, to evaluate whether CGA affects PPARγ2 subcellular distribution, we investigated the distribution of endogenous PPARγ2 by immunostaining and confocal microscopy of mouse preadipocytes (Figure 6). On D0 and D2, immunostaining revealed PPARγ2 in the nucleus, with RG treatment significantly increasing the green

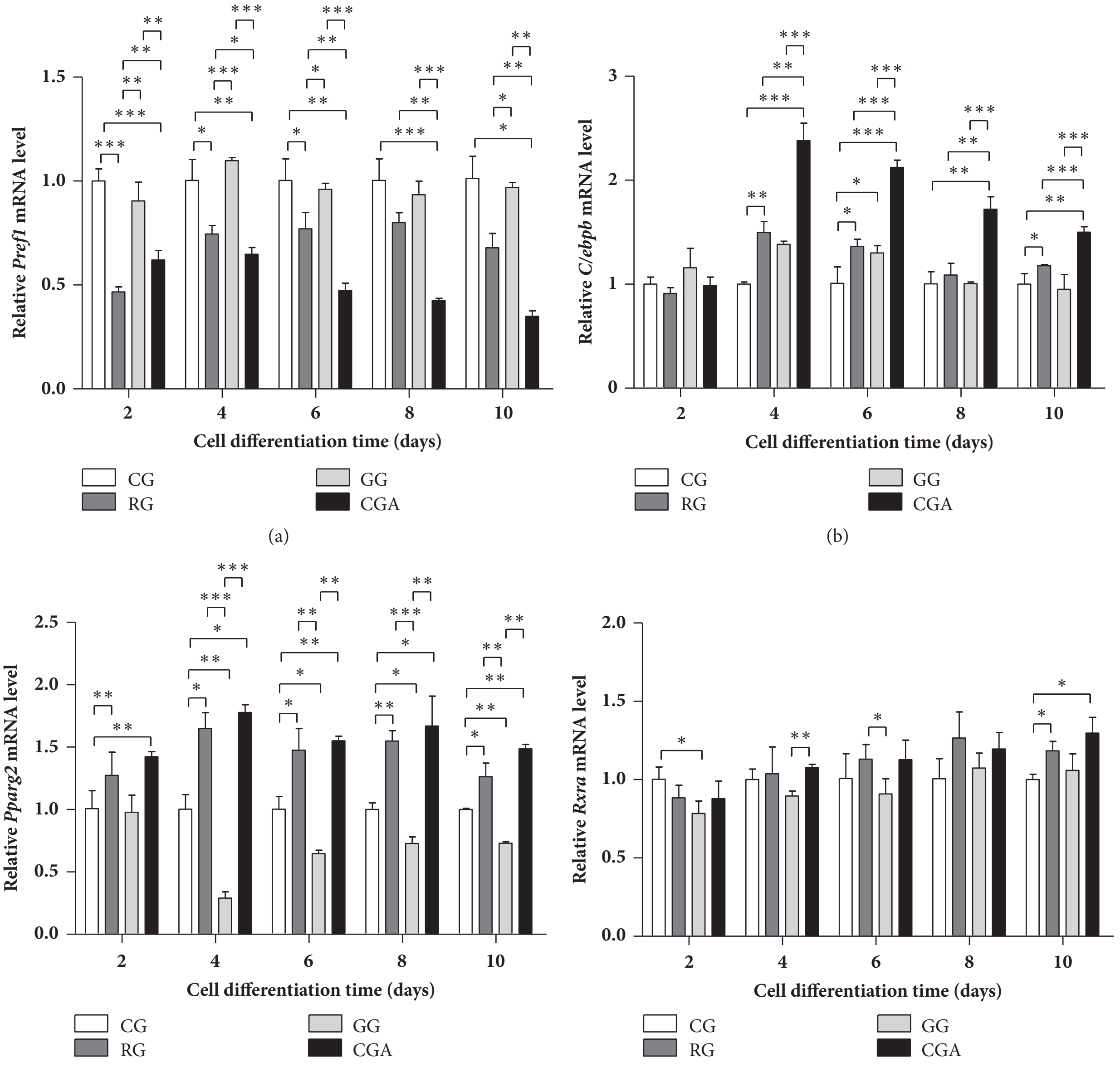

(a) (b) (c) (d)

Figure 4: Effects of chlorogenic acid (CGA) on the expression of key differentiation-related genes during the differentiation process of mouse 3T3-L1 preadipocytes. Rosiglitazone group (RG) was used as a positive control. GW9662 was used as a negative control (GG). CG, control group. (a) *Pref1*; (b) *Cebpb*; (c) *Pparg2*; (d) *Rxra*. Data are shown as the means ± SD (n = 3). $^*P < 0.05$, $^{**}P < 0.01$.

(PPARγ2):blue (nucleus) fluorescence ratio by 65.55% as compared with that of the control group ($P < 0.01$), whereas no difference was detected between the GW9662-treated and control groups (Figure 6(c)). By contrast, this ratio in the CGA-treated group was significantly (26.71%) higher than that of the control group ($P < 0.01$) and significantly lower (24.07%) than that of the RG-treated group ($P < 0.01$) (Figure 6(c)). Figure 6(d) shows a robust enhancement in blue fluorescence intensity on D8 relative to that on D2, suggesting an increased PPARγ2 distribution outside of the nucleus. Although we found no significant difference between the RG-treated and control groups, PPARγ2 levels in the CGA-treated group were slightly higher than those in the other three groups, with green:blue fluorescence ratio 30.17% higher than that of the control group ($P < 0.05$), 48.6% higher than that of the GW9662-treated group ($P < 0.01$), and 22.47% higher than that of the RG-treated group ($P > 0.05$) (Figure 6(e)). These results indicated that CGA and RG promoted PPARγ2 expression and subcellular distribution similarly during adipocyte differentiation.

4. Discussion

RG is a full agonist of PPARγ, activates the PPARγ nuclear receptor, and is widely used as a therapeutic agent for type

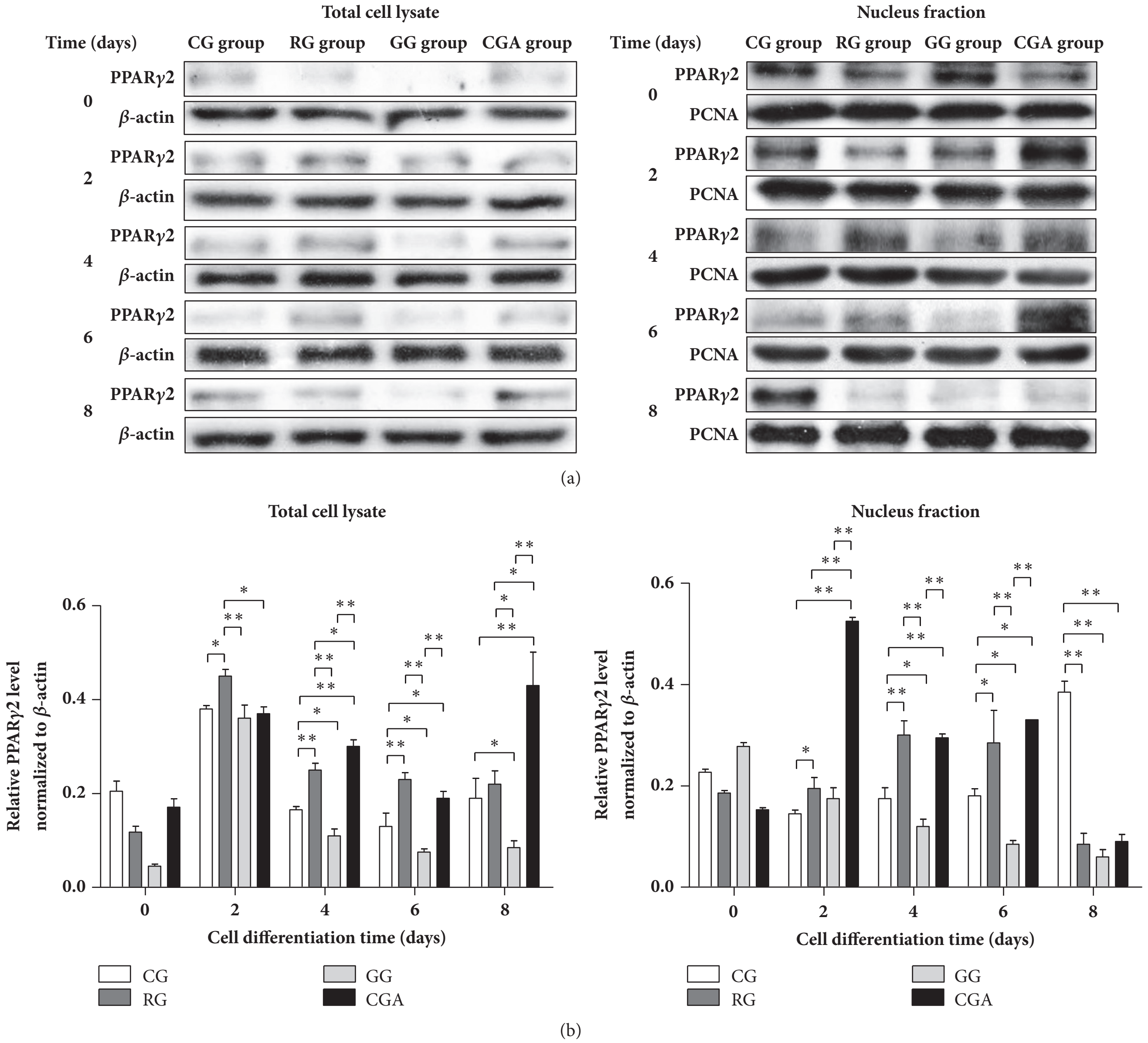

Figure 5: Chlorogenic acid (CGA) activates PPARγ2 during the differentiation process of mouse 3T3-L1 preadipocytes. (a) Mouse 3T3-L1 preadipocytes were treated with control (control group; CG), rosiglitazone (RG), GW9662 (GG), and CGA for 2, 4, 6, and 8 days, respectively. The samples were lysed and subjected to western blot analysis with indicated antibodies. Left: total cell lysate; Right: nucleus fraction. (b) The intensity of the band was quantified using densitometric imaging. Data are shown as the means ± SD (n = 3). $^{*}P < 0.05$, $^{**}P < 0.01$.

2 diabetes. However, studies indicate that partial PPARγ agonists have lower risks of causing side effects (*e.g.*, edema, fractures, and heart failure) relative to full PPARγ agonists, although they exhibit similar effects associated with insulin sensitivity. Therefore, it is necessary to identify safer and more effective partial PPARγ agonists [37, 38].

Many studies report that the CGA complex can be promoted as an active ingredient in the nutritional management of obesity [16, 39, 40]. In the present study, we investigated whether CGA could also affect preadipocyte differentiation through its lipid-lowering effect, as well as the molecular mechanism associated with CGA-mediated adipogenesis. We treated mouse 3T3-L1 preadipocytes with different doses of CGA, significant inhibition of 3T3-L1 cell viability in a time- and dose-dependent manner (Figure 1).

Lee *et al.* [41] reported changes in morphology of 3T3-L1 preadipocytes from a predifferentiation spindle-like shape to a round shape during early differentiate, with subsequent development of lipid droplets indicating preadipocyte differentiation into adipocytes and their accumulation signaling adipocyte maturity [42]. In the present study, ORO staining indicated that CGA promoted adipocyte differentiation, albeit to a lesser degree than that observed following RG treatment [Figure 2(A)(a)]. We found that the shape of the

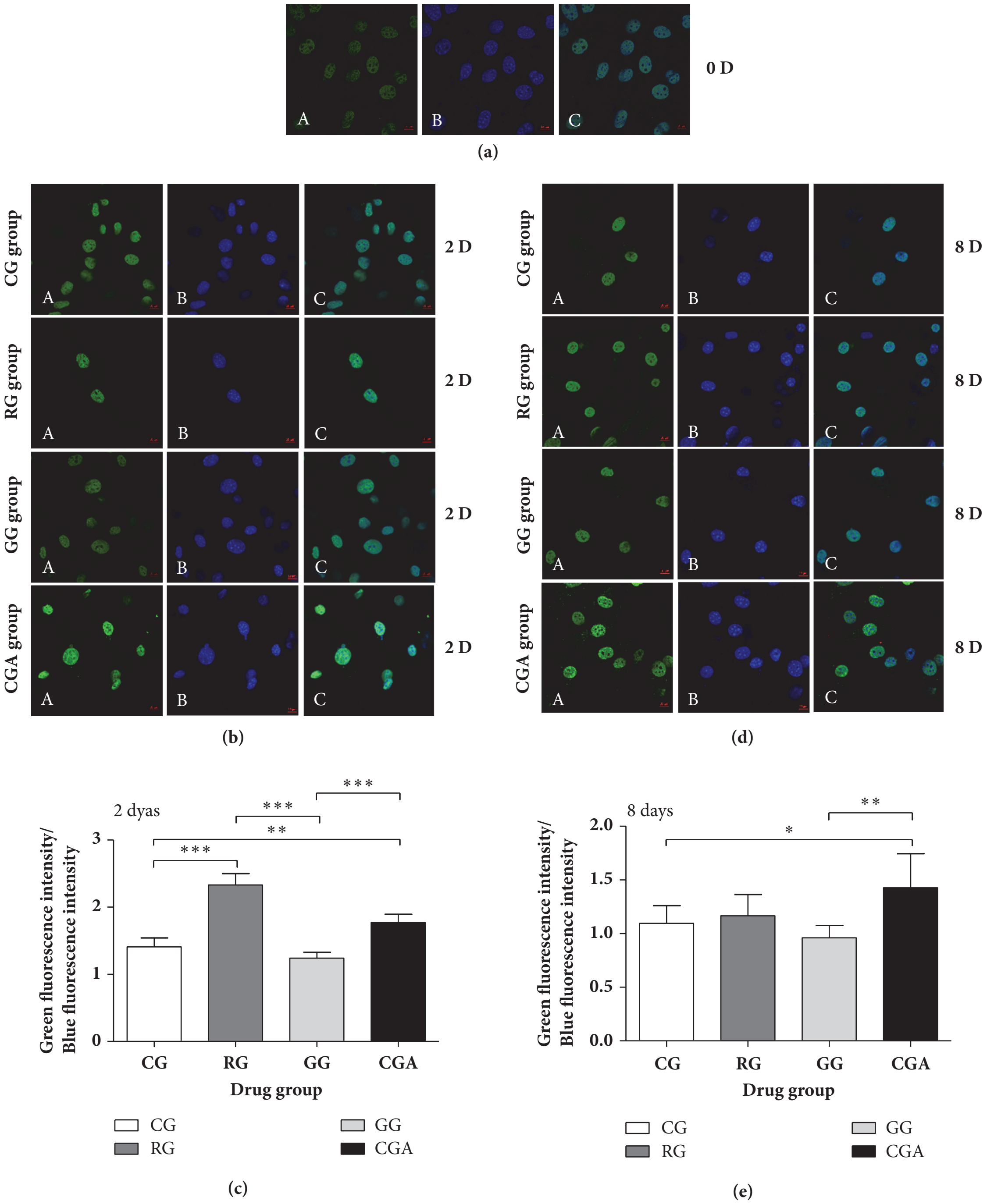
0 D
A
B
C
CG group
RG group
GG group
CGA group
2 D
8 D
2 dyas
8 days
***
**
*
Green fluorescence intensity/
Blue fluorescence intensity
0
1
2
3
0.0
0.5
1.0
1.5
2.0
CG
RG
GG
CGA
Drug group

(a)

(b)

(d)

(c)

(e)

Figure 6: Chlorogenic acid (CGA) enhances the expression of PPARγ2 during the differentiation process of mouse 3T3-L1 preadipocytes. Mouse 3T3-L1 preadipocytes were immunostained for PPARγ2 protein (*green*) (A), while nuclei were simultaneously revealed by DAPI staining (*blue*) (B). Colocalization is rendered in the merge panels (*cyan*) (C). Subcellular distribution of PPARγ2 and nuclei was analyzed by microscopic confocal analysis. (a) 0 days (630 ×); (b) 2 days (630 ×); (d) 8 days (630 ×). ((c) and (e)) The intensity of the green and blue fluorescence was quantified using ZEN 2 lite software. Data are shown as the means ± SD (n = 3). $^{*}P < 0.05$, $^{**}P < 0.01$, $^{***}P < 0.001$.

lipid droplets differed in the CGA-treated group relative to those in the RG-treated group (*i.e.*, small and not ring-like) [Figure 2(A)(a, d)] and implying that lipid accumulation in the CGA-treated group differed from that in the RG-treated group. Moreover, this morphological change was consistent with those reported previously [40].

According to the biological processes associated with adipocyte differentiation, we evaluated the expression levels of *Plin* and *Srebp*, which comprise important factors related to lipid homeostasis in 3T3-L1 cells. Lipid droplets store a large amount of TAGs, thereby regulating the storage and hydrolysis of lipids in mammalian adipocytes. The stability of lipid droplets is dependent upon PLINs, the most well-known coat proteins embedded in the phospholipid monolayer of lipid droplets [43] and that bind to and stabilize newly formed lipid droplets in order to protect them from breakdown by HSL [34, 43]. Ruiz *et al.* [38] reported that SREBP1 levels are significantly elevated in obese patients and animal models of obesity and type 2 diabetes, with other studies indicating that SREBP1 contributes to hepatic lipid accumulation and insulin resistance. In the present study, we found that CGA treatment significantly enhanced *Plin* and *Srebp1* expression as compared with levels in the control group, thereby contributing to lipid accumulation in 3T3-L1 cells. However, levels of both genes following CGA treatment were significantly lower than those in the RG-treated group (Figures 2(B) and 2(C)), suggesting increased lipid accumulation following RG treatment relative to that observed after CGA treatment.

Interestingly, Zheng *et al.* [39] demonstrated that CGA treatment decreased serum levels of TAG, a marker for lipid homeostasis, in mice, and that hepatic TAG concentrations were decreased by CGA + caffeine administration. Moreover, a previous study reported that CGA treatment decreased TAG levels in the liver and plasma of Sprague-Dawley rats on a high-energy diet [44]. In the present study, the TAG content of CGA-treated 3T3-L1 cells increased by only 12.25%, whereas TAG levels increased significantly by 101.02% following RG treatment relative to levels in the control group (Figure 3(a)). These results suggested that CGA treatment promoted adipocyte differentiation but had a weak effect on lipid accumulation in 3T3-L1 cells.

The *Hsl* gene is expressed in adipose tissue, where it hydrolyzes stored triglycerides to free fatty acids and mobilizes the stored lipids [45]. Therefore, HSL constitutes the rate-limiting enzyme in TAG catabolism, whereas DGAT1 is the key enzyme associated with TAG synthesis [17]. Figure 2(B) shows similar *Plin* expression between the CGA- and RG-treated groups during the differentiation process, whereas *Hsl* expression was lower in the CGA-treated group relative to that in the RG-treated group (Figure 3(b)). These results suggested that the rate of lipid degradation following CGA treatment was lower than that following RG treatment, contradicting the results of ORO and TAG staining (Figures 2(A) and 3(a)). However, it is worth noting that *Dgat1* expression in the RG-treated group was ~1.5-fold higher than that in the CGA-treated group from the initial stage of differentiation to D8 and that *Dgat1* expression in the CGA-treated group was similar to that in the control group. On D6 of differentiation, *Dgat1* expression in the CGA-treated group was lower than that in the GW9662 group (Figure 3(c)), implying that lipid synthesis following CGA treatment was inhibited as compared with that following RG treatment. Additionally, during the primary differentiation stage, *Srebp1* expression in the CGA-treated group was lower than that in the RG-treated group (Figure 3(c)). This might represent one of the mechanisms associated with the differences in the results of ORO staining observed between the CGA- and RG-treated groups and suggests that CGA intervention led to the accumulation of intracellular TAG during adipocyte differentiation, although to levels significantly lower than those in the RG-treated group.

Moreover, we observed that expression of key adipocyte-differentiation-related factors (*Pref1*, *Pparg2*, and *Cebpb*) changed during adipocyte differentiation. Our results agreed with a previous study reporting abundant *Pref1* expression in preadipocytes but a dramatic decrease in these levels during adipocyte differentiation [46]. Moreover, constitutive expression of *Pref1* in preadipocytes inhibits adipocyte differentiation [46]. PREF1 obstructs adipocyte differentiation by combining the promoter regions of *Cebpb* and *Cebpd* and inactivating C/EBPα and PPARγ [47]. Furthermore, *Pref1* overexpression decreases adipocyte-marker expression [46], and dexamethasone-mediated inhibition of *Pref1* expression in preadipocytes activates PPARγ and stimulates preadipocyte differentiation and maturation [48]. As an important transcription factor and master regulator of adipogenesis, PPARγ plays an important role in regulating the expression of genes involved in fatty acid β oxidation, lipid homeostasis, and controlling adipogenesis [49].

PPARγ has at least two subtypes: PPARγ1 is expressed in most tissues, and PPARγ2 is expressed specifically in adipose tissue [36]. C/EBPα shares a pathway with PPARγ associated with regulating preadipocyte differentiation, with C/EBPα activity dependent upon PPARγ status. Both proteins regulate the expression of *activating protein (Ap)-2*, *Fas*, and *Hsl*, as well as other factors related to preadipocyte differentiation [50]. Additionally, PPARγ promotes the transformation of cultured myoblasts into adipocytes, especially when coexpressed with C/EBPα [41]. During the early stage of adipocyte differentiation, *Cebpb* is highly expressed and initiates mitotic clonal expansion to enable entry of preadipose cells into the cell-proliferation cycle. After approximately two rounds of mitosis, cells exit this cycle and enter the differentiation stage, at which point C/EBPβ activates the expression of *Pparg* and other adipokines by binding to their promoter regions [51–54]. Additionally, C/EBPβ can also promote non-fat cell differentiation into adipocytes [55]; however, this requires PPARγ formation of a dimer with RXRα, which promotes transcriptional activity via binding to DNA [56]. PPARγ1 and PPARγ2 effectively stimulate adipocyte differentiation, although, under low-ligand (RXRα) concentrations, PPARγ2 stimulation of adipose-tissue formation is significantly stronger than that of PPARγ1 [57]. Moreover, Ren *et al.* [58] demonstrated that PPARγ2 rather than PPARγ1 plays a role in promoting cell differentiation.

In the present study, CGA and RG treatment, respectively, downregulated *Pref1* expression and upregulated *Pparg2* and *Cebpb* expression in all stages of 3T3-L1 cell differentiation and relative to levels observed in the control and GW9662-treated groups (Figures 4(a)–4(c)), whereas only minimal increases in *Rxra* levels were observed relative to controls (Figure 4(d)). These expression levels during adipocyte differentiation were consistent with those reported previously [46, 49, 51–54]. Notably, the effect of CGA treatment was more pronounced than that of RG treatment, with CGA treatment having a greater effect on *Pref1* expression. These data suggested that the number of preadipocytes in the CGA- and RG-treated groups was lower than that in the two control groups and that the majority of these adipocytes were able to differentiate into mature adipocytes. This finding was consistent with the results of ORO staining (Figure 2(A)). Additionally, several studies reported that downregulating *Plin*, *Srebp*, *Pparg*, and *Cebpa* inhibits adipogenesis in 3T3-L1 preadipocytes [34, 54, 59–61]. The results of the present study indicated that CGA treatment promoted adipogenesis specifically by affecting activation of adipogenic transcription factors and regulating adipogenesis-related gene expression.

Besten *et al.* [62] reported that short-chain fatty acids (SCFAs) prevent and reverse HFD-induced obesity in mice via a PPARγ-dependent switch from lipid synthesis to fat oxidation. SCFAs also stimulate mitochondrial fatty acid oxidation by activating the uncoupling protein 2 (UCP2)-AMPK-acetyl-CoA carboxylase (ACC) pathway in 3T3-L1 preadipocytes. Moreover, activating or inhibiting PPARγ activity via the PPARγ agonist RG or the PPARγ antagonist GW9662 abolishes SCFA-induced increases in UCP2-pAMPK-pACC signaling [63]. In the present study, we observed significantly lower TAG accumulation in 3T3-L1 cells following CGA treatment relative to that following RG treatment; however, whether this was due to CGA-mediated activation of UCP2-pAMPK-pACC signaling to promote β oxidation of fatty acids remains unknown.

Analysis of PPARγ2 levels revealed significant increases in *Pparg*2 expression in both CGA- and RG-treated groups, and that in the GW9662-treated group was significantly lower, relative to that observed in the control during the course of adipocyte differentiation and especially on D4 (Figure 4(c)). Our analysis of PPARγ2 levels agreed with qPCR results (Figures 4(c), 5, and 6) and with those reported previously [17]. These findings supported a role for CGA in promoting adipocyte through PPARγ2 expression and activity.

Zheng *et al.* [39] reported that supplementation of culture medium with 0.2% CGA reduced hepatic *Pparg* expression in mice, and Ryohei *et al.* [64] demonstrated that 5% caffeine downregulated PPARγ levels; however, the major bioactive constituent of CGA in coffee extract showed no effect on *Pparg* expression at concentrations of 100 μM. These results were inconsistent with the findings reported in the present study. Notably, numerous studies reported results consistent with our findings [17, 22, 25]. Sanchez *et al.* [22] reported that CGA acted as either an insulin secretagogue or a PPARα/γ dual agonist, and Ghadieh *et al.* [25] demonstrated that CGA/chromium supplementation alleviates insulin resistance. Additionally, our previous *in vivo* study [14] showed that supplementation with either low or high doses of CGA (20 and 90 mg/kg, respectively) significantly increased adipose-tissue PPARγ2 mRNA and protein levels, with these levels of CGA supplementation equivalent to physiological concentrations present in humans [17]. Moreover, Du *et al.* [65] demonstrated that intravenous injection of a 5-fold higher level of CGA than the recommended daily amount induced inflammation reactions and oxidative-stress injury in rats, with these findings supporting our use of 20 μM CGA in the present study. These findings suggest that the CGA concentration used in the present study was significantly lower than those of previous studies. Furthermore, the majority of CGA is hydrolyzed to caffeic acid and quinic acid before being absorbed in the gastrointestinal tract by gut microbiota esterases in both the small and large intestine [63]. Therefore, differences in dosage, CGA hydrolysis, or differentiation conditions might have contributed to inconsistencies in results. Nevertheless, our findings showed that CGA treatment activated PPARγ to a degree similar to RG treatment, potentially explaining the ability of CGA to increase insulin sensitivity and inhibit chronic inflammation caused by obesity [17, 21, 22, 25].

Previous studies reported strong links between PPARγ2 and the inflammatory response associated with obesity. PPARγ2 inhibits the inflammatory response via the NF-κB, Janus kinase-signal transducers and activators of transcription (STAT), AP-1, and nuclear factor of activated T cell pathways [66, 67]. As early as 1998, Ricote *et al.* [68] demonstrated that activation of PPARγ results in reduced transcriptional activity of cytokine-induced inflammation-associated factors, such as *Ap-1*, *Nfkb*, and *Stat* genes in mouse myeloid progenitor cells. Additionally, PPARγ reportedly plays an important role in improving insulin sensitivity [69], with clinical studies showing improvements in metabolic disorders and reduced inflammatory responses in type 2 diabetes patients treated with the PPARγ agonist RG within 6 months after receiving coronary artery intervention [70]. In the present study, CGA treatment promoted preadipocyte differentiation by activating PPAPγ2 in a similar manner to RG treatment, although RG treatment promoted a greater increase in lipid accumulation relative to that observed following CGA treatment. These results implied that CGA prevented lipid accumulation, even in the presence of activated PPAPγ2, suggesting its potential efficacy as a PPARγ agonist for clinical application.

5. Conclusions

This represents the first validation that CGA constitutes a PPAPγ2 agonist capable of effectively stimulating 3T3-L1 preadipocyte differentiation. However, our findings showed that CGA acted differently from RG in the area of fat metabolism during adipocyte differentiation and that TAG content was significantly higher in the RG-treated group relative to that in the CGA-treated group. This might be due to CGA enhancing lipolysis but not lipid synthesis, resulting in decreased lipid accumulation prior to preadipocyte differentiation. These data indicated that CGA represents a novel PPARγ2 agonist different from RG; however, further study of the regulation mechanism associated with CGA-mediated activity on lipid metabolism is necessary to provide insight to its potential application for preventing insulin resistance and hyperglycemia.

Data Availability

All the data are available from Professor Zheng Wang (zhengw@hunau.edu.cn) upon reasonable request.

Conflicts of Interest

The authors declare no conflicts of interest.

Authors' Contributions

Shu-guang Peng and Yi-lin Pang are equal contributors.

Acknowledgments

This study was supported by the National Natural Science Foundation of China (31071531) and the Foundation of the Research Institute of Hunan Tobacco Science (15-17Aa04).

References

[1] D. M. Nathan, "Diabetes: advances in diagnosis and treatment," *The Journal of the American Medical Association*, vol. 314, no. 10, pp. 1052–1062, 2015.

[2] J. Ye, "Challenges in drug discovery for thiazolidinedione substitute," *Acta Pharmaceutica Sinica B (APSB)*, vol. 1, no. 3, pp. 137–142, 2011.

[3] K. Ogurtsova, J. da Rocha Fernandes, Y. Huang et al., "IDF Diabetes Atlas: Global estimates for the prevalence of diabetes for 2015 and 2040," *Diabetes Research and Clinical Practice*, vol. 128, pp. 40–50, 2017.

[4] X. Song, H. Jia, Y. Jiang et al., "Anti-atherosclerotic effects of the glucagon-like peptide-1 (GLP-1) based therapies in patients with type 2 Diabetes Mellitus: A meta-analysis," *Scientific Reports*, vol. 5, 2015.

[5] S. Chatterjee, K. Khunti, and M. J. Davies, "Type 2 diabetes," *The Lancet*, vol. 389, no. 10085, pp. 2239–2251, 2017.

[6] S. E. Nissen and K. Wolski, "Effect of rosiglitazone on the risk of myocardial infarction and death from cardiovascular causes," *The New England Journal of Medicine*, vol. 356, no. 24, pp. 2457–2471, 2007.

[7] W. Wei, X. Wang, M. Yang, L. C. Smith, and P. C. Dechow, "PGC1beta mediates PPARgamma activation of osteoclastogenesis and rosiglitazone-induced bone loss," *Cell Metabolism*, vol. 11, no. 6, pp. 503–516, 2010.

[8] T. J. Orchard, "The effect of rosiglitazone on overweight subjects with type 1 diabetes," *Diabetes Care*, vol. 29, no. 3, pp. 746-747, 2006.

[9] K.-H. Zhang, Q. Huang, X.-P. Dai et al., "Effects of the peroxisome proliferator activated receptor-γ coactivator-1α (PGC-1α) Thr394Thr and Gly482Ser polymorphisms on rosiglitazone response in Chinese patients with type 2 diabetes mellitus," *Clinical Pharmacology and Therapeutics*, vol. 50, no. 9, pp. 1022–1030, 2010.

[10] Y. Lu, D. Ma, W. Xu, S. Shao, and X. Yu, "Effect and cardiovascular safety of adding rosiglitazone to insulin therapy in type 2 diabetes: a meta-analysis," *Journal of Diabetes Investigation*, vol. 6, no. 1, pp. 78–86, 2015.

[11] I. Schreiber, G. Dörpholz, C.-E. Ott et al., "BMPs as new insulin sensitizers: Enhanced glucose uptake in mature 3T3-L1 adipocytes via PPARγ and GLUT4 upregulation," *Scientific Reports*, vol. 7, no. 1, 2017.

[12] Y. Toyota, S. Nomura, M. Makishima, Y. Hashimoto, and M. Ishikawa, "Structure-activity relationships of rosiglitazone for peroxisome proliferator-activated receptor gamma transrepression," *Bioorganic & Medicinal Chemistry Letters*, vol. 27, no. 12, pp. 2776–2780, 2017.

[13] M. N. Clifford, "Miscellaneous phenols in foods and beverages - Nature, occurrence and dietary burden," *Journal of the Science of Food and Agriculture*, vol. 80, no. 7, pp. 1126–1137, 2000.

[14] A. A. Adedapo, B. O. Adeoye, M. O. Sofidiya, and A. A. Oyagbemi, "Antioxidant, antinociceptive and anti-inflammatory properties of the aqueous and ethanolic leaf extracts of Andrographis paniculata in some laboratory animals," *Journal of Basic and Clinical Physiology and Pharmacology*, vol. 26, no. 4, pp. 327–334, 2015.

[15] S. Ahuja, S. Kohli, S. Krishnan, D. Dogra, D. Sharma, and V. Rani, "Curcumin: A potential therapeutic polyphenol, prevents noradrenaline- induced hypertrophy in rat cardiac myocytes," *Journal of Pharmacy and Pharmacology*, vol. 63, no. 12, pp. 1604–1612, 2011.

[16] N. Tajik, M. Tajik, I. Mack, and P. Enck, "The potential effects of chlorogenic acid, the main phenolic components in coffee, on health: a comprehensive review of the literature," *European Journal of Nutrition*, vol. 56, no. 7, pp. 2215–2244, 2017.

[17] S.-L. Liu, B.-J. Peng, Y.-L. Zhong, Y.-L. Liu, Z. Song, and Z. Wang, "Effect of 5-caffeoylquinic acid on the NF-κB signaling pathway, peroxisome proliferator-activated receptor gamma 2, and macrophage infiltration in high-fat diet-fed Sprague-Dawley rat adipose tissue," *Food & Function*, vol. 6, no. 8, pp. 2779–2786, 2015.

[18] R. Jiang, J. M. Hodgson, E. Mas, K. D. Croft, and N. C. Ward, "Chlorogenic acid improves ex vivo vessel function and protects endothelial cells against HOCl-induced oxidative damage, via increased production of nitric oxide and induction of Hmox-1," *The Journal of Nutritional Biochemistry*, vol. 27, pp. 53–60, 2016.

[19] S. J. Deka, S. Gorai, D. Manna, and V. Trivedi, "Evidence of PKC binding and translocation to explain the anticancer mechanism of chlorogenic acid in breast cancer cells," *Current Molecular Medicine*, vol. 17, no. 1, pp. 79–89, 2017.

[20] Z. Zhang, D. Wang, S. Qiao et al., "Metabolic and microbial signatures in rat hepatocellular carcinoma treated with caffeic acid and chlorogenic acid," *Scientific Reports*, vol. 7, no. 1, 2017.

[21] N. Xue, Q. Zhou, M. Ji et al., "Chlorogenic acid inhibits glioblastoma growth through repolarizating macrophage from M2 to M1 phenotype," *Scientific Reports*, vol. 7, no. 1, 2017.

[22] M. B. Sanchez, E. Miranda-Perez, J. C. G. Verjan, M. de los Angeles Fortis Barrera, J. Perez-Ramos, and F. J. Alarcon-Aguilar, "Potential of the chlorogenic acid as multitarget agent: Insulin-secretagogue and PPAR α/γ dual agonist," *Biomedicine & Pharmacotherapy*, vol. 94, pp. 169–175, 2017.

[23] Z. Hakkou, A. Maciuk, V. Leblais et al., "Antihypertensive and vasodilator effects of methanolic extract of Inula viscosa: Biological evaluation and POM analysis of cynarin, chlorogenic acid as potential hypertensive," *Biomedicine & Pharmacotherapy*, vol. 93, pp. 62–69, 2017.

[24] O. Palócz, E. Pászti-Gere, P. Gálfi, and O. Farkas, "Chlorogenic acid combined with lactobacillus plantarum 2142 reduced LPS-induced intestinal inflammation and oxidative stress in IPEC-J2 cells," *PLoS ONE*, vol. 11, no. 11, 2016.

[25] H. E. Ghadieh, Z. N. Smiley, M. W. Kopfman, M. G. Najjar, M. J. Hake, and S. M. Najjar, "Chlorogenic acid/chromium supplement rescues diet-induced insulin resistance and obesity in mice," *Journal of Nutrition and Metabolism*, vol. 12, no. 1, 2015.

[26] G. Martínez, M. Regente, S. Jacobi, M. Del Rio, M. Pinedo, and L. de la Canal, "Chlorogenic acid is a fungicide active against phytopathogenic fungi," *Pesticide Biochemistry and Physiology*, vol. 140, pp. 30–35, 2017.

[27] L. Wang, C. Bi, H. Cai et al., "The therapeutic effect of chlorogenic acid against Staphylococcus aureus infection through sortase A inhibition," *Frontiers in Microbiology*, vol. 6, 2015.

[28] D. Wu, C. Bao, L. Li et al., "Chlorogenic acid protects against cholestatic liver injury in rats," *Journal of Pharmacological Sciences*, vol. 129, no. 3, pp. 177–182, 2015.

[29] H. Ye, J. Jin, L. Jin, Y. Chen, Z. Zhou, and Z. Li, "Chlorogenic Acid Attenuates Lipopolysaccharide-Induced Acute Kidney Injury by Inhibiting TLR4/NF-κB Signal Pathway," *Inflammation*, vol. 40, no. 2, pp. 523–529, 2017.

[30] Y. Mikami and T. Yamazawa, "Chlorogenic acid, a polyphenol in coffee, protects neurons against glutamate neurotoxicity," *Life Sciences*, vol. 139, pp. 69–74, 2015.

[31] J. J. Park, S. J. Hwang, J.-H. Park, and H.-J. Lee, "Chlorogenic acid inhibits hypoxia-induced angiogenesis via down-regulation of the HIF-1α/AKT pathway," *Cellular Oncology*, vol. 38, no. 2, pp. 111–118, 2015.

[32] S. Q. Zheng, X. B. Huang, T. K. Xing, A. J. Ding, G. S. Wu, and H. R. Luo, "Chlorogenic acid extends the lifespan of caenorhabditis elegans via insulin/IGF-1 signaling pathway," *Journal of Gerontology Series A Biological Sciences and Medical Sciences*, vol. 72, pp. 464–472, 2017.

[33] A.-S. Cho, S.-M. Jeon, M.-J. Kim et al., "Chlorogenic acid exhibits anti-obesity property and improves lipid metabolism in high-fat diet-induced-obese mice," *Food and Chemical Toxicology*, vol. 48, no. 3, pp. 937–943, 2010.

[34] B.-C. Jang, "Artesunate inhibits adipogeneis in 3T3-L1 preadipocytes by reducing the expression and/or phosphorylation levels of C/EBP-α, PPAR-γ, FAS, perilipin A, and STAT-3," *Biochemical and Biophysical Research Communications*, vol. 474, no. 1, pp. 220–225, 2016.

[35] R. Ruiz, V. Jideonwo, M. Ahn et al., "Sterol regulatory element-binding protein-1 (SREBP-1) is required to regulate glycogen synthesis and gluconeogenic gene expression in mouse liver," *The Journal of Biological Chemistry*, vol. 289, no. 9, pp. 5510–5517, 2014.

[36] S. Tyagi, P. Gupta, A. S. Saini, C. Kaushal, and S. Sharma, "The peroxisome proliferator-activated receptor: a family of nuclear receptors role in various diseases," *Journal of Advanced Pharmaceutical Technology & Research*, vol. 2, no. 4, pp. 236–240, 2011.

[37] R. M. Lago, P. P. Singh, and R. W. Nesto, "Congestive heart failure and cardiovascular death in patients with prediabetes and type 2 diabetes given thiazolidinediones: a meta-analysis of randomised clinical trials," *The Lancet*, vol. 370, no. 9593, pp. 1129–1136, 2007.

[38] R. Agrawal, P. Jain, and S. N. Dikshit, "Balaglitazone: a second generation peroxisome proliferator-activated receptor (PPAR) gamma (γ) agonist," *Mini-Reviews in Medicinal Chemistry*, vol. 12, no. 2, pp. 87–97, 2012.

[39] G. Zheng, Y. Qiu, Q.-F. Zhang, and D. Li, "Chlorogenic acid and caffeine in combination inhibit fat accumulation by regulating hepatic lipid metabolism-related enzymes in mice," *British Journal of Nutrition*, vol. 112, no. 6, pp. 1034–1040, 2014.

[40] D. De Souza Marinho Do Nascimento, R. M. Oliveira, R. B. G. Camara et al., "Baccharis trimera (Less.) DC exhibits an anti-adipogenic effect by inhibiting the expression of proteins involved in adipocyte differentiation," *Molecules*, vol. 22, no. 6, 2017.

[41] E. Hu, P. Tontonoz, and B. M. Spiegelman, "Transdifferentiation of myoblasts by the adipogenic transcription factors PPARγ and C/EBPα," *Proceedings of the National Acadamy of Sciences of the United States of America*, vol. 92, no. 21, pp. 9856–9860, 1995.

[42] H. Lee, J. Kim, J. Y. Park, K. S. Kang, J. H. Park, and G. S. Hwang, "Processed panax ginseng, sun ginseng, inhibits the differentiation and proliferation of 3T3-L1 preadipocytes and fat accumulation in caenorhabditis elegans," *Journal of Ginseng Research*, vol. 41, no. 3, pp. 257–267, 2017.

[43] T. Fujimoto, Y. Ohsaki, J. Cheng, M. Suzuki, and Y. Shinohara, "Lipid droplets: a classic organelle with new outfits," *Histochemistry and Cell Biology*, vol. 130, no. 2, pp. 263–279, 2008.

[44] K. Huang, X.-C. Liang, Y.-L. Zhong, W.-Y. He, and Z. Wang, "5-Caffeoylquinic acid decreases diet-induced obesity in rats by modulating PPARα and LXRα transcription," *Journal of the Science of Food and Agriculture*, vol. 95, no. 9, pp. 1903–1910, 2015.

[45] C. W. Liew, J. Boucher, J. K. Cheong et al., "Ablation of TRIP-Br2, a regulator of fat lipolysis, thermogenesis and oxidative metabolism, prevents diet-induced obesity and insulin resistance," *Nature Medicine*, vol. 19, no. 2, pp. 217–226, 2013.

[46] C. M. Smas and H. S. Sul, "Pref-1, a protein containing EGF-like repeats, inhibits adipocyte differentiation," *Cell*, vol. 73, no. 4, pp. 725–734, 1993.

[47] C. S. Hudak and H. S. Sul, "Pref-1, a gatekeeper of adipogenesis," *Frontiers in Endocrinology*, vol. 4, 2013.

[48] H. S. Sul, C. Smas, B. Mei, and L. Zhou, "Function of pref-1 as an inhibitor of adipocyte differentiation," *International Journal of Obesity*, vol. 24, pp. S15–S19, 2000.

[49] J. Jang, Y. Jung, S. Chae et al., "Gangjihwan, a polyherbal composition, inhibits fat accumulation through the modulation of lipogenic transcription factors SREBP1C, PPARγ and C/EBPα," *Journal of Ethnopharmacology*, vol. 210, pp. 10–22, 2018.

[50] E. D. Rosen, C. H. Hsu, X. Wang et al., "C/EBPalpha induces adipogenesis through PPARgamma: a unified pathway," *Genes & Development*, vol. 16, no. 1, pp. 22–26, 2002.

[51] R. Herrera, H. S. Ro, G. S. Robinson, K. G. Xanthopoulos, and B. M. Spiegelman, "A direct role for C/EBP and the AP-I-binding site in gene expression linked to adipocyte differentiation," *Molecular and Cellular Biology*, vol. 9, no. 12, pp. 5331–5339, 1989.

[52] R. J. Christy, K. H. Kaestner, D. E. Geiman, and M. Daniel Lane, "CCAAT/enhancer binding protein gene promoter: Binding of nuclear factors during differentiation of 3T3-L1 preadipocytes," *Proceedings of the National Acadamy of Sciences of the United States of America*, vol. 88, no. 6, pp. 2593–2597, 1991.

[53] C.-S. Hwang, S. Mandrup, O. A. MacDougald, D. E. Geiman, and M. D. Lane, "Transcriptional activation of the mouse obese (ob) gene by CCAAT/enhancer binding protein α," *Proceedings of the National Acadamy of Sciences of the United States of America*, vol. 93, no. 2, pp. 873–877, 1996.

[54] K. M. Sprott, M. J. Chumley, J. M. Hanson, and R. T. Dobrowsky, "Decreased activity and enhanced nuclear export of CCAAT-enhancer-binding protein β during inhibition of adipogenesis by ceramide," *Biochemical Journal*, vol. 365, no. 1, pp. 181–191, 2002.

[55] Z. Wu, Y. Xie, N. L. Bucher, and S. R. Farmer, "Conditional ectopic expression of C/EBP beta in NIH-3T3 cells induces PPAR gamma and stimulates adipogenesis," *Genes & Development*, vol. 9, pp. 2350–2363, 1995.

[56] J. L. Oberfield, J. L. Collins, C. P. Holmes et al., "A peroxisome proliferator-activated receptor gamma ligand inhibits adipocyte differentiation," *Proceedings of the National Acadamy of Sciences of the United States of America*, vol. 96, no. 11, pp. 6102–6106, 1999.

[57] E. Mueller, S. Drori, A. Aiyer et al., "Genetic analysis of adipogenesis through peroxisome proliferator-activated receptor γ isoforms," *The Journal of Biological Chemistry*, vol. 277, no. 44, pp. 41925–41930, 2002.

[58] D. Ren, T. N. Collingwood, E. J. Rebar, A. P. Wolffe, and H. S. Camp, "PPARgamma knockdown by engineered transcription factors: exogenous PPARgamma2 but not PPARgamma1 reactivates adipogenesis," *Genes & Development*, vol. 16, pp. 27–32, 2002.

[59] A. M. Rashid, K. Lu, Y. M. Yip, and D. Zhang, "Averrhoa carambola L. peel extract suppresses adipocyte differentiation in 3T3-L1 cells," *Food & Function*, vol. 7, no. 2, pp. 881–892, 2016.

[60] L. Y. Cheong, S. Suk, N. R. Thimmegowda et al., "Hirsutenone directly targets PI3K and ERK to inhibit adipogenesis in 3T3-L1 preadipocytes," *Journal of Cellular Biochemistry*, vol. 116, no. 7, pp. 1361–1370, 2015.

[61] K. Kowalska, A. Olejnik, J. Rychlik, and W. Grajek, "Cranberries (Oxycoccus quadripetalus) inhibit adipogenesis and lipogenesis in 3T3-L1 cells," *Food Chemistry*, vol. 148, pp. 246–252, 2014.

[62] G. Den Besten, A. Bleeker, A. Gerding et al., "Short-chain fatty acids protect against high-fat diet-induced obesity via a PPARgamma-dependent switch from lipogenesis to fat oxidation," *Diabetes*, vol. 64, no. 7, pp. 2398–2408, 2015.

[63] Y. Konishi and S. Kobayashi, "Transepithelial transport of chlorogenic acid, caffeic acid, and their colonic metabolites in intestinal caco-2 cell monolayers," *Journal of Agricultural and Food Chemistry*, vol. 52, pp. 2518–2526, 2004.

[64] R. Aoyagi, M. Funakoshi-Tago, Y. Fujiwara, and H. Tamura, "Coffee inhibits adipocyte differentiation via inactivation of PPARγ," *Biological & Pharmaceutical Bulletin*, vol. 37, no. 11, pp. 1820–1825, 2014.

[65] W.-Y. Du, C. Chang, Y. Zhang et al., "High-dose chlorogenic acid induces inflammation reactions and oxidative stress injury in rats without implication of mast cell degranulation," *Journal of Ethnopharmacology*, vol. 147, no. 1, pp. 74–83, 2013.

[66] R. B. Clark, D. Bishop-Bailey, T. Estrada-Hernandez, T. Hla, L. Puddington, and S. J. Padula, "The nuclear receptor PPARγ and immunoregulation: PPARγ mediates inhibition of helper T cell responses," *The Journal of Immunology*, vol. 164, no. 3, pp. 1364–1371, 2000.

[67] H. Lee, W. Shi, P. Tontonoz et al., "Role for peroxisome proliferator-activated receptor α in oxidized phospholipid-induced synthesis of monocyte chemotactic protein-1 interleukin-8 by endothelial cells," *Circulation Research*, vol. 87, no. 6, pp. 516–521, 2000.

[68] M. Ricote, A. C. Li, T. M. Willson, C. J. Kelly, and C. K. Glass, "The peroxisome proliferator-activated receptor-gamma is a negative regulator of macrophage activation," *Nature*, vol. 391, no. 6662, pp. 79–82, 1998.

[69] Z.-Y. Li, J. Song, S.-L. Zheng et al., "Adipocyte Metrnl Antagonizes Insulin Resistance Through PPARγ Signaling," *Diabetes*, vol. 64, no. 12, pp. 4011–4022, 2015.

[70] G. Wang, J. Wei, Y. Guan, N. Jin, J. Mao, and X. Wang, "Peroxisome proliferator-activated receptor-γ agonist rosiglitazone reduces clinical inflammatory responses in type 2 diabetes with coronary artery disease after coronary angioplasty," *Metabolism - Clinical and Experimental*, vol. 54, no. 5, pp. 590–597, 2005.

Hindawi
BioMed Research International
Volume 2018, Article ID 8343052, 7 pages
https://doi.org/10.1155/2018/8343052

Research Article

Effect of Quercetin Monoglycosides on Oxidative Stress and Gut Microbiota Diversity in Mice with Dextran Sodium Sulphate-Induced Colitis

Zhu Hong [1] **and Meiyu Piao** [2]

[1]Department of Anal and Intestinal Surgery, Tianjin Union Medical Center (Nankai University Affiliated Hospital), Tianjin, China
[2]Department of Gastroenterology and Hepatology, Tianjin Medical University, General Hospital, Tianjin 300052, China

Correspondence should be addressed to Meiyu Piao; ypiao01@tmu.edu.cn

Received 16 October 2018; Accepted 7 November 2018; Published 12 November 2018

Guest Editor: Hengjia Ni

Copyright © 2018 Zhu Hong and Meiyu Piao. This is an open access article distributed under the Creative Commons Attribution License, which permits unrestricted use, distribution, and reproduction in any medium, provided the original work is properly cited.

The pathogenesis of inflammatory bowel disease (IBD) is linked to an intricate association of environmental, microbial, and host-related factors. This study examined the potential effects of dietary addition of two preparations from onion, one comprising quercetin aglycone alone (Q: 0.15% polyphenols, quercetin aglycone:quercetin monoglycosides, 98:2) and another comprising quercetin aglycone with monoglycosides (Q+MQ: 0.15% total polyphenols, quercetin aglycone:quercetin monoglycosides, 69:31), on dextran sodium sulphate- (DSS-) induced colitis in mice. The results revealed a significant decrease in the body weight gain of the mice with DSS-induced colitis, which was counteracted by the dietary Q or Q+MQ supplementation. Meanwhile, the oxidative stress indicated by myeloperoxidase (MPO), reduced glutathione (GSH), malondialdehyde (MDA), and serum nitrate (NO) concentrations was higher in mice with DSS-induced colitis than in the control group mice, but dietary Q or Q+MQ supplementation counteracted this trend. The colitis mice demonstrated reduced Chao1, angiotensin-converting enzyme (ACE), and Shannon indices and an increased Simpson index, but the colitis mice receiving dietary Q or Q+MQ exhibited higher Chao1, ACE, and Shannon indices and a reduced Simpson index. In conclusion, this research showed that even at a low dose, dietary Q or Q+MQ supplementation counteracts DSS-induced colitis in mice, indicating that Q or Q+MQ may be used as an adjuvant therapy for IBD patients.

1. Introduction

Inflammatory bowel disease (IBD) is a chronic immune system-mediated inflammatory disorder that comprises a range of conditions predominantly affecting the gastrointestinal tract [1]. These conditions include Crohn's disease, ulcerative colitis, and indeterminate colitis, a rare condition. The pathogenesis of IBD is linked to an intricate association of environmental, microbial, and host-related factors, including genetic factors; however, the precise mechanism underlying the condition remains unknown [2, 3].

Numerous contributing factors influence the pathology of IBD, including genetic, environmental, and inflammatory factors, intestinal microbiota, and oxidative stress conditions [4–6]. Oxidative stress is associated with protein, lipid, and DNA damage due to oxidation reactions and is thus considered to be responsible for the development of many pathological disorders or exacerbation of symptoms, such as inflammation [7–9]. Recently, the significant role of intestinal microbiota in the pathophysiology of IBD has been emphasized. Most studies have reported reduced diversity of intestinal microbiota in IBD patients [10, 11], with reduced Firmicutes population and increased Proteobacteria population being the most commonly observed variations [3, 11]. The reduced diversity of intestinal microbiota observed in IBD patients is considered to be predominantly caused by a reduction in Firmicute diversity.

Although therapeutic drugs, such as steroids, immunomodulators, and antibodies, are available to treat IBD, their administration is limited due to their serious side-effects, including infection, malignancy, and general health concerns [12, 13]. Several studies that have investigated nutritional controls for IBD, with particular focus on polyphenols, have reported that a variety of polyphenols can be used as potential therapeutic approaches for IBD [14].

Onions are known to contain high levels of polyphenols, the most abundant of which is quercetin [15, 16]. Quercetin mostly occurs in the glycoside form, although the free aglycone form is also reasonably common [16]. Studies have shown that quercetin exhibits antihypertensive, antidepressant, and anti-inflammatory properties by participating in several intracellular biochemical mechanisms [17]. However, different polyphenolic compounds within the diet may have different effects on the host physiology, either locally within the intestinal tract or on other tissues [18]. The present study investigated the protective effects of dietary addition of two preparations from onion, one rich in quercetin aglycone alone (Q) and another containing quercetin aglycone with monoglycosides (Q+MQ), on dextran sodium sulphate- (DSS-) induced colitis in mice.

2. Materials and Methods

2.1. Preparation of Quercetin and Quercetin Monoglycosides. Quercetin and quercetin monoglycosides were prepared according to the method described by Katarzyna Grzelak-Błaszczyk et al. [18]. In brief, raw onions (50 kg) were subjected to extraction by immersing them in 50% aqueous ethanol solution (1:5) in a dynamic large-scale laboratory extractor at 35°C for 6 h. The extract was then evaporated to obtain 5% ethanol extract, followed by purification in a column filled with Amberlite XAD 1600N. Gravitational elution was performed at a flow rate of 1.6–7 ml/min using 10%–70% ethanol solutions. Of these, 10%–40% fractions were rejected, and only 50%–70% fractions were used to obtain a fraction of quercetin monoglycosides with quercetin aglycone and a separate fraction containing a high concentration of quercetin aglycone. The fractions were concentrated to 10–12°Bx and freeze-dried under 0.26 mbar vacuum for 48 h. The two resulting preparations were (1) quercetin aglycone with quercetin monoglycosides (Q+MQ) and (2) quercetin aglycone (Q). Polyphenol concentrations were then confirmed using ultra-high-performance liquid chromatography as described by Katarzyna Grzelak-Błaszczyk et al. [18].

The obtained onion polyphenol preparations had different polyphenol compositions. The Q+MQ preparation comprised 42.5% polyphenols, the main polyphenol of which was free quercetin (68.4% of the total polyphenols) and remaining polyphenols were quercetin monoglycosides (31.6%). The Q preparation contained a high concentration of polyphenols of approximately 73.7%, comprising quercetin aglycone as the predominant polyphenol (97.8% of the total polyphenols) with small quantities of quercetin monoglycosides.

2.2. Experimental Design. The experiment was performed in accordance with the Guidelines for Animal Welfare and Experimental Protocol and was approved by the Animal Care and Use Committee of Nankai University Affiliated Hospital. Forty female ICR mice, each weighing approximately 21 g, were used in this experiment. The mice were kept in separate cages maintained at 24°C ± 3°C, 49% ± 5% humidity, and a 12-h light–dark cycle.

The 40 female mice were randomly assigned to four equal groups: the control group (CTRL), which received a basal rodent diet; a DSS treatment group (DSS); a QUE group (QUE); and a QMQ group (QMQ). All groups received a basal rodent diet [19]; however, the control and DSS group diets were devoid of polyphenols, whereas the QUE group diet was supplemented with 0.21% Q preparation comprising 0.15% polyphenols (quercetin aglycone:quercetin monoglycosides, 98:2) and the QMQ diet was supplemented with 0.36% Q+MQ preparation comprising 0.15% polyphenols (quercetin aglycone:quercetin monoglycosides, 69:31). The mice were allowed free access to their respective diets and clean water for 7 days. On the eighth day, the CTRL group mice were permitted free access to clean water, but the DSS, QUE, and QMQ group mice received drinking water containing 3% DSS solution (Kayon Biological Technology Co. Ltd.) for 7 days to induce colitis [19]. Each mouse was weighed at the start and end of the experimental procedure. At the end of this experiment, each mouse was sacrificed for measuring the colon length and weight. Further histological evaluations were performed as described by Jie Yin et al. [2]. Furthermore, colon contents from each mouse were collected and immediately frozen in liquid nitrogen for storage at −70°C until use.

2.3. Assessment of Serum Oxidative Stress. Myeloperoxidase (MPO), reduced glutathione (GSH), and malondialdehyde (MDA) concentrations were assessed using commercial kits (Nanjing Jiancheng Bioengineering Institute, Nanjing, Jiangsu, China) in accordance with the manufacturer's instructions. Serum nitrate (NO) concentrations were approximated by measuring the absorbance of the azo-product resulting from the reaction between nitrite, sulfonamide, and N-(1-napthyl)ethylenediamine at 543 nm, in accordance with the methods described by Miranda et al. [20].

2.4. Microbial DNA Isolation and Sequencing. Microbial DNA was purified from mouse colon contents using a QIAamp DNA Stool Mini Kit (Qiagen) in accordance with the manufacturer's instructions. Microbial community diversity and composition for each sample was assessed and calculated by sequencing the V4 region of 16S rDNA. The total DNA was amplified with primers 515F (5′-GTGCCAGCMGCCGCGGTAA-3′) and 806R (5′-GGACTACHVGGGTWTCTAAT-3′) as described previously [21]. The DNA samples were then forwarded to a commercial service provider (Novogene, Beijing, China) for sequencing on an Illumina MiSeq platform in accordance with the manufacturer's guidelines [22]. Raw data were acquired prior to screening and assembly using the QIIME [23] and FLASH [22] software packages. Sequencing reads were assigned to samples according to the barcodes. Reads flagged as chimeric were eliminated to obtain an effective sequence collection for every sample. The QIIME software package and UPARSE pipeline were used to evaluate these effective sequences and

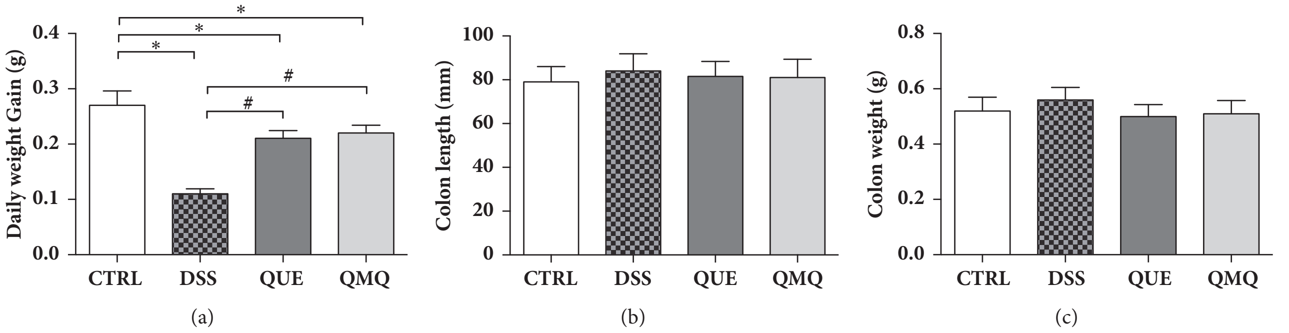

Figure 1: Illustration showing the effect of administering Q or Q+MQ on (a) average daily weight gain, (b) colon length, and (c) colon weight following DSS treatment. ∗ indicates significant difference compared with the CTRL group ($P < 0.05$); # indicates significant difference compared with the DSS group ($P < 0.05$) (all, $n = 10$).

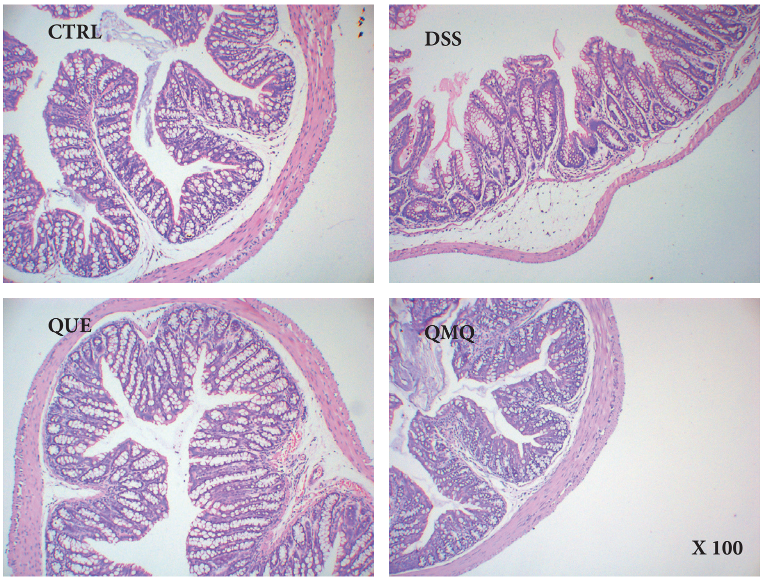

Figure 2: Histological evaluation of the hematoxylin and eosin-stained sections of the colon (×100) from the four groups (all, $n = 10$).

identify operational taxonomic units (OTUs). Subsequently, the UCLUST algorithm was used to cluster sequences with a 97% identity into the same OTU. Each OTU was allotted to a specific taxonomic level using the RDP Classifier [24].

2.5. Statistical Analysis. All data are presented as the mean and standard error of the mean (SEM). Statistical analysis was performed using SPSS 22.0 software (SPSS, Chicago, IL). The results were statistically evaluated using one-way analysis of variance, and significant differences between groups were determined using Duncan's multiple range test with statistical significance set at $P < 0.05$.

3. Results

The results demonstrated a significant reduction ($P < 0.05$) in the average daily gain in the DSS group, but the dietary Q and Q+MQ in the QUE and QMQ groups, respectively, seemed to significantly counteract this DSS-induced growth suppression ($P < 0.05$) (Figure 1(a)). In addition, the length and weight of the colon showed no significant differences between the four groups (Figures 1(b) and 1(c)).

Figure 2 presents the results of histological evaluation of the colon. No histological injury was observed in the colon of the CTRL group, whereas mice exposed to DSS in the DSS, QUE, and QMQ groups showed scattered villi, neutrophil infiltration, and desquamation in the colon. The histological status of the QUE and QMQ groups was much better than that of the DSS group.

The MPO activity significantly increased ($P < 0.05$) in DSS-treated mice compared with that in the CTRL group mice. However, Q and Q+MQ administration in the QUE and QMQ groups, respectively, significantly counteracted this increase in the MPO activity ($P < 0.05$) compared with that in the DSS group (Figure 3(a)). Further, the GSH level significantly decreased ($P < 0.05$) in DSS-treated mice compared with that in the CTRL group mice. However, Q and Q+MQ administration in the QUE and QMQ groups, respectively, significantly counteracted this reduction in the GSH activity ($P < 0.05$) compared with that in the DSS

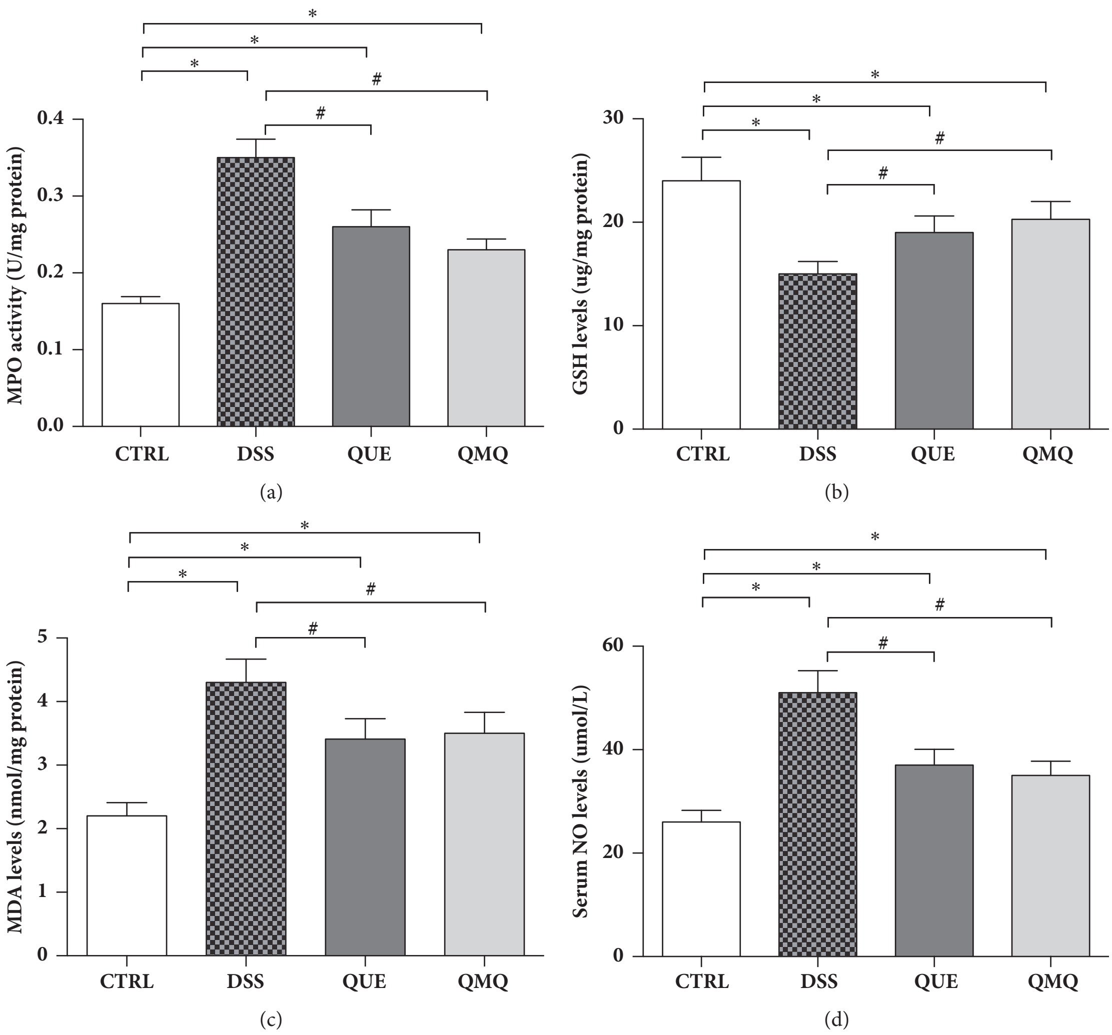

(a) (b)

(c) (d)

FIGURE 3: Effect of quercetin on (a) MPO, (b) reduced GSH, (c) MDA, and (d) serum NO concentrations in DSS-induced IBD in mice (n = 10). $*$ indicates significance at $P < 0.05$ relative to the CTRL group; # indicates significance at $P < 0.05$ relative to the DSS group.

TABLE 1: Alpha diversity indices of the colonic contents of mice with DSS-induced IBD.

Items	CTRL	DSS	QUE	QMQ	SEM	P
OTU	1239	1028	1144	1122	98.4	0.37
Chao1	1189.23	998.45*	1104.81$^{*\#}$	1096.45$^{*\#}$	45.6	0.039
ACE	1230.14	1057.48*	1155.47$^{*\#}$	1136.74$^{*\#}$	76.3	0.045
Shannon	5.39	4.81*	5.07$^{*\#}$	5.11$^{*\#}$	0.212	0.035
Simpson	0.84	0.93$^{*\#}$	0.89$^{*\#}$	0.88$^{*\#}$	0.064	0.041

$*$ indicates significance at $P < 0.05$ relative to the CTRL group; # indicates significance at $P < 0.05$ relative to the DSS group.

group (Figure 3(b)). Moreover, the MDA and serum NO concentrations significantly increased ($P < 0.05$) in DSS-treated mice compared with that in the CTRL group mice. However, Q and Q+MQ administration in the QUE and QMQ groups, respectively, significantly counteracted this increase in MDA and serum NO concentrations ($P < 0.05$) compared with that in the DSS group (Figures 3(c) and 3(d)).

To evaluate the effects of Q and Q+MQ on microbial communities, the V4 region of the 16S rRNA gene was sequenced. In total, 1,064,746 sequences (25,038 ± 1432 per sample) were obtained, including 38135, 39198, 37542, and 39011 raw reads obtained from samples in the CTRL, DSS, QUE, and QMQ groups, respectively. Following trimming, assembly, and quality filtering, 4563 OTUs were identified, and the indices of community richness and diversity are presented in Table 1. Compared with the CTRL group, the DSS, QUE, and QMQ groups demonstrated reduced Chao1, angiotensin-converting enzyme (ACE), and Shannon indices and an increased Simpson index ($P < 0.05$). Conversely, compared with the DSS group, the QUE and QMQ groups

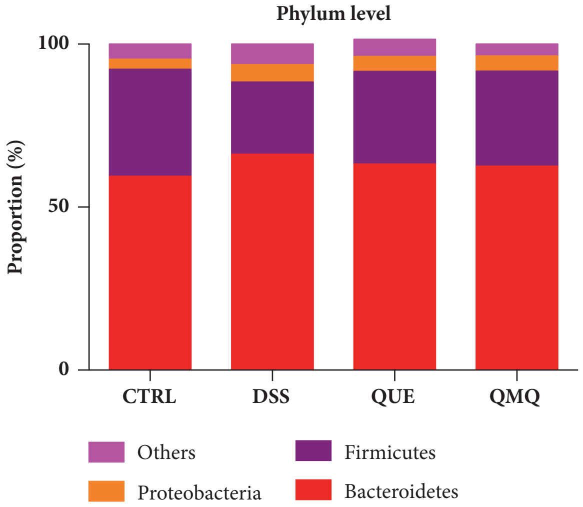

Figure 4: Effect of quercetin on colonic microbiota at the phylum level in mice with DSS-induced IBD ($n = 10$).

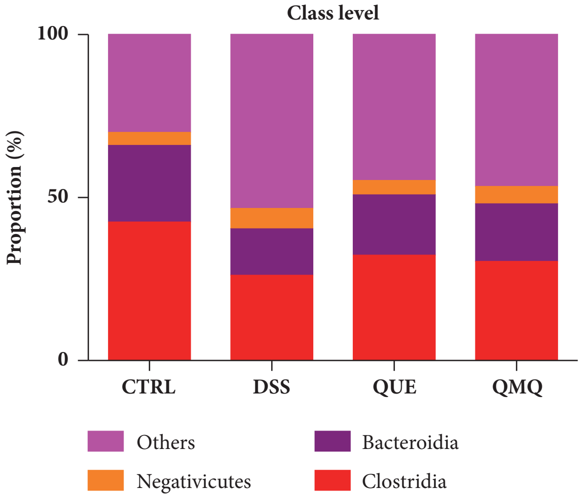

Figure 5: Effect of quercetin on colonic microbiota at the class level in mice with DSS-induced IBD ($n = 10$).

exhibited higher Chao1, ACE, and Shannon indices ($P < 0.05$) and a reduced Simpson index ($P < 0.05$). Nevertheless, no significant alpha diversity was detected in the microbiota in the QUE and QMQ groups.

Intestinal microbiota diversity was evaluated using taxon-dependent analysis. Six phyla were detected in the colonic contents across all four groups. The three most predominant phyla across all four groups were Bacteroidetes, Firmicutes, and Proteobacteria. The proportion of Bacteroidetes, Firmicutes, and Proteobacteria populations were 59.45%, 32.87%, and 3.05% of the total microbiota, respectively, in the CTRL group; 66.19%, 22.16%, and 5.34%, respectively, in the DSS group; 63.24%, 28.42%, and 4.54%, respectively, in the QUE group; and 62.53%, 29.15%, and 4.68%, respectively, in the QMQ group (Figure 4).

The three most predominant classes across all four groups were Clostridia, Bacteroidia, and Negativicutes, in addition to small quantities of Bacilli, Gammaproteobacteria, and Erysipelotrichia. The proportions of Clostridia, Bacteroidia, and Negativicutes populations were 42.48%, 23.49%, and 3.95%, respectively, in the CTRL group; 26.14%, 14.22%, and 6.24%, respectively, in the DSS group; 32.33%, 18.43%, and 4.46%, respectively, in the QUE group; and 30.37%, 17.63%, and 5.36%, respectively, in the QMQ group (Figure 5).

4. Discussion

Preparations from onion were demonstrated to be good sources of polyphenols. The extraction and purification procedures delivered preparations with high-purity polyphenols of varying concentrations. This study showed that dietary Q and Q+MQ were effective in reducing DSS-induced colitis in mice, which is thought to manifest via reduction in oxidative stress and colonic microbiota diversity. To the best of our knowledge, only a limited number of studies have focused on investigating natural compounds capable of reversing experimental colitis. In the current study, 3% DSS was used to induce acute colitis so that the effect of Q and Q+MQ on DSS-induced colitis could be investigated. Weight loss is the traditional clinical index for IBD [25], and the results of this study showed that DSS-containing water caused neutrophil infiltration and scattered villi in the colon and a significant decrease in average daily weight gain, consistent with the results of previous studies [2, 26]. However, both Q and Q+MQ ameliorated these changes.

Increased oxidative stress is associated with mucosal inflammation in ulcerative colitis, and it may be a contributing factor to the progression to malignancy associated with this disorder [27, 28]. The biological tests performed in the current study validated the antioxidant effects of the preparations, which included free quercetin in addition to free Q and Q+MQ, on the DSS-induced colitis in mice. Compared with the CTRL group mice, a significant increase ($P < 0.05$) was observed in the MPO, MDA, and NO concentrations in mice receiving DSS water. However, compared with the DSS group, both Q and Q+MQ significantly counteracted this increase in MPO, MDA, and NO concentrations ($P < 0.05$) in the QUE and QMQ groups, respectively. The MPO activity in the colonic mucosa is used as an inflammatory response marker and is linearly correlated with neutrophil infiltration [29]. Several studies have shown that MPO is present at high concentrations in IBD patients [29, 30]. Inflammation is associated with the recruitment and activation of mucosal phagocytic leukocytes, which release high levels of reactive oxygen species (ROS), e.g., superoxide anion [31]. Such unregulated overproduction of ROS may overwhelm protective mechanisms, leading to cellular oxidative damage [32].

Both the Shannon and Simpson indices indicate diversity within any community and are affected by parameters of species richness and species evenness within that sample community. With respect to same species richness, the greater the uniformity of the species within the community, the greater the diversity of the microbial community. Consistent with previous findings [3, 11], our findings indicated that DSS treatment reduces colonic microbiota diversity. The human intestines contain large populations of microorganisms, and extensive alterations in the microbial composition and the regular function of the intestinal microbiota have been associated with IBD [10, 11]. Typically, the Firmicutes-to-Bacteroidetes ratio is a key indicator of intestinal microbiota composition, and lower Firmicutes-to-Bacteroidetes ratios may be associated with weight loss because reduced Firmicutes populations reduce the additional energy provided to the host by them via fermentation of polysaccharides to short-chain fatty acids [25]. The present study demonstrated that DSS treatment reduces Firmicutes population and increases Proteobacteria population but that Q or Q+MQ supplementation can ameliorate these effects. The results also indicated that dietary Q or Q+MQ supplementation may alter the outcomes of microbiota-associated disorders. In IBD patients, intestinal microbiota dysbiosis is frequently noted. This condition is frequently characterized by an increased abundance of facultative anaerobic bacteria (e.g., Enterobacteriaceae and Bacilli) and simultaneous reduction of obligate anaerobic bacteria from the Bacteroidia and Clostridia classes [33, 34].

In conclusion, this study demonstrated that DSS treatment for 7 days results in signs of colitis, including growth reduction and colonic inflammation. Dietary Q or Q+MQ supplementation, even at a low dose, was found to counteract DSS-induced colitis in mice. Because quercetin is a ubiquitous phytochemical present in a variety of fruits and vegetables, implementation of a quercetin-supplemented diet for treating IBD represents a feasible approach with considerable potential. Thus, Q or Q+MQ may be administered as an adjuvant therapy for IBD patients. Additional mechanistic and toxicity investigations to examine the efficacy of this phytochemical for IBD prevention and treatment are recommended.

Data Availability

The data used to support the findings of this study are available from the corresponding author upon request.

Conflicts of Interest

All coauthors have seen and agree with the contents of the manuscript and there is no financial interest to report.

Acknowledgments

This study was supported by the National Natural Science Foundation of China (no. 81600509).

References

[1] K. Clarke and J. Chintanaboina, "Allergic and Immunologic Perspectives of Inflammatory Bowel Disease," *Clinical Reviews in Allergy & Immunology*, 2018.

[2] J. Yin, M. Wu, J. Duan et al., "Pyrrolidine Dithiocarbamate Inhibits NF-KappaB Activation and Upregulates the Expression of Gpx1, Gpx4, Occludin, and ZO-1 in DSS-Induced Colitis," *Applied Biochemistry and Biotechnology*, vol. 177, no. 8, pp. 1716–1728, 2015.

[3] D. Zhu, Y. Ma, S. Ding, H. Jiang, and J. Fang, "Effects of melatonin on intestinal microbiota and oxidative stress in colitis mice," *BioMed Research International*, vol. 2018, Article ID 2607679, 6 pages, 2018.

[4] K. Matsuoka and T. Kanai, "The gut microbiota and inflammatory bowel disease," *Seminars in Immunopathology*, vol. 37, no. 1, pp. 47–55, 2015.

[5] B. Khor, A. Gardet, and R. J. Xavier, "Genetics and pathogenesis of inflammatory bowel disease," *Nature*, vol. 474, no. 7351, pp. 307–317, 2011.

[6] A. N. Ananthakrishnan, "Environmental risk factors for inflammatory bowel disease," *Gastroenterol Hepatol*, vol. 9, no. 6, pp. 367–374, 2013.

[7] S. Salim, N. Sarraj, M. Taneja, K. Saha, M. V. Tejada-Simon, and G. Chugh, "Moderate treadmill exercise prevents oxidative stress-induced anxiety-like behavior in rats," *Behavioural Brain Research*, vol. 208, no. 2, pp. 545–552, 2010.

[8] S. Salim, "Oxidative stress and psychological disorders," *Current Neuropharmacology*, vol. 12, no. 2, pp. 140–147, 2014.

[9] S.-Y. Hu, X.-Y. Jia, J.-N. Li et al., "T cell infiltration is associated with kidney injury in patients with anti-glomerular basement membrane disease," *Science China-Life Sciences*, vol. 59, no. 12, pp. 1282–1289, 2016.

[10] M. Tong, X. Li, L. W. Parfrey et al., "A modular organization of the human intestinal mucosal microbiota and its association with inflammatory bowel disease," *PLoS ONE*, vol. 8, no. 11, Article ID e80702, 2013.

[11] B. P. Willing, J. Dicksved, J. Halfvarson et al., "A pyrosequencing study in twins shows that gastrointestinal microbial profiles vary with inflammatory bowel disease phenotypes," *Gastroenterology*, vol. 139, no. 6, pp. 1844.e1–1854.e1, 2010.

[12] L. P. McLean and R. K. Cross, "Adverse events in IBD: to stop or continue immune suppressant and biologic treatment," *Expert Review of Gastroenterology & Hepatology*, vol. 8, no. 3, pp. 223–240, 2014.

[13] J.-F. Colombel, B. E. Sands, P. Rutgeerts et al., "The safety of vedolizumab for ulcerative colitis and Crohn's disease," *Gut*, vol. 66, no. 5, pp. 839–851, 2016.

[14] S. Ding, H. Jiang, and J. Fang, "Regulation of immune function by polyphenols," *Journal of Immunology Research*, vol. 2018, Article ID 1264074, 8 pages, 2018.

[15] A. N. Panche, A. D. Diwan, and S. R. Chandra, "Flavonoids: an overview," *Journal of Nutritional Science*, vol. 5, 2016.

[16] S. Chen, H. Jiang, X. Wu, and J. Fang, "Therapeutic effects of quercetin on inflammation, obesity, and type 2 diabetes," *Mediators of Inflammation*, vol. 2016, Article ID 9340637, 5 pages, 2016.

[17] Q. Su, M. Peng, Y. Zhang et al., "Quercetin induces bladder cancer cells apoptosis by activation of AMPK signaling pathway," *American Journal of Cancer Research*, vol. 6, no. 2, pp. 498–508, 2016.

[18] K. Grzelak-Błaszczyk, J. Milala, M. Kosmala et al., "Onion quercetin monoglycosides alter microbial activity and increase antioxidant capacity," *The Journal of Nutritional Biochemistry*, vol. 56, pp. 81–88, 2018.

[19] W. Ren, J. Yin, M. Wu et al., "Serum amino acids profile and the beneficial effects of L-arginine or L-glutamine supplementation in dextran sulfate sodium colitis," *PLoS ONE*, vol. 9, no. 2, article e88335, 2014.

[20] P. C. H. Hollman, J. M. P. van Trijp, M. N. C. P. Buysman et al., "Relative bioavailability of the antioxidant flavonoid quercetin

from various foods in man," *FEBS Letters*, vol. 418, no. 1-2, pp. 152–156, 1997.

[21] X.-F. Kong, Y.-J. Ji, H.-W. Li et al., "Colonic luminal microbiota and bacterial metabolite composition in pregnant Huanjiang mini-pigs: Effects of food composition at different times of pregnancy," *Scientific Reports*, vol. 6, 2016.

[22] T. Magoč and S. L. Salzberg, "FLASH: fast length adjustment of short reads to improve genome assemblies," *Bioinformatics*, vol. 27, no. 21, pp. 2957–2963, 2011.

[23] J. G. Caporaso, J. Kuczynski, J. Stombaugh et al., "QIIME allows analysis of high-throughput community sequencing data," *Nature Methods*, vol. 7, no. 5, pp. 335-336, 2010.

[24] Q. Wang, G. M. Garrity, J. M. Tiedje, and J. R. Cole, "Naïve Bayesian classifier for rapid assignment of rRNA sequences into the new bacterial taxonomy," *Applied and Environmental Microbiology*, vol. 73, no. 16, pp. 5261–5267, 2007.

[25] S. Chen, M. Wang, L. Yin et al., "Effects of dietary tryptophan supplementation in the acetic acid-induced colitis mouse model," *Food & Function*, vol. 9, no. 8, pp. 4143–4152, 2018.

[26] J. J. Kim, M. S. Shajib, M. M. Manocha, and W. I. Khan, "Investigating intestinal inflammation in DSS-induced model of IBD," *Journal of Visualized Experiments*, no. 60, article e3678, 2012.

[27] T. A. Ullman and S. H. Itzkowitz, "Intestinal inflammation and cancer," *Gastroenterology*, vol. 140, no. 6, pp. 1807–1816, 2011.

[28] A. Bhattacharyya, R. Chattopadhyay, S. Mitra, and S. E. Crowe, "Oxidative stress: an essential factor in the pathogenesis of gastrointestinal mucosal diseases," *Physiological Reviews*, vol. 94, no. 2, pp. 329–354, 2014.

[29] Y. Iba, Y. Sugimoto, C. Kamei, and T. Masukawa, "Possible role of mucosal mast cells in the recovery process of colitis induced by dextran sulfate sodium in rats," *International Immunopharmacology*, vol. 3, no. 4, pp. 485–491, 2003.

[30] H. H. Arab, S. A. Salama, A. H. Eid, H. A. Omar, E.-S. A. Arafa, and I. A. Maghrabi, "Camel's milk ameliorates TNBS-induced colitis in rats via downregulation of inflammatory cytokines and oxidative stress," *Food and Chemical Toxicology*, vol. 69, pp. 294–302, 2014.

[31] H. Zhu and Y. R. Li, "Oxidative stress and redox signaling mechanisms of inflammatory bowel disease: updated experimental and clinical evidence," *Experimental Biology and Medicine*, vol. 237, no. 5, pp. 474–480, 2012.

[32] K. P. Pavlick, F. S. Laroux, J. Fuseler et al., "Role of reactive metabolites of oxygen and nitrogen in inflammatory bowel disease," *Free Radical Biology & Medicine*, vol. 33, no. 3, pp. 311–322, 2002.

[33] Y. Minamoto, C. C. Otoni, S. M. Steelman et al., "Alteration of the fecal microbiota and serum metabolite profiles in dogs with idiopathic inflammatory bowel disease," *Gut Microbes*, vol. 6, no. 1, pp. 33–47, 2015.

[34] B. Stecher, "The roles of inflammation, nutrient availability and the commensal microbiota in enteric pathogen infection," *Microbiology Spectrum*, vol. 3, no. 3, 2015.

Hindawi
BioMed Research International
Volume 2018, Article ID 8063647, 10 pages
https://doi.org/10.1155/2018/8063647

Review Article

Immunomodulatory Effects of Probiotics on Cytokine Profiles

Md. Abul Kalam Azad,[1,2] Manobendro Sarker,[3,4,5] and Dan Wan[1,6]

[1] *Hunan Province Key Laboratory of Animal Nutritional Physiology and Metabolic Process, Key Laboratory of Agroecological Processes in Subtropical Region, Institute of Subtropical Agriculture, Chinese Academy of Sciences, National Engineering Laboratory for Pollution Control and Waste Utilization in Livestock and Poultry Production, Changsha, Hunan 410125, China*
[2] *University of Chinese Academy of Sciences, Beijing 100049, China*
[3] *Biomass Energy Engineering Research Centre, School of Agriculture and Biology, Shanghai Jiao Tong University, 800 Dongchuan Road, Shanghai 200240, China*
[4] *Key Laboratory of Urban Agriculture (South), Ministry of Agriculture, 800 Dongchuan Road, Shanghai 200240, China*
[5] *Department of Food Engineering and Technology, State University of Bangladesh, Dhaka 1205, Bangladesh*
[6] *Academician Workstation of Hunan Baodong Farming Co., Ltd., Hunan 422001, China*

Correspondence should be addressed to Dan Wan; w.dan@isa.ac.cn

Received 15 September 2018; Accepted 8 October 2018; Published 23 October 2018

Guest Editor: Deguang Song

Copyright © 2018 Md. Abul Kalam Azad et al. This is an open access article distributed under the Creative Commons Attribution License, which permits unrestricted use, distribution, and reproduction in any medium, provided the original work is properly cited.

Probiotics confer immunological protection to the host through the regulation, stimulation, and modulation of immune responses. Researchers have shifted their attention to better understand the immunomodulatory effects of probiotics, which have the potential to prevent or alleviate certain pathologies for which proper medical treatment is as yet unavailable. It has been scientifically established that immune cells (T- and B-cells) mediate adaptive immunity and confer immunological protection by developing pathogen-specific memory. However, this review is intended to present the recent studies on immunomodulatory effects of probiotics. In the early section of this review, concepts of probiotics and common probiotic strains are focused on. On a priority basis, the immune system, along with mucosal immunity in the human body, is discussed in this study. It has been summarized that a number of species of *Lactobacillus* and *Bifidobacterium* exert vital roles in innate immunity by increasing the cytotoxicity of natural killer cells and phagocytosis of macrophages and mediate adaptive immunity by interacting with enterocytes and dendritic, Th1, Th2, and Treg cells. Finally, immunomodulatory effects of probiotics on proinflammatory and anti-inflammatory cytokine production in different animal models have been extensively reviewed in this paper. Therefore, isolating new probiotic strains and investigating their immunomodulatory effects on cytokine profiles in humans remain a topical issue.

1. Introduction

Probiotics are living microorganisms that confer several health benefits when administrated in adequate amounts to the host [1, 2]. Adhering to human intestines, probiotics stimulate, regulate, and modulate various different functions, including digestion, metabolism, epithelial innate immunity, competitive exclusion of pathogens, and brain-gut communication [3, 4]. Gut microorganisms produce several nontoxic metabolites and play important roles in nutritional and clinical applications [5–7]. Therefore, the microecology of the gastrointestinal tract, consisting of intestine, microbiota, and nondigestible food within the tract, is crucial for probiotic action in the host.

Probiotics act symbiotically by fermenting nondigestible food, known as prebiotics, for their energy and exert elite properties including antipathogenicity, antiobesity, and diabetic, antidiabetic, anti-inflammatory, anticancer, and angiogenic activities and efficacy on the brain and central nervous system [8]. However, the functions of probiotics can be classified as metabolic, protective, and trophic [9], since the trophic role has garnered attention in studies of immunomodulation. Typically, the immune system in vertebrates can be divided into innate and adaptive immunity. Innate immunity is a nonspecific defense mechanism exerting immediate or near-immediate responses to the presence of pathogens in body. On the other hand, adaptive immunity is highly specific and is able to destroy individual invading pathogens in vertebrates. Besides, a pathogen-specific long-lasting protective memory enables the adaptive immune system to attack and destroy pathogens when reencountered [10]. Lymphocytes, especially B cells and T cells, exert adaptive immune responses by recognizing antigens with their specific receptors.

In the last few years, probiotics have been extensively studied and reported, with humoral, cellular, and nonspecific immunity modulation, as well as promoting the immunological barrier [11, 12]. Probiotics have been evaluated for *in vivo* effects, such as increased peripheral immunoglobin production, stimulation of IgA secretion, and decreased proinflammatory cytokine production [13]. It has been reported that homogenates prepared from several probiotics, including *Lactobacillus rhamnosus GG*, *Lactobacillus acidophilus*, *Lactobacillus delbrueckii* sub sp. *bulgaricus*, *Bifidobacterium lactis*, and *Streptococcus thermophiles,* have the ability to suppress the proliferation of mononuclear cells [14]. It has also been reviewed that *Bifidobacterium bifidum* has a significant effect in enhancing antibody responses to ovalbumin, whereas *B. breve* has an increased humoral immune response after stimulation with IgA [15].

However, published articles regarding the immune responses of probiotics are few in number, while a number of research articles have focused on the metabolic actions of probiotics. In the treatment of various diseases, including inflammation, intestinal bowel diseases, and colon cancer, there is an urgent need to study probiotic strains and their effects on immune modulation. In this review article, particular attention has been paid to probiotics and their immunomodulatory effects on cytokine profiles in terms of pro- and anti-inflammatory cytokines in the host.

2. Background and Concept of Probiotics

In scientific and clinical research, *Lactobacillus* (*L. acidophilus*, *L. casei*, *L. salivarius*, and *L. lactis*) and *Bifidobacterium* (*B. bifidum* and *B. lactis*) are commonly found in healthy intestines and are noted as being prominent probiotics [2, 15] having different culture conditions, variability, and diverse characteristics, including sensitivity to low pH, gastric juice, pancreatic and intestinal fluids, bile acid, intestinal or respiratory mucus, adherence to intestinal cells, and interactions with other pathogenic microorganisms in the intestine [7, 8, 16]. Probiotics have been reported to produce a number of nonviable metabolic byproducts, such as bacteriocins, organic acids, acetaldehydes, diacetyl, ethanol, and hydrogen peroxide, which are nontoxic, nonpathogenic, and resistant to enzyme systems in mammals, and have been remarked on as an alternative to antibiotics due to their biological activity and inhibitory properties toward pathogenic microbes in the host [17, 18].

In the gut, probiotic microorganisms act symbiotically and modulate immunity [5, 6, 19]. Several studies have reported that probiotics also produce antioxidants (glutathione) and stimulate activity in reducing oxidative stress. Probiotic microorganisms, including *L. acidophilus* NCDC14 and *L. casei* NCDC19, inhibit lipid peroxidation and decrease streptozotocin- (STZ-) induced oxidative damage in pancreatic tissues of rats [20]. According to Sengul et al. [21], probiotic strains *L. delbrueckii* subsp. *bulgaricus* A13 and *L. delbrueckii* subsp. *Bulgaricus* B3 have a significant effect in reducing oxidative stress in colitis. A probiotic supplement containing freeze-dried beneficial strains, namely, *L. acidophilus*, *L. casei*, *L. rhamnosus*, *L. bulgaricus*, *B. breve*, *B. longum*, and *S. thermophiles*, has been found to increase the plasma total glutathione (GSHt) significantly [22]. However, the health benefits of probiotic microorganisms include prevention of infectious diseases of the intestinal and urinary tracts, prevention of diarrhea, reductions in allergy symptoms, serum cholesterol concentration, blood pressure, stimulation and modulation of the immune system, modulation of gene expression (cytokines, in particular), regression of tumors, and reduction in cocarcinogen production [23]. Researchers are now shifted to discerning deeper understanding of whether probiotics exert health benefits; proposed reaction mechanisms include inhibitory effects of lactate on pathogens, production of short chain fatty acids, lowering the production of toxic substances contributing to pathologies such as inflammatory bowel disease (IBD), and adherence of microbes to the gut through controlling water flow from the blood serum to the intestinal lumen [24]. Most common probiotic microorganisms are presented in Table 1.

In the small intestine, probiotic microorganisms ferment nondigestible carbohydrates, such as fructooligosaccharide, oligofructose, inulin, galactose, and xylose-containing oligosaccharides from various natural sources, including vegetables, fruits, and grains, and readily fulfill their energy requirements [25]. Common prebiotics used in the preparation of synbiotics and their natural sources are summarized in Table 2. *In vivo*, *Lactobacillus casei* has been found to produce significant amounts of GSHt, GSH, and -SH free groups by fermenting inulin, whereas physiological stress results in lower GSH concentrations with large amounts of oxidative stress markers [26]. Verma and Shukla [27] revealed that *L. rhamnosus* and *L. acidophilus* lead to the formation of large quantities of antioxidants, mainly GSH, with inulin being a nondigestible carbohydrate in the small intestine. In another study by Kavitha et al. [28], increased GSH concentrations have been reported due to the combined effects of insulin, pioglitazone, and probiotics in STZ-induced diabetic rats. In a very recent study, the effects of *Lactobacillus plantarum* HII11 are remarkable in preventing adrenomedullin- (ADM-) mediated colon cancer in the rat [29].

3. Human Immune System

In the human gut, M cells present in Peyer's patches are crucial due to their capacity to transport macromolecules, antigens, and microorganisms and inert particles from the lumen into the lymphoid tissue by adsorptive endocytosis. In addition, enterocytes and M cells may uptake such as macromolecules, antigens, and microorganisms through a

Table 1: Most used probiotic microorganisms.

Probiotic genera	Probiotic strains	References
Lactobacillus	*L. acidophilus, L. amylovorus, L. bulgaricus, L. crispatus, L. casei, L. gasseri, L. helveticus, L. johnsonii, L. pentosus, L. reuteri, L. paracasei, L. plantarum, L. rhamnosus*	[17, 18, 30]
Bifidobacterium	*B. animalis, B. breve, B. infantis, B. bifidum, B. lactis, B. catenulatum, B. longum, B. adolescentis*	[31–34]
Enterococcus	*Enterococcus faecium*	[35]
Streptococcus	*Streptococcus thermophilu*	[36]
Lactococcus	*Lactococcus lactis, L. lactis, L. reuteri, L. rhamnosus, L. casei, L. acidophilus, L. curvatus, L. plantarum*	[37]
Bacillus	*Bacillus clausii, B. coagulans, B. subtilis, B. laterosporus*	[38, 39]
Pediococcus	*Pediococcus acidilactici, P. pentosaceus*	[40]
Propionibacterium	*P. jensenii, P. freudenreichii*	[30]
Streptococcus	*Streptococcus sanguis, S. oralis, S. mitis, S. thermophiles, S. salivarius*	[36]
Bacteroides	*Bacteroides uniformis*	[41]
Enterococcus	*Enterococcus faecium*	[35]
Peptostreptococcus	*Peptostreptococcus productus*	[39]
Escherichia	*Escherichia coli Nissle 1917*	[38]
Faecalibacterium	*Faecalibacterium prausnitzii*	[42]
Akkermansia	*A. muciniphila*	[41]
Saccharomyces	*Saccharomyces cerevisiae, S. boulardi*	[43]

Table 2: A list of common prebiotics for the preparation of synbiotics*.

Prebiotics	Sources	References
Fructooligosaccharides	Fructooligosaccharides Onion, Leek, Asparagus, Chicory, Jerusalem artichoke, Garlic, Wheat, Oat	[44]
Inulin	Agave, banana, burdock camas, chicory, coneflower, costus, elecampane, globe artichoke, dandelion, Jerusalem artichoke, jicama, wild yam, mugwort root, yacon, garlic, onion	[45]
Isomaltooligosaccharides	Miso, soy, sauce, sake, honey	[46]
Lactulose	Skim milk	[47]
Lactosucrose	Milk sugar	[48]
Galactooligosaccharides	Lentil, human milk, chickpea/hummus, green pea, lima bean, kidney bean	[49, 50]
Soybean oligosaccharides	Soybean	[51]
Xylooligosaccharides	Bamboo shoot, milk, honey	[34]
Fructooligosaccharides	Onion, chicory, garlic, asparagus, banana, artichoke	[52]
Arabinoxylan	Bran of grasses	[53]
Arabinoxylan oligosaccharides	Cereals	[54]
Resistant starch-1,2,3,4	Beans, legumes, starchy fruits and vegetables, whole grains	[55]

*This information was reproduced from Kerry et al. [8].

transepithelial vesicular transport mechanism. When antigenic molecules cross the intestinal barrier, they stimulate the innate and adaptive immune systems in the body [56].

3.1. Innate and Adaptive Immunity. Humans may come into contact with millions of pathogenic organisms through ingestion, inhalation, and many other ways, while the innate immune system plays a vital role in preventing infection by specific pathogen. Innate immunity is recognized as a first-line defense system against pathogens and can remember previous encounters while attacking again. Phagocytic cells, including neutrophils, monocytes, macrophages, and NK cells, enable this first-line defense system against pathogenic microorganisms in the human body, which destroys pathogens and protects from the corresponding infection. These key players are not specific in recognizing their targets, unlike adaptive immune responses. However, this first-line defense system largely depends on the number of phagocytic cells and proteins, which then activate the adaptive immune response in vertebrates through the activation of antigen-presenting cells (APCs) [57, 58].

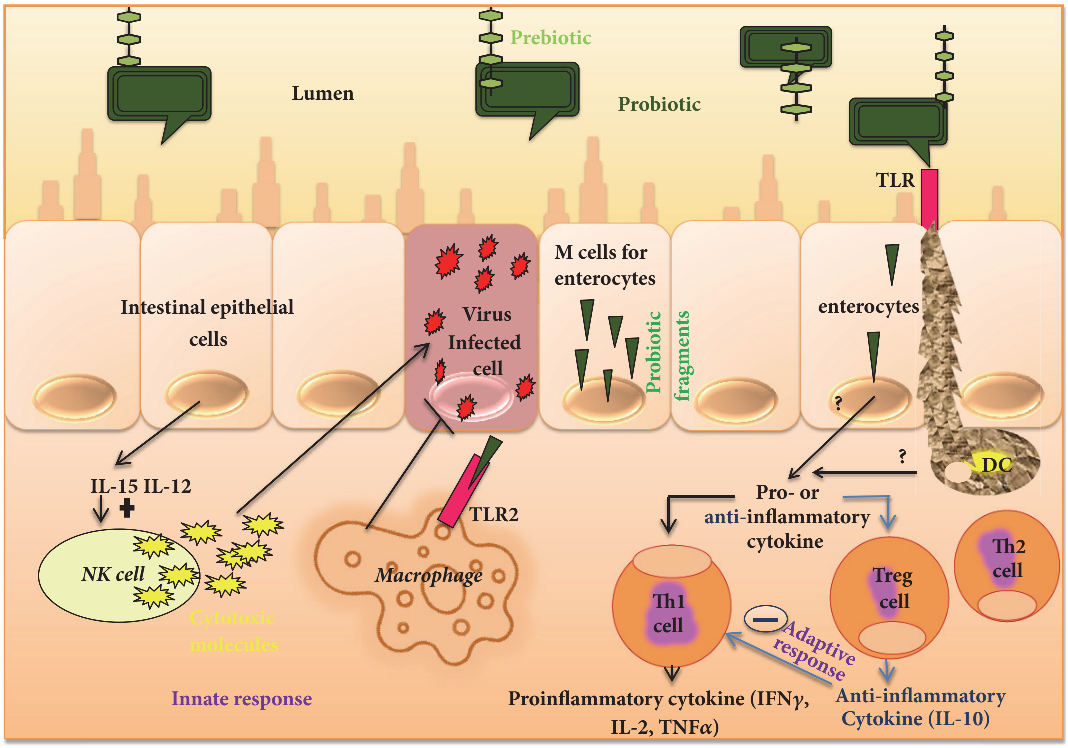

Figure 1: Immunomodulation of probiotics.

On the other hand, development of adaptive immune responses to a new pathogen in the body is comparatively slower than innate immune responses. Usually, lymphocytes (B and T) are key players in the adaptive immune response, which exerts more effective immune responses, having specific antigen receptors, namely, the B cell receptor (BCR) for B cells and T cell receptor (TCR) for T cells [59]. Furthermore, antigen receptors of each naive lymphocyte possess unique specificity. Interestingly, B cells contribute to adaptive immunity, through the secretion of antibodies, known as humoral immunity, while T cells contribute cell-mediated immunity through subdivision into T helper cells (CD4+, called Th) and cytotoxic T cells (CD8+) [60]. It has been well known that B cells recognize specific antigens via BCRs, whereas CD8+ cells recognize antigens as peptide/MHC class I complexes, and CD4+ cells recognize antigens as peptide/MHC class II complex [61]. Once ACPs are activated, T cells proliferate and differentiate into CD8+ T cells and CD4+ T helper cells. Furthermore, CD8+ T cells convert into cytotoxic T lymphocytes (CTLs), whereas CD4+ T helper cells activate and regulate macrophages and B cells to respond to the adaptive immune system.

3.2. Mucosal Immunity. The mucosal immune system is very specific in protecting the whole inner surface, involving the oral-pharyngeal cavity, respiratory tract, gastrointestinal (GI) tract, and urogenital tract, as well as the exocrine glands in the human body. The mucosal immune system exerts similar features and anatomical organization for whole inner surface, although organs have different locations in the human body. The GI immune system can represent the mucosal immune system, as shown in Figure 1, while three major compartments, namely, the epithelial layer, lamina propria (LP), and mucosal-associated lymphoid tissue (MALT), are reported to be involved in the GI tract [62, 63]. Lymphoid tissue in the GI tract consists of Peyer's patches, which are characterized by follicle-associated epithelium (FAE) and are distributed in the intestinal epithelium and in secretory sites within the mucosa. However, the epithelial layer and lamina propria are battlefronts, while MALTs act as headquarters and initiate adaptive immune responses. APCs in Peyer's patches capture immunoglobulin A (IgA) antigen from epithelium and microfold cells. Usually, T cells become activated after antigen recognition, and, finally, APCs migrate antigen to lymphoid follicles, lymphoid tissue (LP), and mesenteric lymph nodes. IgA exerts first-line immune defense in the mucosal immune defense with two isotypes of IgA, one being IgA1 in the small intestine and the other being IgA2 in the colonic mucosa produced by B cells [64]. Nevertheless, activated T cells differentiate into effector cells and ensure the integrity of the mucosal barrier and GI environment. However, an application of *Bifidobacterium bifidum* R0071, *Bifidobacterium infantis* R0033, and *Lactobacillus helveticus* R0052 was reported to boost the immunity of infants with changes in salivary immunoglobulin A (SIgA) and the digestive system [65]. Probiotic fermented milk containing *L. casei* DN 114001was found to be effective for gut mucosal immunity in a BALC/c mouse model, with an increased number of T and IgA+B lymphocytes, macrophages, and cells from the nonspecific barrier (goblet cells), while IgA+B was also reported to activate the transcriptional factor NFAT, which is also a nuclear factor of activated T cells [66]. Dogi et al. [67] introduced nonpathogenic Gram-positive and Gram-negative bacteria in some animal models, while only Gram-positive strains, including *L. acidophilus* (strains CRL 1462 and A9) and *L. casei* (CRL 431), have been reported to increase TLR-9 expression.

4. Immunomodulation of Cytokine Profiles

Immunomodulatory effects and clinical health benefits of probiotics have been attractive in the treatment of various degenerative diseases. Researchers are now concentrating on identifying the elite properties of probiotics, and some of these include effects on immunity, such as antipathogenicity, antiobesity and diabetic, anti-inflammatory, anticancer, antiallergic, and angiogenic activities and result in effects on the central nervous system (CNS), while efficacy largely depends on the mechanism of action. A number of studies have reported basic molecular mechanisms, such as enhanced IgA secretion, production of cytokines, production of antibacterial substances, enhanced tight junctions of the intestinal barrier against intercellular bacterial invasion, and competition with new pathogenic microorganisms for enterocyte adherence, by which probiotics regulate intestinal epithelial health, although the immunomodulatory effects of probiotics are not the same in every individual and largely depend on environment and epigenetic interactions with the host. In the immunomodulation, probiotic antigenic fragments, such as cell wall compounds, have the ability to cross the intestinal epithelial cells and M cells in Peyer's patches and to then modulate the innate and adaptive immune responses in the body, as illustrated in Figure 1 [68].

The immunomodulatory effect of probiotics is attributed to the release of cytokines, including interleukins (ILs), tumor necrosis factors (TNFs), interferons (IFNs), transforming growth factor (TGF), and chemokines from immune cells (lymphocytes, granulocytes, macrophages, mast cells, epithelial cells, and dendritic cells (DCs)) [69] which further regulate the innate and adaptive immune system [70]. It has been reported that cell wall components of *Bifidobacteria* and *Lactobacilli*, such as lipoteichoic acid, stimulate NO synthase, which is potential in pathogen-infected cell death mechanism (NO) presented by macrophages through TNF-α secretion. In addition, two surface phagocytosis receptors (FcγRIII and tool-like receptor (TLR)) are also upregulated by NO [61, 71]. Probiotics have been reported to interact with enterocytes and dendritic, Th1, Th2, and Treg cells in the intestine and to modulate the adaptive immunity into pro- and/or anti-inflammatory action. Studies with BALB/c (20–30 g) inbred mice and Fisher-344 inbred rats demonstrated that *Lactobacillus paracasei* subsp. *Paracasei* DC412 strain and *L. acidophilus* NCFB 1748 induced early innate immune responses and specific immune markers through phagocytosis, polymorphonuclear (PMN) cell recruitment, and TNF-alpha (TNF-α) production [72]. In another experimental animal model involving BALB/c mice, oral administration of *L. casei* favored rapid activation of immune cells and produced a higher number of specific markers such as CD-206 and TLR-2 cells [73], while TLRs improve the immunological defense mechanism in terms of pro- and anti-inflammatory cytokine production upon the detection of foreign objects [74].

4.1. Pro- and Anti-Inflammatory Cytokines. Probiotic strains have a significant influence on the gut barrier by stimulating B cells for the production of IgA. In *in vitro* studies with enterocyte cells (HT-29, caco-2, and dendritic cells derived from PBMC), probiotics have been reported to influence cytokine production by APCs, which initiates adaptive responses. Cytokines also enhance the defense system against invasion by bacterial, fungal, viral, and any pathogenic components. A number of researchers studying the immune system in animal models found that the importance of cytokines lies in binding to specific receptors on cell membrane and in triggering cellular cascades for the induction and improvement, as well as inhibition of several cytokine-regulated genes in the nucleus [75, 76]. The inflammatory process depends on proinflammatory and anti-inflammatory cytokines, where the anti-inflammatory cytokine, interleukin-10 (IL-10), is produced by monocytes, T cells, B cells, macrophages, natural killer cells, and dendritic cells, which inhibit proinflammatory cytokines, chemokines, and chemokine receptors, responsible for intestinal inflammation. A mechanism of immune regulation, involving two distinct categories probiotics (immunostimulatory and immunoregulatory), is shown in Figure 2. Immunostimulatory probiotics have the ability to act against infection and cancer cells, inducing IL-12 production, which activates NK cells and develops Th1 cells. These probiotics also act against allergy through a balance between Th1 and Th2. On the other hand, immunoregulatory probiotics have been characterized with IL-10 and Treg cell production, which results in decreases in allergy, IBD, autoimmune diseases, and inflammatory responses [77].

In an *in vitro* study with Caco-2 cells [78], proinflammatory cytokines (IL-1β, IL-8, and TNF-α) were induced by *Lactobacillus sakei*, whereas *Lactobacillus johnsonii* influenced the production of TGF-β (anti-inflammatory). It has been revealed that IL-6 favors the clonal expansion of IgA B lymphocytes and stimulates the production of antibodies such as IgM, IgG, and reduced secretion of IgE [79]. In addition, anti-inflammatory cytokines, such as IL-4, IL-5, IL-6, IL-10, and IL-13, are produced by Th2 cells, DCs, monocytes, B cells, and Tregs and induce adaptive immune response in the body [80]. In an earlier study, Borruel et al. [81] cultured intestinal mucosa of Crohn's disease patient with nonpathogenic bacteria including *Lactobacillus casei, Lactobacillus bulgaricus, Lactobacillus crispatus*, and *Escherichia coli* to investigate bacterial modulating effects on cytokine responses. Considering a significant reduction in the proinflammatory cytokine TNF-α in inflamed mucosa cultured with *L. casei* and *L. bulgaricus*, the authors noted that probiotics interact with immunocompetent cells and modulate the production of proinflammatory cytokines. In an interleukin-10-deficient mouse model, *Lactobacillus salivarius* and *Bifidobacterium infantis* have been used to evaluate their impact on the immune system of hosts in terms of mucosal and systemic cytokine profiles [82]. Significant

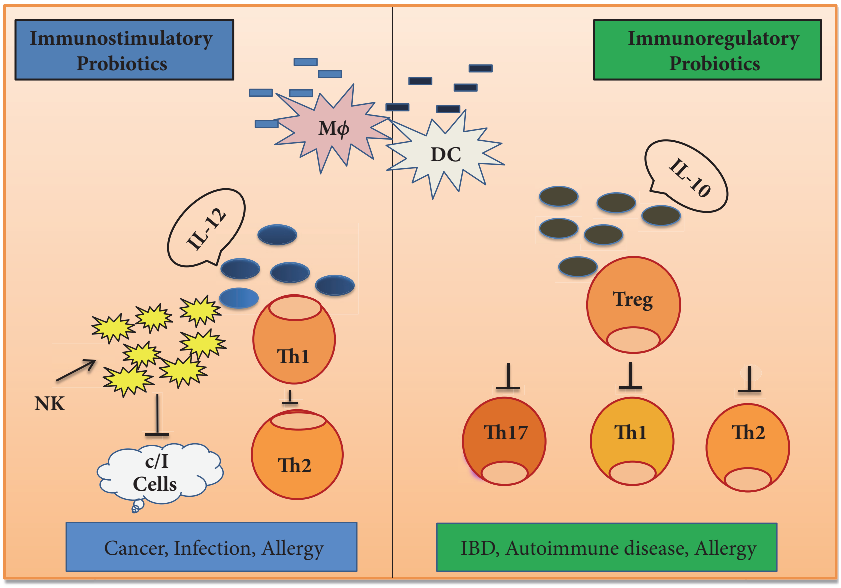
Immunostimulatory Probiotics
Immunoregulatory Probiotics
Mϕ
DC
IL-12
IL-10
Treg
Th1
Th2
Th17
Th1
Th2
NK
c/I Cells
Cancer, Infection, Allergy
IBD, Autoimmune disease, Allergy

Figure 2: Mechanism of immune regulation by probiotics.

reductions in interferon-γ (INF-γ) and TNF-α by Peyer's patch lymphocytes and proinflammatory cytokine production by spleen cells were found in probiotic-treated mice. The administration of a mixture of *L. paracasei* and *L. reuteri* to IL-10-deficient mice infected with *Helicobacter hepaticus* resulted in reductions in mucosal proinflammatory cytokines and, consequently, reduced the development of colitis [83]. Yan and Polk [84] found that *Lactobacillus rhamnosus* GG plays a vital role in activating antiapoptotic Akt/protein kinase B and in the inhibition of proapoptotic factors through the p38 MAPK pathway. Recently, Karamese et al. [85] administrated a mixture of *Lactobacillus* and *Bifidobacterium* species to rats for evaluation of the immunomodulatory effects of probiotics, where modulation or regulation of immune responses is evident through the upregulation of IL-10 (an anti-inflammatory cytokine) and the downregulation of TNF-α and IL-6 (proinflammatory cytokines). It has also been reported that application of probiotics leads to significant increases in IgA and IgG concentrations in rats, although this is dose-dependent.

Probiotics also have potential as immunomodulators with the ability to interact with epithelium and DCs, monocytes/macrophages, and lymphocytes. Borruel et al. [81] cultured mucosal samples from Crohn's disease patients with *Escherichia coli, Lactobacillus casei, Lactobacillus bulgaricus,* and *Lactobacillus crispatus* and reported that *Lactobacillus casei* and *Lactobacillus bulgaricus* significantly reduced the production of the proinflammatory cytokine TNF-α through interaction with immunocompetent cells. The oral administration of lactic acid bacteria, such as *Lactobacillus casei, L. acidophilus, L. rhamnosus, L. delbrueckii subsp. bulgaricus, L. plantarum, Lactococcus lactis,* and *Streptococcus thermophiles,* increases the number of IgA-producing cells associated with lamina propria in mucosa and this effect is dose-dependent. It has been reported that most of the lactic acid bacteria assayed induced inflammatory immune responses, although none of them are unable to induce cytotoxicity mechanisms [86]. Livingston et al. [87] treated bone-marrow-derived dendritic cells (BMDCs) with *Lactobacillus reuteri* 100-23, which were then incubated with splenic T cells from ovalbumin T cell receptor transgenic mice. Anti-inflammatory cytokine IL-10, induced by BMDCs, resulted in lower IL-2 production and increased TGF-β production. Different *Lactobacillus* and *Bifidobacterium* strains demonstrate the potential to trigger epithelial cell expression of IL-10, TGF-β, and IL-6 and further stimulate the immunoglobulin production (IgA). Probiotic strains stimulate the immunoglobulin receptors of intestinal epithelial cells [88]. Various animal models suggest that the effects of probiotics on the immunomodulation of cytokines are strain-specific; therefore, combinations of different probiotic strains are beyond the scope of further study to treat inflammation-associated tissue damage and gastrointestinal inflammation in humans.

5. Conclusions

Probiotic treatment is a promising research arena in the medical sciences, since probiotics alone, or together with prebiotics, have potential in the modulation of gut microbiota and immune responses in the host. However, a number of scientific reports are identical in terms of the role of probiotics in preventing obesity, inflammatory diseases, and cancer. The immunomodulatory effects of probiotics have gained much attention for the treatment of degenerative and other diseases caused by pathogenic microorganisms. Probiotics have a positive influence on the innate immunity, exerting several antiviral properties. Furthermore, it has been established that probiotics increase gut barrier functions by stimulating B cells and by influencing cytokine production, which initiates adaptive responses in the host body, although there are insufficient research publications regarding how probiotics induce immunomodulatory effects in the treatment of inflammation.

It is also urgent to understand cytokine secretion by Th2 cells, DCs, monocytes, B cells, and Tregs in order to establish new strains of probiotics. Further studies can be suggested to determine the precise action of probiotics on inflammation because these findings will be key routes in the medical sector and for better human health.

Disclosure

This review article does not contain any studies involving human participants or animals performed by any of the authors.

Conflicts of Interest

The authors declare that there are no conflicts of interest regarding the publication of this article.

Authors' Contributions

Md. Abul Kalam Azad and Manobendro Sarker contributed equally to this manuscript.

Acknowledgments

This work was supported by the National Key R&D Program of China (2016YFD0501201, 2016YFD0200900, and 2016YFD0500504) and the National Natural Science Foundation of China (31702127).

References

[1] C. Hill, F. Guarner, G. Reid et al., "Expert consensus document: the International Scientific Association for Probiotics and Prebiotics consensus statement on the scope and appropriate use of the term probiotic," *Nature Reviews Gastroenterology & Hepatology*, vol. 11, no. 8, pp. 506–514, 2014.

[2] M. A. K. Azad, M. Sarker, T. Li, and J. Yin, "Probiotic Species in the Modulation of Gut Microbiota: An Overview," *BioMed Research International*, vol. 2018, Article ID 9478630, 8 pages, 2018.

[3] S. C. Rao, G. K. Athalye-Jape, G. C. Deshpande, K. N. Simmer, and S. K. Patole, "Probiotic supplementation and late-onset sepsis in preterm infants: A meta-analysis," *Pediatrics*, vol. 137, no. 3, Article ID e20153684, 2016.

[4] N. B. Kristensen, T. Bryrup, K. H. Allin, T. Nielsen, T. H. Hansen, and O. Pedersen, "Alterations in fecal microbiota composition by probiotic supplementation in healthy adults: A systematic review of randomized controlled trials," *Genome Medicine*, vol. 8, no. 1, article no. 52, 2016.

[5] A. L. Kau, P. P. Ahern, N. W. Griffin, A. L. Goodman, and J. I. Gordon, "Human nutrition, the gut microbiome and the immune system," *Nature*, vol. 474, no. 7351, pp. 327–336, 2011.

[6] M. Bermudez-Brito, J. Plaza-Díaz, S. Muñoz-Quezada, C. Gómez-Llorente, and A. Gil, "Probiotic mechanisms of action," *Annals of Nutrition and Metabolism*, vol. 61, no. 2, pp. 160–174, 2012.

[7] P. Bin, M. A. K. Azad, G. Liu, D. Zhu, S. W. Kim, and Y. Yin, "Effects of different levels of methionine on sow health and plasma metabolomics during late gestation," *Food & Function*, vol. 9, no. 9, pp. 4979–4988, 2018.

[8] R. George Kerry, J. K. Patra, S. Gouda, Y. Park, H. Shin, and G. Das, "Benefaction of probiotics for human health: A review," *Journal of Food and Drug Analysis*, vol. 26, no. 3, pp. 927–939, 2018.

[9] Z. Küskü-Kiraz, S. Genc, S. Bekpınar et al., "Effects of betaine supplementation on nitric oxide metabolism, atherosclerotic parameters, and fatty liver in guinea pigs fed a high cholesterol plus methionine diet," *Nutrition Journal* , vol. 45, pp. 41–48, 2018.

[10] C. Tan, H. Wei, H. Sun et al., "Effects of dietary supplementation of oregano essential oil to sows on oxidative stress status, lactation feed intake of sows, and piglet performance," *BioMed Research International*, vol. 2015, Article ID 525218, 9 pages, 2015.

[11] H. S. Gill, "Dietary probiotic supplementation to enhance cellular immunity in the elderly," *British Journal of Biomedical Science*, vol. 58, pp. 94–96, 2001.

[12] C. Wood, S. Keeling, S. Bradley, P. Johnson-Green, and J. M. Green-Johnson, "Interactions in the mucosal microenvironment: Vasoactive intestinal peptide modulates the down-regulatory action of Lactobacillus rhamnosus on LPS-induced interleukin-8 production by intestinal epithelial cells," *Microbial Ecology in Health and Disease*, vol. 19, no. 3, pp. 191–200, 2007.

[13] J. Villena, M. Medina, E. Vintiñi, and S. Alvarez, "Stimulation of respiratory immunity by oral administration of Lactococcus lactis," *Canadian Journal of Microbiology*, vol. 54, no. 8, pp. 630–638, 2008.

[14] P. Kankaanpää, Y. Sütas, S. Salminen, and E. Isolauri, "Homogenates derived from probiotic bacteria provide down-regulatory signals for peripheral blood mononuclear cells," *Food Chemistry*, vol. 83, no. 2, pp. 269–277, 2003.

[15] P. Bodera and A. Chcialowski, "Immunomodulatory effect of probiotic bacteria," *Recent Patents on Inflammation & Allergy Drug Discovery*, vol. 3, no. 1, pp. 58–64, 2009.

[16] M. A. K. Azad, P. Bin, G. Liu, J. Fang, T. Li, and Y. Yin, "Effects of different methionine level on offspring piglets during late gestation and lactation," *Food & Function*, 2018.

[17] S. U. Islam, "Clinical Uses of Probiotics," *Medicine*, vol. 95, no. 5, p. e2658, 2016.

[18] M. F. Ooi, N. Mazlan, H. L. Foo et al., "Effects of carbon and nitrogen sources on bacteriocin-inhibitory activity of postbiotic metabolites produced by Lactobacillus plantarum I-UL4," *Malaysian Journal of Microbiology*, vol. 11, no. 2, pp. 176–184, 2015.

[19] D. L. Topping and P. M. Clifton, "Short-chain fatty acids and human colonic function: roles of resistant starch and nonstarch polysaccharides," *Physiological Reviews*, vol. 81, no. 3, pp. 1031–1064, 2001.

[20] H. Yadav, S. Jain, and P. R. Sinha, "Oral administration of dahi containing probiotic *Lactobacillus acidophilus* and *Lactobacillus casei* delayed the progression of streptozotocin-induced diabetes in rats," *Journal of Dairy Research*, vol. 75, no. 2, pp. 189–195, 2008.

[21] N. Şengul, S. Isik, B. Aslim, G. Ucar, and A. E. Demirbag, "The effect of exopolysaccharide-producing probiotic strains on gut oxidative damage in experimental colitis," *Digestive Diseases and Sciences*, vol. 56, no. 3, pp. 707–714, 2011.

[22] Z. Asemi, Z. Zare, H. Shakeri, S.-S. Sabihi, and A. Esmaillzadeh, "Effect of multispecies probiotic supplements on metabolic profiles, hs-CRP, and oxidative stress in patients with type 2 diabetes," *Annals of Nutrition and Metabolism*, vol. 63, no. 1-2, pp. 1–9, 2013.

[23] R. M. Patel and P. W. Denning, “Therapeutic Use of Prebiotics, Probiotics, and Postbiotics to Prevent Necrotizing Enterocolitis. What is the Current Evidence?” *Clinics in Perinatology*, vol. 40, no. 1, pp. 11–25, 2013.

[24] A. Saadatzadeh, “Biochemical and pathological evidences on the benefit of a new biodegradable nanoparticles of probiotic extract in murine colitis,” *Fundamental & Clinical Pharmacology*, vol. 26, no. 5, pp. 589–598, 2012.

[25] R. W. Hutkins, J. A. Krumbeck, L. B. Bindels et al., “Prebiotics: why definitions matter,” *Current Opinion in Biotechnology*, vol. 37, pp. 1–7, 2016.

[26] P. Kleniewska and R. Pawliczak, “Influence of Synbiotics on Selected Oxidative Stress Parameters,” *Oxidative Medicine and Cellular Longevity*, vol. 2017, 2017.

[27] A. Verma and G. Shukla, “Synbiotic (Lactobacillus rhamnosus+ Lactobacillus acidophilus+inulin) attenuates oxidative stress and colonic damage in 1,2 dimethylhydrazine dihydrochloride-induced colon carcinogenesis in Sprague’Dawley rats: A long-term study,” *European Journal of Cancer Prevention*, vol. 23, no. 6, pp. 550–559, 2014.

[28] K. Kavitha, A. G. Reddy, K. K. Reddy, C. S. V. S. Kumar, G. Boobalan, and K. Jayakanth, “Hypoglycemic, hypolipidemic and antioxidant effects of pioglitazone, insulin and synbiotic in diabetic rats,” *Veterinary World*, vol. 9, no. 2, pp. 118–122, 2016.

[29] C. Chaiyasut, T. Pattananandecha, S. Sirilun, P. Suwannalert, S. Peerajan, and B. S. Sivamaruthi, “Synbiotic preparation with lactic acid bacteria and inulin as a functional food: In vivo evaluation of microbial activities, and preneoplastic aberrant crypt foci,” *Food Science and Technology*, vol. 37, no. 2, pp. 328–336, 2017.

[30] Y. Dixit, A. Wagle, and B. Vakil, “Patents in the Field of Probiotics, Prebiotics, Synbiotics: A Review,” *Journal of Food: Microbiology Safety & Hygiene*, pp. 01-02, 2016.

[31] C. Westermann, M. Gleinser, S. C. Corr, and C. U. Riedel, “A Critical Evaluation of Bifidobacterial Adhesion to the Host Tissue,” *Frontiers in Microbiology*, vol. 7, 2016.

[32] S. Bartosch, E. J. Woodmansey, J. C. M. Paterson, M. E. T. McMurdo, and G. T. Macfarlane, “Microbiological effects of consuming a synbiotic containing Bifidobacterium bifidum, Bifidobacterium lactis, and oligofructose in elderly persons, determined by real-time polymerase chain reaction and counting of viable bacteria,” *Clinical Infectious Diseases*, vol. 40, no. 1, pp. 28–37, 2005.

[33] G. T. Macfarlane, H. Steed, and S. Macfarlane, “Bacterial metabolism and health-related effects of galacto-oligosaccharides and other prebiotics,” *Journal of Applied Microbiology*, vol. 104, no. 2, pp. 305–344, 2008.

[34] A. A. Aachary and S. G. Prapulla, “Xylooligosaccharides (XOS) as an Emerging Prebiotic: Microbial Synthesis, Utilization, Structural Characterization, Bioactive Properties, and Applications,” *Comprehensive Reviews in Food Science and Food Safety*, vol. 10, no. 1, pp. 2–16, 2011.

[35] F. Onyenweaku et al., “Health benefits of probiotics,” *International Journal of Innovative and Applied Research*, vol. 4, no. 3, pp. 21–30, 2016.

[36] T. Arora, S. Singh, and R. K. Sharma, “Probiotics: interaction with gut microbiome and antiobesity potential,” *Nutrition Journal* , vol. 29, no. 4, pp. 591–596, 2013.

[37] J. El Jakee, R. Eid, and A. Rashidy, “Potential Antimicrobial Activities of Probiotic Lactobacillus Strains Isolated from Raw Milk,” *Journal of Probiotics & Health*, pp. 04-02, 2016.

[38] European Food Safety Authority (EFSA), “Scientific Opinion on the update of the list of QPS-recommended biological agents intentionally added to food or feed as notified to EFSA (2017 update),” *EFSA Journals*, vol. 15, pp. 1–177, 2017.

[39] H.-T. Nguyen, D.-H. Truong, S. Kouhoundé, S. Ly, H. Razafindralambo, and F. Delvigne, “Biochemical engineering approaches for increasing viability and functionality of probiotic bacteria,” *International Journal of Molecular Sciences*, vol. 17, no. 6, article no. 867, 2016.

[40] P. Sornplang and S. Piyadeatsoontorn, “Probiotic isolates from unconventional sources: a review,” *Journal of Animal Science and Technology*, vol. 58, no. 1, 2016.

[41] N. Kobyliak, C. Conte, G. Cammarota et al., “Probiotics in prevention and treatment of obesity: a critical view,” *Nutrition & Metabolism*, vol. 13, no. 1, 2016.

[42] G. Giorgetti, G. Brandimarte, F. Fabiocchi, S. Ricci, P. Flamini, G. Sandri et al., “Interactions between Innate Immunity, Microbiota, and Probiotics,” *Journal of Immunology Research*, vol. 2015, Article ID 501361, 7 pages, 2015.

[43] X. Chen, G. Yang, J. H. Song et al., “Probiotic yeast inhibits VEGFR signaling and angiogenesis in intestinal inflammation,” *PLoS ONE*, vol. 8, no. 5, Article ID e64227, 2013.

[44] M. Sabater-Molina, E. Larqué, F. Torrella, and S. Zamora, “Dietary fructooligosaccharides and potential benefits on health,” *Journal of Physiology and Biochemistry*, vol. 65, no. 3, pp. 315–328, 2009.

[45] J. Slavin, “Fiber and prebiotics: mechanisms and health benefits,” *Nutrients*, vol. 5, no. 4, pp. 1417–1435, 2013.

[46] S. Patel and A. Goyal, “The current trends and future perspectives of prebiotics research: a review,” *3 Biotech*, vol. 2, no. 2, pp. 115–125, 2012.

[47] R. P. De Souza Oliveira, A. C. Rodrigues Florence, P. Perego, M. N. De Oliveira, and A. Converti, “Use of lactulose as prebiotic and its influence on the growth, acidification profile and viable counts of different probiotics in fermented skim milk,” *International Journal of Food Microbiology*, vol. 145, no. 1, pp. 22–27, 2011.

[48] X. Zhou, Z. Ruan, X. Huang, Y. Zhou, S. Liu, and Y. Yin, “The prebiotic lactosucrose modulates gut metabolites and microbiota in intestinal inflammatory rats,” *Food Science and Biotechnology*, vol. 23, no. 1, pp. 157–163, 2014.

[49] D. P. M. Torres, M. D. P. F. Gonçalves, J. A. Teixeira, and L. R. Rodrigues, “Galacto-Oligosaccharides: Production, properties, applications, and significance as prebiotics,” *Comprehensive Reviews in Food Science and Food Safety*, vol. 9, no. 5, pp. 438–454, 2010.

[50] J. Vulevic, A. Juric, G. Tzortzis, and G. R. Gibson, “A mixture of *trans*-galactooligosaccharides reduces markers of metabolic syndrome and modulates the fecal microbiota and immune function of overweight adults1-3,” *Journal of Nutrition*, vol. 143, no. 3, pp. 324–331, 2013.

[51] C. E. Rycroft, M. R. Jones, G. R. Gibson, and R. A. Rastall, “A comparative in vitro evaluation of the fermentation properties of prebiotic oligosaccharides,” *Journal of Applied Microbiology*, vol. 91, no. 5, pp. 878–887, 2001.

[52] G. Moro, S. Arslanoglu, B. Stahl, J. Jelinek, U. Wahn, and G. Boehm, “A mixture of prebiotic oligosaccharides reduces the incidence of atopic dermatitis during the first six months of age,” *Archives of Disease in Childhood*, vol. 91, no. 10, pp. 814–819, 2006.

[53] M. Le Barz, F. F. Anhê, T. V. Varin et al., "Probiotics as Complementary Treatment for Metabolic Disorders," *Diabetes & Metabolism Journal*, vol. 39, no. 4, p. 291, 2015.

[54] C. Grootaert, P. van den Abbeele, M. Marzorati et al., "Comparison of prebiotic effects of arabinoxylan oligosaccharides and inulin in a simulator of the human intestinal microbial ecosystem," *FEMS Microbiology Ecology*, vol. 69, no. 2, pp. 231–242, 2009.

[55] E. Fuentes-Zaragoza, E. Sánchez-Zapata, E. Sendra et al., "Resistant starch as prebiotic: A review," *Starch - Stärke*, vol. 63, no. 7, pp. 406–415, 2011.

[56] V. Snoeck, B. Goddeeris, and E. Cox, "The role of enterocytes in the intestinal barrier function and antigen uptake," *Microbes and Infection*, vol. 7, no. 7-8, pp. 997–1004, 2005.

[57] B. Alberts, "Pathogens, infection, and innate immunity," in *Molecular Biology of the Cell*, M. Anderson and S. Granum, Eds., pp. 1485–1537, Garland Science, Taylor & Francis Group, New York, NY, USA, 5th edition, 2008.

[58] P. Gourbeyre, S. Denery, and M. Bodinier, "Probiotics, prebiotics, and synbiotics: Impact on the gut immune system and allergic reactions," *Journal of Leukocyte Biology*, vol. 89, no. 5, pp. 685–695, 2011.

[59] J. L. Sanchez-Trincado, M. Gomez-Perosanz, and P. A. Reche, "Fundamentals and Methods for T- and B-Cell Epitope Prediction," *Journal of Immunology Research*, vol. 2017, Article ID 2680160, 14 pages, 2017.

[60] M. Molero-Abraham, J.-P. Glutting, D. R. Flower, E. M. Lafuente, and P. A. Reche, "EPIPOX: Immunoinformatic Characterization of the Shared T-Cell Epitome between Variola Virus and Related Pathogenic Orthopoxviruses," *Journal of Immunology Research*, vol. 2015, 2015.

[61] V. Delcenserie et al., "Immunomodulatory Effects of Probiotics in the Intestinal Tract," *Current Issues in Molecular Biology*.

[62] F. van Wijk and H. Cheroutre, "Intestinal T cells: Facing the mucosal immune dilemma with synergy and diversity," *Seminars in Immunology*, vol. 21, no. 3, pp. 130–138, 2009.

[63] K. P. Murphy, *Janeway's immunobiology*, London/New York: Garland Science, Taylor & Francis Group, 8th edition, 2011.

[64] M. A. Otten and M. van Egmond, "The Fc receptor for IgA (FcαRI, CD89)," *Immunology Letters*, vol. 92, no. 1-2, pp. 23–31, 2004.

[65] L. Xiao, G. Ding, Y. Ding et al., "Effect of probiotics on digestibility and immunity in infants," *Medicine*, vol. 96, no. 14, p. e5953, 2017.

[66] C. M. Galdeano, A. De Moreno De Leblanc, E. Carmuega, R. Weill, and G. Perdigón, "Mechanisms involved in the immunostimulation by probiotic fermented milk," *Journal of Dairy Research*, vol. 76, no. 4, pp. 446–454, 2009.

[67] C. A. Dogi, F. Weill, and G. Perdigón, "Immune response of non-pathogenic Gram(+) and Gram(-) bacteria in inductive sites of the intestinal mucosa. Study of the pathway of signaling involved," *Immunobiology*, vol. 215, no. 1, pp. 60–69, 2010.

[68] C. M. Galdeano and G. Perdigón, "Role of viability of probiotic strains in their persistence in the gut and in mucosal immune stimulation," *Journal of Applied Microbiology*, vol. 97, no. 4, pp. 673–681, 2004.

[69] R. Savan and M. Sakai, "Genomics of fish cytokines," *Comparative Biochemistry and Physiology Part D: Genomics and Proteomics*, vol. 1, no. 1, pp. 89–101, 2006.

[70] B. Foligné, J. Dewulf, J. Breton, O. Claisse, A. Lonvaud-Funel, and B. Pot, "Probiotic properties of non-conventional lactic acid bacteria: Immunomodulation by Oenococcus oeni," *International Journal of Food Microbiology*, vol. 140, no. 2-3, pp. 136–145, 2010.

[71] R. Schwandner, R. Dziarski, H. Wesche, M. Rothe, and C. J. Kirschning, "Peptidoglycan- and lipoteichoic acid-induced cell activation is mediated by Toll-like receptor 2," *The Journal of Biological Chemistry*, vol. 274, no. 25, pp. 17406–17409, 1999.

[72] A. Kourelis, I. Zinonos, M. Kakagianni et al., "Validation of the dorsal air pouch model to predict and examine immunostimulatory responses in the gut," *Journal of Applied Microbiology*, vol. 108, no. 1, pp. 274–284, 2010.

[73] C. M. Galdeano and G. Perdigón, "The probiotic bacterium *Lactobacillus casei* induces activation of the gut mucosal immune system through innate immunity," *Clinical and Vaccine Immunology*, vol. 13, no. 2, pp. 219–226, 2006.

[74] K. V. Anderson, "Toll signaling pathways in the innate immune response," *Current Opinion in Immunology*, vol. 12, no. 1, pp. 13–19, 2000.

[75] I. E. Mulder, S. Wadsworth, and C. J. Secombes, "Cytokine expression in the intestine of rainbow trout (Oncorhynchus mykiss) during infection with Aeromonas salmonicida," *Fish and Shellfish Immunology*, vol. 23, no. 4, pp. 747–759, 2007.

[76] G. Biswas, H. Korenaga, R. Nagamine et al., "Elevated cytokine responses to vibrio harveyi infection in the japanese pufferfish (Takifugu rubripes) treated with lactobacillus paracasei spp. paracasei (06TCa22) isolated from the mongolian dairy product," *Fish and Shellfish Immunology*, vol. 35, no. 3, pp. 756–765, 2013.

[77] Y. Chiba, K. Shida, S. Nagata et al., "Well-controlled proinflammatory cytokine responses of Peyer's patch cells to probiotic Lactobacillus casei," *The Journal of Immunology*, vol. 130, no. 3, pp. 352–362, 2010.

[78] D. Haller, C. Bode, W. P. Hammes, A. M. A. Pfeifer, E. J. Schiffrin, and S. Blum, "Non-pathogenic bacteria elicit a differential cytokine response by intestinal epithelial cell/leucocyte co-cultures," *Gut*, vol. 47, no. 1, pp. 79–87, 2000.

[79] C. M. Galdeano, A. De Moreno De Leblanc, G. Vinderola, M. E. Bibas Bonet, and G. Perdigón, "Proposed model: mechanisms of immunomodulation induced by probiotic bacteria," *Clinical and Vaccine Immunology*, vol. 14, no. 5, pp. 485–492, 2007.

[80] K. W. Moore, R. de Waal Malefyt, R. L. Coffman, and A. O'Garra, "Interleukin-10 and the interleukin-10 receptor," *Annual Review of Immunology*, vol. 19, pp. 683–765, 2001.

[81] N. Borruel, M. Carol, F. Casellas et al., "Increased mucosal tumour necrosis factor α production in Crohn's disease can be downregulated ex vivo by probiotic bacteria," *Gut*, vol. 51, no. 5, pp. 659–664, 2002.

[82] J. McCarthy, L. O'Mahony, L. O'Callaghan et al., "Double blind, placebo controlled trial of two probiotic strains in interleukin 10 knockout mice and mechanistic link with cytokine balance," *Gut*, vol. 52, no. 7, pp. 975–980, 2003.

[83] J. A. Peña, A. B. Rogers, Z. Ge et al., "Probiotic Lactobacillus spp. diminish Helicobacter hepaticus-induced inflammatory bowel disease in interleukin-10-deficient mice," *Infection and Immunity*, vol. 73, no. 2, pp. 912–920, 2005.

[84] F. Yan and D. B. Polk, "Probiotic bacterium prevents cytokine-induced apoptosis in intestinal epithelial cells," *The Journal of Biological Chemistry*, vol. 277, no. 52, pp. 50959–50965, 2002.

[85] M. Karamese, H. Aydin, E. Sengul et al., "The Immunostimulatory Effect of Lactic Acid Bacteria in a Rat Model," *Iranian journal of immunology : IJI*, vol. 13, no. 3, pp. 220–228, 2016.

[86] E. Vitiñi, S. Alvarez, M. Medina, M. Medici, M. V. de Budeguer, and G. Perdigón, "Gut mucosal immunostimulation by lactic acid bacteria," *Biocell*, vol. 24, no. 3, pp. 223–232, 2000.

[87] M. Livingston, D. Loach, M. Wilson, G. W. Tannock, and M. Baird, "Gut commensal *Lactobacillus reuteri* 100–23 stimulates an immunoregulatory response," *Immunology & Cell Biology*, vol. 88, no. 1, pp. 99–102, 2010.

[88] A. A. Reséndiz-Albor, H. Reina-Garfias, S. Rojas-Hernández et al., "Regionalization of pIgR expression in the mucosa of mouse small intestine," *Immunology Letters*, vol. 128, no. 1, pp. 59–67, 2010.